

**11th Montreux Symp. on LC-MS,  
SFC-MS, CE-MS and MS-MS  
Montreux, 9-11 November 1994**

JOURNAL OF

# CHROMATOGRAPHY A

INCLUDING ELECTROPHORESIS AND OTHER SEPARATION METHODS

## EDITORS

U.A.Th. Brinkman (Amsterdam)  
R.W. Giese (Boston, MA)  
J.K. Haken (Kensington, N.S.W.)  
C.F. Poole (London)  
L.R. Snyder (Orinda, CA)  
S. Terabe (Hyogo)

EDITORS, SYMPOSIUM VOLUMES,  
E. Heftmann (Orinda, CA), Z. Deyl (Prague)

## EDITORIAL BOARD

D.W. Armstrong (Rolla, MO)  
W.A. Aue (Halifax)  
P. Boček (Brno)  
P.W. Carr (Minneapolis, MN)  
J. Crommen (Liège)  
V.A. Davankov (Moscow)  
G.J. de Jong (Groningen)  
Z. Deyl (Prague)  
S. Dilli (Kensington, N.S.W.)  
Z. El Rassi (Stillwater, OK)  
H. Engelhardt (Saarbrücken)  
M.B. Evans (Hatfield)  
S. Fanali (Rome)  
G.A. Guiochon (Knoxville, TN)  
P.R. Haddad (Hobart, Tasmania)  
I.M. Hais (Hradec Králové)  
W.S. Hancock (Palo Alto, CA)  
S. Hjertén (Uppsala)  
S. Honda (Higashi-Osaka)  
Cs. Horváth (New Haven, CT)  
J.F.K. Huber (Vienna)  
J. Janák (Brno)  
P. Jandera (Pardubice)  
B.L. Karger (Boston, MA)  
J.J. Kirkland (Newport, DE)  
E. sz. Kováts (Lausanne)  
C.S. Lee (Ames, IA)  
K. Macek (Prague)  
A.J.P. Martin (Cambridge)  
E.D. Morgan (Keele)  
H. Poppe (Amsterdam)  
P.G. Righetti (Milan)  
P. Schoenmakers (Amsterdam)  
R. Schwarzenbach (Dübendorf)  
R.E. Shoup (West Lafayette, IN)  
R.P. Singhal (Wichita, KS)  
A.M. Siouffi (Marseille)  
D.J. Strydom (Boston, MA)  
T. Takagi (Osaka)  
N. Tanaka (Kyoto)  
K.K. Unger (Mainz)  
P. van Zoonen (Bilthoven)  
F. Verpoorte (Leiden)  
Gy. Vigh (College Station, TX)  
J.T. Watson (East Lansing, MI)  
B.D. Westerlund (Uppsala)

## EDITORS, BIBLIOGRAPHY SECTION

Z. Deyl (Prague), J. Janák (Brno), V. Schwarz (Prague)

ELSEVIER

# JOURNAL OF CHROMATOGRAPHY A

INCLUDING ELECTROPHORESIS AND OTHER SEPARATION METHODS

**Scope.** The *Journal of Chromatography A* publishes papers on all aspects of **chromatography, electrophoresis** and related methods. Contributions consist mainly of research papers dealing with chromatographic theory, instrumental developments and their applications. In the *Symposium volumes*, which are under separate editorship, proceedings of symposia on chromatography, electrophoresis and related methods are published. *Journal of Chromatography B: Biomedical Applications*—This journal, which is under separate editorship, deals with the following aspects: developments in and applications of chromatographic and electrophoretic techniques related to clinical diagnosis or alterations during medical treatment; screening and profiling of body fluids or tissues related to the analysis of active substances and to metabolic disorders; drug level monitoring and pharmacokinetic studies; clinical toxicology; forensic medicine; veterinary medicine; occupational medicine; results from basic medical research with direct consequences in clinical practice.

**Submission of Papers.** The preferred medium of submission is on disk with accompanying manuscript (see *Electronic manuscripts* in the Instructions to Authors, which can be obtained from the publisher, Elsevier Science B.V., P.O. Box 330, 1000 AH Amsterdam, Netherlands). Manuscripts (in English; *four* copies are required) should be submitted to: Editorial Office of *Journal of Chromatography A*, P.O. Box 681, 1000 AR Amsterdam, Netherlands, Telefax (+31-20) 485 2304, or to: The Editor of *Journal of Chromatography B: Biomedical Applications*, P.O. Box 681, 1000 AR Amsterdam, Netherlands. Review articles are invited or proposed in writing to the Editors who welcome suggestions for subjects. An outline of the proposed review should first be forwarded to the Editors for preliminary discussion prior to preparation. Submission of an article is understood to imply that the article is original and unpublished and is not being considered for publication elsewhere. For copyright regulations, see below.

**Publication information.** *Journal of Chromatography A* (ISSN 0021-9673): for 1995 Vols. 683–714 are scheduled for publication. *Journal of Chromatography B: Biomedical Applications* (ISSN 0378-4347): for 1995 Vols. 663–674 are scheduled for publication. Subscription prices for *Journal of Chromatography A*, *Journal of Chromatography B: Biomedical Applications* or a combined subscription are available upon request from the publisher. Subscriptions are accepted on a prepaid basis only and are entered on a calendar year basis. Issues are sent by surface mail except to the following countries where air delivery via SAL is ensured: Argentina, Australia, Brazil, Canada, China, Hong Kong, India, Israel, Japan, Malaysia, Mexico, New Zealand, Pakistan, Singapore, South Africa, South Korea, Taiwan, Thailand, USA. For all other countries airmail rates are available upon request. Claims for missing issues must be made within six months of our publication (mailing) date. Please address all your requests regarding orders and subscription queries to: Elsevier Science B.V., Journal Department, P.O. Box 211, 1000 AE Amsterdam, Netherlands. Tel.: (+31-20) 485 3642; Fax: (+31-20) 485 3598. Customers in the USA and Canada wishing information on this and other Elsevier journals, please contact Journal Information Center, Elsevier Science Inc., 655 Avenue of the Americas, New York, NY 10010, USA, Tel. (+1-212) 633 3750, Telefax (+1-212) 633 3764.

**Abstracts/Contents Lists** published in Analytical Abstracts, Biochemical Abstracts, Biological Abstracts, Chemical Abstracts, Chemical Titles, Chromatography Abstracts, Current Awareness in Biological Sciences (CABS), Current Contents/Life Sciences, Current Contents/Physical, Chemical & Earth Sciences, Deep-Sea Research/Part B: Oceanographic Literature Review, Excerpta Medica, Index Medicus, Mass Spectrometry Bulletin, PASCAL-CNRS, Referativnyi Zhurnal, Research Alert and Science Citation Index.

**US Mailing Notice.** *Journal of Chromatography A* (ISSN 0021-9673) is published weekly (total 52 issues) by Elsevier Science B.V., (Sara Burgerhartstraat 25, P.O. Box 211, 1000 AE Amsterdam, Netherlands). Annual subscription price in the USA US\$ 5389.00 (US\$ price valid in North, Central and South America only) including air speed delivery. Second class postage paid at Jamaica, NY 11431. **USA POSTMASTERS:** Send address changes to *Journal of Chromatography A*, Publications Expediting, Inc., 200 Meacham Avenue, Elmont, NY 11003. Airfreight and mailing in the USA by Publications Expediting.

**See inside back cover** for Publication Schedule, Information for Authors and information on Advertisements.

© 1995 ELSEVIER SCIENCE B.V. All rights reserved.

0021-9673/95/\$09.50

No part of this publication may be reproduced, stored in a retrieval system or transmitted in any form or by any means, electronic, mechanical, photocopying, recording or otherwise, without the prior written permission of the publisher, Elsevier Science B.V., Copyright and Permissions Department, P.O. Box 521, 1000 AM Amsterdam, Netherlands.

Upon acceptance of an article by the journal, the author(s) will be asked to transfer copyright of the article to the publisher. The transfer will ensure the widest possible dissemination of information.

**Special regulations for readers in the USA**—This journal has been registered with the Copyright Clearance Center, Inc. Consent is given for copying of articles for personal or internal use, or for the personal use of specific clients. This consent is given on the condition that the copier pays through the Center the per-copy fee stated in the code on the first page of each article for copying beyond that permitted by Sections 107 or 108 of the US Copyright Law. The appropriate fee should be forwarded with a copy of the first page of the article to the Copyright Clearance Center, Inc., 222 Rosewood Drive, Danvers, MA 01923, USA. If no code appears in an article, the author has not given broad consent to copy and permission to copy must be obtained directly from the author. The fee indicated on the first page of an article in this issue will apply retroactively to all articles published in the journal, regardless of the year of publication. This consent does not extend to other kinds of copying, such as for general distribution, resale, advertising and promotion purposes, or for creating new collective works. Special written permission must be obtained from the publisher for such copying.

No responsibility is assumed by the Publisher for any injury and/or damage to persons or property as a matter of products liability, negligence or otherwise, or from any use or operation of any methods, products, instructions or ideas contained in the materials herein. Because of rapid advances in the medical sciences, the Publisher recommends that independent verification of diagnoses and drug dosages should be made.

Although all advertising material is expected to conform to ethical (medical) standards, inclusion in this publication does not constitute a guarantee or endorsement of the quality or value of such product, or of the claims made of it by its manufacturer.

Ⓢ The paper used in this publication meets the requirements of ANSI/NISO Z39.48-1992 (Permanence of Paper).

Printed in the Netherlands

**For Contents see p. VII.**

JOURNAL OF CHROMATOGRAPHY A

VOL. 712 (1995)



# JOURNAL OF CHROMATOGRAPHY A

INCLUDING ELECTROPHORESIS AND OTHER SEPARATION METHODS

## EDITORS

U.A.Th. BRINKMAN (Amsterdam), R.W. GIESE (Boston, MA), J.K. HAKEN (Kensington, N.S.W.),  
C.F. POOLE (London), L.R. SNYDER (Orinda, CA), S. TERABE (Hyogo)

## EDITORS, SYMPOSIUM VOLUMES

E. HEFTMANN (Orinda, CA), Z. DEYL (Prague)

## EDITORIAL BOARD

D.W. Armstrong (Rolla, MO), W.A. Aue (Halifax), P. Boček (Brno), P.W. Carr (Minneapolis, MN), J. Crommen (Liège), V.A. Davankov (Moscow), G.J. de Jong (Groningen), Z. Deyl (Prague), S. Dilli (Kensington, N.S.W.), Z. El Rassi (Stillwater, OK), H. Engelhardt (Saarbrücken), M.B. Evans (Hatfield), S. Fanali (Rome), G.A. Guiochon (Knoxville, TN), P.R. Haddad (Hobart, Tasmania), I.M. Hais (Hradec Králové), W.S. Hancock (Palo Alto, CA), S. Hjertén (Uppsala), S. Honda (Higashi-Osaka), Cs. Horváth (New Haven, CT), J.F.K. Huber (Vienna), J. Janák (Brno), P. Jandera (Pardubice), B.L. Karger (Boston, MA), J.J. Kirkland (Newport, DE), E. sz. Kováts (Lausanne), C.S. Lee (Ames, IA), K. Macek (Prague), A.J.P. Martin (Cambridge), E.D. Morgan (Keele), H. Poppe (Amsterdam), P.G. Righetti (Milan), P. Schoenmakers (Amsterdam), R. Schwarzenbach (Dübendorf), R.E. Shoup (West Lafayette, IN), R.P. Singhal (Wichita, KS), A.M. Siouffi (Marseille), D.J. Strydom (Boston, MA), T. Takagi (Osaka), N. Tanaka (Kyoto), K.K. Unger (Mainz), P. van Zoonen (Bilthoven), R. Verpoorte (Leiden), Gy. Vigh (College Station, TX), J.T. Watson (East Lansing, MI), B.D. Westerlund (Uppsala)

## EDITORS, BIBLIOGRAPHY SECTION

Z. Deyl (Prague), J. Janák (Brno), V. Schwarz (Prague)



ELSEVIER

Amsterdam – Lausanne – New York – Oxford – Shannon – Tokyo

---

*J. Chromatogr. A*, Vol. 712 (1995)

© 1995 ELSEVIER SCIENCE B.V. All rights reserved.

0021-9673/95/\$09.50

No part of this publication may be reproduced, stored in a retrieval system or transmitted in any form or by any means, electronic, mechanical, photocopying, recording or otherwise, without the prior written permission of the publisher, Elsevier Science B.V., Copyright and Permissions Department, P.O. Box 521, 1000 AM Amsterdam, Netherlands.

Upon acceptance of an article by the journal, the author(s) will be asked to transfer copyright of the article to the publisher. The transfer will ensure the widest possible dissemination of information.

*Special regulations for readers in the USA* – This journal has been registered with the Copyright Clearance Center, Inc. Consent is given for copying of articles for personal or internal use, or for the personal use of specific clients. This consent is given on the condition that the copier pays through the Center the per-copy fee stated in the code on the first page of each article for copying beyond that permitted by Sections 107 or 108 of the US Copyright Law. The appropriate fee should be forwarded with a copy of the first page of the article to the Copyright Clearance Center, Inc., 222 Rosewood Drive, Danvers, MA 01923, USA. If no code appears in an article, the author has not given broad consent to copy and permission to copy must be obtained directly from the author. The fee indicated on the first page of an article in this issue will apply retroactively to all articles published in the journal, regardless of the year of publication. This consent does not extend to other kinds of copying, such as for general distribution, resale, advertising and promotion purposes, or for creating new collective works. Special written permission must be obtained from the publisher for such copying.

No responsibility is assumed by the Publisher for any injury and/or damage to persons or property as a matter of products liability, negligence or otherwise, or from any use or operation of any methods, products, instructions or ideas contained in the materials herein. Because of rapid advances in the medical sciences, the Publisher recommends that independent verification of diagnoses and drug dosages should be made.

Although all advertising material is expected to conform to ethical (medical) standards, inclusion in this publication does not constitute a guarantee or endorsement of the quality or value of such product or of the claims made of it by its manufacturer.

Ⓢ The paper used in this publication meets the requirements of ANSI/NISO Z39.48-1992 (Permanence of Paper).

Printed in the Netherlands

SYMPOSIUM ISSUE



**11TH MONTREUX SYMPOSIUM ON LIQUID  
CHROMATOGRAPHY-MASS SPECTROMETRY,  
SUPERCRITICAL FLUID CHROMATOGRAPHY-MASS  
SPECTROMETRY, CAPILLARY ELECTROPHORESIS-  
MASS SPECTROMETRY AND TANDEM  
MASS SPECTROMETRY**

*Montreux (Switzerland), 9-11 November 1994*

*Guest Editor*

**J. VAN DER GREEF**

(Leiden)





## CONTENTS

(Abstracts/Contents Lists published in Analytical Abstracts, Biochemical Abstracts, Biological Abstracts, Chemical Abstracts, Chemical Titles, Chromatography Abstracts, Current Awareness in Biological Sciences (CABS), Current Contents/Life Sciences, Current Contents/Physical, Chemical & Earth Sciences, Deep-Sea Research/Part B: Oceanographic Literature Review, Excerpta Medica, Index Medicus, Mass Spectrometry Bulletin, PASCAL-CNRS, Referativnyi Zhurnal, Research Alert and Science Citation Index)

### 11TH MONTREUX SYMPOSIUM ON LIQUID CHROMATOGRAPHY-MASS SPECTROMETRY, SUPERCRITICAL FLUID CHROMATOGRAPHY-MASS SPECTROMETRY, CAPILLARY ELECTROPHORESIS-MASS SPECTROMETRY AND TANDEM MASS SPECTROMETRY

Foreword by J. van der Greef (Leiden, Netherlands) . . . . .	1
---	---

### LIQUID CHROMATOGRAPHY-MASS SPECTROMETRY

#### Technical aspects

Application of a new atmospheric pressure ionization source for double focusing sector instruments by P. Dobberstein and H. Muenster (Bremen, Germany) . . . . .	3
Application of liquid chromatography-atmospheric pressure chemical ionization mass spectrometry to a sector mass spectrometer by K. Nojima and S. Fujimaki (Tokyo, Japan) and R.C. Hertsens and T. Morita (Zaventem, Belgium) . . . . .	17
Effect of ion source pressure on ion formation of carbamates in particle-beam chemical-ionisation mass spectrometry by M. Honing and D. Barceló (Barcelona, Spain) and M.E. Jager, J. Slobodnik, B.L.M. van Baar and U.A.Th. Brinkman (Amsterdam Netherlands) . . . . .	21
Comparison of softwares used for the detection of analytes present at low levels in liquid chromatographic-mass spectrometric experiments by J. Visentini and E.C. Kwong (Quebec, Canada) and A. Carrier, D. Zidarov and M.J. Bertrand (Montreal, Canada) . . . . .	31

#### Pharmaceutical applications

Enantiospecific determination of nimodipine in human plasma by liquid chromatography-tandem mass spectrometry by W.M. Mück (Wuppertal, Germany) . . . . .	45
Estimation of ranolazine and eleven Phase I metabolites in human plasma by liquid chromatography-atmospheric pressure chemical ionisation mass spectrometry with selected-ion monitoring by W.J. Herron, J. Eadie and A.D. Penman (Edinburgh, UK) . . . . .	55
Metabolic studies of an orally active platinum anticancer drug by liquid chromatography-electrospray ionization mass spectrometry by G.K. Poon, F.I. Raynaud, P. Mistry, D.E. Odell, L.R. Kelland and K.R. Harrap (Surrey, UK) and C.F.J. Barnard and B.A. Murrer (Reading, UK) . . . . .	61
Rapid analysis of $\beta$ -agonists in urine by thermospray tandem mass spectrometry by J.A. van Rhijn (Wageningen, Netherlands), M. O'Keefe (Dublin, Ireland), H.H. Heskamp (Wageningen, Netherlands) and S. Collins (Dublin, Ireland) . . . . .	67
Determination of an endothelin receptor antagonist in human plasma by narrow-bore liquid chromatography and ionspray tandem mass spectrometry by B. Lausecker and G. Hopfgartner (Basle, Switzerland) . . . . .	75

#### Environmental applications

Determination of the pesticide diflubenzuron in mushrooms by high-performance liquid chromatography-atmospheric pressure chemical ionisation mass spectrometry by K.A. Barnes, J.R. Startin, S.A. Thorpe, S.L. Reynolds and R.J. Fussell (Norwich, UK) . . . . .	85
Identification of diflubenzuron by packed-capillary supercritical fluid chromatography-mass spectrometry with electron-capture negative ionization by C. Brede and E. Lundanes (Oslo, Norway) . . . . .	95

Determination of organophosphorus pesticides and their transformation products in river waters by automated on-line solid-phase extraction followed by thermospray liquid chromatography–mass spectrometry by S. Lacorte and D. Barceló (Barcelona, Spain) . . . . .	103
Trace determination of herbicides in estuarine waters by liquid chromatography–high-flow pneumatically assisted electrospray mass spectrometry by C. Molina (Barcelona, Spain), G. Durand (Brest, France) and D. Barceló (Barcelona, Spain) . . . . .	113
Polar organic pollutants in the Elbe river. Liquid chromatographic–mass spectrometric and flow-injection analysis–mass spectrometric analyses demonstrating changes in quality and concentration during the unification process in Germany by H.F. Schröder (Aachen, Germany) . . . . .	123
<i>Other applications</i>	
Identification of phosphocysteine by electrospray mass spectrometry combined with Edman degradation by C. Weigt, H. Korte, R.P. von Strandmann, W. Hengstenberg and H.E. Meyer (Bochum, Germany) . . . . .	141
Separation and detection of 4-hexadecylaniline maltooligosaccharide derivatives with packed capillary liquid chromatography–frit fast atom bombardment–mass spectrometry by L. Johansson, H. Karlsson and K.-A. Karlsson (Göteborg, Sweden) . . . . .	149
Liquid chromatography combined with thermospray and continuous-flow fast atom bombardment mass spectrometry of glycosides in crude plant extracts by J.-L. Wolfender and K. Hostettmann (Lausanne, Switzerland) and F. Abe, T. Nagao, H. Okabe and T. Yamauchi (Fukuoka, Japan) . . . . .	155
Liquid chromatographic–mass spectrometric studies on the enzymatic degradation of $\beta$ -endorphin by endothelial cells by M. Brudel, U. Kertscher, D. Schröder, M.F. Melzig and B. Mehlig (Berlin, Germany) . . . . .	169
Enhanced sensitivity for peptide mapping with electrospray liquid chromatography–mass spectrometry in the presence of signal suppression due to trifluoroacetic acid-containing mobile phases by A. Apffel, S. Fischer, G. Goldberg, P.C. Goodley and F.E. Kuhlmann (Palo Alto, CA, USA) . . . . .	177
Qualitative liquid chromatographic–atmospheric-pressure chemical-ionisation mass spectrometric analysis of polyethylene terephthalate oligomers by K.A. Barnes, A.P. Damant, J.R. Startin and L. Castle (Norwich, UK) . . . . .	191

## ELECTROMIGRATION METHODS–MASS SPECTROMETRY

### *Technical aspects*

Development of an instrumental configuration for pseudo-electrochromatography–electrospray mass spectrometry by S.E.G. Dekkers, U.R. Tjaden and J. van der Greef (Leiden, Netherlands) . . . . .	201
Performance of an electrospray-interfaced thermospray ion source in hyphenated techniques by R.A.M. van der Hoeven, B.A.P. Buscher, U.R. Tjaden and J. van der Greef (Leiden, Netherlands) . . . . .	211
On-line coupling of micellar electrokinetic chromatography to electrospray mass spectrometry by M.H. Lamoree, U.R. Tjaden and J. van der Greef (Leiden, Netherlands) . . . . .	219
Combined liquid–liquid electroextraction–isotachopheresis for loadability enhancement in capillary zone electrophoresis–mass spectrometry by E. van der Vlis, M. Mazereeuw, U.R. Tjaden, H. Irth and J. van der Greef (Leiden, Netherlands) . . . . .	227

### *Miscellaneous applications*

Analysis of inositol phosphates and derivatives using capillary zone electrophoresis–mass spectrometry by B.A.P. Buscher, R.A.M. van der Hoeven and U.R. Tjaden (Leiden, Netherlands), E. Andersson (Perstorp, Sweden) and J. van der Greef (Leiden, Netherlands) . . . . .	235
Optimization of conditions for the analysis of a peptide mixture and a tryptic digest of cytochrome <i>c</i> by capillary electrophoresis–electrospray-ionization mass spectrometry with an improved liquid-sheath probe by J.F. Banks (Branford, CT, USA) . . . . .	245
Mass spectral analyses of microcystins from toxic cyanobacteria using on-line chromatographic and electrophoretic separations by K.P. Bateman, P. Thibault, D.J. Douglas and R.L. White (Halifax, Canada) . . . . .	253
Industrial applications of capillary zone electrophoresis–mass spectrometry by M.W.F. Nielen (Arnhem, Netherlands) . . . . .	269



ELSEVIER

Journal of Chromatography A, 712 (1995) 1

---

---

JOURNAL OF  
CHROMATOGRAPHY A

---

---

---

## Foreword

---

The 11th Montreux symposium on LC-MS, CE-MS and MS-MS was held in Montreux on 9-11 November 1995. Many scientists and vendors from over the world gathered to exchange information on new technologies, novel strategies and practical approaches.

The maturity of LC-MS was clearly reflected by the many contributions on real problem solving often demonstrating robust high-throughput quantitation at low concentration levels. Important driving forces in achieving these levels originate from pharmaceutical and biotechnological R&D efforts although an increase in other areas such as environmental and food related topics, is also noted.

On the instrumental side mainly atmospheric pressure ionization (API) techniques such as electrospray/ion spray and heated nebulizer/APCI form the basis of the majority of new efforts, although some new ionization techniques such as hyperthermal surface ionization (HSI) and matrix assisted laser desorption ionization LC-MS were presented as well. Fundamental considerations contributed to a further improvement of the understanding of the underlying ionization mechanisms and principles. The developments in analyzers have provided improved performance or lower cost bench-top instruments to appear on the market. All types of analyzers are examined, in addition to quadrupoles and magnetic sectors such as Fourier transform MS, time-of-flight and ion trap systems.

Important new challenges have come from the separation science developments to improve the existing techniques or open new areas of application. Especially electromigration techniques were addressed and elegant solutions were presented to overcome loadability and compatibility limitations in CE-MS using isotachophoretic principles and coupled capillary approaches for achieving micellar electrokinetic chromatography-MS. Applications of a bio-analytical nature as well as elegant biomacromolecular analysis show that CE-MS is developing, steadily entering important problem solving areas.

In LC-MS, the separation side of the developments was also emphasized by applying perfusion chromatography for fast analysis, new electro-extraction sample preparation in combination with CE- or LC-MS and by combining chromatographic and electromigration selectivity in pseudo-electrochromatography.

The growing interest and enthusiasm of the participants clearly reflected that the technologies of interest of this symposium can no longer be missing from the modern analytical laboratory.

*Leiden, Netherlands*

**J. van der Greef**



# Application of a new atmospheric pressure ionization source for double focusing sector instruments

P. Dobberstein\*, H. Muenster

*Finnigan MAT, Barkhausenstr. 2, 28197 Bremen Germany*

---

## Abstract

In three application examples we demonstrate how the capabilities of a modern atmospheric pressure ionization (API) source, as a universal LC–MS coupling tool, are supplemented by the high mass resolution available on double focusing sector instruments. The examples include charge state determination in complex electrospray ionization–collisional induced dissociation (ESI–CID) spectra of multiply charged ions, mixture analysis of multicomponent samples without prior chromatographic separation, and very sensitive and highly specific detection of pesticides using atmospheric pressure chemical ionization (APCI).

---

## 1. Introduction

The utilization of electrospray ionization (ESI) [1–3] and atmospheric pressure chemical ionization (APCI), also known as heated pneumatic nebulizer/corona discharge ionization [4,5], has induced a breakthrough for the online LC–MS coupling. On the one hand the generation of multiple charged ions from large biomolecules by ESI has opened entirely new fields of application for mass spectrometry, on the other hand the relatively simple operation of the new ionization techniques ESI and APCI in combination with their broad application kDa range has made them to the preferred LC–MS techniques over the previously developed techniques like thermospray (TSP), particle beam interface (PBI) and continuous-flow fast-atom bombardment (CF-FAB).

In both techniques, ESI and APCI, ions are generated from liquid sprays at atmospheric pressure and transferred through several differential pumping stages into the mass analyzer, a principle, which was introduced as atmospheric pressure ionization (API) by Horning et al. [6], but initially applied with a different type of ionization. During the last years the abbreviation API has been used for this principle, independent of the type of ionization applied [7].

Most ESI and APCI applications are performed on quadrupole instruments. The relatively low mass range of these instruments, typically up to  $m/z$  2000, is sufficient for most analytic measurements, because the high charge state  $z$  of the generated ions causes the  $m/z$  values to fall into this mass range even for molecular masses in the  $M_r$  100 kDa range [1]. The low resolving power of quadrupoles, however, limits their analytical capabilities and therefore ESI was also combined with high-res-

---

\* Corresponding author.

olution mass analyzers, like double focusing sector instruments [8-17], Fourier transform ion cyclotron resonance (FTICR) instruments [18] and quadrupole ion traps, modified for high-resolution operation [19], but up to now only ESI on sector instruments has reached such a mature state that it is applied for daily routine analysis.

The new API source for sector instruments is based on a similar design for quadrupoles [20]. The main components are (Fig. 1): a heated metal capillary, patented by Chowdhury et al. [21], a tube lens, a skimmer and a radio frequency (rf)-only octapole. The octapole has a high transmission for ions and is nearly transparent for neutrals, such as liquid vapor- and residual gas-molecules, and therefore is the ideal focusing device for this type of source. It is responsible for the main contribution to the about ten-fold increase in sensitivity compared to the previous API source for sector instruments, based on the Analytica design [11].

The source manifold is entirely built from plastic material, allowing to keep the source elements at  $\pm 5$  kV ion acceleration potential and the vacuum pumps in the source region, a 16

$\text{m}^3/\text{h}$  forepump and two 260 l/s turbomolecular pumps at ground potential.

The API source can be equipped either with an ESI- or with an APCI-sprayer, accepting a large range of flow-rates ( $1 \mu\text{l}/\text{min}$  up to  $1 \text{ ml}/\text{min}$  or in case of APCI up to  $2 \text{ ml}/\text{min}$ ), thus allowing coupling with all modern liquid chromatographic techniques ranging from CZE to HPLC.

Three typical examples from the daily practice are chosen in order to demonstrate the capabilities of API combined with high-resolution sector instruments. These examples cover a relative low molecular mass range (below  $M_r$  4000). An application of this API source for accurate mass determination at a resolution of  $R = 20\,000$  on a protein (myoglobin) with a higher  $M_r$  resulting in a mass deviation of 1 ppm has already been published [24].

## 2. Experimental

The new API source in combination with the MAT 95 (example 1) and the MAT 900 (exam-

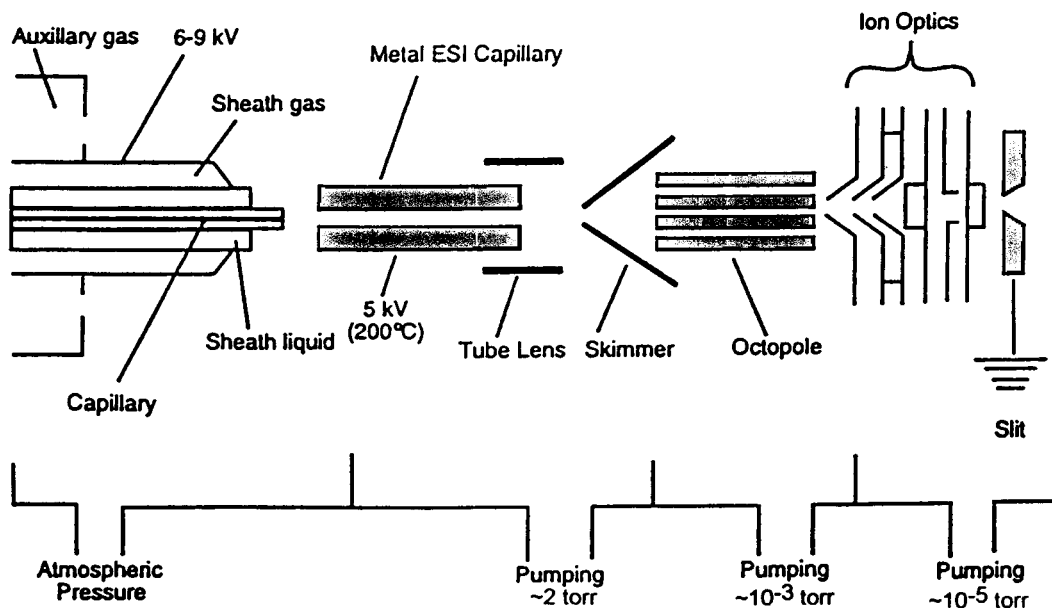


Fig. 1. Schematics of the new API source.

ples 2 and 3) double focusing mass spectrometers, has been used in these experiments. The API source was either equipped with the ESI-sprayer (examples 1 and 2) or with the APCI-sprayer (example 3). In the following examples a resolution  $R = 3000$  to  $10\,000$  (at 5% peak height) was applied, which was found to be a good compromise between peakwidth and sensitivity for the individual analytical problem; this resolution is much lower than the maximum resolution obtainable in the ESI mode.

### 3. Results and discussion

#### 3.1. Example 1

Sequence elucidation of peptides by means of ESI-MS, combined with collisional induced dissociation (CID), has become an attractive technique since the introduction of ESI [27]. The following example demonstrates how the specificity of this type of experiment is increased,

if a high-resolution sector instrument is applied. The Kaplan peptide with the following sequence (one letter code) was chosen for this demonstration:

S-A-I-S-L-D-G-E-K-V-D-F-N-B-F-R-G-R-A-V-K

N-terminus: free amino; C-terminus: free acid; B: acetylated Thr; the elemental composition ( $M_r$  2352.6) is:  $C_{103}H_{166}N_{30}O_{33}$ .

With the mass spectrometer tuned to  $R = 3000$ , the ESI spectrum (Fig. 2) was measured under the following conditions: flow-rate  $2\ \mu\text{l}/\text{min}$ ; solvent water-methanol (1:1); sample concentration  $5\ \text{pmol}/\mu\text{l}$ , continuous infusion of sample. Transforming the mass-to-charge data from the measured spectrum (Fig. 2) to a plot of relative abundance vs. mass, as per the deconvolution algorithm Biomass<sup>TM</sup> [25] (see also Ref. [26]), is presented in Fig. 3. It shows the resolved isotope pattern of the peptide in accordance with the theoretical isotope pattern.

A simple and effective method to obtain CID

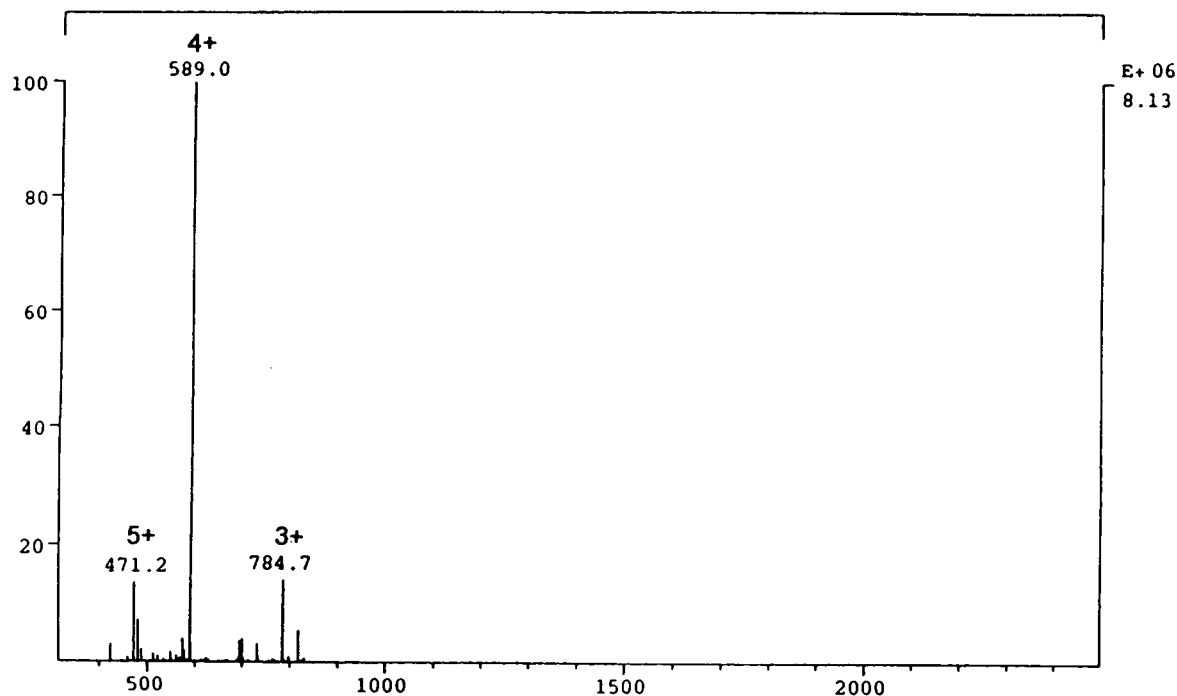


Fig. 2. ESI spectrum of Kaplan peptide, measured at resolution  $R = 3000$ .

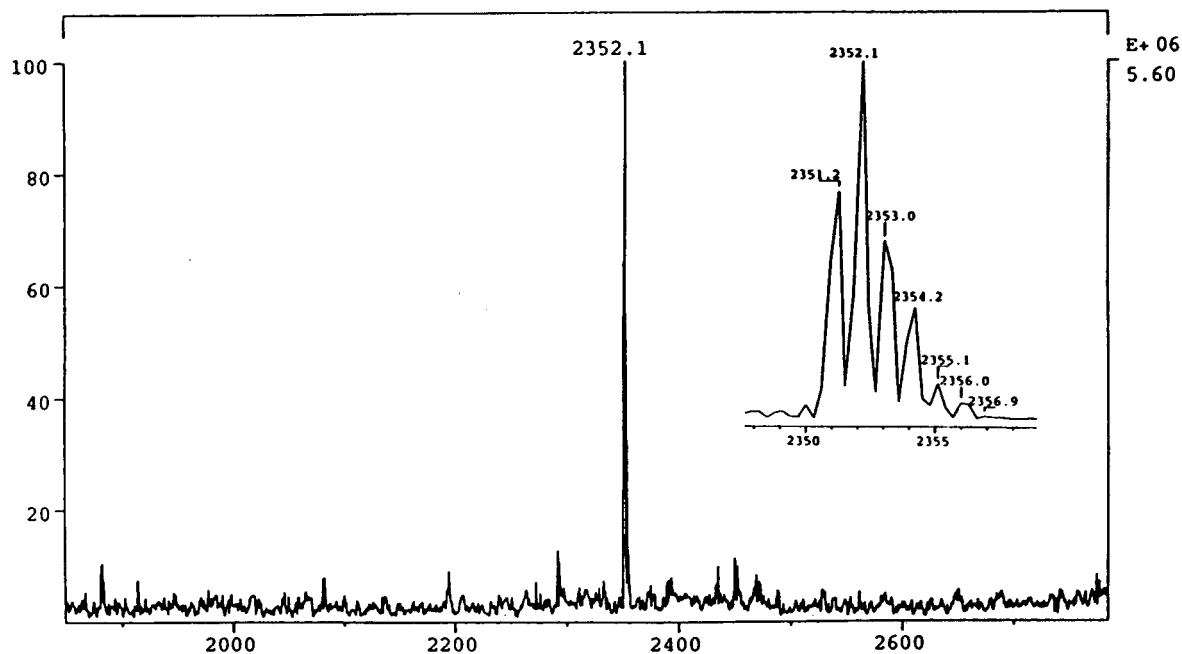


Fig. 3. The Biomass transformation of ESI spectrum from Fig. 2. Inset is expanded section of base peak. The corresponding calculated masses of the Kaplan peptide are: 2351.22 (76.6%), 2352.22 (100%), 2353.22 (69.7%), 2354.23 (34.2%), 2355.23 (13.2%), 2356.23 (4.2%)

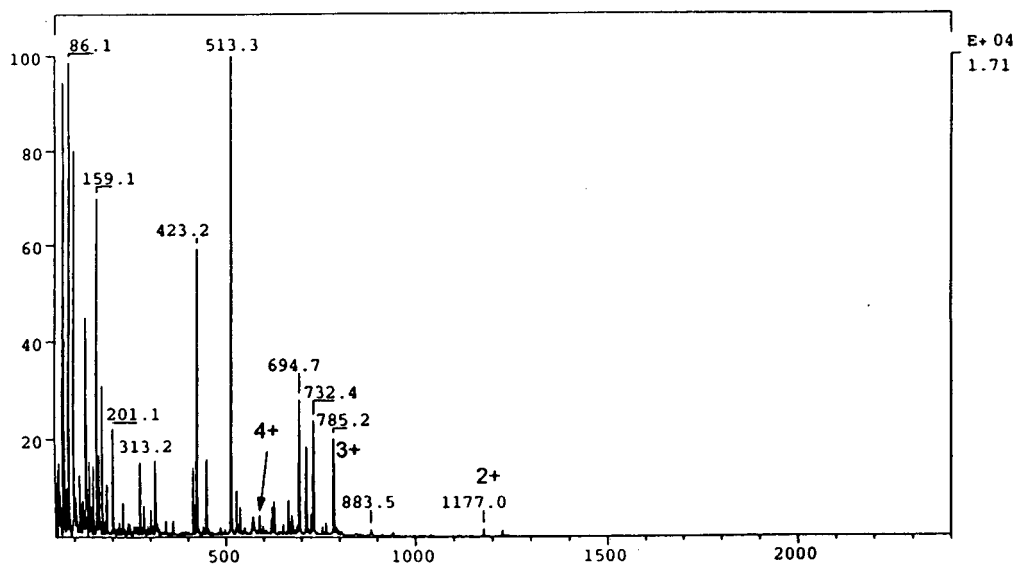


Fig. 4. Octapole CID spectrum of Kaplan peptide at  $R = 3000$ , mother ions marked by charge number.



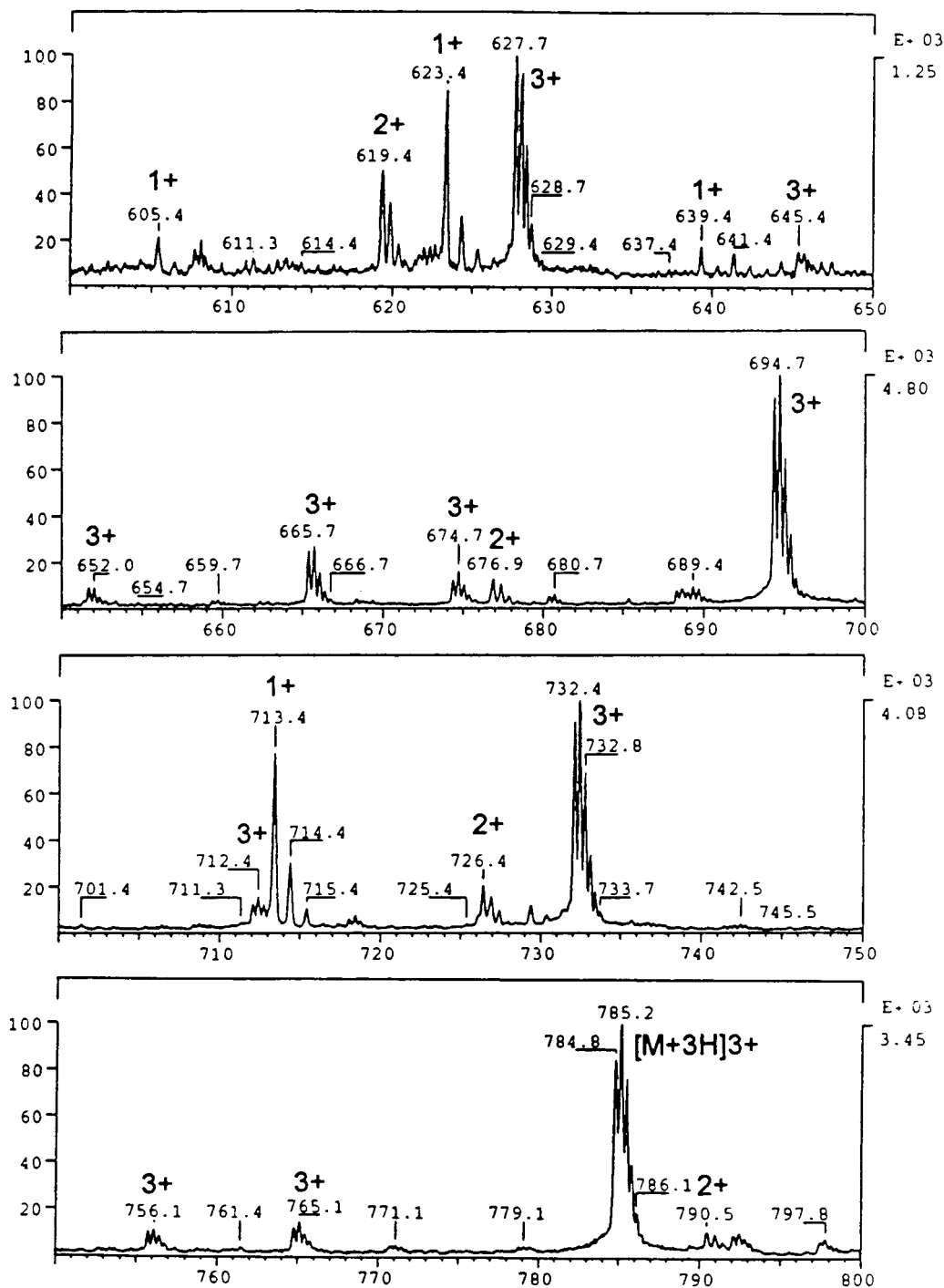


Fig. 5. Enlarged section (higher mass range) of CID spectrum from Fig. 4 showing triply charged mother ion (marked  $[M + 3H]^{3+}$ ) and numerous fragment ions with charges between 1+ and 3+.

spectra with an API source is octapole CID. For this purpose the potentials of the heated ESI capillary and the tube lens (see Fig. 1) are raised by approximately 50 V for positive ions (lowered by 50 V for negative ions), so that the ions enter the rf-only octapole with an increased translational energy and undergo collisions with the residual gas molecules, a process similar to the one applied in triple-stage quadrupoles.

The daughter ions generated by this CID method appear with the parent ions in the same spectrum, because both types of ions are accelerated in the ion optics of the source to the same final energy (5 kV in case of MAT 95 and MAT 900).

The octapole CID spectrum of the Kaplan peptide (Fig. 4) shows parent ions with charge states 2+ to 4+ as well as numerous daughter ions. The charge state of the parents in this spectrum is one charge unit lower than the charge state of the ions in the normal ESI spectrum (Fig. 2), because of a charge-stripping process within the rf-only octapole.

The daughter ions at the low mass end of the spectrum are all singly charged, so the spectrum is relatively simple to interpret, but the situation changes if one looks at higher masses (Fig. 5). Charge states between 1+ and 3+ appear in the daughter spectrum and spectra interpretation is made much more straightforward on the basis

of a high-resolution measurement, where the charge state is made visible by the spacing of the isotope peaks, than on a low-resolution spectrum, where no indication of the charge state is available in the spectrum. In addition the mass values from the high-resolution spectrum are much more exact due to the resolved isotope pattern than the mass values from quadrupole instruments, which very much improves the capability for correct assignment of the fragment ions to fragments of the amino acid chain.

We leave the method of structure elucidation of peptides at this point and refer to the literature (e.g. [27]) for more details.

### 3.2. Example 2

The sample “*Haemophilus influenzae* A2 LOS” (Table 1) is a complex mixture of 11 lipo-oligosaccharides (LOS); these components behave like detergents in HPLC and CZE and therefore the chromatographic separation is very difficult [28]. High-resolution ESI-MS, without prior chromatographic separation, can help to verify the proposed composition much more easily.

In a first analysis step, using a low-resolution instrument in negative ESI mode, an overlapping of 2 pairs of components in the multiple charged ion peaks was proposed due to the postulated

Table 1  
Proposed composition of *Haemophilus influenzae* A2 LOS

LOS	$M_r$	Proposed composition
A	2277.8	2 Hex, 3 Hep, PEA, P, KDO, lipid A*
B	2438.4	3 Hex, 3 Hep, PEA, P, KDO, lipid A*
C	2561.1	3 Hex, 3 Hep, 2 PEA, P, KDO, lipid A*
D	2600.8	4 Hex, 3 Hep, PEA, P, KDO, lipid A*
E	2723.1	4 Hex, 3 Hep, 2 PEA, P, KDO, lipid A*
F	2762.4	5 Hex, 3 Hep, PEA, P, KDO, lipid A*
G	2925.9	6 Hex, 3 Hep, PEA, P, KDO, lipid A*
H	3086.4	7 Hex, 3 Hep, PEA, P, KDO, lipid A*
I	3249.0	8 Hex, 3 Hep, PEA, P, KDO, lipid A*
J	3256.2	NANA, HexNAc, 5 Hex, 3 Hep, PEA, P, KDO, lipid A*
K	3416.4	NANA, HexNAc, 6 Hex, 3 Hep, PEA, P, KDO, lipid A*

Abbreviations used [28]: Hex = hexose (glucose or galactose); Hep = heptose; PEA = phosphoethanolamine; P = phosphate; KDO = 2-keto-3-deoxy-D-manno-octulosonic acid; NANA = 5-N-acetyl-neuraminic acid (sialic acid); HexNAc = N-acetyl-hexosamine; lipid A\* = diphosphorylated O-deacylated lipid A.

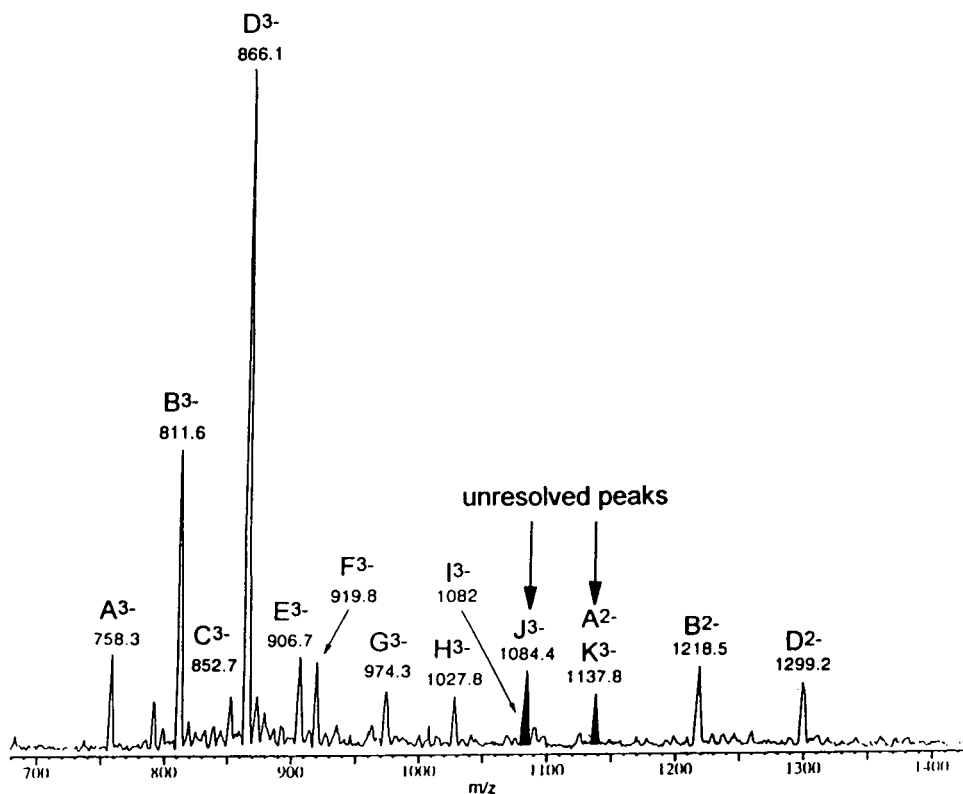


Fig. 6. Low-resolution negative ion ESI spectrum of *H. influenzae* A2 LOS.

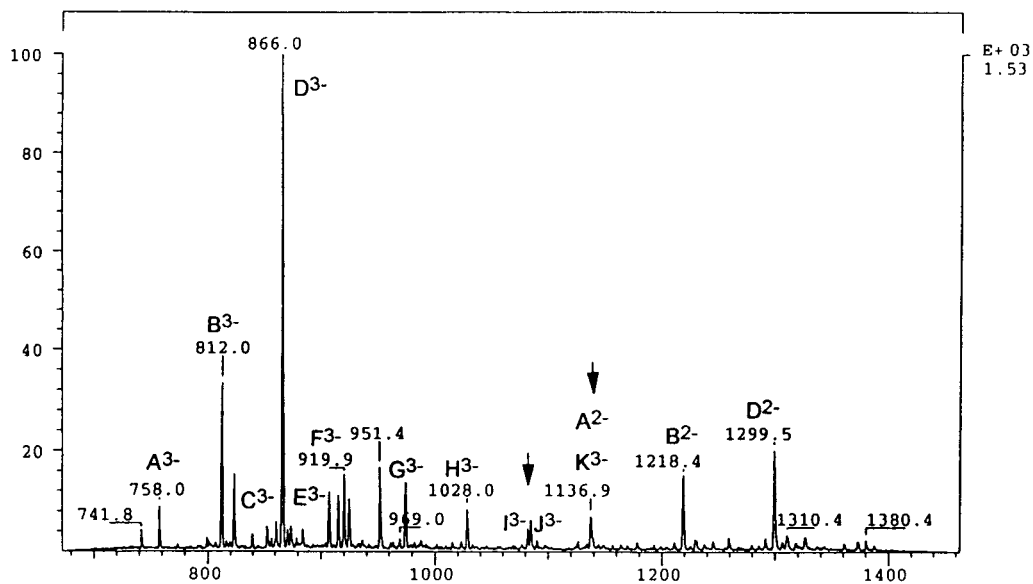


Fig. 7. Negative ion ESI spectrum of *H. influenzae* A2 LOS, obtained with sector instrument at R = 2500.

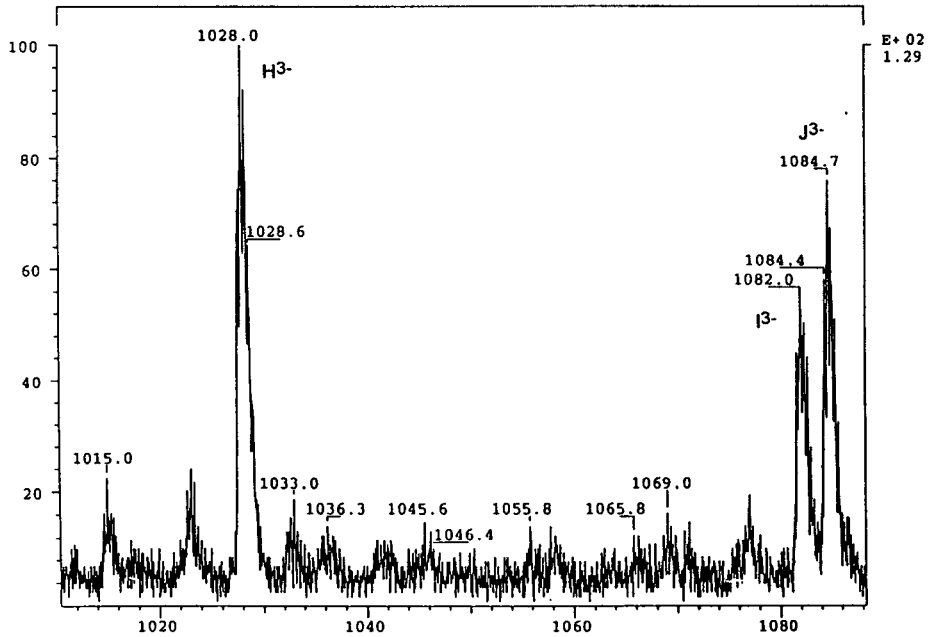


Fig. 8. Enlarged section of ESI spectrum from Fig. 7, showing mass resolved peaks I<sup>3-</sup> and J<sup>3-</sup>.

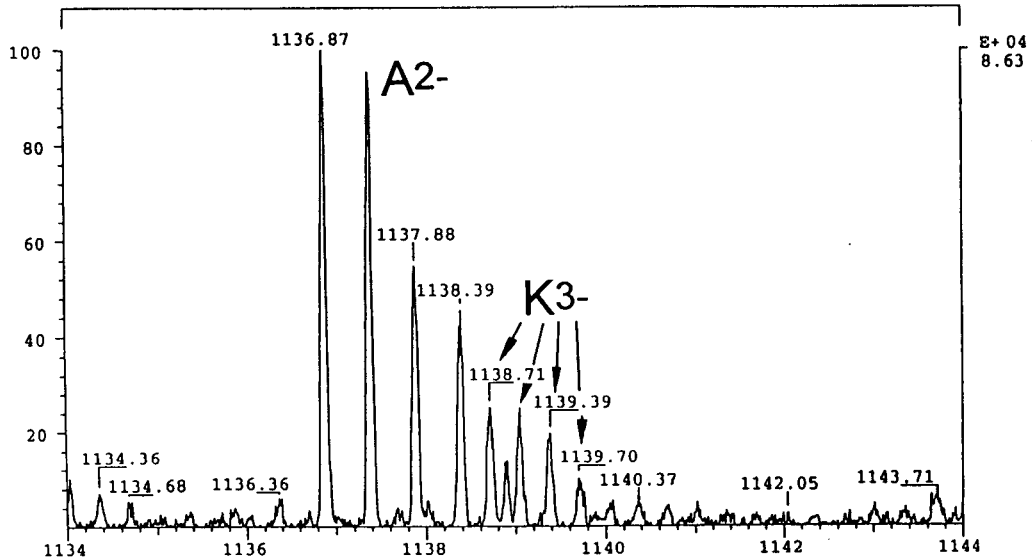


Fig. 9. Enlarged section of high-resolution negative ion ESI spectrum at  $R = 10\,000$ , showing resolved isotope clusters of components A and K.

structure (Fig. 6), hindering the unequivocal conformation of the proposed structure.

For analysis on a MAT 900 sector instrument, the sample was dissolved in H<sub>2</sub>O at a concentration of 2 µg/µl total and 20 µl of this solution was injected into the flow to the ESI-sprayer. The ESI-sprayer was operated in negative-ion mode at a flow-rate of 10 µl/min of H<sub>2</sub>O-CH<sub>3</sub>CN (1:1) with 1% acetic acid.

A first measurement using the position and time resolved ion counting detector (PATRIC<sup>TM</sup> [29]) at a resolution of  $R = 2500$ , entirely separated two of the interfering peaks, I<sup>3-</sup> and J<sup>3-</sup>, but the other pair of peaks was still unresolved (Figs. 7 and 8).

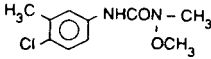
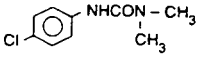
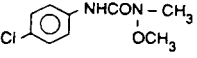
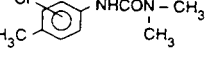
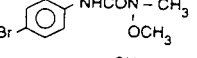
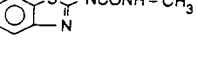
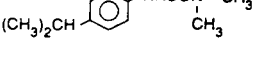

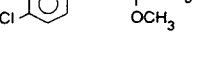
Switching to the point detector (slit and sec-

ondary electron multiplier) and setting the resolution to  $R = 10\,000$  helped to separate also the other pair of overlapping peaks, A<sup>2-</sup> and K<sup>3-</sup> (see Fig. 9), allowing verification of all of the 11 components of the proposed mixture.

### 3.3. Example 3

High specificity and high sensitivity for pesticides are required for the analysis of drinking water as well as residual analysis of food. Because these compounds are very labile and tend to fragment applying other ionization techniques [30,31], APCI allows the measurement of underivatized pesticides with good sensitivity. In

Table 2  
List of pesticides used

A	Metoxuron	
B	Monuron	
C	Monolinuron	
D	Chlortoluron	
E	Metobromuron	
F	Metabenzthiazuron	
G	Isoproturon	
H	Diuron	
I	Linuron	

order to demonstrate the capabilities of a high-resolution mass spectrometer with this respect, the following analysis was performed on a MAT 900 sector instrument using the point detector at a resolution of  $R = 5000$ .

An artificial mixture of 9 pesticides in water (Table 2) at different concentrations (see Fig. 11) under the following LC conditions was used as the test mixture for the LC-MS experiments:

-HPLC: pump, LDC 4100 MS; flow-rate, 0.7 ml/min; solvent, water-methanol (1:1); column, Supelcosil RP-18; sample concentration, 1-1000 pg/ $\mu$ l per component; injector volume, 20  $\mu$ l

-APCI: vaporizer temperature, 300°C; capillary temperature, 170°C; corona voltage, 3 kV.

-Reference: sample, PPG 400 (4 ng/ $\mu$ l); flow-rate, 30  $\mu$ l/min (added postcolumn).

Poly propylene glycol (PPG) as an internal mass calibrant was added postcolumn. The aims of this experiment were sample identification (step 1) and sample quantitation (step 2).

For step 1 the mass spectrometer was operated

in full-scan mode, using electrical scanning in the mass range 185 to 270.

For the reconstructed ion chromatogram (RIC) in Fig. 10 a sample concentration of 1 ng/ $\mu$ l per component (20 ng injected) was applied.

Averaged spectra taken from the peak regions were mass calibrated using the PPG masses ( $M_r$  193 or  $M_r$  251). For all calibrated spectra the elemental compositions of the used pesticides were found with an average mass deviation of 1 to 2 milli mass units (mmu) (Table 3).

In step 2 the mass spectrometer was operated in the multiple-ion detection (MID) mode in order to find the detection limits for the different pesticides. Five time windows have been defined to get the utmost sensitivity by a maximum dwell time. The sum of all MID windows for three separate MID runs (Fig. 11) demonstrates that the detection limits for the individual pesticides are between 0.5 and 5 pg/ $\mu$ l (10 and 100 pg).

In additional experiments the response curves

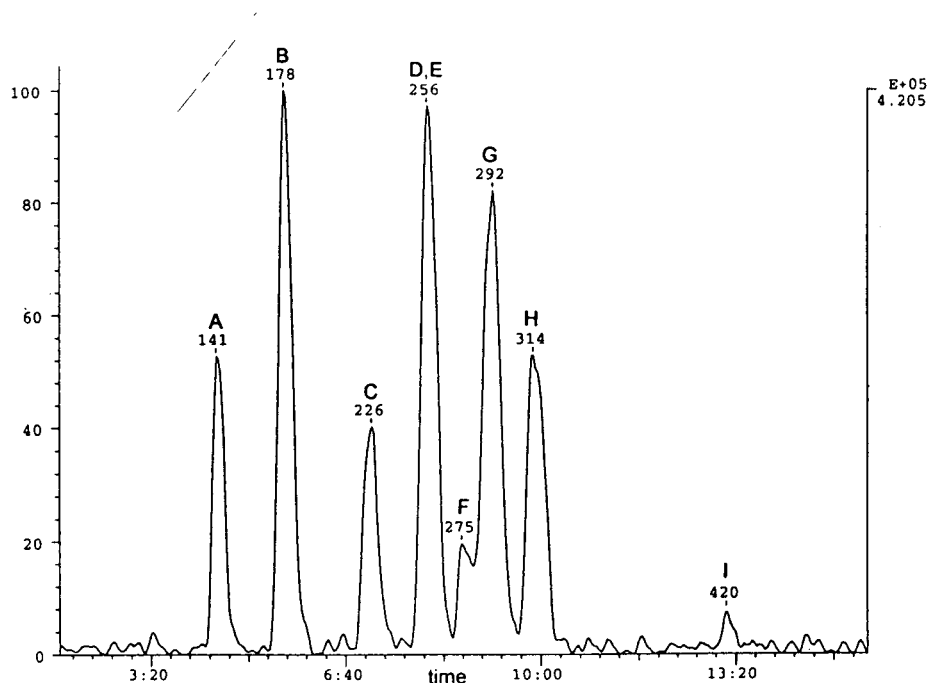


Fig. 10. Background subtracted RIC trace for HPLC separation of pesticide mixture, measured at  $R = 5000$ .

Table 3

Elemental compositions related to mass spectra taken from peaks A-I of Fig. 10, calculated and observed mass of the most abundant isotope peak

Peak	Elemental composition	Mass calculated	Mass observed
A	$C_{10}H_{14}N_2O_2Cl_1$	229.0744	229.0747
B	$C_9H_{12}N_2O_1Cl_1$	199.0639	199.0655
C	$C_9H_{12}N_2O_2Cl_1$	215.0587	215.0569
D	$C_{10}H_{14}N_2O_1Cl_1$	213.0794	213.0800
E	$C_9H_{12}N_2Br_1O_2$	259.0082	259.0103
F	$C_{10}H_{12}N_3O_1S_1$	222.0701	222.0696
G	$C_{12}H_{19}N_2O_1$	207.1498	207.1506
H	$C_9H_{11}N_2O_1Cl_2$	233.0248	233.0251
I	$C_9H_{11}N_2O_2Cl_2$	249.0198	249.0233

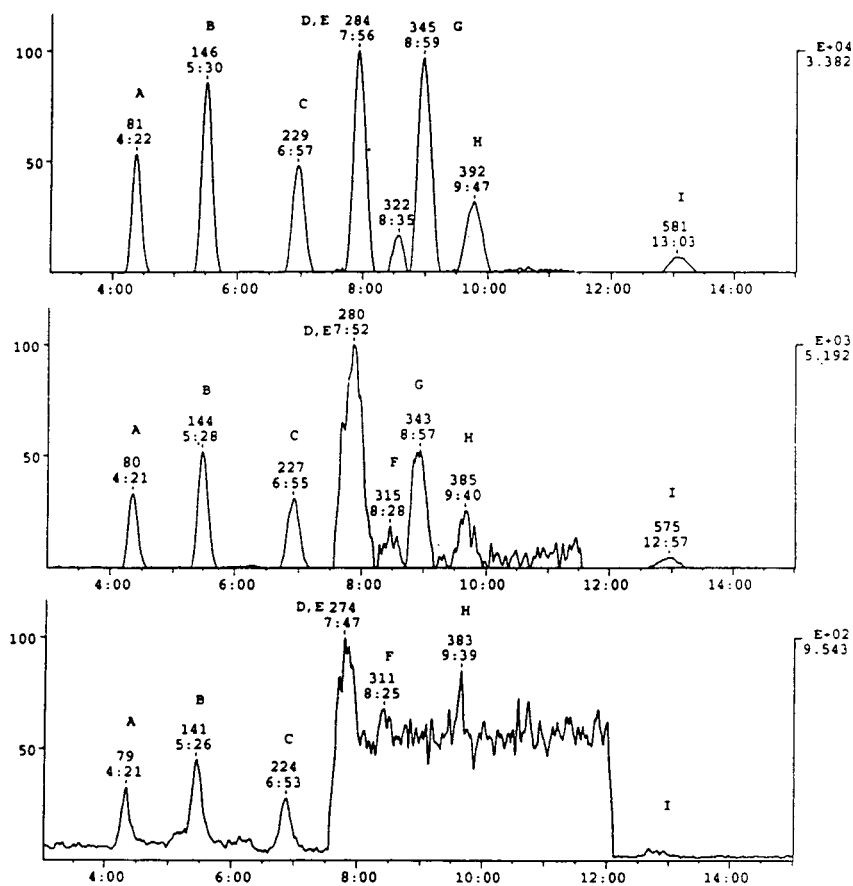


Fig. 11. ID traces for different dilutions of pesticide mixture: upper, 100  $\mu\text{g}/\mu\text{l}$  (2 ng); middle, 10  $\mu\text{g}/\mu\text{l}$  (200 pg); lower, 1  $\mu\text{g}/\mu\text{l}$  (20 pg); measured at  $R = 5000$ .

for the 9 pesticides have been determined by performing double injections of the pesticide mixture at four different concentrations between 1 and 1000 pg/ $\mu$ l onto the HPLC column. The response curves are all absolutely linear and typically a standard deviation of better than 2% was achieved.

#### 4. Conclusions

High-resolution mass spectrometry is complementing the capabilities of modern API sources by providing additional information, which is not available on quadrupole instruments, such as the unequivocal determination of the charge state of multiple charged ions and a more exact mass value, both making sequence elucidation of peptides much more straightforward.

Complex sample mixtures can be analyzed by high-resolution ESI-MS without prior chromatographic separation, which might be the only choice in cases where chromatographic separation is not possible.

The new API source equipped with the APCI sprayer allows to perform LC-MS measurements of underivatized pesticides in the low picomol range with good reproducibility and accuracy. Detection limits in MID mode range from 10 to 100 pg.

API on sector instruments has become a routine ionization technique, which is replacing more and more the former LC-MS methods like TSP, PBI and CFFAB.

#### Acknowledgements

We thank Prof. Dr. Bradford W. Gibson from the School of Pharmacy at the University of California at San Francisco, CA, USA for providing us the sample "*Haemophilus influenzae* A2 LOS" and the permission to publish the spectra taken from this sample. We thank Mrs.

Monika Hoehn for assistance with the measurements and the data evaluation.

#### References

- [1] J.B. Fenn, M. Mann, C.K. Meng, S.F. Wong and C.M. Whitehouse, *Mass Spectrom. Rev.*, 9 (1990) 37.
- [2] R.D. Smith, J.A. Loo, C.G. Edmonds, C.J. Barinaga and H.R. Udseth, *Anal. Chem.*, 62 (1990) 882.
- [3] P. Kebarle and L. Tang, *Anal. Chem.*, 65 (1993) 972A.
- [4] J.D. Henion, B.A. Thomson and P.H. Dawson, *Anal. Chem.*, 54 (1982) 451.
- [5] T.R. Covey, E.D. Lee, A.P. Bruins and J.D. Henion, *Anal. Chem.*, 58 (1986) 1451A.
- [6] E.C. Horning, M.G. Horning, D.I. Carroll, I. Dzidic and R.N. Stillwell, *Anal. Chem.*, 45 (1973) 936.
- [7] A.P. Bruins, *Mass Spectrom. Rev.*, 10 (1991) 53–77.
- [8] C.K. Meng, C.N. McEwen and B.S. Larsen, *Rapid Commun. Mass Spectrom.*, 4 (1990) 147.
- [9] R.T. Callagher, J.R. Chapman and M. Mann, *Rapid Commun. Mass Spectrom.*, 4 (1990) 369.
- [10] B.S. Larsen and C.N. McEwen, *J. Am. Soc. Mass Spectrom.*, 2 (1991) 205.
- [11] P. Dobberstein, U. Giessmann and E. Schroeder, *Proc. 39th Annu. Conf. Mass Spectrom.*, Nashville, TN, 1991, p. 238.
- [12] R.H. Bateman, H.J. Major and A.R. Woolfit, *Proc. 39th Annu. Conf. Mass Spectrom.*, Nashville, TN, 1991, p. 244.
- [13] J.R. Chapman, R.T. Callagher, E.C. Barton, J.M. Curtis and P.J. Derrick, *Org. Mass Spectrom.*, 27 (1992) 195.
- [14] C.N. McEwen and B.S. Larsen, *Rapid Commun. Mass Spectrom.*, 6 (1992) 173.
- [15] R.B. Cody, J. Tamura and B.D. Musselman, *Anal. Chem.*, 64 (1992) 1561.
- [16] A.M. Starrett and G.C. DiDonato, *Rapid Commun. Mass Spectrom.*, 7 (1993) 12.
- [17] J.A. Loo and A.B. Giordani, *Rapid Commun. Mass Spectrom.*, 7 (1993) 186.
- [18] R.D. Smith, S.A. Hofstadler, J.E. Bruce, B.E. Wigner and A.L. Rockwood, *Proc. 41st. Annu. Conf. Mass Spectrom.*, San Francisco, CA, 1993, Paper 3a.
- [19] J.C. Schwartz, J.E.P. Syka and I. Jardine, *J. Am. Soc. Mass Spectrom.*, 2 (1991) 198.
- [20] M. Hail and I. Mylchreest, *Proc. 41st Annu. Conf. Mass Spectrom.*, San Francisco, CA, 1993, Paper 1074a.
- [21] S. Chowdhury, V. Katta and B.T. Chait, *Rapid Commun. Mass Spectrom.*, 4 (1990) 91, and U.S. Patent 4,977,320.
- [24] P. Dobberstein and E. Schroeder, *Rapid Commun. Mass Spectrom.*, 7 (1993) 861.
- [25] P.J.F. Watkins, I. Jardine and J.X.G. Zhou, *Biochem. Soc. Trans.*, 19 (1991) 957.



- [26] M. Mann, C.K. Meng and J.B. Fenn, *Anal. Chem.*, 61 (1989) 1702.
- [27] D.M. Desiderio (Editor), *Mass Spectrometry of Peptides*, CRC Press, Boca Raton, FL, 1990.
- [28] N.J. Phillips, M.A. Apicella, J.M. Griffiss and B.W. Gibson, *Biochemistry*, 32 (1993) 2003.
- [29] C. Brunnee, R. Pesch and E. Schroeder, *Rapid Commun. Mass Spectrom.* 4 (1990) 173.
- [30] L.M. Shalaby and R.W. Reiser, in C.N. McEwen and B.S. Larson (Editors), *Mass Spectrometry of Biological Materials*, Marcel Dekker, New York, NY, 1990, Ch. 11.
- [31] L.M. Shalaby, F.Q. Bramble and P.W. Lee, *J. Agric. Food Chem.*, 40 (1992) 513.





ELSEVIER

Journal of Chromatography A, 712 (1995) 17–19

JOURNAL OF  
CHROMATOGRAPHY A

Short communication

# Application of liquid chromatography–atmospheric pressure chemical ionization mass spectrometry to a sector mass spectrometer

K. Nojima<sup>a</sup>, S. Fujimaki<sup>a</sup>, R.C. Hertsens<sup>b,\*</sup>, T. Morita<sup>b</sup>

<sup>a</sup>JEOL Ltd., Musashino 3-1-2, Akishima, Tokyo 196, Japan

<sup>b</sup>JEOL Europe, Ikaroslaan, 7a, B-1930 Zaventem, Belgium

## Abstract

Combined liquid chromatography–mass spectrometry (LC–MS) is increasingly used as a powerful technique in research and quality control. Among thermospray, FAB and electrospray, atmospheric pressure chemical ionization (APCI) is a powerful technique for high flow-rate LC–MS. APCI has primarily been used with a quadrupole mass spectrometer, where only low mass resolution experiments are possible. In this article we describe a newly designed APCI source for high-accelerating-voltage and high-resolution double focusing mass spectrometers. Detection in the pg range is possible.

## 1. Introduction

Atmospheric pressure chemical ionization (APCI) is a powerful technique for high flow-rate liquid chromatography–mass spectrometry (LC–MS). However, APCI has primarily been used with quadrupole mass spectrometer, and LC–MS analysis was made under low mass resolutions.

We designed and constructed a new APCI source for high-ion-accelerating voltage and high-resolution double focusing mass spectrometers.

## 2. Experimental

All data shown were obtained with a JEOL JMS-SX102A reversed geometry (BE) mass spectrometer operating at an accelerating voltage of 5 kV. Flow injection and HPLC analysis were carried out by using an HP 1090 LC system. The flow-rate was 1 ml/min into the APCI source. The absorbance was measured by placing a UV detector between the column and the APCI interface. The APCI ion source is constructed with a heated nebulizer, a discharge electrode and skimmers (Fig. 1). Skimmer 1 has an aperture of 300  $\mu\text{m}$  in diameter and skimmer 2 of 400  $\mu\text{m}$ . Skimmers and lenses are all on axis to obtain high transmission. No contamination of

\* Corresponding author.

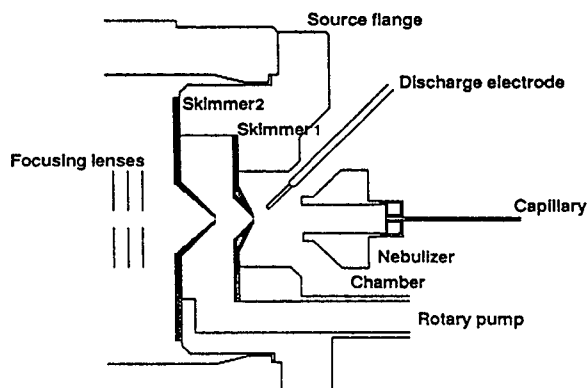


Fig. 1. Schematic block diagram of the APCI source.

the analyzer by neutral fragments is to be expected since we are using a sector mass spectrometer. Two experiments were performed. In the reserpine experiment a Develosil ODS-5 150 mm  $\times$  4.6 mm I.D. column was used with a flow-rate of 1 ml/min, a mobile phase consisting of water-methanol (30:70), an internal standard of 100 ppm PEG300-methanol, and a resolution of 1000. The nebulizer temperature was 300°C, the ion source chamber temperature was 400°C, and the accelerating voltage was +5 kV. No nebulizer gas was used. A calibration curve of reserpine between 10 pg and 1 ng was made to test the linearity.

In the second experiment we used four different hormones (cortisone, hydrocortisone, cor-

ticosterone, progesterone). We injected 10  $\mu$ l of a mixture of 100 ppm each on a Develosil ODS-5 150 mm  $\times$  4.6 mm I.D. column at a flow-rate of 1 ml/min, a mobile phase of water (A)-methanol (B), with a linear gradient of B = 50-90% in 15 min, an internal standard of 100 ppm PEG300-methanol, and a resolution of 3000. The nebulizer temperature was 290°C, the ion source chamber temperature was 400°C and the accelerating voltage was +5 kV. No nebulizer gas was used.

### 3. Results and discussion

Fig. 2 shows a typical positive APCI mass spectrum of reserpine ( $M_r = 608$ ) which gave an intense protonated molecular ion. No characteristic fragment peaks of reserpine were detected. The small ion peaks present are due to not fully subtracted background noise. Fig. 3 shows the selected-ion monitoring (SIM) chromatogram of reserpine from 10 pg to 1 ng. Fig. 4 presents a calibration curve of reserpine for the same concentration range as in Fig. 3. Excellent linearity is obtained. This result provides significantly better sensitivity on sector MS, also shown in Fig. 3.

The use of high-resolution accurate mass measurements in APCI LC-MS allows the determination of elemental compositions of the ions

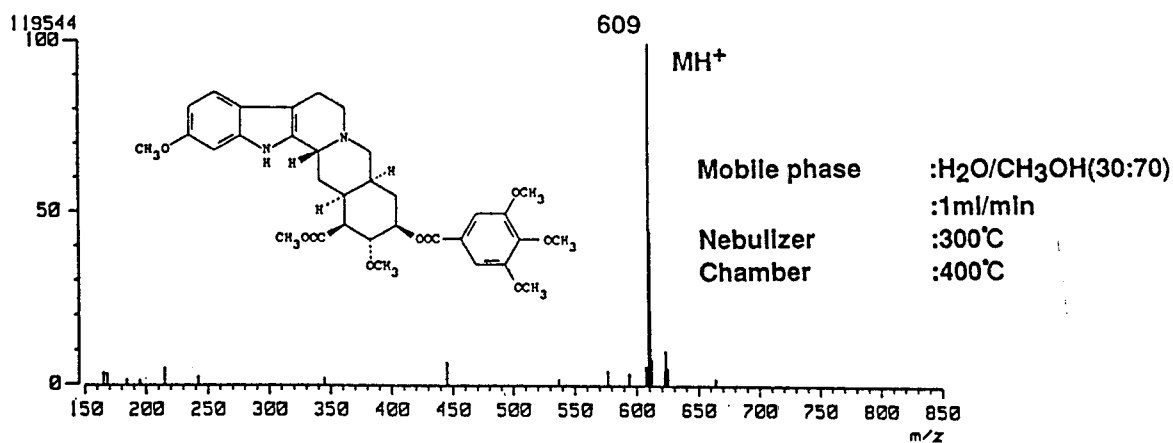


Fig. 2. APCI spectrum of reserpine.

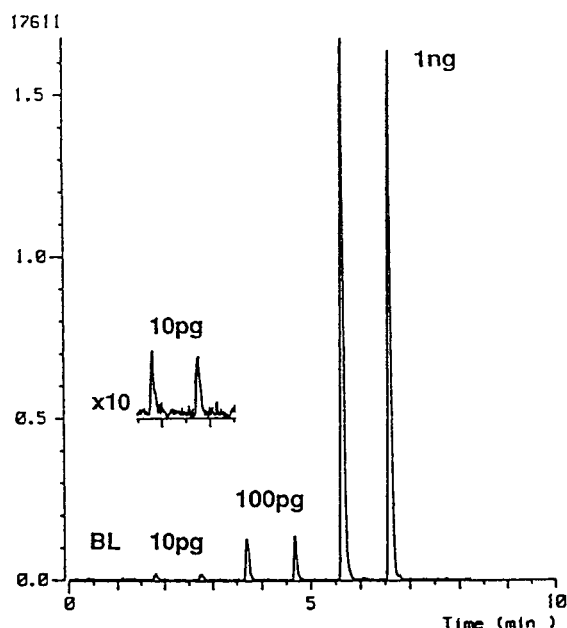


Fig. 3. Selected-ion monitoring (SIM) chromatogram of reserpine (10 pg to 1 ng).

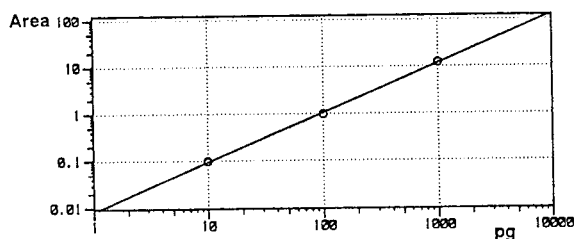


Fig. 4. Calibration curve of reserpine (10 pg to 1 ng).

from the component represented in the LC peaks. Fig. 5 and Table 1 presents the accurate mass measurements of protonated molecules of cortisone, hydrocortisone, corticosterone and progesterone. The observed mass values are typically within 2.6 mmu of the theoretical values

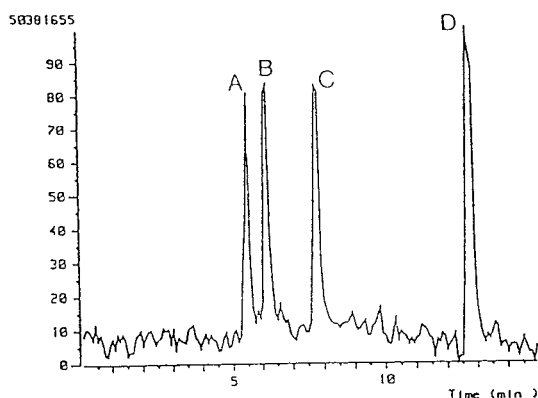


Fig. 5. Total ion current (TIC) of APCI LC-MS measurement.

Table 1  
High-resolution accurate mass measurement with APCI LC-MS

Sample	Observed	Theoretical	Error (mmu)
(A) Cortisone	361.2014	361.2015	-0.1
(B) Hydrocortisone	363.2162	363.2172	-1.0
(C) Corticosterone	347.2248	347.2222	+2.6
(D) Progesterone	315.2332	315.2324	+0.8

and the root mean square (rms) error is within 4 mmu (three consecutive injections).

#### 4. Conclusion

APCI LC-MS on sector MS is well-suited for the quantification of reserpine at concentration levels higher than a few picograms.

The selectivity of the detection can be increased by using high-resolution mass spectrometry which also allows accurate mass measurements of the components represented in the LC peaks.





ELSEVIER

Journal of Chromatography A, 712 (1995) 21–30

JOURNAL OF  
CHROMATOGRAPHY A

## Effect of ion source pressure on ion formation of carbamates in particle-beam chemical-ionisation mass spectrometry

M. Honing<sup>a,\*</sup>, D. Barceló<sup>a</sup>, M.E. Jager<sup>b</sup>, J. Slobodnik<sup>b</sup>, B.L.M. van Baar<sup>c</sup>,  
U.A.Th. Brinkman<sup>b</sup>

<sup>a</sup>Department of Environmental Chemistry, CID/CSIC, Jordi Girona 18-26, 08034 Barcelona, Spain

<sup>b</sup>Department of Analytical Chemistry, Free University, De Boelelaan 1083, 1081 HV Amsterdam, Netherlands

<sup>c</sup>Department of Organic Chemistry, Free University, De Boelelaan 1083, 1081 HV Amsterdam, Netherlands

### Abstract

In this study the mass spectra of fourteen carbamate pesticides, obtained with desorption chemical ionisation (DCI) and flow injection (FIA)–particle beam (PB)–ammonia positive chemical ionisation (PCI)–mass spectrometry (MS), are compared. The mass spectra from the FIA–PB–PCI–MS experiments exhibit higher relative abundances for fragment ions. The influence of the ion source pressure and temperature on the ion abundances under ammonia positive chemical ionisation conditions was studied. The results indicate that thermal degradation of the carbamate pesticides takes place in the FIA–PB–MS system. In addition, the  $[M + NH_3 + H]^+$  and  $[M + NH_3 + H - CH_3NCO]^+$  ion intensities are strongly dependent on the ion source pressure, especially for carbofuran as an extreme. Both the ion source pressure and the temperature cause irreproducibility of the ammonia PCI mass spectra of carbamates under liquid chromatography PB–PCI–MS conditions and it is therefore of utmost importance to use well defined experimental conditions for the quantitative determination of carbamates.

### 1. Introduction

Under conventional conditions, the gas chromatographic (GC) quantitation of carbamates and some of their transformation products is rather unreliable, because thermal degradation may occur. Nevertheless, it has been shown that GC with electron ionisation mass spectrometric detection (GC–EI–MS) generally leads to irrefutable identification of the compounds [1,2]. Recently, it was observed that GC with positive chemical ionisation (PCI)–MS detection, using methane as the reagent gas, results in a better sensitivity of detection by a factor of 2 for

carbofuran and carbaryl [3]. Similarly, in a previous study, the use of ammonia as a reagent gas [4] resulted in a 3–7 times lower limit of detection for these carbamates. Therefore, PCI–MS with ammonia may be expected to generally provide the lower limits of detection. In addition, specific fragmentation of the most widely used N-methylcarbamates under PCI conditions, in particular the loss of methylisocyanate ( $CH_3NCO$ ) from the protonated molecule, provides some structural confirmation. Thus, GC with ammonia PCI–MS detection would provide an ideal method for carbamate analysis if the problem of thermal degradation could be circumvented.

Several modified GC procedures have been

\* Corresponding author.

developed to prevent thermal decomposition: reducing the analysis time by using shorter columns [5,6], application of programmed temperature vaporisation (PTV) injection [7], and the use of special types of stationary phases [8]. However, these procedures have not led to analytical methods that are generally applicable to carbamates. Moreover, transformation products of carbamates, which tend to be even more polar, cannot be determined by GC–MS without prior derivatisation. The application of liquid chromatography (LC) is to be preferred, because of both the lack of thermal decomposition during separation and the additional possibility to simultaneously analyse the transformation products.

Various liquid chromatographic–mass spectrometric (LC–MS) interfacing methods have been applied in the determination of carbamates and their transformation products, e.g. direct liquid introduction (DLI) [9,10], thermospray (TSP) [11–16], electrospray (ESP) [17,18], atmospheric pressure chemical ionisation (APCI) [19,20] and particle beam (PB) [20–26]. In general, carbamates can be detected with all these methods with good sensitivity, i.e. typically in the low ng range. However, LC–PB–MS is to be preferred for the confirmation of carbamates in real samples [27] because it can provide solvent-independent CI and electron ionisation (EI) mass spectra.

In the PB interface the column effluent is pneumatically nebulised in a heated desolvation chamber at nearly atmospheric pressure. The solutes are selectively separated from the solvent vapour molecules in a two-stage momentum separator and subsequently transported into the ion source. It was postulated that the particles evaporate upon collision with the heated ion source wall and that the released molecules may become ionised [28]. Unfortunately, high limits of detection and non-linear calibration curves at low concentrations [20,24,25] are encountered with the PB interface. Many parameters, e.g. ion source temperature and alignment of the nebuliser, have to be optimised [29]. Moreover, the design of the nebuliser is important for the stability of the signal [23]. In a recent review all the aspects of this interface were discussed [30].

The use of LC–PB–MS for the detection of carbamates and their transformation products requires a systematic approach. It has, for example, been observed that thermal degradation of chlorophenoxy acetic acid pesticides occurs in PB–MS [31]; given the above-mentioned experience with GC, thermal degradation may also occur with the N-methyl carbamates. Moreover, differences between the methane CI mass spectra with either GC or direct inlet systems (desorption chemical ionisation, DCI) have been reported for aldicarb, butocarboxim and their oxime and nitrile derivatives [32,33]; these differences were explained to be due to thermal processes in the GC column. In order to gain insight in the applicability of LC–PB–PCI–MS to carbamate analysis, we studied the effects of various parameters on the ion formation of carbamate pesticides in flow injection (FIA)–PB–PCI–MS, by comparing the mass spectra of selected carbamate pesticides in both positive ion DCI and FIA–PB–PCI–MS experiments, using ammonia as the reagent gas.

## 2. Experimental

### 2.1. Chemicals

All carbamate pesticides, including aldicarb-sulphone, were obtained from Riedel–de Haën (Seelze, Germany), the EPA (Research Triangle Park, NC, USA) or from Dr. Ehrenstorfer (Augsburg, Germany). These compounds were of 96–99% purity, and were used as received. Standard solutions (20 mg/l) of all carbamates were made in methanol and were stored, for a maximum of 1 year, in the dark at  $-20^{\circ}\text{C}$ .

Acetonitrile (99.9% purity) was obtained from Westburg (Leusden, Netherlands). HPLC-grade water, methanol and ammonium acetate (min. 97%) were purchased from Baker (Deventer, Netherlands). All eluents were purged with helium for at least 1 h, before starting an analysis. Helium gas for the particle beam interface and methane and ammonia reagent gases,



all with a purity of 99.99%, were obtained from Hoekloos (Schiedam, Netherlands).

## 2.2. Mass spectrometry

Particle beam experiments were performed with a HP Model 5988A quadrupole (“MS Engine”) mass spectrometer (Hewlett-Packard, Palo Alto, CA, USA) coupled with a Model 1090 Series II liquid chromatograph (Hewlett-Packard, Waldbronn, Germany). The latter was equipped with an autosampler, and interfaced to the mass spectrometer by a Model 59980A particle beam interface.

The temperature of the desolvation chamber and the analyser were maintained at 100°C. Pressure dependencies were recorded at source temperatures of 125, 175 and 225°C; a source temperature of 125°C was used for all other PB-MS experiments. Full scan spectra were acquired from  $m/z$  85 to 350 in the PCI mode at (2.4 s/scan).

Desorption chemical ionisation mass spectra were obtained with a Finnigan MAT 90 mass spectrometer (Finnigan MAT, Bremen, Germany), using the standard direct inlet (DI) probe. Samples were introduced over a longer period of time, with the probe temperature not

exceeding 60°C. Ionisation was performed with 150 eV electrons at an emission current of 0.2 mA and using ammonia as the reagent gas (at an indicated source pressure of  $4 \cdot 10^{-4}$  Torr). The pressure dependence was recorded at ion source temperatures of 115, 170 and 210°C; a source temperature of 125°C was used for all other DCI experiments. Metastable ion kinetic energy (MIKE) mass spectra of  $[M + H]^+$  and  $[M + NH_3 + H]^+$  were obtained.

## 2.3. Pressure measurement

Pressure measurement was performed with the available gauges; unfortunately the pressure values cannot be mutually compared. The MAT 90 source pressure is measured by an ionisation gauge, inserted in a side tube of the source manifold. The MS Engine source pressure can be read as a fore vacuum pressure, as it is measured by a cold cathode manometer. Fig. 1 gives a schematic representation of the PB and the CI ion source; the fore vacuum (“auxiliary”) pressure is measured at the CI gas inlet (indicated by the arrow “CI reagent gas”). An auxiliary pressure of approximately 0.6 Torr corresponds to a source manifold pressure (measured above the inlet of the roughing pump) of  $1 \cdot 10^{-4}$  Torr.

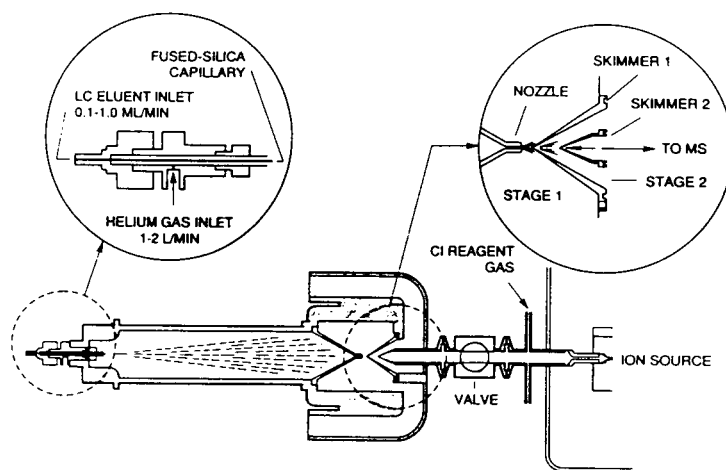


Fig. 1. Schematic representation of the particle beam interface and ion source of the MS Engine.

### 3. Results and discussion

Fourteen carbamates (including the transformation product aldicarbulsulphone) were selected to represent the various subclasses. Mass spectra of these selected carbamates were obtained at an ion source temperature of 125°C and with ammonia as the reagent gas, using both positive ion DCI and PB-PCI; these spectra are summarised in Table 1. More fragmentation appears to occur under PB-PCI than under DCI conditions. As was reported before for TSP [15], an increase of the relative abundance of the specific fragment ion of the N-methyl carbamates,  $[M + H - CH_3NCO]^+$ , is related to their thermal degradation, prior to ionisation. The concomitant ion signal increase is generally masked in the EI mode, because the intensity of the molecular ion peak is 50 to 100 times lower than that of the  $[M - CH_3NCO]^{+\bullet}$  ion peak; hence, an increase in the thermolysis of molecules will only result in a small contribution to the  $[M - CH_3NCO]^{+\bullet}$  signal. That  $[M - CH_3NCO]^{+\bullet}$  and  $[M + H - CH_3NCO]^+$  are indeed formed by fragmentation of  $M^{+\bullet}$  and  $[M + H]^+$  ions, respectively, has been shown by metastable ion studies using deuterated methane as the reagent gas [34,35]. Thus, the  $[M - CH_3NCO]^{+\bullet}$  signal, in EI, and the  $[M + H - CH_3NCO]^+$  signal, in PCI, result from ionic fragmentation and from ionisation of the thermolysis product.

Under conditions of ammonia PCI the situation becomes even more complicated, because ammonia adduct ions,  $[M + NH_3 + H]^+$ , may be generated. This gives rise to the formation of  $[M + NH_3 + H - CH_3NCO]^+$ , either from fragmentation or from adduct ion formation of the thermolysis product. Metastable ion (MIKE) spectra were recorded from  $[M + NH_3 + H]^+$ , as generated under DCI conditions, confirm that  $CH_3NCO$  is lost from the adduct ions, albeit that the intensity is only 1–5% of the ammonia loss. An additional problem was especially distinct in the case of carbofuran: a dramatic pressure dependence was observed under ammonia DCI conditions. Although pressure dependence in CI has been reported before and is considered a general characteristic of the method [36], the

pressure dependence is only rarely problematic in the pressure regimes used for DCI and PB-CI. In the case of carbofuran, however, the relative abundances of the  $[M + H]^+$  ion, the specific fragment ion,  $[M + H - CH_3NCO]^+$ , and their ammonia adduct ions, at  $m/z$ , 222, 165, 239 and 182, respectively, change completely between manifold pressures of  $4 \cdot 10^{-5}$  to  $4 \cdot 10^{-4}$  Torr. This dependence is depicted in Fig. 2, where the relative abundances of  $m/z$  222 and 239 are plotted against the manifold pressure at three different source temperatures: 115, 170 and 210°C. The ammonium adduct ion,  $[M + NH_3 + H]^+$ , is seen to dominate the spectrum at higher ion source pressures, but the adduct ion abundance decreases with increasing ion source temperature. The formation of the ammonium adduct ions results in the suppression of the fragment ion,  $[M + H - CH_3NCO]^+$ , at  $m/z$  165. At the higher ion source temperatures the relative abundances of  $[M + H]^+$ ,  $m/z$  222, and  $[M + NH_3 + H]^+$ ,  $m/z$  239, are less sensitive to pressure changes than at 115°C. Such a strong dependence of the mass spectra upon the ion source pressure is shown by none of the other carbamates studied here; intensity ratio differences may be as high as 20–30%.

The possible origin of ion signals in the ammonia PCI mass spectra of carbamates is depicted in Fig. 3. Note that the ammonium adduct ions,  $[M + NH_3 + H]^+$ , are formally reaction intermediates in the protonation process. For example, a change in the intensity of the  $[M + H - CH_3NCO]^+$  ion may be due to more or less thermolysis (process T), to the deposition of more or less energy in the product ions (in the processes A and F) or to a more or less efficient formation of the ammonium adduct ion (process A). Under ammonia PCI conditions and using either DCI or PB-CI, it is not possible to distinguish between the contributions of the various processes to the spectrum abundances of thermally labile compounds. However, it is clear that quantitation in ammonia PCI might be difficult, especially when selected-ion monitoring is used.

In order to study the effect of source pressure and temperature on ion abundances in FIA–PB-

Table 1

Main ions and their relative abundances of fourteen carbamates, obtained with ammonia PCI at an ion source temperature of 125°C and using direct probe or particle beam inlet (at  $5 \cdot 10^{-4}$  Torr and 0.6 Torr indicated source pressure, respectively)

Compound Ion composition	<i>m/z</i>	Relative intensity (%)	
		DCI	PB-PCI
<i>Aldicarb Sulphone</i>			
[M + H + NH <sub>3</sub> ] <sup>+</sup>	240	100	–
[M + H] <sup>+</sup>	223	1	1
[M + H – CH <sub>3</sub> NCO + NH <sub>3</sub> ] <sup>+</sup>	183	10	–
[M + H – CH <sub>3</sub> NHCOOH + NH <sub>3</sub> ] <sup>+</sup>	165	8	100
<i>Aminocarb</i>			
[M + H] <sup>+</sup>	209	100	33
[M + H – CH <sub>3</sub> NCO] <sup>+</sup>	152	10	100
<i>Asulam</i>			
[M + H + NH <sub>3</sub> ] <sup>+</sup>	248	100	32
[M + H + NH <sub>3</sub> – CH <sub>3</sub> OH] <sup>+</sup>	216	–	45
[M + H – 58] <sup>+</sup>	190	2	100
<i>Barban</i>			
[M + H + (NH <sub>3</sub> ) <sub>2</sub> ] <sup>+</sup>	292	13	–
[M + H + NH <sub>3</sub> ] <sup>+</sup>	275	100	67
[M + H] <sup>+</sup>	258	1	–
[M + H – HCl + NH <sub>3</sub> ] <sup>+</sup>	239	1	56
[M + H – HCl] <sup>+</sup>	222	1	24
[C <sub>10</sub> H <sub>4</sub> NCO] <sup>+</sup>	153	–	100
<i>Bromocarbamate</i>			
[M + H + (NH <sub>3</sub> ) <sub>2</sub> ] <sup>+</sup>	292	10	–
[M + H + NH <sub>3</sub> ] <sup>+</sup>	275	100	100
[M + H] <sup>+</sup>	258	1	25
<i>Carbaryl</i>			
[M + H + NH <sub>3</sub> ] <sup>+</sup>	219	100	100
[M + H] <sup>+</sup>	202	2	16
[M + H – CH <sub>3</sub> NCO + NH <sub>3</sub> ] <sup>+</sup>	162	29	16
[M + H – CH <sub>3</sub> NCO] <sup>+</sup>	145	6	18
<i>Carbendazim</i>			
[M + H + NH <sub>3</sub> ] <sup>+</sup>	209	4	–
[M + H] <sup>+</sup>	192	100	100
<i>Carbofuran</i>			
[M + H + NH <sub>3</sub> ] <sup>+</sup>	239	100	25
[M + H] <sup>+</sup>	222	3	53
[M + H – CH <sub>3</sub> NCO + NH <sub>3</sub> ] <sup>+</sup>	182	13	100
[M + H – CH <sub>3</sub> NCO] <sup>+</sup>	165	–	23
<i>Dioxacarb</i>			
[M + H + NH <sub>3</sub> ] <sup>+</sup>	241	100	20
[M + H] <sup>+</sup>	224	2	15
[M + H – CH <sub>3</sub> NCO] <sup>+</sup>	167	21	100

(Continued on p. 26)

Table 1. (Continued)

Compound Ion composition	<i>m/z</i>	Relative intensity (%)	
		DCI	PB-PCI
<i>Desmedipham</i>			
$[(M - C_6H_5NCO)_2 + H + NH_3]^+$	380	3	–
$[M + H + NH_3]^+$	318	2	–
$[M + H + (NH_3)_2 - C_6H_5NCO]^+$	216	13	–
$[M + H + NH_3 - C_6H_5NCO]^+$	199	100	100
$[M + H - C_6H_5NCO]^+$	182	1	33
<i>Ethiofencarb</i>			
$[M + H + NH_3]^+$	243	100	100
$[M + H]^+$	226	2	32
$[M + H - CH_3NCO + NH_3]^+$	186	8	–
$[M + H - CH_3NCO]^+$	169	5	85
<i>Pirimicarb</i>			
$[M + H]^+$	239	100	100
<i>Promecarb</i>			
$[M + H + NH_3]^+$	225	100	100
$[M + H]^+$	208	1	48
$[M + H - CH_3NCO + NH_3]^+$	168	4	–
$[M + H - CH_3NCO]^+$	151	3	39
<i>Propoxur</i>			
$[M + H + NH_3]^+$	227	100	100
$[M + H]^+$	210	47	95
$[M + H - CH_3NCO + NH_3]^+$	170	14	–

PCI-MS five representative carbamates were selected, of which the structures are depicted in Fig. 4. The N-methylcarbamates carbofuran, dioxacarb and carbaryl were selected, because they primarily form ammonium adduct ions; in addition, we suspected dioxacarb to be extremely thermally labile because of the relatively high abundance of  $[M + H - CH_3NCO]^+$  ions observed in preliminary measurements. The N-methylcarbamate aminocarb and the N,N-dimethylcarbamate pirimicarb were selected, because they show no ammonium adduct ions in their mass spectra; we suspected aminocarb to be thermolabile (on the same grounds as given above for dioxacarb), whereas pirimicarb cannot eliminate an isocyanate-type molecule and must be thermally stable. The pressure dependence of the intensity of  $[M + H]^+$ ,  $[M + NH_3 + H]^+$ ,  $[M + H - CH_3NCO]^+$  and  $[M + NH_3 + H -$

$CH_3NCO]^+$  ions (if present) was recorded at three different source temperatures, using FIA-PB-PCI-MS with ammonia; the results are briefly discussed below.

The pressure dependencies of the ion intensities for carbofuran are depicted in Fig. 5. The behaviour of carbofuran parallels that observed in the DCI experiments. At higher temperatures the fragment ion at *m/z* 165 becomes the base peak. In addition one should note the decline of all ion intensities at higher pressures; a similar decline is not observed in the DCI experiments.

The results for dioxacarb are given in Fig. 6. The  $[M + H - CH_3NCO]^+$  ion, *m/z* 167, yields the base peak already at 125°C. At a source temperature of 125°C the intensity of the ammonia adduct ions, *m/z* 184 and 241, and of the protonated molecule, *m/z* 224, increases with the ion source pressure. At higher source tem-



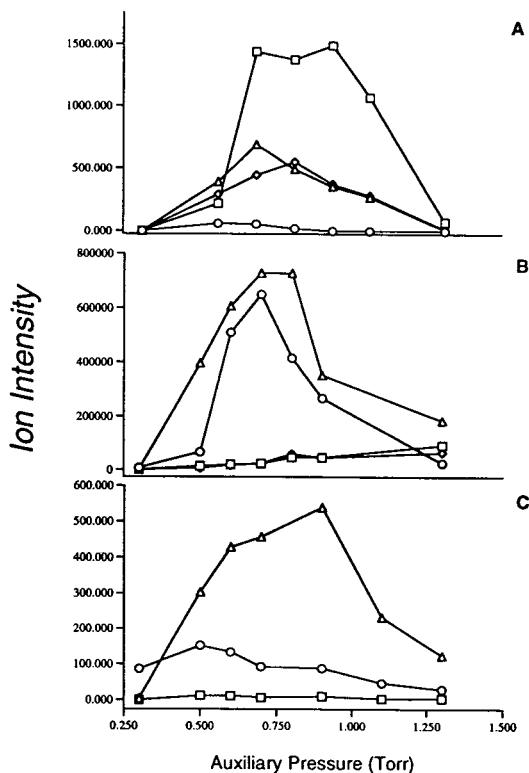


Fig. 5. Ion intensities of ions  $m/z$  165 ( $\circ$ ), 182 ( $\Delta$ ), 222 ( $\square$ ) and 239 ( $\diamond$ ) of carbofuran at different reagent gas pressures, and at ion source temperatures of 125 (A), 175 (B) and 225°C (C).

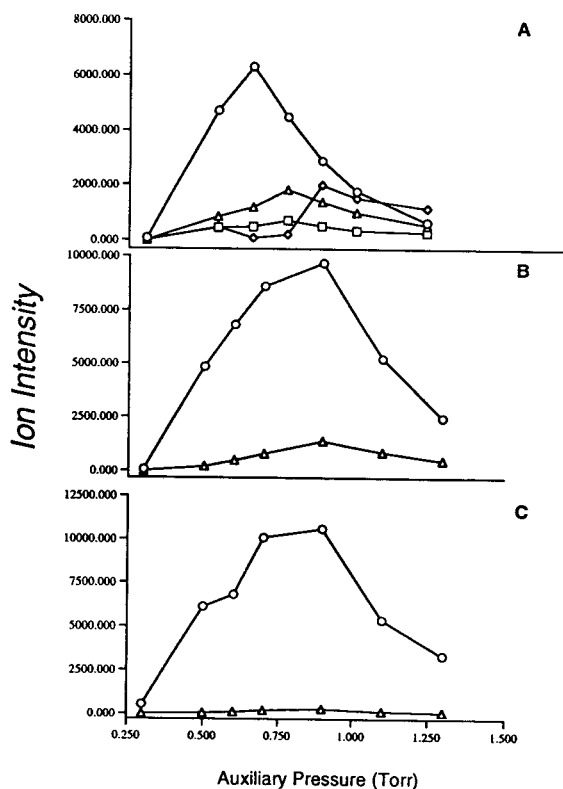


Fig. 6. Ion abundances of ions  $m/z$  167 ( $\circ$ ), 184 ( $\Delta$ ), 224 ( $\square$ ), and 241 ( $\diamond$ ) of dioxacarb at different reagent gas pressures, and at ion source temperatures of 125 (A), 175 (B) and 225°C (C).

209, and  $[M+H-CH_3NCO]^+$  ions,  $m/z$  152. At an ion source temperature of 125°C the protonated molecule is the base peak. At higher temperatures the  $[M+H-CH_3NCO]^+$  ion becomes the base peak; at 225°C the relative intensity of the protonated molecule is even decreased to less than 10% of the  $m/z$  152 base peak. This is due to the thermal degradation of the compound in the ion source, as was mainly observed for dioxacarb (see above).

The results for pirimicarb are given in Fig. 7. The protonated molecule,  $m/z$  239, provides the base peak at all pressures and temperatures used. Although we considered this compound to be thermally stable, the ion with  $m/z$  166, which appears at higher source temperatures, shows

that pirimicarb can lose dimethylformamide,  $(CH_3)_2NC(O)H$ . Because we also observe  $m/z$  166 ions in the MIKE spectra of protonated pirimicarb obtained under ammonia DCI conditions, this fragment may arise through stimulated fragmentation of  $[M+H]^+$  or through thermolysis of neutral pirimicarb. Thus, even pirimicarb may give problems in quantitation via PCI experiments.

All base peaks of the compounds tested in PB-PCI-MS show an optimum in their intensity between an indicated ion source pressure of 0.6 and 0.8 Torr, at all temperatures applied. This is in the same order of magnitude as results from earlier reports, where an optimum ion source pressure of approximately 0.4 Torr for methane

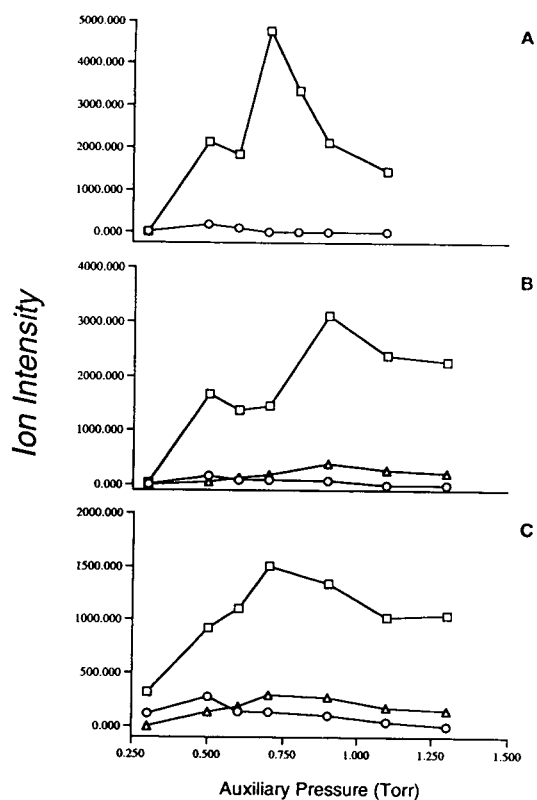


Fig. 7. Ion abundances of ions  $m/z$  166 (○), 225 (△) and 239 (□) of pirimicarb at different reagent gas pressures, and at ion source temperatures of 125 (A), 175 (B) and 225°C (C).

NCI in PB-MS was found [37,38]. The upper limit is probably due to the fact that less particles reach the ion source wall; therefore, evaporation of the particles remains incomplete and, consequently, less analyte molecules are available for ionisation. The lower limit is probably determined by the efficiency of the ion formation process, indiscriminate of the type of ions formed. The pressure dependence is not compound-specific, as is evident from our experimental data.

The pressure dependence is less important at higher ion source temperatures, of, typically, 175–225°C. Consequently, the ion intensity data at these temperatures show better repeatability. As expected, an increase of the  $[M + H -$

$CH_3NCO]^+$  and  $[M + NH_3 + H - CH_3NCO]^+$  ion intensities with the ion source temperature is observed for all N-methyl carbamates and although the mechanism of formation of these ions remains unclear, a comparison of DCI and PB-PCI spectra makes it likely that they are mainly due to thermal degradation of these compounds. The use of higher ion source temperatures, up to 225°C, is favourable for the total ion current quantitation of some of the carbamates. However, under these conditions, the intensities of the  $[M + H]^+$  and  $[M + NH_3 + H]^+$  ions of all test analytes decrease markedly and selected-ion monitoring is best carried out at low source temperatures, typically 125°C.

#### 4. Conclusions

Mass spectra of selected carbamates were obtained under ammonia PCI conditions and using direct probe or FIA-PB inlet systems. Comparison of spectra from both inlet methods shows that an increase in fragment ion intensities with the ion source temperature under FIA-PB-PCI-MS conditions is due to thermal degradation.

It is observed that both the ion source pressure and the temperature cause irrepeatability of the ammonia PCI mass spectra of carbamates under FIA-PB-MS conditions, with strongest variations for carbofuran. The use of higher ion source temperatures, up to 225°C, is favourable for the total ion current quantitation of some of the carbamates. However, under these conditions, the intensities of the  $[M + H]^+$  and  $[M + NH_3 + H]^+$  ions of all test analytes decrease markedly and selected-ion monitoring is best carried out at low source temperatures, typically 125°C. As a consequence it is of utmost importance to use well defined experimental conditions for the quantitative determination of carbamates with LC-PB-PCI-MS. A study on the quantitative determination of carbamates by LC-PB-MS, using on-line preconcentration, will be published in the near future [26].

## Acknowledgements

M.H. has a fellowship from the Community Bureau of Reference (BCR) of the Commission of European Communities (BCR\*-913001). J.S. acknowledges support from the EU Environmental project ENVI-CT92-0109.

## References

- [1] Y.Y. Wigfield, R. Grant and N. Snider, *J. Chromatogr. A*, 657 (1993) 219.
- [2] L.G.M.Th. Tuinstra, F.R. Povel and A.H. Roos, *J. Chromatogr.*, 552 (1991) 259.
- [3] S. Lartiges and P. Carrigues, *Analisis*, 21 (1993) 157.
- [4] R.P. Morgan, E.J. Howard and G. Steel, *Org. Mass Spectrom.*, 14 (1979) 627.
- [5] M.L. Trehy, R.A. Yost and J.J. McCreary, *Anal. Chem.*, 56 (1984) 1281.
- [6] M.L. Trehy, R.A. Yost and J.G. Dorsey, *Anal. Chem.*, 58 (1986) 14.
- [7] H.J. Stan and H.M. Müller, *J. High Resolut. Chromatogr. Chromatogr. Commun.*, 11 (1988) 140.
- [8] R.C. Hall and D.E. Harris, *J. Chromatogr.*, 169 (1979) 245.
- [9] R.D. Voyksner and J.T. Bursey, *Anal. Chem.*, 56 (1984) 1582.
- [10] R.D. Voyksner, J.T. Bursey and E.D. Pellizzari, *J. Chromatogr.*, 312 (1984) 221.
- [11] D.E. Games and N.C.A. Weerasinghe, *J. Chromatogr. Sci.*, 18 (1980) 106.
- [12] G. Durand, N. de Bertrand and D. Barceló, *J. Chromatogr.*, 544 (1991) 233.
- [13] D. Volmer and K. Levsen, *J. Am. Soc. Mass Spectrom.*, 5 (1994) 655.
- [14] D. Volmer, A. Preiss, K. Levsen and G. Wunsch, *J. Chromatogr.*, 647 (1993) 235.
- [15] M. Honing, D. Barceló, B.L.M. van Baar, R.T. Ghijsen and U.A.Th. Brinkman, *J. Am. Soc. Mass Spectrom.*, 5 (1994) 913.
- [16] H. Bagheri, E.R. Brouwer, R.T. Ghijsen and U.A.Th. Brinkman, *J. Chromatogr.*, 647 (1993) 121.
- [17] H.-Y. Lin and R.D. Voyksner, *Anal. Chem.*, 65 (1993) 451.
- [18] G. Hopfgartner, T. Wachs, K. Bean and J.D. Henion, *Anal. Chem.*, 65 (1993) 439.
- [19] D.R. Doerge and S. Bajic, *Rapid Commun. Mass Spectrom.*, 6 (1992) 663.
- [20] S. Pleasance, J.F. Anacleto, M.R. Bailey and D.H. North, *J. Am. Soc. Mass Spectrom.*, 3 (1992) 378.
- [21] R.C. Willoughby and R.F. Browner, *Anal. Chem.*, 56 (1991) 2626–2631.
- [22] P.C. Winkler, D.D. Perkins, W.K. Williams and R.F. Browner, *Anal. Chem.*, 60 (1988) 489.
- [23] C.J. Miles, D.R. Doerge and S. Bajic, *Arch. Environ. Contam. Toxicol.*, 22 (1992) 247.
- [24] T.D. Behymer, T.A. Bellar and W.L. Budde, *Anal. Chem.*, 62 (1990) 1686.
- [25] T.A. Bellar, T.D. Behymer and W.L. Budde, *J. Am. Soc. Mass Spectrom.*, 1 (1989) 92.
- [26] J. Slobodnik, M.E. Jager, S.J.F. Hoekstra-Oussoren, M. Honing, B.L.M. van Baar and U.A.Th. Brinkman, *Org. Mass Spectrom.*, submitted (1995).
- [27] A.P. Tinke, R.A.M. van der Hoeven, W.M.A. Niessen, U.R. Tjaden and J. van der Greef, *J. Chromatogr.*, 554 (1991) 119.
- [28] A.P. Tinke, R.A.M. van der Hoeven, W.M.A. Niessen, U.R. Tjaden and J. van der Greef, *J. Chromatogr.*, 647 (1993) 63.
- [29] R.D. Voyksner, C.S. Smith and P.C. Knox, *Biomed. Environ. Mass Spectrom.*, 19 (1990) 523.
- [30] C.S. Creaser and J.W. Stygall, *Analyst*, 118 (1993) 1467.
- [31] L.D. Betowski, C.M. Pace and M.R. Roby, *J. Am. Soc. Mass Spectrom.*, 3 (1992) 823.
- [32] L. Muszkat and N. Aharonson, *Int. J. Mass Spectrom. Ion Processes*, 48 (1983) 323.
- [33] L. Muszkat and N. Aharonson, *J. Chromatogr. Sci.*, 21 (1983) 411.
- [34] J.J. Stamp, E.G. Siegmund, T. Cairns and K.K. Chan, *Anal. Chem.*, 58 (1986) 873.
- [35] T. Cairns, E.G. Siegmund and J.J. Stamp, *Biomed. Environ. Mass Spectrom.*, 11 (1984) 301.
- [36] A.G. Harrison, *Chemical Ionization Mass Spectrometry*, CRC Press, Boca Raton, FL, 1992, 2nd ed.
- [37] B.C. Lynn Jr., G.D. Marbury and J.R. Tuschall Jr., *Org. Mass Spectrom.*, 23 (1988) 736.
- [38] B.C. Lynn Jr., G.D. Marbury and J.R. Tuschall Jr., *Proc. 36th ASMS Conference on Mass Spectrometry*, San Fransisco, CA, June 1988, American Society of Mass Spectrometry, Washington, DC, 1988, p. 908.





ELSEVIER

Journal of Chromatography A, 712 (1995) 31–43

JOURNAL OF  
CHROMATOGRAPHY A

## Comparison of softwares used for the detection of analytes present at low levels in liquid chromatographic–mass spectrometric experiments

J. Visentini<sup>a</sup>, E.C. Kwong<sup>a</sup>, A. Carrier<sup>b</sup>, D. Zidarov<sup>b</sup>, M.J. Bertrand<sup>b,\*</sup>

<sup>a</sup>Merck Frosst Centre for Therapeutic Research, P.O. Box 1005, Pointe Claire-Dorval, Quebec H9R 4P8, Canada

<sup>b</sup>Regional Center for Mass Spectrometry, Department of Chemistry, University of Montreal, P.O. Box 6128, Montreal H3C 3J7, Canada

### Abstract

A comparison has been made between different approaches for detecting low-level analytes in the TIC traces of sample mixtures analysed by different liquid chromatographic–mass spectrometric (LC–MS) techniques. The approaches studied were contour mapping or “eagle’s view” and a background treatment software, TICFilt, recently developed. Typical pharmaceutical samples including standards and plasma containing common drugs such as propranolol, phenothiazine, acetaminophen have been analysed in LC–MS experiments using ionspray, atmospheric-pressure chemical ionization and direct liquid introduction interfaces. The data obtained were examined by contour mapping and treated by TICFilt in order to detect low level elution peaks. Contour mapping can be efficient at higher masses ( $> M_r$  250) where the background is generally weaker but cannot always detect elution peaks at lower masses where background contribution is important. Furthermore, it cannot distinguish actual peaks from spikes which are often present in these experiments. Background treatment algorithms such as TICFilt, however, can not only eliminate spikes from the TIC trace but also offer a peak detection efficiency for unknown compounds which is constant throughout the mass range and independent of the mobile phase composition and the ionization technique used. Furthermore, background treatment algorithms also provide mass spectra with enhanced spectral information which is important in the identification of unknown drug-related species.

### 1. Introduction

The development of interfaces allowing the direct introduction of liquid samples into the mass spectrometer has considerably increased the range of compounds amenable to mass spectral analysis. For example, direct liquid introduction (DLI) [1], thermospray (TSI) [2,3], continuous-flow fast atom bombardment (CF-

FAB) [4] and more recently atmospheric-pressure chemical ionization (APCI) [5–7], electrospray (ESI) [8,9], and IonSpray (ISP) [10–12] have all been used to identify eluents from an HPLC column. Since these techniques allow the eluent to enter partially or entirely into the ionization source, the solvents and buffers present in the mobile phase are also ionized, thereby generally producing high levels of chemical noise in the total-ion current (TIC) traces. The contribution of this background signal can lead to

\* Corresponding author.

problems in the analysis of unknown samples. For example, in pharmaceutical samples, metabolites or degradation products present at levels as low as 0.1% of the parent drug must often be identified. In screening for these substances in the full-scan mode, the degradation product peaks are often lost in background signal. This masking of low-level eluent peaks by background signal is worst in the low mass range ( $< M_r$ , 250–300).

Several approaches for the post-process background treatment of mass spectral data have appeared in the literature [13–22]. For LC–MS data, in particular, the TIC traces do not generally provide easily observed eluent peaks due to the abundance of mobile phase ions. Although peaks of interest can usually be detected by thorough screening of reconstructed mass chromatograms, which is necessary for unknowns, examination of all reconstructed mass chromatograms in a typical full-scan analysis is tedious and impractical. Furthermore, the traditional background subtraction routines involving the subtraction of a background spectrum from the spectrum of the analyte of interest is often of little use for low-level degradation products masked by chemical noise. This method is further complicated with gradient HPLC methods where the background spectra change with time.

Polynomial smoothing techniques [13] which can enhance the signal-to-noise ratios of low-level analyte peaks, improve the appearance of the profile but are of limited use since they do not extract significant ions hidden in the chemical noise. One of the most common approaches for the extraction of significant peaks from LC–MS data is contour mapping or “eagle’s view” [14]. By plotting three axes (mass, time, and intensity) in a two-dimensional display (mass–time), the elution peaks appear over a few scans depending on the width of the chromatographic peak. The background noise in this type of plot will appear as a continuous band over a wide time-span, often occurring throughout the entire analysis time. This technique is most effective at higher mass ranges ( $> M_r$ , 400) where background noise is less abundant for most LC–MS interfaces. Pharmaceutical compounds, however,

are often small molecules which fall in the lower mass range where background interferences are high.

An ideal background filter for LC–MS data would eliminate the contribution of solvent and buffer ions to the acquired mass spectra, recognize and remove noise spikes caused by experimental variations, and extract weak eluent peaks containing significant ions from the overall TIC trace. This type of approach would provide a background-corrected TIC trace indicating low-level eluent peaks as well as other more visible components. It would also provide treated mass spectra with enhanced intensities of significant analyte ions. A background treatment algorithm, TICfilt, has been developed with the above criteria in mind. The filtering of LC–MS data by TICfilt is based on the premise that the occurrence of background ions is more frequent than that of ions due to analytes. Its performance will be compared to the commonly used contour mapping approach.

## 2. Experimental

Acetaminophen ( $M_r$  151) and propranolol ( $M_r$  259) used in these experiments are USP reference standards obtained from American Chemicals (Rockville, MD, USA), phenothiazine ( $M_r$  199) was purchased from Fluka Chemika (Ronkonkoma, NY, USA). Compound X ( $M_r$  454) was synthesized in-house. All compounds were used without further purification. The mobile phases used in these experiments were composed of given ratios of HPLC grade acetonitrile and distilled deionized water and contained 0.1% formic acid (approx. 99%, Sigma, St. Louis, MO, USA). All sample solutions were prepared in acetonitrile.

The liquid chromatographic system used for DLI analyses consisted of a Carlo Erba Phoenix-20 high-pressure syringe pump (Carlo Erba Str. Milano, Italy) connected to a Valco C14W 60 nL valve (Valco Instrument Co., Houston, TX, USA) in order to minimize dead volume between the pump and capillary tubing or liquid chromatographic columns. The columns used in

the DLI-LC-MS experiments consisted of laboratory made capillary reversed-phase columns (Spherisorb ODS-2, particle diameter 5  $\mu\text{m}$ , 200 mm  $\times$  250  $\mu\text{m}$  I.D.). Mass spectral analyses were performed on a VG Trio-1 mass spectrometer equipped with differential pumping (analyzer 50 l/s, source 240 l/s) and using an in-source  $\mu$ -thermospray interface [23]. Data handling and control of the mass spectrometer were provided by the LAB BASE (version 2.01) data system. All spectra were recorded in the filament-on mode. The TICfilt program version for this instrument was written in Borland C<sup>++</sup> on an IBM compatible computer PC (80386 or above with Windows software) and execution time for moderate data files requires only a few seconds.

All APCI and ESI LC-MS experiments were performed on a HP 1090 liquid chromatograph equipped with an Intersil (Metachem, Torrance, CA, USA) 5  $\mu\text{m}$  ODS-2 (100  $\times$  3 mm I.D.) column and coupled to a PE/Sciex API III triple quadrupole mass spectrometer via an IonSpray or an APCI interface operating at atmospheric pressure. Full-scan mass spectra over the mass range  $m/z$  120–600 were acquired and examined using PE/Sciex Tune 2.4 and MacSpec 3.22 softwares respectively. The contour mapping feature of the API III MacSpec software was used as a typical example of this type of approach for treating LC-MS data. The background treatment algorithm, TICfilt, was written in C language and runs on Macintosh or IBM compatible computers with Windows. Execution time of this version of TICfilt is in the order of 1 min. Treated data can be accessed and viewed through MacSpec software.

### 3. Results and discussion

Although direct introduction interfaces have made the routine use of LC-MS possible, the problem of dealing with background interferences remains an important challenge. Current background treatment softwares associated with LC-MS systems often represent mass spectral data through contour mapping which plots mass

vs. scan number vs. intensity as shown below by the typical contour plot in Fig. 1a. This contour mapping approach can be used to distinguish peaks from the constant chemical background signal due to mobile phase ions. For example, a chromatographic peak will appear as a discrete band such as that observed at about  $m/z$  150 and 2.1 min in Fig. 1a while the background ions are observed as constant bands throughout the analysis time.

Once a peak is found on the contour plot, spectra immediately before and after the elution peak are subtracted from the spectrum or average spectrum due to the species of interest in order to improve the signal-to-background ratio. Other methods simply subtract baseline noise from the TIC chromatogram. These methods, however, do not filter data and are therefore vulnerable in cases where background is intense. It is very difficult to find elution peaks at low levels amidst heavy noise levels due to mobile phase ions unless background ions are distinguished from elution peak ions. Furthermore, the presence of spikes in the TIC chromatogram may complicate the analysis of data and the contour plot. The whole process may become rather time-consuming.

A background treatment algorithm which filters data will enhance the quality of the TIC chromatogram and of the mass spectra simultaneously, thereby saving data treatment time. Furthermore, if data are filtered, the number of cases where elution peaks are lost in the mass of background peaks will be minimized. An efficient computer algorithm for LC-MS data treatment of sample mixtures containing unknowns must, therefore, be able to remove background signal without eliminating low-level analyte peaks. TICfilt, a background treatment algorithm developed by our group [15], is based on the hypothesis that background ion signals in a mass spectrum will occur with a higher frequency than ion peaks due to analyte species which should have intensities distributed in a random fashion. The algorithm which basically includes three steps—background treatment, noise and spikes treatment and elution peak recognition—will from the raw data generate a treated TIC

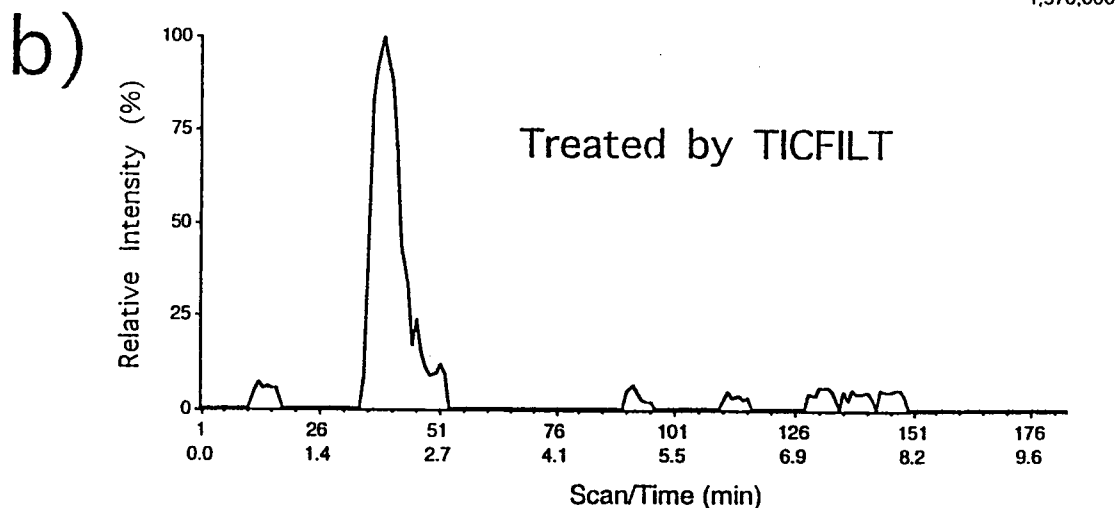
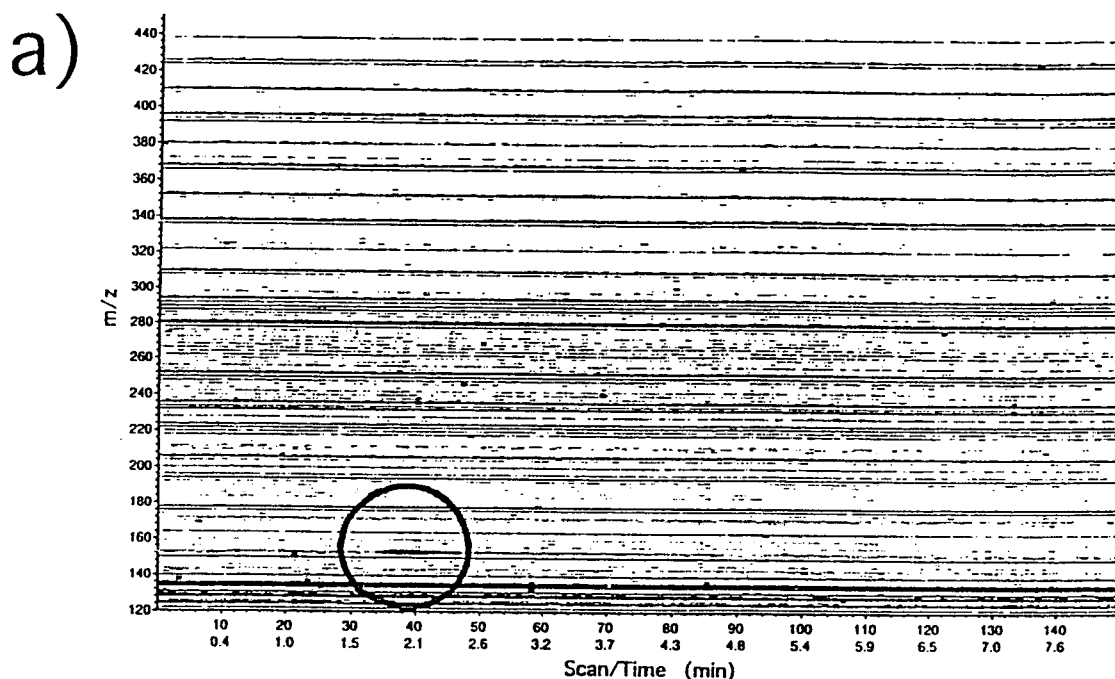


Fig. 1. (a) Contour plot and (b) TICFilt treated data for a 0.025 mg/ml solution of acetaminophen in acetonitrile obtained by LC-APCI (heated nebulizer)-MS.

and treated mass spectra from which most interferences are eliminated.

Upon entering the TICFilt program, the user must select the files to be treated and may define

parameters to be used, such as mass range or scan interval of interest, if they are different from the default conditions (entire acquisition ranges). Once these values are established, TIC-

Filt uses the mass/intensity lists of the raw data file and calculates the frequency of occurrence of each mass in order to perform its background treatment [15]. Noise and spike treatment is then performed by defining appropriate parameters which are related to experimental conditions. Signals which adhere to the given definition of spikes are then eliminated from the data file. Finally, the elution peak recognition portion of TICFilt determines the total number of elution peaks and filters each mass with respect to the elution peaks found. The treated mass/intensity list is then plotted by the commercial software from which raw data was taken. The data output from this program consists of a treated TIC trace with enhancement of elution peaks and its corresponding mass spectra which have been background treated.

The TICFilt data filtering method was compared to the contour plot approach for LC-MS data obtained using IonSpray, APCI and DLI interfaces. Fig. 1a, for example, illustrates the contour plot of a 0.025 mg/ml solution of acetaminophen analyzed by LC-APCI-MS. An elution peak can be observed as a distinct band (highlighted) at about 2.1 min in this contour plot. When this data was treated by TICFilt, a peak at this retention time is isolated from the total TIC trace as shown in Fig. 1b. The results given in Fig. 2 indicated that when LC-MS analyses are performed at a lower concentration (0.5  $\mu\text{g/ml}$ ), the peak due to acetaminophen (highlighted) at about 2.1 min and  $m/z$  150 is not easily observed on the contour plot (Fig. 2a) but that TICFilt is still able to extract significant ions from the overall acquired data (Fig. 2b). This efficiency of TICFilt in extracting elution peaks from the TIC trace is particularly more important at lower masses ( $< M_r$  250) where the constant and often intense background signal masks the elution peak bands.

Fig. 3a presents the TIC obtained for compound X in rat plasma, which contributes a substantial background signal, obtained by LC-IonSpray-MS. Although a signal is not easily observed in the original TIC trace (Fig. 3a), TICFilt indicates that an elution peak occurs at approximately 10 min (Fig. 3b). The mass spec-

trum at the apex of this peak contains a base peak at  $m/z$  455 that corresponds to the parent ion of compound X. TICFilt also allows a narrow scan range to be selected which is useful when the elution peak is quite small in the normalized TIC. The effect of this option is demonstrated in Fig. 3c where the elution peak of compound X now appears as prominent. This option also enhances the elution profile of another peak which was revealed in Fig. 3b. This compound shows a base peak at  $m/z$  416 in its mass spectrum and although it may be a by-product of compound X its origin is still uncertain.

Similarly, results obtained from experiments conducted by LC-APCI-MS for a phenothiazine sample in rat plasma (Fig. 4a) also showed that TICFilt is efficient at extracting elution peaks from the overall signal acquired (Fig. 4b). The elution peak for phenothiazine was found to be clearly distinguished from background signal (Fig. 4b). Again the narrow scan option can be advantageous in enhancing low-level elution peaks as shown in Fig. 4c where the scan range to be treated was limited to scans 50–183. Another small elution peak is also revealed in the TIC around 9 min with a base peak at  $m/z$  417. Similar results were also obtained for an acetaminophen standard analyzed by DLI (Fig. 5). From this figure it can be seen that the noise-filtering ability of TICFilt is very efficient in eliminating the heavy background fluctuations in the TIC that could otherwise be mistaken for analyte signals. The results from these experiments indicate that regardless of the ionization technique employed for the LC-MS analysis, TICFilt can successfully isolate significant ions from the mass of ions produced in the source.

When employing background filters to treat LC-MS data, it is also important to enhance the quality of the mass spectra. For example, in Fig. 6a, the parent ion of acetaminophen at  $m/z$  152 is lost in the legion of background peaks of the raw mass spectrum. When the spectra immediately before and after the peak of interest identified using the contour plot are subtracted from the mass spectra of the acetaminophen (Fig. 6b), the parent ion at  $m/z$  152 is now the base peak but there are also several other

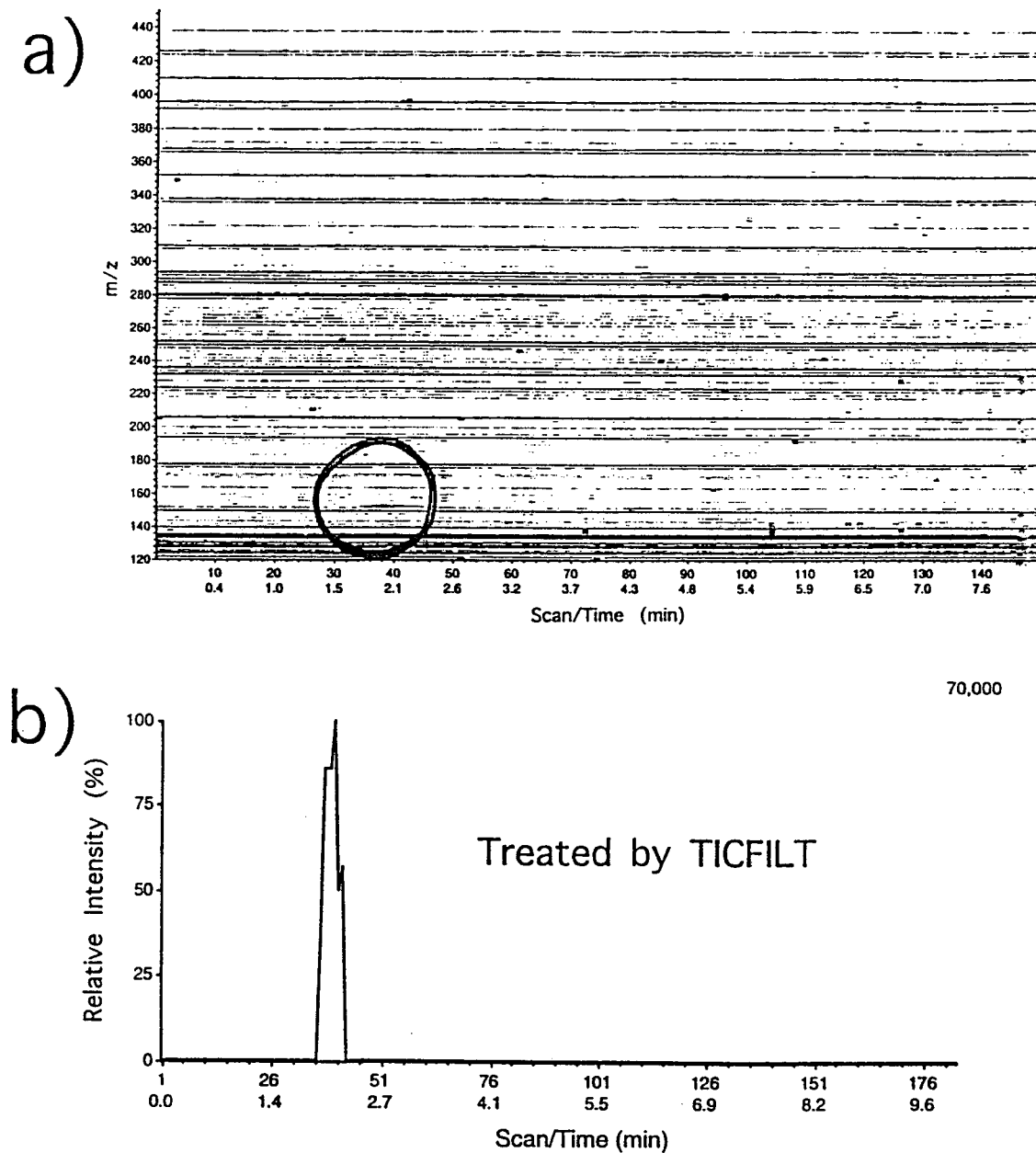


Fig. 2. (a) Contour plot and (b) TICFilt treated data for a 0.5  $\mu\text{g/ml}$  solution of acetaminophen in acetonitrile obtained by LC-APCI (heated nebulizer)-MS.

background peaks which can be seen in this background-corrected spectrum. The corresponding TICFilt treated spectrum (Fig. 6c)

however contains only a few peaks with the base peak at  $m/z$  152. This improvement in signal-to-noise ratio due to background treatment can be

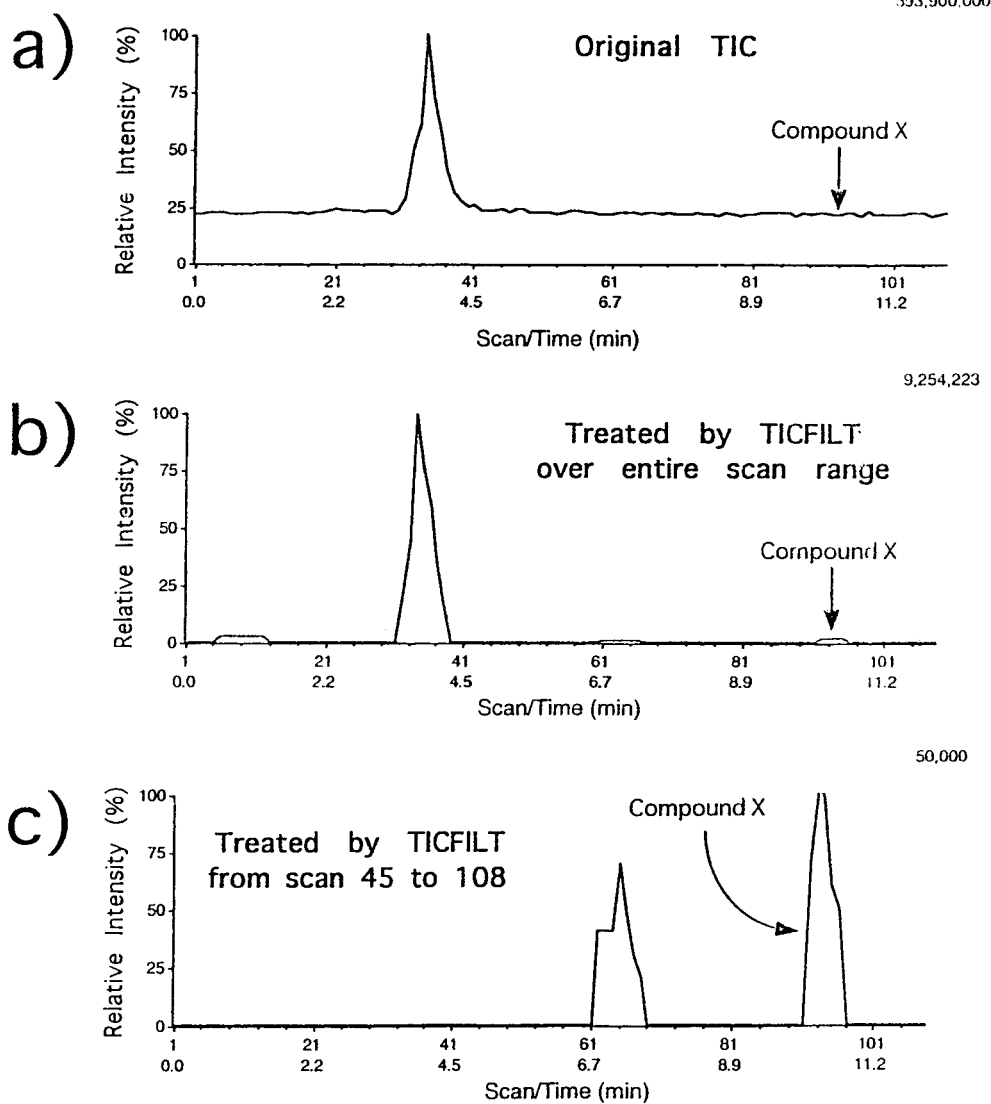


Fig. 3. Total-ion chromatograms of compound X (0.0025 mg/ml) in rat plasma obtained by LC–IonSpray-MS. (a) Original TIC, (b) TICFilt treated TIC and (c) TICFilt treated TIC over the limited scan range 45–108.

particularly useful for the analysis of unknown samples where the analyst must identify parent ions of compounds in a sample mixture.

Fig. 7 compares the quality of spectra obtained for a propranolol sample by examining the raw mass spectrum, the contour mapping background-subtracted spectrum, and the TICFilt treated spectrum. In the original mass spectrum (Fig.

7a), again the parent ion at  $m/z$  260 is lost in the legion of background ions. When the contour plot was used to guide in background subtraction (Fig. 7b), the parent ion became the base peak with several other background ion peaks present in the treated spectrum. The TICFilt treated spectrum (Fig. 7c) illustrates that the extraction of significant ions from the overall raw spectrum,

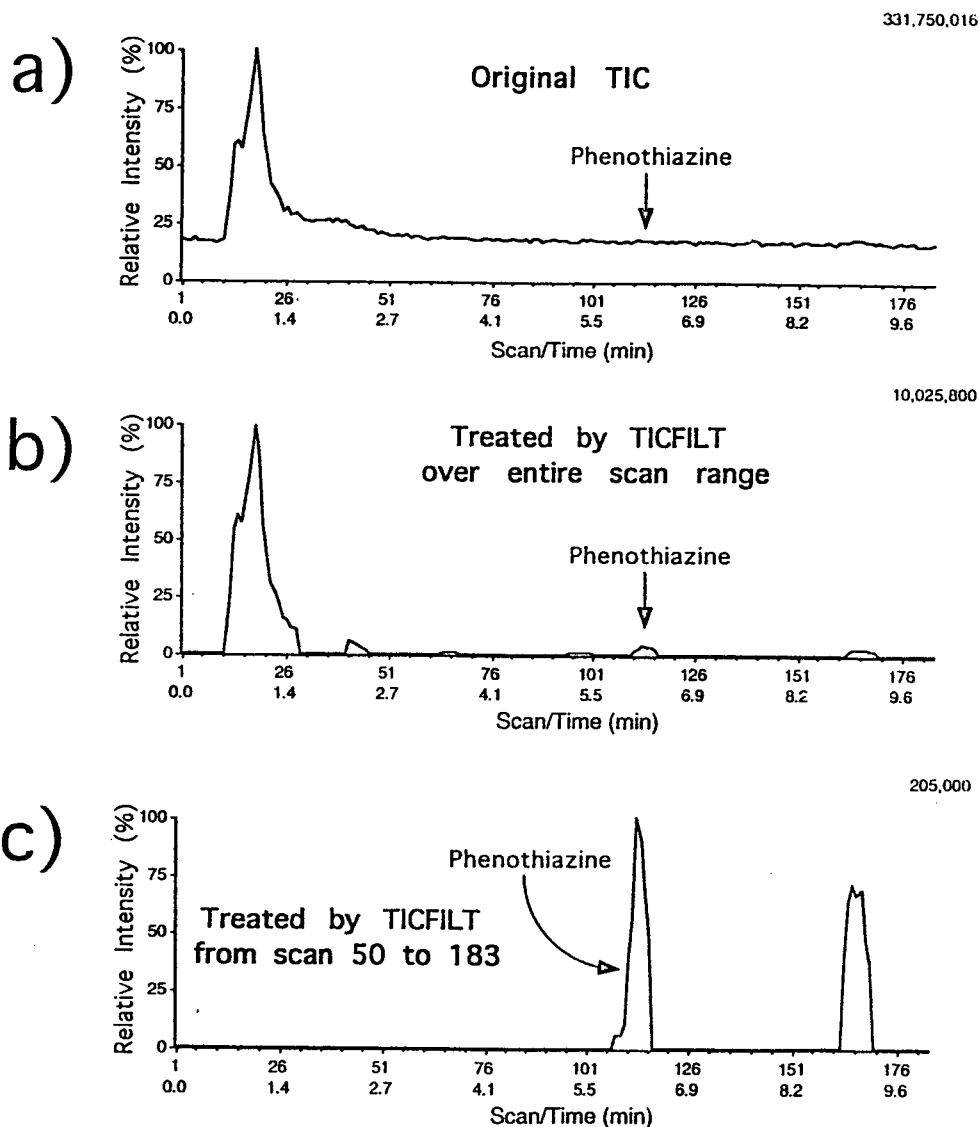


Fig. 4. Total-ion chromatograms of phenothiazine (0.0025 mg/ml) in rat plasma obtained by LC-APCI (heated nebulizer)-MS. (a) Original TIC, (b) TICFilt treated TIC and (c) TICFilt treated TIC over the limited scan range 50–183.

in this case, is more efficient and less time-consuming when TICFilt is used for data treatment. Another example of the efficiency of TICFilt to produce significant treated spectra is given in Fig. 8. This figure presents the raw and treated spectra of acetaminophen (150 ng) obtained by LC-DLI-MS. Since this technique uses the mobile phase as a reagent gas for chemical

ionization, the intensities of the mobile phase ions are often very important which causes problems in identifying the signal due to the analyte in the normalized spectrum. As can be seen from Fig. 8 (lower spectrum) the spectrum of the analyte is clearly enhanced after data treatment by the algorithm clearly showing the protonated molecular ion at  $m/z$  152 and frag-



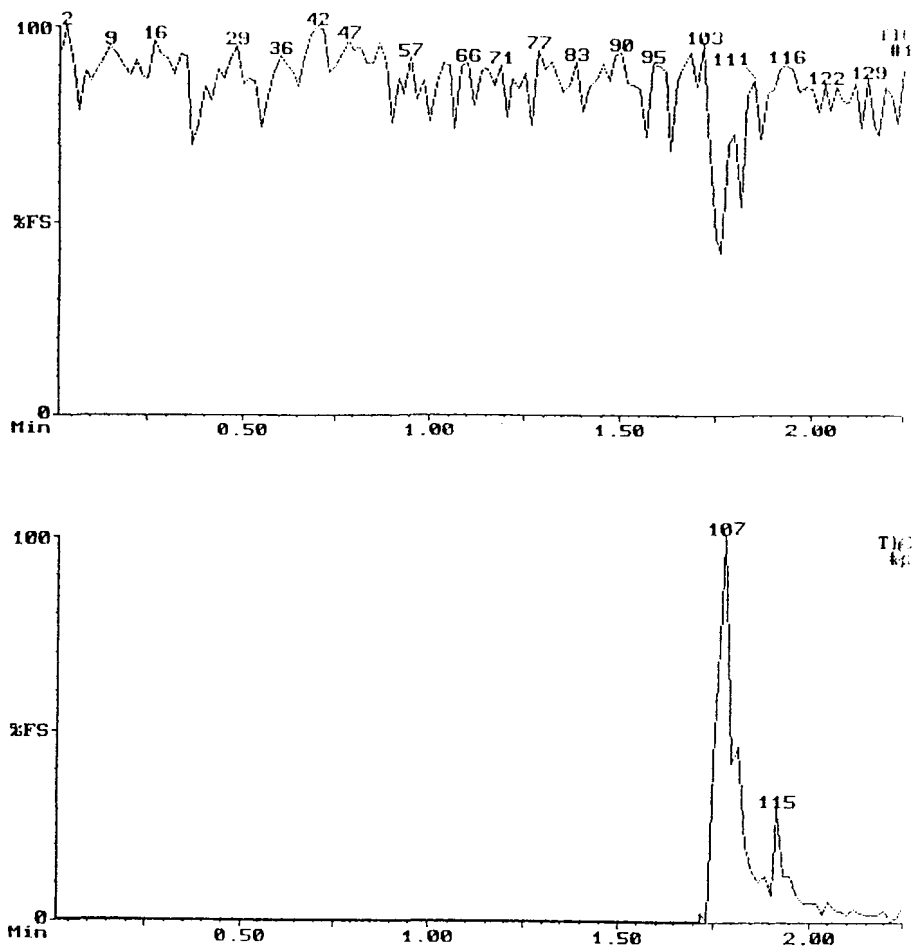


Fig. 5. Total-ion chromatograms obtained for a 150-ng injection of acetaminophen by LC-DLI-MS.

ment at  $m/z$  134. In spite of their relatively high intensities, plasma ions at  $m/z$  42 and 83 due to the protonated monomer and dimer of acetonitrile are absent from the treated spectrum (lower spectrum).

#### 4. Conclusion

The data presented in this comparative study indicate that peak detection approaches can be extremely useful in identifying elution peaks of low-level components in TIC chromatograms obtained by current direct introduction LC-MS

techniques. Contour mapping types of approaches can be efficient at higher masses because background is generally lower but they are limited at lower masses ( $< M_r$  250) where the background generated by the mobile phase is usually more intense. Background treatment algorithms such as TICfilt, however, tend to be efficient throughout the mass range. Furthermore, background treatment algorithms are independent of the ionization technique and the composition of the mobile phase used. When elution peaks or spikes are observed in the TIC, contour mapping will detect both as elution peaks varying only in their width. Background treatment algorithms such as TICfilt can, how-

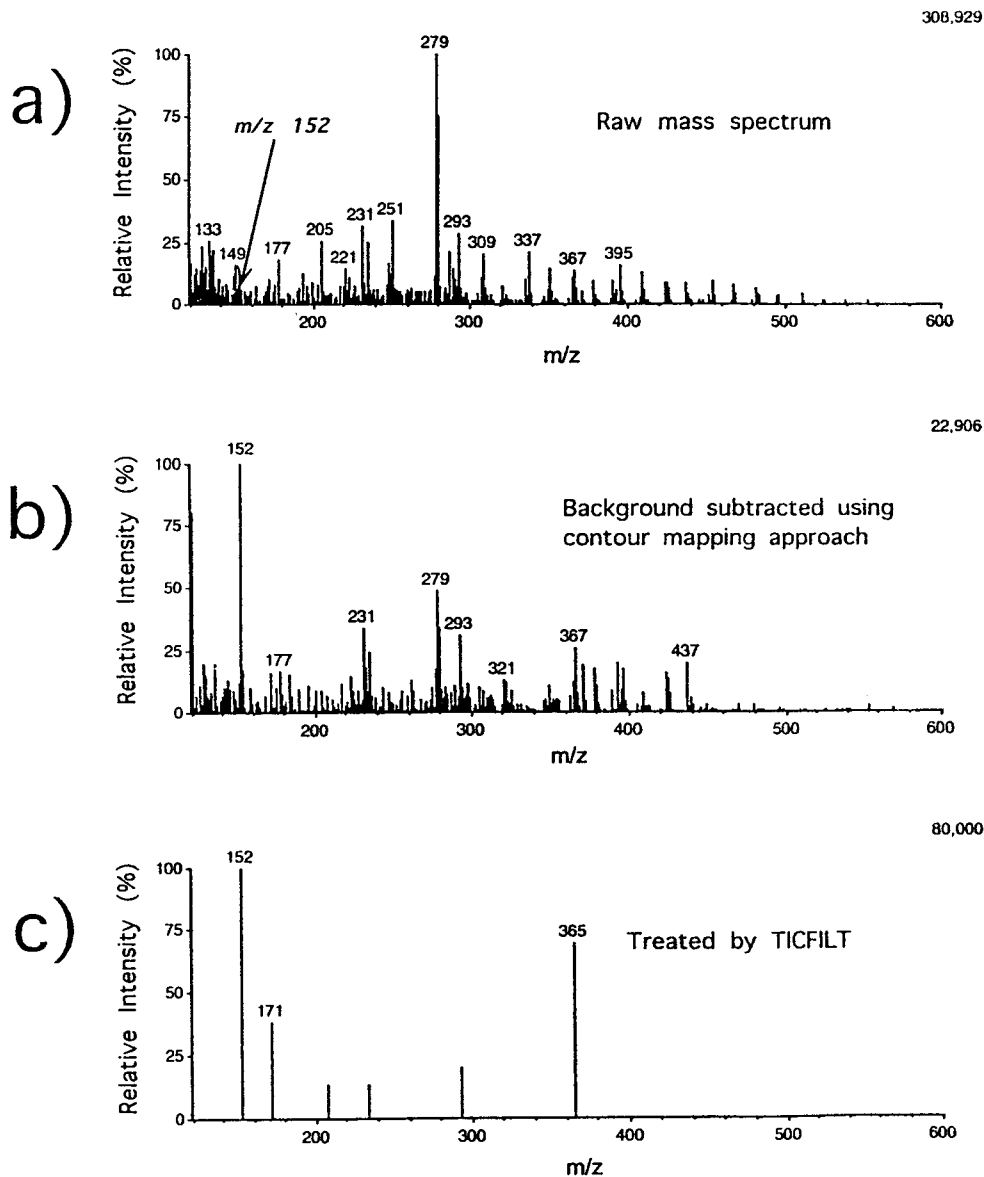


Fig. 6. Comparison of mass spectral quality for: (a) raw data, (b) data treated using the contour mapping approach and (c) data treated by TICFILT for a 0.5  $\mu\text{g/ml}$  acetaminophen standard analyzed by LC-APCI (heated nebulizer)-MS.

ever, remove spikes present in the TIC and reveal only analyte components. A further advantage of background treatment algorithms resides in their ability to produce treated mass spectra in which most of the interfering signals

have been eliminated. This feature is useful in revealing the masses due to the analyte especially at lower masses where analyte peaks are often not observed in the raw spectrum because of their low relative intensities. Thus, background

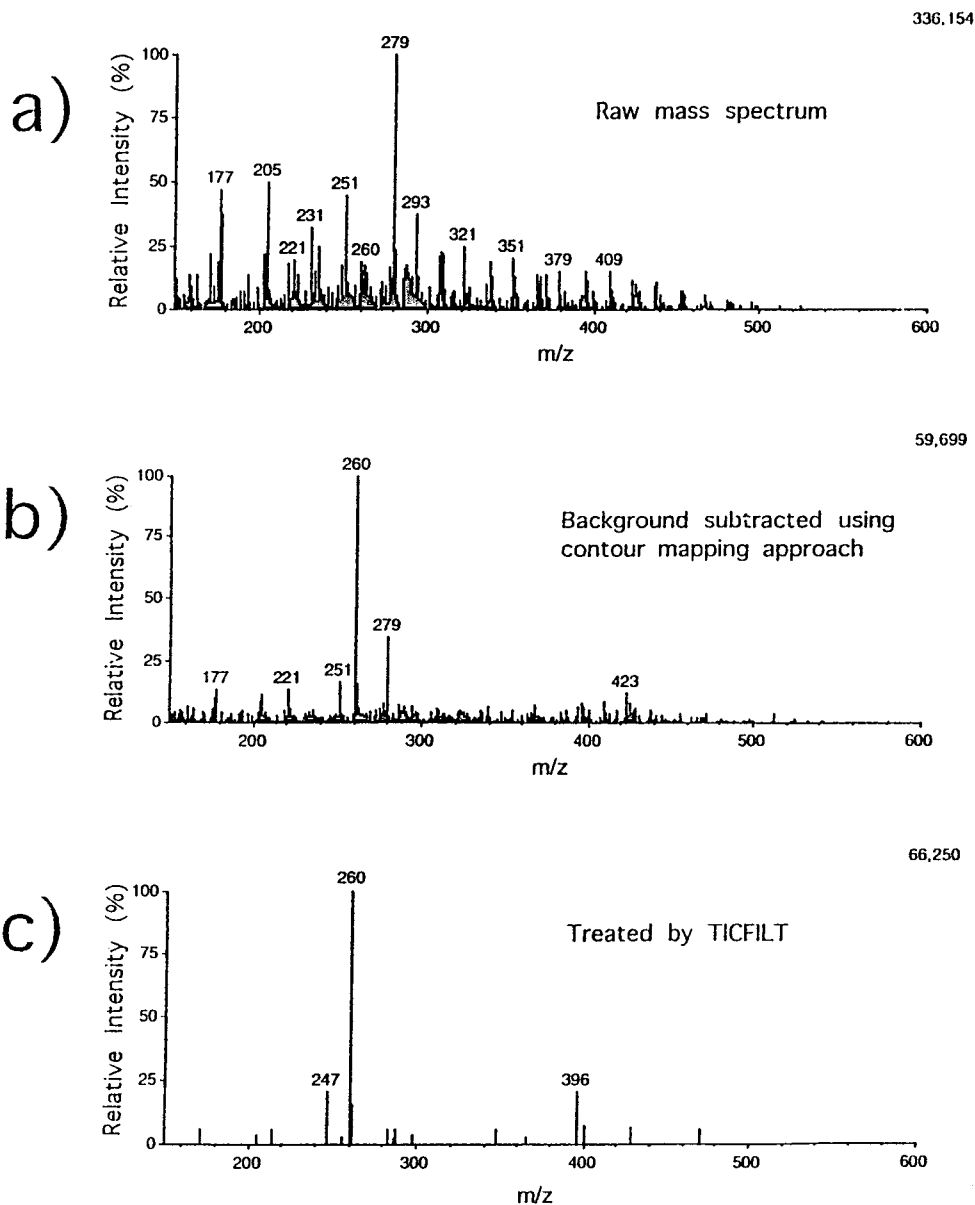


Fig. 7. Comparison of mass spectral quality for: (a) raw data, (b) data treated using the contour mapping approach and (c) data treated by TICFILT for a 0.0025 mg/ml propranolol standard analyzed by LC–IonSpray-MS.

treatment algorithms such as TICFilt, provide high quality TIC and mass spectral data simultaneously, thereby saving data processing time and facilitating data interpretation involving un-

known species as in the case of degradation or metabolic studies. The algorithm is in all aspects equivalent to single-ion chromatograms traces, however, TICFilt is more advantageous because

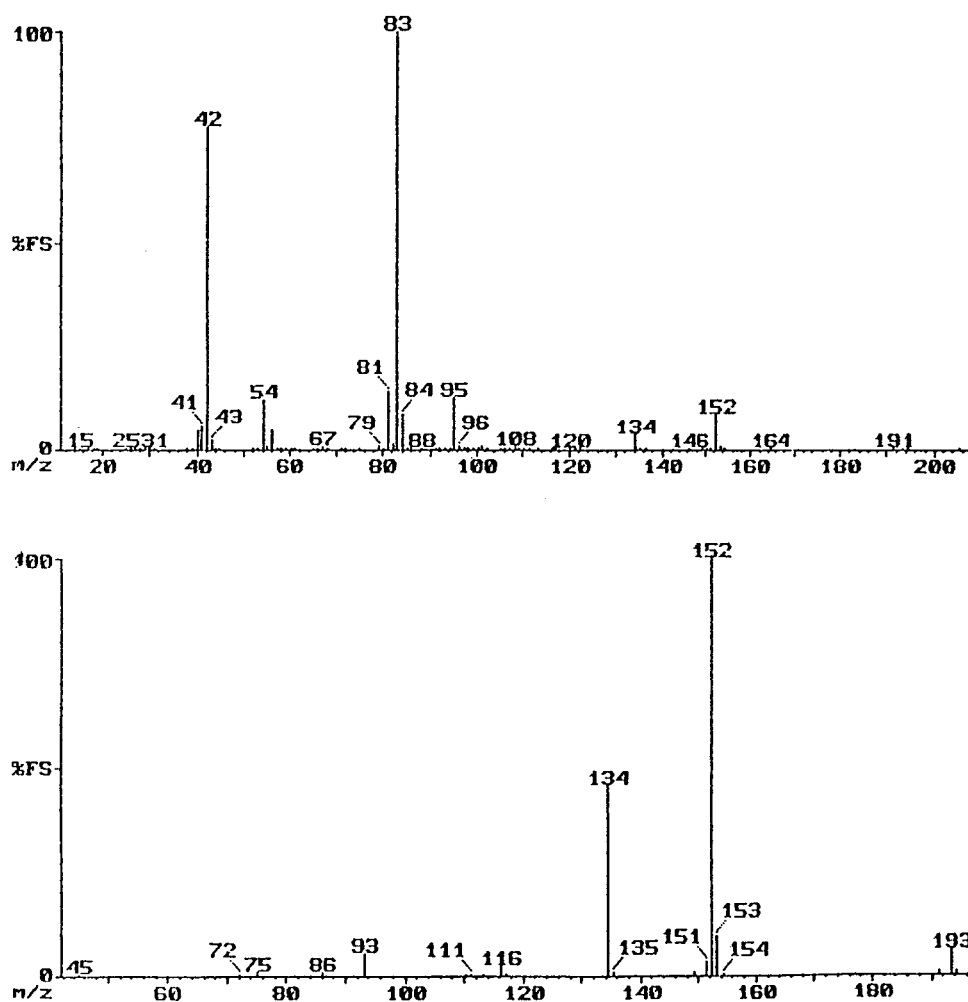


Fig. 8. Comparison of mass spectral quality for (top) raw data and (bottom) data treated by TICFilter for a 150-ng injection of acetaminophen analyzed by LC-DLI-MS.

it can detect the elution peaks without requiring any information on the nature of the eluting compound.

#### Acknowledgements

The authors wish to acknowledge the financial support of the Natural Sciences and Engineering Research Council of Canada (NSERC) and Hydro-Quebec that has permitted this work.

#### References

- [1] R.D. Voyksner and J.T. Burse, *Anal. Chem.*, 56 (1984) 1582.
- [2] I. Hammond, K. Moore, H. James and C.J. Watts, *J. Chromatogr.*, 474 (1989) 175.
- [3] C.R. Blakely, J.J. Carmody and M.L. Vestal, *J. Am. Chem. Soc.*, 102 (1980) 5931.
- [4] R.M. Caprioli, T. Fan and S.J. Cottrel, *Anal. Chem.*, 58 (1986) 2946.
- [5] J.D. Gilbert, T.V. Olah, A. Barrish and T.F. Greber, *Biol. Mass Spectrom.*, 21 (1992) 341.
- [6] B.A. Olsen, S.W. Baertschi and R.M. Riggin, *J. Chromatogr.*, 648 (1993) 165.

- [7] P.V. Macrae, B.C. Jones and J.F.J. Todd, *Rapid Commun. Mass Spectrom.*, 7 (1993) 605.
- [8] C.G. Whitehouse, R.N. Dreyer, M. Yamashita and J.B. Fenn, *Anal. Chem.*, 57 (1985) 675.
- [9] M. Yamashita and J.B. Fenn, *J. Phys. Chem.*, 88 (1984) 4451.
- [10] M.A. Quilliam, M. Janecek and J.F. Lawrence, *Rapid Commun. Mass Spectrom.*, 7 (1993) 482.
- [11] L. Weidolf and T.R. Covey, *Rapid Commun. Mass Spectrom.*, 6 (1992) 192.
- [12] S. Pleasance, P. Blay, M.A. Quilliam and G. O'Hara, *J. Chromatogr.*, 558 (1991) 155.
- [13] C.G. Enke and T.A. Nieman, *Anal. Chem.*, 48 (1976) 705A.
- [14] J. Hau and M. Linscheid, *Spectrochimica Acta*, 48B (1993) E1047.
- [15] A. Carrier, D. Zidarov and M.J. Bertrand, *Proceedings of the 42nd ASMS Conference on Mass Spectrometry and Allied Topics*, Chicago, IL, 1994, p. 490.
- [16] D. Zidarov, D. Faubert, J. Visentini and M.J. Bertrand *Proceedings of the 39th ASMS Conference on Mass Spectrometry and Allied Topics*, Nashville, TN, 1991, p. 1123.
- [17] T.A. Lee, L.M. Headley and J.K. Hardy, *Anal. Chem.*, 63 (1991) 357.
- [18] P. Geladi and B.R. Kowalski, *Anal. Chim. Acta*, 185 (1986) 1.
- [19] J.E. Biller and K. Biemann, *Anal. Letters*, 7 (1974) 515.
- [20] R.B. Lam, D.T. Sparks and T.L. Isenhour, *Anal. Chem.*, 54 (1982) 1927.
- [21] J.M. Laeven and H.C. Smit, *Anal. Chim. Acta*, 176 (1985) 77.
- [22] R.P.J. Doursma and H.C. Smit, *Anal. Chim. Acta*, 133 (1981) 67.
- [23] A. Carrier and M.J. Bertrand, *Proceedings of the 41th ASMS Conference on Mass Spectrometry and Allied Topics*, San Francisco CA, May 31–June 4, 1993, p. 1047.



# Enantiospecific determination of nimodipine in human plasma by liquid chromatography–tandem mass spectrometry

Wolfgang M. Mück

*Clinical Pharmacology International, Bayer AG, Aprather Weg, D-42096 Wuppertal, Germany*

## Abstract

A direct enantiospecific HPLC assay using tandem mass spectrometric (MS–MS) detection via pneumatically-assisted electrospray has been developed for the determination of the calcium antagonist nimodipine in human plasma. By the addition of ammonium acetate (2 mM) to the purely organic eluent ethanol–*n*-heptane (20:80, v/v) charged species ( $M + NH_4^+$ ) were producible by electrospray ionization at sufficient sensitivity. Routine determination of nimodipine enantiomers in human plasma in the working range of 0.5–75  $\mu\text{g/l}$  plasma for each isomer with an accuracy  $\leq \pm 10\%$  and a precision of about 10% (20% close to the limit of quantification) was possible. This was comparable to the available LC–GC–MS assay, however, the time required for routine analysis of ca. 150 unknowns could be reduced from 4 weeks to 1 week.

## 1. Introduction

The calcium antagonist nimodipine (Nimotop<sup>®</sup>) is known for its preferential action on cerebral blood vessels and its suggested cytoprotective effects by reducing calcium influx into nerve cells [1,2]. It is approved for the prevention or treatment of delayed ischaemic dysfunction following subarachnoid haemorrhage, and is currently widely studied in impaired brain function in old age and in senile dementia.

With its asymmetrical substitution at the dihydropyridine ring nimodipine is a racemate (Fig. 1). A stereospecific assay to describe the pharmacokinetic behaviour of its enantiomers has recently been reported [3,4]. The liquid chromatography–gas chromatography–mass spectrometry (LC–GC–MS) assay is based on liquid–liquid extraction with a 1:1 mixture of diethyl ether–*n*-heptane, separation of racemic

nimodipine into its enantiomers via chiral stationary phase HPLC, and collection of the two isomer fractions followed by off-line GC–MS for quantification.

To increase the sample throughput, especially by simplifying this tedious procedure and reducing manual operations, a direct HPLC assay using tandem mass spectrometry (MS–MS) detection in the single reaction monitoring (SRM) mode via pneumatically-assisted electrospray (IonSpray<sup>®</sup>) has been developed. Details of the method and performance data in routine use are presented.

## 2. Experimental

### 2.1. Reference compounds and chemicals

Nimodipine, isopropyl-2-methoxyethyl-1,4-dihydro-2,6-dimethyl-4-(3-nitrophenyl)-3,5-





termine inter-assay accuracy and precision of the assay for each enantiomer and as a tool for quality assurance during routine analysis of the unknowns.

### 2.3. Sample preparation

A 1.0-ml aliquot of plasma from the unknowns (or a 1.0-ml calibration sample spiked as described above, or a 1.0-ml QC sample), 30  $\mu$ l (24 ng) of ISTD solution, 0.3 ml of 1 M sodium hydroxide and 5 ml of diethyl ether-*n*-heptane (1:1, v/v) were thoroughly mixed for 5 min at 400 rpm on a mini-shaker. The samples were centrifuged for 5 min at ca. 3000 g, 4°C. The upper organic layer was transferred to another glass tube and was evaporated in a metal heating block at 40°C under a gentle stream of nitrogen. The residue was reconstituted in 200  $\mu$ l of mobile phase and transferred to the autosampler vials for HPLC analysis.

### 2.4. Instrumentation and operating conditions

A modular instrument HP 1050 (Hewlett-Packard, Waldbronn, Germany) was used in conjunction with an API III<sup>+</sup> tandem mass spectrometer (Sciex, Toronto, Canada). The injection volume was 50  $\mu$ l. Nimodipine enantiomers were separated with a Chira OJ MOD column (250  $\times$  2 mm I.D., 8  $\mu$ m) with a guard column (10  $\times$  2 mm I.D.), supplied by Grom (Herrenberg, Germany). The column was operated at 35°C. The mobile phase consisted of ethanol-*n*-heptane (20:80, v/v) including 2 mM ammonium acetate, with a constant flow-rate of 300  $\mu$ l/min. A split was applied to reduce the flow-rate into the IonSpray interface of the MS system to approximately 50  $\mu$ l/min.

The API III<sup>+</sup> triple quadrupole mass spectrometer was operated with a standard atmospheric pressure ionization (API) source and the pneumatically-assisted electrospray (IonSpray) interface. The potential hazard by using flammable eluents and the occurrence of discharge at the tip of the sprayer has to be carefully addressed by creating an oxygen-free atmosphere within the API source (filling with nitrogen), and

applying moderate voltage to the IonSpray interface to avoid discharge phenomena.

For optimizing the MS conditions a constant infusion of 1–2 mg/ml nimodipine dissolved in ethanol-*n*-heptane containing potassium acetate (Fig. 2A), sodium acetate (Fig. 2B), formic acid (Fig. 2C) and ammonium acetate (Fig. 3A) was used, delivered by a Harvard syringe pump (Harvard Apparatus, SouthNatick MA, USA) at a flow-rate of 10  $\mu$ l/min. For the MS spectra the scan range was 200–500 amu with a step-size of 1 amu and a dwell time of 4 ms each; the result is the average of 15 scans. For the MS–MS spectra the scan range was 50–450 amu with a step-size of 1 amu and a dwell time of 4 ms each; the result is the average of 10 scans.

Both mass analyzers were always operated under unit mass resolution conditions (10% valley definition). The high vacuum in the analyzer region was  $3 \cdot 10^{-5}$  Torr under MS–MS conditions. Collision-induced dissociation in the second quadrupole was obtained at  $3.1 \cdot 10^{14}$  atoms/cm<sup>2</sup> argon gas thickness and a collision energy of 33 eV. The IonSpray interface was floated at +4.2 kV. Single reaction monitoring (SRM) was based on the observation of the parent ions (M + NH<sub>4</sub>)<sup>+</sup> *m/z* 436 for nimodipine and *m/z* 443 for the ISTD and the common fragment *m/z* 301 (Fig. 3). The dwell time for each selected ion pair was 200 ms.

### 2.5. Assay calibration, quality control and validation

Each set of samples analyzed included a set of calibration samples in duplicate, a set of QC samples, analyzed in triplicate during routine analysis, and unknowns, all processed identically during sample pretreatment and LC–MS–MS analysis. Each set of samples included also a blank plasma sample to check for interferences.

The samples were processed as described and peak height ratios of analyte–internal standard were calculated. Calibration curves were constructed by weighted least squares linear regression analysis; as weights the reciprocals of the squared response (i.e., peak height ratio) were used.

Before starting the analysis of unknowns two validation runs with replicates of QC samples ( $n = 5$ ) were performed. Overall assay performance was assessed by calculating inter-assay accuracy and precision of all QC samples analyzed ( $n = 16$ ) for each concentration level.

### 3. Results and discussion

#### 3.1. Optimization of MS conditions

Starting with the existing LC–GC–MS procedure, there were three options for a direct HPLC–MS assay:

(i) Changing the separation system completely to attain reversed-phase conditions commonly applied to electrospray ionization, e.g., a stationary-phase based on  $\alpha_1$ -acid glycoprotein [5] combined with an appropriate buffer–organic modifier system

(ii) Keeping the successful separation, but changing the effluent before entrance into the API source by post-column addition–sheath flow of water–buffer–organic modifier amenable to electrospray ionization

(iii) Adapting the eluent to directly allow electrospray operation without sacrificing the enantiomeric separation.

Although the use of 100% organic mobile phases is not very common in LC–MS with electrospray ionization [6], the latter strategy was selected. While no signal could be acquired with pure ethanol–*n*-heptane (20:80, v/v), charged species of the type  $(M + X)^+$ , (where  $X = H$ , when formic acid was added, or Na, K,  $NH_4$ , when the respective acetate salts of these cations were added into the ethanol before mixing) were obtained. Fig. 2 and 3A show typical electrospray mass spectra of nimodipine under these conditions.

For the  $(M + H)^+$  spectrum with formic acid the sensitivity was dependent on the amount of formic acid (0.1% vs. 1%); beyond 1%, however, no further increase was achieved. The  $(M + Na)^+$  adduct ion was always present in the formic acid experiment, possibly due to the purity of the reagent used. The ratio of signal

intensity of the ions at  $m/z$  419 and  $m/z$  441 could be controlled by the applied orifice voltage. The mass spectra of the ammonium acetate medium showed both the  $(M + NH_4)^+$  adduct and the protonated ion  $(M + H)^+$  depending on the orifice voltage (fragmentation energy) chosen. Fig. 3A shows the mass spectrum under conditions optimized for highest sensitivity (orifice voltage: 33 V).

Though all modifiers were able to produce charged nimodipine species in ethanol–*n*-heptane and showed satisfactory and comparable sensitivity for the  $(M + X)^+$  ion, no adequate fragmentation could be obtained in the MS–MS experiment (collision-induced dissociation with argon) for the alkali adducts. Only the parent ion itself and the alkali ion at  $m/z$  23 or  $m/z$  39, respectively, could be detected, even at increased collision energy. In contrast, the CID spectrum of the  $(M + NH_4)^+$  parent ion showed fragmentation with a dominant daughter ion at  $m/z$  301 (or at  $m/z$  343, depending on the applied collision energy). A detailed interpretation of the CID spectrum was not undertaken, but both fragments at  $m/z$  343 and  $m/z$  301 show loss of the labelled isopropyl side chain (Fig. 1). Fig. 3B shows the nimodipine MS–MS spectrum under final conditions (collision energy: 33 eV).

Based on these optimized MS and MS–MS conditions for  $(M + NH_4)^+$ , single reactions of both  $m/z$  436 and  $m/z$  443 (ISTD) to  $m/z$  301 were selected to monitor the enantiomeric HPLC separation.

#### 3.2. Chromatographic performance

Various aspects of the chromatographic performance have already been discussed together with the LC–GC–MS assay [3,4] and will not be repeated herein. All four considered modifiers, i.e., formic acid, sodium, potassium and ammonium acetate, were tested and did not change the separation, at least not in the concentrations mentioned. An example of the separation in the direct LC–MS–MS assay is given in Fig. 4, showing chromatograms of duplicate injections at various concentrations. The slightly reduced

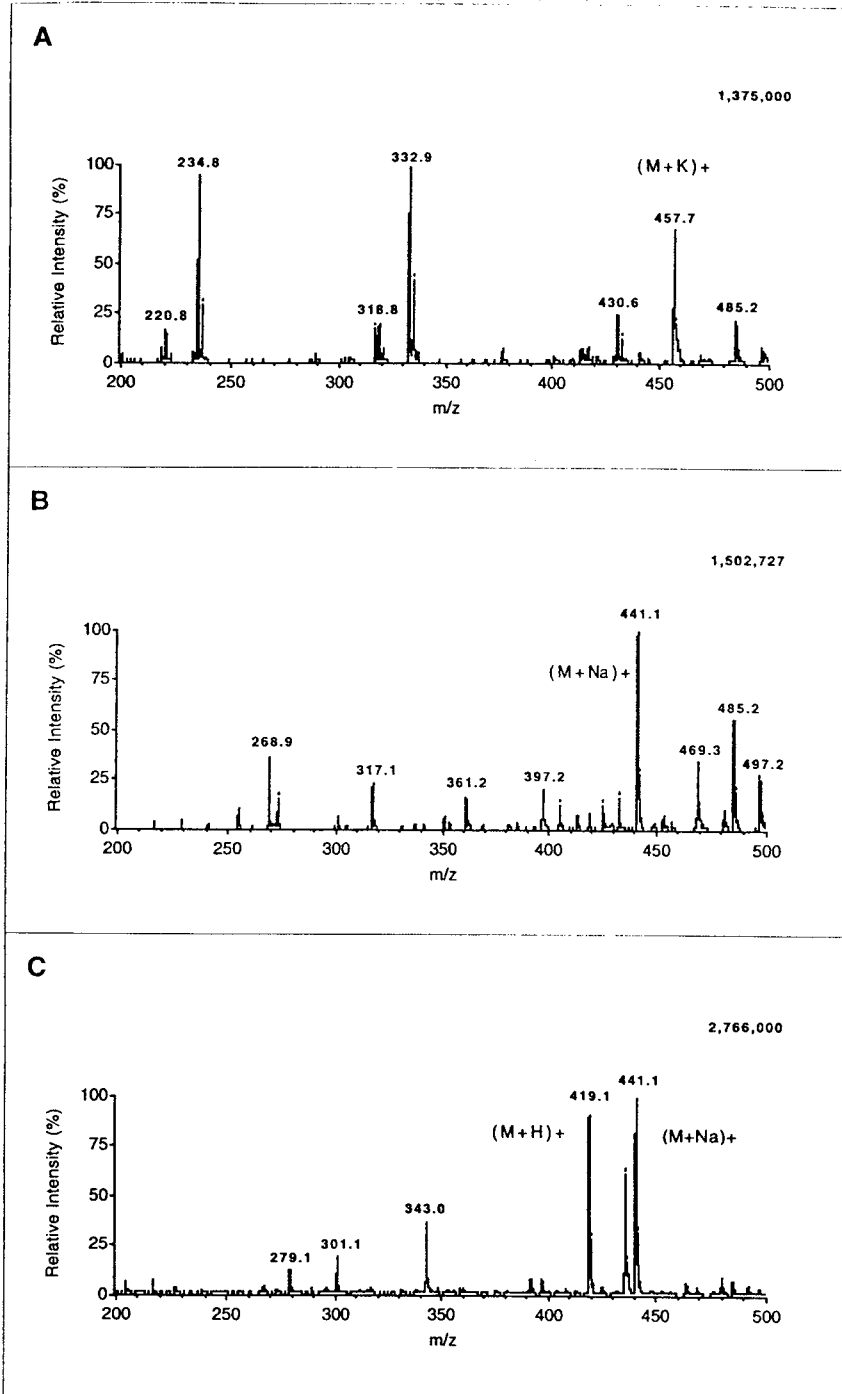


Fig. 2. Mass spectra of nimodipine (2 mg/l constant infusion) dissolved in ethanol-*n*-heptane (20:80, v/v) including 2 mM of (A) potassium acetate (B) sodium acetate or (C) 1% formic acid.

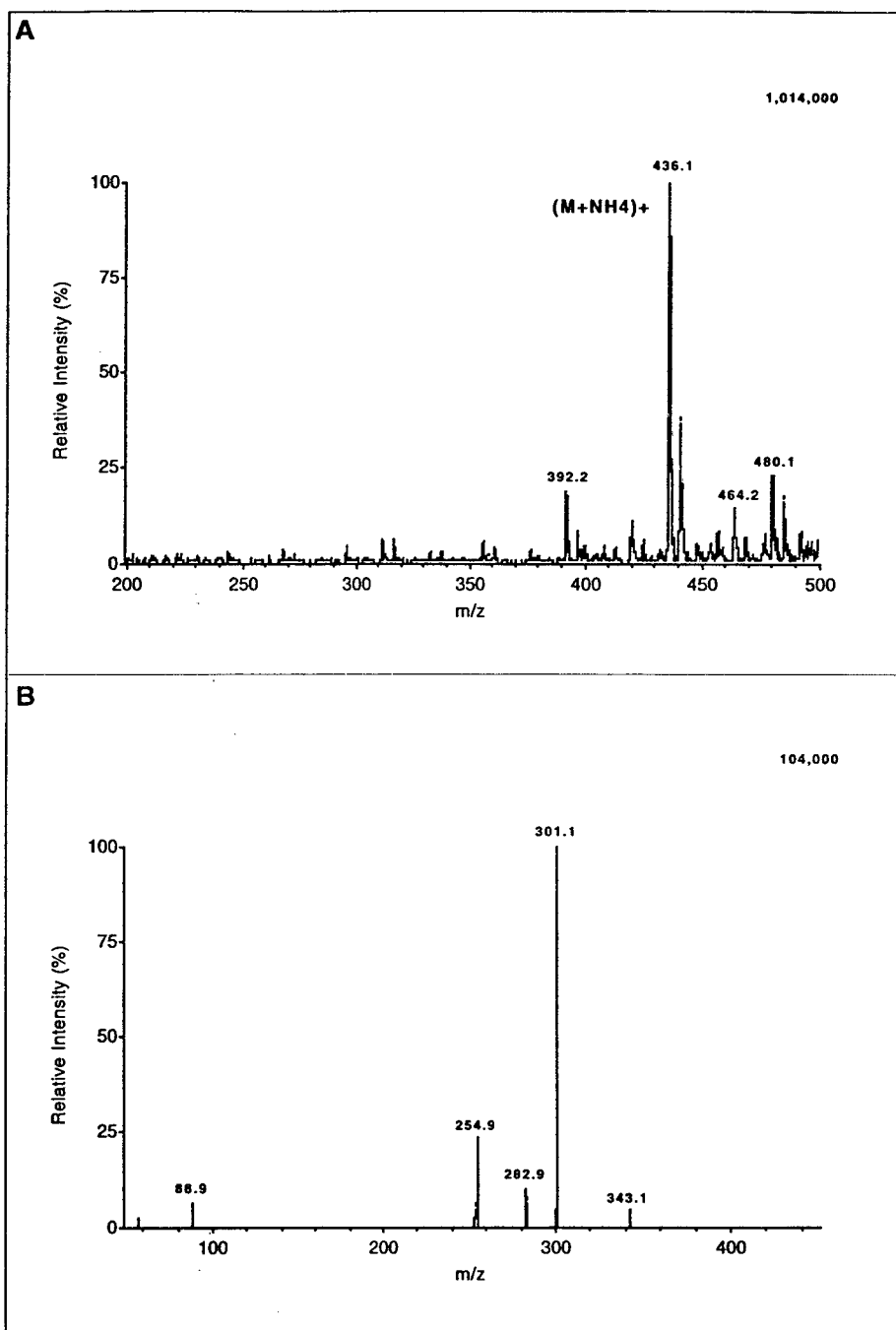


Fig. 3. Mass spectrum (A) and CID-spectrum (B) of nimodipine (1 mg/l constant infusion [dissolved in ethanol-*n*-heptane (20:80, v/v)] including 2 mM ammonium acetate).

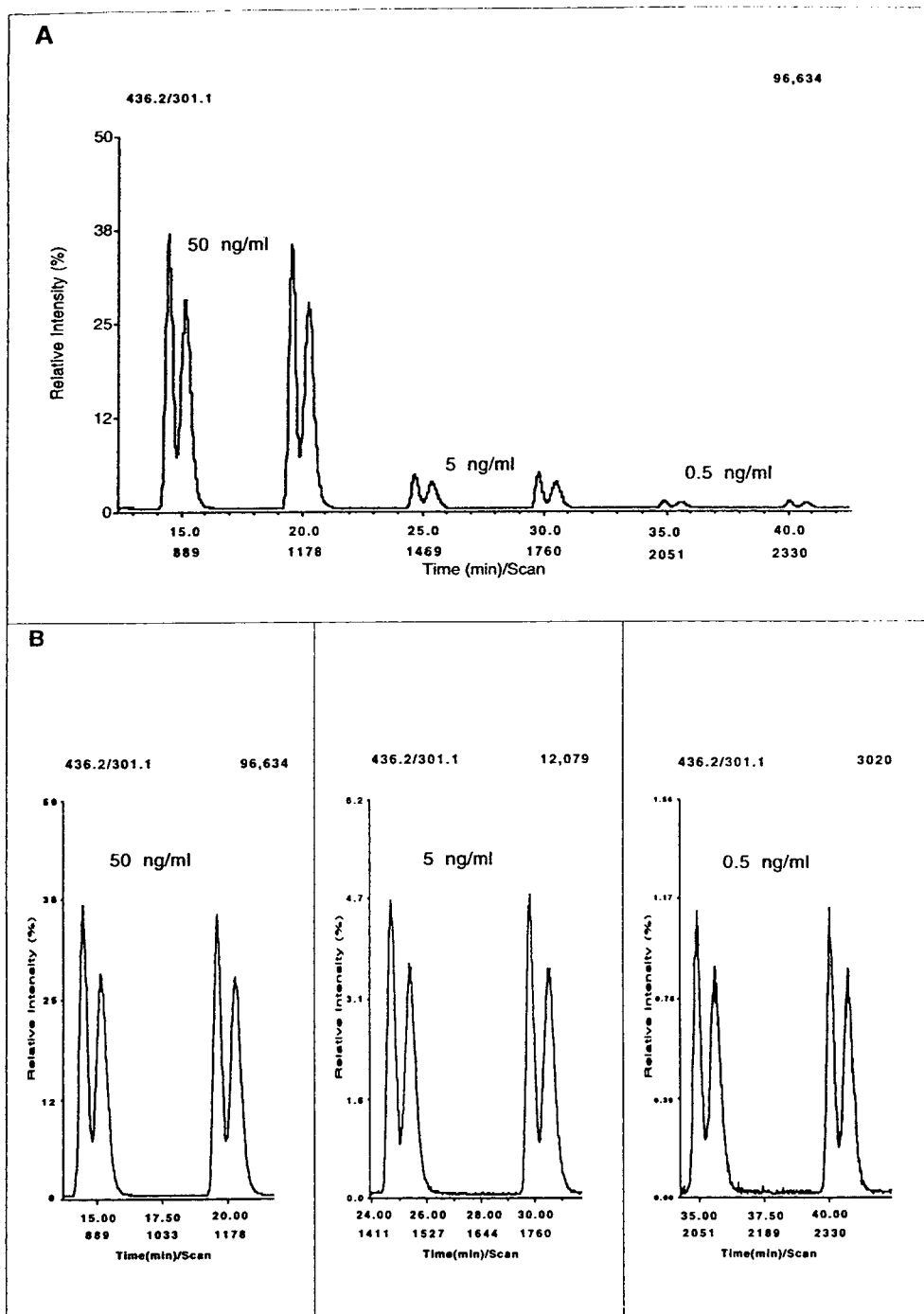


Fig. 4. (A) LC–MS–MS separation of nimodipine enantiomers (50, 5, and 0.5  $\mu\text{g/l}$  of each enantiomer, duplicate injection). (B) Normalized ion chromatograms of each concentration level.

separation efficiency compared with chromatograms from the LC–GC–MS assay, may be due to the different column size (4.6 vs. 2 mm I.D.) or due to the different supplier used.

The effluent split of approx. 1:10 used before entering the atmospheric pressure ionization chamber resulted in a flow of ca. 50  $\mu\text{l}/\text{min}$ . This flow-rate was used to keep the amount of non-aqueous solvent entering the API source as low as possible and was not due to sensitivity requirements. A separate experiment investigating the dependence of the SRM signal on the flow-rate exhibited no decrease in sensitivity at increasing flow-rates up to 250  $\mu\text{l}/\text{min}$  (highest flow tested). On the contrary, a decrease in signal could be monitored at lower flow-rates than 30  $\mu\text{l}/\text{min}$ , e.g., 10  $\mu\text{l}/\text{min}$ . This needs further investigation, but an explanation may be found in the rapid desolvation of the ions in the non-aqueous medium.

### 3.3. Method specifications

The validity of the sample pretreatment with an extraction efficiency of about 90% has been previously presented [3].

For both enantiomers, linear calibration curves could be established in the range from 0.25–75  $\mu\text{g}/\text{l}$ . Inter-assay precision and accuracy data were derived from all QC results (two validation runs and two series including unknowns,  $n=16$  each) at the defined six concentration levels. Accuracy, expressed as the deviation from the nominal value in percentage, was between  $-0.6\%$  and  $-4.9\%$  for *S*-nimodipine and between  $-0.3\%$  and  $-7.0\%$  for *R*-nimodipine. The precision (coefficient of variation CV) was between 8.2% and 13.7% for *S*-nimodipine and between 5.7% and 11.7% for *R*-nimodipine. Thus, over the whole working range an overall accuracy of  $\leq \pm 10\%$  and a precision of  $\leq 10\%$  could be attained, comparable to the LC–GC–MS method [3]. No mutual interference of the enantiomers was observed. When comparing the sum of nimodipine enantiomers with the total (racemic) concentrations determined independently with the achiral GC assay with electron-capture detection [3], good

agreement could be observed (see Fig. 5 as example): differences between both determinations were in general below 10%, only in a few cases higher up to 20%.

The limit of quantification (LOQ), i.e., the concentration level with an accuracy  $\leq 15\%$  and a precision  $\leq 20\%$ , was defined at 0.5  $\mu\text{g}/\text{l}$  for both enantiomers in an additional experiment where six replicates of this concentration level showed an accuracy of  $-13.0\%$  *S*-(-) and  $+16.8\%$  *R*-(+), respectively, and a precision of

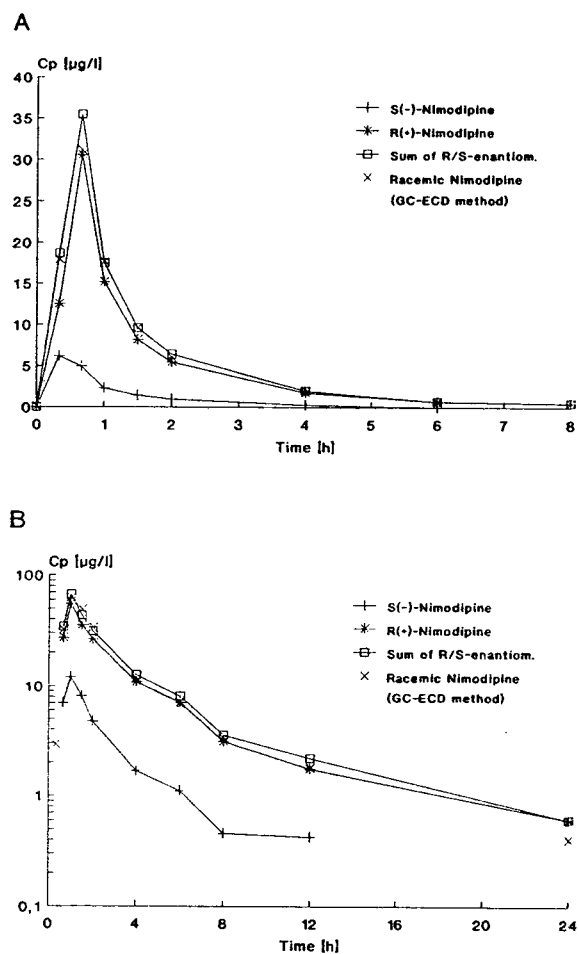


Fig. 5. Plasma concentration–time profiles of nimodipine enantiomers, their sum, and of racemic nimodipine (determined previously by an achiral GC–ECD assay). (A) after a single oral dose of 30 mg to a fasting healthy volunteer (linear scale); (B) after a single oral dose of 60 mg to a fasting healthy volunteer (semi-logarithmic scale).

14.9% and 20%, respectively. The limit of detection (LOD) was estimated at 0.25  $\mu\text{g/l}$  for each enantiomer (an even lower LOD was restricted by the  $^2\text{H}_0$  impurity from the ISTD which was observed in the blank samples in the order of ca. 0.1  $\mu\text{g/l}$ ).

### 3.4. Application

Fig. 5 shows representative plasma concentration–time data obtained from a healthy volunteer using this LC–MS–MS assay. Plasma concentrations were higher for *R*-(+)-nimodipine than for *S*-(-)-nimodipine, suggesting similar stereoselective disposition of nimodipine to that reported earlier [7].

The gain in time required for routine analysis of 150 study samples — one working week with the new LC–MS–MS assay — was considerable when compared to the four weeks needed with the established LC–GC–MS procedure. When comparing the flow charts of both assays, however, this gain in sample throughput is not unexpected since the tedious time-consuming steps of fractionation, collection of isomer fractions, and GC analysis could be omitted.

## 4. Conclusions

Based on the existing LC–GC–MS assay for determination of nimodipine enantiomers, the development of a direct enantiospecific HPLC assay with MS–MS detection via pneumatically-assisted electrospray (IonSpray) was straightforward. By the addition of suitable modifiers to the non-aqueous eluent, charged species could be produced by electrospray with sufficient sensitivity. This makes electrospray, in principal, compatible with ‘normal-phase’ separation conditions, provided that any potential hazard by using flammable eluents and the occurrence of discharge at the tip of the sprayer can be excluded.

The reported stereospecific LC–MS–MS assay is not only successful for the quantification of nimodipine in human plasma, but allows fast method development and highly specific and sensitive routine determination of enantiomers in biological matrix in general. A method transfer to other dihydropyridines where successful separations using the described chromatographic system have already been reported, e.g., nitrendipine, felodipine, nisoldipine [8–10], should be straightforward. In addition, similar chromatographic separation systems should also be amenable to MS detection via the outlined approach. Since the gain in sample throughput may be considerable, the efforts should be worth undertaking.

## Acknowledgement

The excellent technical realization of the presented work by C. Schüttler and W. Marter is gratefully acknowledged.

## References

- [1] M.S. Langley and E.M. Sorkin, *Drugs*, 37 (1989) 669.
- [2] A.N. Wadworth and D. McTavish, *Drugs Aging*, 2 (1992) 262.
- [3] W. Mück and H. Bode, *Pharmazie*, 49 (1994) 130.
- [4] C. Fischer, F. Schönberger, W. Mück, K. Heuck and M. Eichelbaum, *J. Pharm. Sci.*, 82 (1993) 244.
- [5] E. Delee, I. Jullien and L. Le Garrec, *J. Chromatogr.* 450 (1988) 191.
- [6] K.L. Duffin, J.J. Shieh and J.D. Henion, *Anal. Chem.* 63 (1991) 1781.
- [7] K. Sporckmann and M. Eichelbaum, *Naunyn Schmiedeberg's Arch. Pharmacol.*, 343 (1991) R 124.
- [8] P.A. Soons, M.C.M. Roosemalen and D.D. Breimer, *J. Chromatogr.*, 528 (1990) 343.
- [9] R. Heinig, V. Muschalek and G. Ahr, *J. Chromatogr. A*, 655 (1994) 286.
- [10] D. Zimmer and V. Muschalek, *J. Chromatogr. A*, 666 (1994) 241.





# Estimation of ranolazine and eleven Phase I metabolites in human plasma by liquid chromatography–atmospheric pressure chemical ionisation mass spectrometry with selected-ion monitoring

W.J. Herron\*, J. Eadie, A.D. Penman

*Department of Drug Metabolism and Pharmacokinetics, Quintiles Scotland Ltd. (formerly Syntex Research Centre), Heriot Watt University Research Park, Riccarton, Edinburgh EH14 4AP, UK*

## Abstract

The estimation of ranolazine, a novel piperazine derivative, and eleven of its Phase I metabolites has been undertaken by liquid chromatography–atmospheric pressure chemical ionisation mass spectrometry (LC–APCI–MS). Plasma samples, taken on day 5 of a multiple-dose study, were extracted by solid-phase extraction (SPE) and analysed, using a gradient HPLC system coupled to the APCI source of a Finnigan MAT TSO 700 mass spectrometer. Metabolites were analysed in selected-ion monitoring (SIM) mode, using an instrument control language (ICL) procedure. The LC–MS combination allowed resolution of all eleven metabolites, including four hydroxylated metabolites and five unresolved components. The results from the linear regression showed good correlation ( $r^2 > 0.980$ ) for all the metabolites. Plasma concentrations indicated that three metabolites were present at levels higher than 10% of the parent compound.

## 1. Introduction

The introduction of APCI mass spectrometers as routine, robust, and very sensitive analytical instruments has led to a much wider use of mass spectrometry in drug metabolism departments throughout the pharmaceutical industry. These instruments have been used to develop very specific and sensitive assay methods [1,2], as well as for the characterisation of drug and metabolites [3,4].

Ranolazine (RS-43285; Fig. 1) is a novel piperazine derivative that has been indicated in

the treatment of both angina and intermittent claudication [5,6]. Previous *in vitro* and *in vivo* studies had allowed the identification of the extensive metabolic pathway for ranolazine. These proposed metabolites were synthesised to

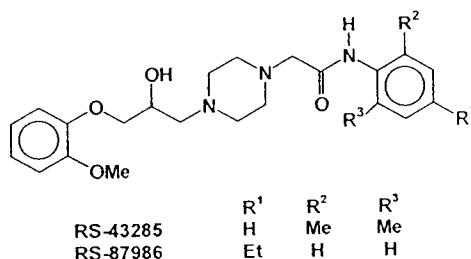


Fig. 1. Chemical structures of ranolazine and RS-87986.

\* Corresponding author.

allow confirmation of retention times and mass spectra. Plasma samples, taken on day 5, of a multi-dose clinical study were initially analysed by LC–MS to provide qualitative metabolite identification information. In this study semi-quantitation of the observed metabolites was undertaken to provide preliminary concentration data to determine which metabolites were at levels greater than 10% of parent drug for which a fully validated method would subsequently be developed.

## 2. Experimental

### 2.1. Chemicals

All chemical used were of analytical grade or better and were supplied by Fisons (Loughborough, UK), BDH (Poole, Dorset, UK) and Aldrich (Gillingham, Dorset, UK).

RS-87986 (internal standard; Fig. 1), RS-43285 and its metabolites were supplied by Recherche Syntex France (RSF) (Leuville, France), or the Institute of Organic Chemistry (IOC) (Palo Alto, CA, USA).

### 2.2. Sample extraction

Human plasma (1 ml), spiked with RS-87986 (25  $\mu$ l, 15  $\mu$ g/ml), was thoroughly mixed and loaded onto a Bond-Elut (C<sub>18</sub>, 3 ml) SPE cartridge (supplied by Crawford Scientific, Strathaven, UK.) conditioned by successively washing with methanol (3 ml), distilled water (3 ml) and sodium hydroxide (0.1 M, 0.5 ml). The plasma was allowed to elute under gravity. The SPE cartridge was washed with distilled water (2 ml), dried with positive pressure, and transferred to a clean culture tube. The absorbed components were eluted by washing the cartridge with methanol (2 ml) followed by methanolic ammonium acetate (0.1 M, 2 ml). The combined extract was evaporated to dryness under a stream of nitrogen at 40°C, and the residue reconstituted in distilled water (300  $\mu$ l) by whirl-mixing before centrifuging for 5 min at 3000

rpm. The supernatant was transferred to a 300- $\mu$ l autosampler microvial for analysis.

For the analysis of ranolazine 0.1 ml of plasma was spiked with RS-87986 (25  $\mu$ l, 15  $\mu$ g/ml) and extracted as described above.

### 2.3. Calibration curves

Calibration curves, from 20 to 1000 ng/ml, were constructed by spiking varying volumes of stock solutions (4  $\mu$ g/ml and 20  $\mu$ g/ml) containing the eleven metabolites into control human plasma (1 ml in duplicate). RS-87986 (25  $\mu$ l, 15  $\mu$ g/ml) was added and the samples extracted as described above.

A calibration curve for ranolazine, over the range 0.5–5  $\mu$ g/ml, was constructed by spiking varying volumes of a stock solution (10  $\mu$ g/ml) into control human plasma (0.1 ml in duplicate). RS-87986 (25  $\mu$ l, 15  $\mu$ g/ml) was added and the samples extracted as described above.

### 2.4. HPLC conditions

Aliquots (200  $\mu$ l) of the plasma extracts were injected using an ISS-100 autosampler (Perkin-Elmer, Beaconsfield, UK) and chromatographed on a Waters 600MS HPLC system (Waters Associates, Watford, UK) at 1 ml/min using an Ultrasphere ODS (150  $\times$  4.6 mm I.D.) HPLC column (Beckman Instruments UK) maintained at 50°C in a column oven.

For the analysis of the metabolites a gradient system was developed in order to resolve four hydroxylated metabolites. Solvent A was composed of aqueous ammonium acetate (20 mM) and trifluoroacetic acid (TFA, 0.12%) at pH 3.0, and Solvent B was methanolic ammonium acetate (20 mM) and TFA (0.12%). The HPLC gradient was linearly increased from 10 to 55% B in 30 min, then linearly from 55 to 100% B in 3 min, held at 100% B for 2 min before returning to 10% B in 1 min. The column was allowed to re-equilibrate for 4 min before injection of the next sample.

For the analysis of ranolazine an isocratic mobile phase of A–B (40:60, v/v) was used.

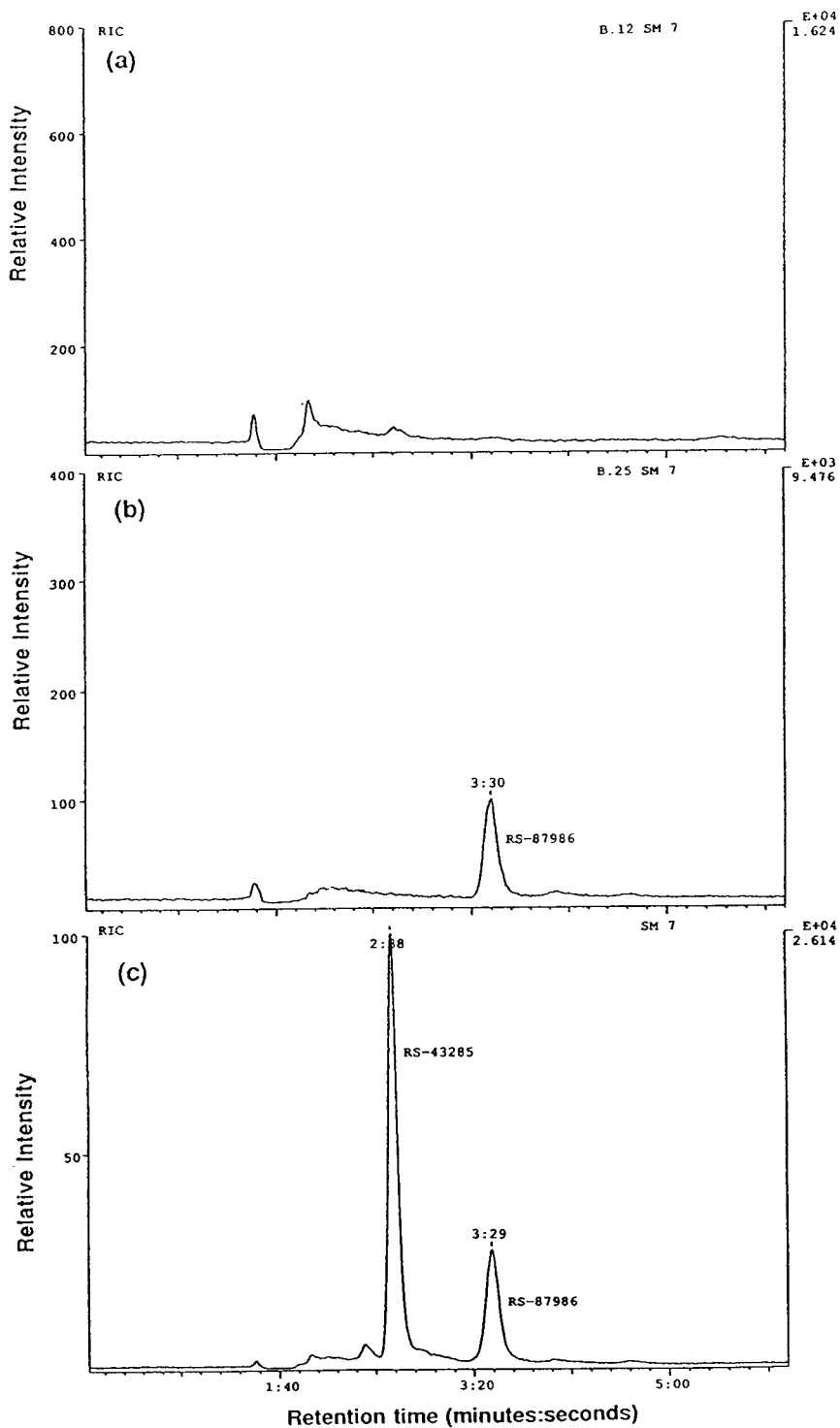


Fig. 2. SIM chromatograms for the estimation of ranolazine. (a) Control human plasma, (b) pre-dose (day 1), (c) 1 h post-dose (day 5).

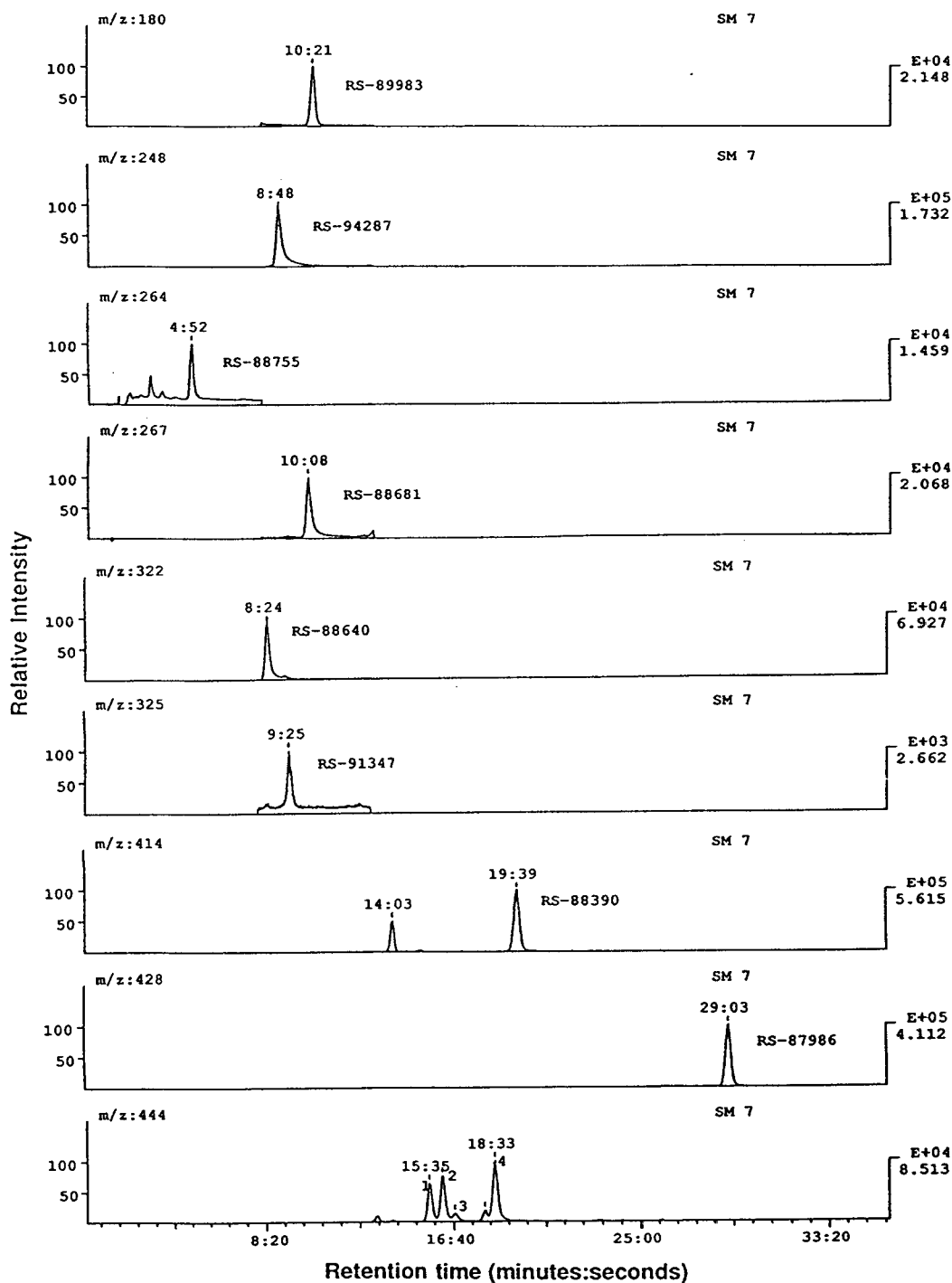


Fig. 3. SIM chromatograms for the estimation of ranolazine metabolites on day 5 (1 h post-dose). Peaks labelled 1–4 are identified as RS-88772, RS-88597, RS-88835 and RS-89961 respectively. The additional peak observed in the  $m/z$  414 trace (14:03 min:s) is a glucuronide metabolite.

### 2.5. Mass spectrometric conditions

The eluate from the HPLC column was plumbed directly into the APCI probe assembly of a Finnigan MAT APCI source which was fitted to a Finnigan MAT TSQ 700 triple quadrupole mass spectrometer (Finnigan MAT, Hemel Hempstead, UK). The HPLC flow was nebulised using  $N_2$  as both a sheath gas, at a pressure of  $3.1 \cdot 10^5$  Pa, and an auxiliary gas, at a flow-rate of 2 l/min. The APCI vapouriser and capillary heaters were held at 500°C and 250°C respectively to assist in the desolvation and declustering of the HPLC solvent. A corona discharge of 5  $\mu A$  was also applied to assist in ionisation. Capillary, tube lens and octapole voltages of respectively 40 V, 100 V and  $-3.0$  V were also applied to assist in the focusing of ions into the mass spectrometer.

Analysis in the mass spectrometer was carried out in positive ion mode with unit mass resolution. The mass spectrometer was operated in the selected-ion monitoring (SIM) mode using an ICL procedure written to allow the mass spectrometer to switch between the metabolite masses at specific retention times, and a 100-ms dwell-time for each mass was used. Ranolazine and RS-87986 have the same molecular mass ( $M_r$  427) and therefore the mass spectrometer was operated in SIM for  $m/z$  428  $[M + H]^+$  continually.

Peak areas for all components were automatically integrated using CHRO software on the TSQ 700 and peak-area ratios (area of drug or metabolite/area RS-87986) were plotted versus concentration using unweighted linear regression. From the calibration lines obtained concentrations of unknown samples were determined by interpolation.

### 3. Results

SIM chromatograms are shown for the analysis of ranolazine in Fig. 2. SIM chromatograms for the analysis of the metabolites are shown in Fig. 3 and show the HPLC separation obtained for four hydroxylated metabolites ( $m/z$  444) and the

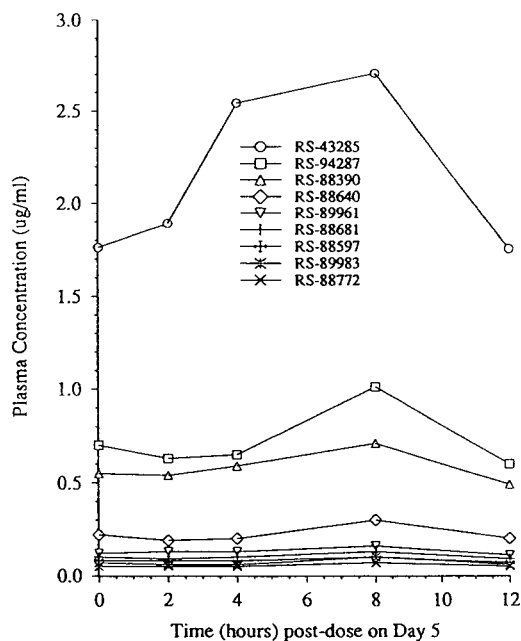


Fig. 4. Plasma concentration profiles of ranolazine and eight Phase I metabolites on day 5.

mass resolution of five co-eluting components (8:24–10:21). For the linear regression of ranolazine an  $r^2$  value of 0.996 was obtained;  $r^2$  values of between 0.980 and 0.999 were obtained for the linear regression of the metabolites. The plasma concentration profiles for ranolazine and the metabolites are shown in Fig. 4 and indicated that three of the metabolites (RS-94287, RS-88390 and RS-88640) were at levels greater than 10% of parent drug. Three of the metabolites (RS-88755, RS-88835 and RS-91347) gave levels below the limit of quantitation of this method and are not shown in Fig. 4. The plasma concentrations of ranolazine and RS-88390, obtained by this method, were compared with results previously obtained using a validated HPLC–UV method and were found to give a mean inter-assay variation of 18.5% for ranolazine and 13.1% for RS-88390.

### 4. Conclusions

The results of this experiment indicate the tremendous selectivity and specificity that can be

achieved by the use of LC–MS techniques. The quantitation, by mass resolution, of the five components with retention times between 8:24 and 10:21 (min:s) would not be possible using this HPLC system with UV detection. Likewise, the quantitation of the four hydroxylated components would not have been possible without the separation by HPLC. Excellent  $r^2$  values were also obtained for the linear regression considering the differences in the metabolite structures and the use of only one internal standard, but may also in part be due to the stability of the signal obtained by APCI. The presence of only three metabolites at levels greater than 10% of the parent drug also allows the possibility of modifying the HPLC conditions

to give a shorter run time thus increasing the sample throughput for future studies. The simplicity of the SPE methodology may also allow its transfer to automated sample processors, i.e. ASPEC.

### References

- [1] B. Kaye et al., *Biol. Mass Spectrom.*, 21 (1992) 585.
- [2] S. Pleasance et al., *Biol. Mass Spectrom.*, 21 (1992) 675.
- [3] B.M. Warrack et al., *Biol. Mass Spectrom.*, 22 (1993) 101.
- [4] J. Liu et al., *J. Chromatogr.*, 632 (1993) 45.
- [5] B. Clarke et al., *Br. J. Pharmacol.*, 109 (1993) 748.
- [6] D. Jain et al., *Eur. J. Clin. Pharmacol.*, 38 (1990) 111.



ELSEVIER

Journal of Chromatography A, 712 (1995) 61–66

JOURNAL OF  
CHROMATOGRAPHY A

# Metabolic studies of an orally active platinum anticancer drug by liquid chromatography–electrospray ionization mass spectrometry

G.K. Poon<sup>a,\*</sup>, F.I. Raynaud<sup>a</sup>, P. Mistry<sup>a</sup>, D.E. Odell<sup>a</sup>, L.R. Kelland<sup>a</sup>,  
K.R. Harrap<sup>a</sup>, C.F.J. Barnard<sup>b</sup>, B.A. Murrer<sup>b</sup>

<sup>a</sup>CRC Centre for Cancer Therapeutics, Institute of Cancer Research, Sutton, Surrey SM2 5NG, UK

<sup>b</sup>Johnson Matthey Technology Centre, Sonning Common, Reading, UK

## Abstract

Bis(acetato)amminedichloro(cyclohexylamine) platinum(IV) (JM216) is a new orally administered platinum complex with antitumor properties, and is currently undergoing phase II clinical trials. When JM216 was incubated with human plasma ultrafiltrate, 93% of the platinum species were protein-bound and 7% were unbound. The unbound platinum complexes in the ultrafiltrates of human plasma were analysed using a liquid chromatography–electrospray ionization–mass spectrometry (LC–ESI–MS) method. Apart from the parent drug, four metabolites were identified and characterised. These include JM118 [amminedichloro(cyclohexylamine) platinum(II)], JM383 [bis(acetato)ammine(cyclohexylamine)dihydroxo platinum(IV)] and the two isomers JM559 and JM518 [bis(acetato)amminechloro(cyclohexylamine) hydroxo platinum(IV)]. Their elemental compositions were determined by accurate mass measurement during the LC analysis, to confirm their identities. Quantitation of these metabolites by off-line LC atomic absorption spectroscopy demonstrated that JM118 is the major metabolite in plasma from patients receiving JM216 treatment.

## 1. Introduction

Bis (acetato) amminedichloro (cyclohexylamine) platinum(IV) (JM216) [1] is a mixed amine platinum(IV) dicarboxylate complex and an analogue of cisplatin [*cis*-diamminedichloro platinum(II)] [2] designed for oral administration. In preclinical studies the complex exhibited cytotoxic activity against a panel of human ovarian and testicular carcinoma cell lines including those with acquired resistance to cisplatin [3,4]. In addition, *in vivo* antitumor activity after oral dosing was reported to be far superior to that

observed for cisplatin, carboplatin or tetraplatin in the cisplatin-sensitive murine ADJ/PC6 plasmacytoma tumor model [3]. JM216 is currently undergoing phase II clinical trials for the treatment of a variety of tumors, particularly ovarian and lung. The present study investigated the *in vitro* biotransformation of JM216 by incubating the drug with human plasma. Identification of metabolites was carried out by comparing chromatograms and mass spectra of metabolites with those of synthesized authentic standards using LC–ESI–MS. The high-resolution magnetic sector mass spectrometer used was fitted with an atmospheric pressure ionization (API) source which could accommodate a high LC flow-rate

\* Corresponding author.

(600  $\mu\text{l}/\text{min}$ ). Simultaneous on-line LC–ESI–MS and accurate mass measurements on the platinum complexes provided the elemental compositions of these compounds, as required for verification of the structures of the metabolites. Quantitative analysis of JM216 and its metabolites was conducted by off-line LC–flameless atomic absorption spectroscopy (LC–AAS), the most commonly used analytical technique for quantifying platinum complexes [5].

## 2. Experimental

### 2.1. Reagents

JM216, JM118, JM383, JM518, JM559 were synthesized and provided by Johnson Matthey Technology Centre. HPLC grade solvents were purchased from Merck (Darmstadt, Germany) and Romil Chemicals (Cambridgeshire, UK).

### 2.2. Preparation of human plasma ultrafiltrate

Pre-treatment, 3-h post-treatment plasma obtained from patients receiving JM216 (an oral single dose of 700 mg/m<sup>2</sup>) or control human plasma (4 ml) was incubated with JM216 (120  $\mu\text{M}$ ) in darkness for 1 h at 37°C and was ultrafiltered at 1900 g at 4°C using an Amicon Centrifree Micropartition System, molecular mass cut-off 10 000 (Silverstone, Gloucester, UK). Aliquots of the samples [50  $\mu\text{l}$  for the human plasma ultrafiltrate (HPUF) and 100  $\mu\text{l}$  for the patient plasma ultrafiltrate] were analysed by LC–MS. An incubation containing JM216 and saline at pH 7 was used as control.

### 2.3. On-line LC–MS analysis

The HPLC system consisted of a LDC MS 4100 pump (Thermo Separation, Riviera Beach, FL, USA) and a 250  $\times$  4.6 mm PLRP-S polymer column (Polymer Laboratories, Shropshire, UK) operated at 600  $\mu\text{l}/\text{min}$ . The mobile phase was water (A) and methanol (B) and the sample was eluted using a linear gradient of 30–95% B in 30 min.

MS was performed on a Finnigan MAT 900 magnetic sector mass spectrometer equipped with an ESI source (Bremen, Germany). The spray voltage was set to 3 kV and the heated capillary temperature was maintained at 250°C. The instrument was optimized in the positive ion mode by constantly infusing (via a syringe pump) a 4 pmol/ $\mu\text{l}$  solution of gramicidin S. Ion detection was in the centroid mode with an array-type focal plane detector (PATRIC, position and time resolved ion counter). Data was acquired over the mass range  $m/z$  200–700 at a resolving power of 1200 (full width at half height) during normal acquisition. During the accurate mass measurement, the resolving power of the instrument was adjusted to approximately 4000. Polypropylene glycol (PPG 425, 10 pmol/ $\mu\text{l}$ ) dissolved in water–methanol (1:1, v/v) was chosen as the reference compound. The solution was infused into the mass spectrometer via the sheath liquid inlet of the ESI source at 5  $\mu\text{l}/\text{min}$  during the LC analysis. The scan range was  $m/z$  410–530 in 2.5 s. Tandem mass spectrometry was performed on a Finnigan MAT TSQ 700 triple quadrupole mass spectrometer operated with an ESI source (San Jose, CA, USA). Argon was used as the collision gas, at a pressure of 40 kPa and the collision energy was maintained at –30 eV. All the data acquisition analysis was controlled by a DEC data system with Finnigan ICIS and ICL software.

### 2.4. Off-line LC–AA analysis

LC analyses were performed using a Waters Model 510 pump (Millipore, Herts., UK) and a PLRP-S column at 600  $\mu\text{l}/\text{min}$  flow-rate. Plasma ultrafiltrates (50  $\mu\text{l}$ ) were analysed and the eluent was collected by a LKB fraction collector at 0.2-min intervals. The platinum absolute levels were determined on a Perkin-Elmer Model 1100B atomic absorption spectrophotometer (Ueberlingen, Germany) equipped with a graphite furnace Model 700. Samples (50  $\mu\text{l}$ ) were injected at 60°C and the absorbance of the atomized platinum was measured at 266 nm. Calibration was achieved by injecting standards at concentrations of 100, 50, 20, 10 and 5 ng/ml.



Quality controls were added in each run of 30 unknown samples at the level of 50 and 20 ng/ml, and 15% deviation from nominal concentration was allowed. The lower limit of quantification is 3 ng/ml (20% C.V.).

### 3. Results and discussion

Once in circulation, platinum complexes are taken up by the tissue. They then either bind irreversibly to the plasma protein, or undergo metabolism and excretion. Most platinum complexes, including cisplatin, are heavily bound to protein in the plasma, subsequently losing their cytotoxicity and therapeutic values [6–8]. On the other hand, the ultrafiltrable fraction contains the intact drug and metabolites. These non-protein-bound species react with DNA or intracellular enzymes, and are responsible for the antitumor and toxic properties of the drug [9]. When the ultrafiltrates were analysed by AAS, 93% of the platinum species (including JM216) was bound and only 7% was present in the ultrafiltrate as “free” components.

When the human plasma ultrafiltrate was analysed by LC–ESI–MS, the reconstructed ion chromatograms indicated that the sample contained four metabolites (Fig. 1). A typical ESI mass spectrum of platinum complex displays a characteristic cluster pattern [10] due to the platinum ( $^{194}\text{Pt}$ ,  $^{195}\text{Pt}$ ,  $^{196}\text{Pt}$ ) and chloride ion ( $^{35}\text{Cl}$  and  $^{37}\text{Cl}$ ) isotopes, and is usually dominated by a sodiated molecule as the base peak with minimal fragmentation. The parent drug which eluted at 29 min showed a pseudo-molecular ion at  $m/z$  521 ( $[\text{M} + \text{Na}]^+$ ). Two less intense signals at  $m/z$  499 and 537 were observed, which represented the  $[\text{M} + \text{H}]^+$  and  $[\text{M} + \text{K}]^+$  ions, respectively (Fig. 2a). Accurate mass measurement indicated that the sodiated adduct of JM216 had a molecular mass of 521.0473 (calculated molecular mass of  $^{194}\text{Pt}^{35}\text{Cl}_2\text{C}_{10}\text{H}_{22}\text{N}_2\text{O}_4\text{Na}$  is 521.0482). The component at 27:12 min was an endogenous constituent and did not contain platinum.

The retention time (19:18 min) and the mass spectrum of metabolite I (at  $m/z$  403,  $[\text{M} +$

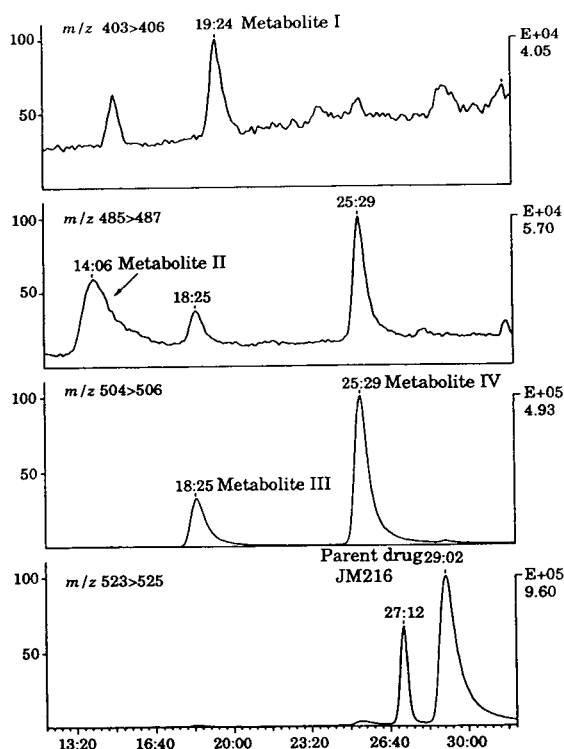


Fig. 1. Reconstructed ion chromatograms of HPUF after incubation of plasma with JM216 and analysed by LC–ESI–MS. Metabolite I: JM118; metabolite II: JM383; metabolites III and IV: two isomers of JM518; and the parent drug JM216. Each peak is labelled with the scan time. The two peaks at 18:25 and 25:29 min with  $m/z$  485 > 487 were derived from metabolites III and IV.

$\text{Na}]^+$ ), resembled the results obtained from the authentic reference material [amminedichloro(cyclohexylamine) platinum(II)] (JM118) (Fig. 2b). The less intense cluster at  $m/z$  419 corresponds to the  $[\text{M} + \text{K}]^+$  ion. Further confirmation was achieved by comparing the accurate mass data of the  $[\text{M} + \text{K}]^+$  ion at  $m/z$  418.9962 with the calculated accurate mass data ( $^{194}\text{Pt}^{35}\text{Cl}_2\text{C}_6\text{H}_{16}\text{N}_2\text{K}$  is 418.9956). JM118 is a Pt(II) complex, it reflects the reduction of JM216 via loss of the two axial carboxylate groups. Metabolic conversion of Pt(IV) complexes to Pt(II) complexes is well documented (i.e. iprop-latin and tetraplatin) [11–14]. Pt(II) complexes such as cisplatin readily react with DNA, causing a variety of intra-strand and a small proportion

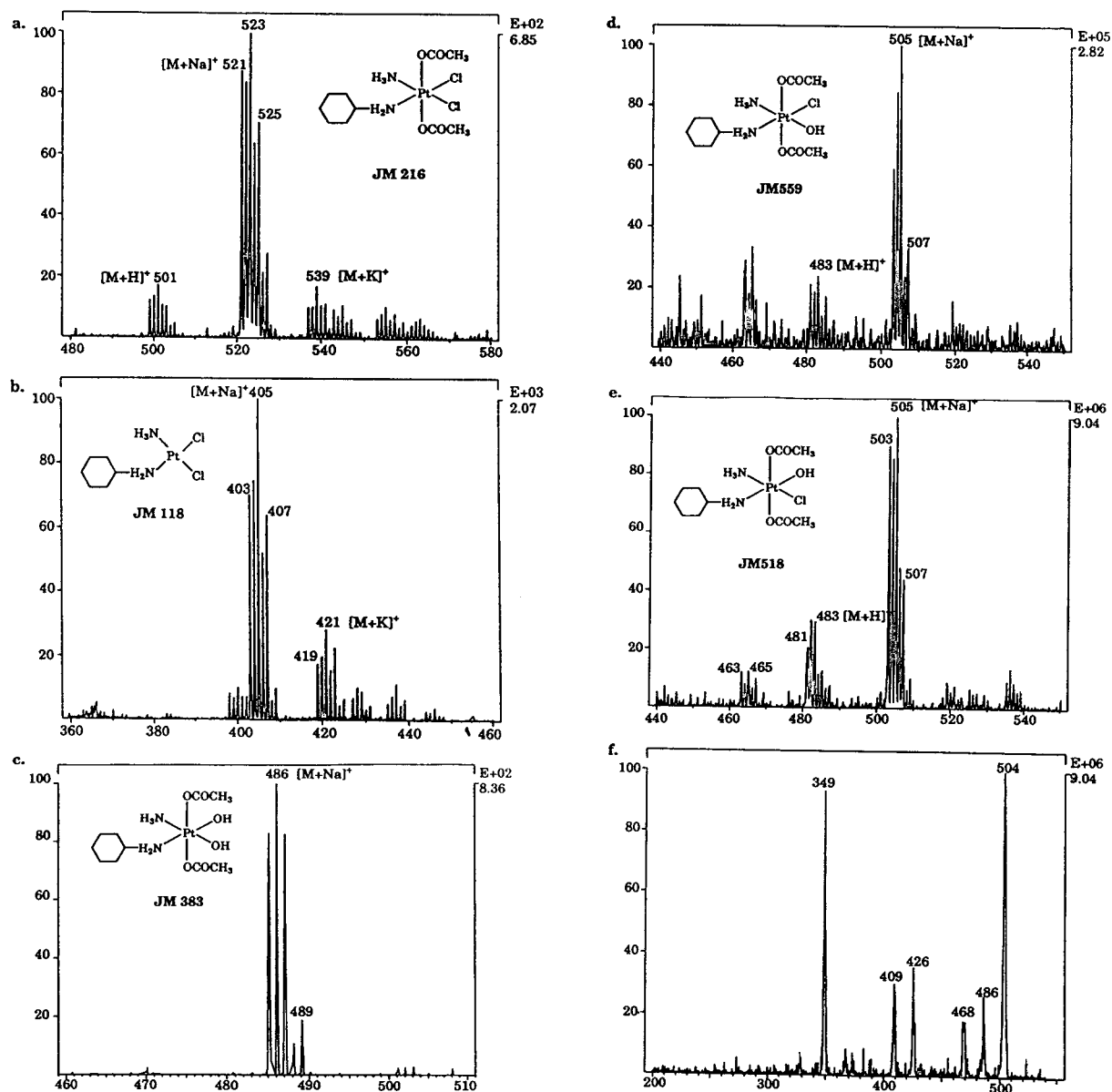


Fig. 2. ESI mass spectra of the metabolites: (a) parent JM216; (b) JM118; (c) JM383; (d) and (e) the two isomers of JM518; (f) product-ion mass spectrum of the metabolite JM518.

of inter-strand crosslinks and cytotoxicity [15]. When JM118 was examined against six ovarian carcinoma cell lines, it was approximately 4.8-fold more potent than cisplatin [16]. Moreover, JM118 has been shown to circumvent acquired

resistance in both a human ovarian and a human cervical carcinoma cell line [17,18].

The mass spectrum of metabolite II (Fig. 2c) is consistent with the sodiated pattern of bis(acetato)amine(cyclohexylamine)dihydroxo

platinum(IV), JM383. The mass spectrum showed a different isotopic cluster ion to that of JM118 or JM216, which strongly suggested that the two chloride ions of JM216 had been displaced. The LC elution time (14:06 min) and the accurate mass measurement of the metabolite were identical to those obtained from an authentic sample of JM 383 (calculated for  $^{194}\text{PtC}_{10}\text{H}_{24}\text{N}_2\text{O}_6\text{Na}$  is 485.1160; measured: 485.1142). The two components observed at 18:25 min and 25:29 min with  $m/z$  485–487 were derived from metabolites III and IV.

The mass spectra of metabolites III and IV ( $t_R = 18:25$  and  $25:30$  min) primarily gave pseudomolecular ion at  $m/z$  503, coinciding with the sodiated molecule of bis(acetato)amminechloro(cyclohexylamine)hydroxo platinum(IV) (Fig. 2d,e). The elution time of metabolite IV was identical to that of JM518, and metabolite III is thus tentatively identified as its isomer JM559. Additional evidence confirming the structural assignment of these two isomers was elicited from tandem mass spectrometry. A collision-induced dissociation mass spectrum of  $m/z$  505 gave fragment ions at  $m/z$  486 ( $[\text{M} + \text{Na} - \text{H}_2\text{O}]^+$ ),  $m/z$  468 ( $[\text{M} + \text{Na} - \text{HCl}]^+$ ) and  $m/z$  426 ( $[\text{M} + \text{Na} - \text{H}_2\text{O} - \text{CH}_3\text{COOH}]^+$ ). Elimination of the entire ( $[\text{M} + \text{Na} - \text{CH}_3\text{COOH} - \text{Cl}]^+$ ) moiety gave rise to the abundant peaks at  $m/z$  409; and the base peak at  $m/z$  349 was attributed to loss of ( $[\text{M} + \text{Na} - 2\text{CH}_3\text{COOH} - \text{Cl}]^+$ ) (Fig. 2f). The measured molecular mass of the JM518 sodiated adduct is 503.0825, in good agreement with the calculated value ( $^{194}\text{Pt}^{35}\text{ClC}_{10}\text{H}_{23}\text{N}_2\text{O}_5\text{Na}$ : 503.0821). However, the signal intensity of metabolite III was insufficient for accurate mass measurement.

Displacement of the chloride ligand by a hydroxy-group is an established metabolic route of platinum complexes, and the resulting hydroxo group forms a stable bond with platinum with variable antitumor activities [19]. The cytotoxicity of JM518 is similar to that of JM216 against the ovarian cell lines, while JM383 is less cytotoxic (F. Raynaud, pers. commun.).

Off-line LC–AAS was used to determine the level of platinum complexes in the ultrafiltrates. JM518 and JM383 were the major metabolites

observed and represented approximately 1.15 and 1.18  $\mu\text{g}/\text{ml}$  of plasma, respectively, whereas JM118, JM216 and the isomer of JM518 were present at 0.66, 1.15 and 0.238  $\mu\text{g}/\text{ml}$  of plasma, respectively. Some unidentified components eluted in the solvent front were probably glutathione or methionine adducts and accounted for <10% of the unbound platinum complexes. Only trace amounts of JM118 and JM383 were detected in the control incubation.

Fig. 3 represents the selected-ion monitoring chromatograms of the patient plasma ultrafiltrate when examined by LC–ESI–MS on a quadrupole mass spectrometer. Two metabolites were detected, i.e. JM383 and JM118. As indicated by off-line LC–AAS, JM118 was the major metabolite in the patient plasma ultrafiltrate, and the sample contained only trace amounts of unchanged parent drug (<2%). Neither JM518 nor its isomer were detected in the post-treat-

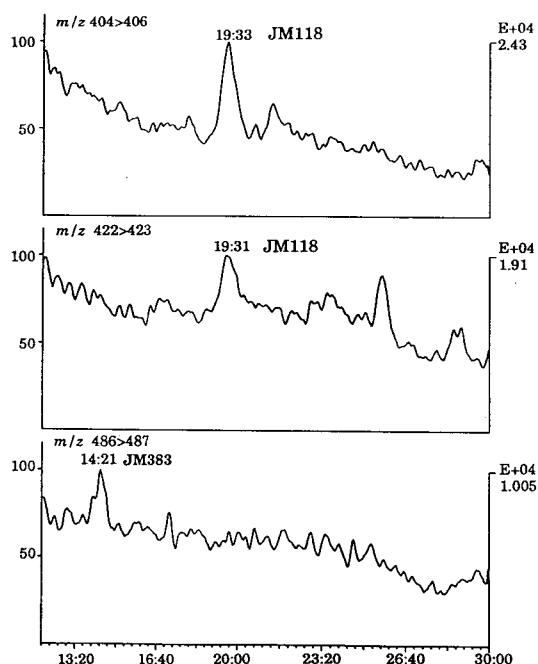


Fig. 3. Selected-ion chromatograms of the plasma ultrafiltrate obtained from patients treated with JM216 and analysed by LC–ESI–MS showing the presence of metabolite I, JM118, and metabolite II, JM383.

ment plasma sample. No platinum complexes were observed in the patient pre-treatment plasma ultrafiltrate sample.

#### 4. Conclusions

Information on the biotransformation products from patients treated with platinum complexes has previously been limited by the lack of analytical techniques capable of determining these species at a sufficiently low level. In the present study LC–ESI–MS with accurate mass measurement and tandem mass spectrometry has been successfully applied to the study of platinum complexes, affording unambiguous identification of four metabolites of JM216 in human plasma ultrafiltrate, JM118 and JM383 in patient plasma ultrafiltrate.

#### Acknowledgements

This work was supported by the Cancer Research Campaign, UK. We thank Dr. H. Muenster of Finnigan MAT, Bremen for providing the LC–MS analysis of our samples on the MAT 900 mass spectrometer.

#### References

- [1] M.J. McKeage, P. Mistry, J. Ward, F.E. Boxall, S. Loh, C. O'Neill, P. Ellis, L.R. Kelland, S.E. Morgan, B. Murrer, P. Santabarbara, K.R. Harrap and I.R. Judson, *Clin. Pharmacol. (Proceedings of ASCO)*, 12 (1993) A230.
- [2] B. Rosenberg, L. van Camp, J.E. Trosko and V.H. Mansour, *Nature (London)*, 222 (1969) 385.
- [3] L.R. Kelland, G. Abel, M.J. McKeage, J. Jones, P.M. Goddard, M. Valenti, B.A. Murrer and K.R. Harrap, *Cancer Res.*, 53 (1993) 2581.
- [4] L.R. Kelland, *Drugs of the Future*, 18 (1993) 551.
- [5] W.A. de Waal, F.J.M. Maessen and J.C. Kraak, *J. Chromatogr.*, 407 (1987) 253.
- [6] H. Calvert, I. Judson and W.I.M. van der Vijgh, *Cancer Surv.*, 17 (1993) 189.
- [7] F.F. Farris, F.G. King, R.L. Dedrick and C.L. Litterst, *J. Pharm. Biopharm.*, 13 (1985) 13.
- [8] E. Heinen, R. Basdeer and L.C. DeSaive, *Eur. J. Cancer*, 14 (1978) 1005.
- [9] J.E. Melvik, J.M. Dornish and E.O. Pettersen, *Br. J. Cancer*, 24 (1992) 73.
- [10] G.K. Poon, P. Mistry and S. Lewis, *Biol. Mass Spectrom.*, 20 (1991) 687.
- [11] L. Pendyala, J.R. Walsh, M.M. Huq, A.V. Arakali, J.W. Cowens and P.J. Creaven, *Cancer Chemother. Pharmacol.*, 25 (1989) 15.
- [12] L. Pendyala, B.S. Krishnan, J.R. Walsh, A.V. Arakali, J.W. Cowens and P.J. Creaven, *Cancer Chemother. Pharmacol.*, 25 (1989) 10.
- [13] G.R. Gibbons, S. Wyrick and S.G. Chaney, *Cancer Res.*, 49 (1989) 1402.
- [14] S.G. Chaney, G.R. Gibbons, S.D. Wyrick and P. Podhasky, *Cancer Res.*, 51 (1991) 969.
- [15] A.L. Pinto and S.J. Lippard, *Biochim. Biophys. Acta*, 780 (1985) 167.
- [16] L.R. Kelland, *Crit. Rev. Oncol. Hematol.*, 15 (1993) 191.
- [17] S.Y. Loh, P. Mistry, L.R. Kelland, G. Abel and K.R. Harrap, *Br. J. Cancer*, 66 (1992) 1109.
- [18] K.J. Mellish, L.R. Kelland and K.R. Harrap, *Br. J. Cancer*, 68 (1993) 240.
- [19] T. Yamashita, J. Hirose, M. Noji, R. Saito, H. Tomida and Y. Kidani, *Biol. Pharm. Bull.*, 16 (1993) 1014.

## Rapid analysis of $\beta$ -agonists in urine by thermospray tandem mass spectrometry

J.A. van Rhijn<sup>a,\*</sup>, M. O’Keeffe<sup>b</sup>, H.H. Heskamp<sup>a</sup>, S. Collins<sup>b,1</sup>

<sup>a</sup>State Institute for Quality Control of Agricultural Products (RIKILT-DLO), Bornsesteeg 45, 6708 PD Wageningen, Netherlands

<sup>b</sup>National Food Centre, Dunsinea, Castleknock, Dublin 15, Ireland

---

### Abstract

A method is described for the analysis of  $\beta$ -agonists in urine of cattle. The method uses solid-phase extraction (SPE), followed by analysis of the resulting extract by flow injection thermospray tandem mass spectrometry (TSP-MS-MS). Sample preparation is performed using a mixed-bed SPE procedure using a sorbent having both hydrophobic and ionic properties. MS-MS analysis following thermospray ionization, is performed in single-reaction monitoring parent mode. In that way isotope dilution can be used for quantitation of clenbuterol. Data are presented on precision and accuracy for clenbuterol and related compounds. Furthermore, data acquisition was performed in full-scan neutral loss mode to indicate the suitability of flow injection analysis (FIA)-TSP-MS-MS for exploratory analysis. Detection of  $\beta$ -agonists in this mode is based on the presence of the *N-tert.*-butyl- $\beta$ -ethanolamino moiety and, in that respect, detection of known as well as unknown compounds having this moiety will take place. This feature is exemplified by the analysis of samples containing several compounds.

---

### 1. Introduction

In the EC the use of  $\beta$ -agonists as growth promoting agents in the fattening of animals for human consumption is banned. Nevertheless these compounds are frequently found in the urine of cattle and analysis for the purpose of regulatory control is carried out in most, if not all, countries. Besides regulatory control, there is a growing interest in methods suitable for “real-time” analysis to perform process control. Within the FLAIR (Food-Linked Agro-Industrial Research) Concerted Action nr. 8 this subject was studied extensively and part of the

presented work was carried out within the framework of this EC project.

Furthermore, an additional analytical problem is the use of slightly modified compounds for growth promotion. These compounds are usually not detected whenever a target-compound approach is applied.

For regulatory control, the analysis is usually carried out using GC-MS in the multiple ion detection (MID) mode [1,2]. Although a very effective technique, it has three major drawbacks: the compounds are targeted, so related compounds will not be detected, derivatization is usually necessary and this may impart unwanted selectivity and variability and, furthermore, the procedure typically takes two days to carry out.

Whenever the results of analysis should be

---

\* Corresponding author.

<sup>1</sup> Author deceased.

available on a short term, as for “real-time” analysis, GC–MS methods generally are not very suitable. In that case application of LC–MS–MS techniques may offer better performance.

We present here a flow injection (FIA)–TSP–MS–MS method that may be used in either of two ways: (a) a method for semi-quantitative target-compound analysis that is suitable for very rapid analysis of residues of  $\beta$ -agonists and (b) a method for rapid qualitative group-specific analysis of nanogram amounts of known as well as unknown  $\beta$ -agonists.

## 2. Experimental

### 2.1. Materials and instrumentation

All reagents used were of analytical grade. The absence of  $\beta$ -agonists in the blank urine used for spiking experiments was demonstrated using a method based on GC–MS with a limit of detection of 0.2 ng/ml [1].

Clenbuterol- $d_6$ , the analogue of clenbuterol where six protons at the *tert.*-butyl moiety are substituted with six deuterons, was used as an internal standard, allowing quantitation by isotope dilution.

Sample preparation was performed using XtrackT columns XRDAF515 (World Wide Monitoring, Bristol, PA, USA) containing 500 mg of a sorbent having ionic and hydrophobic properties. The clean-up procedure was adapted from the procedure published by Montrade et al. [3]. In brief, samples are hydrolyzed using glucuronidase/arylsulfatase from *Helix pomatia* at pH 4.8, using acetate buffer for pH adjustment. Following hydrolysis, the pH is adjusted to 6.0 using 0.1 M phosphate buffer and the extract is applied to a column conditioned with 3 ml each of methanol, water and 0.1 M phosphate buffer. The column is washed with 0.1 M phosphate buffer and the analytes are eluted with methanol containing 3% concentrated ammonium hydroxide.

The analysis is carried out using a Finnigan MAT TSQ70 (San Jose, CA, USA) mass spec-

trometer equipped with a thermospray II interface. The interface is operated at 200°C block temperature and 90°C vaporizer temperature. The repeller was at 80 V, no discharge ionization was used. Argon was used as collision gas at a pressure reading of 1.2 mTorr and a collision offset of –13 eV was applied. The carrier eluent consisted of 30% methanol in water with an overall concentration of 0.05 M ammonium acetate. The solvent was pumped at a flow-rate of 1.0 ml/min by a Gilson 305 pump (Villiers-le-Bel, France) equipped with an additional pulse damper. Aliquots of 50  $\mu$ l were injected directly into the carrier eluent by means of a Gilson 231-401 autosampler.

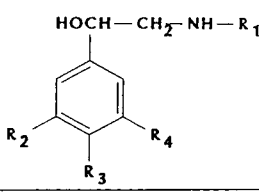
### 2.2. Data acquisition

To perform semi-quantitative analysis, a procedure for single reaction monitoring (SRM) in parent mode was used, monitoring the loss of water ( $M_r$  18) and methylpropene ( $M_r$  56) from the molecular ions. For cimaterol and clenbuterol- $d_6$  corresponding losses were monitored (Table 1). By applying parent mode data acquisition, the data system will record the masses of the precursor ions rather than the masses of the product ions. In this way the use of clenbuterol- $d_6$  as an internal standard becomes possible regardless of the fact that the mass of the product ion monitored is the same as for unlabelled clenbuterol.

Urine samples were spiked with five  $\beta$ -agonists (cimaterol, clenbuterol, terbutaline, mabuterol and salbutamol) at 1, 2 and 5 ng/ml, respectively. Aliquots of 5 ml of urine each from each spiking level were analyzed in triplicate. Following clean-up, to each extract 15 ng of clenbuterol- $d_6$ , corresponding to 3 ng/ml in the urine, was added as an internal standard. The extracts were evaporated to dryness and redissolved in 0.50 ml of carrier eluent. Subsequently the extracts were analyzed using FIA–TSP–MS–MS in SRM parent mode. Aliquots of 50  $\mu$ l, corresponding to 0.5 ml of urine, were injected in duplicate.

To perform group-specific qualitative analysis, data acquisition is performed in full-scan neutral

Table 1  
Molecular structure and SRM data for the investigated analytes

Name					SRM
	R <sub>1</sub>	R <sub>2</sub>	R <sub>3</sub>	R <sub>4</sub>	
Clenbuterol (CLEN)	C(CH <sub>3</sub> ) <sub>3</sub>	Cl	NH <sub>2</sub>	Cl	277 → 203
Clenbuterol-d <sub>6</sub> (CLEN-d <sub>6</sub> )	C(C <sup>2</sup> H <sub>3</sub> ) <sub>2</sub> CH <sub>3</sub>	Cl	NH <sub>2</sub>	Cl	283 → 203
Mabuterol (MAB)	C(CH <sub>3</sub> ) <sub>3</sub>	Cl	NH <sub>2</sub>	CF <sub>3</sub>	311 → 237
Terbutaline (TER)	C(CH <sub>3</sub> ) <sub>3</sub>	OH	H	OH	226 → 152
Salbutamol (SAL)	C(CH <sub>3</sub> ) <sub>3</sub>	CH <sub>2</sub> OH	OH	H	240 → 166
Cimaterol (CIM)	CH(CH <sub>3</sub> ) <sub>2</sub>	CN	NH <sub>2</sub>	H	220 → 160

loss mode. The scanning range of the first quadrupole is from 200 to 370 amu at one scan per second. Consequently the scan range of the second quadrupole is from 126 to 296 amu.

### 3. Results and discussion

#### 3.1. Semi-quantitative determination

Fig. 1 shows a typical result for the analysis of urine samples spiked at 1 ng/ml. Table 2 presents the corresponding quantitative data of the three spiking levels tested. From Fig. 1 it is clear that detection of all analytes except salbutamol is readily performed at 1 ng/ml level with sufficient signal-to-noise ratio. For salbutamol, signal-to-noise ratio is low and, although this compound is detected, the limit of detection (LOD) is equal to 1 ng/ml. For the other compounds, based on signal-to-noise ratio, a LOD of at least 0.5 ng/ml in the urine is achievable. Reagent blanks do not

indicate the presence of any of the analytes. Analysis of the blank urine extract, however, seems to indicate the presence of cimaterol and clenbuterol. For cimaterol this is most likely caused by interfering compounds, because all urine blanks analyzed during this study show a comparable blank offset. These interferences were not characterized any further. Consequently, for cimaterol the clean-up has to be improved or, alternatively, chromatographic separation of the analyte and the interference may be applied. For clenbuterol, other urine blanks did not show an offset, so for this compound it may have been incidental contamination. However, especially for clenbuterol the signal is rather small and quantitation yields a blank offset of approximately 0.3 ng/ml.

Quantitation is carried out by using clenbuterol-d<sub>6</sub> as an internal standard. For clenbuterol the quantitative results are therefore acceptable, especially when taking into account that clenbuterol-d<sub>6</sub> is only added after clean-up

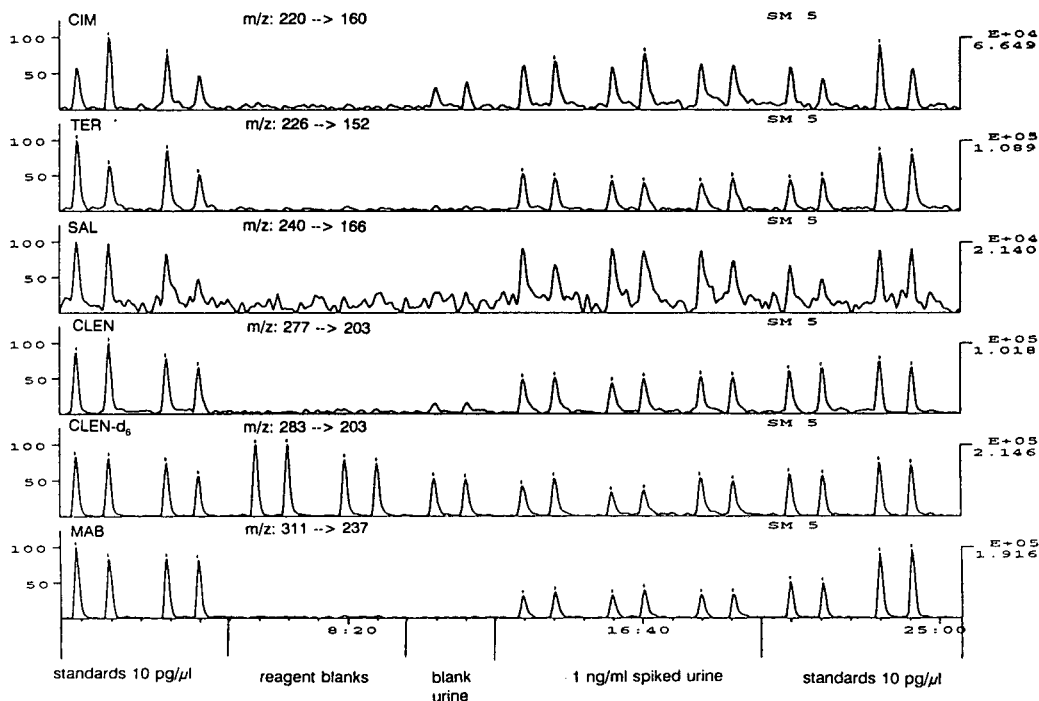


Fig. 1. SRM profiles for the FIA-TSP-MS-MS analysis of urine samples spiked at 1 ng/ml with five  $\beta$ -agonists.

so recovery losses are not corrected. For the other compounds, quantitative results should be improved. Repeatability is again acceptable for clenbuterol and perhaps for mabuterol and terbutaline, but also here improvements have to be made. However, as the use of these compounds in the fattening of animals for human consumption is banned within the EC, indication of the presence itself is more important than accurate quantitative results. Improvement of quantita-

tion may be achieved by using isotope-labelled standards added before clean-up. Particularly for salbutamol the use of salbutamol- $d_6$  as an internal standard could improve quantitation. The results of analysis justify the statement that the presented method yields at least semi-quantitative information, except for salbutamol.

Together with the clean-up, not including hydrolysis, the entire procedure, including calibration, can be performed within two hours for a

Table 2

Results for the analysis of clenbuterol (CLEN), salbutamol (SAL), cimaterol (CIM), terbutaline (TER) and mabuterol (MAB) in spiked urine samples purified on XtrackT SPE columns

Spike level (ng/ml)	CLEN		SAL		CIM		TER		MAB	
	Mean (ng/ml)	C.V. (%)	Mean (ng/ml)	C.V. (%)	Mean (ng/ml)	C.V. (%)	Mean (ng/ml)	C.V. (%)	Mean (ng/ml)	C.V. (%)
1.0	1.1	15	1.6	28	1.5	25	1.0	21	0.7	21
2.0	2.4	18	4.3	31	2.7	19	1.9	9	1.5	18
5.0	4.4	12	12.2	19	5.9	7	5.6	14	2.9	8



set of 20 samples. In that respect the method is far more rapid than any GC-MS method now available.

### 3.2. Qualitative determination

Tandem mass spectrometry may also be used for exploratory analysis to detect the possible presence of unknown compounds. Using neutral loss scanning, the loss of 74 amu can be monitored, corresponding to the loss of water followed by the loss of methylpropene from the molecular ion. It is assumed that for all *N-tert.*-butyl substituted  $\beta$ -ethanolamines, this fragmentation will occur when using alike experimental parameters. For all known compounds this has been confirmed in our laboratory.

Fig. 2 shows the analysis of a 50- $\mu$ l aliquot, corresponding to 0.5 ml of urine, of a urine extract spiked prior to clean-up, at 3 ng/ml, with several  $\beta$ -agonists. The presence of the peak at 4.4 min indicates the presence of one or more compounds that comply with the scanning requirement: the loss of 74 amu.

The inset in Fig. 2 shows the CID spectrum averaged over the peak at 4.4 min. This spectrum indicates the presence of salbutamol  $[M+H]^+$  at  $m/z$  240 and  $[M+H-H_2O]^+$  at  $m/z$  222, terbutaline  $[M+H]^+$  at  $m/z$  226, clenbuterol  $[M+H]^+$  at  $m/z$  277/279 and mabuterol  $[M+H]^+$  at  $m/z$  311/313. It is obvious that these compounds are readily detected at this concentration level. The presence of two fragment ions for salbutamol may be the reason for the low sensitivity in the semi-quantitative analysis, because there the loss of 74 amu from only one ion ( $m/z$  240) is monitored.

To exemplify the detection of possible unknowns, a rather artificial experiment was carried out. Recently the abuse of the brominated analog of clenbuterol was discovered [4]. At that time, in our laboratory, GC-MS was used for the analysis. One of these samples was analyzed using the presented method. Experimental conditions were the same as in Fig. 2. Again an aliquot equivalent to 0.5 ml of urine was injected while scanning the mass spectrometer for the loss of 74 amu. Fig. 3 indicates the presence of compound(s) losing 74 amu, and the averaged

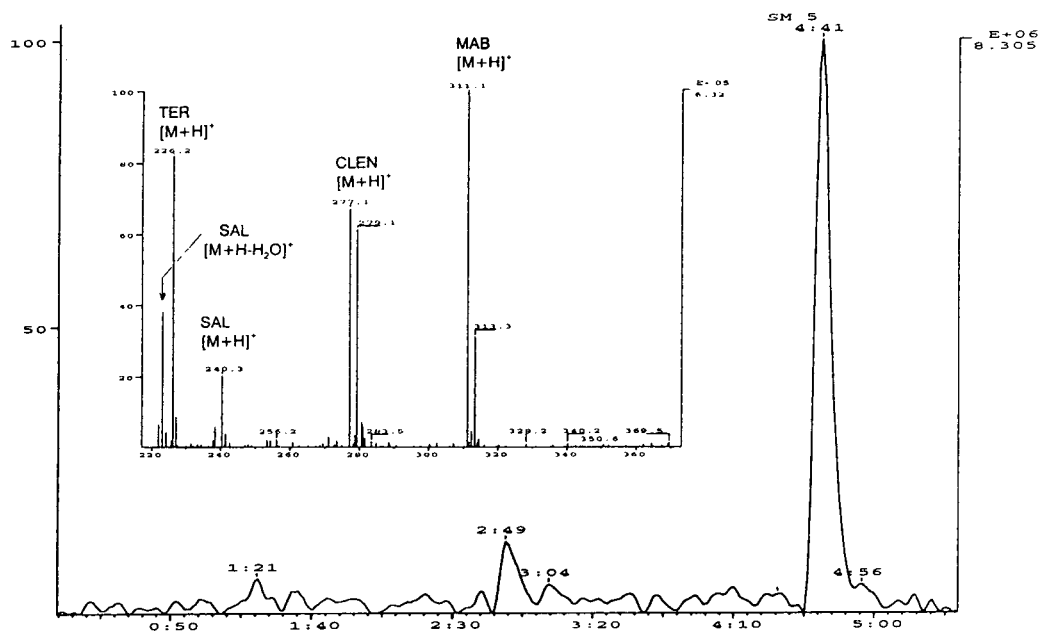


Fig. 2. Injection of an extract of a urine sample spiked at 3 ng/ml, indicating the simultaneous detection of all *N-tert.*-butyl substituted compounds present. The mass spectrometer was operated in full-scan neutral loss (74 u) mode.

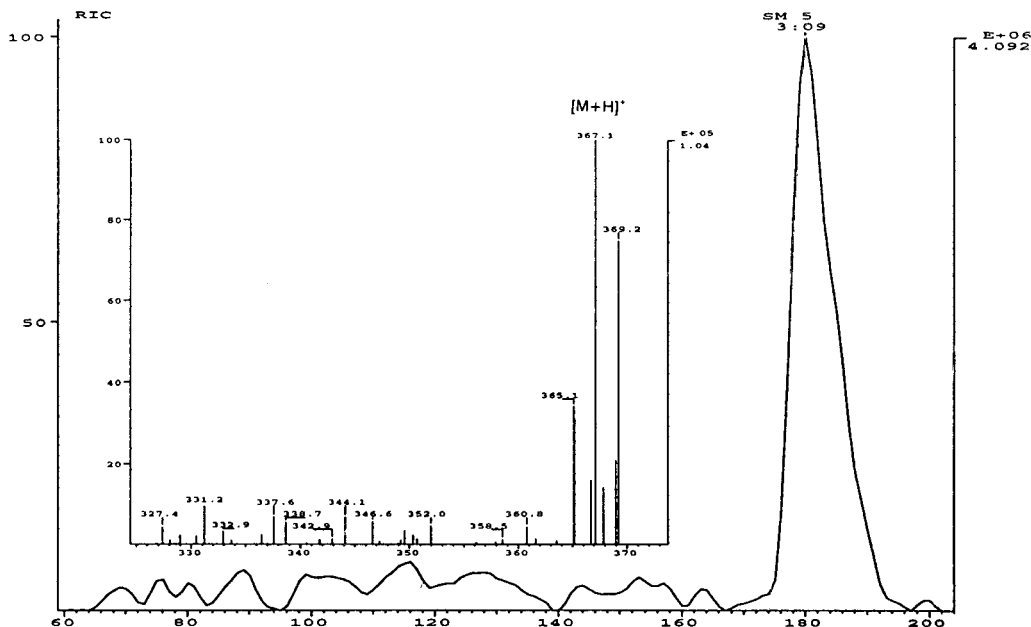


Fig. 3. Injection of an extract of a urine sample exemplifying the detection of a possible unknown compound. The CID spectrum reveals the presence of bromobuterol. The amount was estimated at 0.7 ng/ml in the urine.

CID spectrum reveals the presence of a compound containing two bromine atoms with a mono-isotopic molecular mass of 364,  $[M+H]^+ = 365$ . This compound was previously identified as bromobuterol, the brominated analog of clenbuterol. Using GC-MS, the amount was estimated at 0.7 ng/ml assuming a response per mass unit equal to clenbuterol.

From the above examples, the possibilities of tandem MS for group-specific detection, in this case specific for *N-tert.*-butyl substituted  $\beta$ -ethanolamines, are apparent even for low concentration levels like 1 ng/ml, although this strongly depends on the compound. It should be emphasized, however, that the loss of 74 amu may not be an exclusive feature of *N-tert.*-butyl substituted  $\beta$ -ethanolamines alone, so interference may occur. Only the analysis of a large number of samples from as diverse origin as possible will indicate whether or not the specificity is sufficient. Currently this item is under investigation.

#### 4. Conclusion

The presented method may be used for rapid analysis of several  $\beta$ -agonists in urine in a semi-quantitative fashion at sub-ng/ml levels. Analysis is rapid but specificity should be studied more extensively. Operating the mass spectrometer in full-scan neutral loss mode, the possibilities of tandem mass spectrometry for group-specific detection of structure-related compounds are indicated. Detection of an unknown as well as known compounds at ng/ml levels is demonstrated.

#### Acknowledgements

This work was in part performed within the framework of the FLAIR Concerted Action nr. 8 and presented at the FLAIR Workshop in Porto, April 1994. The authors wish to thank the managing committee for their support. Other

participants are acknowledged for their contributions to stimulating discussions on the subject.

## References

- [1] J.A. van Rhijn, W.A. Traag and H.H. Heskamp, *J. Chromatogr.*, 619 (1993) 243.
- [2] L.A. van Ginkel, R.W. Stephany and H.J. van Rossum, *J. Assoc. Off. Anal. Chem.*, 75 (1992) 554.
- [3] M.P. Montrade, B. Le Bizec, F. Monteau, B. Siliart and F. Andre, *Anal. Chim. Acta*, 275 (1993) 253.
- [4] L. Leyssens, J. van der Greef, H. Penxten, J. Czech, J.P. Noben, P. Adriaensens, J. Gelan and J. Raus, in N. Haagsma, A. Ruiter and P.B. Czedik-Eysenberg (Editors), *Residues of Veterinary Drugs in Food—Proceedings of the EuroResidue II Conference*, Veldhoven, Netherlands, 3–5 May 1993, Vol. 2, p. 444.



# Determination of an endothelin receptor antagonist in human plasma by narrow-bore liquid chromatography and ionspray tandem mass spectrometry

B. Lausecker, G. Hopfgartner\*

*F. Hoffmann-La Roche Ltd., Department of Drug Metabolism and Kinetics, Bioanalytical Section, CH-4002 Basle, Switzerland*

## Abstract

A method is described for the determination of a new endothelin receptor antagonist, Bosentan Ro 47-0203, in human plasma using narrow-bore liquid chromatography and ionspray tandem mass spectrometry. After protein precipitation with acetonitrile, the compounds were extracted with dichloromethane at pH 11. The compounds were chromatographed on a 2 mm I.D. reversed-phase column and introduced into the mass spectrometer with an ionspray (pneumatically assisted electrospray) interface at a flow-rate of 170  $\mu\text{l}/\text{min}$  without postcolumn splitting. Two different internal standards were used for the assay: either a structural analogue or a deuterated analogue. The limit of quantification was 0.5 ng/ml using a 0.5-ml aliquot of plasma. Concentrations of the drug were determined in the range 0.5–200 ng/ml. The recovery from human plasma was 87%. The new API IIIplus collision cell was about five times more sensitive than the original API III cell. The assay was demonstrated to be sensitive, selective and robust for the analysis of over 1500 samples.

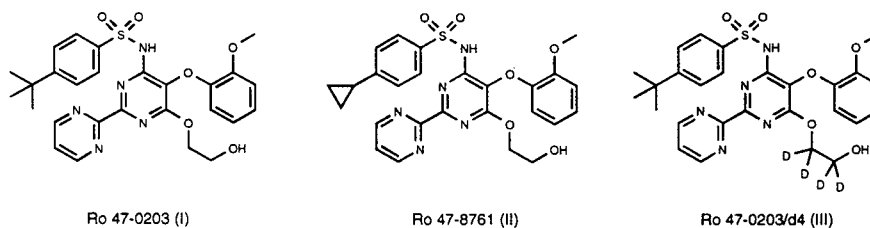
## 1. Introduction

Liquid chromatography is widely used for the determination pharmaceutical compounds with UV, fluorescence or electrochemical detection. More recently, mass spectrometry (MS) has been introduced as a highly specific and sensitive detector for HPLC. Several approaches have been used to combine LC and MS, including direct liquid introduction (DLI) [1], thermospray (TS) [2], particle beam (PB) [3] and more recently electrospray [4] and ionspray [5]. For quantitative analysis, LC–MS, in particular with

atmospheric pressure ionization (API), is rapidly becoming a powerful analytical tool with respect to sensitivity and selectivity compared with HPLC with UV detection. Ionspray can handle flow-rates from a few nanolitres per minute [6] to over 1000  $\mu\text{l}/\text{min}$  [7]. For quantitative ionspray mass spectrometry, narrow-bore HPLC columns of 2 mm I.D. are a practical alternative to standard-bore columns owing to the lower solvent consumption and increased analyte response with good chromatographic performance [8].

Endothelin is a bicyclic 21-amino acid peptide and a very potent long-lasting vasoconstrictor. It is also a growth factor for vascular smooth muscle and mesangial and cancer cells and is a

\* Corresponding author.



Scheme 1. Structures of compounds I–III.

potent bronchoconstrictor [9–11]. A non-peptidic endothelin receptor antagonist, Bosentan [12] (Ro 47-0203, Scheme 1), is currently under development for the treatment of diseases such as hypertension, sub-arachnoid haemorrhage and Raynaud's syndrome. For pharmacokinetic studies, an HPLC–UV assay [13] was developed, but was insufficiently sensitive for complete characterization of the kinetics in man. Therefore, it was necessary to validate a sensitive and robust assay with ionspray tandem mass spectrometry for the determination of the drug at low levels in human plasma.

## 2. Experimental

### 2.1. Chemicals

Ro 47-0203 (I,  $M_r = 552$ ), Ro 47-8761 (II,  $M_r = 536$ ) and Ro 47-0203/002 (III,  $M_r = 556$ ) (Scheme 1) were provided by F. Hoffmann-La Roche (Basle, Switzerland). Dichloromethane was obtained from Fluka (Buchs, Switzerland) and was of analytical-reagent grade. Acetonitrile, ethanol, ammonium acetate, Titrisol buffer solution (pH 11) and acetic acid were obtained from Merck (Darmstadt, Germany) and were of chromatographic or pro analysis grade. Water was doubly distilled in-house or was of chromatographic grade obtained from Merck.

### 2.2. Liquid chromatography

The mobile phase, acetonitrile–5 mM ammonium acetate–acetic acid (75:25:1 or 70:30:1, v/v),

was delivered by a Model 6200A LC pump (Merck–Hitachi, Tokyo, Japan). The extracts were injected with an AS 4000 autosampler (Merck–Hitachi) equipped with a 100- $\mu$ l injection loop on to a 125  $\times$  2 mm I.D. column with a 10  $\times$  2 mm I.D. guard column (Superspher RP-18, 4  $\mu$ m; Stagroma, Wallisellen, Switzerland). The column temperature was held constant at 35°C using a Jones Chromatography (Llanbradach, UK) Model 9730 column thermostat. The mobile phase was degassed on-line using an SDU 2003 solvent degasser unit (Labsource, Basle, Switzerland).

### 2.3. Mass spectrometry

A Perkin-Elmer SCIEX (Thornhill, Canada) API III triple-quadrupole biomolecular mass analyser or the same instrument upgraded to a Perkin-Elmer SCIEX API IIIplus triple-quadrupole biomolecular mass analyser was used. The original collision cell was an open type with a crossed-flow jet, which suffered from a significant energy spread. The improved confined collision cell requires less gas flow and uses improved optics, but operates at pressures about ten times higher than the old cell. This high pressure (<0.66 Pa) causes ions, under the influence of r.f. fields, to relax into a narrow beam with well defined kinetic energy, which results in better sensitivity and better fragment ion resolution [14].

The mass spectrometer was equipped with an in-house constructed articulated ionspray device. This articulated ion spray device uses an 80 cm  $\times$  100  $\mu$ m I.D.  $\times$  500  $\mu$ m O.D. stainless-steel capillary as a sprayer capillary. The tip of the

capillary was biased at approximately 60° and electropolished. This capillary was placed inside a 35 mm × 800 μm I.D. × 1.59 mm O.D. stainless-steel capillary used as the nebulizer capillary. The tip of this capillary was shrunk to 650 μm. The nebulizer gas (nitrogen, +99.999% purity) was introduced using a T-piece. The other end of the sprayer capillary was connected to a ca. 100 mm × 100 μm I.D. × 170 μm O.D. fused-silica capillary through a zero-dead-volume union. The fused-silica capillary used for electrical isolation was connected to the column outlet through a Swagelok connector. The mass axis of the mass spectrometer was calibrated with a standard solution of quaternary alkylammonium salts in acetonitrile at a flow-rate of 10 μl/min covering a molecular mass range from 200 to 600.

Infusion experiments were performed with a Harvard syringe pump. Prior to quantitative analysis, the resolution of the quadrupoles was tuned with 1 ng/μl Ro 47-0203 solution [acetonitrile–5 mM ammonium acetate–acetic acid (30:70:1, v/v/v)] to be better than 1 u at the peak half-height for Q1 on both devices, better than 2 u at the peak half-height for Q3 using the API III and better than 1 u at the peak half-height for Q3 using API IIIplus. Argon was used as the collision gas in Q2 with a collision gas thickness (CGT) of  $500 \cdot 10^{12}$  atoms/cm<sup>2</sup> (API III) or with a CGT of  $250 \cdot 10^{13}$  atoms/cm<sup>2</sup> (API IIIplus). The collision energy used was set at 50 eV (API III) or 35 eV (API IIIplus).

The LC–UV trace was recorded with a ABI (Ramsey, NJ, USA) Model 783A UV detector, equipped with 2.4-μl volume, 6-mm path length micro detection cell in-line between the column outlet and the articulated ionspray device. The wavelength was set at 270 nm.

Method development and routine work were carried out using the standard software Tune 2.4, RAD 2.5 and Mac Quant 1.3 (Perkin-Elmer SCIEX).

#### 2.4. Preparation of standard solutions

Stock standard solutions of compound I–III were prepared by dissolving about 4 mg in 100

ml of ethanol. Aliquots of the stock standard solution were diluted with ethanol to provide working standard solutions. The plasma standards were obtained by spiking blank plasma (20 ml) with 100 μl of working solution, providing concentrations between 0.5 and 200 ng/ml of the analyte. The standards were divided into aliquots of 0.5 ml and stored deep frozen at –20°C until required for analysis.

The stability of analyte I was investigated by preparing control plasma samples at concentrations of 2.5 and 80 ng/ml. Aliquots were frozen and stored at –20°C. Fresh calibration samples were prepared to provide 100% values and the data indicated that compound I was stable for 7 months in human plasma under the conditions investigated.

#### 2.5. Sample preparation

An aliquot of human plasma (0.5 ml) was mixed with 10 μl of internal standard (I.S.) solution containing 50 ng of Ro 47-0203/002 or Ro 47-8761 in ethanol. Acetonitrile (0.75 ml) was added to the sample, which was homogenized by vortex mixing. To complete protein precipitation, the sample was kept in a refrigerator at 5°C for 10 min. The supernatant was extracted with dichloromethane (7 ml) at pH 11 by shaking (20 min) on a rotating shaker (Heidolph, Kelheim, Germany). After centrifugation (5 min) and removal of the upper aqueous phase, the organic phase was transferred into a new tube and evaporated to dryness in a vacuum centrifuge (Savant, Farmingdale, NY, USA). To remove lipids, the extract was dissolved in acetonitrile (1 ml) and centrifuged (5 min). The sample was transferred to a conical tube (1.1 ml) and evaporated to dryness in a vacuum centrifuge. Prior to LC–MS analysis, the extract was dissolved in 100 μl of acetonitrile–5 mM ammonium acetate–acetic acid (30:70:1, v/v/v). Volumes of 30 or 90 μl were injected.

#### 2.6. Calibration and calculations

Along with the unknown samples, quality control samples and ten plasma standards with

appropriate drug concentrations were processed as described above. The concentrations in all samples were determined using peak areas with a calibration graph obtained by weighted linear least-squares regression (weighting factor =  $1/y^2$ ) of the peak-area ratios of the calibration samples.

### 3. Results and discussion

#### 3.1. Analytical system and chromatography

Pharmacokinetic studies required the quantification of **I** at levels below 1 ng/ml. This sensitivity could not be achieved by the standard HPLC–UV method. However, flow injection analysis

indicated a very good sensitivity for **I** with ionspray MS. In LC–MS, the mobile phase composition plays an important role regarding sensitivity, and one is restricted to the use of volatile buffers such as ammonium acetate and acetic acid. The chromatography of **I** is relatively uncritical on reversed-phase material, and the choice of a narrow-bore column was dictated by a high organic content of the mobile phase and a sharp peak shape. For interfacing LC and MS, two approaches are possible: the heater nebulizer which allows gas-phase (APCI) and ionspray, which is a condensed-phase ionization process. Ionspray was selected because it provided the best response for the analytes with the HPLC mobile phase used. API produces mainly charged protonated molecular ions, which can be

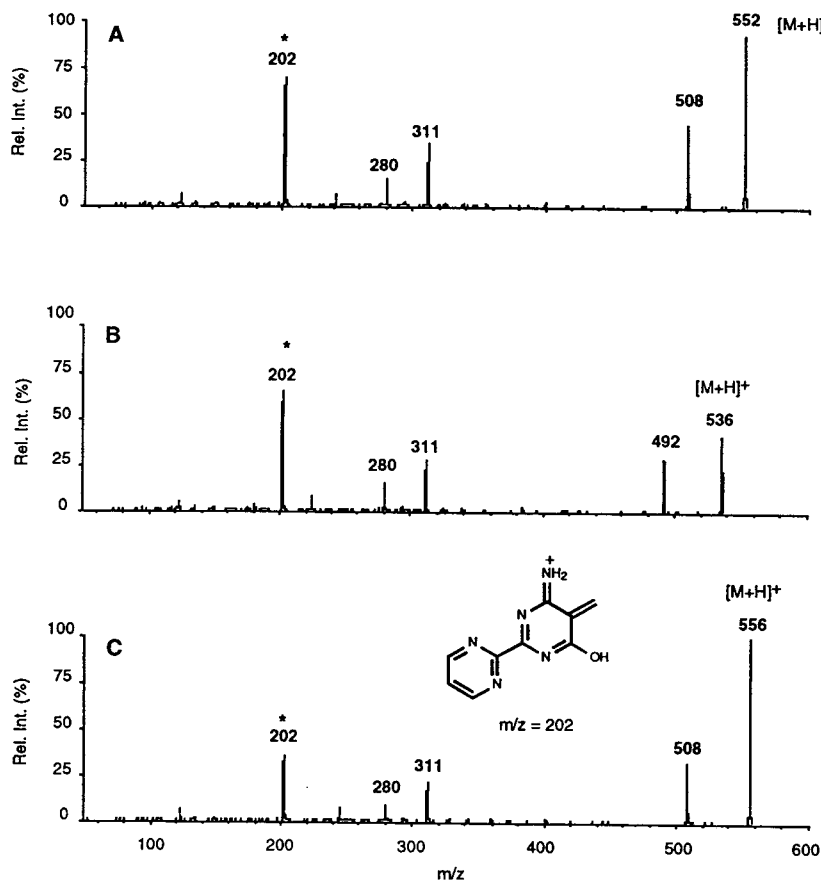


Fig. 1. Product ion spectra of (A) Ro 47-0203 (**I**), (B) Ro 47-8761 (**II**) and (C) Ro 47-0203/d4 (**III**) at a collision energy of 25 eV and a collision gas thickness of  $300 \cdot 10^{13}$  atoms/cm<sup>2</sup>.



fragmented in the collision cell (Q2) of a tandem mass spectrometer. Fig. 1 shows the product ion spectrum of **I** and the two internal standards **II** and **III**. For all three compounds, an intense product ion was observed at  $m/z$  202 which was selected for the selected reaction monitoring (SRM) mode.

A major concern in standard HPLC–UV is co-elution of endogenous compounds with the analytes. Ro 47-0203 has a relatively intense chromophore, and a few nanograms of a standard solution can be detected easily. However, adequate selectivity could not be achieved with a plasma extract (2.5 ng/ml of **I** and 50 ng/ml of

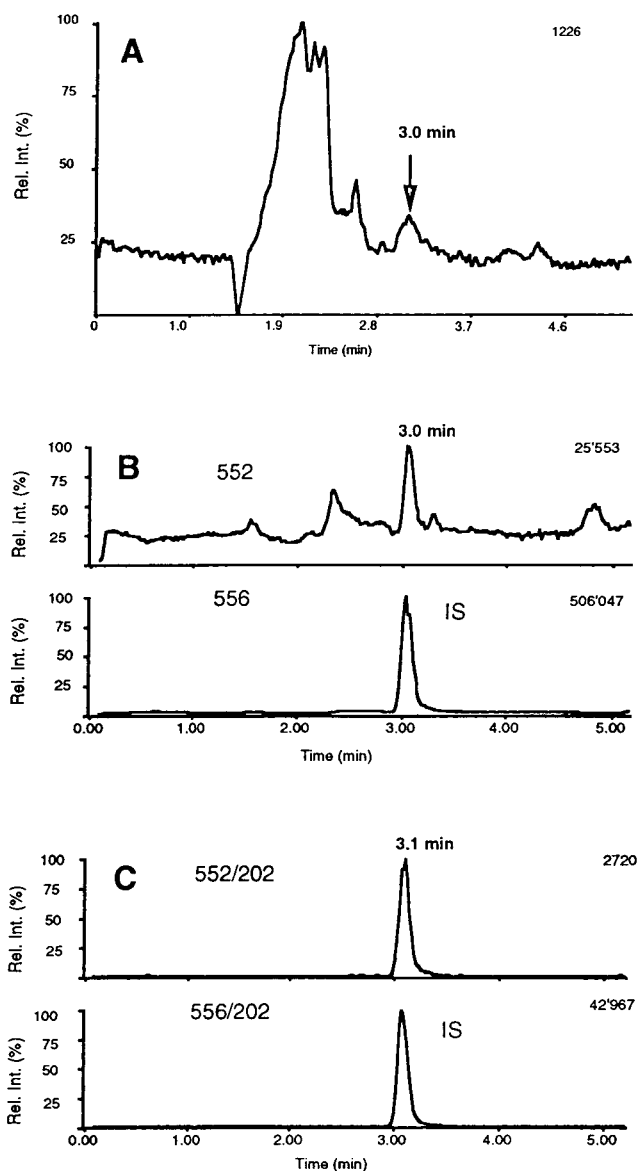


Fig. 2. Analysis of a human plasma extract spiked with 2.5 ng/ml of Ro 47-0203 and 50 ng/ml of Ro 47-0203/d4 by (A) LC–UV, (B) selected-ion monitoring (SIM) and (C) selected reaction monitoring (SRM).

III as I.S.), as illustrated in Fig. 2A, where the analyte and the I.S. are co-eluting with endogenous compounds. Even LC-MS with SIM did not give sufficient selectivity, as shown in Fig. 2B, where the upper trace at  $m/z$  552 represents 2.5 ng/ml of I. The use of a gradient instead of an isocratic chromatographic system would certainly help to improve the selectivity, but analysis time would increase considerably. The SRM mode brings the required selectivity to overcome this problem efficiently, as illustrated in Fig. 2C, especially when short retention times are desired. During the analysis of clinical samples, no significant interferences from plasma were observed. To minimize possible interferences from plasma, the resolution of the quadrupoles Q1 and Q3 should not be compromised to improve the sensitivity.

The use of standard-bore columns with the ionspray interface generally requires postcolumn splitting. When biological extracts are analysed, splitting may affect the robustness of the assay. It has been reported that standard ionspray mass spectrometry in the flow-rate range 20–200  $\mu\text{l}/\text{min}$  behaves like a concentration-sensitive detector. When using a concentration-sensitive detector, a decrease in the column I.D. from 4.6 to 2 mm will result in a ca. fivefold increase in sensitivity [8]. A further decrease in column diameter to 1 mm or less will result in an increase in sensitivity; however, 2 mm I.D. columns are a good compromise between sensitivity, low solvent consumption and good chromatographic performance. Once the sprayer settings have been optimized for 20  $\mu\text{l}/\text{min}$ , an increase in the flow-rate up to 170  $\mu\text{l}/\text{min}$  results in a decrease in response of about 40%. When the sprayer position, nebulizer gas flow-rate and interface plate temperature were reoptimized at 170  $\mu\text{l}/\text{min}$ , slightly better sensitivity was obtained than at 20  $\mu\text{l}/\text{min}$ .

### 3.2. Internal standard

In the first development phase of the assay, no deuterated internal standard was available. When using short retention times, the choice of the internal standard may be critical because it

could interfere with possible metabolites. At this stage, some metabolites were known from *in vitro* experiments and no interference could be observed from the metabolites or the cyclopropyl analogue used as the IS. Subsequently, a tetra-deuterated analogue became available. For mass spectrometry, deuterated internal standards are ideal because they compensate for matrix effects during extraction and matrix suppression during the ionization process. However, pure material is difficult to obtain and often traces of the parent compound are present.

### 3.3. Assay performance

The precision of the method was evaluated for I over the concentration range 0.5–200 ng/ml by replicate analysis of each concentration over a period of several weeks. The data given in Table 1 demonstrate good precision whichever internal standard was used. The assay was linear in the range 0.5–200 ng/ml using a 0.5-ml aliquot of plasma. The recovery from replicate analysis was 87%. A quantification limit of 0.5 ng/ml was found to be sufficient. However, better sensitivity can be achieved, in particular with the new collision cell (API IIIplus). After upgrading the instrument with the new collision cell, the assay was revalidated. The new collision cell allows better mass resolution for Q3 in the MS-MS mode and a fivefold sensitivity increase was obtained. The analyte I and the internal standards have different precursor ions, but generate the same product ion; therefore, the setting of the pause time to 50 ms with the new collision cell is very important to avoid carryover.

### 3.4. Application to biological samples

The method has been applied successfully to the analysis of more than 1500 human plasma samples from clinical trials. Figs. 3 and 4 show representative chromatograms of the analyte with the two different internal standards. In Fig. 4A a peak is observed at a retention time of 3.2 min (280 counts) in the predose trace of the analyte, which corresponds to Ro 47-0203 present at trace levels in the internal standard.

Table 1  
Precision and accuracy of the method with the two different internal standards

Amount added (ng/ml)	Ro 47-8761 (n = 5)				Ro 47-0203/d4 (n = 5)			
	Amount found (ng/ml)	S.D. (ng/ml)	R.S.D. (%)	Inaccuracy (%)	Amount found (ng/ml)	S.D. (ng/ml)	R.S.D. (%)	Inaccuracy (%)
0.50	0.504	0.04	8.91	-0.73	0.485	0.03	5.29	3.10
0.75	0.778	0.05	6.03	-3.76	0.755	0.05	7.07	-0.71
1.00	0.987	0.04	4.25	1.27	1.014	0.07	6.53	-1.43
2.00	2.190	0.11	5.45	-9.52	2.035	0.12	6.03	-1.77
5.00	5.120	0.21	4.17	-2.41	5.208	0.14	2.73	-4.17
10.00	10.60	0.22	2.18	-6.01	10.27	0.34	3.30	-2.68
50.00	53.40	1.98	3.96	-6.79	50.69	0.96	1.89	-1.38
100.00	101.4	2.79	2.79	-1.44	103.5	3.59	3.46	-3.55
175.00	173.5	2.67	1.53	0.86	161.9	6.74	4.16	7.46
200.00	193.6	6.75	3.38	3.21	198.5	6.18	3.11	0.74

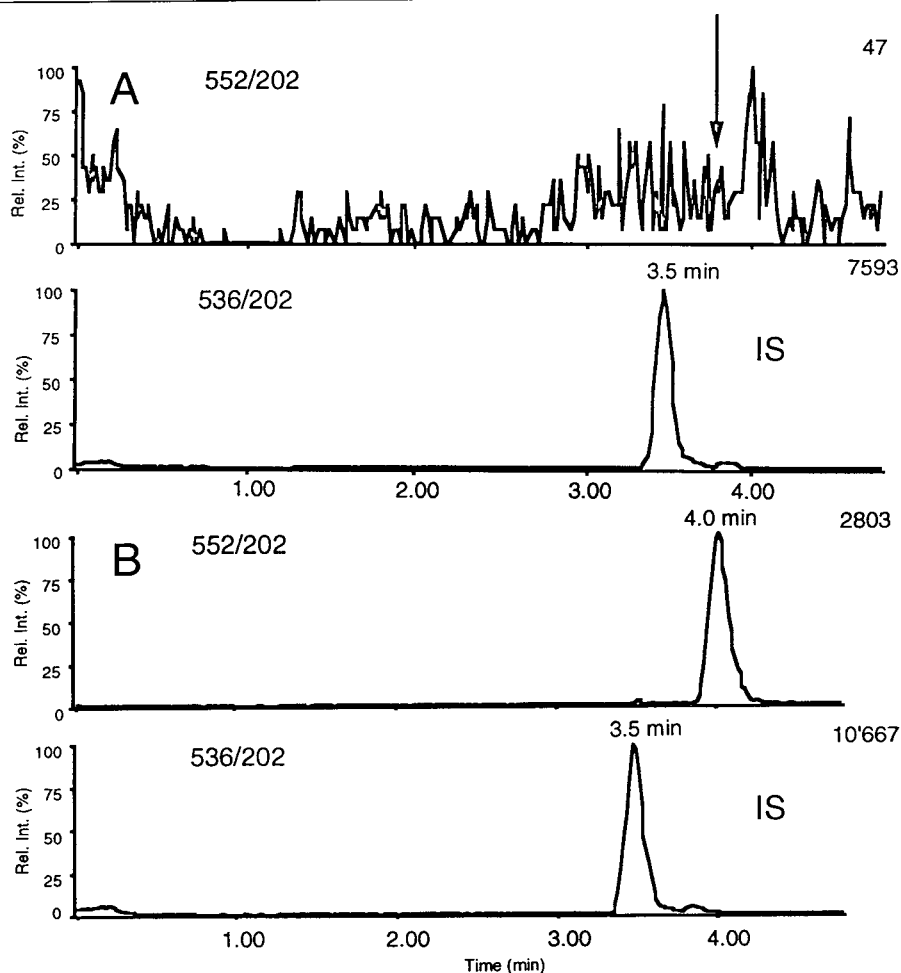


Fig. 3. Selected reaction monitoring (SRM) chromatograms of human plasma with the non-deuterated I.S.: (A) predose and (B) collected after 24 h after a single oral dose of 100 mg p.o. of I; measured concentration, 6.63 ng/ml.

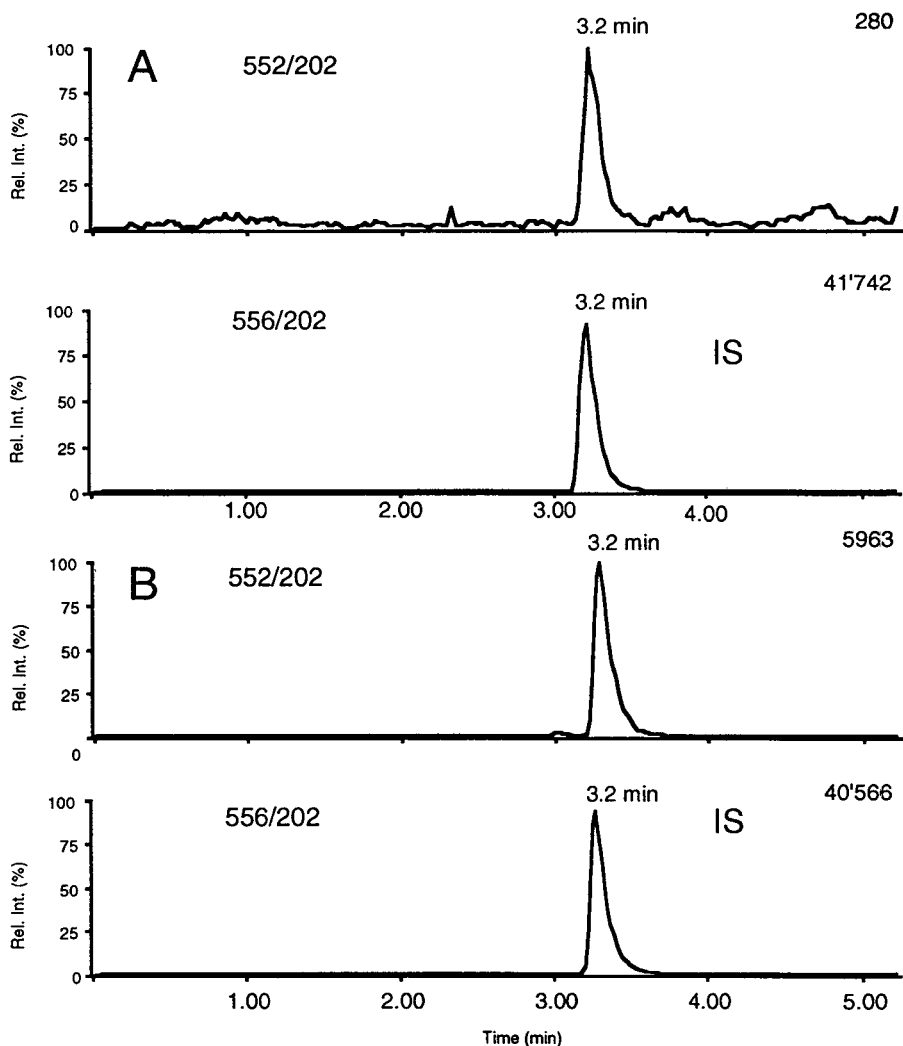


Fig. 4. Selected reaction monitoring (SRM) chromatograms of human plasma with deuterated I.S.: (A) predose and (B) collected after 24 h after a single oral dose of 200 mg p.o. of I; measured concentration, 12.58 ng/ml.

Using MS–MS, the selectivity of the assay was found to be very good and no interfering peaks were observed. The retention time of the analyte was in the range 3–4 min, allowing a short cycle time in the isocratic mode and the analysis of 100 samples can be performed overnight. The narrow-bore columns were found to be reliable and over 500 plasma extracts were injected on to the same column without significant decrease in performance.

#### Acknowledgement

The authors thank Dr. D. Dell for correcting the manuscript.

#### References

- [1] E.D. Lee and J.D. Henion, *J. Chromatogr. Sci.*, 23 (1985) 253.

- [2] P. Arpino, *Mass Spectrom. Rev.* 11 (1992) 3.
- [3] P.C. Winkler, D.D. Perkins, W.K. Williams and R.F. Browner, *Anal. Chem.*, 60 (1988) 489.
- [4] S.F. Wong, C.K. Meng and J.B. Fenn, *J. Phys. Chem.*, 92 (1988) 546.
- [5] A.P. Bruins, T.R. Covey and J.D. Henion, *Anal. Chem.*, 59 (1987) 2642.
- [6] M. Wilm and M. Mann, *Int. J. Mass Spectrom. Ion Phys.*, 136 (1994) 167.
- [7] G. Hopfgartner, T. Wachs, K. Bean and J. Henion, *Anal. Chem.*, 65 (1993) 439.
- [8] G. Hopfgartner, K. Bean, J.D. Henion and R. Henry, *J. Chromatogr.*, 647 (1993) 51.
- [9] M.H. Yanagisawa, H. Kurihara, S. Kimura, Y. Tomobe, Y. Mitsui, Y. Yazaki, K. Goto and T. Masaki, *Nature*, 332 (1988) 411.
- [10] C. Advenier, B. Sarria, E. Naline, L. Puybasset and V. Lagente, *Br. J. Pharmacol.*, 100 (1990) 168.
- [11] Y. Yada, K. Higushi and G. Omokawa, *J. Biol. Chem.*, 226 (1991) 18352.
- [12] M. Clozel, V. Breu, G.A. Gray, B. Kalina, B.M. Löffler, K. Burri, J.M. Cassal, G. Hirth, M. Müller, W. Neidhart and H. Ramuz, *J. Pharmacol. Exp. Ther.*, 270 (1994) 118.
- [13] H. Eggers and A. Götschi, personal communication.
- [14] D.J. Douglas and J.B. French, *J. Am. Soc. Mass Spectrom.*, 3 (1992) 398.





ELSEVIER

Journal of Chromatography A, 712 (1995) 85–93

JOURNAL OF  
CHROMATOGRAPHY A

# Determination of the pesticide diflubenzuron in mushrooms by high-performance liquid chromatography–atmospheric pressure chemical ionisation mass spectrometry

Karen A. Barnes\*, James R. Startin, Stephen A. Thorpe, Stewart L. Reynolds,  
Richard J. Fussell

Ministry of Agriculture, Fisheries and Food, CSL Food Science Laboratory, Norwich Research Park, Colney, Norwich,  
NR4 7UQ, UK

## Abstract

A method using high-performance liquid chromatography–atmospheric pressure chemical ionisation mass spectrometry (HPLC–APCI-MS) has been developed and validated for the determination of the insecticide diflubenzuron [1-(4-chlorophenyl)-3-(2,6-difluorobenzoyl)urea] in mushrooms. Samples were homogenised with acetone, extracted into dichloromethane–cyclohexane and further cleaned-up by size-exclusion chromatography (SEC). HPLC was performed on an ODS column with methanol–water at 1 ml/min. The limit of detection was 0.02 ng/ $\mu$ l (equivalent to 0.017 mg/kg in the crop). The calibration was linear over the range 0.025–1.0 ng/ $\mu$ l. Recovery of diflubenzuron from spiked mushrooms (0.06–0.58 mg/kg) was 85.5% with a relative standard deviation of 14.5% ( $n = 56$ ).

## 1. Introduction

Diflubenzuron [1-(4-chlorophenyl)-3-(2,6-difluorobenzoyl)urea,  $M_r$  310.0321, Fig. 1], first reported by Van Daalen et al. in 1972 [1], belongs to a group of insecticides which are effective as stomach and contact poisons and act by inhibi-

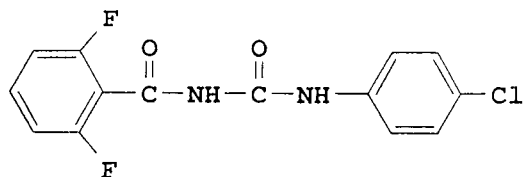


Fig. 1. Structure of diflubenzuron.

tion of chitin synthesis, thus interfering with the formation of the insect cuticle [2,3]. Therefore, all insect stages in which new cuticles are formed should be susceptible to diflubenzuron. It has a broad range of applications including use against the larvae of *Sciaridae* and *Phoridae* in mushrooms [4].

A number of analytical methods have previously been reported for the determination of diflubenzuron in various matrices. Although diflubenzuron is not itself amenable to GC, its thermal decomposition in the GC injector to form 4-chlorophenyl isocyanate, 4-chloroaniline, and 2,6-difluorobenzamide, has been used as the basis of a GC–MS method [5].

Methods involving HPLC with UV detection have been reported for various matrices includ-

\* Corresponding author.

ing bolti fish (*Oreochromis niloticus*) [6], forestry substrates [7], cabbage under sub-tropical conditions [8], a range of environmental samples including soil, sediment, agricultural crops, milk, eggs and animal tissues [9], and adult stable flies [10]. However, for the analysis of both chillies and plums, Wilkins has reported that a method based on multiple-wavelength UV detection was very prone to interferences [11].

An HPLC–MS method using thermospray (TSP) ionisation in the positive ion mode for the determination of diflubenzuron in foodstuffs was reported by Wilkins [11]. The base peak of the spectrum was the 2,6-difluorobenzamide ion ( $m/z$  175) produced by loss of *p*-chlorophenyl isocyanate, and the protonated molecule ( $m/z$  311) was present with an intensity of 80% of the base peak. Due to interferences at  $m/z$  175 quantitation was based on the protonated molecule which resulted in a detection limit equivalent to 0.25 mg/kg of analyte in the crop.

Recently the HPLC–MS ionization technique of atmospheric pressure chemical ionisation (APCI), shown in several reports to be viable for the determination of various classes of pesticide residues [12,13], has become particularly attractive for routine application following the introduction of relatively low cost, dedicated instrumentation [14]. APCI is a gas-phase ion–molecule reaction process which leads to the ionisation of analyte molecules under atmospheric pressure conditions. The process is analogous to chemical ionisation but the reactant ions are produced from the effect of a corona discharge on a nebulised aerosol of solvent. Due to the atmospheric pressure conditions the high frequency of analyte/reactant ion collisions ensures a high sample ionisation efficiency. The ionisation is soft and results predominantly in protonated molecules  $[M+H]^+$  in the positive ion mode or deprotonated molecules  $[M-H]^-$  in the negative ion mode.

Our laboratory has previously carried out the analysis of diflubenzuron in mushrooms using a HPLC–UV method [15] which provides a detection limit of 0.10 mg/kg, limited by matrix-derived interferences. Although this detection

limit is equivalent to the Codex maximum residue level (MRL) [16], higher sensitivity and a more specific technique for confirmation were desirable. We now report the application of HPLC–MS using APCI to the measurement of residues at lower concentrations.

## 2. Experimental

### 2.1. Materials

HPLC grade methanol and cyclohexane and glass-distilled grade acetone and hexane were obtained from Rathburn Chemicals (Walkern, UK). HPLC water was obtained from Fisons Scientific Equipment (Loughborough, UK) and pesticide grade dichloromethane from Merck (Leicestershire, UK). Granular AR anhydrous sodium sulphate was obtained from Fisons and was heated at 420°C for 4 h prior to use.

Polyethylene glycol (PEG) was a mixture of PEG 300, 600, and 1000 obtained from Koch Light (Haverhill, Suffolk, UK) and BDH (Dagenham, Essex, UK). Diflubenzuron standard was obtained from Promochem (Welwyn Garden City, UK) with a certified purity of 99%. Cultivated mushrooms were purchased from various retail outlets.

### 2.2. Preparation of standards and spiked samples

Two separate sets of calibration standards at concentrations of 0.025, 0.05, 0.10, 0.20, 0.50 and 1.0 ng/ $\mu$ l were prepared in (a) methanol–water (80:20) and (b) pooled extracted sample matrix (known to be blank).

Spiked mushrooms samples for recovery determination were prepared by the addition of an appropriate amount of a standard stock solution (7  $\mu$ g/ml in hexane) to finely chopped mushrooms (30 g) which were left to stand for a few minutes before extraction to allow the spike solution to penetrate the mushrooms. Spiked



concentrations were 0.06, 0.12, 0.23 and 0.58 mg/kg.

### 2.3. Extraction and clean-up

Extraction of diflubenzuron was based on the method reported by Andersson and Palsheden [17]. Samples were homogenised with 100 ml of acetone for 3 min using a laboratory blender (Ultra-Turrax) and filtered under vacuum through a sintered glass funnel. The filtrate was transferred to a 500-ml separating funnel and shaken with 200 ml cyclohexane–dichloromethane (1:1). On standing two distinct layers were formed, with the lower layer containing water originating from the sample matrix. The lower layer was transferred to a second separating funnel and the upper organic layer was decanted through anhydrous sodium sulphate into a 500-ml round-bottom flask. The aqueous layer was further extracted with two successive 70-ml portions of dichloromethane. At each successive extraction the organic layer was decanted through anhydrous sodium sulphate and combined with the organic fraction from the first extraction. Using a rotary evaporator (controlled at 30°C and 300 mbar) the organic extract was concentrated to near dryness, transferred to a volumetric flask (5 ml) and made to volume with cyclohexane–dichloromethane (1:1). The extract was filtered through an Anachem (Luton, UK) 0.45- $\mu\text{m}$  Nylon 66 syringe filter, and an aliquot (1 ml) injected on to a size-exclusion chromatography (SEC) system consisting of a glass column (500  $\times$  10 mm I.D.) packed with Bio-Beads S-X3 (Bio-Rad, Hemel Hempstead, UK), a Gilson (Villiers-le-Bel, France) 232-401 automated sample processor and a Spectra-Physics (San-Jose, California) Isochrom HPLC pump. The mobile phase for SEC was cyclohexane–dichloromethane (1:1) at a flow-rate of 1 ml/min. (The dump time and collect time of 16 and 30 min respectively were determined by injecting extracts of mushrooms spiked with diflubenzuron and calculating the recoveries obtained.) The collected fraction was taken to very near dryness under a gentle stream of oxygen-free nitrogen. The

cleaned up extract was transferred to a volumetric flask (5 ml) with methanol–water (80:20) and made up to volume.

### 2.4. HPLC

HPLC was performed using a Hichrom (Berkshire, UK) S50DS2 (250  $\times$  4.6 mm I.D.) column preceded by a S50DS2 (10  $\times$  4.6 mm I.D.) guard column. The mobile phase was methanol–water delivered at a flow-rate of 1 ml/min by a Spectra-Physics SP8800-20 pump, with a composition gradient consisting of 80% methanol for 8 min, a linear increase over 0.1 min to 95% methanol which was maintained for 9.9 min, a decrease to 80% methanol over 0.1 min and re-equilibration at 80% methanol for 7.9 min giving a total run time of 26 min. Both solvents were degassed by helium sparging prior to use and filtered through 10- $\mu\text{m}$  inlet filters.

Partial-loop (50  $\mu\text{l}$ ) injections were made via a Gilson 231 XL autosampler fitted with a 100- $\mu\text{l}$  loop on a Rheodyne (Cotati, CA, USA) 7125 injection valve. A solid-block column heater was used to maintain the column at a temperature of 45°C (Jones Chromatography, Mid Glamorgan, UK). Injections were made on to the HPLC column at 26.5 min intervals. Each sample or standard was analysed in duplicate.

### 2.5. Mass spectrometry

Mass spectra were obtained on a VG Platform “Classic” (Fisons Instruments, Altrincham, UK) bench-top mass spectrometer. Following preliminary evaluation of positive and negative ion modes (see below) all measurements were made using the latter. The instrument was initially tuned on background ions and mass calibrated in the positive ion mode on a mixture of PEG 300, 600 and 1000. Tuning parameters were then optimised in the negative ion mode on the deprotonated molecule ( $m/z$  309) of diflubenzuron [10 ng/ $\mu\text{l}$  solution in methanol–water (80:20, v/v) injected directly into the mass spectrometer via a 500- $\mu\text{l}$  Rheodyne loop]. Typical operating conditions were: corona 2.74 kV,

high voltage lens 0 kV, extraction 5 V, focus 10 V, source temperature 120°C, probe temperature 450°C, low mass resolution 14.0, high mass resolution 15.0, ion energy 0.7 V, ion energy ramp 0.0, multiplier 650.

Scanned acquisitions were made over the mass range 60–500 with a scan time of 1 s.

Single-ion monitoring (SIM) was performed at  $m/z$  289.02, 291.03, 309.02, 310.03 and 311.04. The dwell time for each channel was 0.1 s, the interchannel delay was 0.02 s and the mass span was 1 mass unit. SIM data were collected during the first 10 min of the 26-min chromatographic run. The retention time of diflubenzuron was approximately 5.5 min. Quantitation was based on the area under the peak in the mass chromatogram of the deprotonated molecule ( $m/z$  309).

### 3. Results

In preliminary experiments using full scanned acquisitions and loop injections containing 1  $\mu$ g of diflubenzuron, both positive and negative ionisation modes were evaluated. No ions attributable to diflubenzuron were observed in the positive mode whilst the negative mode gave an intense  $[M - H]^-$  ion ( $m/z$  309) and consequent-

ly negative ionisation was used for all further studies.

As noted by Kawasaki et al. [18], in HPLC–APCI-MS the APCI probe temperature can have a large effect on sensitivity. Fig. 2 shows the effect of temperature on the peak area of the deprotonated molecule ( $m/z$  309). The response clearly optimised at a probe temperature of 450°C which was used for subsequent measurements.

Fig. 3a shows the spectrum of diflubenzuron obtained at low extraction and focus voltages (5 and 10 V respectively) where  $[M - H]^-$  was the base peak. Higher extraction and focus voltages (30 and 35 V respectively) caused increased fragmentation (Fig. 2b) and under these conditions the deprotonated difluorobenzamide fragment ( $m/z$  156) was the base peak. Such “cone voltage” induced fragmentation provides the potential for generation of alternative confirmatory ions but at the expense of molecular ion sensitivity. To minimise fragmentation and thus maximise the sensitivity for the deprotonated molecule ( $m/z$  309) on which quantitation was based, low extraction and focus voltages were used for quantitation experiments.

Fig. 4 shows the five ions monitored by SIM from a 0.10 ng/ $\mu$ l diflubenzuron standard (equivalent to 0.085 mg/kg in the matrix assuming a

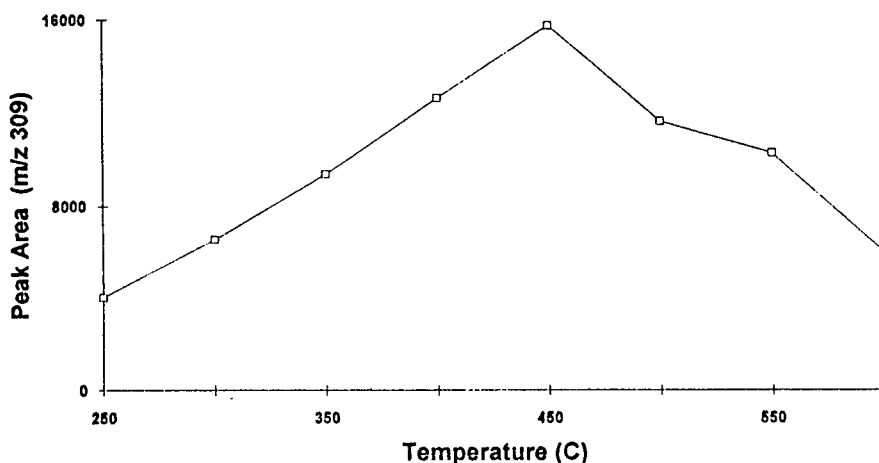


Fig. 2. Effect of the APCI probe temperature (°C) on peak area (arbitrary units) of the deprotonated diflubenzuron molecule ( $m/z$  309). The peak area was measured on 10- $\mu$ l loop injections of a 1 ng/ $\mu$ l standard.

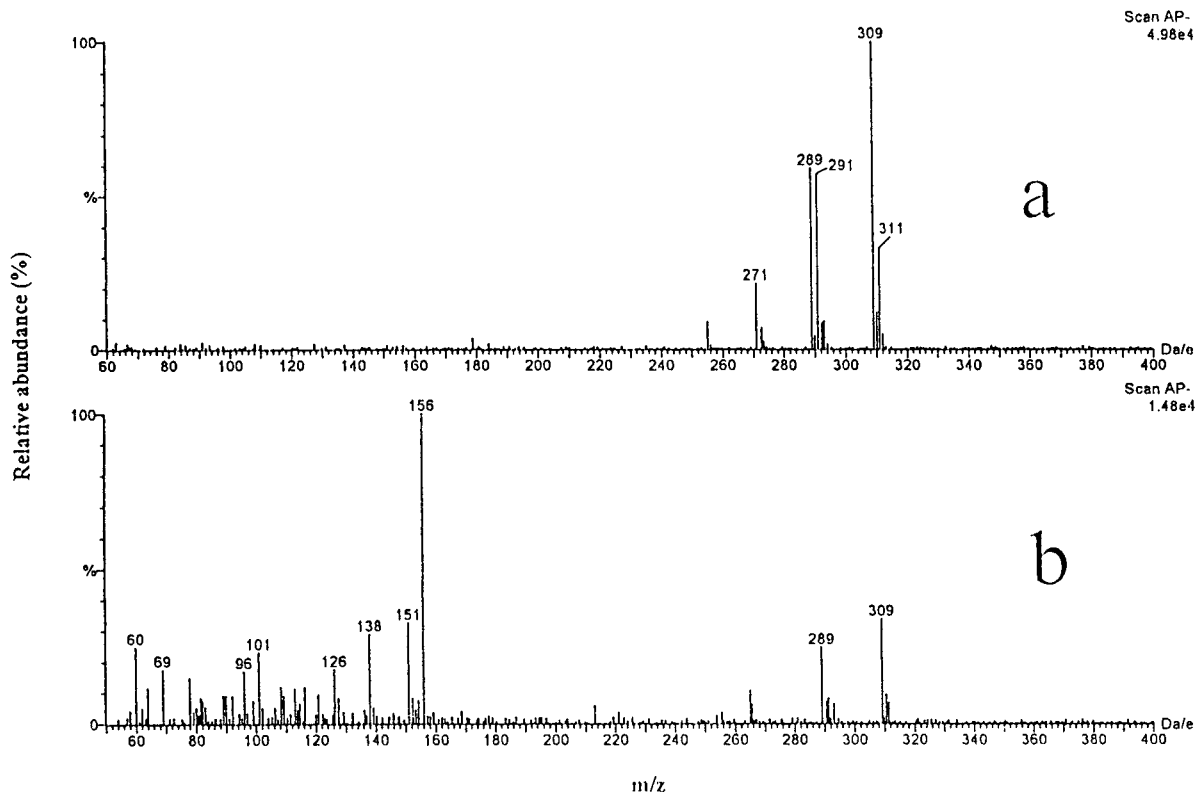


Fig. 3. Spectrum of diflubenzuron obtained at (a) low extraction and focus voltages (5 and 10 V, respectively), the base peak of which is the deprotonated molecule at  $m/z$  309 and (b) higher extraction and focus voltages (30 and 35 V, respectively) the base peak of which is the deprotonated difluorobenzamide fragment at  $m/z$  156.

100% recovery) prepared in the mobile phase. The isotope ratio observed for the deprotonated molecule was as expected for a compound with a single chlorine atom, with a ratio of 3 between the ions at  $m/z$  309 and 311. For a total of 249 injections, including both standards and extracts, the relative standard deviation of the observed ratio (mean 2.97) was 9%, giving an indication of the measurement precision of the mass spectrometer.

Calibration curves for standards in methanol–water were found to be linear over the 0.025–1.0 ng/ $\mu$ l range (Fig. 5). Over a 5-week period, during which time the high voltage electrode and skimmer cone were cleaned several times, the mean correlation coefficient was 0.993 with a standard deviation of 0.020 ( $n = 18$ ). However, the sensitivity on different occasions varied considerably, the extremes differing by a factor of

30. In the absence of an internal standard frequent recalibration was thus essential.

The calibration obtained when using standards prepared in matrix extracts was examined on two separate occasions and was also found to be linear (correlation coefficients of 0.994 and 0.988). Differences in slope were observed compared with calibrations using methanol–water solutions, but on one occasion the slope was greater (ratio 1.3) and on the other less (ratio 0.84) than the slope from the solvent standards. In view of this, and since the series compared were analysed consecutively and not interspersed, we believe the difference in slope reflects changes in instrument sensitivity rather than an effect attributable to the presence of co-extractives.

The use of methanol–water or matrix extract standards was found to influence precision. Thus

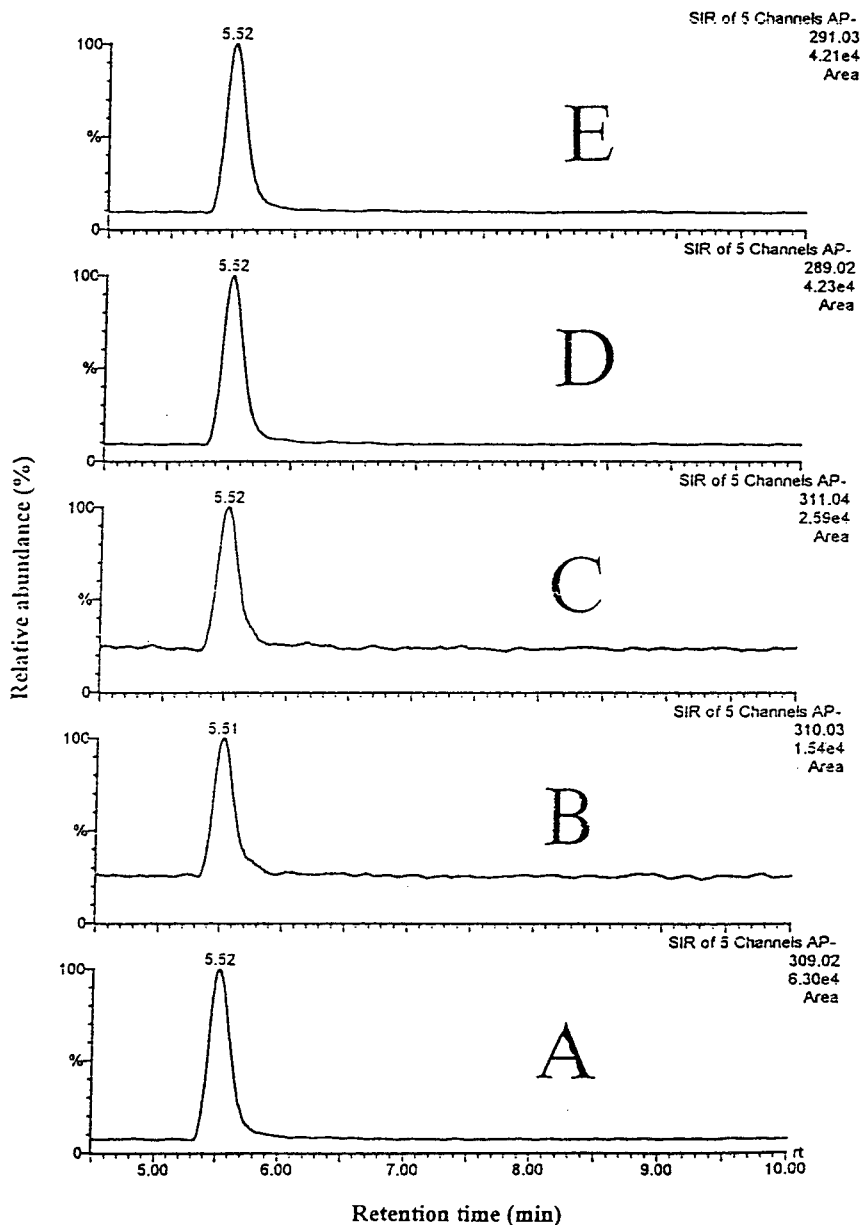


Fig. 4. The five ions monitored by SIM in a 0.10 ng/ $\mu$ l diflubenzuron standard prepared in methanol–water (80:20) mobile phase. (A)  $m/z$  309, (B)  $m/z$  310, (C)  $m/z$  311, (D)  $m/z$  289, (E)  $m/z$  291.

the relative standard deviation at the 0.10 ng/ $\mu$ l level for standards prepared in solvent was 3% ( $n = 9$ ) but for the same concentration in matrix extract was higher at 8% ( $n = 9$ ). Consequently

solvent-based standards were used throughout to quantitate the extracts.

Having established linearity, quantitation of extracts was routinely based on calibrations

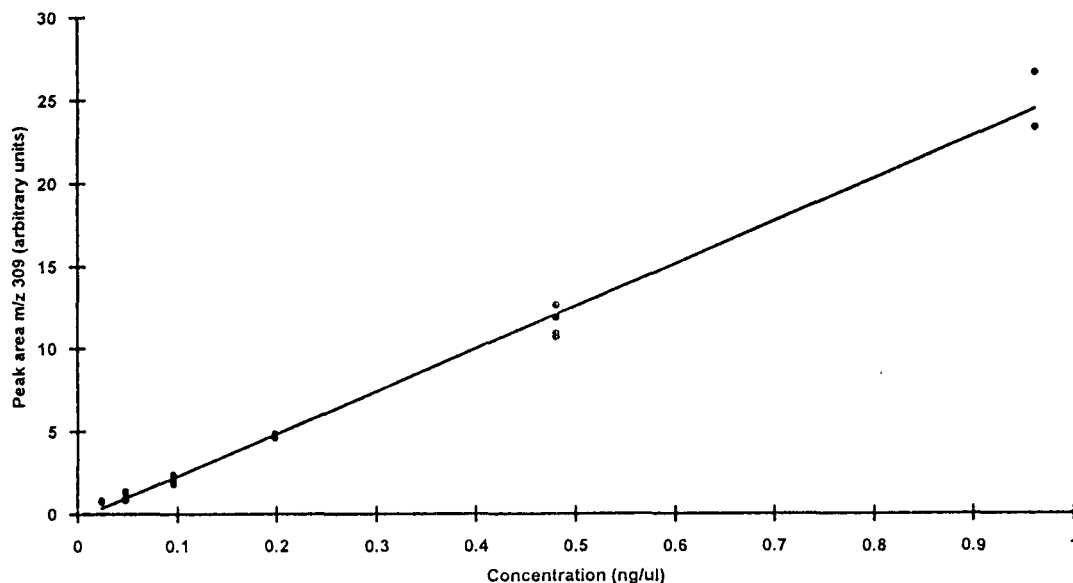


Fig. 5. Calibration of peak area ( $m/z$  309) over the concentration range 0.025–1.0  $\text{ng}/\mu\text{l}$ .

derived from standards in methanol–water at concentrations of 0.05, 0.20 and 0.50  $\text{ng}/\mu\text{l}$  which were analysed before and after each batch of extracts (typically 10). The mean slope was used in calculations unless large deviations between the two sets of standards were observed, in which case the whole batch was re-analysed.

For quality control additional diflubenzuron standards (0.025–0.50  $\text{ng}/\mu\text{l}$  in methanol–water) were also analysed at intervals. Over a 5-week period the measured concentrations had a mean of 96% of the theoretical value ( $n = 35$ ), corresponding to a bias of  $-4\%$ , and a relative standard deviation of 11%, thus demonstrating good accuracy and precision. The mean of results for standards prepared in blank extract was 92% of their theoretical value ( $n = 20$ ), corresponding to a greater bias of  $-8\%$ , and a relative standard deviation of 10%. Both sets of data were quantified from solvent standard calibrations and the accuracy of the results for the extract standards justifies the decision to use solvent based standards for quantitation.

Extrapolation based on a number of determinations of the 0.05  $\text{ng}/\mu\text{l}$  standard prepared in

blank extract gave a limit of detection (LOD) of 0.017  $\text{ng}/\mu\text{l}$  [3 times the total standard deviation ( $n = 14$ )] which is equivalent to 0.0142  $\text{mg}/\text{kg}$  in the crop with the extraction method employed and assuming 100% recovery. This theoretical LOD was consistent with the observed response for a 0.025  $\text{ng}/\mu\text{l}$  extract standard.

Fig. 6 shows the channel for the diflubenzuron  $[\text{M} - \text{H}]^-$  ion at  $m/z$  309 for 0.06, 0.12, 0.23 and 0.58  $\text{mg}/\text{kg}$  spiked extracts and for an extract blank.

The recovery of diflubenzuron spiked into mushrooms before extraction at concentrations from 0.06  $\text{mg}/\text{kg}$  to 0.58  $\text{mg}/\text{kg}$  was assessed in a series of seven replicate extraction batches (Table 1). The mean recovery was 85.5% with a relative standard deviation of 14.5% ( $n = 56$ ). Allowing for recovery the average limit of detection of the method was 0.017  $\text{mg}/\text{kg}$  in the crop.

#### 4. Conclusions

This HPLC–APCI–MS method relies for quantitation on the deprotonated molecule of

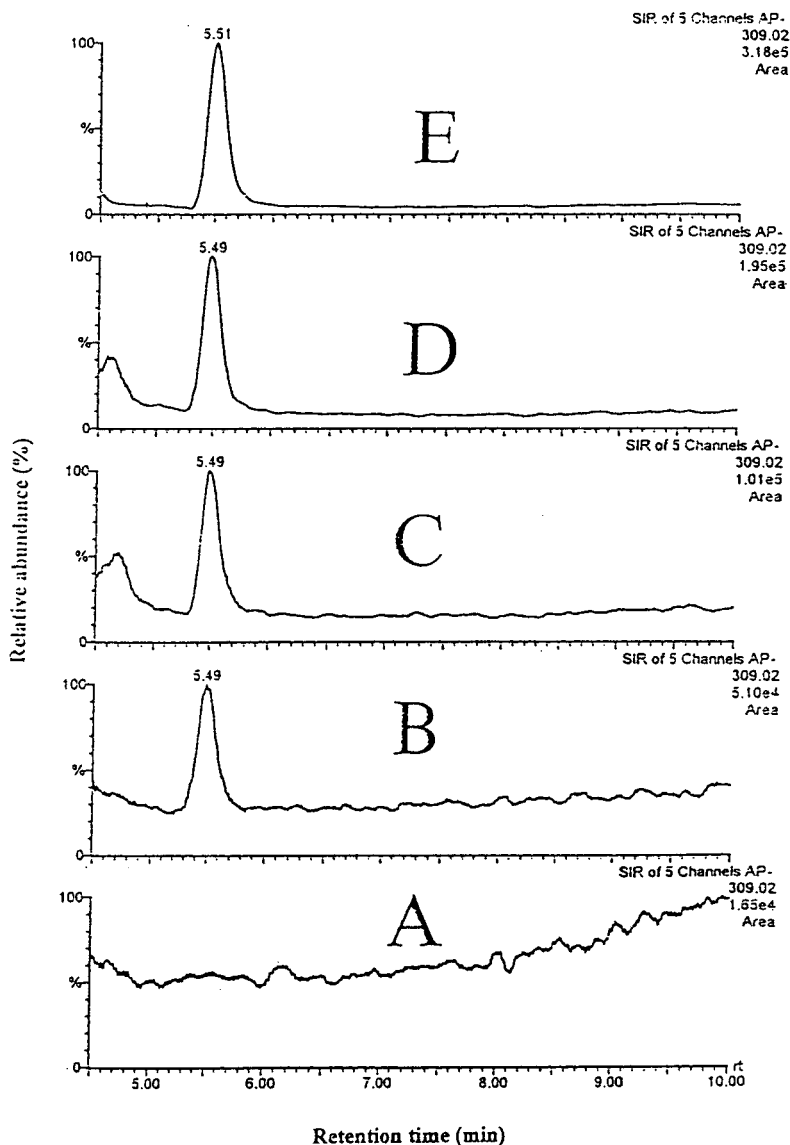


Fig. 6. The diflubenzuron  $[M-H]^-$  ion at  $m/z$  309 for an extract blank and spiked extracts. (A) Extract blank, (B) 0.06 mg/kg spike, (C) 0.12 mg/kg spike, (D) 0.23 mg/kg spike, (E) 0.58 mg/kg spike.

diflubenzuron which is the base peak of the scanned spectrum. This has the advantage over previously described GC and TSP methods which rely on either fragment ions or non-base peak ions for quantitation. The limit of detection is an order of magnitude better than that obtained by HPLC–TSP–MS, and six times less than the MRL. Once optimised, tuning was

found to be stable and data have been acquired for up to 72 h non-stop. Some changes in sensitivity were encountered over time but this was adequately compensated for by frequent calibration. For the determination of diflubenzuron in mushroom extracts this HPLC–APCI–MS method has proven robust with suitable accuracy and precision.

Table 1  
Recovery of diflubenzuron from spiked mushrooms determined at four concentrations and in seven separate extraction batches

Spiking concentration (mg/kg)	Trial No.	Extraction batch							Between batch	
		1	2	3	4	5	6	7	Mean	R.S.D. (%)
0.06	1	78.4	107.0	98.5	77.9	76.8	86.6	85.3	88.8	10.7
	2	93.5	86.3	96.6	74.1	63.4	99.8	93.2	88.1	12.3
0.12	1	76.2	78.0	107.3	86.8	91.0	120.2	99.7	94.1	14.8
	2	72.7	80.0	115.9	79.5	84.5	102.7	91.3	89.6	14.0
0.23	1	53.0	75.0	88.6	60.4	88.3	91.8	103.1	79.6	16.7
	2	58.7	71.0	90.5	59.3	82.3	87.7	101.5	78.4	15.1
0.58	1	80.1	69.6	106.0	84.9	83.7	96.9	72.8	84.0	11.9
	2	80.5	65.9	106.0	82.7	77.6	94.0	74.6	82.2	12.2
Within-batch	Mean	74.1	79.1	101.2	75.7	81.0	97.5	90.2		
Within-batch	R.S.D. (%)	12.9	13.0	9.3	10.6	8.6	10.8	11.7		

A single extract of each spiking concentration was prepared in each batch and analysed in duplicate ( Trial 1 or 2 ). The overall mean recovery was 85.5% with a relative standard deviation of 14.5%

## References

- [1] J.J. Van Daalen, J. Meltzer, R. Mulder and K. Wellinga, *Naturwissenschaften*, 59 (1972) 312.
- [2] K. Wellinga, R. Mulder and J.J. Van Daalen, *J. Agric. Food Chem.*, 21 (1973) 348.
- [3] K. Wellinga, R. Mulder and J.J. Van Daalen, *J. Agric. Food Chem.*, 21 (1973) 993.
- [4] C.R. Worthing and R.J. Hance (Editors), *The Pesticide Manual, A World Compendium*, The British Crop Protection Council, 9th ed., 1991, pp. 281–282.
- [5] M.J. Wimmer, R.R. Smith and J.P. Jones, *J. Agric. Food Chem.*, 39 (1991) 280–286.
- [6] M.T. Ahmed and A.H. Eid, *Nahrung*, 35 (1991) 27–31.
- [7] K.M.S. Sundaram and R. Nott, *J. Liq. Chromatogr.*, 12 (1989) 2333–2343.
- [8] P. Singh, B. Singh, K.K. Chahal and R.L. Kalra, *J. Insect Sci.*, 4 (1991) 182–184.
- [9] S.J.D. Prima, R.D. Cannizaro, J.C. Roger and C.D. Ferrell, *J. Agric. Food Chem.*, 26 (1978) 968–971.
- [10] G.E. Spates and J.E. Wright, *J. Econ. Entomol.*, 73 (1980) 595–598.
- [11] J.P.G. Wilkins, *Anal. Proc.*, 30 (1993) 396–397.
- [12] S. Pleasance, J.F. Anacleto, M.R. Bailey and D.H. North, *J. Am. Soc. Mass Spectrom.*, 3 (1992) 378–397.
- [13] S. Kawasaki, F. Nagumo, H. Ueda, Y. Tajima, M. Sano and J. Tadano, *J. Chromatogr.*, 620 (1993) 61–71.
- [14] S. Bajic, D.R. Doerge, S. Lowes and S. Preece, *Am. Laboratory*, 25 (1993) 40B.
- [15] A.R.C. Hill, CSL Harpenden UK, personal communication (unpublished).
- [16] Status of Codex Maximum Residue Limits for Pesticides in Food and Animal Feed, Codex Alimentarius Commission, Joint FAO/WHO Food Standards Programme CX/PR 2-1993.
- [17] A. Andersson and H. Palsheden, *Fresenius J. Anal. Chem.*, 339 (1991) 365–367.
- [18] S. Kawasaki, H. Ueda, H. Itoh and J. Tadano, *J. Chromatogr.*, 595 (1992) 193–202.







ELSEVIER

Journal of Chromatography A, 712 (1995) 95–101

JOURNAL OF  
CHROMATOGRAPHY A

# Identification of diflubenzuron by packed-capillary supercritical fluid chromatography–mass spectrometry with electron-capture negative ionization

Cato Brede, Elsa Lundanes\*

*Department of Chemistry, University of Oslo, P.O. Box 1033, Blindern, 0315 Oslo, Norway*

## Abstract

The thermolabile insecticide diflubenzuron [1-(4-chlorophenyl)-3-(2,6-difluorobenzoyl)urea] was successfully chromatographed by supercritical fluid chromatography on a 320  $\mu\text{m}$  I.D. Inertsil  $\text{C}_8$  column using neat carbon dioxide as mobile phase.

Detection and electron-capture negative ionization (ECNI) mass spectrometric characterization were accomplished using a double focusing mass spectrometer with a modified ion source and coaxial direct fluid introduction. Detection limits of 1.0  $\mu\text{g}/\text{ml}$  and 0.03  $\mu\text{g}/\text{ml}$  were obtained in full-scan and selected-ion monitoring (SIM) mode, respectively. The restrictor heater temperature was found to have a major influence on the signal intensity and fragmentation pattern, as thermal degradation was believed to take place or be initiated on the hot restrictor wall. The relative abundance of the molecular ion amounted to 100% using restrictor temperatures of 160°C and 170°C, while it was completely absent at 190°C. At the lower temperatures,  $[\text{M} - \text{HF}]^{-\bullet}$  was the most significant fragment ion.

## 1. Introduction

Diflubenzuron [1-(4-chlorophenyl)-3-(2,6-difluorobenzoyl) urea] is a thermolabile insect growth regulator [1] and direct determination by gas chromatography is impossible due to thermal degradation [2]. The methods available for direct quantitation are based upon high-performance liquid chromatography (HPLC) with UV detection [3]. However, due to the non-specific detection, long clean-up procedures are often required. Gas chromatographic methods including derivatization and subsequent electron capture, as well as nitrogen–phosphorus or mass spectrometric detection have been used for quantifi-

cation [4–6]. Diflubenzuron has also been quantified by a GC–MS method using deuterated diflubenzuron as internal standard, by quantitation of the heat decomposition products [2].

However, methods including direct compound identification as well as quantitation are preferable. Supercritical fluid chromatography (SFC) has been recognized as a potential technique for the determination of thermolabile pesticides [7–9]. The combination SFC–MS has been shown to be applicable for the identification of different pesticides [10–13]. This work focuses primarily upon the possibility of using SFC–MS for the determination of diflubenzuron. Due to the limitations of the MS, relatively small volumetric flow-rates are allowed in the SFC system. Thus, packed capillary columns appear to be the col-

\* Corresponding author.

umn of choice because of their higher sample loadability as compared to open capillary columns. High sample loadability is important since low concentrations are expected to be present in real samples. Determination of diflubenzuron in real samples usually requires a sample preparation step including preconcentration and purification; however, this was not the subject of our work.

The halogen-containing diflubenzuron should be applicable to negative-ion detection in the MS. The rate constant for ion formation in EC depends strongly on the collision cross-section and can exceed  $10^{-7} \text{ cm}^3 \text{ s}^{-1}$  for polyhalogenated compounds [14]. In such cases, sensitivity might be 100 times better as compared to positive chemical ionization (PCI). ECNI was therefore our choice for detection.

Since the standard ion source for electron ionization (EI) and chemical ionization (CI) was found to be unsatisfactory for negative-ion detection [13], the second aim of this study was to design a better interface-ion source system for negative-ion detection in SFC-MS

## 2. Experimental

### 2.1. Chemicals

Both packing and chromatography were performed using neat  $\text{CO}_2$  (99.998%) supplied by Aga Norgas (Oslo, Norway). The solvents used were  $\text{CS}_2$  (>99.0%) from J.T. Baker Chemicals (Deventer, Netherlands), HPLC grade tetrahydrofuran (THF) (Rathburn, Walkerburn, UK) and pro-analysis grade formamide (Merck, Darmstadt, Germany). The THF was filtered through aluminium oxide prior to use. Potassium silicate solution was purchased from Kebo Lab. (Oslo, Norway). Analytical grade diflubenzuron was obtained from the Agricultural University of Norway (Aas, Norway) and dissolved in THF or  $\text{CS}_2$ . MS-calibration was carried out using low boiling perfluorokerosene (PFK) (Tokyo Kasei, Japan).

### 2.2. Columns and restrictors

Fused-silica 320  $\mu\text{m}$  I.D. and 450  $\mu\text{m}$  O.D. from Polymicro Tech. (Composite Metal Services, UK) was used for the columns. The packing material was 5  $\mu\text{m}$  silica-based Inertsil  $\text{C}_8$  (Keystone, USA) or 4  $\mu\text{m}$  Nova-Pak  $\text{C}_{18}$  (Waters, USA). Both columns were 60 cm long and prepared in the laboratory, according to the method described by Malik et al. [15]. A 2-mm ceramic frit was used at the outlet of the column. Valco zero dead volume unions (1/16 in. to 1/16 in.) and one piece fused-silica adapter ferrules were utilized for column fitting.

The integral restrictor [16] was made from fused-silica capillary (I.D. 50  $\mu\text{m}$ , O.D. 365  $\mu\text{m}$ ). For the purpose of fast analyses, a flow was chosen that gave a  $t_0$  value of ca. 3–4 min at 100 bar of pump pressure.

### 2.3. Instrumentation

Supercritical fluid chromatography was performed with a Model 602 system from Lee Scientific (Salt Lake City, UT, USA). A CI4W injector from Valco Instruments (Houston, TX, USA), equipped with a 0.2- $\mu\text{l}$  loop, was used with timed split injection at room temperature. A small piece of fused-silica capillary (I.D. 50  $\mu\text{m}$ ) was used to connect the column to the injector. In order to prevent backflushing of packing material, a small stainless-steel frit (No. 24000, Keystone Scientific) was placed in the union connected to the column entrance. The whole column was kept in the oven at a constant temperature of 60°C. The restrictor was attached directly to the column end union.

The mass spectrometer used for detection was a JMS-DX303 from JEOL (Tokyo, Japan). It is a double focusing instrument with EB-geometry. Ion detection was done by the ion multiplier equipped with a 10-kV post-acceleration conversion dynode unit. Detector sensitivity adjustments were kept constant while performing these experiments, making it possible to compare results. The ion source pressure, as referred to in this work, was actually the pressure measured by

a gauge placed some distance from the ion source. The pressure inside the ion source was considerably higher, since the ion source was made as small and sealed as possible. Cryopumping was used in all experiments. The modified CI ion source, made at the institute, had a channel drilled through its metal block. To achieve cooling, nitrogen gas, at room temperature and slightly above ambient pressure, was led through this channel. An even lower ion source temperature was reached by precooling the nitrogen in a copper tube placed in a mixture of methanol and dry ice at  $-77^{\circ}\text{C}$ .

Direct fluid introduction (DFI) was made possible by designing a simple restrictor heating interface (Fig. 1), consisting of a 4-cm steel tubing (I.D. 1.0 mm) containing both the restrictor and an insulated heater. Two pieces of fused-silica capillary were used to insulate the thermowire applied as heater. The fluid was allowed to enter the ion source coaxially, toward the analyzer, by making the DFI-interface a part of the repeller (Fig. 2). The ion source side entrance was plugged with a Teflon-insulated thermocouple, making accurate ion source temperature measurements possible. The thermocouple tip was placed less than 1 mm inside the ion source. The LC controller of the MS supplied the electric current for the heater and restrictor temperature monitoring (at the outside of the stainless-steel tubing). The heat from the filament generally kept a stable ion source temperature of  $150^{\circ}\text{C}$ , when no cooling gas was added.

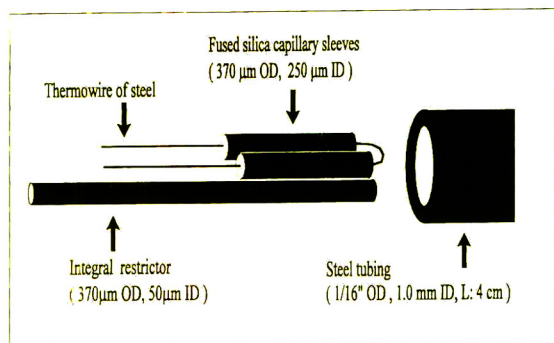


Fig. 1. Restrictor heater.

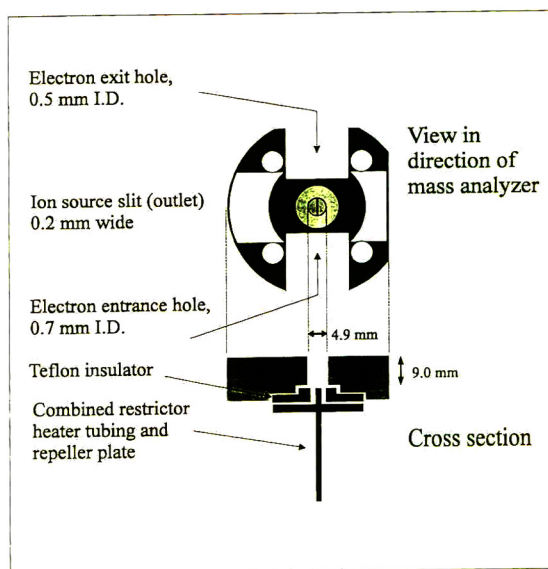


Fig. 2. Modified ion source (not to scale).

A rhenium filament was used, despite the background  $\text{ReO}_3^-$  and  $\text{ReO}_4^-$  ions associated with it. Rhenium was preferred instead of thoriated irridium [13], because of its relative low cost and ease of replacement. The internal diameter of the electron entrance hole was increased from 0.5 to 0.7 mm in order to make filament positioning less critical. The effect of this modification on detector sensitivity was not examined. A  $100\text{-}\mu\text{A}$  ionization current was set, and electrons accelerated through 230 V. The repeller voltage was kept at 0 V.

The resolution, at 25% valley, was kept at 500 throughout. The cycle and scan times were set to 2.3 and 2.0 s, respectively, with a  $m/z$  range of 10 to 500 in full-scan mode.

### 3. Results and discussion

#### 3.1. Chromatography.

Since diflubenzuron is capable of forming hydrogen bonds with free silanol groups, an inert packing material was sought. An inert packing material is also of importance when analyzing

real samples containing other components which can adsorb irreversibly to silanol groups and change the stationary phase characteristics. The highly endcapped  $C_8$  Inertsil and Nova-Pak  $C_{18}$  materials were examined for the determination of diflubenzuron. As shown in Fig. 3, the chromatography of diflubenzuron on the  $C_8$  Inertsil material is acceptable, avoiding the need for a modified  $CO_2$  mobile phase. In fact, the addition of 5% (w/w) methanol to the  $CO_2$ , resulted in up to 100-fold reduction of the MS detection sensitivity for some halogenated compounds. A reduction was also observed for diflubenzuron. The Nova-Pak  $C_{18}$  material also seemed to be sufficiently deactivated for chromatography of diflubenzuron with neat  $CO_2$ . The  $C_8$  group on Inertsil provided a decrease in retention compared to the Nova-Pak  $C_{18}$  material (data not shown), leading to shorter analysis time and elution at a lower pressure and was therefore preferred.

Using SFC with flame ionization detection an acceptable reduced plate height of about 7 was obtained for anthracene at  $k$  values of 4-5 on these columns. Evaluation of columns prepared by this method has been done recently by Tong et al. [17]. They have reported a reduced plate height as low as 2.33. This indicates the potential of such columns for separation of complex mixtures. As we did, they also found the columns to

be very stable. No void volume was observed at the column entrance, even after months of use.

With the high flow-rate required to obtain fast elution on these columns, the ion source pressure was higher than the optimum value, which was about  $5 \cdot 10^{-6}$  Torr at the gauge.

### 3.2. Detection

Preliminary experiments included cooling of the modified ion source to study the effect of temperature upon signal response since lower temperatures were previously shown to be beneficial for the detection of some chlorinated pesticides [13]. However with 1-chloroanthracene, 9,10-dichloroanthracene, hexachlorobenzene and 2,3-dichloronaphthoquinone a small decrease in peak heights measured on the molecular ion RIC (reconstructed ion current) chromatogram was observed, when reducing the ion source temperature from 150° to 100°C (data not shown). The detection of diflubenzuron was therefore performed at 150°C, since lowering the ion source temperature was not believed to seriously affect sensitivity and since cooling was avoided.

The modified ion source also provided the possibility of comparing the effect on signal response of two different introduction angles, either from the left side or coaxially. When introducing the fluid coaxially, toward the ana-

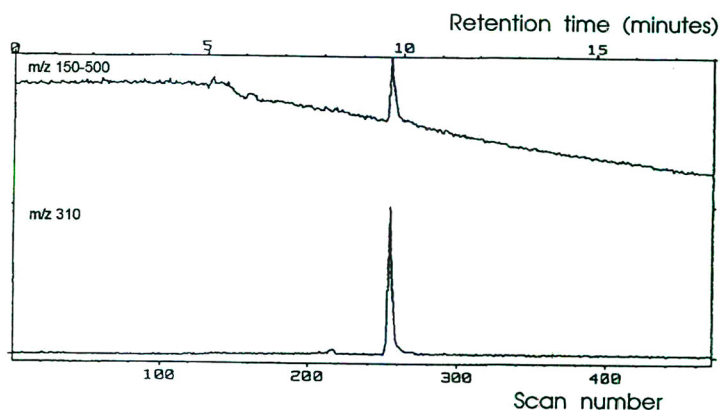


Fig. 3. RIC chromatograms of diflubenzuron on 5  $\mu$ m Inertsil  $C_8$  with EC detection. About 50 nl of a 0.05 mg/ml solution was injected. SFC conditions: column temperature 60°C and pressure programming 100 bar (3 min), then increased from 100 bar to 250 bar at 10 bar/min (linear gradient). MS conditions, see text. Restrictor temperature 160°C.

lyzer, increased molecular ion signals were generally found for the halogenated compounds investigated. This was therefore the preferred method.

A sufficient heating of the restrictor is vital for the success of any SFC system, since it prevents restrictor plugging and gives a stable flow. The mass spectrum of diflubenzuron in ECNI-MS turned out to be quite dependent on the restrictor temperature. The mass spectra at restrictor temperatures of 190°C (Fig. 4a) and 170°C (Fig. 4b) revealed a large degree of fragmentation in the former case and the molecular ion ( $m/z$  310) was completely absent at 190°C. However, some of these fragment ions were suspected to be due to thermal degradation products.

Pathways for the thermal degradation of diflubenzuron have been reported in the literature [2]. Some of these thermal degradation products were detected by EC using a restrictor temperature of 190°C (Fig. 4a); the  $m/z$  156 and 157 ions can be assigned to difluorobenzamide. The  $m/z$  156 was the most abundant of the two and would likely be due to detachment of a hydrogen radical. The ion  $m/z$  183, present at a lower abundance, probably corresponds to 2,6-difluorobenzoyl-isocyanate. Ions corresponding to the thermal degradation products 4-chloroaniline and 4-chlorophenylisocyanate were not observed, perhaps as a result of chloride anion detachment, as indicated by  $m/z$  35/37.

The fragment ion  $[M - HF]^{-\bullet}$  at  $m/z$  290

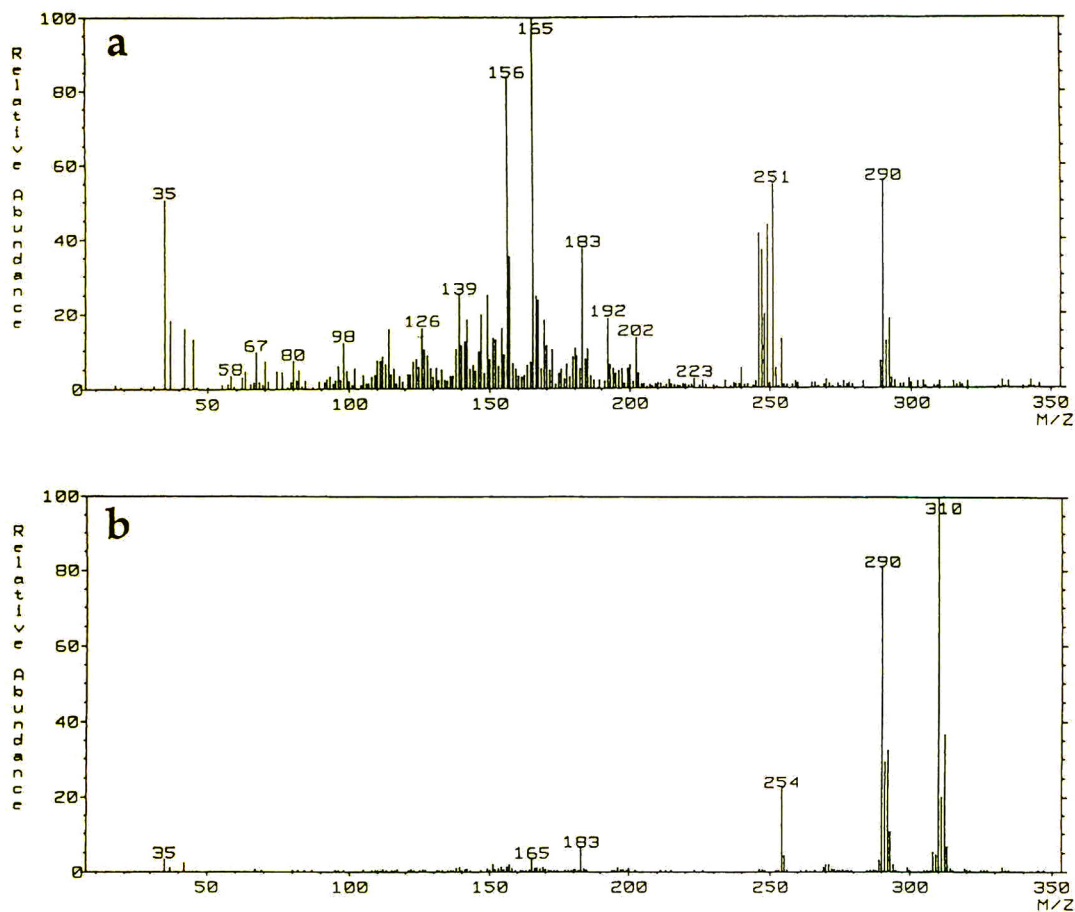


Fig. 4. The mass spectra of diflubenzuron at restrictor temperature of (a) 190°C, and (b) 170°C.

results from loss of neutral HF from the molecule. The reaction mechanism for this process could be via a ring formation. The large intensity of  $m/z$  165 could be due to a similar mechanism to produce the molecule shown in Fig. 5b. As expected, no chloride patterns were found for the  $m/z$  156, 165 and 183 ions. The  $m/z$  246–248 remain unidentified. The ions at 249 and 251 may be assigned to rhenium oxide from the filament.

At lower restrictor temperature (170°C) the mass spectrum was dominated by  $[M]^{-\bullet}$  and  $[M - HF]^{-\bullet}$  (Fig. 4b). Almost no chloride was observed in the mass spectra. The  $m/z$  254 may originate from a  $[M - HF - HCl]^{-\bullet}$  fragment. By comparing the RIC chromatograms of the above-mentioned  $m/z$  values, it was observed that the peak maxima of  $m/z$  35/37, 156, 165 and 183 were slightly delayed compared to  $m/z$  310, 290 and 254. A delay may be explained by the laminar flow through the heated zone and decomposition of diflubenzuron at the hot wall of the restrictor. This indicates that  $m/z$  156, 165 and 183 originate from thermal decomposition occurring in the heated zone of the restrictor. Since  $m/z$  290 and 254 have peak maxima identical to  $M^{-\bullet}$ , these fragment ions may be produced in the ion source. However, the possibility of these ions being formed by thermolysis must be considered.

The sensitivity was also found to be strongly dependent on restrictor temperature. Increased TIC (total ion current) peak heights with lower restrictor temperatures were found (Fig. 6). This would partly be explained if the degradation

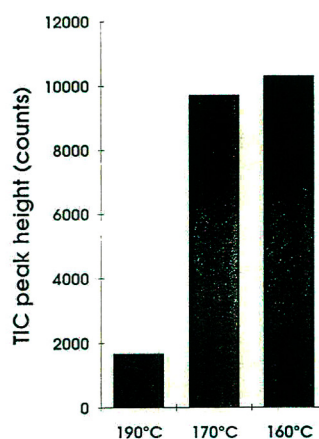


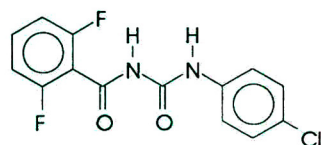
Fig. 6. TIC peak heights of diflubenzuron at three different restrictor temperatures.

products had a total cross-section for the EC processes which was lower than that of the analyte itself, thus producing a weaker total ion current. Another possibility is the effect of restrictor temperature on  $CO_2$  cluster formation and production of fewer thermalized electrons.

The minimum detectable amount of diflubenzuron was estimated to be 100 pg and 3 pg injected onto the column in full-scan and SIM mode, respectively, using a signal-to-noise ratio of 3. This corresponds to detection limits of 1.0  $\mu g/ml$  and 0.03  $\mu g/ml$ .

Less thermal degradation and lower limit of detection (LOD) might be achieved by heating only the part of the restrictor where adiabatic expansion finds place. A restrictor heater with a more local heat zone would therefore be suitable. Such devices have been designed and used elsewhere [18,19].

a)



Diflubenzuron, MW: 310.7

b)

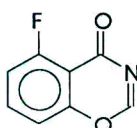


Fig. 5. Diflubenzuron (a) and a possible structure for the main decomposition product at 190°C restrictor temperature (b).

#### 4. Conclusions

Neat  $CO_2$  can be used as the mobile phase for the chromatography of diflubenzuron on the highly deactivated Inertsil  $C_8$  packing material. Ionization and detection by ECNI was obtained utilizing the mobile phase  $CO_2$  as moderating gas. Generally lower limits of detection were observed using the modified ion source with

coaxial introduction used in this work compared to the earlier design [13].

The detection limits for diflubenzuron obtained in this work are not as low as those obtained by HPLC [3], mainly due to the lower acceptable sample introduction volume. However, the much better selectivity as well as the possibility of compound confirmation makes SFC–MS a promising complementary method for the determination of diflubenzuron in different samples.

The restrictor temperature was found to have a major effect on the signal intensity (TIC) and fragmentation pattern. To obtain molecular ions, a restrictor temperature of 160–170°C was found to be suitable for the detection of diflubenzuron using an ion source temperature of 150°C. The additional fragment ions observed at this restrictor temperature are advantageous for identification.

## References

- [1] B. Rabenort, P.C. de Wilde, F.G. de Boer, P.K. Korver, S.J. DiPrima and R.D. Cannizzaro, in G. Zweig and J. Sherma (Editors), *Analytical Methods for Pesticides and Plant Growth Regulators*, Academic Press, New York, NY, 1978, p. 57.
- [2] M.J. Wimmer, R.R. Smith and J.P. Jones, *J. Agric. Food Chem.*, 39 (1991) 280.
- [3] K.M.S. Sundaram and R. Nott, *J. Liq. Chromatogr.*, 12 (1989) 2333.
- [4] H.-J. Stan and P. Klaffenbach, *Fresenius J. Anal. Chem.*, 339 (1991) 40.
- [5] B.L. Worobey and G.R.B. Webster, *J. Assoc. Off. Anal. Chem.*, 60 (1977) 213.
- [6] F.P.M. Karg, *J. Chromatogr.*, 634 (1993) 87.
- [7] B.N. Zegers, A.C. Hagenboom, S.E.G. Dekkers, H. Lingeman and U.A.Th. Brinkman, *J. Microcol. Sep.*, 6 (1994) 55.
- [8] T.A. Berger, W.H. Wilson and J.F. Deye, *J. Chromatogr. Sci.*, 32 (1994) 179.
- [9] T.A. Berger, *J. Chromatogr. Sci.*, 32 (1994) 25.
- [10] H.T. Kalinoski and R.D. Smith, *Anal. Chem.*, 60 (1988) 529.
- [11] E.C. Huang, B.J. Jackson, K.E. Markides and M.L. Lee, *J. Microcol. Sep.*, 2 (1990) 88.
- [12] R.J. Houben, P.A. Leclercq and C.A. Cramers, *J. Chromatogr.*, 554 (1991) 351.
- [13] A. Jablonska, M. Hansen, D. Ekeberg and E. Lundanes, *J. Chromatogr.*, 647 (1993) 341.
- [14] H. Budzikiewicz, *Mass Spectrom. Rev.*, 5 (1986) 345.
- [15] A. Malik, W. Li and M.L. Lee, *J. Microcol. Sep.*, 5 (1993) 361.
- [16] E.J. Guthrie and H.E. Schwartz, *J. Chromatogr. Sci.*, 24 (1986) 236.
- [17] D. Tong, K.D. Bartle and A.A. Clifford, *J. Microcol. Sep.*, 6 (1994) 249.
- [18] E.C. Huang, B.J. Jackson, K.E. Markides and M.L. Lee, *Anal. Chem.*, 60 (1988) 2715.
- [19] V.N. Reinhold, D.M. Sheeley, J. Kuei and G.-R. Her, *Anal. Chem.*, 60 (1988) 2719.





# Determination of organophosphorus pesticides and their transformation products in river waters by automated on-line solid-phase extraction followed by thermospray liquid chromatography–mass spectrometry

S. Lacorte\*, D. Barceló

*Department of Environmental Chemistry, CID-CSIC, c/Jordi Girona 18–26, 08034 Barcelona, Spain*

## Abstract

The trace-level determination of ten priority organophosphorus (OP) pesticides (e.g. chlorpyrifos-methyl, diazinon, disulfoton, fenthion, fenamiphos) and various transformation products (TPs; e.g. disulfoton sulfoxide, fenthion sulfoxide etc.) using automated on-line solid-phase extraction (SPE) with  $C_{18}$  precolumns followed by LC–MS and thermospray interface with time-scheduled selected-ion monitoring (SIM) was developed.

Two main ions (usually  $[M + H]^+$  and  $[M + NH_4]^+$  or  $[M + CH_3CN]^+$ ) were used for each pesticide in the positive ion (PI) detection mode, while  $[M - H]^-$  and  $[M + HCOO]^-$  ions were used in the negative ion (NI) mode. The proposed method requires 100 ml of sample for a limit of detection (LOD) of 0.01–0.1  $\mu\text{g/l}$ . Calibration graphs were constructed by preconcentrating 100 ml of water spiked with the pesticide mixture at various concentrations (from 0.025 to 2  $\mu\text{g/l}$ ). Good linearity was observed for most of the analytes studied.

The experimental setup described in this paper was applied to study the kinetics of degradation of ten organophosphorus pesticides in spiked river water samples. The different samples were first analyzed by an automated on-line precolumn exchange system (OSP-2) followed by LC with diode array detection. To confirm the identity of the organophosphorus pesticides detected, the samples were then analyzed by automated on-line SPE–LC–MS. The method permitted unequivocal identification of many of the TPs formed during the experiments, e.g. the oxo-derivatives of chlorpyrifos-methyl, temephos and pyridafenthion, fenamiphos sulfoxide. Many of these TPs are here reported for the first time since previously used MS-based techniques were not sensitive enough.

## 1. Introduction

The determination of organophosphorus (OP) pesticides is of concern because of their extensive use as insecticides in different types of cultivation, e.g. rice [1], and their use in

the elimination of pests [2]. Residue levels of OP pesticides such as pyridafenthion and fenitrothion have been reported in environmental matrices [3,4]. These compounds can persist in the environment for several days, and biotic and abiotic degradation can occur [5], with the subsequent formation of various transformation products (TPs). Such TPs may be more toxic than the parent compounds [6], and therefore,

\* Corresponding author.

pesticide degradation and their stability in the environment are becoming study subjects of increasing interest. Proof that OP pesticides are of concern is their inclusion in different water monitoring programs such as the National Pesticide Survey (NPS) and the Commission of the European Communities (CEC). In this respect, the CEC 76/464/EEC council directive list of pesticides to be monitored in the aquatic environment includes different OP pesticides, e.g., parathion, methyl-azinphos, fenitrothion, demeton, fenthion, and malathion.

On-line solid-phase extraction (SPE) techniques coupled to liquid chromatography and thermospray mass spectrometry (LC-TSP-MS) are currently applied for the determination of different pesticide groups, including organophosphorus [7], triazines [8,9], and chlorinated phenoxyacids [9,10], in different environmental water matrices. Up to now, no studies dealing with the coupling of on-line SPE followed by LC-TSP-MS for the trace determination of OP pesticides in water samples have been reported.

In our Department, we are also particularly interested in following the degradation of OP pesticides in river waters in order to measure the degradation kinetics and half-lives of pesticides under real environmental conditions [1,4]. In this respect, on-line SPE-LC-TSP-MS is a useful technique for the confirmation of unknown pesticide TPs formed during the degradation experiments.

The objectives of the present paper are: (i) the development of an on-line SPE-LC-TSP-MS method for the direct determination of trace levels of OP pesticides in water samples and the establishment of analytical parameters such as linearity and limit of detection of the analytical method, and (ii) the application of the on-line method to the quantitation of OP pesticides in river waters submitted to natural degradation with special emphasis on the degradation products formed, such as sulfoxide and oxo-metabolites. The information obtained by the developed on-line system will be of interest to environmental water analysis.

## 2. Experimental

### 2.1. Chemicals

HPLC grade water, acetonitrile, and methanol (Baker, Deventer, Netherlands) were filtered through a 0.45- $\mu\text{m}$  filter before use. Ammonium formate was purchased from Fluka (Buchs, Switzerland). Chlorpyrifos-methyl, diazinon, disulfoton, fenamiphos, fenthion, isofenphos, malathion, metidathion, pyridafenthion, and temephos were obtained from Promochem (Wesel, Germany).

### 2.2. Chromatographic conditions

The eluent was delivered by two Model 510 high-pressure pumps coupled to a Model 680 automated gradient controller (Waters, Milford, MA, USA). The automated SPE device (OSP-2, Merck, Darmstadt, Germany) was connected on-line with the gradient pumps. The OSP-2 consists of a cartridge magazine containing the precolumns, which are held in a ring. Two electrically operated six-port switching valves are arranged in such a way that preconcentration is carried out in the preparation clamp, and afterwards the ring rotates so that the precolumn is transferred to the elution position, and the analytes are desorbed (Fig. 1). A LiChroGraph Model L-6200A intelligent pump (Merck-Hitachi) was used to deliver the solvents to condition the precolumns and the water that contained the pesticides. The precolumns were conditioned by flushing 10 ml of methanol and then 10 ml of HPLC grade water at 1 ml/min. Water volumes of 100 ml spiked with pesticides were preconcentrated on disposable precolumns (Merck, Darmstadt, Germany) prepacked with 10  $\mu\text{m}$  LiChrospher Si100 RP-18. Prior to SPE, river water samples were filtered through 0.45- $\mu\text{m}$  filters (Millipore) to remove suspended matter.

A Superspher cartridge column (250  $\times$  4 mm I.D.) packed with 4  $\mu\text{m}$  Superspher C<sub>8</sub> (Merck) was used. The LC mobile phase was acetonitrile-water with 0.05 M ammonium formate with

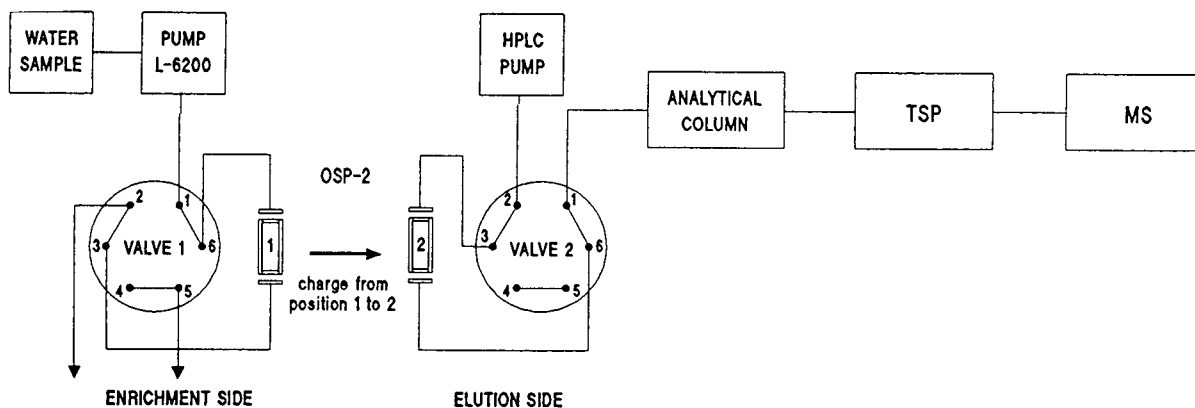


Fig. 1. General diagram of the system used for on-line preconcentration and determination of pesticides in water samples.

the following gradient: from 15:85 (v/v) to 30:70 (v/v) in 15 min, and from there to 90:10 in 15 min, and subsequently kept isocratic for 10 min. Return to the initial conditions was accomplished in 5 min.

Flow-injection (FI) TSP-MS experiments without the use of the column were performed with acetonitrile–water (50:50, v/v) with 0.05 M ammonium formate. In all cases, the flow-rate was set at 1 ml/min, and the amount injected was 200 ng.

### 2.3. Mass spectrometric analysis

A Hewlett-Packard (Palo Alto, CA, USA) Model 5988A thermospray LC-MS quadrupole mass spectrometer and a Hewlett-Packard Model 35741B instrument for data acquisition and processing were employed. The thermospray temperatures varied from 98 to 95°C (stem), and the tip was maintained at 198°C at the beginning and end of the gradient. The ion source was set at 250°C. The filament-on ionization mode was used in all experiments, with positive (PI) and negative (NI) ion chemical ionization.

### 2.4. Calibration graphs

The linearity and reproducibility of the on-line SPE system were examined. Calibration graphs were constructed for all parent pesticides by percolating 100 ml of HPLC grade water spiked

at six different concentrations (from 0.025 to 2  $\mu\text{g/l}$ ) through  $\text{C}_{18}$  precolumns. Analytical conditions were as described above. Quantitation was performed with an external standard calibration method, using time-scheduled selected-ion monitoring (SIM); the ions selected for quantitation are italicized in Table 1.

### 2.5. Water analysis

Ebre river water samples were collected, filtered through 0.45- $\mu\text{m}$  filters (Millipore) to remove suspended particles, and spiked with each individual pesticide (listed in Table 2) at a level of 50  $\mu\text{g/l}$ , lower than the amount applied for treatment purposes (200  $\mu\text{g/l}$ ). These waters were placed in a transparent glass bottle on a terrace roof in Barcelona on January 19th. After four weeks they were collected and analyzed by on-line SPE-LC-TSP-MS. Chromatograms were recorded under full scan mode from  $m/z$  150 to 550 in the PI mode. The water sample which contained chlorpyrifos-methyl was also analyzed in the NI mode.

## 3. Results and discussion

### 3.1. Mass-spectral information

Even though there is ample literature concerning the determination of OP pesticides by

Table 1  
Mass fragments and relative abundances (%) observed in flow-inject thermospray LC-MS in PI and NI modes and filament-on conditions

Compound	$M_r$	Ions ( $m/z$ ) (% abundance) PI mode	Ions ( $m/z$ ) (% abundance) NI mode
Chlorpyrifos-methyl	322	323(58) [M + H] <sup>+</sup>	186(100) [M - HCl] <sup>-</sup>
Diazinon	304	340(100) [M + NH <sub>4</sub> ] <sup>+</sup>	169(100) [(C <sub>2</sub> H <sub>5</sub> O) <sub>2</sub> POS] <sup>-</sup>
Disulfoton	274	305(100) [M + H] <sup>+</sup>	303(4) [M - H] <sup>-</sup>
		153(75) [CH <sub>3</sub> CH <sub>2</sub> O) <sub>2</sub> PS] <sup>+</sup>	185(100) [(C <sub>2</sub> H <sub>5</sub> O) <sub>2</sub> PS <sub>2</sub> ] <sup>-</sup>
		275(100) [M + H] <sup>+</sup>	
Disulfoton sulfone	306	292(26) [M + NH <sub>4</sub> ] <sup>+</sup>	185(100) [(C <sub>2</sub> H <sub>5</sub> O) <sub>2</sub> PS <sub>2</sub> ] <sup>-</sup>
		307(100) [M + H] <sup>+</sup>	
Disulfoton sulfoxide	290	324(44) [M + NH <sub>4</sub> ] <sup>+</sup>	185(100) [(C <sub>2</sub> H <sub>5</sub> O) <sub>2</sub> PS <sub>2</sub> ] <sup>-</sup>
		159(73)	
Fenamiphos	303	291(100) [M + H] <sup>+</sup>	153(15) [CH <sub>3</sub> S - C <sub>6</sub> H <sub>3</sub> - CH <sub>3</sub> O]
		308(15) [M + NH <sub>4</sub> ] <sup>+</sup>	302(100) [M - H] <sup>-</sup>
Fenamiphos sulfone	335	304(100) [M + H] <sup>+</sup>	185(65) [M - 150] <sup>-a</sup>
		321(17) [M + NH <sub>4</sub> ] <sup>+</sup>	320(98) [M - CH <sub>3</sub> ] <sup>-</sup>
		336(30) [M + H] <sup>+</sup>	334(100) [M - H] <sup>-</sup>
Fenamiphos sulfoxide	319	353(100) [M + NH <sub>4</sub> ] <sup>+</sup>	380(42) [M + HCOO] <sup>-</sup>
		377(11) [M + H + CH <sub>3</sub> CN] <sup>+</sup>	169(100) [M - 150] <sup>-a</sup>
		320(93) [M + H] <sup>+</sup>	185(82) [169 + HCOOH - CH <sub>2</sub> O] <sup>-</sup>
		337(100) [M + NH <sub>4</sub> ] <sup>+</sup>	215(29) [169 + HCOOH] <sup>-</sup>
Fenthion	278	361(17) [M + H + CH <sub>3</sub> CN] <sup>+</sup>	318(85) [M - H] <sup>-</sup>
		183(53)	153(28) [M - (CH <sub>3</sub> O) <sub>2</sub> PS] <sup>-</sup>
		279(25) [M + H] <sup>+</sup>	279(48) [M + H] <sup>-</sup>
		296(100) [M + NH <sub>4</sub> ] <sup>+</sup>	340(100) [M + HCOOH + HCOO - CO] <sup>-</sup>
Fenthion oxon	262	171(13) [C <sub>6</sub> H <sub>5</sub> OS + NH <sub>4</sub> ] <sup>+</sup>	153(100) [M - (CH <sub>3</sub> O) <sub>2</sub> PO] <sup>-</sup>
		263(24) [M + H] <sup>+</sup>	194(40)
		280(100) [M + NH <sub>4</sub> ] <sup>+</sup>	
		304(8) [M + H + CH <sub>3</sub> CN] <sup>+</sup>	
Isofenphos	345	287(100) [M - NHCH(CH <sub>3</sub> ) <sub>2</sub> ] <sup>+</sup>	344(100) [M - H] <sup>-</sup>
		346(89) [M + H] <sup>+</sup>	
Malathion	330	331(12) [M + H] <sup>+</sup>	157(100) [(CH <sub>3</sub> O) <sub>2</sub> PS <sub>2</sub> ] <sup>-</sup>
		348(100) [M + NH <sub>4</sub> ] <sup>+</sup>	329(33) [M - H] <sup>-</sup>
Malaoxon	314	315(54) [M + H] <sup>+</sup>	172(100) [(CO <sub>2</sub> CH <sub>2</sub> CH <sub>3</sub> ) <sub>2</sub> - C <sub>2</sub> H <sub>2</sub> ] <sup>-</sup>
		332(100) [M + NH <sub>4</sub> ] <sup>+</sup>	230(48) [172 + CH <sub>3</sub> COO + H] <sup>-</sup>
			313(18) [M - H] <sup>-</sup>
Metidathion	302	303(18) [M + H] <sup>+</sup>	157(100) [(CH <sub>3</sub> O) <sub>2</sub> PS <sub>2</sub> ] <sup>-</sup>
		320(100) [M + NH <sub>4</sub> ] <sup>+</sup>	287(6) [M - CH <sub>3</sub> ] <sup>-</sup>
Pyridafenthion	340	341(100) [M + H] <sup>+</sup>	169(100) [(C <sub>2</sub> H <sub>5</sub> O) <sub>2</sub> POS] <sup>-</sup>
			203(10) [M - (C <sub>2</sub> H <sub>5</sub> O) <sub>2</sub> PO] <sup>-</sup>
			340(11) [M] <sup>-</sup>
Temephos	466	466(53) [M] <sup>+</sup>	341(35) [M - (CH <sub>3</sub> O) <sub>2</sub> PS] <sup>-</sup>
		484(100) [M + NH <sub>4</sub> ] <sup>+</sup>	451(100) [M - CH <sub>3</sub> ] <sup>-</sup>
Temephos sulfoxide	482	348(44) [M - (OCH <sub>3</sub> ) <sub>2</sub> P + CH <sub>3</sub> CN] <sup>+</sup>	341(6) [M - (CH <sub>3</sub> O) <sub>2</sub> POS] <sup>-</sup>
		482(45) [M] <sup>+</sup>	373(22) [M - (CH <sub>3</sub> O) <sub>2</sub> PO] <sup>-</sup>
		483(100) [M + H] <sup>+</sup>	451(100) [M - CH <sub>3</sub> O] <sup>-</sup>

Eluent: acetonitrile-water (50:50, v/v) with ammonium formate 0.05 M. Amount injected = 200 ng.

<sup>a</sup> 150 = PO(OC<sub>2</sub>H<sub>5</sub>) + NHCH(CH<sub>3</sub>)<sub>2</sub>.

Table 2

Calibration graphs constructed by preconcentrating 100 ml of river water sample, spiked with the pesticide mixture at six different concentrations (from 0.025 to 2  $\mu\text{g/l}$ )

Compound	Calibration equation	$R^2$	Linear range ( $\mu\text{g/l}$ )	LOD ( $\mu\text{g/l}$ )
Chlorpyrifos-m	$Y = 571066X + 45888$	0.9955	0.100–2	0.088
Diazinon	$Y = 58415859X + 2785451$	0.9833	0.025–2	0.004
Disulfoton	$Y = 11124131X + 1431491$	0.8666	0.025–2	0.002
Fenamiphos	$Y = 15544948X + 827158$	0.9803	0.025–2	0.012
Isofenphos	$Y = 2608255X + 22174$	0.9987	0.025–2	0.011
Malathion	$Y = 3688033X + 201632$	0.9831	0.025–2	0.029
Metidathion	$Y = 2555832X + 645204$	0.9860	0.025–2	0.016
Pyridafenthion	$Y = 12968626X + 1132752$	0.9947	0.025–2	0.011
Temephos	$Y = 47078X + 32472$	0.9920	0.050–2	0.038

Chromatograms were recorded under time-scheduled selected-ion monitoring (SIM).

TSP-MS [10–18], few consider the need for characterization of TPs for further studies on the biodegradation of pesticides [14,15]. For this reason, the parental pesticides selected in this study were characterized by TSP-MS together with those TPs that were commercially available. Table 1 shows the main fragment ions and relative abundances of the parent pesticides studied and all their TPs in both PI and NI mode of operation. The spectral information obtained from the different TPs was mandatory for the further identification and characterization of such compounds in spiked river water submitted to degradation.

(a) Positive ions. The favored formation of  $[\text{M} + \text{NH}_4]^+$  as the base peak for OP indicates that the proton affinity for these compounds is slightly lower than that of ammonia (858 kJ/mol), as reported previously [15]. There are three exceptions among the different OPs studied that certainly show  $[\text{M} + \text{H}]^+$  as base peak, i.e. fenamiphos, diazinon, and pyridafenthion. This has been explained in previous articles by our group [11,14,17]. However, the formation of  $[\text{M} + \text{H}]^+$  ion as the second most abundant ion (relative abundance varying from 12% to 93%) indicates that these compounds exhibit intermediate basicity, with an equal or lower proton affinity than ammonia, favoring both the formation of  $[\text{M} + \text{NH}_4]^+$  and  $[\text{M} + \text{H}]^+$  ion. The relative abundances of both ions can be slightly

different when compared to those of the parent compounds (temephos or fenamiphos) and the corresponding TPs (sulfoxide and sulfone), as shown in Table 1. In the case of fenamiphos sulfoxide and sulfone, these TPs have a decreased proton affinity, and then  $[\text{M} + \text{NH}_4]^+$  ion is formed. In the case of temephos, its sulfoxide presents a  $[\text{M} + \text{H}]^+$  ion.

(b) Negative ions. Table 1 presents the NI ions of the pesticides studied using filament-on ionization. The pesticides which produced the strongest signal and fragmentation were the electronegative compounds. In this sense, the NI mode of ionization is advantageous for the determination and identification of pesticides and their TPs from environmental matrices, since it yields more structural information and is usually more selective.

The characterization of OPs by TSP-MS in the NI mode yielded specific fragment ions, as reported previously [12,16], which correspond to molecular ions or adducts with formate as the base peaks. However, under the conditions used in this experiment, strong fragmentation occurred for diazinon, disulfoton and its TPs, fenamiphos sulfoxide, fenthion oxon, malathion, malaoxon, metidathion, pyridafenthion, and temephos and its sulfoxide. In the case of diazinon and disulfoton, the base peak corresponds to  $m/z$  169  $[(\text{C}_2\text{H}_5\text{O})_2\text{POS}]^-$  and  $m/z$  185  $[(\text{C}_2\text{H}_5\text{O})_2\text{PS}_2]^-$ , respectively. This be-

havior has already been observed for some OP pesticides [18]. For fenamiphos, whereas the parent compound and its sulfone exhibited  $[M - H]^-$  as their base peak, the sulfoxide presents an unidentified ion at  $m/z$  169. However, adducts with fragments have been observed for this compound at  $m/z$   $[M + 16]^-$ , which can be attributed to  $[169 + \text{HCOOH} - \text{CH}_2\text{O}]^-$  [18].

Fenthion exhibited an ion at  $m/z$  279, which corresponds to a  $[M - H]^-$  ion similar to that observed by Vreeken et al. [18] for other pesticides. The base peak for fenthion corresponded to  $m/z$  340, which can be tentatively identified as  $[M + 61]^-$ , corresponding to  $[M + \text{HCOOH} + \text{HCOO}^- - \text{CO}]^-$ . The loss of CO from the molecule has also been reported by Vreeken et al. [18] for phenyl urea pesticides. Fenthion oxon presents two fragments at  $m/z$  153 and 194.

### 3.2. Calibration graphs

The calibration data of these pesticides obtained by SIM are presented in Table 2. The linear relationship between the area of each peak versus concentration was evaluated by calculating the correlation coefficient. All compounds showed an  $R^2$  around 0.99 calculated from the limit of detection (LOD), which implies that these compounds exhibit good linearity within this range, and therefore quantitation can be performed at levels of a few  $\mu\text{g/l}$  using on-line SPE-LC-TSP-MS. The exception was fenthion, which could not be determined due to the fact that it is easily degraded in aqueous solution. Its instability in water solution has already been reported [19], and its exclusion from the National Pesticide Survey (USA) list proves that it is unstable in well water within a period of 14 days. The linear range of chlorpyrifos-methyl was from 0.1 to 2  $\mu\text{g/l}$ . This compound was monitored at  $m/z$  323, corresponding to  $[M + H]^+$ , which has an abundance of 58%. A better signal could be obtained at  $m/z$  340, but it was discarded due to a coelution problem with pyridafenthion.

The SIM LODs of the studied pesticides are presented in Table 2. They were calculated by selecting the lowest concentration of the spiked

water sample that gave a signal-to-noise ratio of 3, and measuring the height of the peaks.

The results obtained were far below the limits imposed by the EEC (0.1  $\mu\text{g/l}$ ), indicating the suitability of this method for screening OPs in field studies.

Calibration plots were not constructed for the TPs, since these compounds were qualitatively analyzed in spiked river water submitted to degradation. However, under the analytical conditions used in this work, it can be expected that when percolating 100 ml of water, losses of these compounds due to breakthrough might be expected [20], and thus, the recovery will not reach 100% but the LOD will be augmented. Regardless, the breakthrough value of the TPs is a parameter that has to be taken into account when performing degradation studies.

### 3.3. Environmental application

This technique was used to unequivocally identify the parental pesticides and TPs formed by degradation under semi-natural conditions (Ebre river water spiked at a low concentration level and exposed outdoors). These waters were analyzed four weeks after spiking by both on-line SPE-LC-diode-array detection (DAD) and on-line SPE-LC-TSP-MS in order to detect as many TPs as possible. Table 3 shows the main compounds identified by TSP-MS in the PI mode and summarizes the major ions and their relative abundances. Since not all the TP standards were characterized by flow-injection analysis, the scan mode was used in order to detect as many as possible.

The determination of TPs of OP pesticides is of importance since the oxo-derivatives and sulfoxides, which are more toxic than the parent compounds, can be formed under natural conditions and therefore may cause toxic effects to natural flora and fauna [19]. In this respect, the EEC Directive on the Quality of Water Intended for Human Consumption has already stressed the need for analyzing pesticides and TPs at levels under 0.1  $\mu\text{g/l}$ . Moreover, the NSP has published a list in which pesticides and their TPs detected in ground water were automatically

Table 3

List of the OPs oxo or sulfoxide TPs studied, their molecular mass ( $M_r$ ), retention time (min), and major ions obtained by TSP-MS in the PI mode of Ebre river water samples spiked at a level of 50  $\mu\text{g/l}$  and analyzed four weeks after spiking

Compound	$M_r$	LC-TSP-MS	
		$t_R$	Main ions
Chlorpyrifos-m oxon	322	33.9	323[M + H] <sup>+</sup>
	306	28.5	324[M + NH <sub>4</sub> ] <sup>+</sup>
Diazinon oxon	304	35.8	305[M + H] <sup>+</sup>
	288	29.1	289[M + H] <sup>+</sup>
Disulfoton sulfoxide	274	30.1	275[M + H] <sup>+</sup>
	290	24.6	291[M + H] <sup>+</sup> 308[M + NH <sub>4</sub> ] <sup>+</sup>
Fenamiphos sulfoxide	303	28.7	304[M + H] <sup>+</sup>
	319	20.9	320[M + H] <sup>+</sup> 337[M + NH <sub>4</sub> ] <sup>+</sup>
Fenthion sulfoxide	278	34.1	279[M + H] <sup>+</sup>
	294	24.9	295[M + H] <sup>+</sup> 312[M + NH <sub>4</sub> ] <sup>+</sup> 336[M + CH <sub>3</sub> CN] <sup>+</sup>
Isofenphos oxon	345	30.3	287[M - NHCH(CH <sub>3</sub> ) <sub>2</sub> ] <sup>+</sup> 346[M + H] <sup>+</sup>
	329	25.3	330[M + H] <sup>+</sup>
Malathion	330	31.7	331[M + H] <sup>+</sup> 348[M + NH <sub>4</sub> ] <sup>+</sup>
	302	31.0	303[M + H] <sup>+</sup> 320[M + NH <sub>4</sub> ] <sup>+</sup>
Pyridafenthion oxon	340	29.3	341[M + H] <sup>+</sup>
	324	23.5	325[M + H] <sup>+</sup>
Temephos oxon	466	31.3	484[M + NH <sub>4</sub> ] <sup>+</sup> 525[M + (CH <sub>3</sub> CN)NH <sub>4</sub> ] <sup>+</sup>
	450	31.6	468[M + NH <sub>4</sub> ] <sup>+</sup>

Analytical conditions as described in the Experimental section.

included. For this reason, there is a demand for an analytical method which accomplishes such needs.

It can be observed from Table 3 that some oxons were detected four weeks after the water samples were spiked (chlorpyrifos-methyl, diazinon, isofenphos, pyridafenthion, and temephos). The toxicity of the oxo-derivatives has been demonstrated by Miyamoto et al. [21]. In all cases, the oxygen analogues could be identified since they followed the same adduct formation as the parent pesticide (except for chlorpyrifos-methyl) and eluted before their parent compound. Temephos oxon, however,

eluted after temephos, possibly due to the stronger effect of the P = S group towards the C<sub>8</sub> of the stationary phase compared to the P = O group.

The presence of these compounds in aqueous solution for at least four weeks means that, according to the NPS-EPA, they are stable for at least 14 days, and thus their inclusion in the NPS-US-EPA list of toxic contaminants should be contemplated. Since the NPS-US-EPA stability study was conducted without the use of LC-MS, the TPs were probably also formed but were not detected. In this respect, LC-MS is a very useful technique for the identification of OP pesticide TPs.

The production of sulfoxide derivatives was noted for disulfoton, fenamiphos, and fenthion. In the case of disulfoton sulfoxide, the ions were located at  $m/z$  291 [M + H]<sup>+</sup> and  $m/z$  308 [M + NH<sub>4</sub>]<sup>+</sup>, as indicated by flow-injection information. This compound has been included in the NPS-EPA list.

Fenamiphos sulfoxide was the main TP formed, which is in accordance with Ref. [22], which reports the formation of this compound by photodegradation. In neither case was the sulfone found in the water sample, simply because an other oxidation step is implied for its formation in the environment. Fenamiphos presented also an unidentified peak with a molecular mass of 288 (not shown in Table 3), which was tentatively identified as a loss of CH<sub>3</sub> from the original molecule. Chukwudebe et al. [23] already pointed out that after UV irradiation, dealkylation with loss of CH<sub>3</sub> could occur in phosphorotioate pesticides. To our knowledge, such a TP has not been reported previously as being formed in spiked river water submitted to degradation. The other ions formed were 153(67) (unknown fragment), 289(29) [M + H]<sup>+</sup>, 306(100) [M + NH<sub>4</sub>]<sup>+</sup>, and 317(88) (unknown adduct).

Fenthion is a compound which can degrade easily in aqueous solution but could still be identified at  $m/z$  279 [M + H]<sup>+</sup> four weeks after spiking. Its sulfoxide could also be identified (see Table 3). Fenthion is actually a controversial compound since it has been removed from the

NPS-EPA list, as it is considered unstable in well-water solution over a period of 14 days. However, the conditions used in this experiment permitted the detection of traces of fenthion.

In this list, fenthion sulfoxide has not yet been considered as a toxic substance discharged into the environment. Two more peak were identified as possible TPs of fenthion. Since not for all TPs standards are available, its previous characterization by flame ionization (FI) was not possible, and the identification of TPs with this technique is complex due to the presence of fragments and rearrangements which are hard to interpret. The first unknown TP eluted at 27.5 min and produced an ion at  $m/z$  247 as the main peak, which could correspond to the molecular ion X,  $m/z$  264(45)  $[X + NH_4]^+$  and 296(37)  $[X + (CH_3OH)NH_4]^+$ . More sophisticated techniques are needed to identify this TP, such as MS–MS, as reported for chlorotriazines [24]. The second unidentified peak eluted at 34.02 min and presented  $m/z$  153 as its base peak, 171(52) and 277(28). The ion at  $m/z$  153 could correspond to the loss of  $(CH_3O)_2PS$  from the parent pesticide, yielding  $[C_8H_9OS]^+$ . The ion at  $m/z$  171 is identified as  $[M + NH_4]^+$ , following the same adduct formation as the parent pesticide.

Similarly, waters containing isofenphos hold the parent pesticide, the oxygen derivative, and an unidentified TP at  $m/z$  287(100), at 28.16 min. Since no fragmentation occurred, its molecular structure is uncertain, but as it was similar to isofenphos, it could tentatively be identified with the loss of  $(CH_3)_2CHNH$  from the parent compound.

Fig. 2 shows the LC–DAD of a water sample spiked with chlorpyrifos-methyl and analyzed after four weeks, with two peaks that correspond to chlorpyrifos-methyl and to its oxon. Confirmation was performed by means of MS detection. Water samples spiked with chlorpyrifos-methyl were analyzed in both the PI and NI mode, to gain more structural information. Compounds such as chlorpyrifos-methyl showed good sensitivity [25], and it was found that loss of chlorine was involved. The total ion chromatogram (TIC) in the PI and NI ionization mode and the ion

traces at  $m/z$  323, 324, and 198 are presented, which correspond to the parent compound and the two TPs formed, chlorpyrifos-methyl oxon ( $m/z$  324) and 3,5,6-trichloro-2-pyridinol ( $m/z$  198). The latter exhibited loss of chlorine atoms and proton abstraction, similar to the parent compound. One report [26] also describes the formation of 3,5,6-trichloro-2-pyridinol by hydrolysis. The presence of this compound agrees with other studies on photolysis in water using the suntest apparatus [22] and in different solid surfaces [26]. The toxicity of 3,5,6-trichloro-2-pyridinol is higher than that of chlorpyrifos, with  $EC_{50}$  values of 18.6 and 46.3  $\mu\text{g/ml}$ , respectively, as calculated with the Microtox system [27]. Also, it has been reported that this compound is toxic to soil microorganisms, resulting in lower mineralization and therefore enhanced persistence of chlorpyrifos in soil.

Other samples analyzed with the NI mode of ionization were diazinon, fenamiphos, fenthion, isofenphos, pyridafenthion, and temephos. The use of TSP-NI permitted further confirmation of the results with another detection technique. Of the pesticides mentioned, temephos, fenthion, and fenamiphos gave no signal. As stated by Barceló et al. [25], sensitivity for OP pesticides of the parathion group was higher in the PI than in the NI mode; hence, these compounds could not be detected under NI mode and scanning. The only oxygen derivative found was that of pyridafenthion, with  $m/z$  at 324  $[M]^-$ . The poor formation of oxons in the NI mode of ionization was expected since for oxygen analogues the oxo group enhances the proton affinity compared with the thio group, and therefore, the sensitivity is one order of magnitude higher with PI [25].

Waters spiked with diazinon presented two peaks at  $m/z$  169, at 21.45 and 27.1 min. The second one corresponds to diazinon itself. The former has an unidentified  $m/z$  235 as base peak and an ion at  $m/z$  169(34). Not enough information is given to identify this TP.

Pyridafenthion was detected at  $m/z$  340  $[M]^-$ . Isofenphos was detected under NI mode, together with a TP at 16.1 min, tentatively identified as  $[(CH_3)_2CHNH(CH_3CH_2O)POS]^-$  at



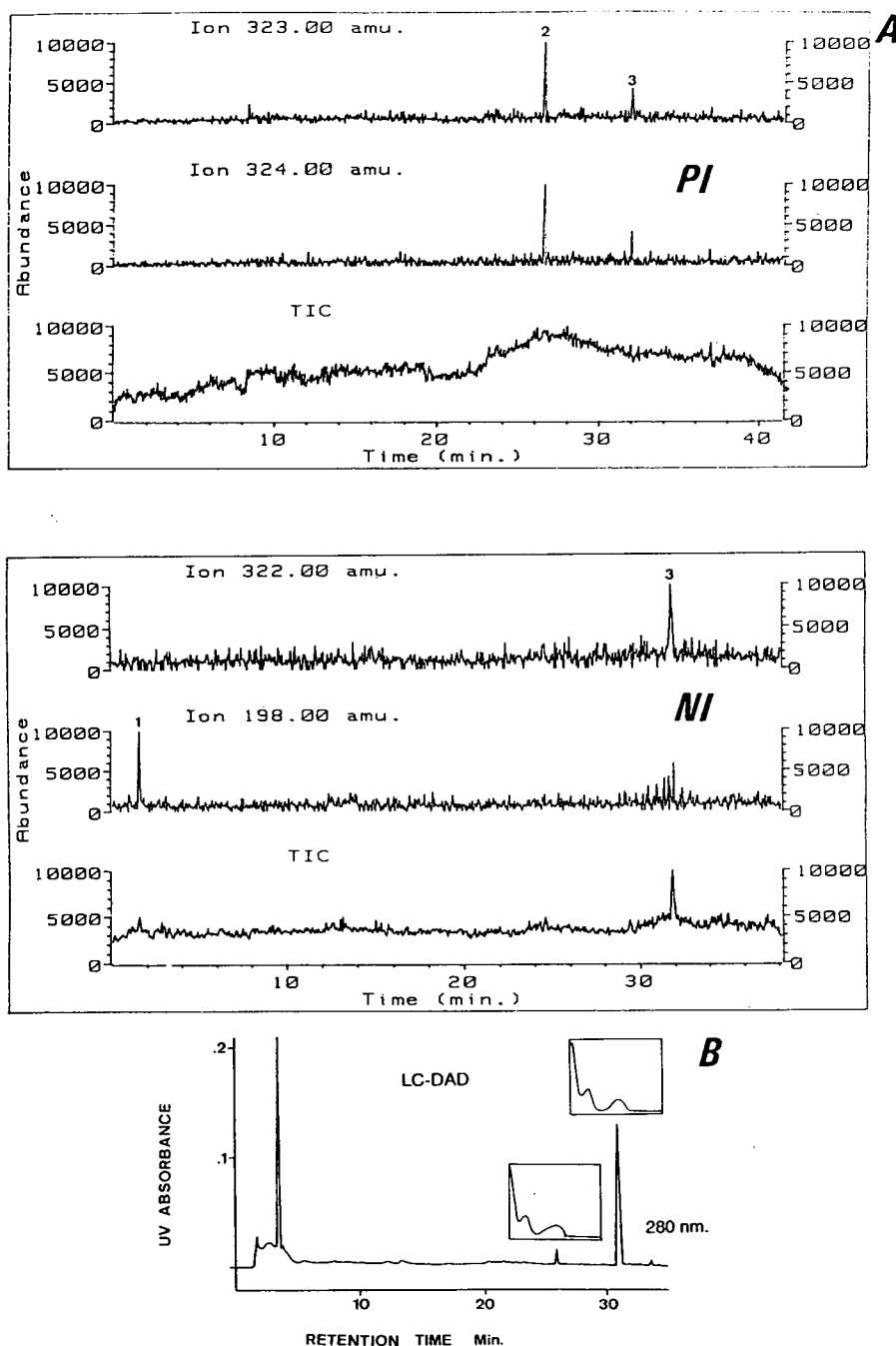


Fig. 2. (A) Reconstructed ion chromatogram obtained with on-line SPE-LC-TSP-MS with PI and NI mode of ionization of an Ebre river water sample spiked with chlorpyrifos-methyl at  $50 \mu\text{g/l}$ ; the water sample was analyzed four weeks after spiking. Peak identification: 1 = 3,5,6-trichloro-2-pyridinol, 2 = chlorpyrifos-methyl oxon, 3 = chlorpyrifos-methyl. (B) Same water sample analyzed by on-line SPE-LC-DAD at 280 nm. In both cases, the same analytical conditions were used (see Experimental section).

$m/z$  182(100). Adducts with formate were present at 228(50)  $[182 + \text{HCOOH}]^-$ . This compound could be formed by hydrolysis.

#### 4. Conclusions

The application of automated on-line SPE (OSP-2) followed by LC-TSP-MS was used for the determination of OPs and their TPs at trace levels in river water samples subjected to natural degradation. It has been shown that the application of highly automated techniques permits the detection of polar TPs determined for the first time in natural waters, e.g. 3,5,6-trichloro-2-pyridinol. The use of such automated techniques combined with MS is useful in environmental degradation studies of pollutants. Few results have been published up to now on the stability of OPs in water. This subject is still a matter of controversy, and conclusions cannot be drawn. In this sense, although a few OPs were rapidly degraded in water, TPs were formed and were stable during a period of more than 3–4 weeks, which led us to pay attention to a more stable contamination in water due to TPs. More research is needed in order to verify the formation of TPs of pollutants in natural waters and to check their stability over time.

#### Acknowledgements

R. Alonso is thanked for laboratory assistance in the LC-MS studies. This work has been supported by the Environment R&D Program 1991–1994 (Commission of the European Communities) (Contract EV5V-CT93-0245) and by PLANICYT (AMB94-1507-CE). S.L. gratefully acknowledges financial support from CICYT (Grant AMB92-0218). Research Agreement 7978/CF from the International Atomic Energy Agency (IAEA) is also acknowledged.

#### References

- [1] D. Barceló, C. Porte, J. Cid and J. Albaigés, *Int. J. Environ. Anal. Chem.*, 38 (1990) 199–209.
- [2] M. Eto, *Organophosphorus pesticides: Organic and Biological Chemistry*, CRC Press, Boca Raton, FL, 1979.
- [3] S. Lacorte, C. Molina and D. Barceló, *Anal. Chim. Acta*, 281 (1993) 71–84.
- [4] S. Lacorte and D. Barceló, *Environ. Sci. Technol.*, 28 (1994) 1159–1163.
- [5] P.H. Pritchard, C.R. Cripe, W.W. Walter and A.W. Bourquin, *Chemosphere*, 16 (1987) 1509.
- [6] K.E. Day, in L. Somasundaram and J.R. Coats (Editors), *Pesticide Transformation Products, Fate and Significance in the Environment*, ACS Symposium series, Vol. 459, American Chemical Society, Washington, DC, 1991, Ch. 16.
- [7] D. Barceló, G. Durand, V. Bouvot and M. Nielen, *Environ. Sci. Technol.*, 27 (1993) 271–277.
- [8] S. Chiron, A. Fernandez-Alba and D. Barceló, *Environ. Sci. Technol.*, 27 (1993) 2352–2358.
- [9] S. Chiron, S. Dupas, P. Scribe and D. Barceló, *J. Chromatogr. A*, 665 (1994) 295–305.
- [10] S. Chiron, E. Martinez and D. Barceló, *J. Chromatogr. A*, 665 (1994) 283–293.
- [11] S. Lacorte, S. Lartigues, Ph. Garrigues and D. Barceló, *Environ. Sci. Technol.*, 29 (1995) 431–438.
- [12] D. Barceló, *Biomed. Environ. Mass Spectrom.*, 17 (1988) 363–369.
- [13] D. Volmer, K. Levsen and G. Wünsch, *J. Chromatogr. A*, 660 (1994) 231–248.
- [14] G. Durand, N. de Bertrand and D. Barceló, *J. Chromatogr.*, 554 (1991) 233–250.
- [15] G. Durand, F. Sanchez-Baeza, A. Messeguer and D. Barceló, *Biol. Mass Spectrom.*, 20 (1991) 3–10.
- [16] D. Barceló, *Anal. Chim. Acta*, 263 (1992) 1–19.
- [17] A. Farran, J. de Pablo and D. Barceló, *J. Chromatogr.*, 455 (1988) 163–172.
- [18] R.J. Vreeken, W.D. van Dongen, R.T. Ghijsen and U.A.Th. Brinkman, *Int. J. Environ. Anal. Chem.*, 54 (1994) 119–145.
- [19] D. Barceló, *J. Chromatogr.*, 643 (1993) 117–143.
- [20] S. Lacorte and D. Barceló, *Anal. Chim. Acta*, 296 (1994) 223–234.
- [21] J. Miyamoto, N. Mikami, K. Mihara, Y. Takimoto, H. Kohda and H. Suzuki, *J. Pesticide Sci.*, 3 (1978) 35–41.
- [22] D. Barceló, G. Durand and N. de Bertrand, *Toxicol. Environ. Chem.*, 38 (1993) 183–199.
- [23] A. Chukwudebe, R.B. March, M. Othman and T.R. Fukuto, *J. Agric. Food Chem.*, 37 (1989) 539–545.
- [24] J. Abian, G. Durand and D. Barceló, *J. Agric. Food Chem.*, 41 (1993) 1264–1273.
- [25] D. Barceló, G. Durand, R.J. Vreeken, G.J. de Jong, H. Lingeman and U.A.Th. Brinkman, *J. Chromatogr.*, 553 (1991) 311–328.
- [26] S. Walia, P. Dureja and S.K. Mukerjee, *Arch. Environ. Contam. Toxicol.*, 17 (1988) 183–188.
- [27] L. Somasundaram, J.R. Coats, K.D. Racke and H.M. Stahr, *Bull. Environ. Contam. Toxicol.*, 44 (1990) 254–259.



ELSEVIER

Journal of Chromatography A, 712 (1995) 113–122

JOURNAL OF  
CHROMATOGRAPHY A

# Trace determination of herbicides in estuarine waters by liquid chromatography–high-flow pneumatically assisted electrospray mass spectrometry

C. Molina<sup>a</sup>, G. Durand<sup>b</sup>, D. Barceló<sup>a,\*</sup>

<sup>a</sup>Department of Environmental Chemistry, CID-CSIC, c/ Jordi Girona 18–26, 08034 Barcelona, Spain

<sup>b</sup>Directorate General des Services, Cellule Environnement, B.P. 883-29279, Communauté Urbaine de Brest, France

## Abstract

High-flow pneumatically assisted electrospray (ESP) was applied to the characterization of triazine (atrazine, simazine, ametryne, cyanazine, deethylatrazine and deisopropylatrazine), phenylurea (chlortoluron, isoproturon, diuron, linuron and diflufenbuzon) and other priority herbicides (alachlor, metolachlor). In LC–ESP–MS the  $[M + Na]^+$  ion was used as the base peak in most cases, with the exception of chlorotriazines, which showed  $[M + H]^+$  as the base peak. When LC–TSP–MS was used,  $[M + H]^+$  was the base peak for many of the pesticides, with the exception of linuron and diflufenbuzon, which showed  $[M + NH_4]^+$  as the base peak. The ESP results were compared with those obtained with thermospray (TSP). LC–TSP–MS offered greater sensitivity for triazines than phenylurea herbicides, whereas the use of LC–ESP–MS offered an enhancement in sensitivity for phenylurea herbicides. As regards the fragmentation obtained using both techniques, ESP offered a considerable amount of structural information for the different chlorotriazines studied when the extraction voltage was increased from 20 to 40 V. Liquid–liquid extraction with dichloromethane was used for the trace enrichment of the different herbicides in estuarine water samples from the Elorn river (France). The presence of the different triazine metabolites, atrazine, simazine, metolachlor, isoproturon and diuron was confirmed by both LC–MS techniques.

## 1. Introduction

Herbicides such as the chlorotriazines and phenylureas, alachlor and metolachlor are compounds used in Europe [1] and the USA [2] for agricultural applications. The various usage lists include atrazine, alachlor, metolachlor, chlortoluron, isoproturon and diuron as the main pesticides used worldwide with amounts of several millions pounds of active ingredient per year. After application, the different pesticide residues constitute a source of pollution of different

environmental waters with levels varying from 1 to 800 ng/l [3–6].

Chlorotriazine pesticides together with alachlor and metolachlor are usually determined by gas chromatography–mass spectrometry (GC–MS) with electron impact (EI) and/or positive- and negative-ion chemical ionization (PCI and NCI, respectively) [3–5,7,8]. GC–MS–MS has also been applied [9,10], offering higher selectivity and additional structural information. Liquid chromatographic techniques, involving diode-array determinations, MS generally with a thermospray (TSP) or particle beam interface and MS–MS have been used for the determi-

\* Corresponding author.

nation of the above-mentioned herbicides and also for phenylurea herbicides [6,11–15].

Although LC–TSP–MS has been widely used for the determination of the above-mentioned herbicides, it was the purpose of this work to use electrospray (ESP) ionization for the determination of the same herbicides. LC–ESP–MS has rarely been used in environmental analysis, as pointed out recently by Budde [16], only 5 out of the 54 presentations on LC–MS in environmental analysis at the 42nd ASMS Conference reported the use of ESP. Atmospheric pressure chemical ionization (APCI) is the most popular LC–MS technique. Recently, high-flow ESP–MS has been developed and is now commercially available. It has the advantage over conventional ESP that it does not require low flow-rates (10  $\mu$ l/min) that need either a split (when using conventional LC pumps) or syringe LC pumps, with the additional time and extra cost involved. In addition, the ideal situation of an environmental laboratory will be to perform the same analysis under conventional LC–UV or LC–diode-array conditions using LC–MS. In a previous paper [17], we evaluated the use of LC with high-flow ESP–MS for the trace determination of thermally labile organophosphorus pesticides in water samples.

In this work, we used high-flow LC–ESP–MS for the determination of a variety of herbicides in estuarine waters. The aims were (i) characterization by LC–ESP–MS of the different herbicides studied and (ii) comparison of the results obtained by LC–ESP–MS with those obtained by LC–TSP–MS for the trace determination of herbicides in estuarine waters.

## 2. Experimental

### 2.1. Chemicals

HPLC-grade water and methanol were obtained from J.T. Baker (Deventer, Netherlands) and were passed through a 0.45- $\mu$ m filter before use. The herbicides were purchased from Promocem (Wesel, Germany).

### 2.2. Liquid chromatography–mass spectrometry

#### *Electrospray*

The eluent was delivered by a gradient system from Waters Model 616 pumps controlled by a Waters Model 600S controller (Waters–Millipore, Milford, MA, USA). The LC eluent conditions varied from methanol–water (30:70) to pure methanol in 15 min, maintaining the latter for 10 min and using a flow-rate of 0.3 ml/min. The LC column was kept at the starting LC conditions for 10 min as the equilibrium time. A 300 mm  $\times$  2.1 mm I.D. column, packed with 10- $\mu$ m particles coated with a C<sub>18</sub> stationary phase (Waters–Millipore) was used.

The gradient LC system was connected to a VG Platform ESP from Fisons Instruments (Manchester, UK) equipped with a Megaflo ESP probe. The design of this ESP consists of a coaxial flow probe; a detailed description of the interface has been published elsewhere (17). The operational parameters of ESP optimized using an eluent flow-rate of 0.3 ml/min and a source temperature of 150°C as follows were: nitrogen drying gas flow-rate, 250–300 l/h; nitrogen ESP nebulizing gas flow rates, 10 l/h; ESP voltage, 3.1 kV; HV lens voltage, 0.3 kV; extraction voltage, 20–40 V; and focus voltage and ion energy as reported previously [17].

After the LC separation, the sample is introduced into the ESP source together with a nebulizing gas, which flows directly through the probe tip, maximizing the efficiency of the nebulizing. A drying gas is added to flush out any solvent which may have entered the gas line by capillary action and as a declustering medium for solvated molecules. The instrument control and data processing utilities included the use of MassLynx application software installed in a Digital DEC PC 466 computer. The high-flow pneumatically assisted ESP using a VG Platform instrument was used at a flow-rate of 0.3 ml/min and a source temperature of 150°C.

#### *Thermospray*

When the TSP interface was used, the LC gradient elution varied from methanol–water (10:90) to pure methanol in 18 min at a flow-rate

of 0.6 ml/min. Ammonium formate (0.05 M) was used as the mobile phase additive and it was added with a T-junction at a flow-rate of 0.4 ml/min using an LC pump from Knauer (Bad-Homburg, Germany).

A Hewlett-Packard (Palo Alto, CA, USA) Model 5988A Thermospray LC/MS quadrupole mass spectrometer and a Hewlett-Packard Model 35741B instrument for data acquisition and processing were employed. The thermospray temperature parameters were programmed from 98 to 90°C at 0.3°C/min with respect to the stem. The tip and ion source temperatures were set at 206 and 250°C, respectively. The filament-on mode and conventional positive-ion TSP ionization were used in all experiments.

### 2.3. Sample preparation

The extraction procedure follows a method reported previously [3,6] involving liquid–liquid extraction (LLE) with dichloromethane (2 × 100 ml) of 2.5 l of estuarine water. After agitation the extract was evaporated to dryness and the residue was dissolved in 400 µl of methanol. Volumes of 10 and 20 µl were injected into the

LC–ESP-MS and LC–TSP-MS systems, respectively.

### 2.4. Quantification

External standard calibration was used with quantification of the extract after LLE with a standard. The system was linear in most cases using 5–8 points from 0.01–0.5 to 20–100 ng. The calibration equations for the different pesticides analysed are given in Table 1. These calibration equations show, in some cases, large non-zero intercepts on the ordinate as compared with the abscissa, e.g., linuron. It should be noted that the linearity range in ESP is very much dependent on the compound, the number of points selected for calibration (usually 5–8) and the concentration linearity range. There is always a deviation from the intercept on the ordinate because it is not linear in the low concentration range (below 0.1–0.2 ng with few exceptions) and that when more points are used for the calibration graphs, this deviation increases. Analysis of the water extracts was achieved by using selected-ion monitoring (SIM) using either the  $[M + H]^+$  or  $[M + Na]^+$  ion, depending on the compound.

Table 1  
Calibration data for herbicides in the range 0.2–40 ng (0.0016–0.32 µg/l)

Analyte	Peak No.	Calibration equation	$R^2$	L.O.D. (pg)	
				ESP	TSP
Deisopropylatrazine	1	$y = 55513x + 22130$	0.997	450	200
Deethylatrazine	2	$y = 15801x + 1714$	0.999	450	200
Cyanazine	3	$y = 29652x + 8548$	0.998	300	150
Simazine	4	$y = 13444x + 3220$	0.999	450	200
Atrazine	5	$y = 18642x + 138$	0.999	450	200
Ametryne	6	$y = 234535x + 18696$	0.999	10	150
Alachlor	7	$y = 188311x + 5655$	0.999	20	400
Metolachlor	8	$y = 270930x + 18715$	0.999	15	300
Chlortoluron	9	$y = 56747x + 18106$	0.999	35	90
Isoproturon	10	$y = 119637x + 16901$	0.999	120	200
Diuron	11	$y = 33416x + 61515$	0.999	230	250
Linuron	12	$y = 6744x + 27869$	0.993	500	500
Diflubenzuron	13	$y = 27895x + 2924$	0.998	130	150

Calibration was performed by plotting peak area ( $y$ ) versus amount injected ( $x$ ). For ametryne, alachlor, metolachlor and chlortoluron, the linearity started at 0.01 ng whereas for atrazine and linuron from 0.5 to 120 ng (0.004 to 1.0 µg/l).

### 3. Results and discussion

#### 3.1. General considerations

Although TSP has been used extensively for the determination of pesticides, nowadays the use of APCI techniques is replacing this popular interfacing system. There are different APCI interfacing systems in LC-MS based on ultrasonic nebulization [18] and pneumatically assisted [17] and heated ESP [19] for the ionization of the analytes. The system shown in this paper was described in detail in a previous paper [17] and it is based on the use of pneumatically assisted ESP-MS. It does not heat the interface or the tip, but the nebulization is assisted by nitrogen nebulizing gas at 10 l/h. There is no heat in the interface itself and only the source is kept at 150°C. The nitrogen drying gas is used at 250 l/h. Both gases are introduced at room temperature.

A flow-rate of the LC eluent of 0.3 ml/min was used. This was not changed, although we performed a few experiments (not reported here) that showed a substantial decrease in sensitivity when the flow-rate was increased up to 0.5–0.6 ml/min.

The calibration equations for the different herbicides when using LC-TSP-MS have already been given previously [20,21] and indicate that LC-TSP-MS offers good linearity for many of the herbicides studied here. However, compounds such as alachlor and metolachlor elute at the end of the chromatographic trace at 100% of organic modifier with difficulties associated with maintaining a stable TSP tip temperature, and consequently high standard deviations were observed with no linearity in the quantification values [20]. The use of LC-ESP-MS is advantageous, specially in this case, for the accurate determination of these two analytes. Basically, because of the interface design with no heat in the interface, instability of the tip temperature was avoided. The fact that no heat is applied in the interface permitted the accurate determination of the thermally labile organophosphorus pesticide trichlorfon [17].

Fig. 1 shows different chromatograms ob-

tained for the herbicide standards using both LC-TSP-MS and LC-ESP-MS.

#### 3.2. Structural information

Table 2 shows the main ions obtained for the different herbicides using LC-ESP-MS at two extraction voltages. The first consideration is that when using a higher extraction voltage, generally much more fragmentation is obtained, as shown previously for organophosphorus pesticides [17]. The second question arises from the fact that on changing the extraction voltage from 20 to 40 V, the sensitivity usually decreases from 50 to 25%. Of the different herbicides studied, chlorotriazines gave good structural information on increasing the extraction voltage. The fragmentation obtained resembles the use of MS-MS [10,12,14]. This is known and it has been reported previously that this occurs by changing the capillary-skimmer potential difference. The spectra generated by ESP in the transport region at a capillary-skimmer potential difference of 30–50 V closely resembles those obtained from the  $[M + H]^+$  ion by a triple quadrupole mass spectrometer using a 30-eV collision energy [22].

The ion at  $m/z$  71 of deisopropylatrazine, commonly found using TSP-MS-MS, corresponds to  $[\text{CH}_3\text{CH}_2\text{NHCN} + \text{H}]^+$ . Ions corresponding to ring-opening reactions such as the ion at  $m/z$  132, which are common to deisopropylatrazine and simazine, corresponds to the  $[\text{CH}_3\text{CH}_2\text{NHC}(\text{NH})\text{NCCl}]^+$  moiety. Loss of HCl from this ion generates a signal at  $m/z$  96, and loss of the  $\text{CH}_2\text{CH}_2$  group generates a signal at  $m/z$  104. Pesticides bearing an isopropyl group (such as atrazine and deethylatrazine) show an ion derived from the loss of this moiety at  $m/z$  174 and 104. Elimination of HCN in the case of cyanazine affords the  $m/z$  214 ion. In addition to the above-mentioned diagnostic ions of the chlorotriazines, there is the possibility of the formation of adduct ions with  $\text{Na}^+$  of different diagnostic ions as reported for organophosphorus pesticides. This is a typical feature in high-flow pneumatically assisted ESP-MS [17], an example of which is the signal at  $m/z$  236 for cyanazine.

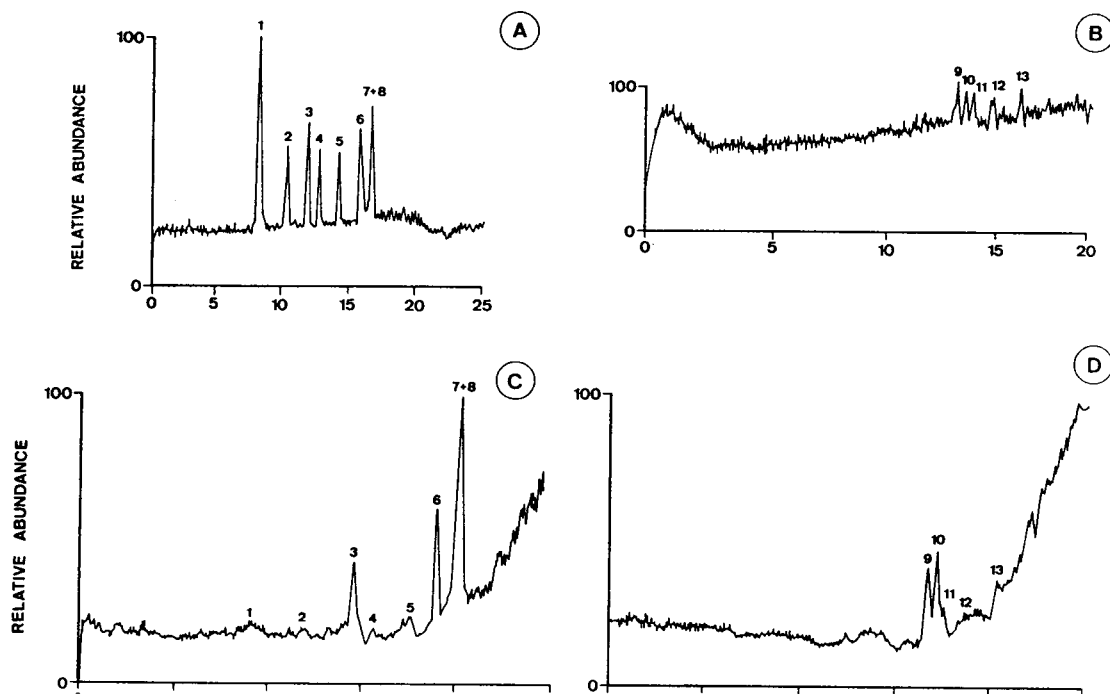


Fig. 1. (A and B) LC-TSP-MS and (C and D) LC-ESP-MS under full-scan conditions of herbicide standards injected at 200 ng (TSP) or 100 ng (ESP) for compounds corresponding to peaks 1–8 and at 100 ng (TSP) or 50 ng (ESP) for compounds corresponding to peaks 9–13. For peak identification, see Table 1. For gradient and column conditions, see Experimental.

Fig. 2 shows the increasing fragmentation observed for deethylatrazine when the extraction voltage was increased from 20 to 40 V. This feature is particularly relevant for environmental analysis, since it shows that for chlorotriazines high-flow pneumatically assisted ESP-MS can be used as a screening method for the identification of unknown chlorotriazine compounds. This is possible because the spectra obtained at an extraction voltage of 40 V resembles the fragmentation obtained under MS-MS conditions.

The remaining pesticides investigated showed virtually the same features when the extraction voltage was increased from 20 to 100 V, with  $[M + Na]^+$  as the base peak. The increased fragmentation observed for the chlorotriazines relative to the other groups of herbicides could be attributed to the facility of bond cleavage in such pesticides as compared with the other herbicides studied, which generally have an

aromatic structure that is more difficult to fragment under ESP-MS conditions.

### 3.3. Environmental analysis

Typical chromatograms of an estuarine water extract of 15‰ salinity from the Elorn river (France) obtained using LC-TSP-MS and LC-ESP-MS with SIM are shown in Fig. 3. The concentration of the different herbicides present in river water varied between 20 and 1000 ng/l. Both techniques permitted the different compounds present in the river water to be identified. The different intensities of the ions using the two techniques have been already discussed and the real sample follows expectations. In this respect, LC-TSP-MS offers higher sensitivity for chlorotriazines (peaks 1–5) whereas LC-ESP-MS offers considerably higher sensitivity than for

Table 2

Important mass spectral fragments, relative intensities of herbicides using methanol–water (50:50) as LC eluent and extraction voltages of 20 and 40 V under ESP-MS conditions

$M_r$	$m/z$	Compounds and ions: tentative identification	Relative intensity (%)	
			20 V	40 V
173		Deisopropylatrazine		
	174	$[M + H]^+$	100	100
	132	$[\text{CH}_3\text{CH}_2\text{NHC}(\text{NH})\text{NCCl}]^+$	–	26
	104	$[132 - \text{C}_2\text{H}_4]^+$	–	14
	96	$[132 - \text{HCl}]^+$	–	40
	71	$[\text{CH}_3\text{CH}_2\text{NHCN} + \text{H}]^+$		6
187		Deethylatrazine		
	188	$[M + H]^+$	100	62
	146	$[\text{CH}_3\text{CH}_2\text{CH}_2\text{NHC}(\text{NH})\text{NCCl}]^+$	–	100
	104	$[146 - \text{C}_3\text{H}_6]^+$	–	6
240		Cyanazine		
	263	$[M + \text{Na}]^+$	100	100
	236	$[M - \text{HCN} + \text{Na}]^+$	20	33
	214	$[M - \text{HCN} + \text{H}]^+$	–	5
201		Simazine		
	224	$[M + \text{Na}]^+$	4	35
	202	$[M + H]^+$	100	100
	166	$[M - \text{HCl}]^+$	–	10
	132	$[\text{CH}_3\text{CH}_2\text{NHC}(\text{NH})\text{NCCl}]^+$	–	54
	104	$[132 - \text{C}_2\text{H}_4]^+$	–	8
215		Atrazine		
	238	$[M + \text{Na}]^+$	–	100
	216	$[M + H]^+$	100	26
	174	$[M - \text{C}_3\text{H}_6]^+$	–	74
227		Ametryne		
	250	$[M + \text{Na}]^+$	21	100
	228	$[M + H]^+$	100	69
	186	$[M - \text{C}_3\text{H}_6]^+$	–	36
269		Alachlor		
	292	$[M + \text{Na}]^+$	100	100
283		Metolachlor		
	306	$[M + \text{Na}]^+$	100	100
303		Chlortoluron		
	326	$[M + \text{Na}]^+$	100	100
206		Isoproturon		
	229	$[M + \text{Na}]^+$	100	100
232		Diuron		
	255	$[M + \text{Na}]^+$	100	100
248		Linuron		
	271	$[M + \text{Na}]^+$	100	100
310		Diflubenzuron		
	333	$[M + \text{Na}]^+$	100	100



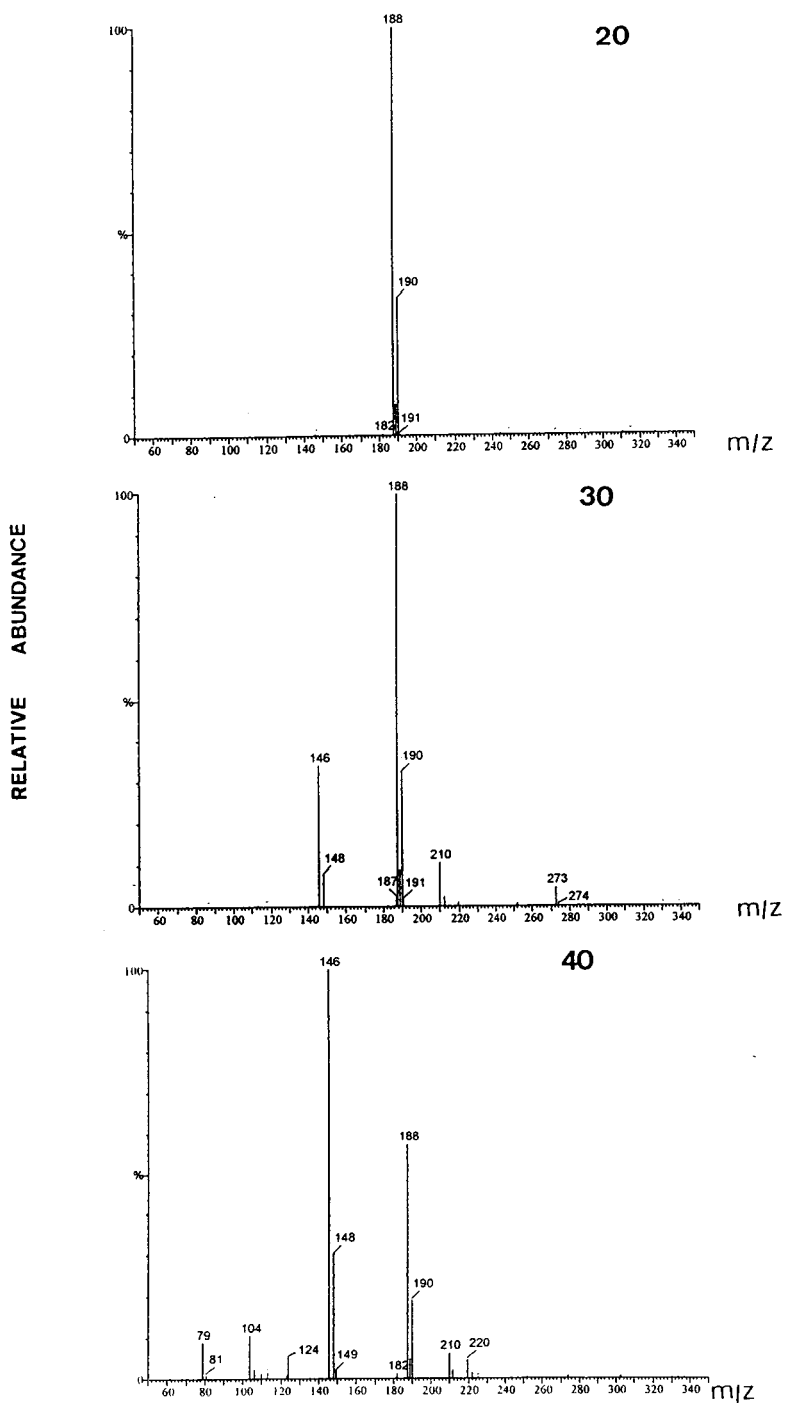


Fig. 2. LC-ESP-MS of deethylatrazine at extraction voltages of 20, 30 and 40 V. For identification of fragments, see Table 2.

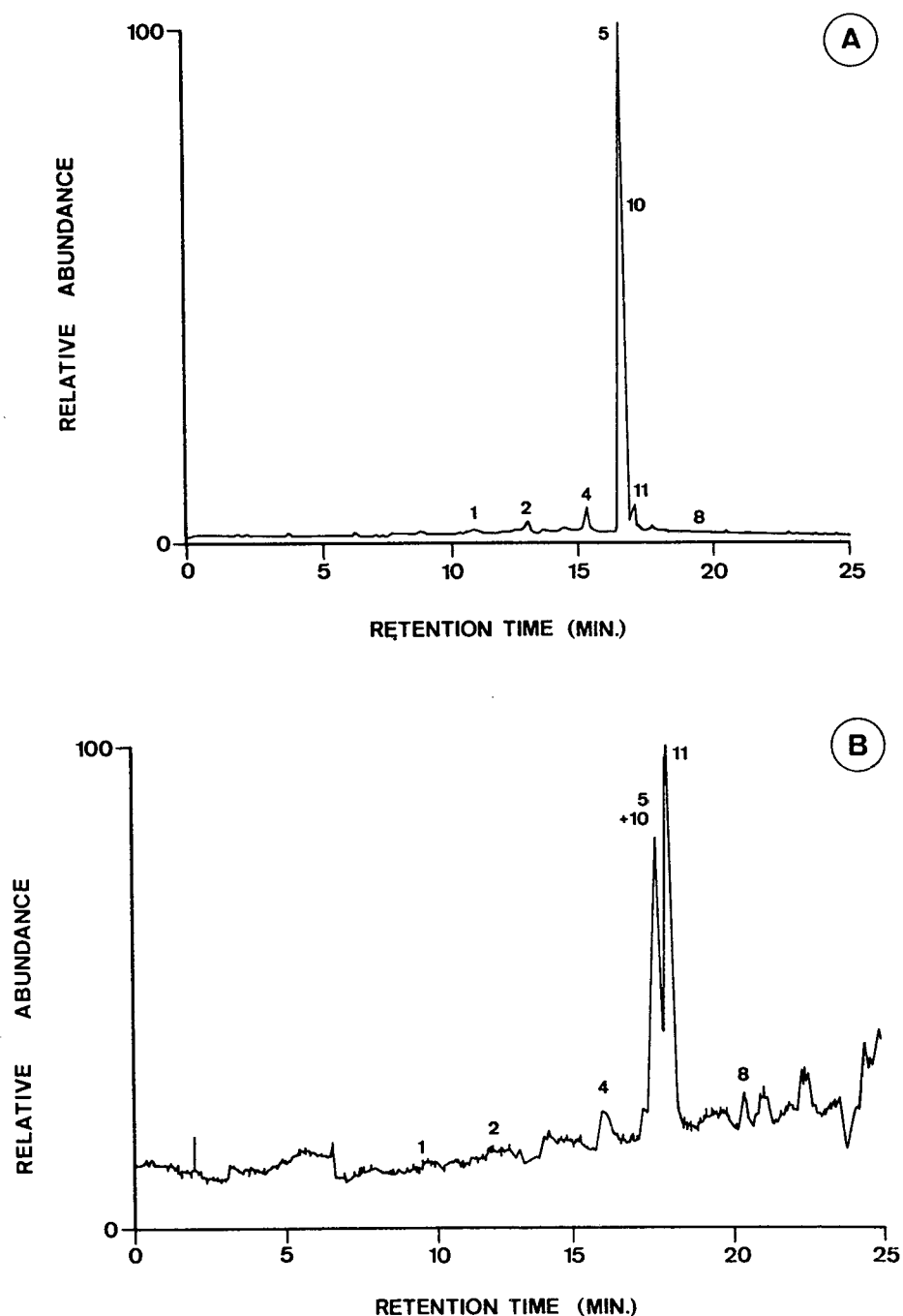


Fig. 3. (A) LC-TSP-MS and (B) LC-ESP-MS SIM traces obtained after dichloromethane LLE of 2.5 l of natural river water sample. The water sample contained (1) 20 ng/l of deisopropylatrazine, (2) 80 ng/l of deethylatrazine, (4) 400 ng/l of simazine, (5) 1000 ng/l of atrazine, (8) 200 ng/l of metolachlor, (10) 50 ng/l of isoproturon and (11) 600 ng/l of diuron. For gradient and column conditions, see Experimental and Fig. 1.

phenylureas and metolachlor (peaks 8, 10 and 11).

LC-ESP-MS can be applied to the determination of herbicides in natural estuarine water samples and has been demonstrated to be a useful technique that can easily compete with other LC-MS techniques in this field of application. From the results reported in Table 1 we can conclude that in general LC-TSP-MS give better limits of detection (L.O.D.s) for chlorotriazines (twofold). LC-ESP-MS is a much better method for alachlor, metolachlor, ametryne and chlortoluron, which show L.O.D.s in the range 10–30 pg (see Table 1). The L.O.D.s varied from 10 to 500 pg using the two techniques and were calculated by using a signal-to-noise ratio of 3–6 (the ratio between the peak intensity with SIM conditions and intensity of the noise was used). The reported L.O.D.s correspond to herbicides spiked into estuarine river waters. When using clean river water or drinking water samples, the L.O.D.s will be better, owing to less matrix interferences and/or better extraction recoveries of the pesticides from the water matrices.

#### 4. Conclusions

The application of LC-ESP-MS for the determination of different herbicides in environmental waters has been established. As regards fragmentation, the use of this technique achieves a comparable fragmentation pattern to TSP-MS-MS for chlorotriazines, whereas phenylurea, alachlor and metolachlor did not show fragmentation when the extraction voltage was increased. LC-ESP-MS offers greater fragmentation than conventional LC-TSP-MS for chlorotriazines although the sensitivity is poor. The L.O.D.s varied from 10 to 500 pg, making it a useful technique for environmental analysis. Of particular attention are the low L.O.D.s for compounds such as ametryne, alachlor, metolachlor and chlortoluron, from 10 to 30 pg, which makes the sensitivity of this technique competitive with GC-MS approaches. Another advantage for compounds not amenable to GC, such as the phenylurea herbicides, it is the much

better L.O.D. than other LC-MS techniques such as TSP or particle beam.

In view of the results obtained, we are interested in using LC-ESP-MS at high extraction voltages as a screening method for compounds that can give good structural information, e.g., chlorotriazines. This will be useful for detecting so-called "alarm" levels of chlorotriazine pesticides in different rivers, which are set at 2–5  $\mu\text{g/l}$ .

#### Acknowledgements

This work was supported by the Environment R & D Program 1991–1994 (Commission of the European Communities) (Contract EV5V-CT94-0524) and CICYT (AMB95-1230-CE). C. Molina received a grant from PLANICYT (AMB94-0950-CE).

#### References

- [1] M. Fielding, D. Barceló, A. Helweg, S. Galassi, L. Torstenson, P. van Zoonen, R. Wolter and G. Angeletti, Pesticides in Ground and Drinking Water, in Water Pollution Research Reports, No. 27, Commission of the European Communities, Brussels, 1992, p. 48.
- [2] A.L. Aspelin, Pesticide Industry Sales And Usage. 1992 and 1993 Market Estimates, Office of Pesticide Programs, Environmental Protection Agency, Washington, DC, 1994, p. 19.
- [3] G. Durand, V. Bouvot and D. Barceló, *J. Chromatogr.*, 607 (1992) 319.
- [4] G. Durand and D. Barceló, *Talanta*, 40 (1993) 1665.
- [5] J.W. Readman, T.A. Albanis, D. Barceló, S. Galassi, J. Tronczynski and G.P. Gabrielides, *Mar. Pollut. Bull.*, 26 (1993) 613.
- [6] S. Chiron, A. Fernandez-Alba and D. Barceló, *Environ. Sci. Technol.*, 27 (1993) 2352.
- [7] W.E. Pereira, C.E. Rostad and T.J. Leiker, *Anal. Chim. Acta*, 228 (1990) 69.
- [8] G. Durand and D. Barceló, *Anal. Chim. Acta*, 243 (1991) 259.
- [9] C.E. Rostad, W.E. Pereira and T.J. Leiker, *Biomed. Environ. Mass Spectrom.*, 18 (1989) 820.
- [10] G. Durand, Ph. Gille, D. Fraisse and D. Barceló, *J. Chromatogr.*, 603 (1992) 175.
- [11] D. Barceló, G. Durand, V. Bouvot and M. Nielsen, *Environ. Sci. Technol.*, 27 (1993) 271.

- [12] J. Abián, G. Durand and D. Barceló, *J. Agric. Food Chem.*, 41 (1993) 1264.
- [13] D. Barceló, G. Durand, R.J. Vreeken, G.J. De Jong, H. Lingeman and U.A.Th. Brinkman, *J. Chromatogr.*, 553 (1991) 311.
- [14] R.J. Vreeken, W.D. van Dongen, R.T. Ghijsen and U.A.Th. Brinkman, *Int. J. Environ. Anal. Chem.*, 54 (1994) 119.
- [15] C.S. Creaser and J.W. Stygall, *Analyst*, 118 (1993) 1467.
- [16] W.L. Budde, presented at the 42nd ASMS Conference on Mass Spectrometry and Allied Topics, Chicago, USA, May 29–June 3, 1994.
- [17] C. Molina, M. Honing and D. Barceló, *Anal. Chem.*, 66 (1994) 4444.
- [18] R.D. Voyskner, *Environ. Sci. Technol.*, 28 (1994) 118A.
- [19] M.G. Ikonomou and P. Kebarle, *J. Am. Soc. Mass Spectrom.*, 5 (1994) 791.
- [20] S. Chiron, S. Dupas, P. Scribe and D. Barceló, *J. Chromatogr. A*, 665 (1994) 295.
- [21] H. Bagheri, E.R. Brouwer, R.T. Ghijsen and U.A.Th. Brinkman, *J. Chromatogr.*, 647 (1993) 121.
- [22] R.D. Voyskner and T. Pack, *Rapid Commun. Mass Spectrom.*, 5 (1991) 263.



ELSEVIER

Journal of Chromatography A, 712 (1995) 123–140

---

---

JOURNAL OF  
CHROMATOGRAPHY A

---

---

# Polar organic pollutants in the Elbe river Liquid chromatographic–mass spectrometric and flow-injection analysis–mass spectrometric analyses demonstrating changes in quality and concentration during the unification process in Germany

Horst Fr. Schröder

*Institut für Siedlungswasserwirtschaft, Aachen University of Technology, Templergraben 55, D-52056 Aachen, Germany*

---

## Abstract

During the unification process of the two German states from 1989 to 1994, water extracts from the Elbe river were analyzed by gas chromatography–mass spectrometry (GC–MS) and by high-performance liquid chromatography (HPLC) combined with ultraviolet (UV) and/or mass spectrometric detection (MS) in order to monitor the pollutants in one of the most contaminated European rivers. After column chromatography (LC) or flow-injection analysis (FIA) bypassing the analytical column, ionization was performed by a thermospray interface (TSP). Semiquantitative estimations of the pollution of the Elbe were made from the total-ion current traces (TIC) of the extracts. Determination of the total dissolved organic carbon (DOC) indicated a reduction of more than 55% of pollutants in the water phase. The pollutants were identified by tandem mass spectrometry (MS–MS), generating daughter-ion spectra by collision-induced dissociation (CID) using either column chromatography or direct mixture analysis. Compound-specific analyses indicated a reduction in the amount of pollutants as well as a change in their composition. This could be explained by reduced industrial production and by intensified construction of biological sewage treatment plants.

---

## 1. Introduction

Today as well as over the last ten years, the production of drinking water from surface waters, i.e. from the Rhine and Elbe rivers, supplies more than 20% of the demand in Germany. While in the 1980s the Rhine water quality was rapidly improved, fewer efforts were made in that respect for the Elbe in the former German Democratic Republic (GDR), existing as an independent state up to 1990, and in former Czechoslovakia where the Elbe has its source.

As biological sewage treatment plants did not exist in these states, municipal and industrial waste water was formerly at most mechanically purified before discharge into the Elbe and its tributaries. Due to these insufficiently treated discharges, the Elbe became one of the most polluted rivers in Europe. Up to the unification of the two German states, the results of investigations on the water quality of the Elbe carried out in the GDR were kept strictly under lock and key. Information on the condition of the Elbe was only available from water samples

taken downstream from river km 474.5, i.e. at Schnackenburg. Here the river left GDR territory and was accessible for sampling.

Our own investigations in 1989 found a dissolved organic carbon content (DOC) in the Elbe water of about 16 mg/l. This confirmed estimations of specialists about the state of pollution of the Elbe. While the spectrum of nonpolar organic pollutants and organo-metallic compounds in this river was subject to numerous investigations [1–3], there was still limited knowledge on the polar organic substances because of a lack of analytical detection methods. Compounds which can be recorded by sum parameter analysis might either be of anthropogenic or biogenic origin. Polar and nonpolar organic pollutants [4] in the Elbe differed considerably from those in other West German rivers. The reasons were, on the one hand, the differing industrial production processes applied in the GDR and Czechoslovakia and the way of life of their inhabitants. On the other hand, a pollutant spectrum generally different from that in the rivers of the Federal Republic of Germany (FRG) had to be expected because of the lack of biological sewage treatment plants.

Though only the results of a few selected samples can be presented here, it is possible to recognize trends. Comparisons with the first results from 1989, i.e. from the time before unification, and further investigations during the years following the unification process by means of LC- and flow-injection analysis (FIA)-MS and -MS-MS allow us to describe the changes in the spectrum of polar organic compounds in the Elbe, which went on for years and years.

## 2. Experimental

### 2.1. Materials

Water samples from the Elbe were taken at the beginning of the research work from the Elbe monitoring station at Schnackenburg and additionally in 1994 from the Elbe monitoring station at Magdeburg. Water pollutants were extracted using continuous liquid-liquid or solid-phase extraction. For liquid-liquid extraction,

hexane was used. Solid-phase extraction cartridges were either filled with C<sub>18</sub> material from Baker (Deventer, Netherlands) or with LiChrolut EN from Merck (Darmstadt, Germany) during the last sampling period. From the beginning of 1994, XAD 2 and XAD 4 (Amberlite) from Serva (Heidelberg, Germany) were additionally used for the enrichment and concentration of pollutants.

Inorganic salts were removed from the water phase by an anionic (Duolite A 102 D col) and a cationic ion exchanger (Duolite C 20 col), both from Merck, before freeze-drying.

Solid-phase extraction materials were conditioned as prescribed by the manufacturers. Glass-fibre and membrane filters used for pre-treatment of the water samples were obtained from Schleicher and Schüll (Dassel, Germany) or Sartorius (Göttingen, Germany). Before use, the glass-fibre and membrane filters were heated to 400°C or were treated with ultra-pure water obtained with a Milli-Q system from Millipore (Milford, MA, USA) for 24 h and then washed with 100 ml of the same water. Hexane for liquid-liquid extraction and hexane, diethyl ether, ethyl acetate and methanol used for desorption of water pollutants from the solid-phase material, and acetone and methanol for cleaning purposes were Nanograde solvents from Promochem (Wesel, Germany). Acetonitrile, chloroform, dimethyl sulphoxide and methanol used for column-cleaning purposes were of analytical-reagent grade from Merck. Nitrogen for drying of solid-phase cartridges was of 99.999% purity (Linde, Germany).

LC separations were done on a Nucleosil C<sub>18</sub> (5 µm, spherical) column (25 cm × 4.6 mm I.D.) (CS, Langerwehe, Germany). The mobile phase was methanol (HPLC grade) from Promochem and Milli-Q-purified water. Ammonium acetate for TSP ionization, stored always at 4°C, was of analytical-reagent grade from Merck.

### 2.2. Sampling and sample preparation

All samples were taken as composite samples in glass bottles. Prior to use the bottles were rinsed carefully with Nanograde acetone and methanol and dried at 105°C. The bottles were

rinsed directly before use with several small portions of the same water that was subsequently stored in them. The storage temperature was 4°C. The cold bottles from refrigerator storage were placed in an insulated packaging and were then transported by a parcel service within 24 h from the sampling point to the research laboratory.

Depending on the degree of pollution as monitored by DOC, different amounts of water were used for solid-phase extraction. Water samples for FIA- and LC-MS analysis were forced through the solid-phase extraction cartridges after passage through a glass-fibre filter. To ensure complete adsorption, the water samples were forced through two cartridges in series. The adsorbed pollutants were desorbed more or less separately. Solvents of different polarities (hexane, hexane-diethyl ether, diethyl ether, water-methanol and methanol) were used for this purpose in combination with C<sub>18</sub> and LiChrolut material. The pollutants adsorbed by Amberlite were desorbed continuously under reflux, first with 150 ml of methanol and then with 150 ml methanol-ethyl acetate (1:1, v/v). All eluates from the solid-phase extraction except the methanol and methanol-water eluates were evaporated to dryness with a nitrogen stream at 30°C. Mixtures of solvents and pollutants from XAD 2 and 4 desorption were brought to dryness by rotary evaporation. The residues from both desorption procedures were dissolved in methanol and could be used for injection during FIA- and LC-MS analysis.

The samples were put into glass bottles after solid-phase extraction or XAD adsorption, and freeze-drying was applied to enrich non-adsorbable compounds after the removal of inorganic salts using an additional ion-exchange step. After freeze-drying, the compounds were desorbed with methanol from the glass walls of the bottles by ultrasonification. The methanolic solutions can be used for FIA- and LC-MS investigations.

For GC-MS analysis, depending on the degree of pollution, 2 or 6 l of water were extracted with hexane. After drying with anhydrous sodium sulphate, the volume of the extract was reduced to 200 µl by rotary evaporation and in

an nitrogen stream. This concentrate (concentration factor: 10 000 or 30 000) could be used for injection into the GC-MS system.

### 2.3. Sum parameter analysis

The dissolved organic carbon (DOC) content of the water samples was measured using a Dohrman total carbon analyzer DC 80. After filtration of the pretreated samples using a glass-fibre filter, wet oxidation with an acidic potassium persulphate solution in water assisted by UV radiation was performed.

### 2.4. Gas chromatographic system

A Varian (Darmstadt, Germany) Model 3400 GC system with a fused-silica capillary column was used. The conditions were as follows: carrier gas, helium; linear gas velocity, 15 cm/s; injector temperature, 250°C; transfer line temperature, 250°C; column, DB-17; film thickness, 0.25 µm (30 m × 0.32 mm I.D.).

Combined with GC, electron-impact (EI) ionization was applied with an ionization energy of 70 eV. Under these conditions the pressure in the ion source was  $8 \cdot 10^{-6}$  Torr (1 Torr = 133.322 Pa) and that in the vacuum system of the mass spectrometer  $3 \cdot 10^{-2}$  Torr. The electron multiplier was operated at 1200 V with the conversion dynode voltage at 5 kV. The temperature in the ion source was 150°C.

### 2.5. Liquid chromatographic system

LC separations coupled with MS, MS-MS and UV detection were achieved with a Waters (Milford, MA, USA) Model 600 MS system. A Waters Model 510 pump was used for post-column addition of 0.1 M ammonium acetate solution in the TSP mode. A Waters Model 490 MS UV detector (up to the beginning of 1994) and then a Waters 996 photodiode-array detector system in combination with a Millennium 2010 data system (Millipore) was connected in-line with the TSP interface. The conditions in FIA bypassing the analytical column were as follows: mobile phase I, methanol-water (60:40); mobile phase II, 0.1 M ammonium acetate in water. The

Table 1  
Gradient elution scheme and composition of mobile phase I

Time (min)	Solvent A (%)	Solvent B (%)
0	10	90
10	30	70
25	60	40
35	90	10

Solvent A = acetonitrile; solvent B = water–methanol (80:20, v/v).

overall flow-rate was 1.5 ml/min, with a ratio of 0.8 ml/min of mobile phase I and 0.7 ml/min of mobile phase II.

The chromatographic separations on the analytical column were carried out after optimization of the conditions by standardized methods, shown in Tables 1 and 2. The flow-rate for column separation was 1.0 ml/min of mobile phase I. After passing the UV detector, 0.5 ml/min of mobile phase II was added, which resulted in an overall flow-rate of 1.5 ml/min.

The reversed-phase column was cleaned once a day with acetonitrile–chloroform–methanol–dimethyl sulphoxide (3:3:3:1, v/v).

## 2.6. MS and MS–MS systems

From 1988 to 1993 a TSQ 70 mass spectrometer (Finnigan MAT, San Jose, CA, USA) combined with a PDP 11/73 data station was used for research work. At the beginning of 1994, the mass spectrometer was upgraded to a TSQ 700 with a DEC 5000/33 data station. The TSP interface was obtained from Finnigan MAT.

Table 2  
Gradient elution scheme and composition of mobile phase II

Time (min)	Solvent A (%)	Solvent B (%)
0	20	80
10	100	0

Solvent A = acetonitrile; solvent B = water–methanol (80:20, v/v).

After upgrading, the TSP interface was adapted to the new system by Finnigan.

For coupling the LC system with the mass spectrometer, the conditions for TSP ionization using ammonium acetate were chosen as: vaporizer temperature, 90°C and jet block temperature, 250°C. The conditions varied during the analytical separations. Under these conditions the ion source pressure was 0.5 Torr, and the pressure in the vacuum system of the mass spectrometer was  $2 \cdot 10^{-5}$  Torr.

The electron multiplier was operated at 1200 V and the conversion dynode at 5 kV. In the MS–MS mode the ion source pressure was also 0.5 Torr. Under CID conditions the pressure in quadrupole 2 (collision cell) normally was 1.3 mTorr, unless otherwise specified in the captions of the figures. The collision energy was adjusted from –10 to –50 eV. The electron multiplier voltage in quadrupole 3 was 1500 V with the conversion dynode voltage at 5 kV.

GC–MS analysis was performed by scanning at 1 s from 45 to 500 u.

FIA and LC analyses were applied, recording TSP mass spectra scanning from 150 to 1200 u at 1 or 3 s, respectively. FIA bypassing the analytical column with MS detection was performed while accumulating a maximum of 50 scans after injection. The mass spectrum averaging the total-ion current from the beginning of the signal up to the end is called the “overview spectrum”.

TSP-ionization was normally carried out in positive and negative modes.

For quantification the mass spectrometer was operated in the selected-ion monitoring (SIM) mode using a dwell time of 200 ms for each mass. Estimations on the concentration of the whole pollutant spectrum were made using the total-ion current trace (TIC) after FIA.

## 3. Results and discussion

Due to the special situation of the two German states, it was still necessary in 1989 to take samples on FRG territory in order to obtain information on the condition of the Elbe. Thus, in 1989, the first samples for these investigations,



carried out at the beginning of an unforeseeable historic change, were taken in Schnackenburg at river km 474.5, where the river enters FRG territory. These samples could serve to determine the state of pollution of the Elbe at that period, with special regard to polar organic compounds.

Screening tests of this 24-h composite sample by GC or LC and FIA-MS, respectively, revealed high concentrations of moderately polar, volatile as well as polar, non-volatile organic pollutants. With 16 mg/l the sum parameter DOC, determined in parallel, was excessive for a surface water serving also for drinking water purposes on GDR territory.

This and the following water samples were analyzed intensively for organic compounds in order to determine especially the polar pollutant spectrum of the Elbe as completely as possible for quantitative assessment and characterization. For this purpose GC-MS, LC-MS and FIA-MS as well as MS-MS analysis with different enrichment procedures were carried out. Fig. 1b shows the GC-MS total-ion current trace of the hexane extract from this composite sample. Many of these pollutants can be identified immediately because of their specific fragmentation pattern or by library search using the NBS library of electron-impact (EI) spectra. These substances, which can be identified without clean-up steps,

are nearly exclusively phthalates of different molar masses in high concentrations. This is proven by the mass trace of the fragment  $m/z$  149, which is characteristic for this class of compounds (Fig. 1a). The majority of the other compounds of this extract, for example tetrabutyl stannane and long-chain hydrocarbons, which can be separated by GC, have an even less polar structure and are therefore not as soluble in water. This is the reason why they were present in the water phase at a considerably lower concentration than the phthalates and should be found in higher concentrations in the river sediment. Due to a lower concentration in the water, they could be detected only after adequate clean-up steps by target analysis, as high phthalate concentrations in the extract predominated in the TICs and prevented the detection of other pollutants during non-targeted screening tests.

At the beginning of our examinations, the polar, non-volatile compounds were obtained by enrichment on  $C_{18}$  material and selective elution with solvents and their mixtures of different polarities [5]. Under the conditions of the pre-separation method applied here, their selective elution behaviour in these samples was only poorly distinct. Some of the overview spectra recorded by FIA-MS of the eluates from "selective elution" are shown in Figs. 2a and 2b,

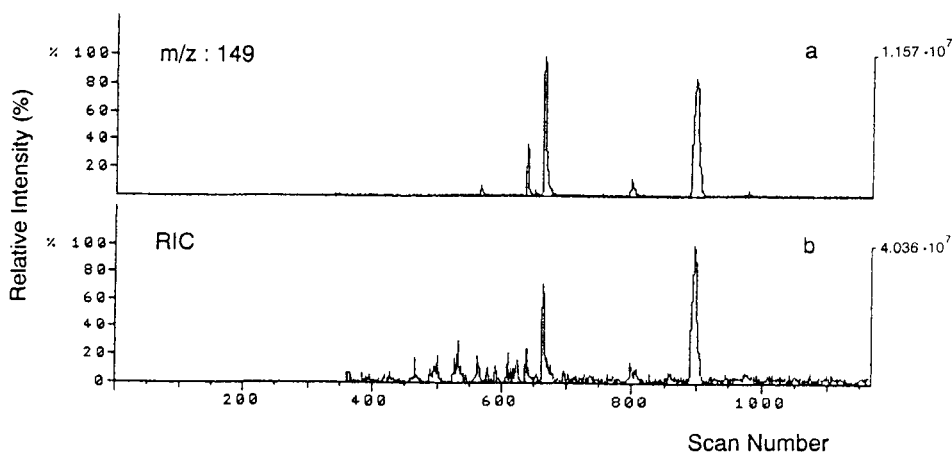


Fig. 1. (a) GC-MS mass trace of fragment ion  $m/z$  149 for water sample no. 1 of the Elbe river. Liquid-liquid extract; solvent, hexane. (b) GC-MS total-ion current trace as in (a). For concentration factor, see Experimental.

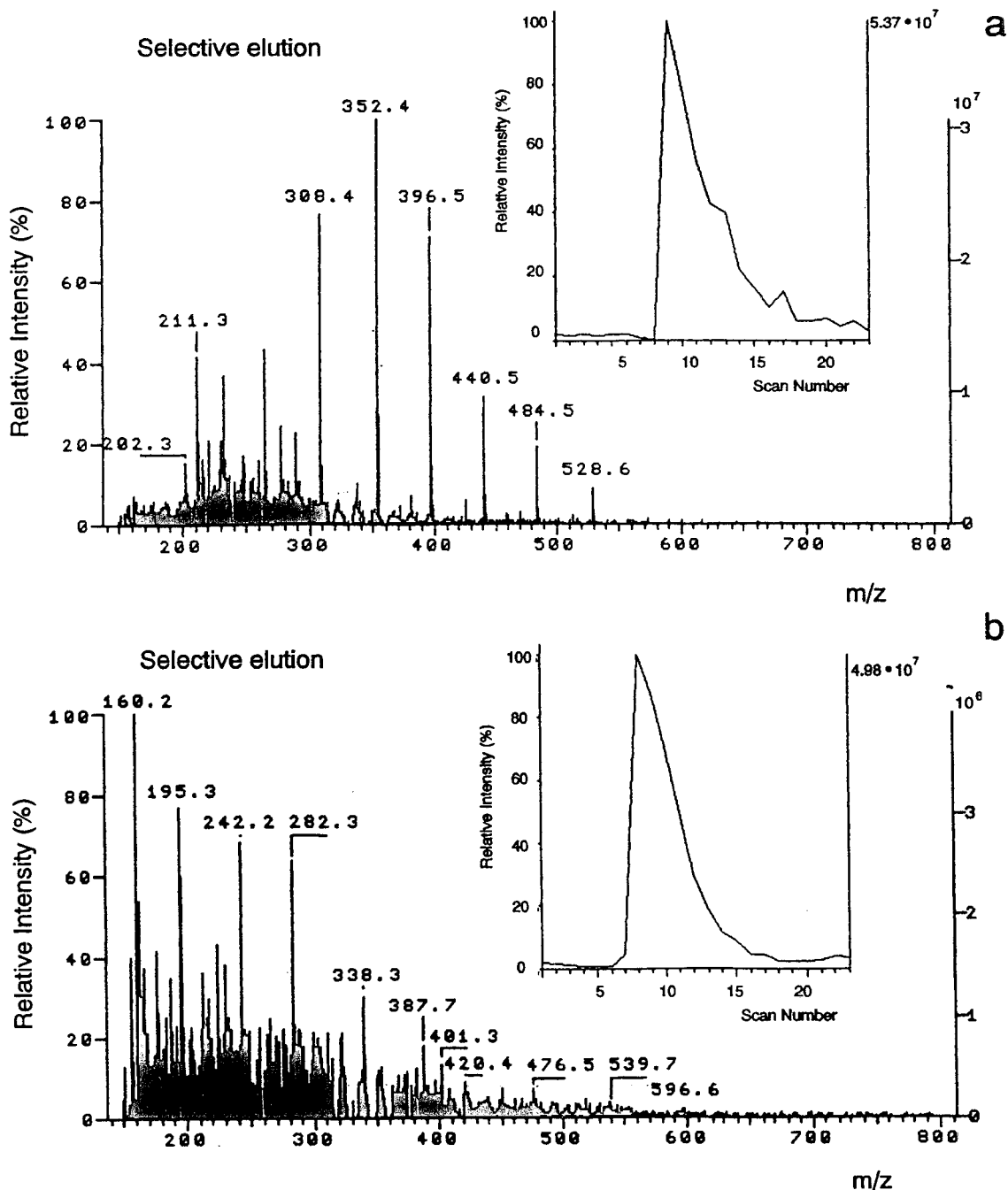


Fig. 2. (a) TSP-MS loop injection spectrum obtained by bypassing the analytical column (FIA-MS), subsequently called "overview spectrum", for water sample no. 1 of Elbe river.  $C_{18}$  solid-phase extract; eluent, diethyl ether. (b) FIA-MS overview spectrum as in (a). Eluent, methanol. Positive TSP ionization. For FIA conditions, see Experimental.

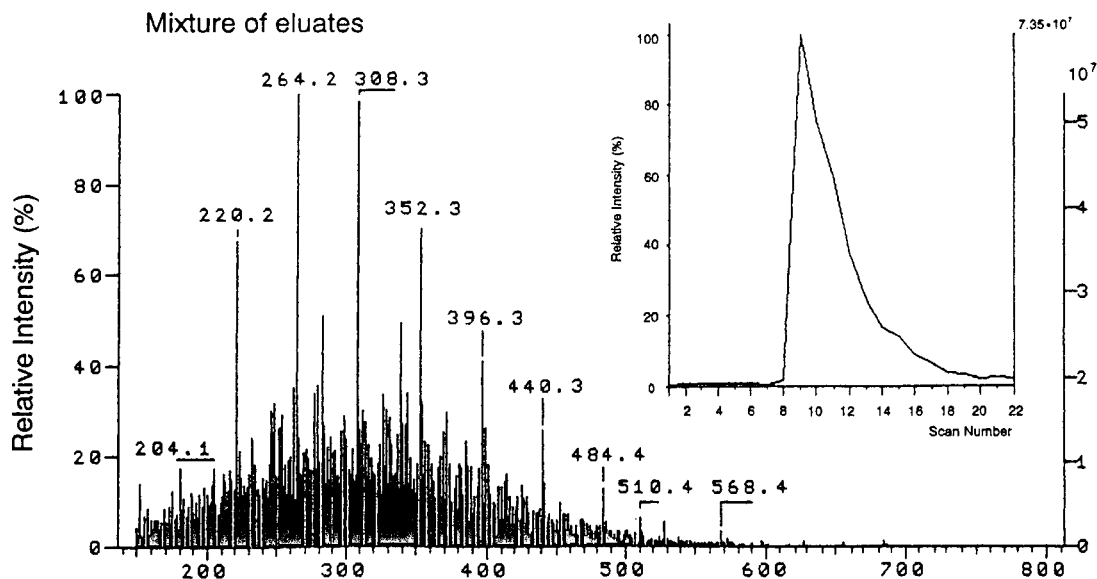


Fig. 3. FIA-MS overview spectrum as in Fig. 2. Mixture of eluates. Eluents, hexane, hexane-ether, ether, water-methanol, methanol.

including their TICs. The overview spectrum in Fig. 3 was recorded from a mixture of all different eluates. The overview spectra here contain their own TIC, which have been inserted into the figures. This method represents a good and quick possibility to make quantitative estimations and to compare the content of pollutants qualitatively. These procedures were possible because the samples to be compared were always handled in the same way and were dissolved in the same solvent.

Examining the compounds of these “selective eluates” by FIA-MS, i.e. bypassing the analytical column without chromatographic separation, but only using the tandem function of the mass spectrometer, some of them can already be identified. This is possible by interpretation of the daughter-ion spectra generated by CID or by comparison of these CID spectra with those contained in our laboratory-made CID library of polar organic water compounds [6].

But also this analytical method has its application limits. Thus FIA-MS analysis with subsequent identification by direct mixture analysis

(MS-MS) is only successful if the mixture consists of a large number of various compounds which differ in their  $m/z$  ratio. Otherwise, the CID spectrum would consist of a mixture of at least two differently dissociating ions [7] and therefore could not be interpreted. Due to the complexity even of the  $C_{18}$  extracts obtained by “selective” elution and to the application limits of mixture analysis, these extracts were also submitted to chromatographic separation on an  $RP_{18}$  phase. Detection followed after TSP ionization by MS and inserted in-line UV detection at 220 nm. The total-ion current trace (TIC) and UV trace are shown in Figs. 4a and 4b. It can be seen that only a small part of the thermospray-active compounds absorbs at 220 nm, i.e. could actually be detected by UV. Although the TIC shows a good total-ion mass trace, only some of the compounds are clearly separated. This can be demonstrated in Fig. 4b, showing the signals of a mixture of compounds hidden under peak 2 (Fig. 4d). These ions are equally spaced with  $\Delta m/z$  44. These compounds are non-ionic surfactants of the alkylpolyglycoether type, as verified

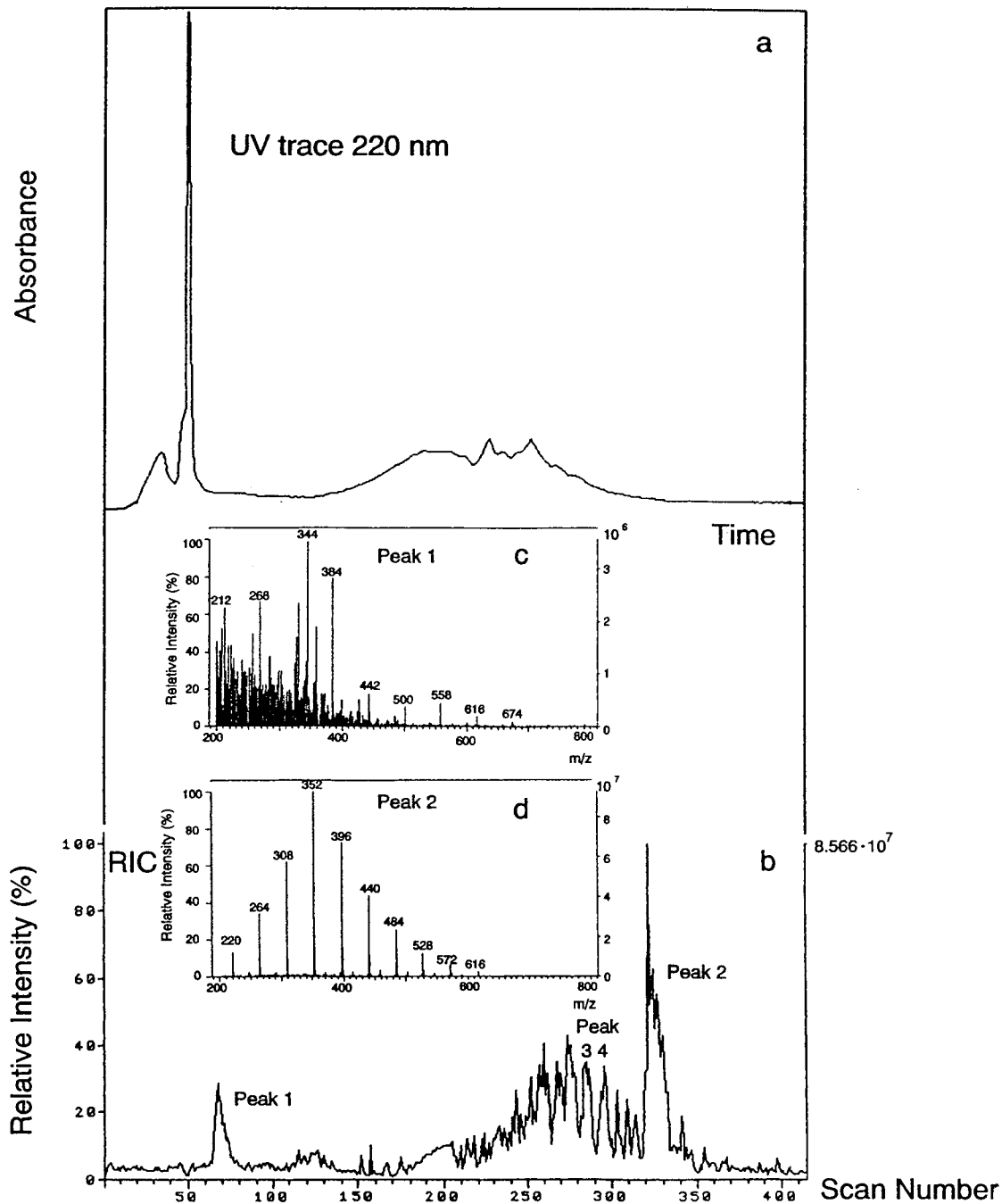


Fig. 4. (a) UV trace (220 nm) for water sample no. 1 of Elbe river.  $C_{18}$  solid-phase extract; mixture of eluates as in Fig. 3; for chromatographic conditions, see Experimental and Table 1. (b) LC-MS total-ion current trace of Elbe river extract in (a) and LC mass spectra of (c) peak 1 and of (d) peak 2; LC conditions as in (a). Positive TSP ionization.

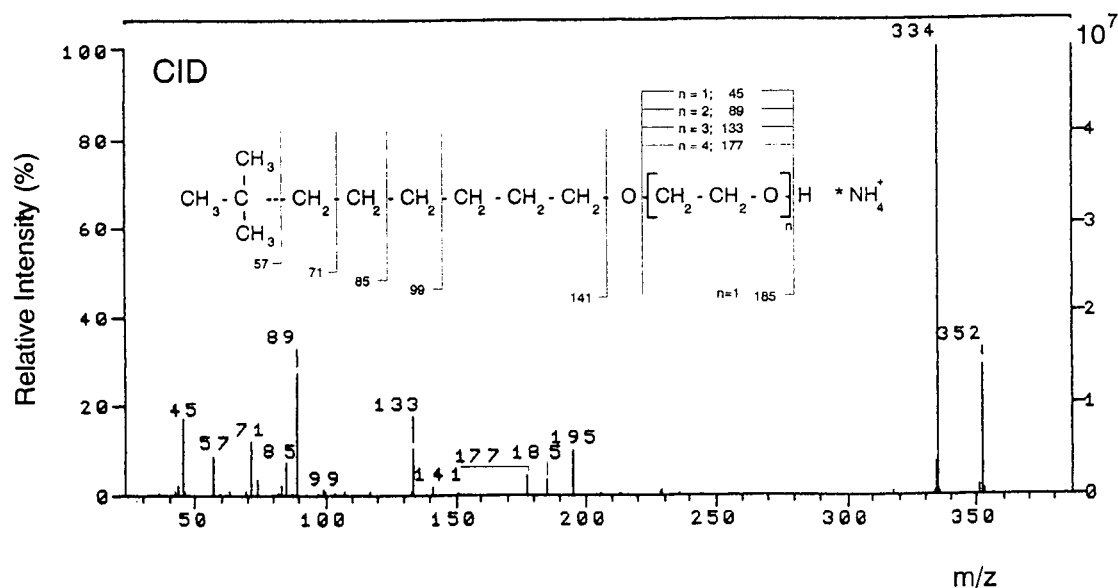


Fig. 5. Daughter-ion mass spectrum (LC-MS-MS) and fragmentation scheme of non-ionic surfactant cluster ion [ $m/z$  352;  $C_{10}H_{21}O(CH_2CH_2O)_nH^+NH_4^+$ ] in peak 2 from Elbe river extract as in Fig. 4b. Collision energy,  $-20$  eV.

by the daughter-ion spectrum of  $m/z$  352 in Fig. 5 [8]. The general empirical formula for this compound is  $C_{10}H_{21}O(CH_2CH_2O)_nH$ , taken from comparison with daughter-ion spectra in our library. For the ammonium adduct ion with  $m/z$  352, the number  $n$  of glycol units is 4. Most signals in the TIC (Fig. 4b) consist of a larger number of very different polar compounds [see Fig. 6a (peak 3 in Fig. 4b) and 6b (peak 4 in Fig. 4b)], such as polyethylene- and polypropyleneglycol and their biochemical oxidation products [9] as well as phthalates and alkyl benzenesulphonic acid (LABS). LABS was also identified by negative TSP ionization [12]. At the same time a large number of non-striking compounds are hidden under nearly each of these signals (Fig. 4b), which cannot be separated or focussed by the applied column, even under strongly varying chromatographic conditions. On the simplifying assumption that the signal height in the mass spectra is a measure of the concentration of compounds, up to 40% of the thermospray-active compounds of the extracts are hidden behind these matrix compounds.

Another 24-h composite sample of the Elbe, taken in 1990 for comparison purposes at exactly

the same location and on the same day as the earlier water sample, is shown as TIC after LC-MS in Fig. 7b. Comparing the results of this sample 2 with those of sample 1, first estimations during GC-MS, FIA-MS and LC-MS analysis point to reduced concentrations of nonpolar as well as polar compounds. This is confirmed by the sum parameter DOC, which had been measured in parallel as 10 mg/l, i.e. the carbon content is reduced by 40%.

While the ion current of the GC-MS analysis is characterized here also by phthalates, as before in sample 1, the spectrum of compounds which can be recorded by LC-MS has considerably changed. In contrast to sample 1, dominant signals suited straightaway for MS-MS characterization were no longer found in the FIA-MS spectra of the extract obtained by selective elution. Therefore, LC separation was carried out directly with the mixture of all eluates. As separation failed with the gradient elution mentioned in Table 1, it was carried out under the chromatographic conditions listed in Table 2. The UV trace at 220 nm and ion-current trace are shown in Fig. 7. The mass spectrum of the signal in the scan region 759–775 of the TIC can

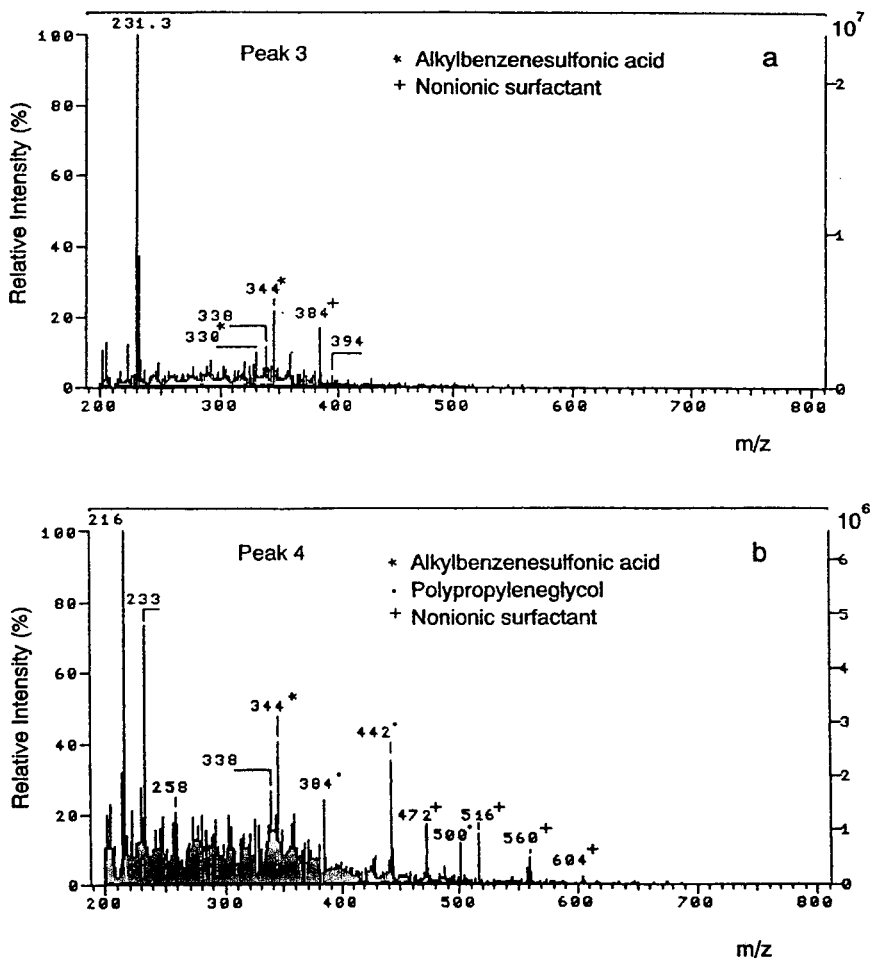


Fig. 6. LC-MS spectra of (a) peak 3 and (b) peak 4 in Fig. 4b.

be identified at once as non-ionic surfactant because of the equidistant signals with  $\Delta m/z$  44 (see Fig. 7c). The daughter-ion spectrum in Fig. 7d allows an unequivocal characterization as nonylphenol ethoxylate. This substance is only rarely detected in surface waters of the FRG. Its application is no longer allowed because of its toxic primary degradation product nonylphenol. The polyglycoether of either anthropogenic or biogenic origin, which could still be observed clearly in Figs. 2 and 3 in the background of the overview spectra of extracts from sample 1, has now almost completely disappeared, as proven by overview spectra.

The examination of another sample from the Elbe (sample 3) taken in 1992, i.e. about three years after first sampling, indicated a further reduction of the pollutant concentration in the river. First proof for this development was the DOC content, being now about 7 mg/l and, thus, more than 55% lower than in sample 1 taken in 1989. Because of the low DOC value, the water volume used for enrichment was tripled for solid-phase as well as hexane extraction. Considerably reduced concentrations of phthalates were detected in the ion-current trace of the GC-MS analysis, so that it was possible to recognize during screening even small quantities

of chloronitrobenzene, chloronitroaniline and hexachlorobenzene in the ion-current trace without special sample preparation.

The observations made for sample 2 apply also to the spectra of this sample 3 generated by FIA-MS; i.e. signals which normally dominate the FIA-MS overview spectra were not found here, except phthalates ( $m/z$  279 and 391) in low concentrations. Therefore, the extract was submitted immediately to LC separation under the same chromatographic conditions as for sample 1. The ion-current trace of the LC separation is

shown in Fig. 8, together with the UV trace. Besides some ions belonging to non-ionic surfactants on a polyethylene or polypropylene glycol basis (see Figs. 8c and 8d), it was not possible to identify other compounds because of the reduced pollutant concentration and, thus, lack of sampling material.

The pollutant content in the 24-h composite sample, taken in 1994 in early summer, was even lower than in all sampling materials from the Elbe analyzed up till then. This sample 4 was taken nearly exactly five years after the first one.

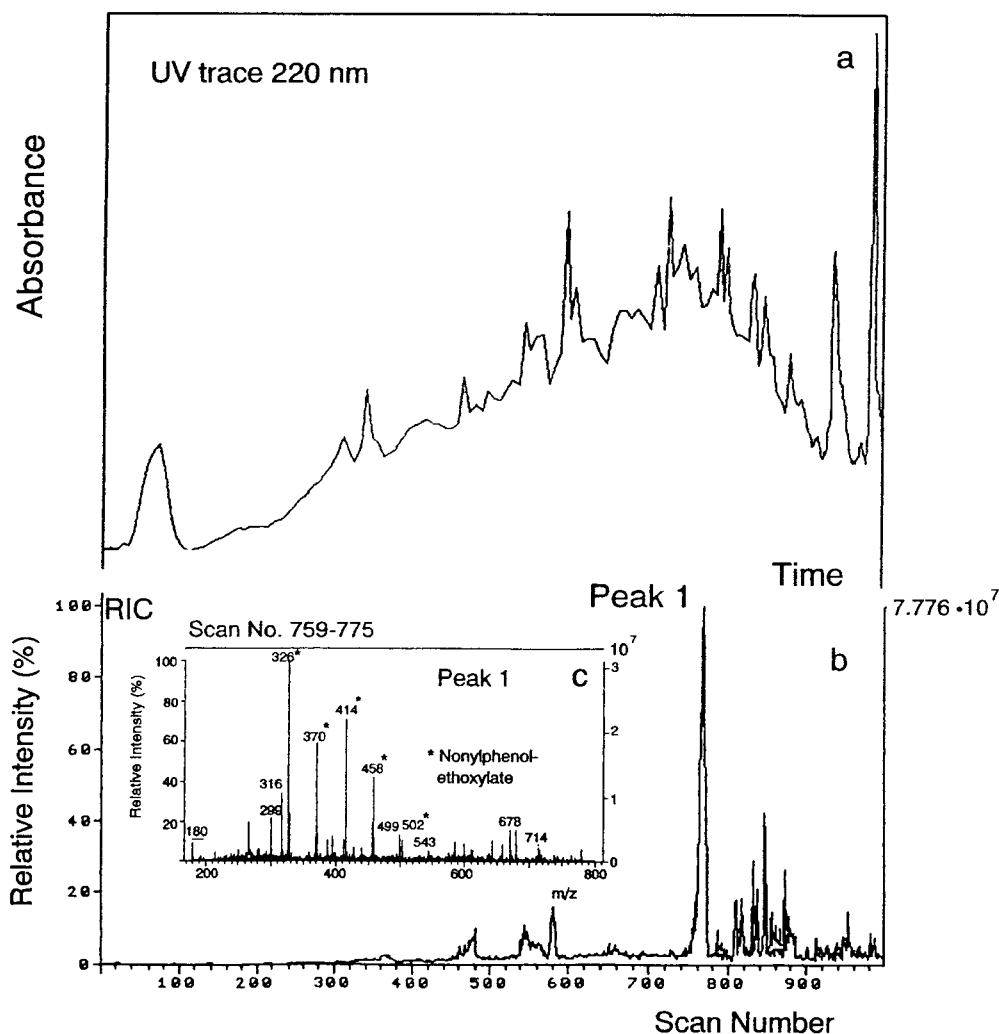


Fig. 7 (continued on p. 134).

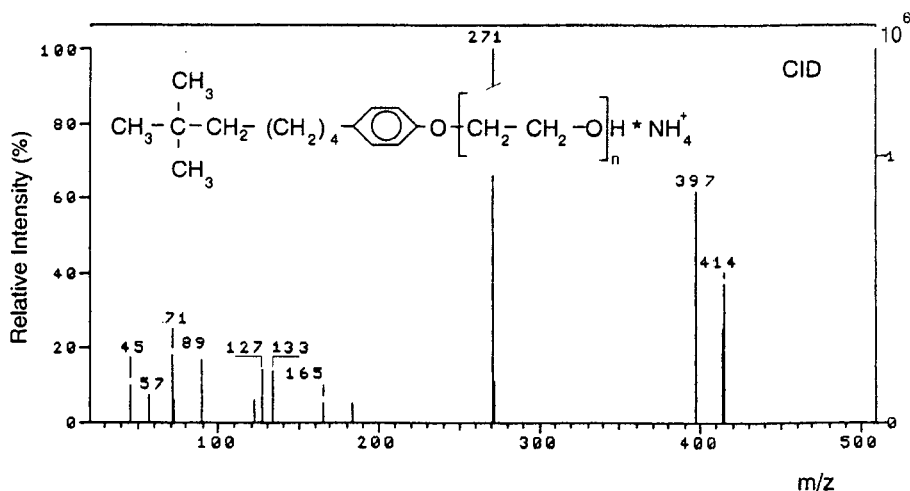


Fig. 7. (a) UV trace (220 nm) for water sample no. 2 of Elbe river.  $C_{18}$  solid-phase extract; mixture of eluates as in Fig. 3; for chromatographic conditions, see Experimental and Table 2. (b) LC-MS total-ion current trace of Elbe river extract in (a) and LC-MS spectrum of (c) peak 1; LC conditions as in (a). Positive TSP ionization. (d) Daughter-ion mass spectrum (LC-MS-MS) and fragmentation scheme of non-ionic surfactant (nonylphenoethoxylate) cluster ion [ $m/z$  414;  $C_9H_{19}(C_6H_4)O-(CH_2CH_2O)_nH^+NH_4^+$ ] in peak 1 from Elbe river extract as in (b). LC conditions as in (a). Collision energy,  $-25$  eV.

It corroborates the trend towards progressive improvement of the water quality which was noted in the earlier samples. So the DOC was with 6 mg/l again lower than in all other tested water samples. Besides hexachlorobenzene, tribromofluoromethane and some phenols, especially phthalates, which are widespread all over the environment, dominate the ion current of the GC-MS analysis. The intensity of the ion current in sample 4 was now only about 20% of that measured in sample 1.

This was nearly the same with the ion-current traces of the extracts obtained by selective elution and examined by FIA-MS, where we tried to compensate for the low concentration of compounds by enrichment of pollutants from a larger water volume. A mass spectrum of the compounds of the whole extract generated by FIA-MS, i.e. without selective elution, shows a Gaussian distribution, and the maximum intensity of the molecule ions is about  $m/z$  300 (Fig. 9), while the ions of the compounds from sample 1 have their maximum at  $m/z$  200.

The chromatographic separation corresponding to LC conditions of sample 1 results in

a TIC which is hardly structured and contains only a few signals (Fig. 10d) and a maximum plot after photodiode-array detection which is not very informative (Fig. 10a). The largest part of the very polar compounds of this extract can be separated only insufficiently under those conditions, except for the ions  $m/z$  257 and 274 (Fig. 10f). This complicates the identification of compounds, as they elute more or less continuously. Thus the specific objective of chromatography, i.e. separation, focussing and, if necessary, identification by CID, is missed. Therefore, we tried to characterize these compounds without preceding LC separation by mixture analysis, using the tandem function of the spectrometer (MS-MS). Even from the confusing mixture in Fig. 9, daughter ions can be generated without problems if the parent ions are accessible to the collision-induced fragmentation process. Besides the parent ions with  $m/z$  257 and 274, which could be separated by LC, we tried to generate daughter ions and to identify the ions with  $m/z$  268 and 270 with their strikingly characteristic isotope pattern. In spite of painstaking optimization of the collision energy and collision gas



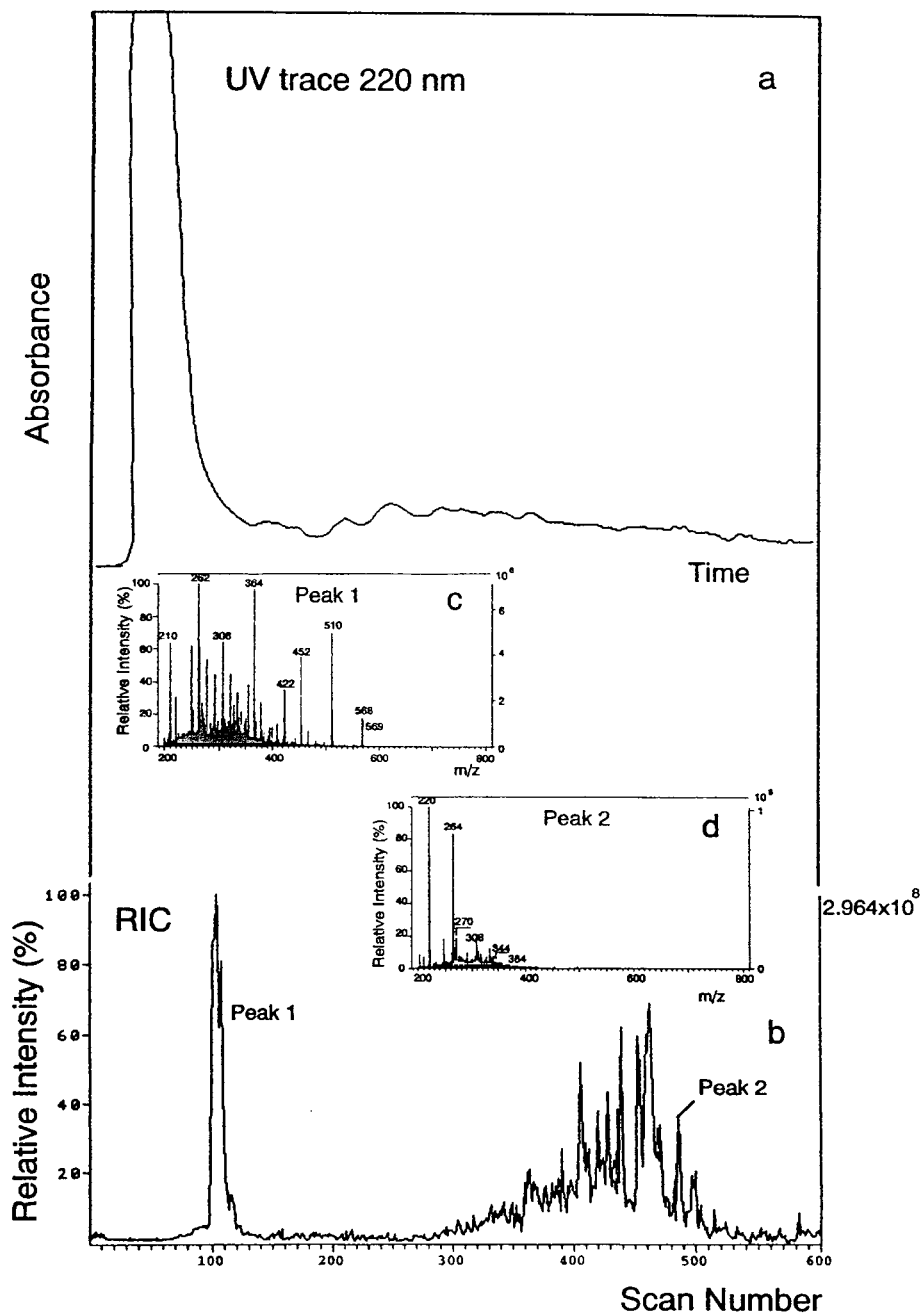


Fig. 8. (a) UV trace (220 nm) for water sample no. 3 of Elbe river.  $C_{18}$  solid-phase extract; mixture of eluates as in Fig. 3; for chromatographic conditions, see Experimental and Table 1. (b) LC-MS total-ion current trace of river Elbe extract in (a) and LC-MS spectrum of (c) peak 1 and of (d) peak 2; LC conditions as in (a). Positive TSP ionization.

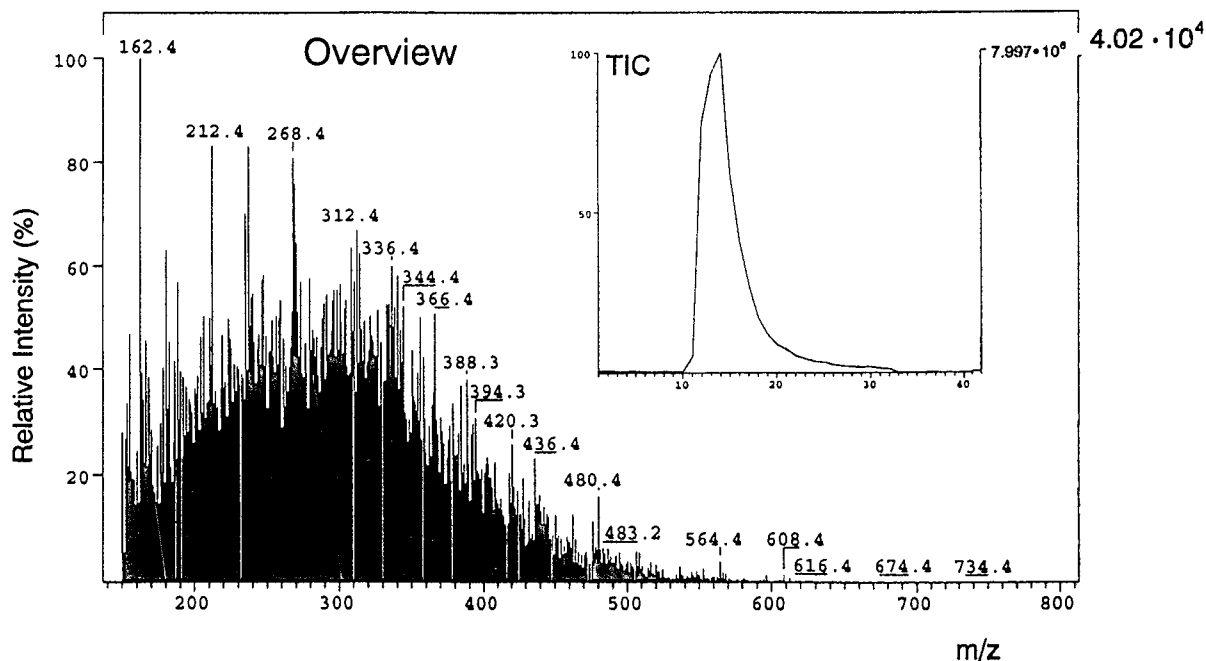


Fig. 9. FIA-MS overview spectrum as in Fig. 2. Mixture of eluates. Eluents, hexane, hexane-ether, ether, water-methanol, methanol.

pressure, the parent ions with  $m/z$  257 and 274 were decomposed into a single daughter ion ( $m/z$  91) only, common to both of them. CID fragmentation of the ions with  $m/z$  268 and 270 resulted in daughter-ion spectra which were very rich in lines and resembled those from electron-impact spectra (Fig. 11).

The concurrence in the daughter ion 91 for both parent ions with  $m/z$  257 and 274 gives rise to the presumption that the same compound is concerned. Ion 257 was formed by the addition of a proton and ion 274 by the addition of an ammonium ion from the ionization agent ammonium acetate to the molecule of molar mass 256. Identification is not possible using a daughter ion spectrum which is so poor in lines.

The daughter-ion spectra of  $m/z$  268 and 270 are rich in lines, which is remarkable for CID spectra. The intensity of the signals of the fragment ions shows that the same compound is concerned, but substituted with different isotopes (see Fig. 11). The different molar masses are caused by the masses of the bromine isotopes

found in the natural environment ( $^{79}\text{Br}/^{81}\text{Br}$ ). Fragments containing bromine (for example in the  $^{79}\text{Br}$ -substituted molecule: 93, 107, 119, 131, 149, 165, 177, 191, 205, 233 and 251) can be recognized very easily because of the mass difference of 2 u in both CID spectra (compare Figs. 11a and 11b). A final characterization has yet to be done. At present, synthesis of reference substances with the empirical formula  $\text{C}_{11}\text{H}_{23}\text{OBr}$  and the molar mass 250/252 is in progress.

#### 4. Conclusions

Sampling from the Elbe, carried out always in early summer in 1989, 1990, 1992 and 1994, and analysis on polar organic compounds showed a clear trend towards ever-decreasing pollutant concentrations. These results were confirmed by sum parameter analysis (DOC) as well as by estimation of the ion-current trace during FIA-

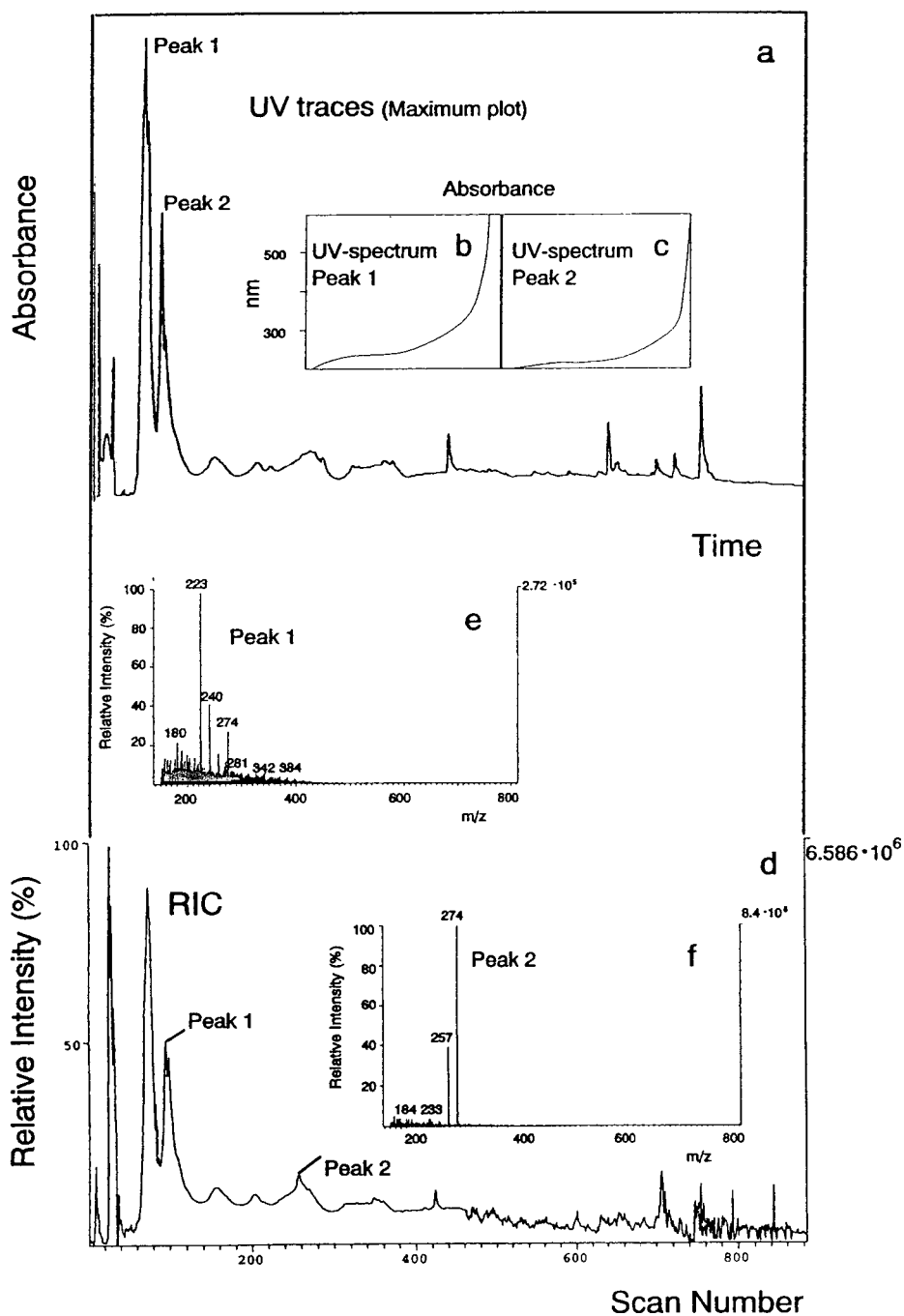


Fig. 10. (a) UV trace (maximum plot) for water sample no. 4 of Elbe river and UV spectra of (b) peak 1 and of (c) peak 2.  $C_{18}$  solid-phase extract; mixture of eluates as in Fig. 3; for chromatographic conditions, see Experimental and Table 1. (d) LC-MS total-ion current trace of Elbe river extract in (a) and LC-MS spectra of (e) peak 1 and of (f) peak 2; LC conditions as in (a). Positive TSP ionization.

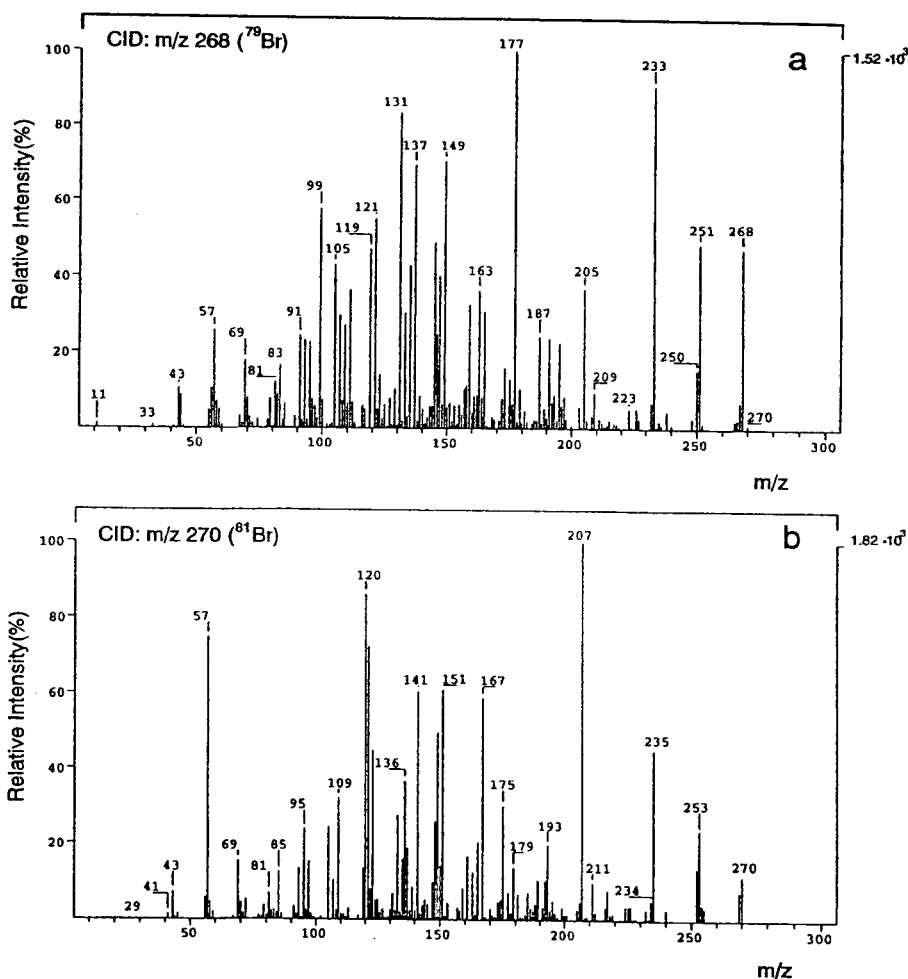


Fig. 11. Daughter-ion mass spectra (FIA-MS-MS) of (a) cluster ion  $m/z$  268 ( $^{79}\text{Br}$ ) and of (b) cluster ion  $m/z$  270 ( $^{81}\text{Br}$ ). Collision energy,  $-15 \text{ eV}$ .

MS and LC-MS analysis. Screening by GC-MS, carried out in parallel, showed the same results.

The pollutant spectrum of the Elbe water, admittedly assessed on the basis of four 24-h composite samples which were taken, however, always at the same seasonal date, showed characteristic changes as to concentration and quality. The quantitative reduction of pollutants is confirmed by the ion-current traces recorded by FIA-MS.

Qualitative changes during the research period can be observed with the help of the overview spectra generated from the TICs which were

recorded by FIA-MS. At the end of the investigation period, they contain only a few compounds which rise above the background of the matrix, in contrast to those recorded at the beginning of this investigation (Figs. 2 and 3). This qualitative change of compounds is also demonstrated by the shift of the maximum intensity of ion distribution in the overview spectra up to higher  $m/z$  ratios (compare Figs. 2 and 3 with Fig. 9).

By combining  $\text{C}_{18}$  material and freeze-drying for enrichment and concentration, respectively, of adsorbable or non-adsorbable pollutants, it

was possible to compare the results of the samples. By this, it was proven that the concentration of individual compounds has become more and more equalized during the sampling period.

The qualitative change in the compounds is shown by the fact that, on the one hand, as already mentioned, the appearance of the overview spectra recorded during FIA–MS analysis of the  $C_{18}$  extracts has changed. On the other hand, approved liquid chromatographic separation conditions, as applied for the successful LC–MS separation of the extracts of samples 1 and 2, could now separate only insufficiently the extracts from samples 3 and 4. With few exceptions, the compounds of these samples do not elute as sharp signals, but continuously. This shows that the polarity of enriched substances has increased from year to year, as always the same  $C_{18}$  column with constant separation efficiency, ensured by standards, had been used.

Direct mixture analysis using FIA–MS and FIA–MS–MS solves part of the difficulty and enables detection and characterization of selected thermospray-active compounds [6,8,10–12]. Direct mixture analysis using the MS–MS option can be applied successfully even in such cases where no dominant signals are observed, but pollutants in similar concentrations are present.

By application of other adsorption materials during the last sampling period, such as LiChrolut EN, XAD 2 or 4, no improvement – except for LiChrolut EN – could be found by comparison of the intensity of the different TICs, i.e. only slightly increased adsorption of polar organic compounds related to the  $C_{18}$  material applied could be observed. In parallel, compounds different in character from the  $C_{18}$ -adsorbable compounds could be adsorbed and should be examined in future.

Unfortunately, the stability of the pollutant mixture from solid-phase extraction, stored in methanolic solution at  $-30^{\circ}\text{C}$ , is limited. Many compounds are already decomposed after 2–3 months, and thus it is no longer possible to compare extracts from old and new samples directly in one run. At present, the stability of sampling material at storage temperatures of

$-86^{\circ}\text{C}$  and at liquid nitrogen temperature is being examined.

The reduction of the concentration of pollutants in the Elbe and their change during the research period of five years can only partly be explained by the increased number of biological sewage treatment plants used to improve the treatment of waste waters discharged into the Elbe. Since the start of the German unification process the discharge of industrial waste waters has also continuously decreased, because of a massive reduction of industrial capacity in the former GDR [13].

As a result of these changes, the concentration of pollutants has decreased, and the pollutant spectrum has changed dramatically. In spite of increased efforts made towards waste water treatment along the Elbe and its tributaries, the concentrations of organic pollutants will hardly change in the future. Other research work [2] suggests that the DOC content will remain as high as that found in the last sample, because the Elbe has normally rather high contents of dissolved organic carbon as matrix. Most of the biogenic compounds hidden behind the DOC are polar, which will continue to complicate the detection of anthropogenic substances.

### Acknowledgements

Generous financial support by the German Minister for Research and Technology in Project 02 WT 9358/2 is gratefully acknowledged. Moreover, I thank Dr. Reincke of Water Quality Monitoring Board Elbe, Hamburg, and Dipl.-Ing. Gerlach of IWW, Mülheim/Ruhr, for the water samples from river Elbe. I thank Mr. Scheduling and Mr. Lohoff for their support in recording spectra and Mr. Gschwendtner for the preparation of numerous samples.

### References

- [1] T. Guderitz, W. Schmidt and H.-J. Brauch, *Vom Wasser*, 81 (1993) 315.

- [2] U. Müller, B. Wricke and H. Sontheimer, *Vom Wasser*, 81 (1993) 371.
- [3] R.-D. Wilken, H. Hintelmann and R. Ebinghaus, *Vom Wasser*, 74 (1990) 383.
- [4] N. Greiser, *Hamb. Küstenforsch.*, 45 (1988) 1.
- [5] H.Fr. Schröder, *Vom Wasser*, 80 (1993) 323.
- [6] H.Fr. Schröder, *J. Chromatogr.*, 554 (1991) 251.
- [7] H.Fr. Schröder, *Vom Wasser*, 82 (1994) 185.
- [8] H.Fr. Schröder, *Vom Wasser*, 73 (1989) 111.
- [9] H.Fr. Schröder, in *DVGW Deutscher Verein des Gas- und Wasserfachs, DVGW-Schriftenreihe Wasser*, No. 108, Wirtschafts- und Verlagsgesellschaft Gas und Wasser mbH, Bonn, 1990, pp. 121–144.
- [10] G.K. Christiansen, R. Brock and G. Bojensen, *Anal. Chem.*, 66 (1994) 3253.
- [11] H.Fr. Schröder, *J. Chromatogr.*, 643 (1993) 145.
- [12] H.Fr. Schröder, *J. Chromatogr.*, 647 (1993) 219.
- [13] Statistisches Bundesamt (Editor), *Statistisches Jahrbuch 1993 für die Bundesrepublik Deutschland*, Wiesbadener Graphische Betriebe GmbH, Wiesbaden, 1993.



ELSEVIER

Journal of Chromatography A, 712 (1995) 141–147

JOURNAL OF  
CHROMATOGRAPHY A

## Identification of phosphocysteine by electrospray mass spectrometry combined with Edman degradation<sup>☆</sup>

Christiane Weigt<sup>a</sup>, Horst Korte<sup>a</sup>, Rembert Pogge von Strandmann<sup>b</sup>,  
Wolfgang Hengstenberg<sup>b</sup>, Helmut E. Meyer<sup>a,\*</sup>

<sup>a</sup>Institut für Physiologische Chemie I, Abteilung Biochemie Supramolekularer Systeme, Protein-Sequenzlabor, MA 2/143,  
Ruhr-Universität Bochum, 44780 Bochum, Germany

<sup>b</sup>Physiologie der Mikroorganismen, NDEF 06/744, Ruhr-Universität Bochum, 44780 Bochum, Germany

### Abstract

Phosphocysteine is an intermediate in the phosphoenolpyruvate-dependent phosphotransferase system (PTS) and in the dephosphorylation of phosphotyrosine residues by protein tyrosine phosphatases. A method is described for the direct and non-radioactive localization of phosphocysteine. The phosphorylated Glu-C peptide of the EII<sup>Mtl</sup> protein of the PTS of *Staphylococcus carnosus* was identified by LC-electrospray MS and isolated for further analysis. Following chemical modification with alkaline ethanethiol, S-ethylcysteine was identified during Edman degradation, demonstrating that phosphocysteine reacts like phosphoserine. As a control, the unphosphorylated cysteine could not be modified by the alkaline ethanethiol.

### 1. Introduction

Cysteine phosphorylation is an essential step in the uptake and transport of carbohydrates by the phosphoenolpyruvate-dependent phosphotransferase system (PTS) in bacteria [1–3]. A second system with a phosphocysteine intermediate is the dephosphorylation of phosphotyrosine residues catalysed by protein tyrosine phosphatases, an important element of many signal transduction pathways [4]. So far, only indirect methods have been available pointing to phosphorylated cysteine, e.g., site-di-

rected mutagenesis or chemical modification with Ellman's reagent, maleimide or iodoacetamide. Additionally, most of these methods required <sup>32</sup>P labelling.

We have developed a non-radioactive method allowing the localization of phosphocysteine in the lower picomolar range by sequence analysis. As a test peptide, we isolated the phosphopeptide from EII<sup>Mtl</sup> protein of the PTS of *Staphylococcus carnosus* which presumably contains phosphocysteine [5]. This peptide was modified with alkaline ethanethiol and subjected to Edman degradation [6]. To prove that S-ethylcysteine was formed from phosphocysteine, we sequenced the non-phosphorylated peptide after alkaline ethanethiol treatment and demonstrated the presence of cysteine by modification with 4-vinylpyridine.

\* Corresponding author.

<sup>☆</sup> Dedicated to Professor Harald Tschesche on the occasion of his 60th birthday.

## 2. Experimental

### 2.1. Protein digestion and HPLC

As starting protein we used the hydrophilic region (amino acids 345–515) of the EII<sup>Mtl</sup> protein of *Staphylococcus carnosus*, an enzyme of the phosphoenolpyruvate-dependent phosphotransferase system. It was purified and phosphorylated as described previously [5,7].

A 20-nmol (400- $\mu$ g) amount of phosphorylated or unphosphorylated EII<sup>Mtl</sup> fragment was dissolved in 25 mM ammonium carbonate buffer (pH 7.8) and digested with 33  $\mu$ g of endoprotease Glu-C in presence of 5% acetonitrile. Incubation was carried out for 18 h at 25°C.

The protein digest was separated on a reversed-phase C<sub>18</sub> column (250 mm  $\times$  4 mm I.D., 250GL4-ODS2-30/5 from SGE, Weiterstadt, Germany) using an ammonium acetate gradient system [8]. The identified phosphocysteine- or cysteine-containing peptides were modified as

described below and subjected to Edman degradation.

### 2.2. Mass spectrometry

All spectra were recorded on a TSQ 7000 triple quadrupole mass spectrometer from Finnigan MAT (Bremen, Germany) equipped with a Finnigan electrospray ion source.

#### Mass spectrometry of the intact proteins

A 150-pmol amount of the phosphorylated or unphosphorylated EII<sup>Mtl</sup> fragment was dissolved in water and subjected to reversed-phase chromatography on a C<sub>4</sub> column (50 mm  $\times$  2 mm I.D., 50GL2-C4-30/5 from SGE). The protein was eluted with a gradient (10% B/min) of 0.6% formic acid (A) vs. 0.6% formic acid–acetonitrile (B) (16:84) at a flow-rate of 80  $\mu$ l/min and injected on-line into the electrospray ionization source.

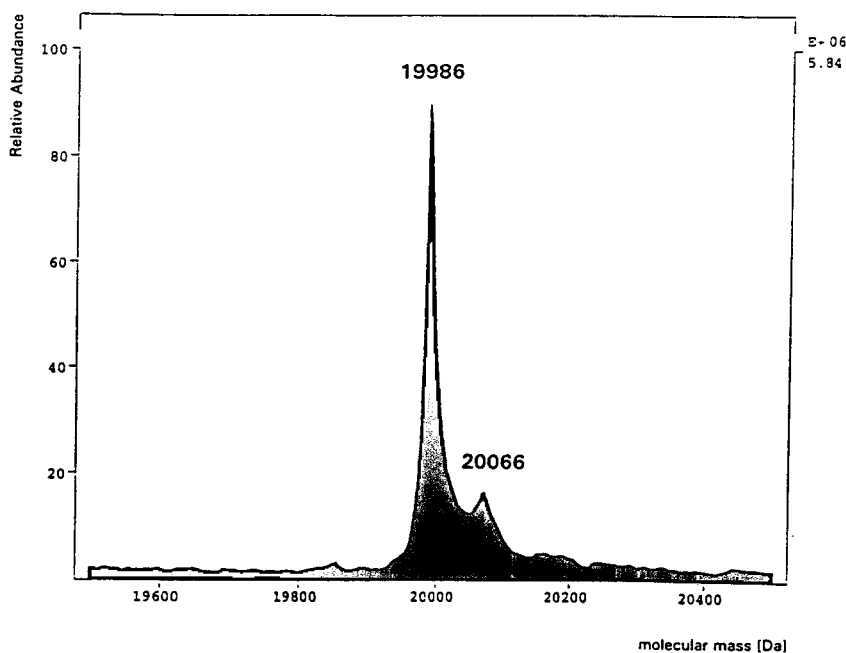


Fig. 1. Deconvoluted ESI mass spectrum of the unphosphorylated EII<sup>Mtl</sup> fragment. A 150-pmol amount of EII<sup>Mtl</sup> fragment was dissolved in water and separated using a C<sub>4</sub> column connected on-line to the electrospray source. For other conditions, see Experimental. The calculated mass of 19 986 corresponds to the mass determined from the amino acid sequence. A small amount of the phosphorylated fragment with  $M_r$  20 066 is also present.



### Mass spectrometry of the protein digests

For analysing the Glu-C digest, 500 pmol of the peptide mixture were separated using a C<sub>18</sub> column (100 mm × 2 mm I.D., 100MGL1-ODS2-30/5 from SGE) connected on-line to the electrospray source. The peptides were eluted with a gradient (2% B/min) of 0.6% formic acid (A) vs. 0.6% formic acid–acetonitrile (B) (16:84) at a flow-rate of 50 μl/min.

The mass spectrometer was operated under unit-mass resolution in the positive-ion mode. Total ion current chromatograms were obtained by scanning the mass range corresponding to *m/z* values between 200 and 2500 every 2 s.

### 2.3. Sequence analysis

Sequence analysis was performed using an Applied Biosystems Model 476A pulse-liquid sequenator or a Model 470A gas-phase sequenator. The S-ethylcysteine modification followed the method described for phosphoserine

in [6]. Modification of cysteine with 4-vinylpyridine was carried out according to a procedure as described in Refs. [9 and 10] and modified in Ref. [11]. In detail, the sample was applied to a biobrene-coated glass filter disc and dried. A 20-μl volume of a reduction–alkylation ‘cocktail’ containing 2 μl of tri-*n*-butylphosphine and 5 μl of 4-vinylpyridine in 100 μl of acetonitrile was added to the sample, the cartridge was immediately reassembled and the sequencing of the modified peptide was started.

### 2.4. Materials

Acetonitrile of HPLC grade was obtained from Scharlau (Barcelona, Spain); water and analytical-reagent grade ethanol, sodium hydroxide and acetic acid were purchased from Merck (Darmstadt, Germany) and ethanethiol, tri-*n*-butylphosphine and 4-vinylpyridine from Aldrich (Steinheim, Germany). All sequencer chemicals and sample discs were obtained from Applied

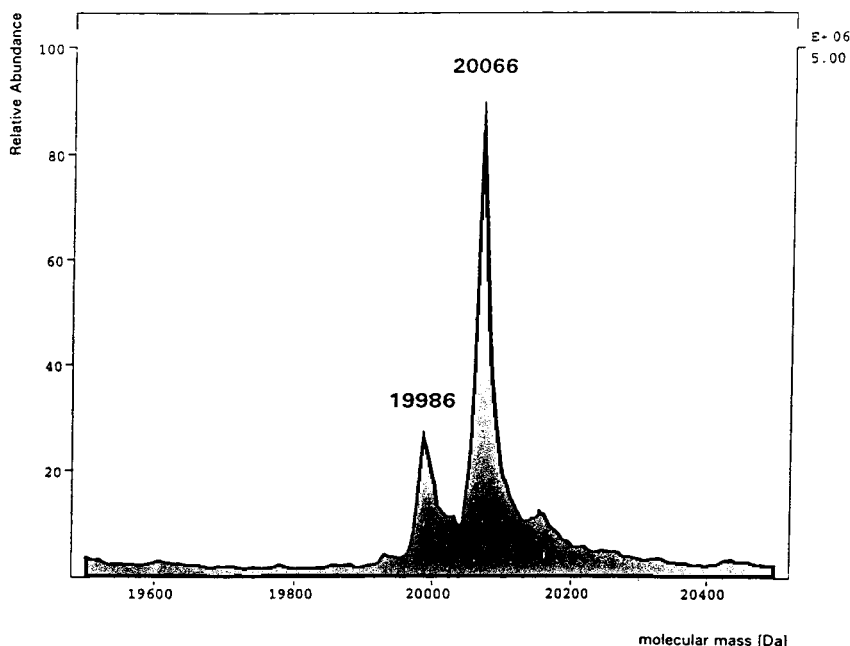


Fig. 2. Deconvoluted ESI mass spectrum of the phosphorylated EII<sup>Mtl</sup> fragment. A 150-pmol amount of phosphorylated EII<sup>Mtl</sup> fragment was dissolved in water and separated using a C<sub>18</sub> column connected on-line to the electrospray source. For other conditions, see Experimental. The phosphorylated form of the EII<sup>Mtl</sup> fragment with a calculated mass of 20 066 predominates over the unphosphorylated form of the fragment.

Biosystems (Weiterstadt, Germany) and endoprotease Glu-C, sequence grade, from Boehringer (Mannheim, Germany). All other chemicals were of the highest purity available.

### 3. Results and discussion

Figs. 1 and 2 show the electrospray mass spectra of the unphosphorylated and phosphorylated form of the EII<sup>Mtl</sup> fragment, respectively. From these spectra, the  $M_r$  of the unphosphorylated protein was calculated to be 19 986 and that of the phosphorylated protein to be 20 066. These calculated masses correspond to the mass determined by the amino acid sequence with one bound phosphate group in the case of the  $M_r$  20 066 species.

For the EII<sup>Mtl</sup> fragment the phosphorylated amino acid was indirectly established by several experiments to be the single cysteine residue in the amino acid sequence [7]. To prove this

hypothesis, we subjected both the phosphorylated and unphosphorylated form of the EII<sup>Mtl</sup> fragment to Glu-C digestion to obtain the phosphopeptide and its unphosphorylated counterpart.

The Glu-C digest was analysed using LC-MS. In Fig. 3 the total ion current chromatogram of the Glu-C digest of the phosphorylated EII<sup>Mtl</sup> fragment is depicted. Additionally, the extracted traces of  $m/z$  values 875–876 and 891–892 are shown. As illustrated in Fig. 4A, the  $m/z$  value 875–876 represents the 5-charged ion  $[M + 5H]^{5+}$  of a peptide with a  $M_r$  4372. The  $m/z$  value 891–892 belongs to a peptide with  $M_r$  4452 (Fig. 4B). These calculated masses agree with the mass of the expected Glu-C peptide 80–120 in the unphosphorylated or phosphorylated state containing a single cysteine in position 17. By this method, it is possible to identify rapidly the phosphopeptides and to subject them to Edman degradation.

The phosphopeptide was sequenced without

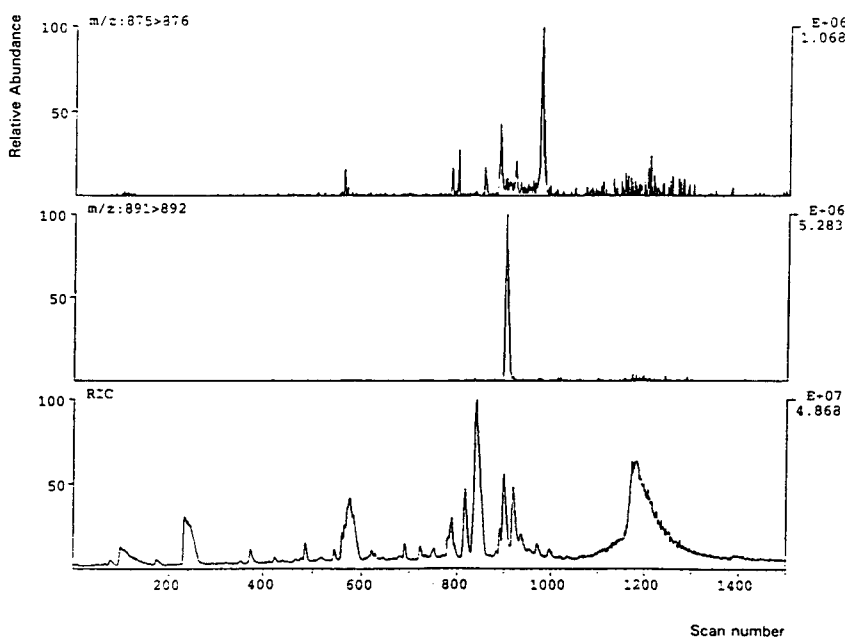


Fig. 3. Total ion current chromatogram of the Glu-C digest of the phosphorylated EII<sup>Mtl</sup> fragment. A 500-pmol amount of the Glu-C digest was separated using a C<sub>18</sub> column connected on-line to the electrospray source. For other conditions, see Experimental. Additionally, the extracted traces of the  $m/z$  875–876 and 891–892 ions are depicted. The former is the 5-charged ion of a peptide with  $M_r$  4372 (see Fig. 4A) and the latter is the 5-charged ion of a peptide with  $M_r$  4452 (see Fig. 4B).

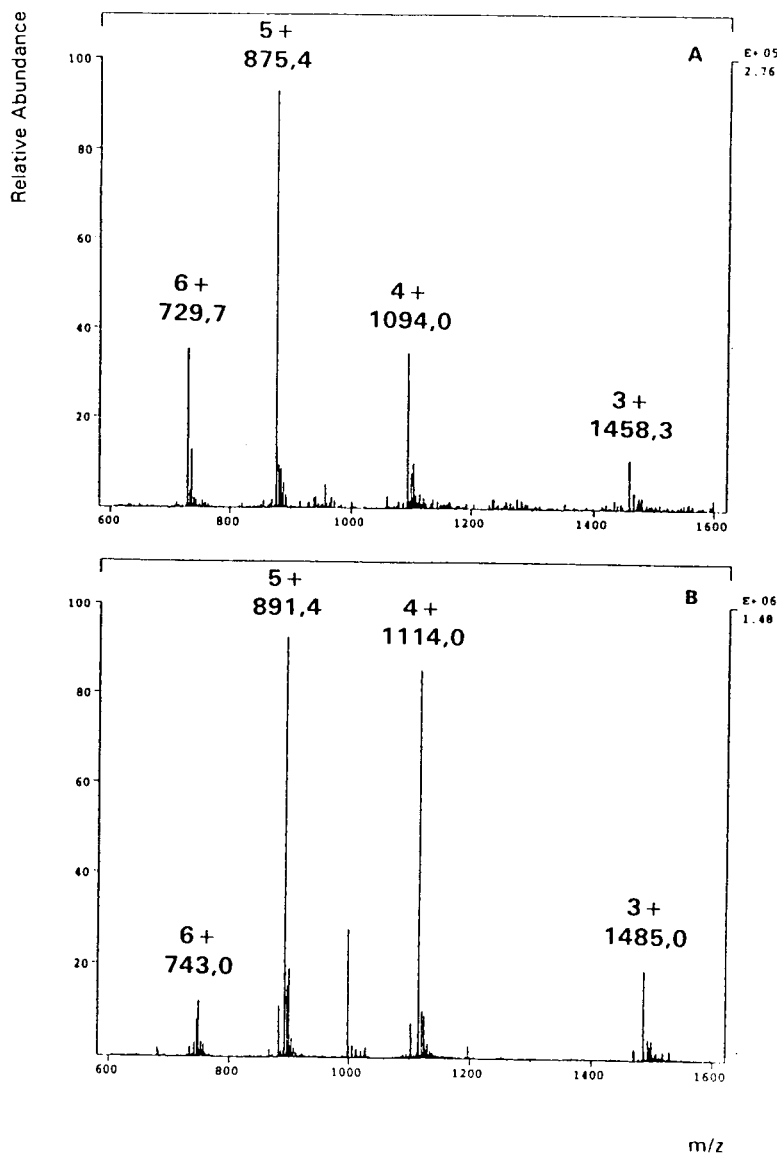


Fig. 4. Extracted ESI mass spectra of peptides with molecular masses of (A) 4372 and (B) 4452. The mass spectra were obtained by summing the scans (A) 967–980 and (B) 894–910 from the total ion chromatogram (Fig. 3) after subtracting the background.

modification or with modification using the alkaline ethanethiol reagent. In Fig. 5, three cycles of the corresponding Edman degradation steps are depicted. Fig. 5A shows the results obtained with the phosphopeptide without further treatment. In cycle 17 only a little DTT-serine appears. This result is expected for a cysteine residue. However, sometimes a small amount of

serine is also detectable, indicating partial hydrolysis of thiophosphate. Fig. 5B depicts the results obtained using the phosphopeptide modified with the alkaline ethanethiol reagent. By this treatment, the cysteine residue in position 17 is transformed into S-ethylcysteine, which is detectable during Edman degradation in cycle 17.

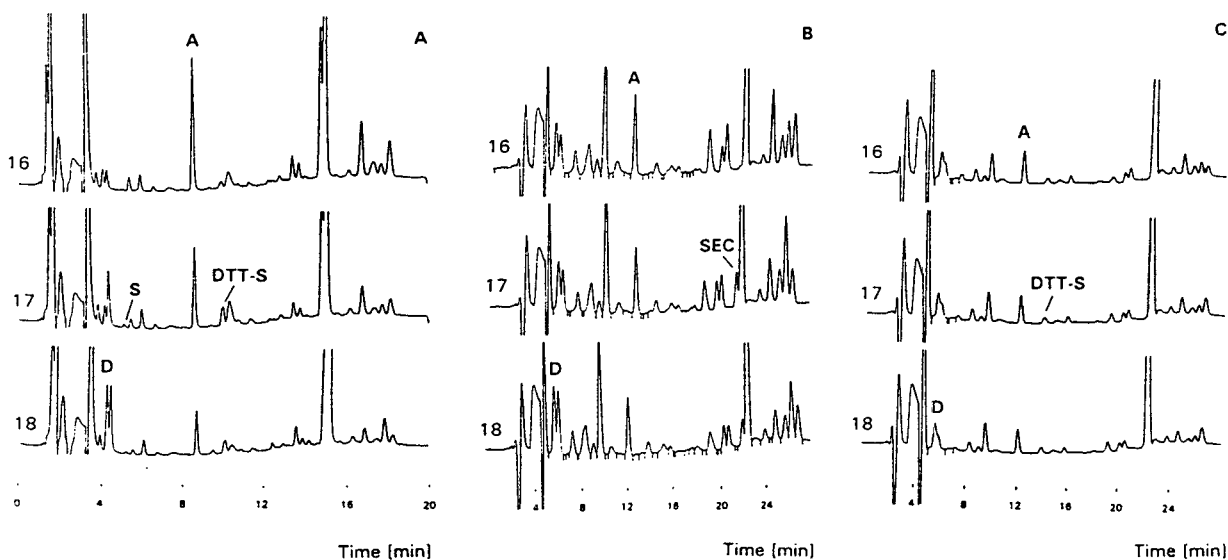


Fig. 5. Sequence analysis of the phosphorylated and unphosphorylated Glu-C peptide 80–120 with a single cysteine in position 17. (A) Results obtained with the phosphopeptide without further modification; (B) results of Edman degradation of the phosphopeptide after treatment with alkaline ethanethiol; (C) Edman degradation of the unphosphorylated peptide after ethanethiol treatment, as a control. The sequence analysis and modifications of the peptides were carried out as described under Experimental. DTT-S denotes DTT-serine and SEC S-ethylcysteine.

As a control, Edman degradation of the unphosphorylated peptide after ethanethiol modification is shown in Fig. 5C. Only a slight increase in DTT-serine in cycle 17 is visible, and no S-ethylcysteine can be detected. This result is expected for a cysteine not post-translationally modified. As an additional control, we subjected the unphosphorylated peptide without ethanethiol modification to Edman degradation. As expected for cysteine, we found only a small amount of DTT-serine in cycle 17 and no serine (data not shown).

To demonstrate the presence of cysteine in the unphosphorylated peptide, we alkylated it with 4-vinylpyridine and obtained S-pyridylethylcysteine in degradation cycle 17 (data not shown).

The results of Edman degradation and of the LC-MS experiments on the differently treated phosphorylated and unphosphorylated forms of the Glu-C peptides reveal some important characteristics of phosphocysteine residues, as follows.

(1) Phosphocysteine is relatively stable in the

presence of dilute formic acid and remains intact during the isolation by reversed-phase HPLC, as could be demonstrated. This allows the application of LC-MS methods for the identification of phosphocysteine-containing peptides in a proteolytic digest.

(2) Phosphocysteine itself is not stable during Edman degradation, but is hydrolysed to cysteine and phosphate and, to a less extent, to serine and thiophosphate. This is in contrast to phosphoserine. The latter is stable during Edman degradation and undergoes  $\beta$ -elimination as soon as the phosphoserine residue is in the N-terminal position and is modified with PITC, yielding DTT-serine quantitatively [12].

(3) Phosphocysteine reacts like phosphoserine [6] or farnesylcysteine [13] during the ethanethiol modification, resulting in the formation of S-ethylcysteine. This means that phosphocysteine undergoes  $\beta$ -elimination followed by the addition of ethanethiol. Hence it can be detected without radioactive labelling by sequence analysis after chemical modification.

In conclusion, LC-MS allows the rapid identi-

fication of phosphocysteine-containing peptides and chemical modification of phosphocysteine to S-ethylcysteine localizes the site of phosphorylation by Edman degradation. The different behaviour during Edman degradation of the unmodified phosphopeptide allows us to distinguish between phosphoserine and phosphocysteine. Hence phosphocysteine can be clearly identified.

### Acknowledgement

This study was supported financially by the Deutsche Forschungsgemeinschaft, Me 765/3-2.

### References

- [1] P.W. Postma, J.W. Lengeler and G.R. Jacobson, *Microbiol. Rev.*, 57 (1993) 543–594.
- [2] G.T. Robillard, H. Boer, R.P. van Weeghel, G. Wolters and A. Dijkstra, *Biochemistry*, 32 (1993) 9553–9562.
- [3] H.H. Pas and G.T. Robillard, *Biochemistry*, 27 (1988) 5835–5839.
- [4] K.L. Guan and J.E. Dixon, *J. Biol. Chem.*, 266 (1991) 17026–17030.
- [5] R. Fischer and W. Hengstenberg, *Eur. J. Biochem.*, 204 (1992) 963–969.
- [6] H.E. Meyer, E. Hoffmann-Posorske, H. Korte and L.M.G. Heilmeyer, Jr., *FEBS Lett.*, 204 (1986) 61–66.
- [7] R. Pogge von Strandmann, C. Weigt, R. Fischer, H.E. Meyer, H.R. Kalbitzer and W. Hengstenberg, *Eur. J. Biochem.*, in press.
- [8] M. Serwe and H.E. Meyer, in R. Kellner, F. Lottspeich, H.E. Meyer (Editors), *Microcharacterization of Proteins*, VCH, Weinheim, 1994, pp. 29–45.
- [9] P.C. Andrews and J.E. Dixon, *Anal. Biochem.*, 161 (1987) 524–528.
- [10] U.T. Ruegg and J. Rudinger, *Methods Enzymol.*, 47 (1977) 111–116.
- [11] D. Hawke and P. Yuan, *Applied Biosystems User Bull.*, December (1987) 28.
- [12] H.E. Meyer, E. Hoffmann-Posorske and L.M.G. Heilmeyer, Jr., *Methods Enzymol.*, 201 (1991) 169–185.
- [13] L.M.G. Heilmeyer, Jr., M. Serwe, C. Weber, J. Metzger, E. Hoffmann-Posorske and H.E. Meyer, *Proc. Natl. Acad. Sci. U.S.A.*, 89 (1992) 9554–9558.



# Separation and detection of 4-hexadecylaniline maltooligosaccharide derivatives with packed capillary liquid chromatography–frit fast atom bombardment–mass spectrometry

Lena Johansson\*, Hasse Karlsson, Karl-Anders Karlsson

*Department of Medical Biochemistry, University of Göteborg, Medicinargatan 9A, S-413 90 Göteborg, Sweden*

## Abstract

A LC–MS method is under development for the separation and detection of mixtures of native glycolipids and of oligosaccharide derivatives. The LC system is based on slurry-packed capillary columns. Frit fast atom bombardment (frit-FAB) is used as the LC–MS interface and ionisation technique and the column is connected to the frit via a 50  $\mu\text{m}$  I.D. fused-silica capillary liner. Post column addition of matrix is achieved using a 50  $\mu\text{m}$  I.D. fused-silica capillary liner with 2.5% (v/v) matrix solution. The two liners are joined through a septum and end side by side against the frit. The detection limit was found to be less than 1 pmole in the negative ion mode. A mixture of tetra to deca maltooligosaccharides reductively aminated with 4-hexadecylaniline ( $M_{4-10}$ -HDA) was separated on a straight phase silica column using gradient elution.

## 1. Introduction

The ionisation of native as well as synthetic glycolipids by fast atom bombardment (FAB) ionisation gives the advantage of intense molecular ions and characteristic fragmentation of the carbohydrate moiety [1]. Derivatisation followed by GC–MS of a mixture of glycolipids is a sensitive analytical tool but limited to glycolipids with up to four sugar units in the carbohydrate moiety [2]. Using a LC column connected to the frit-FAB ion source [3–6] a mixture of underivatized glycolipids can be separated and detected. Even though the sensitivity of the underivatized glycolipids in the negative ion mode is lower

than for derivatised glycolipids in the positive ion mode [7], the amount of sample needed for detection is relatively low. Using packed capillary columns the amount of sample needed for separation, detection and analysis is further decreased since all of the injected sample is chromatographed and then delivered to the frit followed by FAB ionisation, Fig. 1. The use of a gradient mixing valve gives the possibility of gradient elution with optimal chromatographic performance.

The matrix is not included in the eluent because of its negative effects on the chromatographic behaviour; instead post-column addition of the matrix is used. At the column outlet a fused-silica capillary liner is connected using a zero dead-volume union. Another fused-silica

\* Corresponding author.

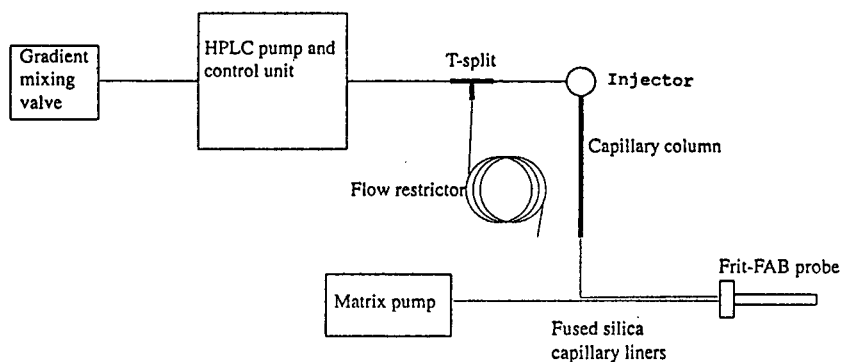


Fig. 1. Schematic of the LC and matrix systems.

capillary liner delivers the matrix solution and the two liners are joined at a septum and end side by side against the frit, Fig. 2. After solvent evaporation the sample is ionised by the matrix upon bombardment with xenon atoms. Mass spectra are continuously recorded and a mass chromatogram is displayed in real-time for either all or selected values of  $m/z$ .

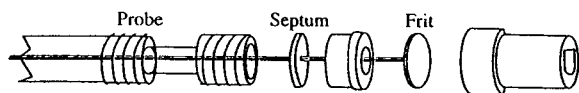


Fig. 2. Frit-FAB interface where one 50  $\mu\text{m}$  fused-silica capillary liner connects the column with the frit and another 50  $\mu\text{m}$  fused-silica capillary liner delivers the matrix solution. The two liners end side by side against the frit.

## 2. Experimental

### 2.1. Eluent and sample

The solvents used for the eluent [chloroform ( $\text{CHCl}_3$ , Fisons), methanol ( $\text{CH}_3\text{OH}$ , Fisons) and distilled water ( $\text{H}_2\text{O}$ )] were degassed using a continuous flow of helium through the solvent bottles.

The sample contained a mixture of tetra to deca maltooligosaccharides ( $\text{M}_{4-10}$ , Sigma) reductively aminated with 4-hexadecylaniline (HDA, Aldrich) [8,9] using dimethylsulfoxide (DMSO) as solvent during the reaction, Fig. 3. A 0.5- $\mu\text{l}$  volume of the 4-hexadecylaniline maltooligosaccharide derivative (1.0  $\mu\text{g}/\mu\text{l}$   $\text{M}_{4-10}$ -HDA) was injected and separated on the col-

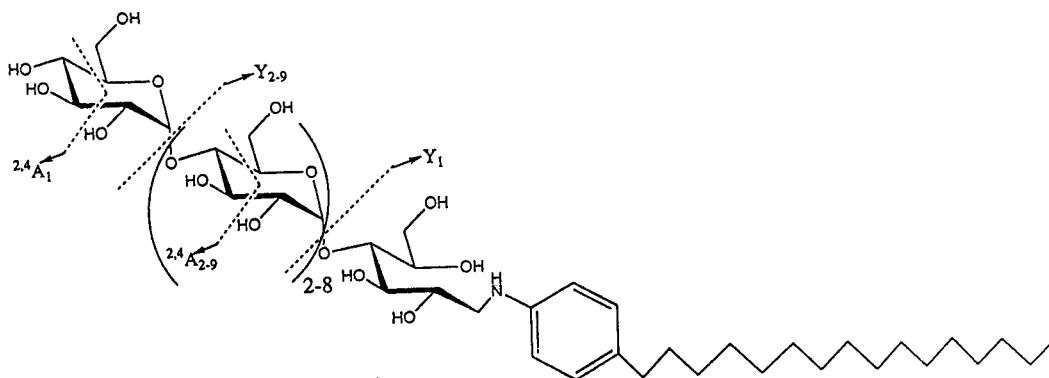


Fig. 3. Reductively aminated tetra to deca maltooligosaccharide ( $\text{M}_{4-10}$ -HDA) and the designations of ions that arise from fragmentations within the carbohydrate portion [1].



umn. Components  $M_{5-8}$ -HDA were present in less than 80 pmole/ $\mu$ l each while the  $M_4$ -HDA and the  $M_{9-10}$ -HDA were present in smaller amounts. The linear gradient used was  $\text{CHCl}_3$ - $\text{CH}_3\text{OH}-\text{H}_2\text{O}$  70:24:1 (v/v) to 60:38.5:1.5 (v/v) over a 10-min period.

Dilutions of N-acetyl-4-hexadecylaniline (ac-HDA) (280, 28, 2.8 and 1.4 pmole/ $\mu$ l) were prepared and chromatographed using isocratic elution with  $\text{CHCl}_3$ - $\text{CH}_3\text{OH}-\text{H}_2\text{O}$  70:24:1 (v/v).

## 2.2. Chromatographic system

The stainless steel capillary (25 cm  $\times$  250  $\mu$ m I.D., Vici) was coupled up to a stainless steel packing reservoir (55  $\times$  4.6 mm I.D.) for slurry packing [10,11]. The slurry was prepared from 15 mg of 5  $\mu$ m straight phase silica particles (Kromasil 100 Å, EKA) in 1.2 ml acetonitrile-toluene-dioxane (2:1:1, v/v) and treated in an ultrasonic bath for a few minutes. The column was packed at 520 bar using an air-driven pump (Maximator LC 72) with heptane as compressor medium during 1.5 h.

A conventional HPLC pump (Pharmacia HPLC pump 2248) and control unit (Pharmacia LKP LCC 2252) delivered the eluent at 0.5 ml/min (Fig. 1). Before the injector the eluent flow was split by a T connection (Vici) where one way goes to the injector/column and the other was restricted by a 2 m  $\times$  100  $\mu$ m I.D. fused-silica capillary, giving a total flow through the column of 3  $\mu$ l/min. Gradient elution was achieved by the use of a gradient mixing valve connected to the pump control unit.

The injected volume was 0.5  $\mu$ l by using a Rheodyne 7520 injector.

## 2.3. Matrix system

Negative matrix effects on the chromatographic behaviour were avoided by post-column addition of the matrix solution (Fig. 1). The matrix solution was delivered by a syringe pump (Harvard apparatus pump 22) at a flow-rate of 0.5  $\mu$ l/min. When operating in the negative ion

mode a 2.5% (v/v) solution of triethanolamine (TEA, Fluka) in  $\text{CH}_3\text{OH}-\text{H}_2\text{O}$  (1:1) was used.

## 2.4. The frit-FAB interface

A 50  $\mu$ m I.D. fused-silica capillary liner was connected to the column outlet using a zero dead-volume union (Vici). Another liner delivers the matrix solution and the two liners are joined in a septum and end side by side at the frit (Fig. 2). The solvents evaporate at the frit leaving the sample dissolved in the remaining matrix where it is ionised by the bombardment.

## 2.5. Mass spectrometric conditions

Mass spectra were acquired on a JEOL SX-102A double-focusing mass spectrometer. In these experiments the mass spectrometer was operated in the negative ion mode, mass range scanned from 500 to 2000, total cycle time 14 s, FAB ionisation with xenon atoms at 6 keV and accelerating voltage at 10 kV. The resolution was set at 1000. During the detection of the smaller

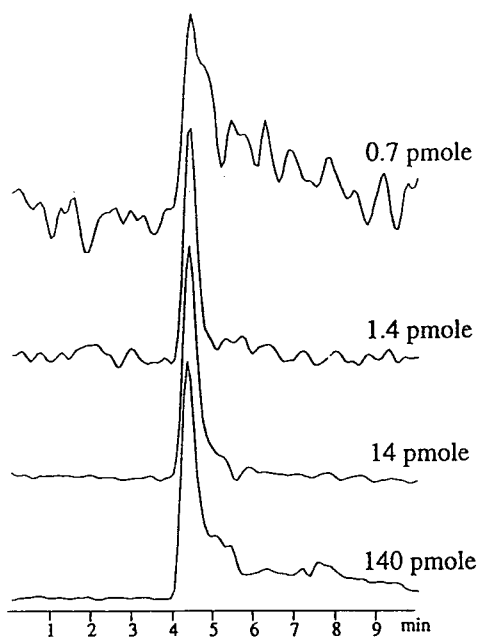


Fig. 4. Mass chromatograms of the pseudo-molecular ion at  $m/z$  642 of ac-HDA for the different amounts analysed.

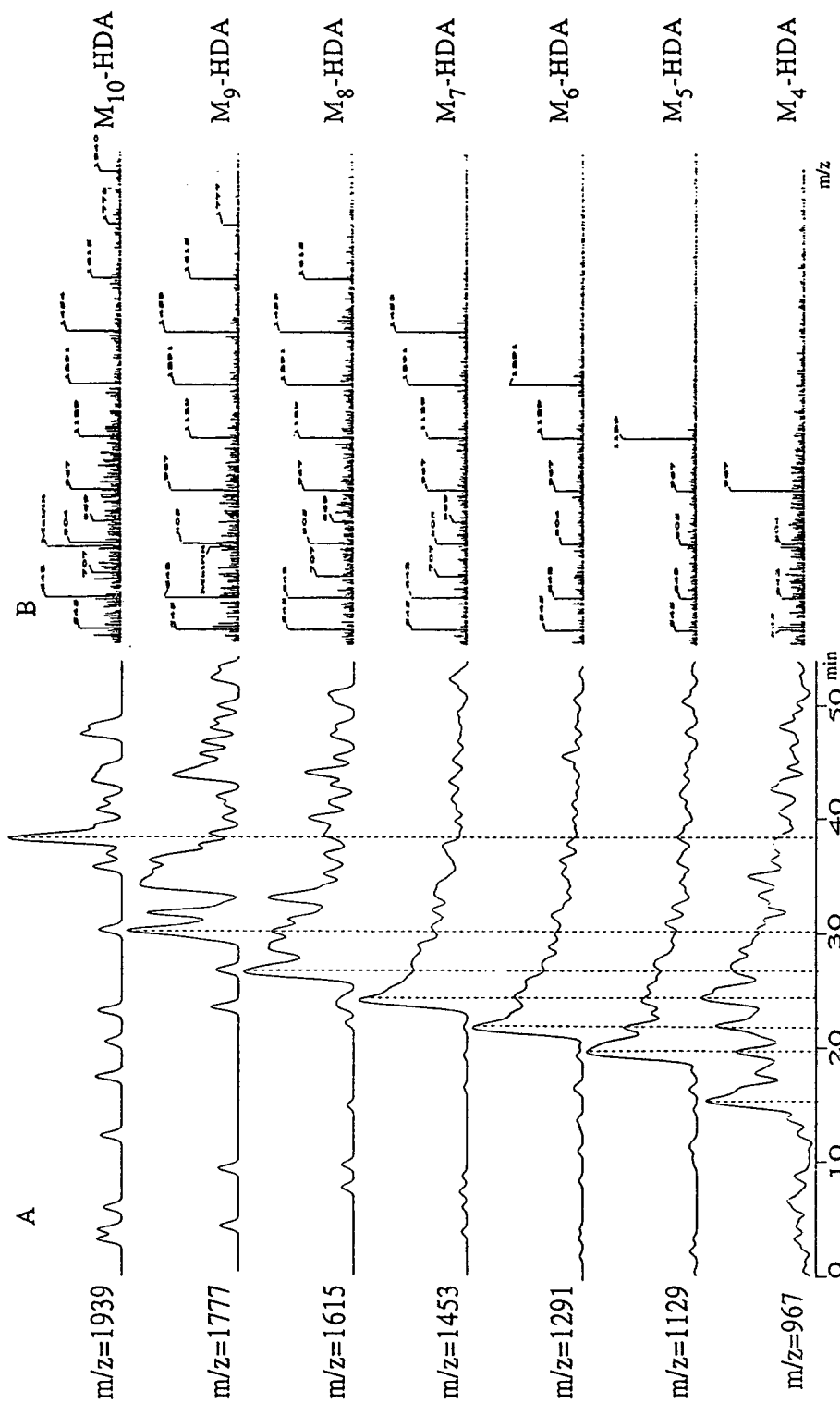


Fig. 5. (A) Mass chromatograms of the pseudo-molecular ion of each component in the mixture of  $M_{4-10}$ -HDA and (B) the corresponding mass spectrum for each component as an average over the major peak intensity with background subtraction by the scans between 1 and 4 min.

ac-HDA the mass range scanned was 100–400 with a total cycle time of 10 s. The ion source block was held at 48°C to prevent formation of ice-plugs in the frit and the liners during the evaporation of solvents. The ion source pressure was  $10^{-4}$  Pa.

Mass chromatograms presented here (Figs. 4 and 5) are reconstructed ion chromatograms of the indicated  $m/z$  and the mass chromatograms for the  $M_{4-10}$ -HDA has been smoothed before presentation.

An average over the peak was chosen to represent the mass spectrum for the component. Background subtraction of the mass spectra was made using scans from the retention time between 1 and 4 min.

### 3. Results and discussion

#### 3.1. Detection limits

In order to evaluate the detection limit of the system a dilution series of ac-HDA was used where 140, 14, 1.4 and 0.7 pmole respectively was injected (Fig. 4). The first three samples, 140, 14 and 1.4 pmole gave mass chromatograms and mass spectra with good signal-to-noise ratio. The 0.7 pmole sample resulted in a less well pronounced mass chromatogram and a weak mass spectrum. Therefore the detection limit was estimated to be 1 pmole in the negative ion mode with the system presented. The detection limit has also been investigated with  $M_2$ -HDA and gradient elution giving similar results. The given values are comparable with the results achieved in static FAB for underivatized glycolipids in the negative ion mode.

Ac-HDA was almost unretarded on the column with a retention time of 4 min which is approximately the value of  $t_0$ .

#### 3.2. Separation and detection of a mixture of 4-hexadecylaniline maltooligosaccharide derivatives

The mass spectra of the 4-hexadecylaniline maltooligosaccharide derivatives (Fig. 5B and

Table 1  
Pseudo-molecular ion masses,  $[M - T]^-$ , and retention times for the components in the analysed mixture

	$[M - H]^-$ (u)	Retention time (min)
$M_4$ -HDA	967	15.6
$M_5$ -HDA	1129	19.6
$M_6$ -HDA	1291	22.6
$M_7$ -HDA	1453	24.6
$M_8$ -HDA	1615	26.9
$M_9$ -HDA	1777	30.2
$M_{10}$ -HDA	1939	33.5

Table 1) are dominated by the Y fragment sequence ions (Table 2). Also present are some fragment ions due to cleavages within the pyranose rings, such as  $^{2,4}A_4$ ,  $^{2,4}A_5$  and  $^{2,4}A_6$  [1] (Table 2).

The separation on the silica column is based on the length and polarity of the carbohydrate moiety. The chromatographic performance is difficult to evaluate from this sample since the sample is made from a homologous series of substituted maltooligosaccharides giving mass spectra with common Y fragment ions. The Y fragment ions of the higher homologues coincide with the pseudo-molecular ions of the lower homologues. This fact results in distorted mass chromatograms of pseudo-molecular ions (Fig. 5A). Still the retention time for each component

Table 2  
Observed fragmentations of the components in the mixture

Fragment ion	$m/z$	Originated from
$Y_2$	642	all
$Y_3$	804	all
$Y_4$	967	$M_{5-10}$ -HDA
$Y_5$	1129	$M_{6-10}$ -HDA
$Y_6$	1291	$M_{7-10}$ -HDA
$Y_7$	1453	$M_{8-10}$ -HDA
$Y_8$	1615	$M_{9-10}$ -HDA
$Y_9$	1777	$M_{10}$ -HDA
$^{2,4}A_4$	545	all
$^{2,4}A_5$	707	$M_{7-8}$ -HDA $M_{10}$ -HDA
$^{2,4}A_6$	869	$M_{7-8}$ -HDA $M_{10}$ -HDA

The designations are indicated in Fig. 3.

is obtained and the differences are in the range of 2–4 min. Glycolipids derived from biological sources do not form a homologous series and the problem above does not occur. The aim of this work is to analyse native and synthetic glycolipids derived from different biological sources.

### Acknowledgements

The sample of  $M_{4-10}$ -HDA was provided by Dr. Maria Ölwegård Halvarsson who is also acknowledged for valuable discussions and help. This work was supported by grants from The Swedish Technical Research Council.

### References

- [1] B. Domon and C.E. Costello, *Glycoconjugate J.*, 5 (1988) 397.
- [2] H. Karlsson, unpublished results.
- [3] Y. Ito, T. Takeuchi, D. Ishii and M. Goto, *J. Chromatogr.*, 346 (1985) 161.
- [4] K. Sato, T. Kumazawa and Y. Katsumata, *J. Chromatogr. A*, 674 (1994) 127.
- [5] M. Suzuki, M. Sekine, T. Yamakawa and A. Suzuki, *J. Biochem.*, 105 (1989) 829.
- [6] M. Suzuki, T. Yamakawa and A. Suzuki, *J. Biochem.*, 108 (1990) 92.
- [7] C.E. Costello and J.E. Vath, in J.A. McCloskey (Editor), *Methods in Enzymology*, Vol. 193, Mass Spectrometry, Academic Press, San Diego, CA, 1990, p. 738.
- [8] M. Stoll, T. Mizuochi, R. Childs and T. Feizi, *J. Biochem.*, 256 (1988) 661.
- [9] H. Towbin, C.-A. Schoenenberger, D. Braun and G. Rosenfelder, *Anal. Biochem.*, 173 (1988) 1.
- [10] T. Tsuda and M. Novotny, *Anal. Chem.*, 50 (1978) 271.
- [11] Y. Hirata, M. Novotny, T. Tsuda and D. Ishii, *Anal. Chem.*, 51 (1979) 475.



ELSEVIER

Journal of Chromatography A, 712 (1995) 155–168

JOURNAL OF  
CHROMATOGRAPHY A

# Liquid chromatography combined with thermospray and continuous-flow fast atom bombardment mass spectrometry of glycosides in crude plant extracts

J.-L. Wolfender<sup>a</sup>, K. Hostettmann<sup>a,\*</sup>, F. Abe<sup>b</sup>, T. Nagao<sup>b</sup>, H. Okabe<sup>b</sup>,  
T. Yamauchi<sup>b</sup>

<sup>a</sup>*Institut de Pharmacognosie et Phytochimie, Ecole de Pharmacie, Université de Lausanne, CH-1015 Lausanne, Switzerland*

<sup>b</sup>*Faculty of Pharmaceutical Sciences, Fukuoka University, 8-19-1 Nanakuma, Jonan-ku, Fukuoka 814-01, Japan*

## Abstract

In crude plant extracts, constituents of biological or pharmaceutical interest often exist in the form of glycosides. Off-line mass spectral investigations of these metabolites require soft ionisation techniques such as desorption chemical ionisation (DCI) or fast atom bombardment (FAB) if information on molecular mass or sugar sequence is desired. In LC–MS, glycosides can be ionised by using thermospray (TSP), continuous-flow fast atom bombardment (CF-FAB) or other interfaces. These techniques are thus potentially applicable to the on-line analysis of glycosides and can be applied to plant extract analysis.

Thermospray (TSP) used with ammonium acetate as buffer provides mass spectra similar to those obtained with DCI–MS using NH<sub>3</sub> and is potentially applicable to the on-line analysis of relatively small glycosides bearing no more than three sugar units. CF-FAB provides cleaner MS spectra than static FAB due to the lower concentration of the matrix used and can be applied to more polar compounds such as glycosides with a larger number of sugars. The use of a special setup involving post-column addition of the buffer or the matrix and splitting allows LC–UV, TSP LC–MS and CF-FAB LC–MS to be performed with the same standard HPLC conditions. Different crude plant extracts containing various types of glycosides with one to eight sugar units have been analysed by both TSP and CF-FAB. Cardenolides from *Nerium odorum* (Apocynaceae) and saponins from *Swarzia madagascariensis* (Leguminosae), *Aster scaber* and *Aster tataricus* (Asteraceae) have been studied by LC–MS. The combination of these two interfaces for the HPLC screening of crude plant extracts is discussed.

## 1. Introduction

Plant constituents often exist in the form of glycosides. These conjugates may or may not occur together with their respective aglycones in the plants. Glycosides are thermally labile, polar and non-volatile compounds. Mass spectral in-

vestigation requires soft ionisation techniques such as desorption chemical ionisation (DCI) or fast atom bombardment (FAB) [1,2] if information on molecular masses or sugar sequences is desired. These off-line techniques, however, require a preliminary isolation and purification of the compounds. The development of LC–MS in the early 1980s allows nowadays MS analysis to be coupled on-line with analytical HPLC separation. Thus, it is possible to analyse many

\* Corresponding author.

classes of non-volatile compounds without isolation from their biological matrices.

In this respect, cardenolides and saponins have been studied by two complementary interfaces, thermospray (TSP) [3] and continuous flow-FAB (CF-FAB) [4]. TSP has already proved to be a valuable technique for the analysis of small glycosides of xanthenes, flavones, monoterpenes and triterpenes [5,6]. In the case of CF-FAB, only very few applications to naturally occurring glycosides have been described. However, the analysis of some saponins has been performed with frit-FAB, a related technique [7,8].

Thermospray LC-MS using ammonium acetate as buffer provides mass spectra nearly identical to those obtained with DCI-MS using  $\text{NH}_3$  and is thus potentially applicable to the on-line analysis of glycosides containing up to three sugar units [2,9]. Due to the use of an additional mechanical pumping in the source chamber of the MS instrument, TSP can be run with high LC flow-rates. Thus standard reversed-phase HPLC conditions (4 mm I.D. column, gradient capability, 1–2 ml/min flow-rate) are compatible with this interface. Parameters developed for routine HPLC-UV analyses of crude plant extracts are directly applicable to TSP LC-MS. Only the use of non-volatile buffer has to be avoided [10].

Continuous flow-FAB produces the same type of soft ionisation as static FAB but cleaner spectra are obtained because less matrix is used (5–20%) [4]. This interface is applicable for all compounds usually analysed with static FAB, including glycosides with large number of sugars. CF-FAB requires very low flow-rates (5–10  $\mu\text{l}/\text{min}$ ) because, contrary to TSP, no additional pumping of the MS source chamber is used.

In order to keep LC-MS conditions as close as possible to those employed in standard reversed-phase HPLC (1 ml/min, gradient with aqueous solvent systems) and with the aim of using the same columns without changing the chromatographic conditions, the LC-UV and TSP LC-MS or LC-UV and CF-FAB LC-MS configurations shown in Fig. 1 have been employed.

An HPLC pump equipped with a gradient controller provides the eluent for the HPLC separation of the plant extracts. A reversed-phase column (I.D. about 4 mm) is most often used. At the column outlet, the eluent passes through a photodiode array detector (DAD) equipped with a high-pressure cell. At the exit of the UV detector, two configurations, according to the LC-MS mode chosen (TSP or CF-FAB), are possible:

For TSP LC-MS operation, post-column addition of the buffer needed for "TSP buffer"

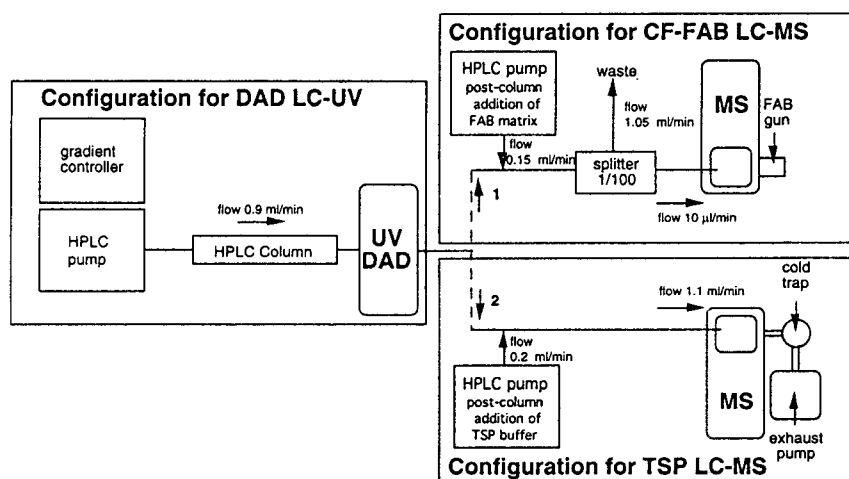


Fig. 1. Schematic representation of the experimental setup used for LC-UV and TSP or CF-FAB LC-MS analysis. The mass spectrometer used is a triple quadrupole instrument.

ionisation is provided by an additional HPLC pump (usually ammonium acetate 0.5 M, 0.2 ml/min). The total eluent (1.2 ml/min) containing the buffer passes through the TSP interface and the exhaust eluent is pumped away by a mechanical pump and trapped in a cold trap.

For CF-FAB operation, the additional HPLC pump allows the post-column addition of the glycerol matrix needed for FAB ionisation (usually glycerol 50%, 0.2 ml/min). The viscous matrix is efficiently mixed in the eluent with a visco mixer. The mobile phase is then split (splitter: 1/100), and only 10  $\mu$ l/min of the total eluent enters the CF-FAB interface through a fused-silica capillary.

With such a setup, standard HPLC conditions for crude extract analysis (1 ml/min, 4 mm I.D. column) can be maintained without alteration in both TSP or CF-FAB LC-MS modes. Furthermore DAD LC-UV detection is not affected by the buffer or the matrix used.

In the context of our studies on the active principles of higher plants [11] and in our search for more rapid and powerful methods for plant extract screening [12], conditions have been established for both TSP LC-MS and CF-FAB LC-MS analysis of different types of naturally occurring glycosides.

In order to compare the potential and limitations of both TSP and CF-FAB ionisation techniques, LC-MS analyses of glycosides bearing one to eight sugar units have been investigated. Crude plant extracts containing cardenolides (Apocynaceae) and saponins (Leguminosae and Asteraceae) were studied.

## 2. Experimental

### 2.1. Chemicals

HPLC grade water was prepared by distillation on a Büchi Fontavapor 210 distillation instrument (Flawil, Switzerland) and passed through a 0.50- $\mu$ m filter Millipore (Bedford, MA, USA). HPLC grade MeCN and MeOH from Maechler AG (Reinach, Basel, Switzerland) were passed through a 0.45- $\mu$ m filter.

Ammonium acetate and trifluoroacetic acid (TFA) were obtained from Merck (Darmstadt, Germany) and glycerol from Fluka (Buchs, Switzerland).

### 2.2. HPLC conditions

Separations were performed on a Nova-Pak C<sub>18</sub> column, 4  $\mu$ m (150  $\times$  3.9 mm I.D.) from Waters (Bedford, MA, USA), equipped with a Nova-Pak Guard-Pak C<sub>18</sub> precolumn. MeCN-H<sub>2</sub>O gradients (0.9 ml/min) were used. To avoid the tailing of phenolic compounds, 0.05% of trifluoroacetic acid was added to the solvents, giving a pH of 3. The eluent delivery was provided by a HPLC 600-MS pump (Waters-Millipore, Bedford, MA, USA) equipped with a gradient controller.

### 2.3. LC-UV (DAD) analyses

The UV trace was recorded on-line with a HP-1050 photodiode array detector from Hewlett-Packard (Palo Alto, CA, USA) (Fig. 1).

### 2.4. TSP LC-MS analyses

A Finnigan MAT TSQ-700 (San Jose, CA, USA) triple quadrupole instrument equipped with a TSP 2 interface was used for the data acquisition and processing. As all the analyses were carried out with approximately the same eluent composition (20 to 50% MeCN), the TSP parameters were set to average values for glycosides. The temperature of the TSP source block was maintained at 280°C and the vaporiser was set to 100°C giving aerosol temperatures varying between 305–330°C (according to the eluent composition). The electron multiplier voltage was 1800 V, dynode 15 kV and the filament and discharge were off in all cases. Usually full-scan spectra from *m/z* 150–1500 in the positive ion (PI) mode were recorded (scan time 3 s). Post-column addition of buffer (ammonium acetate 0.5 M) was achieved by a Waters 590-MS programmable HPLC pump (0.2 ml/min) (Fig. 1).

### 2.5. CF-FAB LC-MS analyses

The same mass spectrometer as described for TSP was used, equipped with the continuous-flow FAB interface series-70 BioProbe from Finnigan MAT. Post-column addition of the matrix (glycerol 50% aqueous solution) was achieved by a Waters 590-MS programmable HPLC pump (0.15 ml/min) producing a matrix concentration of 7% in the eluent. In order to obtain an LC flow-rate compatible with CF-FAB operation, the total eluent flow-rate (1.05 ml/min) was reduced to 10.5  $\mu$ l/min with a splitter [microflow processor splitter: 1/100 (Acurate)] from LC-Packings (Zürich, Switzerland). For stable operation, the copper tip of the CF-FAB interface was maintained at 50°C and the source block was kept at 100°C. The FAB gun was set to 4 kV and 1.2 mA; xenon gas was used for bombardment.

### 2.6. Samples

Extracts were prepared from the dried plant material by maceration at room temperature with MeOH. In the case of *Aster scaber* (Asteraceae), the saponin-rich fraction from the MeOH extract [13] was chromatographed into two fractions (A and B) on a polystyrene resin (Diaion HP-20). These fractions were treated with an ion-exchange resin, Amberlite IRC-84, and the acidic products were converted to methyl esters with  $\text{CH}_2\text{N}_2$ . Solutions to be analysed were usually prepared by dissolving 30–100 mg of extract in 1 ml of a MeOH-H<sub>2</sub>O mixture. The injected volumes varied from 10 to 20  $\mu$ l.

## 3. Results

The crude MeOH extracts of plants and the saponin fractions of *Aster scaber* were separated by HPLC on reversed-phase columns with various MeCN-H<sub>2</sub>O gradients at 0.9 ml/min. Suppression of tailing was achieved with 0.05% TFA. The LC conditions for each extract were first established by LC-UV. For the LC-MS analyses, as the buffer or the matrix needed for

ionisation were added post-column (Fig. 1), no alteration of the chromatographic separation was observed.

### 3.1. TSP tuning

Since glycosides are thermolabile compounds, the ability to observe their molecular ions is a function of the temperatures set for the TSP interface [5,14].

For the study of terpene glycosides, the ionisation of different pure mono-, di- and triglycosylated triterpenes was investigated by repeated loop injection while varying different TSP parameters. In the positive ion mode with ammonium acetate as buffer (0.1 M) at a total flow-rate of 1.1 ml/min (MeCN-H<sub>2</sub>O, 50:50), the vaporiser and the source block temperature were set at average values of 100 and 280°C respectively. These settings represented a compromise, allowing the observation of the molecular ions and a satisfactory total-ion current intensity for the different types of glycosides studied. The influence of the repeller voltage was negligible. The filament "off" mode was preferred as no significant changes were observed in the filament "on" mode.

### 3.2. CF-FAB tuning

In the case of CF-FAB, the different settings were tuned in order to obtain stable operation. The glycerol matrix (glycerol 50% aqueous solution 0.15 ml/min) was efficiently mixed post-column with a visco mixer in order to obtain a homogeneous eluent. The total eluent 1.05 ml/min was split accurately (1/100) with a microflow processor allowing a uniform microflow (10.5  $\mu$ l/min) even in the gradient mode. The temperatures of the source and the FAB tip were optimised by monitoring the intensity of the glycerol ion at  $m/z$  185 in order to obtain stable conditions (variation of intensity of  $m/z$  185 < 10%) at eluent compositions corresponding to the beginning and the end of the LC gradient used. Under these conditions, a source temperature of 100°C and a tip temperature of 50°C were found to be satisfactory for eluent compositions



varying from 20:80 to 50:50 MeCN–H<sub>2</sub>O. Several loop injections of various triterpene glycosides have showed that the negative ion mode produced intense deprotonated molecular ions  $[M - H]^-$  and distinctive fragment ions. The positive ion mode produced less clear results; various salt adduct ions were observed and fragment ions resulting from the sugar losses were not always clearly visible. The negative ion mode was thus chosen for this study.

### 3.3. Cardenolides from *Nerium odorum* (Apocynaceae)

Cardiac glycosides have been isolated from both vegetable and animal sources. Some of them are important drugs. Their characteristic structural features are a C<sub>23</sub> or C<sub>24</sub> steroid aglycone with a sugar moiety containing from one to five sugars attached at position C-3.

In order to illustrate the potentialities of both TSP and CF-FAB LC–MS for the analysis of cardenolides, the crude root bark MeOH extract of *Nerium odorum* (Apocynaceae) has been investigated. This Indian plant is known to possess acetophenones, pregnenolone glucosides, pregnanes, cardiac glycosides and steroid glycosides [15,16].

For a rapid survey of the chemical composition of the MeOH root extract of *N. odorum*, 1 mg was separated by HPLC on a C<sub>18</sub> column (MeCN–H<sub>2</sub>O gradient, 20:80 → 50:50 in 40 min, 0.9 ml/min). The UV chromatogram recorded at 210 nm showed a satisfactory separation of the main metabolites. Under the same LC conditions, this extract was injected twice: once for TSP LC–MS detection and once for CF-FAB LC–MS detection (Fig. 2).

Under the given TSP conditions, the total-ion current trace recorded in TSP LC–MS was very similar to the UV trace at 210 nm, showing the efficient ionisation of the major part of the metabolites detected at 210 nm in the extract. *N. odorum* is known to contain cardenolides bearing only one to three sugar units (Fig. 3). For all these cardiac glycosides, the TSP LC–MS analysis of the crude extract gives on-line molecular mass and sugar sequence information. In order

to illustrate the results obtained, the TSP spectra of four representative cardiac glycosides [15] [odoroside A (1), neritaloside (2), bioside G (3) and odoroside G (4)] have been selected (Fig. 4A). Odoroside A (1) and neritaloside (2) are cardiac monoglycosides. The TSP spectra of 1 and 2, recorded on-line, exhibited the intense protonated molecular ions  $[M + H]^+$  at  $m/z$  519 and 593 respectively and the main fragment ions corresponding to the aglycone moiety  $[A + H]^+$  ( $m/z$  375 and 433). In the case of 1, the mass difference between the proton adduct ion of the aglycone  $[A + H]^+$  and the  $[M + H]^+$  ion was characteristic for the loss of a diginosyl unit (144 u), while for 2, this loss was due to a digitalosyl unit (160 u). The aglycone of 1 is digitoxigenin ( $M_r$  374), which corresponded to the main ion of the TSP spectra at  $m/z$  375. In the case of 2, the aglycone is digitoxigenin-16-acetate ( $M_r$  432). This aglycone was more labile than digitoxigenin and gave, for example, an intense ion at  $m/z$  373 corresponding to the successive loss of the acetyl group and water. Bioside G (3) and odoroside G (4) contain two and three sugar units respectively and have the same aglycone moiety as 1 ( $[A + H]^+$ ,  $m/z$  375). Contrary to 1 and 2, these two polar cardiac glycosides exhibited weak ammonium adduct  $[M + NH_4^+]$  molecular ions and no or very weak protonated molecules. For 3, a first loss of 162 u gave two ions at  $m/z$  552  $[M + NH_4^+ - 162]$  and  $m/z$  535  $[M + H - 162]^+$  which corresponded to the loss of a terminal glucose unit. The loss of 160 u between  $m/z$  535 and  $m/z$  375 was characteristic for a digitalosyl unit. Odoroside G (4) produced identical ions to those described for 3 except that the  $[M + NH_4^+]$  ion was shifted by 162 u to  $m/z$  876, indicating a supplementary terminal glucose unit. The display of the different molecular ions permitted their precise localisation in the chromatogram (Fig. 2A).

Contrary to TSP LC–MS, the total-ion current trace observed in the CF-FAB analysis of the same extract was rather different from the UV trace at 210 nm. The peak sharpness was diminished and the ion intensity differed largely among the peaks compared (Fig. 2). Concerning the spectra recorded on-line, only deprotonated

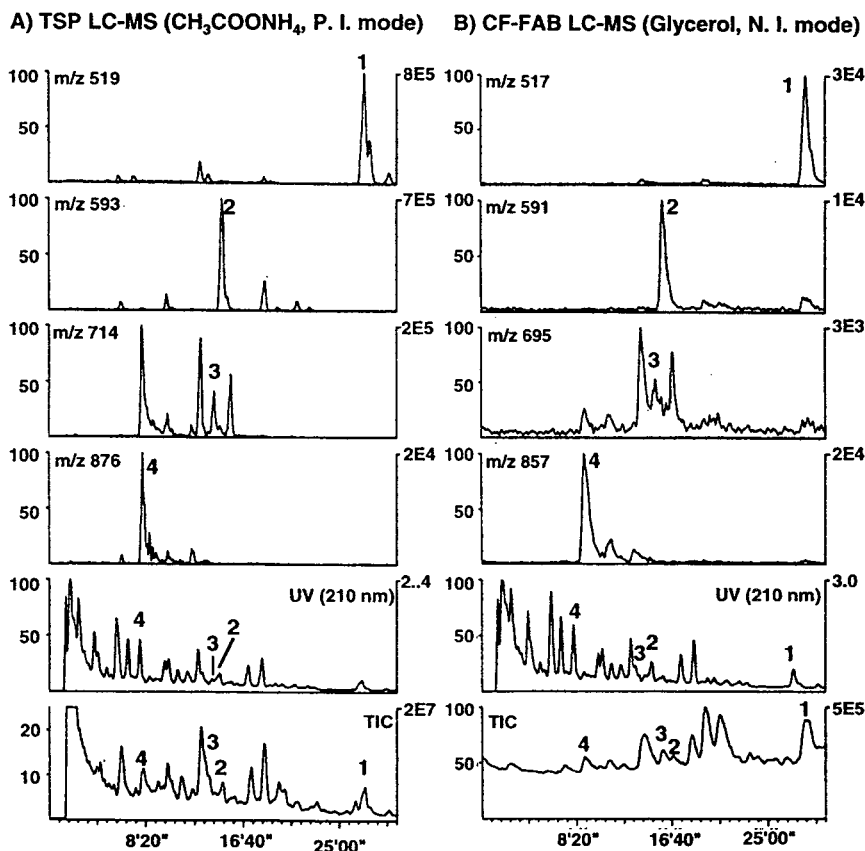


Fig. 2. Combined TSP (A) and CF-FAB (B) LC-MS of the methanolic extract of *Nerium odorum* (Apocynaceae). HPLC:  $\text{C}_{18}$  Nova-Pak ( $4 \mu\text{m}$ ,  $150 \times 3.9 \text{ mm}$  I.D.); gradient,  $\text{CH}_3\text{CN}-\text{H}_2\text{O}$  (0.05% TFA) 20:80  $\rightarrow$  45:55 in 40 min (0.9 ml/min). For conditions of TSP and CF-FAB LC-MS see Experimental.

molecular ions  $[\text{M}-\text{H}]^-$  were observed and no significant fragment ions were recorded (Fig. 4B). Furthermore, the MS responses of these  $[\text{M}-\text{H}]^-$  ions were weaker than those of the corresponding molecular ions in TSP (Fig. 2). The non-labelled ions observable in the CF-FAB

spectra of cardenolides 1–4 were due to the glycerol matrix or attributable to other co-migrating metabolites, as was the case for the ion at  $m/z$  841 in the CF-FAB spectrum of 3.

These results suggest that for the analysis of cardenolides bearing up to three sugar units, TSP LC-MS is probably the method of choice. It enables molecular mass information to be obtained, together with significant sugar sequence and aglycone fragment ions with almost no loss of peak resolution. CF-FAB in this case gives less structural information and is less sensitive. Nevertheless, this latter technique represents a good complement to TSP because it permits a precise confirmation of the on-line molecular mass attribution of the different cardenolides.

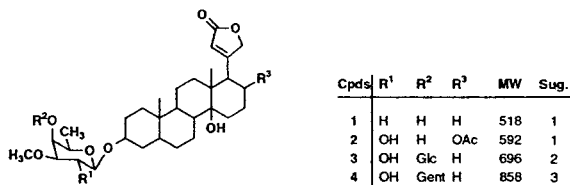


Fig. 3. Structure of selected cardenolides isolated from *Nerium odorum* (Apocynaceae).

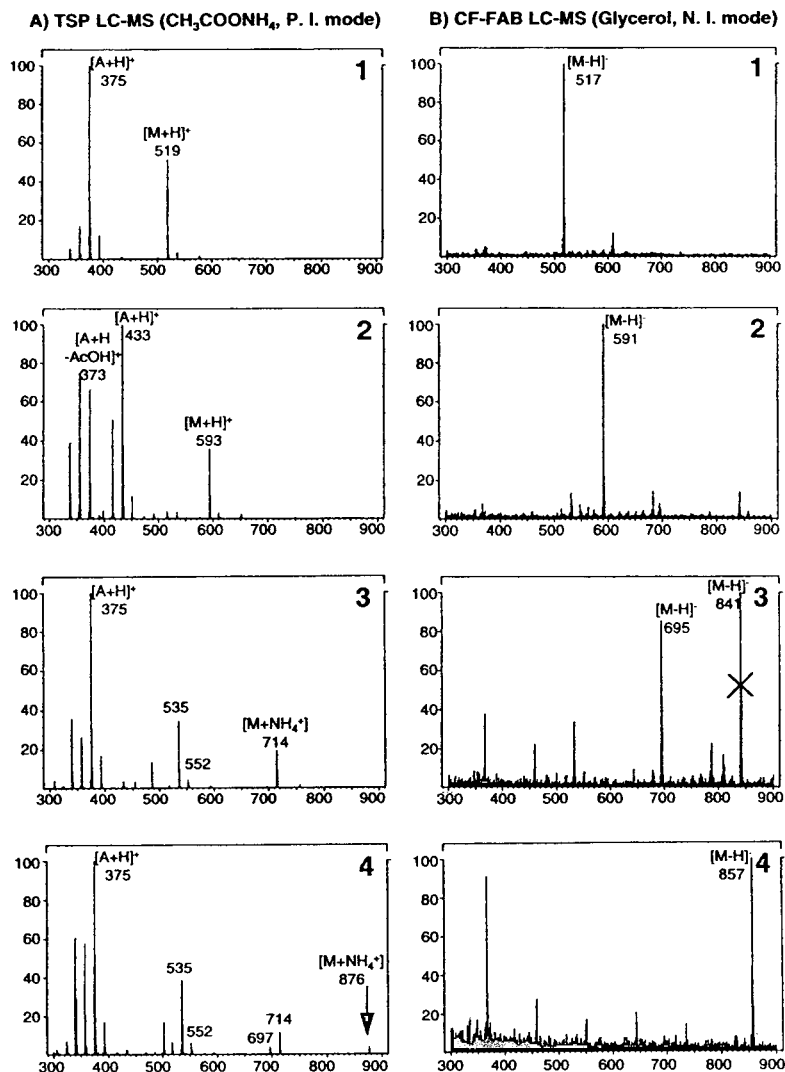


Fig. 4. TSP (A) and CF-FAB (B) MS spectra of cardenolides 1, 2, 3 and 4 from the root methanolic extract of *Nerium odorum* (Apocynaceae). Same experimental conditions as in Fig. 2.

These independent results are particularly useful in this case due to the number of adducts possible in TSP.

### 3.4. Saponins from *Swarzia madagascariensis* (Leguminosae)

Saponins are glycosides that commonly occur in higher plants. They are found in more than 500 species belonging to almost 80 different

families. Their aglycones are triterpenes (usually with oleanane, ursane or dammarane skeletons) or steroid. Monodesmosidic saponins (glycosylated at position C-3 of the aglycone, with a free carboxylic group in position C-28) are known to exhibit important molluscicidal activities [17].

Schistosomiasis (bilharzia) affects millions of people living in African, Asian and South-American countries. This disease is linked to certain species of aquatic snails because they serve as

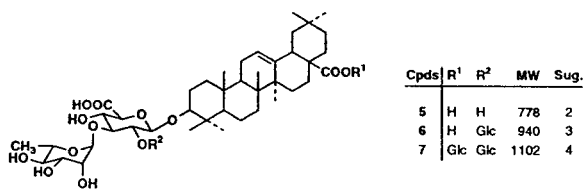


Fig. 5. Structure of selected saponins isolated from *Swartzia madagascariensis* (Leguminosae).

intermediate hosts of the parasite. Molluscicidal plants are of special importance for the control of schistosomiasis as they seem to be less expensive than synthetic compounds. For this reason, a broad screening of snail-killing plants has been undertaken. Different plants containing saponins have thus been studied [17].

In order to have a rapid idea about the saponin content of a plant extract, complemen-

tary TSP and CF-FAB LC-MS analyses have been undertaken. For example, this approach has been used in the study of the molluscicidal water extract of the fruit of *Swartzia madagascariensis* (Leguminosae), a tree widespread in Africa [18]. As in the case of *Nerium odorum* the crude extract of *Swartzia madagascariensis* (0.6 mg) was separated on a C<sub>18</sub> column (MeCN-H<sub>2</sub>O gradient, 30:70→50:50 in 30 min, 0.9 ml/min).

The TSP LC-MS analysis of the extract exhibited the presence of triterpene glycosides derived from oleanolic acid (*M<sub>r</sub>* 456) (Fig. 5). Indeed, strong ionisation of this aglycone moiety was observed for different peaks in the extract (compounds 5, 6 and 7 in Fig. 6A). The ion characteristic of the sapogenin was *m/z* 439 [A + H - H<sub>2</sub>O]<sup>+</sup> (TSP spectra, Fig. 7A). Another ion at *m/z* 502 was not identified but was present in

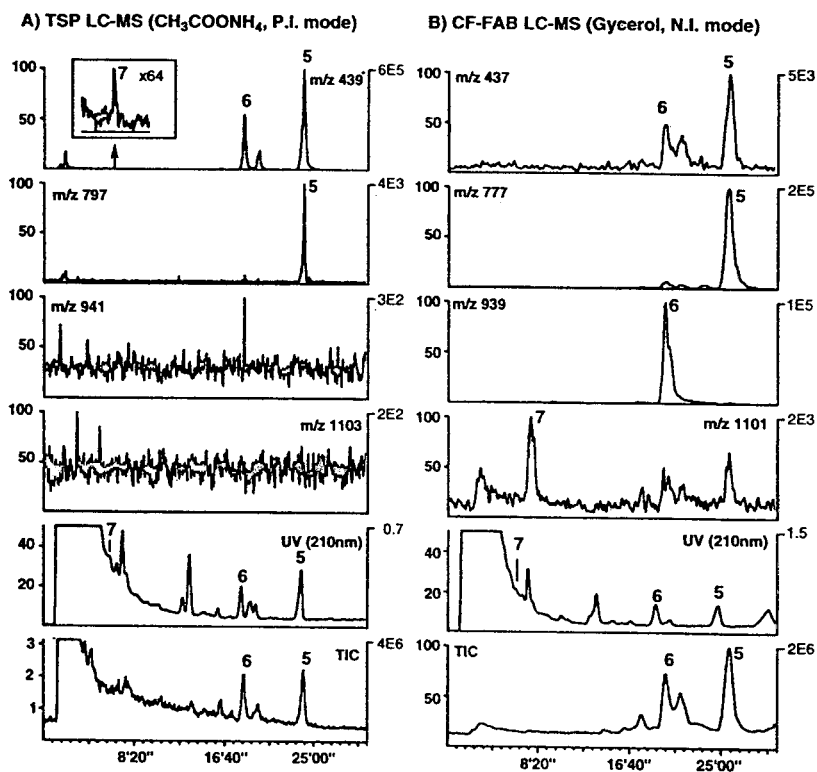
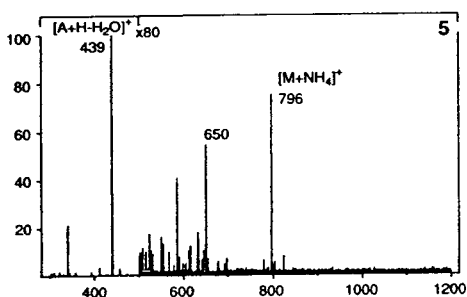


Fig. 6. Combined TSP (A) and CF-FAB (B) LC-MS of the methanolic extract of *Swartzia madagascariensis* (Leguminosae). HPLC: C<sub>18</sub> Nova-Pak (4 μm, 150 × 3.9 mm I.D.); gradient, CH<sub>3</sub>CN-H<sub>2</sub>O (0.05% TFA) 30:70→50:50 in 30 min (0.9 ml/min). For conditions of TSP and CF-FAB LC-MS see Experimental.

A) TSP LC-MS ( $\text{CH}_3\text{COONH}_4$ , P.I. mode)

## B) CF-FAB LC-MS (Glycerol, N.I. mode)

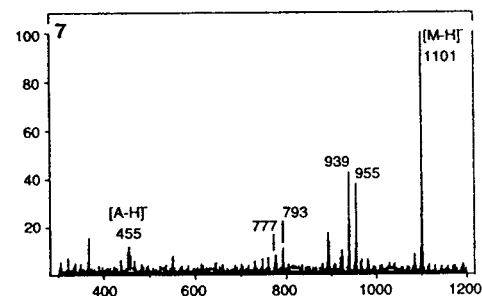
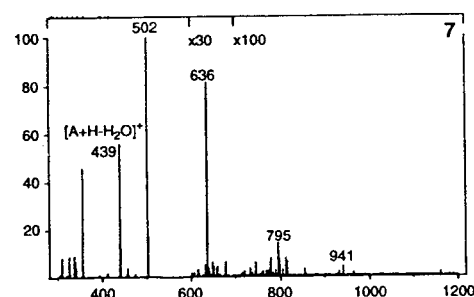
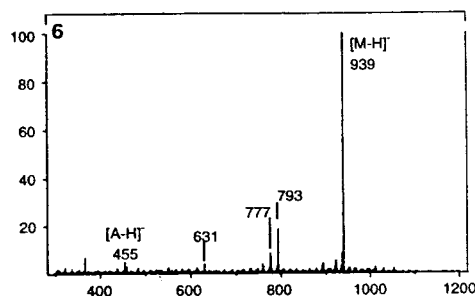
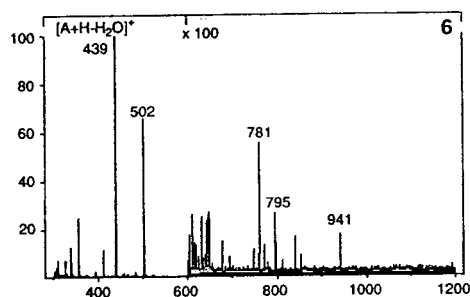
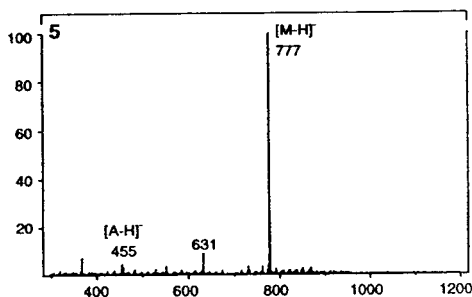


Fig. 7. TSP (A) and CF-FAB (B) MS spectra of saponins 5, 6 and 7 from the root methanolic extract of *Swartzia madagascariensis* (Leguminosae). Same experimental conditions as in Fig. 6.

the extract and the reference sample. In this case and contrary to the cardenolides from *Nerium odorum*, only very weak or no molecular ions of the corresponding saponins were recorded. For 5, a distinctive ion at  $m/z$  796 and a fragment ion at  $m/z$  650 were characteristic for a saponin bearing a diglycosidic moiety consisting of a terminal deoxyhexose unit (146 u) and a glucuronic acid (176 u) moiety. As rhamnose is the most frequent deoxyhexose occurring in saponins, it can be assumed from these on-line MS data that 5 was a saponin of oleanolic acid, substituted by a glucuronic unit and a rhamnose

in the terminal position. The TSP spectra of saponins 6 and 7 were less clear than those of 5. In both cases, characteristic signals for the oleanolic acid moiety were present, and fragment ions at  $m/z$  795 were indicative of the presence of at least glucuronic acid with a hexose unit. No clear molecular ions for tri- or higher glycosylation (TSP spectra, Fig. 7A) were visible. An ion at  $m/z$  941 was discernable in the spectra of 6 and 7 but was so weak that it could not be correlated to any "real" peak (see trace  $m/z$  941 in Fig. 6A). In the case of 7, the ion at  $m/z$  781 arose from a coeluting compound in the

extract and was not recorded on the TSP spectrum of the corresponding pure standard. For these metabolites, the TSP analysis alone could not give enough structural information.

In the CF-FAB analysis of the same extract (Fig. 6B) and unlike the TSP results, all the saponins found in the extract exhibited intense deprotonated molecular ions  $[M - H]^-$  and very weak ions characteristic for the aglycone moiety  $[A - H]^-$  ( $m/z$  455) and  $[A - H - H_2O]^-$  ( $m/z$  437). Furthermore, different characteristic cleavages were distinctive. For 5, ions at  $m/z$  777  $[M - H]^-$ ,  $m/z$  631  $[M - H - 146]^-$  and  $m/z$  455  $[A - H]^-$  confirmed the results obtained with TSP. For 6 an intense  $[M - H]^-$  ion at  $m/z$  939 was observed in the CF-FAB spectrum showing that it was a triglycosylated saponin (Fig. 7B). The different fragments ions recorded in the CF-FAB spectrum of 6 ( $m/z$  777  $[M - H - 162]^-$  and  $m/z$  793  $[M - H - 146]^-$ ) confirmed that 6 is probably similar to 5 with one more hexose unit in position C-28 or branched on the diglycoside moiety. The CF-FAB spectra of 7 exhibited an intense molecular ion at  $m/z$  1101  $[M - H]^-$ . This indicated that 7 has one hexose unit (164 u) more than 6. Saponin 7 was thus a tetraglycosylated triterpene. This was also confirmed by its high polarity (see retention time of 7 in Fig. 6). The molecular ion  $[M + H]^+$  of 7 was not detected during the TSP analysis, showing the limit of TSP in this field.

### 3.5. Saponins from *Aster scaber* and *Aster tataricus* (Asteraceae)

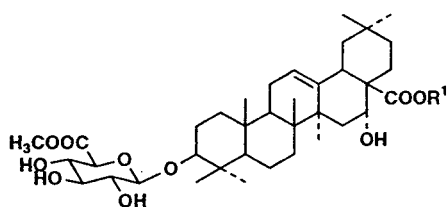
Plants from the Asteraceae family are known to possess a large number of saponins; in particular, triterpenes having long saccharide chains have been described in many species of the genera *Solidago*, *Bellis* and *Aster* [19]. In order to show the potentialities of CF-FAB or TSP for the analysis of these glycosides, two plants from this family, *Aster scaber* and *Aster tataricus*, have been selected.

In the case of *Aster scaber*, two saponin fractions of the root MeOH extract were studied [13,20]. All the acidic saponins known to be

present in the plant were converted into their methyl esters by treatment of the crude fractions with  $CH_2N_2$  before the LC-MS analysis, in order to aid separation (see experimental). The two fractions A and B, which were known to possess triterpenes bearing from 2 to 6 sugar units [13,20], were separated (1 mg each) on a  $C_{18}$  column (MeCN- $H_2O$  gradient, 20:80  $\rightarrow$  50:50 in 60 min, 0.9 ml/min).

The TSP LC-MS analysis of the saponin fractions A and B failed to give any molecular mass information. Nevertheless, intense ions corresponding to the protonated aglycone moieties and their corresponding dehydrated fragments were recorded. These results showed that fraction A consisted mainly of saponins having echinocystic acid as sapogenin ( $M_r$  472), while fraction B was composed of oleanolic acid ( $M_r$  456) glycosides.

On the contrary, the CF-FAB analyses of fractions A and B gave molecular mass and sugar sequence information on-line for all the saponins previously isolated [13,20]. In order to illustrate the results obtained, the CF-FAB analysis of the fraction A containing saponins bearing 4 to 6 sugar units is presented here (Fig. 8). Four saponins, the scaberosides A1, A2, A3 and A4 (8,9,10, and 11 respectively), have been selected (Fig. 8). The CF-FAB spectrum of scaberoside A2 (9) (Fig. 9) exhibited a clearly discernible deprotonated molecular ion  $[M - H]^-$  at  $m/z$  1071. In addition, a main fragment ion was found at  $m/z$  661 and a very intense aglycone ion  $[A - H]^-$  was recorded at  $m/z$  471. These observations suggested that 9 has an oligosaccharide unit of 410 u ( $1071 - 661$ ) esterified at position C-28 and a glucuronic methyl ester unit at C-3 ( $190$  u =  $661 - 471$ ). Indeed the ester bond at C-28 is more easily cleaved than a glycoside ether bond and gave a main fragment ion. The fragment ion recorded at  $m/z$  939 was due to the loss of the terminal pentose unit of the oligosaccharide chain linked at C-28. This oligosaccharide moiety was in fact composed of two xylose units and a rhamnose unit ( $410$  u =  $2 \times 132 + 146$ ). Compound 9 was thus a tetraglycosylated bidesmosidic saponin. Saponin 8 was an isomer of 9 and presented the same



Cpds	R <sup>1</sup>	MW	Sug.
8	-Ara <sup>2</sup> -Rha <sup>3</sup> -Api	1072	4
9	-Xyl <sup>2</sup> -Rha <sup>4</sup> -Xyl	1072	4
10	-Ara <sup>3</sup> -Rha <sup>3</sup> -Api   Xyl <sup>4</sup>	1204	5
11	-Xyl <sup>2</sup> -Rha <sup>3</sup> -Xyl <sup>3</sup> -Xyl   Xyl <sup>4</sup>	1336	6

Fig. 8. Structure of selected saponins isolated from *Aster scaber* (Asteraceae).

CF-FAB spectrum. The difference between 9 and 8 was due to the presence of an apiose and an arabinose unit in 8 instead of the two xylose units in 9. This difference was not detectable by

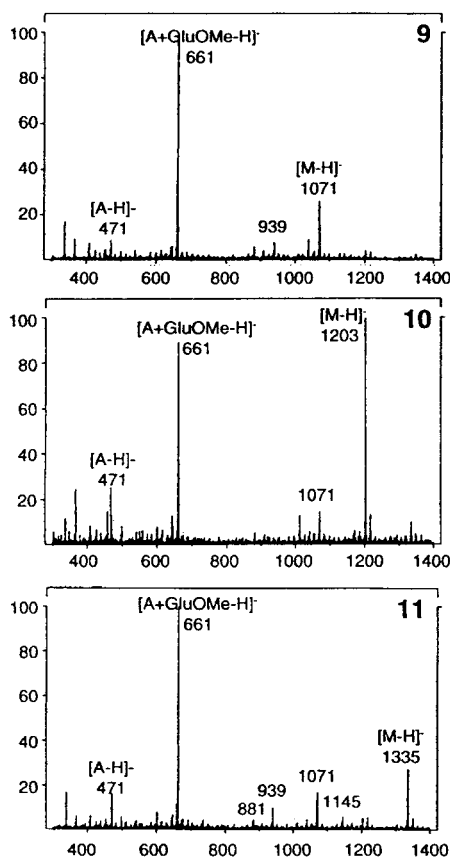


Fig. 9. CF-FAB MS spectra of saponins 9, 10 and 11 from the root methanolic extract of *Aster scaber* (Asteraceae). Same experimental conditions as in Fig. 10.

MS only since these sugars are isomeric. Compound 10 exhibited the same fragments as 9 except that its intense deprotonated molecular ion at  $m/z$  1203 was shifted by 132 u in comparison to 9, indicating a supplementary pentose unit on the oligosaccharide chain at C-28. The saponin 11 had also a protonated molecular ion shifted by 132 u in comparison to 10, indicating in this case that the glycoside had 6 sugar units (5 pentoses and a deoxyhexose) at C-28 and a glucuronic methyl ester unit at C-3. On the  $m/z$  1335 ion trace (Fig. 10) a peak eluting just before 11 was found to be an isomer of the latter having also 5 pentoses and a deoxyhexose at C-28 and a glucuronic methyl ester unit at C-3. The nature of the sugars and/or they interglycosidic linkages were probably different from those of 11. However, this compound, which is a minor constituent of the extract (see UV trace 210 nm), has not been isolated. All these on-line MS results were in good agreement with the data obtained for the isolated scaberosides A1–A4 [20].

In *Aster tataricus*, triterpene glycosides bearing up to eight sugar units (the astersaponins) have been isolated [21]. In order to check the ability of CF-FAB LC–MS to ionise these relatively large molecules, CF-FAB spectra were recorded for different astersaponins. To illustrate these results, the CF-FAB spectrum of an octaglycosylated triterpene, astersaponin D (12), is presented (Fig. 11). An intense deprotonated molecular ion  $[M-H]^-$  at  $m/z$  1585 was obtained and two clearly discernible fragments were observed at  $m/z$  1453 ( $M-H-132$ ) and  $m/z$  765, due to loss of the oligosaccharide chain

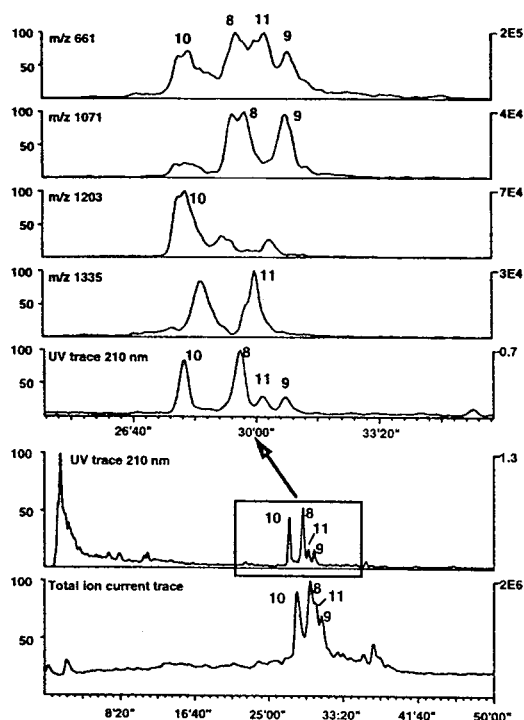


Fig. 10. CF-FAB LC-MS of the saponin fraction A of *Aster scaber* (Asteraceae). HPLC:  $C_{18}$  Nova-Pak ( $4 \mu\text{m}$ ,  $150 \times 3.9$  mm I.D.); gradient,  $\text{CH}_3\text{CN}-\text{H}_2\text{O}$  (0.05% TFA) 30:70  $\rightarrow$  50:50 in 60 min (0.9 ml/min). For conditions of CF-FAB LC-MS see Experimental.

at C-28 ( $820 \text{ u} = 4 \times 132 + 2 \times 146$ ). In this case, the fragment ion corresponding to the aglycone moiety was not clearly observable.

These different LC-MS results obtained for saponins from *Swartzia madagascariensis* and *Aster* species show that CF-FAB provides molec-

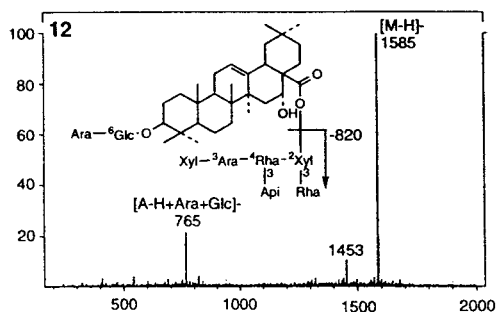


Fig. 11. CF-FAB MS spectrum of astersaponin 12 isolated from *Aster tataricus* (Asteraceae).

ular mass and sugar sequence information on-line for all the saponins, while TSP failed to give reliable molecular mass information as soon as the number of sugar units exceeded two or three. CF-FAB can be thus considered in this case as the method of choice for the LC screening of saponins. Nevertheless, TSP enables the assignment of the molecular mass of the aglycone moieties of the different saponins. This information is complementary to CF-FAB because in certain cases the aglycone ion is not always observed in the CF-FAB spectra. TSP can also be considered as an interesting tool for the detection of saponins in crude extracts. Indeed, due to its sensitivity to aglycone fragments and due to its ability to maintain good LC peak shapes, TSP LC-MS can be used, by displaying the ion traces of specific aglycone moieties, to detect saponins having a weak UV chromophore or present in very small amounts in the extract (Fig 6A).

It should also be stated that TSP remains a powerful tool for the on-line identification of small saponins and thus the use of CF-FAB is not necessary in all cases. For example, LC-MS has proved to be a valuable method for the analysis of mono- and diglycosidic saponins related to aridanin, found in the fruit of *Tetrapleura tetraptera* (Leguminosae) [6].

#### 4. Conclusions

It has been shown that TSP and CF-FAB are two valuable methods for the on-line analysis of glycosides in crude plant extracts. Nevertheless, depending on the nature of the glycosides and the type of information required, the use of one or the other or both techniques is needed.

TSP LC-MS is suitable for the investigation of small glycosides. Due to the thermal instability of glycosides, however, the TSP interface needs to be properly tuned in order to get all the structural information desired. While the technique permits an unambiguous molecular mass determination of mono- and diglycosides, the observation of triglycoside molecular ions is often difficult. The spectra obtained on-line by



TSP LC–MS using ammonium acetate as buffer in the positive ion mode are usually comparable to the DCI (NH<sub>3</sub>) spectra of the corresponding pure products.

CF-FAB LC–MS permits the analysis of a broad range of polar compounds and it has been shown that molecular mass information can be obtained for triterpene glycosides and cardenolides bearing from one to eight sugar units. This technique, however, should be also applicable to larger glycosides. The main drawbacks of CF-FAB are the poor peak sharpness, peak tailing and lack of sensitivity due to the splitting device. The spectra obtained with CF-FAB are comparable to those of static FAB but are much cleaner due to the lower percentage of matrix used. In addition, more structural information can be obtained by the study of these glycosides in CF-FAB LC–MS–MS. LC–MS–MS studies are presently under investigation.

In this paper, examples of TSP and CF-FAB LC–MS of crude plant extracts containing known compounds have been described. The different LC–MS analyses performed have shown that it is possible to efficiently detect glycosides in the crude extracts and that the on-line MS spectra recorded on-line were comparable to those of the isolated products. However, these hyphenated techniques can also be used in order to screen unknown compounds in crude plant extracts and thus to target their isolation. Indeed, the MS information obtained on-line gives a rapid idea of the molecular mass, the number of sugars and also the type of aglycone of the different glycosides. The fragment ions corresponding to the intermediate loss of sugar units sometimes allow the elucidation of the sugar sequence. In combination with chemotaxonomical considerations, these on-line data often permit a partial structural determination of the metabolites of interest. LC–UV, TSP and CF-FAB LC–MS are now used routinely in our laboratories for the LC screening of crude plant extracts. They have already permitted, for example, the efficient targeted isolation of new types of secoiridoid glycosides in a *Gentiana* species (Gentianaceae) [22].

The use of these hyphenated techniques en-

ables the early recognition of known products in extracts with a minute amount of plant material. This avoids their time-consuming isolation and, moreover, allows a targeted isolation of new interesting metabolites.

### Acknowledgement

Financial support was provided by the Swiss National Science Foundation.

### References

- [1] B. Domon and K. Hostettmann, *Phytochemistry*, 24 (1985) 575.
- [2] J.L. Wolfender, M. Maillard, A. Marston and K. Hostettmann, *Phytochem. Anal.*, 3 (1992) 193.
- [3] C.R. Blackley and M.L. Vestal, *Anal. Chem.*, 7 (1983) 750.
- [4] R.M.C. Caprioli, T. Fan and J.S. Cotrell, *Anal. Chem.*, 58 (1986) 2949.
- [5] J.-L. Wolfender, M.P. Maillard and K. Hostettmann, *J. Chromatogr.*, 647 (1993) 183.
- [6] M.P. Maillard and K. Hostettmann, *J. Chromatogr.*, 647 (1993) 147.
- [7] M. Hattori, Y. Kawata, N. Kakiuchi, K. Matsuura and T. Namba, *Shoyakugaku Zasshi*, 42 (1988) 228.
- [8] M. Hattori, Y. Kawata, N. Kakiuchi, K. Matsuura, T. Tomomori and T. Namba, *Chem. Pharm. Bull.*, 36 (1988) 4467.
- [9] D. Schaufelberger, B. Domon and K. Hostettmann, *Planta Med.*, 50 (1984) 398.
- [10] A.L. Vergey, C.G. Edmonds, I.A.S. Lewis and M.L. Vestal, *Liquid Chromatography–Mass Spectrometry*, Plenum, New York, 1989.
- [11] M. Hamburger and K. Hostettmann, *Phytochemistry*, 30 (1991) 3864.
- [12] J.-L. Wolfender, M.P. Maillard and K. Hostettmann, *Phytochem. Anal.*, 5 (1994) 153.
- [13] T. Nagao, R. Tanaka and H. Okabe, *Chem. Pharm. Bull.*, 39 (1991) 1699.
- [14] J. Iida and T. Murata, *Anal. Sciences*, 7 (1991) 963.
- [15] T. Yamauchi, M. Takahashi and F. Abe, *Phytochemistry*, 15 (1976) 1275.
- [16] R. Hanada, F. Abe and T. Yamauchi, *Phytochemistry*, 31 (1992) 3183.
- [17] K. Hostettmann, in H. Wagner, H. Hikino and N.R. Farnsworth (Editors), *Economic and Medicinal Plant Research*, Vol. 3, Academic Press, London, 1989.
- [18] C. Borel and K. Hostettmann, *Helv. Chim. Acta*, 70 (1987) 570.

- [19] K. Hostettmann and A. Marston, *Saponins*, Cambridge University Press, Cambridge, 1995.
- [20] T. Nagao, R. Tanaka, H. Shimokawa and H. Okabe, *Chem. Pharm. Bull.*, 39 (1991) 1719.
- [21] T. Nagao, S. Hachiyama, K. Okabe and T. Yamauchi, *Chem. Pharm. Bull.*, 37 (1989) 1977.
- [22] W.-G. Ma, N. Fuzzati, J.-L. Wolfender and K. Hostettmann, *Helv. Chim. Acta*, 77 (1994) 1660.

# Liquid chromatographic–mass spectrometric studies on the enzymatic degradation of $\beta$ -endorphin by endothelial cells

M. Brudel, U. Kertscher, D. Schröder, M.F. Melzig, B. Mehlis\*

*Institute of Molecular Pharmacology, A. Kowalke Str. 4, D-10315 Berlin, Germany*

## Abstract

An on-line HPLC–mass spectrometric procedure with an electrospray atmospheric pressure ionization (ESI-API) ion source was developed to identify the enzymatic degradation products (peptides) generated by incubation of human  $\beta$ -endorphin (h $\beta$ E) with cultured aortic endothelial cells. The samples from the complex incubation mixture were prepurified and enriched using a small reversed-phase (RP) perfusion precolumn. Flow switching was applied to transfer the peptides from this precolumn to the analytical RP column of 2 or 0.32 mm I.D. and to separate them by gradient elution. The peptides were detected by means of an on-line coupled triple quadrupole mass spectrometer (TSQ 700) with an ESI-API ion source operated in the positive ion mode. This MS system behaves as a concentration sensitive detector at flow-rates from 5 to 150  $\mu$ l/min. MS–MS experiments supported the unambiguous assignment of the peptide structures. Thus most of the peptide fractions were identified and the region 16-17-18 (-L-F-K-) of h $\beta$ E was found to be primarily attacked by the enzymes of the endothelial cells.

## 1. Introduction

The neuropeptide  $\beta$ -endorphin ( $\beta$ E) is known as one of the most active endogenous opioids and is involved in many physiological and pathophysiological processes. It is generated from its precursor pro-opiomelanocortin concomitantly with other neuropeptides by selective proteolytic hydrolysis in the brain and pituitary [1] resulting in a peptide with 31 amino acid residues, i.e. human  $\beta$ E(1–31):

$\text{Y}^1\text{GGFMTSEKS}^{10}\text{QTPLVTLFKN}^{20}\text{AIKNAY-KKGE}^{31}$ .

$\beta$ E is also distributed in many peripheral tissues [2,3].

Secondary peptidolytic processing of  $\beta$ E has been reported to proceed in the pituitary and brain where C-terminal attack results in  $\beta$ E(1–27) and  $\beta$ E(1–26) as the naturally occurring fragments [4,5]. Another cleavage site is the Leu<sup>17</sup>-Phe<sup>18</sup> bond of  $\beta$ E resulting in the biologically active fragment  $\beta$ E(1–17), referred to as  $\gamma$ -endorphin [6,7].

The endothelial cells of the blood vessels are able to process biologically active peptides. This has been reported for Leu-enkephalin [8,9], angiotensin I [10], endothelin [11], bradykinin [12] and natriuretic peptide [13]. However, no reference to the fate of  $\beta$ E in contact with endothelial cells is available.

It was our aim to gain information on this process because exogenous  $\beta$ E, applied in pharmacological experiments, has to pass from the circulation through the continuous monolayer of

\* Corresponding author.

endothelial cells at the inner surface of the blood vessels to its target cells and may be converted by these cells into fragments of changed bioactivity.

Liquid chromatography–mass spectrometry with electrospray ionization is an established method for the identification of peptide molecules. It is also very suitable for the identification of peptide fragments in tryptic or similar peptide digests [14,15]. However, when the peptides have to be identified in a biological matrix where a complex of peptidases of unknown specificity generates a number of fragments, difficulties may arise. The processing of  $\beta$ E, a 31 amino-acid residue peptide, in contact with living cells can serve as a model in this respect. In addition it was our aim to analyze the fractions containing low peptide concentrations that were detected by the UV detector but were below the limit of detection of the mass spectrometer. Therefore, the HPLC–MS system was combined with a flow-switching setup with a small precolumn effecting both fast on-line prepurification and enrichment. Thus we were able to analyze the samples obtained from our pharmacological experiments containing nanomolar peptide concentrations.

## 2. Experimental

### 2.1. Materials

Human  $\beta$ -endorphin,  $h\beta$ E =  $h\beta$ E(1–31), and its partial sequences were supplied by Bachem (Heidelberg, Germany). A small amount (<5%) of oxidized peptide (Met-sulfoxide) was present in these preparations after dissolution. Acetonitrile (HPLC ultra gradient grade) was from Baker (Gross Gerau, Germany). Trifluoroacetic acid (TFA) spectral quality (Uvasol) and all other chemicals were from Merck (Darmstadt, Germany). Deionized water was obtained from a combined Milli-RO/Milli-Q plus water system (Millipore, Eschborn, Germany).

### 2.2. Incubation of cells with $h\beta$ E

Endothelial cells from calf aorta (line BKEz-7) were grown to form a confluent monolayer as

previously described [16]. The culture medium was removed and the cell layer (ca.  $3 \cdot 10^6$  cells) washed two times with an isotonic solution (NaCl 8 g, KCl 0.2 g,  $\text{Na}_2\text{HPO}_4 + 12 \text{H}_2\text{O}$  2.9 g,  $\text{KH}_2\text{PO}_4$  0.2 g in 1000 ml deionized  $\text{H}_2\text{O}$ ). A solution of  $h\beta$ E (1.2 ml, max. concentration 20  $\mu\text{M}$ ) in this isotonic solution was added to cover the cell layer completely and incubated at 37°C with gentle shaking for a maximum of 2 h. Samples of the supernatant were collected at time intervals, taking care not to damage the cells, acidified with TFA (final concentration 1%, pH ca. 1.4), and then centrifuged at 9500 g for 5 min at 4°C to remove cell fragments.

### 2.3. Mass spectrometry

The mass spectrometric equipment was a triple quadrupole mass spectrometer (Finnigan MAT TSQ 700, Bremen, Germany) with an electrospray (API) ion source (Finnigan MAT) operating in the positive mode with a capillary temperature of 200°C, a high voltage of 4.5 kV, nitrogen as auxiliary and sheath gas and without sheath liquid. The off-line mass spectra were obtained by syringe infusion of the sample in methanol–water (1:1) containing 1% acetic acid with a flow of 3 to 5  $\mu\text{l}/\text{min}$  (except for the flow experiments) and with a sheath gas flow corresponding to  $2.1 \cdot 10^5$  Pa without an auxiliary gas flow. In the on-line mode the API ion source was operated at a flow of 5–100  $\mu\text{l}/\text{min}$  (HPLC eluent) depending on the column used and with a sheath and auxiliary gas flow corresponding to  $2.8 \cdot 10^5$  Pa and 235 ml/min, respectively.

Off-line MS–MS experiments were performed with the respective peptide fractions by using a collision gas pressure of 1–3 mTorr, offset voltage of –20 to –30 eV and multiplier voltage of 1.6–1.8 kV.

### 2.4. Chromatographic system

The system used for the on-line LC–MS studies consisted of an Applied Biosystems dual-syringe pump, type 140B and UV detector type 785A equipped with a micro flow cell (light path 8 mm, quartz capillary, type UZ, LC Packings/ICT, Bad Homburg, Germany). Separations

were carried out using columns of Vydac 300 Å, C<sub>18</sub>, 5 μm, 150 × 2 mm I.D. (Promochem, Wesel, Germany) and Vydac 300 Å, C<sub>18</sub>, 5 μm, 150 × 0.32 mm I.D. (LC-Packings/ICT). The flow lines applied for these two columns were similar to those described earlier [17] and included post- and precolumn splitting for the 2 mm and 0.3 mm columns, respectively. In general a split ratio (*X/Y*) of 9:1 for the 2 mm column and 1:19 for the 0.3 mm column was applied (*X* = flow to the MS system). When peptide fractions had to be analyzed off-line, the split ratio at the 2 mm column was reversed (*X/Y* = 1:9, main flow collected). Samples were injected using a trace enrichment setup [18] with a two-position 10-port valve with electric actuator (Valco, type WE C10 WK). The sample loop (PEEK tubing) was filled with the valve in position A, while with the valve in position B the sample was delivered to the precolumn and then flushed with two volumes of water with the aid of an auxiliary pump (LC-6A, Shimadzu, Duisburg, Germany). The precolumns were dry filled with RP perfusion stationary phase POROS 10 R2, 10 μm (PerSeptive Biosystems, Freiburg, Germany). A 20 × 2 mm I.D. precolumn (Upchurch cat. no. C.130B) was used for the 2 mm analytical column and a 10 × 1 mm I.D. precolumn for the 0.3 mm column. Gradient elution was performed with the valve in position A with a mobile phase consisting of A: acetonitrile–water (1:99) containing 0.05% TFA and B: acetonitrile–water (80:20) containing 0.05% TFA. The gradient was run from 15% B to 47% B in 20 min and then in 5 min to 100% B.

Edman sequencing of peptide fractions was performed with a protein sequencer (type 476A, PE/Applied Biosystems, Weiterstadt, Germany).

### 3. Results and discussion

The mass chromatograms (overlay) in Fig. 1 show that hβE is degraded by the enzymes of the endothelial cells into various peptide fragments. Some of the chromatographic peaks (e.g. trace A, no. 11/12 and 14/16; trace B, no. 5/6) detected by the mass spectrometer strongly over-

lap and were not discriminated by the UV detector. Comparison of traces A and B also demonstrates the advantage of the microcolumn (trace A) with a low amount of peptide in the sample. In our experiments a two- to threefold increase in the MS signal intensity was obtained for the microcolumn over that obtained with the 2 mm I.D. column. However, when a sufficient amount of peptide was available, the 2 mm I.D. column was preferred because of its ruggedness. There was also no significant decrease in MS signal intensity when the flow-rate to the MS was increased from 5 μl/min to 150 μl/min (Fig. 2). As can be seen in this figure, the MS system with the ESI-API ion source applied in this study behaves as a concentration sensitive detector over the applied range of flow-rates with a flow optimum indicated around 50 μl/min.

Identification of peptides in biological samples is often difficult because of the low peptide concentrations and matrix effects. The setup for prepurification used in this study significantly improved the MS measurements. Large sample volumes (≤ 2 ml) were applied with high flow-rates (ca. 5 precolumn volumes/min) using RP perfusion stationary phase [15,19]. The dynamic capacity of the 2 mm I.D. precolumn was determined to be ca. 0.1 μmol of peptide (concentration 0.1 μmol/ml). This method can be applied at high salt concentrations (e.g. 0.9% NaCl) provided the samples do not contain high concentrations of proteins competing with the peptides for the stationary phase.

In Table 1 the assignment of the chromatographic peaks (Fig. 1) to the respective hβE fragments is summarized. Most of the fragments were assigned by their double and triple charged ions in the ESI-MS spectra. The structural assignment by mass determination alone (at unit mass resolution) is often not feasible when peptide fragments of this size have to be analyzed. One example are the sequences hβE(19–31) and hβE(7–19), both with *M<sub>r</sub>* 1477.7. Therefore, off-line MS-MS and micro Edman sequencing experiments were performed, where necessary, to confirm the assignment as shown in Table 1. Thus most of the fragments have been unambiguously identified, except the minor peaks 3, 4, 8 and 12. Peak no. 3, which is proposed to be

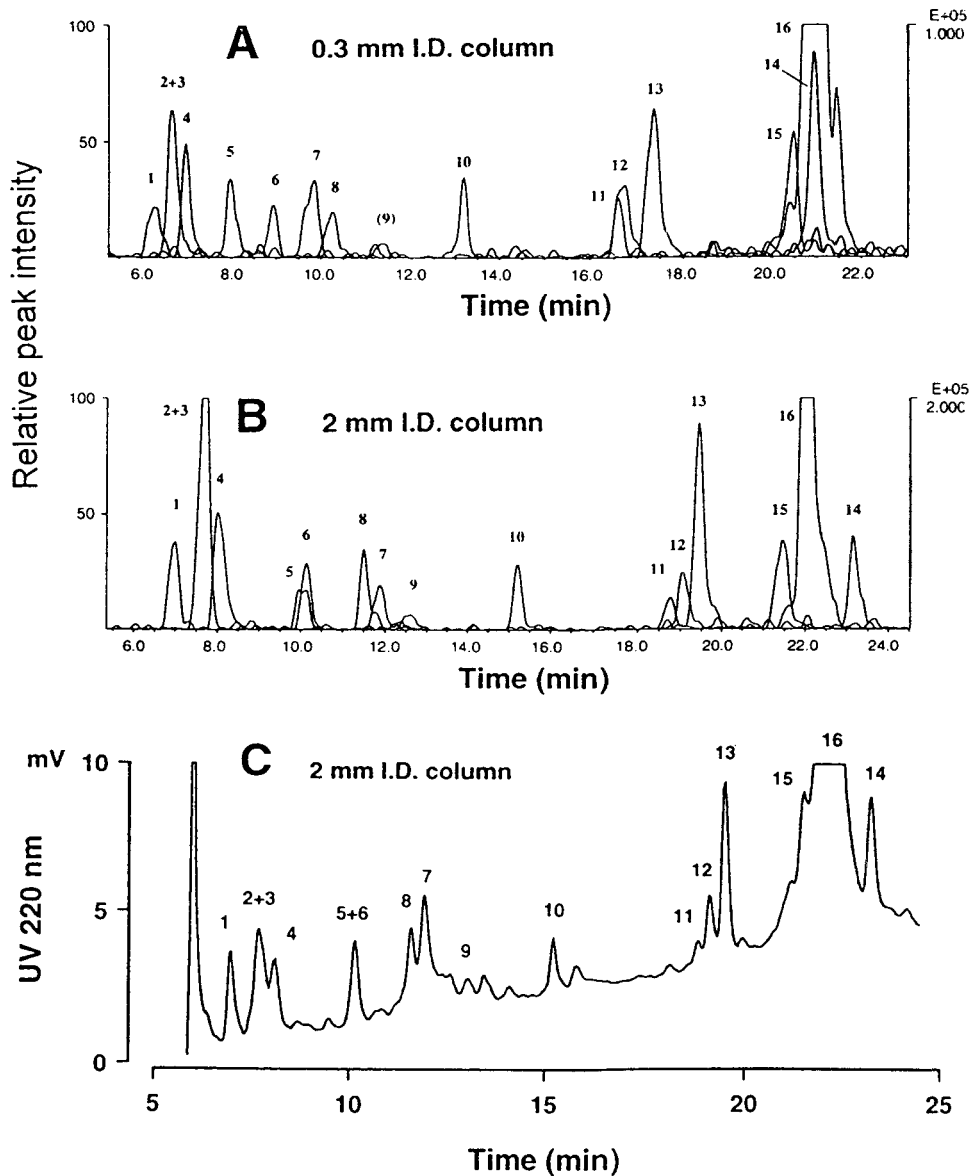


Fig. 1. Mass chromatograms (traces A and B) of the peptide fragments obtained after incubation of h $\beta$ E for 2 h with cultured endothelial cells. The individual mass traces of the  $[M + 2H]^{2+}$  or  $[M + 3H]^{3+}$  ions are superimposed to give the overlap traces. Trace A is the mass chromatogram of the degradation mixture (initial concentration of h $\beta$ E 0.4  $\mu$ M) with the 0.3 mm I.D. column setup while trace B was of an initial 2  $\mu$ M concentration of h $\beta$ E and run with the 2 mm I.D. column setup. The concentrations of the fragments in trace A and B were ca. 0.02–0.1  $\mu$ M and 0.1–0.5  $\mu$ M respectively. In trace C the UV absorption corresponding to trace B is depicted. For the structural assignment of the fragments see Table 1. Peaks no. 16 and 15 are h $\beta$ E and its Met-sulfoxide, respectively. Peaks no. 4 and 12 could not be assigned.

h $\beta$ E(19–30), was detected only when a very shallow gradient was applied (data not shown).

The peptidases of the endothelial cells degrade

about 60% of the h $\beta$ E applied in the incubation mixture within 2 h under the conditions used here for the incubation (Fig. 3, insert). During

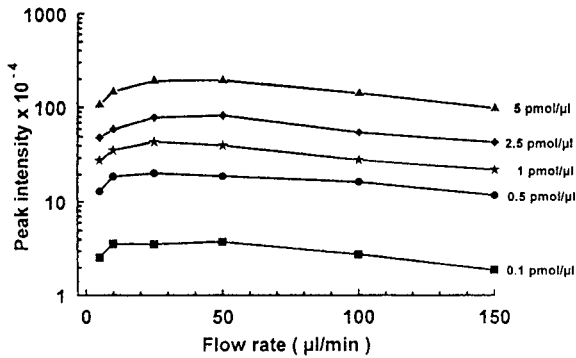


Fig. 2. ESI-API-MS signal intensity at different concentrations and flow-rates. The peptide samples ( $5 \mu\text{l}$ ) of  $0.1\text{--}5 \mu\text{M}$  solutions of h $\beta\text{E}(1\text{--}27)$  in the solvent acetonitrile–water (25:75) containing 0.05% TFA were injected in the flow injection mode into the same solvent. Data points are mean values from two independent sets of experiments with each concentration injected in duplicate (R.S.D.  $\leq 10\%$ ). Spray parameters (sheath gas pressure, auxiliary gas flow, capillary temperature) were optimized at each flow-rate to get a stable spray.

this period the fragments h $\beta\text{E}(1\text{--}17)$  and h $\beta\text{E}(1\text{--}18)$  show the highest concentration. The complementary fragments h $\beta\text{E}(18\text{--}31)$  and h $\beta\text{E}(19\text{--}31)$  also increase with time (Fig. 3) but do not reach the level of the former fragments,

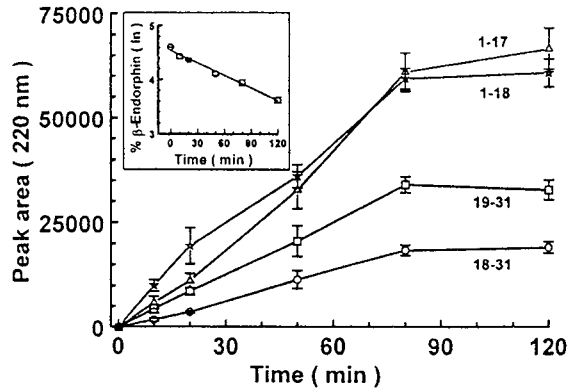


Fig. 3. Time course of the formation of four main degradation products of h $\beta\text{E}$  in the incubation mixture with the endothelial cells. h $\beta\text{E}$  sequences: ( $\Delta$ ) 1–17, ( $\star$ ) 1–18, ( $\square$ ) 19–31, ( $\circ$ ) 18–31. The half-life of h $\beta\text{E}$  (cf. insert) in presence of the endothelial cells was determined to be 82 min ( $n = 5$ ).

probably because of their rapid degradation by amino- and carboxypeptidases, resulting in the intense peak no. 2 + 3, h $\beta\text{E}(20\text{--}31)$  + h $\beta\text{E}(19\text{--}30)$ . The processing of h $\beta\text{E}$  by the endothelial cells may proceed as shown in Fig. 4 with the region 16–17–18 (–L–F–K–) of h $\beta\text{E}$  as the primary site of enzymatic attack. Thus, the fragment

Table 1  
Fragments of human  $\beta$ -endorphin formed by the enzymes of the endothelial cells

Peptide sequence	$\beta$ -Endorphin fragment	Peak No. <sup>a</sup>	$M_r(\text{calc.})^b$	$m/z^c$	
				$[\text{M} + 2\text{H}]^{2+}$	$[\text{M} + 3\text{H}]^{3+}$
YGGFMTSEKSQTP	1–13	7	1432.6	717.4	478.7
GGFMTSEKSQTP	2–13	5	1269.4	635.7	424.2
YGGFMTSEKSQTPLVT	1–16	10	1746.0	873.7	582.6
YGGFMTSEKSQTPLVTL	1–17	13	1859.1	930.8	620.9
GGFMTSEKSQTPLVTL	2–17	11	1696.0	848.9	– <sup>d</sup>
YGGFMTSEKSQTPLVTLF	1–18	14	2006.3	1003.8	670.0
LFKNAIKKNAYKKGE	17–31	9	1737.1	869.3	579.8
FKNAIKKNAYKKGE	18–31	6	1623.9	813.0	542.6
KNAIKKNAYKKGE	19–31	1	1476.8	739.7	493.3
KNAIKKNAYKKG	19–30	3	1347.6	675.2	450.2
NAIKKNAYKKGE	20–31	2	1348.6	675.4	450.6

<sup>a</sup> Peak numbers refer to Fig. 1. Peak no. 16 (h $\beta\text{E}$ ),  $M_r(\text{calc.})$  3465.2 shows  $m/z$  1733.5 and 1156.1 for the double and triple charged ion, respectively.

<sup>b</sup> Calculated relative molecular mass (average mass).

<sup>c</sup>  $m/z$  values of the ions observed in the ES–MS spectra.

<sup>d</sup>  $[\text{M} + 3\text{H}]^{3+}$  ion not observed, found:  $[\text{M} + \text{H}]^+$ ,  $m/z$  1696.5.

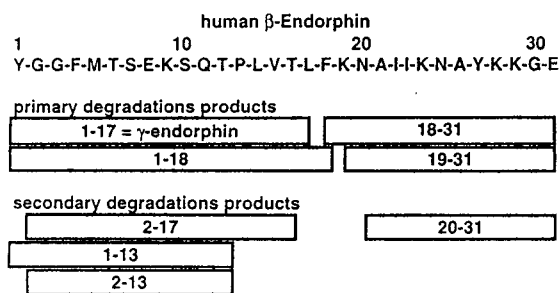


Fig. 4. Degradation pattern of h $\beta$ E produced by the enzymes of the endothelial cells. The site of the primary enzymatic attack is the region 16-17-18. Secondary fragments (only examples shown, see also Table 1) may be generated by amino- and carboxypeptidases from the primary fragments.

h $\beta$ E(1–17),  $\gamma$ -endorphin, identified in some tissues [6,7], is also generated by the enzymes of the endothelial cells from h $\beta$ E. It can not be deduced from these results that enzymes exclusively located at the surface of the endothelial cells are involved. Experiments on the nature and localization of these enzymes are in progress and will be published elsewhere. Apparently, two enzymes are responsible for the splitting in the L-F-K region as shown by the detection of h $\beta$ E(1–18). The sequences h $\beta$ E(1–26) and h $\beta$ E(1–27), also known as naturally occurring fragments [4,5], were not detected and may only be produced (if at all) in very low amounts in this system. Whether the fragment h $\beta$ E(1–13), observed in our experiments, is generated by selective endopeptidase attack or through carboxypeptidase degradation of the larger N-terminal fragments remains to be established.

#### 4. Conclusions

The experimental procedure described in this paper enabled us to structurally assign most of the fragments of the 31 amino acid peptide h $\beta$ E which were produced in the incubation of h $\beta$ E with the endothelial cells. We think that this procedure can be generally applied to the study of enzymatic processing of peptides as a result of their contact with cells.

It is concluded that the on-line HPLC–MS approach gives a valuable fast overview on the

possible peptide fragments. However, if peptides of nearly equal masses have to be considered, unambiguous structural assignment requires additional information. This we obtained from off-line MS–MS experiments which were carried out with fractions collected from the gradient elution. In future it would be desirable to perform the daughter ion experiments on-line as proposed recently by Cary et al. [20].

The applied enrichment procedure using a perfusion stationary phase is fast and reliable. It allows the analysis of low micromolar peptide concentrations in the cell incubation experiments and identification of fragments at nanomolar concentrations. However, further improvements will be necessary for the processing of peptides larger than h $\beta$ E and at nanomolar concentrations to be studied.

#### Acknowledgements

We thank H. Lerch and D. Runald for their skilful technical assistance and Dr. H. Berger for helpful discussions. The authors acknowledge the financial support of the Bundesministerium für Forschung und Technologie (BMFT), grant No. 07 NBL 07-6 TP 06.

#### References

- [1] Y.P. Loh, *Biochem. Pharmacol.*, 44 (1992) 843.
- [2] C.R. DeBold, W.E. Nicholson and D.N. Orth, *Endocrinology*, 66 (1988) 2648.
- [3] A.I. Smith and J.W. Funder, *Endocrine Rev.*, 9 (1988) 159.
- [4] W.R. Millington and D.L. Smith, *J. Neurochem.*, 57 (1991) 775.
- [5] M.D. Hirsch and W.R. Millington, *Brain Res.*, 550 (1991) 61.
- [6] D.M. Dorsa, M.B. Chapman and D.G. Baslin, *Peptides*, 3 (1982) 455.
- [7] J.L.M. Lebouille, R.W. Hendriks, N.M. Soeter and J.P.H. Burbach, *J. Neurochem.*, 52 (1989) 1714.
- [8] G. Heder, M. Melzig, W.E. Siems, *Pharmazie*, 47 (1992) 226.
- [9] S.E. Thompson and K.L. Audus, *Peptides*, 15 (1994) 109.



- [10] R. Auerbach, L. Alby, J. Grieves, J. Joseph, C. Lingren, L.W. Morrissey, Y.A. Sidky, M. Tu and S.L. Watts, *Proc. Natl. Acad. Sci. USA*, 79 (1982) 7891.
- [11] T.J. Opgenorth, J.R. Wu-Wong and K. Shiosaki, *FASEB J.*, 6 (1992) 2653.
- [12] K. Graf, M. Gräfe, C. Bossaller, J. Niehus, K.-D. Schulz, W. Auch-Schweik and E. Fleck, *Eur. J. Clin. Chem. Clin. Biochem.*, 31 (1993) 267.
- [13] S.J. Frost and P.A. Whitson, *J. Cell. Biochem.*, 52 (1993) 227.
- [14] T.R. Covey, E. Huang and J.D. Henion, *Anal. Chem.*, 63 (1991) 1193.
- [15] D.B. Kassel, B. Shushan, T. Sakuma and J.P. Salzmann, *Anal. Chem.*, 66 (1994) 236.
- [16] M. Brudel, U. Kertscher, H. Berger and B. Mehlis, *J. Chromatogr. A*, 661 (1994) 55.
- [17] W. Halle, W.-E. Siems, K.D. Jentsch, E. Teuscher and E. Göres, *Pharmazie*, 39 (1984) 77.
- [18] VICI AG, Valco Europa, Schenkon, Switzerland, Catalogue, 1993, p. 15.
- [19] S.P. Fulton, N.B. Afeyan, N.F. Gordon and F.E. Regnier, *J. Chromatogr.*, 547 (1991) 452.
- [20] A.M. Cary, I. Jardine, M. Wakefield, A. Land and C. Campbell, presented at the *11th Montreux Symposium on Liquid Chromatography–Mass Spectrometry, Montreux, 9–11 November 1994*.



# Enhanced sensitivity for peptide mapping with electrospray liquid chromatography–mass spectrometry in the presence of signal suppression due to trifluoroacetic acid-containing mobile phases

Alex Apffel\*, Steven Fischer, Gerson Goldberg, Paul C. Goodley,  
Frank E. Kuhlmann

*Bay Analytical Operation, Hewlett-Packard Co., 1601 California Ave., Palo Alto, CA 94304, USA*

---

## Abstract

A method is described for improving the sensitivity of peptide mapping with electrospray liquid chromatography–mass spectrometry using trifluoroacetic acid (TFA) containing HPLC mobile phases. The signal suppressing effects of TFA are shown to be due to the combined effect of ion-pairing and surface tension modifications. The post-column addition of a propionic acid–2-propanol (75:25, v/v) in a 1:2 proportion with the HPLC mobile phase counteracts the deleterious effects of TFA resulting in 10–100× improvement of the signal-to-noise ratio. The system described introduces total HPLC flow (plus additive) directly into the electrospray source without splitting. Using 2.1 mm I.D. HPLC columns, minimum detectable quantities are below 40 pmol total protein.

As examples, separations of proteolytic enzyme digests of several proteins are shown using standard HPLC conditions, comparing results with and without the addition of propionic acid. The application of the technique is shown in more depth in the identification of oxidative modification sites in glutamine synthetase. In this application, the enhanced sensitivity allowed location of a modified residue by comparison endoproteinase Lys C digest of native and oxidized forms of the protein without extensive sample preparation or concentration. A third application demonstrates the identification of glycosylation sites in an endoproteinase Arg C digest of single-chain plasminogen activator through the use of in-source collisionally induced dissociation.

---

## 1. Introduction

In the last years, electrospray mass spectrometry (ES-MS) has become the method of choice for introduction of liquids into a mass spectrometer. Although there are applications in pharmaceutical, environmental and general chemical analysis areas, the rapid growth and acceptance of the technique in bioscience is

largely due to the discovery by Fenn et al. [1] that the multiply-charged ions produced by ES-MS could be deconvoluted to determine the molecular mass of large proteins with masses far in excess of the  $m/z$  range of the mass spectrometric analyzer. Using ES-MS, proteins in excess of  $M_r$  500 kDa have been analyzed. For proteins of moderate size ( $M_r < 100$  kDa), typically the mass accuracy is  $< 0.02\%$ . Electrospray ion sources have been successfully coupled with most types of mass analyzers including quad-

---

\* Corresponding author.

rupole, sector [2], ion-trap [3], time-of-flight [4] and Fourier transform mass spectrometry (FTMS) [5] instruments, resulting in a wide range of operational characteristics, cost and ease of use. Currently, the most common configuration consists of an electrospray ion source coupled with a quadrupole (or multiple quadrupole) analyzer.

Early application of liquid chromatography–electrospray mass spectrometry (LC–ES–MS) to “real world” applications suffered from a number of limitations including poor performance with high flow-rates and aqueous mobile phases, inability to accept non-volatile buffer systems and surfactants and signal suppression with strong-acid containing mobile phases such as trifluoro acetic acid (TFA). However, with the rapid development of the technique and the introduction of second and third generation commercial hardware, commonly used mobile phases and flow-rates are routinely accommodated. While non-volatile buffers and surfactants remain problematic, TFA-containing mobile phases can, with the technique described here, be used for a variety of applications.

The use of LC–ES–MS for the characterization of proteolytic enzymatic digests of proteins has greatly increased the ability to identify the resulting digest fragments. Molecular mass data from the mass spectrometer for each of the peaks eluting in a peptide map gives additional qualitative information to the data obtained from the standard UV–Vis detector signal, which can be used to associate a specific peak with a predicted digest fragment. To fulfil this role, it is important that the ES–MS detection system operates with a sensitivity, reproducibility, chromatographic resolution and ease of use comparable to that of the UV–Vis detector. Furthermore, operation of the system should preferably not require modification of established standard HPLC methods. In particular, one should be able to use standard HPLC column-packing materials, column dimensions, flow-rates, and mobile phases.

Trifluoroacetic acid (TFA) is commonly used as an HPLC mobile phase modifier in peptide and protein separations [6]. Its excellent ion pairing and solvating characteristics confer

unique chromatographic selectivity on peptide separations, while its low UV cut-off (192 nm) allows detection of the peptide amide bond at 210 nm with minimal background or interferences from mobile phases, even when using a gradient elution mode. Due to its high volatility, TFA can easily be removed from preparative collected fractions by evaporation. Typical concentrations used are 0.1–0.2% (v/v).

Since the earliest application of electrospray LC–MS to peptide mapping, the difficulty of spraying highly aqueous solutions of TFA has been recognized, resulting in spray instability and analyte signal reduction [7–10]. General agreement exists that both spray instability and signal reduction are due to the high conductivity and surface tension of the eluent [8,11,12]. Both high conductivity and high surface tension require, when operating in pure (unassisted) electrospray mode, the onset voltage for generating a spray to be very close to corona discharge conditions. Consequently, either an unstable (noisy) spray results from operating too close to discharge conditions or low signal results from operating too far from ideal electrospray formation. Several approaches have been used to overcome these difficulties. Attempts have been made to overcome the signal suppressing effects by (i) using low flow-rates and capillary HPLC [13,14] which require lower fields for the onset potential, (ii) by using electrosharpened ES needle tips [11] to increase the field gradient at the point at which the electrospray is generated, (iii) through the use of pneumatically-assisted [12] or ultrasonically-assisted electrospray [15], (iv) through the use of surface tension lowering sheath liquids [13] or (v) the use of discharge suppressing sheath gas [16] and heating of the eluent slightly prior to spraying. Another approach has been to improve sensitivity in other ways in order to overcome the loss of sensitivity due to the signal-suppressing effects of TFA without actually addressing these effects. However, these approaches generally compromise the analytical performance in some aspect in exchange for improved sensitivity. For example, applications have been reported with TFA concentrations reduced to below 0.025% [17], re-

sulting in poor chromatographic performance. The signal-to-noise ratio can be improved by electronic filtering or slow acquisition rates but this may result in reduced chromatographic reliability. A common way to gain signal without decreasing chromatographic performance is to reduce the mass spectral resolution; however, this compromises the mass spectral information such as the ability to accurately differentiate charge states in multiply-charged digest fragments based on information contained in the resolution of isotopic peaks. While under unit resolution conditions it is difficult to identify charge states in this way above  $[M + 3]^{3+}$ , many of the peptide fragments encountered in commonly used proteolytic digests appear as  $[M + 3]^{3+}$  ions.

In this work, it is demonstrated that the signal-suppressing effect of strong acid modifiers, such as TFA, is due not only to the problems introduced during spray generation caused by high conductivity and surface tension, but also to an ion-pairing phenomenon between TFA acid anions and the basic analyte molecules. A method, referred to as the "TFA Fix" which addresses both effects is presented. A number of peptide-mapping applications are demonstrated to characterize the performance of the method.

## 2. Experimental

### 2.1. HPLC

A schematic of the analytical system is shown in Fig. 1. Primary solvent delivery and separations were performed on a Hewlett-Packard (Palo Alto, CA, USA) HP1090 HPLC equipped with a DR-5 ternary solvent delivery system, autosampler with 250- $\mu$ l sample capacity, heated column compartment, column switching valve and diode-array detector (DAD) with 1.9  $\mu$ l high-pressure flow cell. For flow injection analysis (FIA) experiments, the HPLC was connected to the electrospray inlet with approximately 50 cm  $\times$  0.025 mm I.D. peek tubing (Upchurch Scientific, Oak Harbor, WA, USA). For peptide mapping, a 250  $\times$  2.1 mm I.D. 5  $\mu$ m 300A Vydac

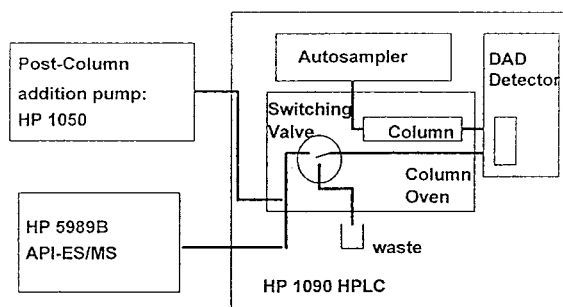


Fig. 1. Schematic of analytical setup for peptide mapping.

Column (The Separations Group, Hesperia, CA, USA) was used. Separations were performed with a linear solvent gradient from 0 to 60% B over a 60-min period at a flow-rate of 0.2 ml/min, unless stated otherwise. Solvent A was 0.2% TFA in water and solvent B was 0.2% TFA in acetonitrile. The column was thermostated at 40°C.

The "TFA Fix" method consisted of post-column addition of propionic acid–2-propanol (75:25) at a flow-rate of 100  $\mu$ l/min. As shown in Fig. 1, the TFA Fix was delivered using an HP 1050 HPLC pump and was teed into the column effluent after the DAD detector and after the column-switching valve. The tee was connected to the electrospray needle via approximately 50 cm  $\times$  6.35 mm I.D. peek tubing (Upchurch). It was not found necessary to include any additional mixing. The column effluent was diverted from the MS for the first 5 min of the chromatogram, during which excess reagents and unretained components eluted.

### 2.2. Mass spectrometry

Mass spectrometry was performed on a Hewlett-Packard 5989B quadrupole mass spectrometer equipped with extended mass range, high-energy dynode detector (HED) and a Hewlett-Packard 59987A atmospheric-pressure ionization (API) electrospray source with high-flow nebulizer option. Both the HPLC and MS were controlled by the HP Chemstation software allowing simultaneous instrument control, data acquisition and data analysis. The high-flow

Table 1  
Electrospray lens settings

ES parameter	Setting
$V_{\text{cap}}$	-4000 V
$V_{\text{end}}$	-3500 V
$V_{\text{cyl}}$	-5500 V
CapEx	100 V
$ES_{\text{Skim1}}$	26.7 V
$ES_{\text{Offs}}$	-0.7 V
$ES_{\text{Skim2}}$	6.2 V
$ES_{\text{Lens2}}$	10 V
$ES_{\text{Lens3}}$	-40 V

nebulizer was operated in a standard mode with  $N_2$  as both nebulizing (1.5 l/min) and drying (15 l/min at 300°C) gases. Typical lens settings for the electrospray source are shown in Table 1.

To characterize the effects of the TFA Fix, FIA of selected samples (listed in Table 2) was done at varying flow-rates and mobile phase conditions with data acquisition in the selected-ion monitoring (SIM) mode at a 100 ms dwell-time.

For peptide mapping, MS data was acquired in the scan mode, scanning from 200 u to 1600 u at an acquisition rate of 1.35 Hz and a stepsize of 0.1 Da. Unit resolution was maintained for all

experiments. Data was filtered in the mass domain with a 0.03-u gaussian mass filter and in the time domain with a 0.05-min gaussian time filter.

### 2.3. Chemicals

HPLC grade water was purified in-house (Barnstaed, Dubuque, IA, USA). Acetonitrile and 2-propanol were HPLC grade (Mallinckrodt, Paris, TX, USA). Formic acid, acetic acid, hydrochloric acid (HCl) and heptafluorobutyric acid (HFBA) (Sigma, St. Louis, MO, USA), trifluoroacetic acid, butyric acid, valeric acid (Aldrich, Milwaukee, WI, USA) and propionic acid (Mallinckrodt) were >99% purity and were not further purified.

Horse heart myoglobin and chicken lysozyme were obtained from Sigma. Native and oxidized glutamine synthetase were obtained by courtesy of Dr. Rodney Levine at National Heart Lung and Blood Institute at the National Institutes of Health. Endoproteinase Arg C digests of single-chain plasminogen activation factor were obtained by courtesy of Erno Pungor, Jr. and Carrie Souders at Berlex Pharmaceuticals. FIA samples (see Table 2) and diphenylthiourea (DPTU) were obtained from Sigma.

Trypsin and endoproteinase Lys C digestion were performed as follows. The samples were

Table 2  
Characteristics of FIA samples

Sample	Concentration <sup>a</sup>	$M_r$	SIM ion monitored
Hydrocortisone	500 pmol/ $\mu$ l	362.4	363 [M + H] <sup>+</sup>
Sulfamethazine	100 pmol/ $\mu$ l	278.3	279.3 [M + H] <sup>+</sup>
Lysine	200 pmol/ $\mu$ l	146.2	147.2 [M + H] <sup>+</sup>
Gly-Tyr	200 pmol/ $\mu$ l	238.2	239.2 [M + H] <sup>+</sup>
Gramacidin S	50 pmol/ $\mu$ l	1141.48	571.6 [M + 2H] <sup>2+</sup>
Reserpine	50 pmol/ $\mu$ l	608.4	609.4 [M + H] <sup>+</sup>
Erythromycin	100 pmol/ $\mu$ l	733.95	734.95 [M + H] <sup>+</sup>
Peptide mixture			
Angiotensin II	50 pmol/ $\mu$ l	1046.21	524 [M + 2] <sup>2+</sup>
ValTyrVal	130 pmol/ $\mu$ l	379.4	380.4 [M + H] <sup>+</sup>
Met-Enkephalin	90 pmol/ $\mu$ l	555.6	556.6 [M + H] <sup>+</sup>
Leu-Enkephalin	90 pmol/ $\mu$ l	573.6	574.6 [M + H] <sup>+</sup>
Biotin	500 pmol/ $\mu$ l	244.31	245.31 [M + H] <sup>+</sup>

<sup>a</sup> Relatively high sample concentrations were used to allow quantitation of performance under unfavorable conditions.

initially reduced and alkylated by reconstituting 10–30 nmols of lyophilized protein in 100  $\mu$ l 6 M guanidine-HCl. A 100- $\mu$ l volume of 0.8 mg/ml dithiothreitol in ammonium bicarbonate (pH 7.8) was added and incubated for 30 min at 37°C. A 100- $\mu$ l volume of 1.1 mg/ml iodoacetic acid in ammonium bicarbonate (pH 7.8) was added and incubated for 30 min at 37°C. To the reduced and alkylated sample, 20  $\mu$ g proteolytic enzyme [TPCK trypsin or endoproteinase Lys C (Promega Chemical, Maddison, WI, USA)] was added in buffer to a final volume of 650  $\mu$ l and a final analyte concentration of 1 nmol/25  $\mu$ l. For modified TPCK trypsin digest, a 50 mM ammonium bicarbonate buffer (pH 7.8) was used. For endoproteinase Lys C digest, a 25 mM Tris, 1 mM EDTA (pH 7.8) buffer was used. For both digests, the samples were incubated at 37°C for 18 h. The digested samples were not further desalted and were stored at <5°C.

### 3. Results and discussion

#### 3.1. TFA Fix

The signal suppressing effects of strong acids such as trifluoroacetic acid have been well docu-

mented and are discussed in the introductory remarks. Fig. 2 shows a comparison of samples run in the FIA mode using 1% acetic acid or 0.2% TFA as a mobile phase. The spectra of the analytes shown in Fig. 2 do not show significant differences between the two acids; this is, however, to be expected since all the analytes, except for gramicidin S and the peptide mixture appear, as singly charged species. The two peptide samples (gramicidin S and the peptide mixture) did not show spectral shifts in the charge states. The chemical equilibria involved in the proposed mechanism are shown in Fig. 3. Equilibrium 1 in the electrospray positive mode generates excess positive charge in the sprayed droplets. If TFA is present in the solvent, the strong acid equilibrium 2 exists. The main ion production mechanism during normal electrospray is shown in equilibrium 3 in which analyte molecules are (multiply-) protonated and can be released into the gas phase by an ion evaporation process. If a weak acid additive, such as propionic acid is also present in solution, the weak acid equilibrium 4 also exists. Equilibrium 5 shows the process primarily responsible for signal suppression by strong acids such as TFA ( $\text{CF}_3\text{COOH}$ ): ion-pair formation between analyte ions formed in equilibrium 3 and TFA

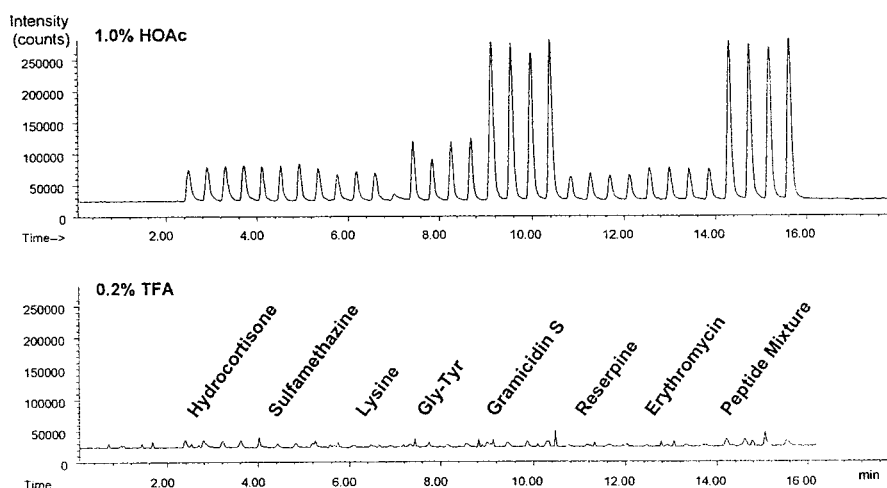


Fig. 2. Signal suppression by TFA containing mobile phases. FIA of probes with 1% acetic acid in 50% acetonitrile (top) or 0.2% TFA in 50% acetonitrile (bottom) at 100  $\mu$ l/min. See Table 1 for analyte characteristics.

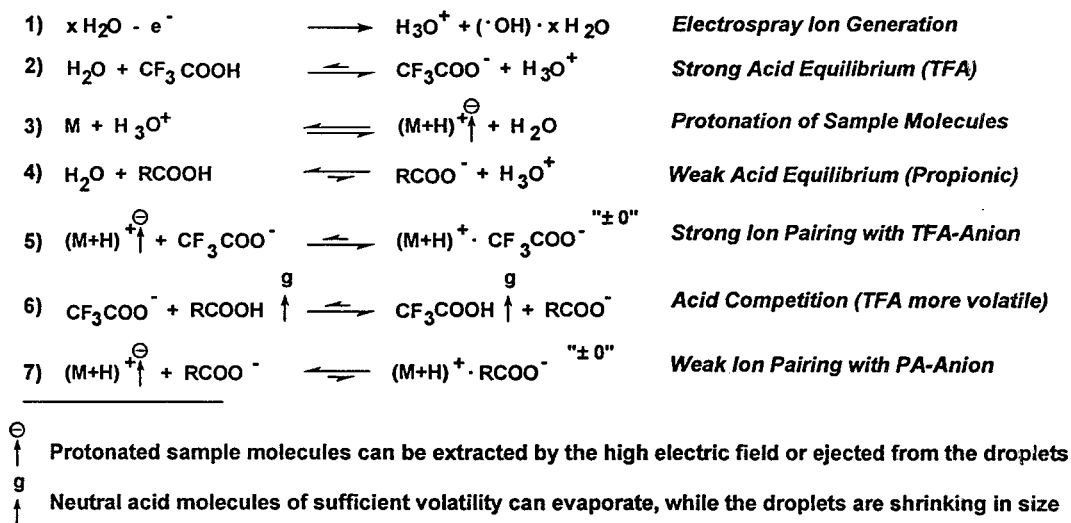


Fig. 3. Proposed mechanism for the TFA signal suppression. See text for discussion.

anions formed in equilibrium 2. Equilibrium 6 shows the basis of TFA Fix; in the presence of high concentrations of a weak acid such as propionic acid (RCOOH), the acid competition between TFA and propionic acid is driven by mass action towards deprotonation of propionic acid. The protonated TFA can be evaporated to some extent from the droplet. Finally, equilibrium 7 shows that the weak ion pairing between the analyte and the weak acid favors the protonated analyte which can be ion evaporated and subsequently focused and mass analyzed.

In optimizing the TFA Fix method, a range of weak organic acids at varying concentrations were evaluated. Fig. 4 shows the effect of adding a series of *n*-alkyl carboxylic acids: formic, acetic, propionic, butyric and valeric acid at concentrations ranging from 0 to 20%. The data shown in this figure represent a plot of the mean effect based on a factorial experiment for a number of FIA probes (see Experimental section) in 0.2% TFA, varying the additive acid and additive concentrations. In a factorial experiment, all combinations of a several variables are evaluated with respect to one or more responses. The effect due to the individual variables can be statistically extracted from this data. Interactions between the variables can also be assessed. For the factorial experiments described in Fig. 4, the

variables were the analyte, organic acid and acid concentrations; the response was the signal intensity. The mean effect shows the statistically calculated effect averaged over different samples caused by a change in acid species and the change in acid concentration. With the exception of formic acid, all these additives gave enhanced performance. The effect increased in the order acetic, propionic and butyric acid and decreased with valeric acid. We speculate that this is due to an optimal volatility. If the acid is too volatile,

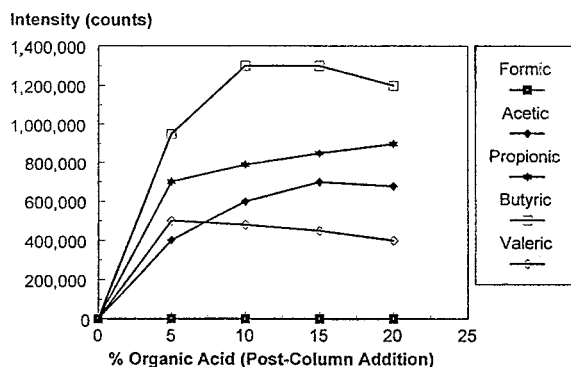


Fig. 4. Effect of different organic acid additives. Signal abundance based on mean main effect for a mixture of peptides (see Table 2). Post-column additive in 2-propanol added at 100  $\mu\text{l}/\text{min}$  for mobile phase flow of 0.2% TFA in 50% acetonitrile at 200  $\mu\text{l}/\text{min}$ .



e.g. acetic acid, the mass action driving the acid equilibrium (in Fig. 3) towards deprotonation of the weak acid will not be as effective and some signal suppression will still occur. On the other hand, if the acid is not volatile enough, as is the case with valeric acid, addition of large amounts of the acid to the droplets prevents rapid desolvation, interfering with the ion evaporation process. For routine work, propionic acid was chosen because the slight performance advantage of butyric acid did not balance its obnoxious odor.

In addition to the weak organic acid, an organic carrier solvent is also added in the TFA Fix method. The role of this solvent is primarily that of a carrier, but the surface tension reducing effects may also play a role in generating a stable enhanced signal. A number of different solvents were evaluated including 2-propanol, acetonitrile, methanol, ethanol, butanol–acetonitrile, 2-methoxyethanol, 2-methoxyethanol–2-propanol and 2-methoxyethanol–butanol. The results are shown in Fig. 5. The data in this plot represent a factorial experiment for a number of FIA probes in 0.2% TFA with varying additives composed of various organic solvents with a constant 15% acetic acid as the weak organic acid additive. In addition, the same samples were run without any additive with and without TFA present. As can be seen from the graph, 2-propanol yielded the best results at approximately 105% of the signal

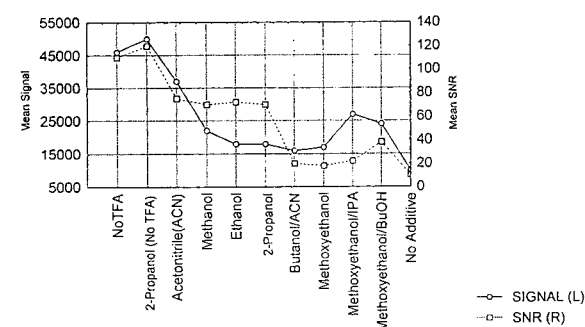


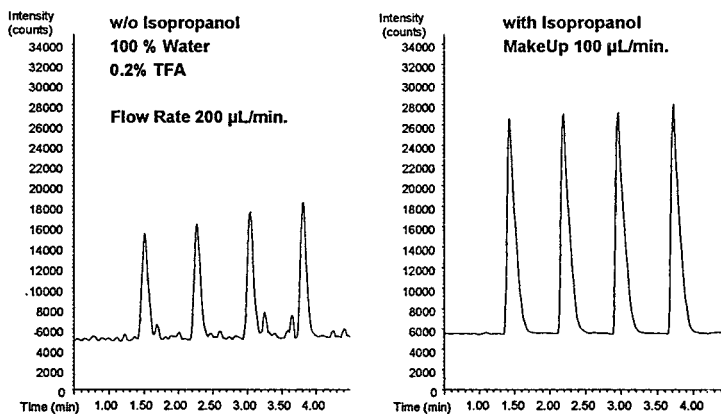
Fig. 5. Effect of organic carrier solvent. Signal abundances and SNRs based on mean main effect for a series of analytes (see Table 1). Post-column additive include 15% acetic acid in organic solvent added at 100  $\mu$ l/min for mobile phase flow of 0.2% TFA in 50% acetonitrile at 200  $\mu$ l/min.

obtained in the absence of TFA. This represents a 10-fold improvement relative to the same samples run in 0.2% TFA in the absence of any additive. With acetonitrile a signal of about 70% is found, with mixtures of 2-methoxyethanol and butanol of ca. 40%, while with 2-methoxyethanol alone a signal of only 20% is found. Experiments were also conducted to evaluate the mutual interaction between organic acid and organic carrier solvent. However, no significant interactions were found. For routine work, 2-propanol was used as the carrier solvent.

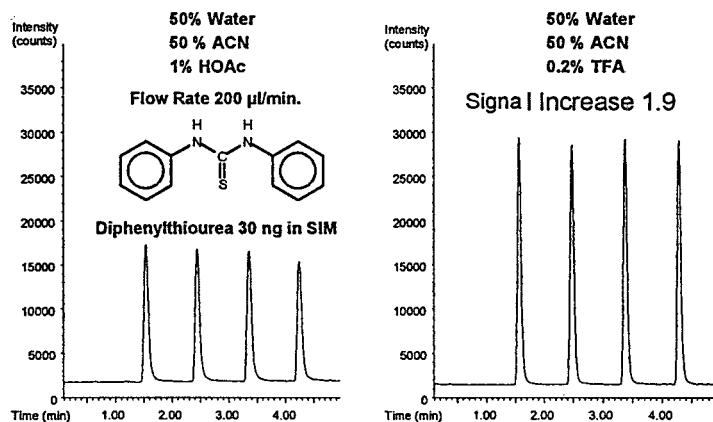
Using an additive of propionic acid–2-propanol, the proportions of the two components and the flow relative to the mobile-phase flow-rate were evaluated. In general, it was found that a maximal signal and signal-to-noise ratio were obtained through post-column addition of a solution of propionic acid–2-propanol (75:25) at a flow-rate approximately half that of the mobile phase.

As mentioned in the introduction, it had been thought previously that the signal suppression was primarily due to conductivity and surface tension effects. If this were the case, then the addition of 2-propanol alone would result in reduction of both the conductivity (by dilution) and the surface tension, and consequently would result in increased performance. However, as can be seen in Fig. 6a, this experiment results in only a 1.8-fold improvement compared to the 30-fold increase in the optimized TFA-Fix experiment (Fig. 6c). The FIA sample shown in Figs. 6a,c consisted of a mixture of ValTyrVal, biotin, reserpine and gramicidin s, each at the concentrations shown in Table 2. Evaluation of the individual extracted ion chromatograms showed improvements similar to those of the total-ion chromatogram of the mixture. The ion-pairing mechanism is further corroborated by the observation that analysis of a weakly basic, “almost neutral” compound such as diphenylthiourea actually shows a 2-fold increase in performance in a 0.2% TFA containing mobile phase relative to a 1% acetic acid containing mobile phase (Fig. 6b). In this case, the strong acid does not ion pair, but does enhance the protonation of the analyte.

### a) Addition of Isopropanol Only



### b) Effect of TFA on Diphenylthiourea



### c) Optimized TFA Fix

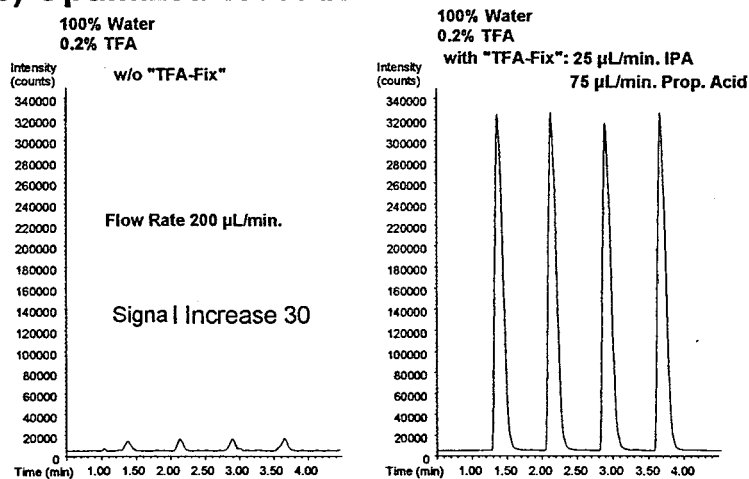


Fig. 6. Mechanism of TFA Fix. See text for discussion.

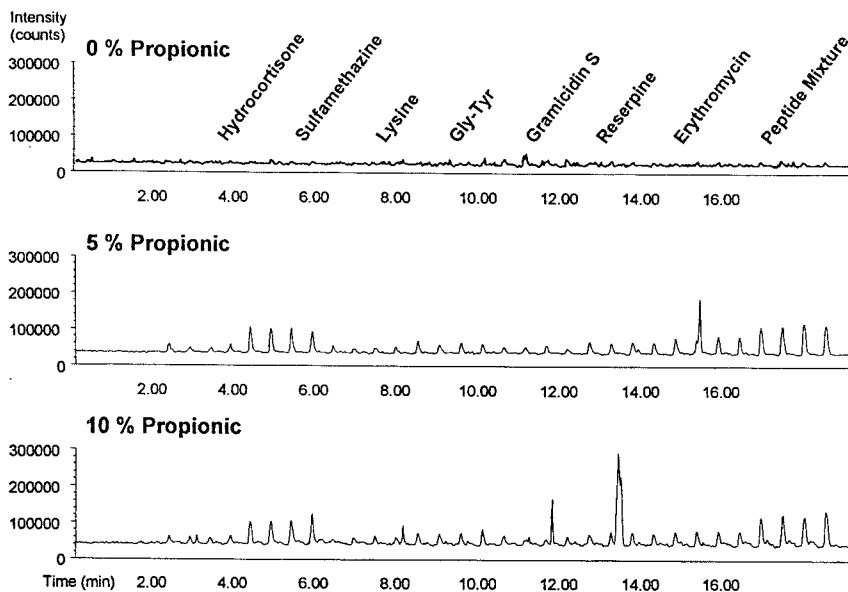


Fig. 7. Effect of TFA Fix on HCl. FIA of probes with 1% HCl in 50% acetonitrile at 100  $\mu\text{l}/\text{min}$ . See Table 1 for analyte characteristics. Post-column additive in 2-propanol added at 100  $\mu\text{l}/\text{min}$  for mobile phase flow of 200  $\mu\text{l}/\text{min}$ .

Although most of the optimization studies and applications presented here were aimed at mobile phases containing trifluoroacetic acid, the

TFA Fix also works for other strong acids that may be used as mobile phase additives. Figs. 7 and 8 show the effect of adding 0, 5 and 10%

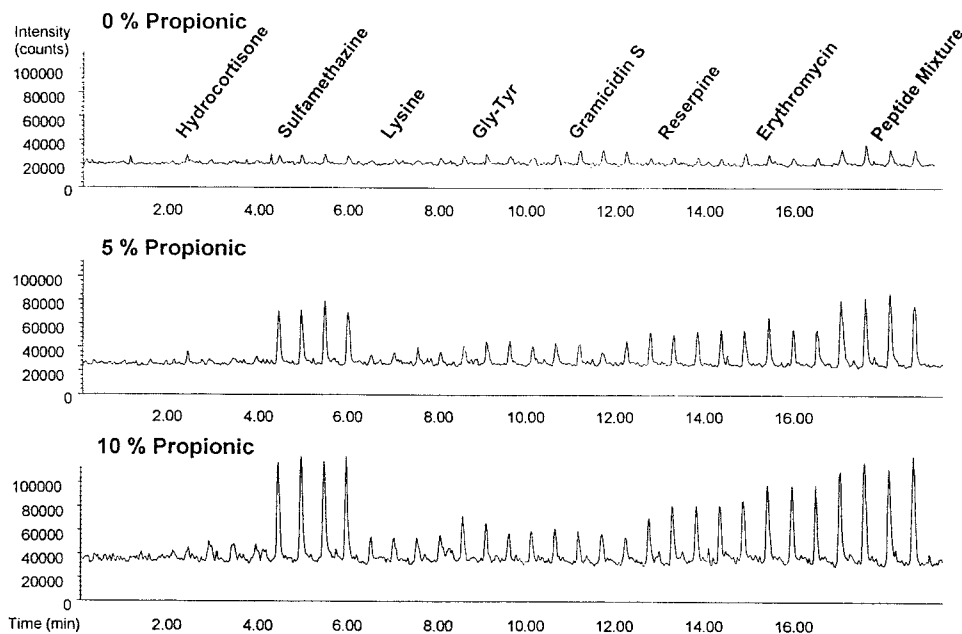


Fig. 8. Effect of TFA Fix on HFBA. FIA of probes with 1% HFBA in 50% acetonitrile at 100  $\mu\text{l}/\text{min}$ . See Table 1 for analyte characteristics. Post-column additive in 2-propanol added at 100  $\mu\text{l}/\text{min}$  for mobile phase flow of 200  $\mu\text{l}/\text{min}$ .

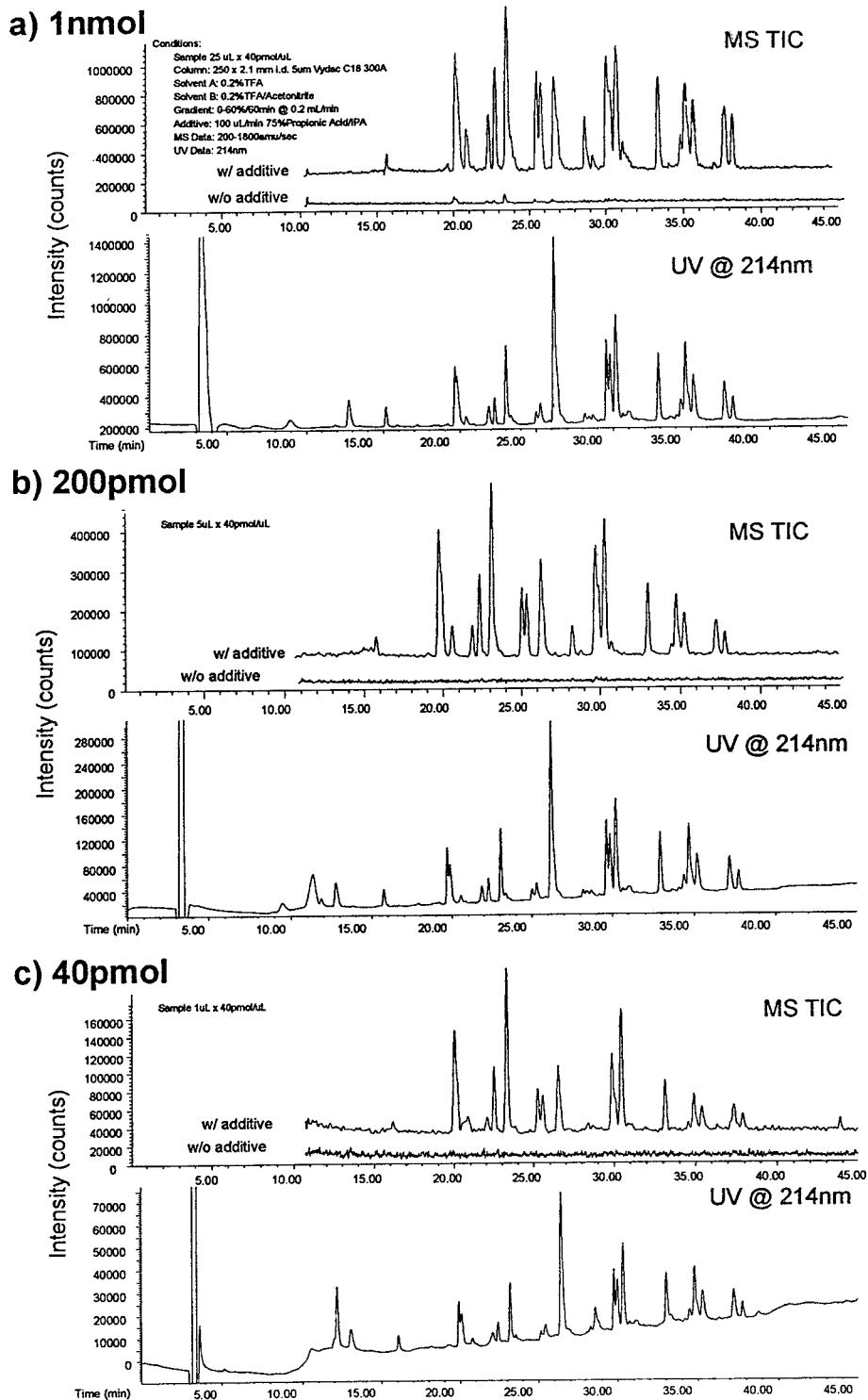


Fig. 9. Peptide maps of tryptic digest of lysozyme.

propionic acid (in 2-propanol) to mobile phases containing HCl and HFBA for a series of FIA probes. The results observed are similar to those obtained in the TFA experiments.

Experiments have shown that TFA Fix works well for peptides and small proteins. However, the effect decreases rapidly as the molecular mass increases: the magnitude of the TFA signal suppression as well as the degree of signal recovery by the TFA Fix is more dependent on the concentration of the sample and the TFA concentration than for smaller molecules such as peptides. For example, for a 1 pmol/ $\mu$ l solution of cytochrome c, infused at 50  $\mu$ l/min, 0.2% TFA will result in a 250-fold decrease in signal intensity relative to the same sample in 1% acetic acid. Adding the TFA Fix results in an approximately 60-fold signal recovery. For larger proteins, it is not possible to break up enough ion pairs with TFA anions to efficiently recover the signal. We speculate that this effect is due to the greater number of protonation sites.

### 3.2. Applications: peptide mapping

As examples of the practical use of the TFA Fix, the following demonstrates a number of peptide mapping applications. For routine operations, the instrumental setup shown in Fig. 1 was used. In this system, the column effluent passes through the diode-array detector and the switching valve before the post-column additive is introduced. This allows UV-Vis signal and spectra to be acquired independent of the spectral characteristics of the additive. The switching valve allows the initial 5 min of the separation to be shunted to waste preventing excess reagent and salts from entering the electrospray chamber. Monitoring the UV signal ensures that no useful peaks are missed during this initial elution period.

Fig. 9 shows the analysis of a tryptic digest of lysozyme. The sample was separated under standard conditions on a 2.1 mm I.D. column at a flow-rate of 200  $\mu$ l/min with a 60-min gradient from 0 to 60% acetonitrile with a constant 0.2% TFA. The amount of total protein was 1 nmol, 200 pmol and 40 pmol in Fig. 9a, b and c,

respectively. At the 1 nmol level, essentially all components that can be seen in the UV (214 nm) signal are present in the MS total-ion chromatogram (TIC). Furthermore, in the absence of the TFA Fix, the signal is markedly reduced, although some peaks can be seen. For the 200 pmol and 40 pmol samples, there are essentially no peaks in the MS TIC trace for the sample run without the TFA Fix, while the sample run with the TFA Fix still shows most peaks seen in the UV signal. At the 40 pmol level, the UV signal shows some increase in baseline which is not present in the MS TIC trace. It should be noted that both solvent A and B in the gradient system contained 0.2% TFA. Carefully balancing the TFA content of the solvents could reduce the increase in baseline in the UV trace.

The sensitivity shown here is not the ultimate that could be obtained. In these experiments, care was taken to use a "standard" HPLC method. Specifically, a 2.1 mm I.D. column was used at conventional flow-rates. It has been shown [18], that electrospray operates as a concentration-, rather than as a mass-sensitive detector. This causes reduction of the HPLC column diameter to result in increased peak concentration for a given amount of sample. In principle, the TFA Fix could be used with miniaturized HPLC systems using 320  $\mu$ m I.D. packed capillaries (or smaller), to take advantage of the concentration sensitivity inherent to all electrospray systems. However, such systems are generally less routinely used and require somewhat more expertise. It should also be noted that the mass spectrometric data acquisition was performed under strict standards. Acquisition rates for all experiments were at least 1 Hz in order to preserve chromatographic resolution. Slower acquisition rates might be used to reduce the noise levels through averaging, but this would result in compromising the chromatographic separation. Additionally, in these experiments, unit resolution was maintained across the mass range of the mass spectrometer. Using lower resolution may result in enhanced sensitivity at the price of spectral resolution. Using a unit resolution is useful in determining charge states of ions in the peptide mass spectra. In

typical digests, common charge states are +5 and less. Unit resolution allows explicit discrimination between singly- and doubly-charged ions. For doubly-charged ions, the isotopic peaks are not completely resolved, but two separate peaks can clearly be seen. For charge states higher than +3, isotopes are generally not resolved, but the unresolved peak width differentiates these ions from singly- and doubly-charged ions.

As a second application, Fig. 10 shows the identification of sites of oxidative modification of glutamine synthetase. Glutamine synthetase is known to undergo oxidative modification *in vivo*, resulting in reduced enzymatic activity [19]. The enzyme can be oxidized in solution using an iron-ascorbate system [20]. Glutamine synthetase is known to have three sites of oxidation. In this applications, endoproteinase Lys C digests of both native and oxidized glutamine synthetase were run under identical conditions. Examination of the MS TIC shows clear differences in the signal at two specific areas. The first, at approxi-

mately 47 min shows a molecular mass of 2770. From the previously determined cDNA-based sequence of glutamine synthetase a Lys C fragment would be predicted with molecular mass of 2784 (L13 + L14). One possible explanation of the 14 Da discrepancy is a DNA point mutation, or more probably, a single point error in the original sequence determination. The fragment at 47 min was collected and sequenced and found to have an Ala instead of a Gly at residue 267. In the oxidized digest, the L13 + L14 fragment disappears and a peak at a slightly later retention time appears with a molecular mass of 2786 Da. The 16 Da difference between the two suggests an oxidation. Collection and sequencing of this fragment in the digest of the oxidized form of glutamine synthetase, the expected His[269] disappeared and a new unidentified peak appeared between Asp and Ser. Subsequent electrospray mass spectral analysis of modified amino acid collected from Edman sequencing indicates a structure consistent with 2-oxo-histidine based

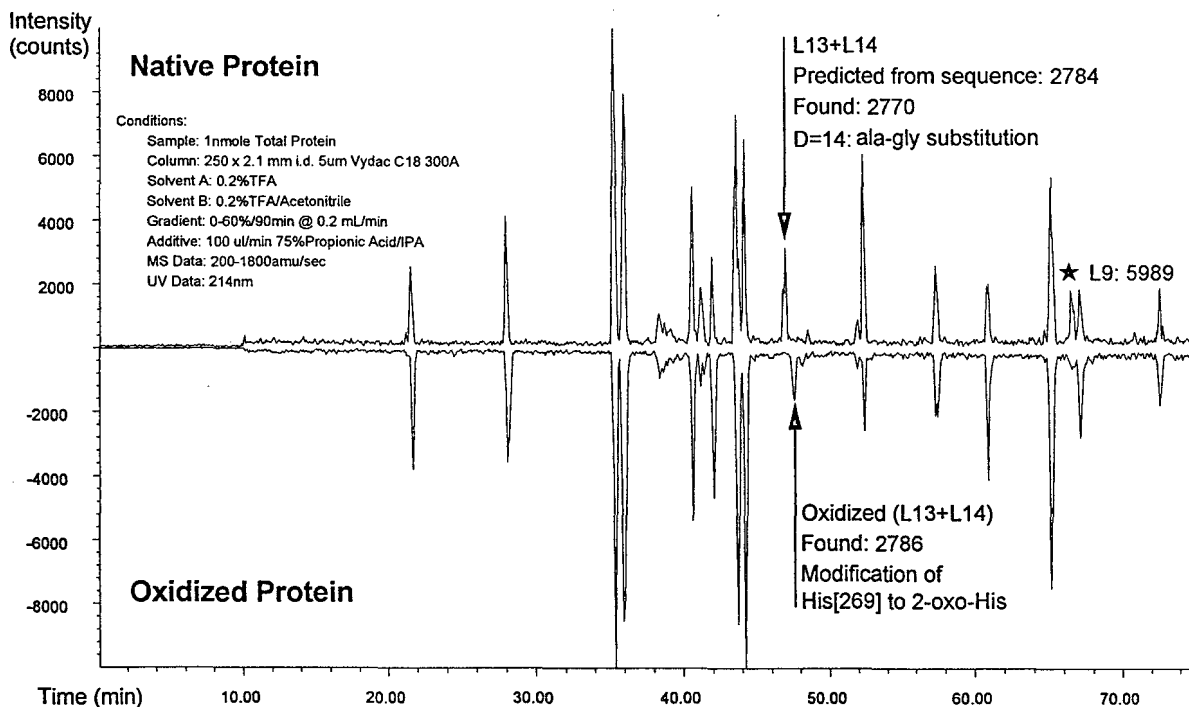


Fig. 10. Identification of oxidative modifications in endoproteinase Lys C digests of glutamine synthetase.

on molecular mass and possible fragmentation.

The second site, at a retention time of 68 min, shows a diminished signal in the oxidized digest, although no corresponding new peak appears. The molecular mass of the component in the native digest is 5989 Da which is consistent with the predicted Lys C digest fragment L9. This fragment, indeed, contains the HHH sequence at residue 177–230 which is also believed to undergo oxidative modification. Similar experiments with trypsin digest (not shown) yielded similar results.

As a final example, the electrospray LC–MS was used with the TFA Fix for the identification of sites of post-translational glycosylation in an endoproteinase Arg C digest of single-chain plasminogen activation factor. In this application, in-source collisionally induced dissociation (CID) was used to generate fragments which can be used as markers for glycosylation. The technique, based on the method described by Carr and co-workers [21,22], tracks glycoforms by looking for fragments characterizing fucose ( $m/z$  147), HexNAc ( $m/z$  204), sialic acid ( $m/z$  292)

and HexNAc + Hex ( $m/z$  366). Fig. 11 shows the results of two separate acquisitions. The top TIC shows a full-scan acquisition with CID energy set relatively low (CapEx voltage, 100 V). Under these conditions, there is very little fragmentation and most digest fragments are detected as singly- or multiply-charged ions with molecular masses corresponding to the nonfragmented peptide. The four lower chromatograms were acquired in a SIM acquisition in which only the ions listed above corresponding to glycosylation markers were recorded. For this acquisition, the set CID potential was higher (CapEx voltage, 200 V) resulting significant structural fragmentation. Although these ion chromatograms could be extracted from full-scan acquisition data, using SIM enhanced the detection limits for the fragmentation. As can be seen from the chromatograms, the glycosylation patterns are relatively complex. Note the relatively broad peaks in the glyco-marker SIM traces compared to the scan TIC. This is due to the microheterogeneity of the glycoforms resulting in broad, un-resolved groups at individually lower levels

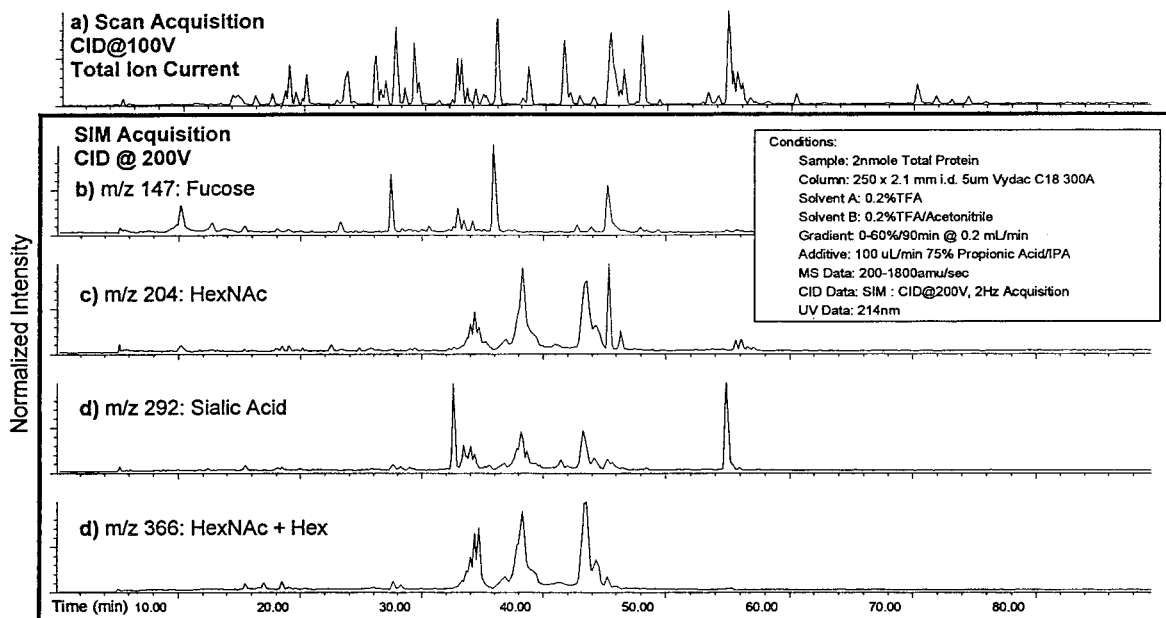


Fig. 11. Detection of glycosylation in endoproteinase Arg C digest of single-chain plasminogen activation factor. (a) Scan acquisition with low CID energy (CapEx, 100 V). (b)–(d) SIM acquisition with high CID energy (CapEx, 200 V).

which are not detected by the scan acquisition. This demonstrates a rapid and easy method to screen samples for glycosylation.

#### 4. Conclusions

In conclusion, the method presented here is able to counteract the signal suppression effects of trifluoroacetic acid containing mobile phases in electrospray LC–MS. The method, termed TFA Fix consists of post-column addition of propionic acid–2-propanol (75:25) at a flow-rate half that of the mobile phase flow-rate. The TFA Fix results in 10–50 fold improvement in signal. The proposed mechanism for both TFA signal suppression and signal recovery by the TFA Fix is based on ion pair formation between analyte and the TFA anion. The TFA Fix acts by competitively interfering with this equilibrium. The method was shown to be useful for a number of different applications of peptide mapping.

#### Acknowledgements

The authors would like to thank the following people and organizations for their help and collaboration: Julie A. Sahakian of Hewlett-Packard Protein Chemistry Systems and Dr. Rodney Levine of the National Heart Lung and Blood Institute of the NIH, for collaboration on the glutamine synthetase application. Dr. Bill Hancock of Hewlett-Packard Laboratories and Carrie Souders and Dr. Erno Pungor, Jr. of Berlex Bioscience for collaboration on the single-chain plasminogen activation factor application. The method described as the TFA Fix is patent pending.

#### References

- [1] J.B. Fenn, M. Mann, C.K. Meng, S.F. Wong and C.M. Whitehouse, *Science*, 246 (1989) 64–71.
- [2] M.H. Allen, J.A.S. Lewis, *Rapid Commun. Mass Spectrom.*, 3 (1989) 255–258.
- [3] G.J. Van Berkel, G.L. Glish and S.A. McLuckey, *Anal. Chem.*, 62 (1990) 1284–1295.
- [4] O.A. Mirgorodskaya, A.A. Shevchenko, I.V. Chernushevich, A.F. Dodonov and A.I. Miroshnikov, *Anal. Chem.*, 66 (1994) 99–107.
- [5] K.D. Henry, E.R. Williams, B.H. Wang, F.W. McLafferty, J. Shabanowitz and D.F. Hunt, *Proc. Natl. Acad. Sci. USA*, 86 (1989) 9075–9078.
- [6] G. Winkler, P. Wolschann, P. Briza, F.X. Heinz and C.J. Kunz, *J. Chromatogr.*, 347 (1985) 83–88.
- [7] S.K. Chowdhury and B.T. Chait, *Anal. Chem.*, 63 (1991) 1660–1664.
- [8] J. Eshraghi and S.K. Chowdhury, *Anal. Chem.*, 65 (1993) 3528–3533.
- [9] R.D. Smith, J.A. Loo, C.G. Edmonds, C.J. Barinaga and H.R. Udseth, *Anal. Chem.*, 62 (1990) 882–899.
- [10] U.A. Mirza and B.T. Chait, *Anal. Chem.*, 66 (1994) 2898–2904.
- [11] S.K. Chowdhury and B.T. Chait, *Anal. Chem.*, 63 (1991) 1660–1664.
- [12] A.P. Bruins, T.R. Covey and J.D. Henion, *Anal. Chem.*, 59 (1987) 2642–2646.
- [13] P.R. Griffin, J.A. Coffman, L.E. Hood and J.R. Yates, *Int. J. Mass Spectrom. Ion Processes*, 111 (1991) 131
- [14] E.C. Huang and J.D. Henion, *Anal. Chem.*, 63 (1991) 732–739.
- [15] J.F. Banks, S. Shen, C.M. Whitehouse and J.B. Fenn, *Anal. Chem.*, 66 (1994) 406–414.
- [16] M.G. Ikononou, A.T. Blades and P. Kebarle, *J. Am. Soc. Mass Spectrom.*, 2 (1991) 497–505.
- [17] G. Neubauer and R.J. Andereg, *Anal. Chem.*, 66 (1994) 1056–1061.
- [18] A.P. Bruins, *Mass Spectrom. Rev.*, 10 (1991) 53–77.
- [19] K. Nakamura and E.R. Stadtman, *Proc. Natl. Acad. Sci. USA*, 81 (1984) 2011–2015.
- [20] R. Levine, *J. Biol. Chem.*, 258 (1983) 11828–11833.
- [21] M.J. Huddleston, M.F. Bean and S.A. Carr, *Anal. Chem.*, 65 (1993) 877–884.
- [22] S.A. Carr, M.J. Huddleston and M.F. Bean, *Prot. Sci.*, 2 (1993) 183–196.





ELSEVIER

Journal of Chromatography A, 712 (1995) 191–199

JOURNAL OF  
CHROMATOGRAPHY A

# Qualitative liquid chromatographic–atmospheric-pressure chemical-ionisation mass spectrometric analysis of polyethylene terephthalate oligomers

Karen A. Barnes, Andrew P. Damant, James R. Startin, Laurence Castle\*

*Ministry of Agriculture Fisheries and Food, CSL Food Science Laboratory, Norwich Research Park, Colney, Norwich NR4 7UQ, UK*

## Abstract

The oligomeric fraction of polyethylene terephthalate (PET) has been studied as it has the potential to migrate to foods and beverages packaged in virgin and recovered PET plastics. We have applied positive ion atmospheric-pressure chemical ionisation (APCI) to extracts of food-grade PET resin and beverage bottles. A reversed-phase HPLC system was connected directly to a VG Platform mass spectrometer. An acetonitrile–water–acetic acid gradient elution was performed. Low APCI probe temperatures (as appropriate for a polyethylene glycol calibrant) produced no significant ions from a PET cyclic trimer standard. A high probe temperature of 500–600°C gave a strong protonated molecular ion.

Characteristic spectra of the cyclic oligomers from the trimer to the heptamer were obtained. A second homologous series of substances 44 mass units higher than each PET oligomer eluted prior to each PET oligomer. The mass spectra indicated these to be oligomers with one monoethylene glycol unit replaced by a diethylene glycol unit. To our knowledge this is the first time that cyclic oligomers above the tetramer have been confirmed by LC–MS. The technique was considerably more sensitive than published thermospray methods and gave good spectra with sub-microgram quantities injected. This work demonstrates the advantages of APCI over thermospray as an MS technique for substances of this type.

## 1. Introduction

The plastic polyethylene terephthalate (PET) is widely used for food packaging. It has excellent heat stability allowing its use in microwave and conventional oven applications as films and containers. It also has good gas barrier properties and is widely used for carbonated drinks bottles. PET is a candidate material for plastics recovery and schemes for chemical and physical recovery along with straightforward re-use (re-

filling) are either in use to a limited extent or are under consideration [1,2].

One factor in assessing the suitability of PET in these applications is the question of chemical migration. PET is relatively free of additives and adventitious low-molecular mass impurities, and so has intrinsic low migration characteristics [3]. It is known to contain small amounts of low-molecular-mass oligomers [4]. APCI is a gas-phase ion-molecule reaction process which leads to the ionisation of analyte molecules under atmospheric pressure conditions. The process is analogous to chemical ionisation but the reactant

\* Corresponding author.

ions are produced from the effect of a corona discharge on a nebulised aerosol of solvent. Due to the atmospheric pressure conditions the high frequency of analyte/reactant ion collisions ensures a high sample ionisation efficiency. A “soft” ionisation results in predominantly protonated molecular ions  $[M + H]^+$  in the positive-ion mode or deprotonated molecular ions  $[M - H]^-$  in the negative-ion mode [5]. The purpose of this work was to develop a sensitive LC-APCI-MS method of analysis for these oligomers so that their chemical migration from virgin and recycled PET could be measured in the future.

## 2. Experimental

### 2.1. Materials

PET bottles (suitable for carbonated soft drinks), bottle pre-forms and PET resin were obtained from manufacturers during April 1994. A standard of PET cyclic trimer was prepared in house [3] and judged to be ca. 90% pure by  $^1\text{H}$  NMR analysis.

### 2.2. Sample preparation

A portion (0.1 g) of polymer was dissolved in a mixture of dichloromethane and hexafluoro-2-propanol (7:3, v/v, 10 ml) and then acetone (8 ml) was added slowly to precipitate the high-molecular-mass polymer. The sample was filtered (pore size 4  $\mu\text{m}$ ), concentrated to almost dryness under a stream of nitrogen, and the residue dissolved in dimethylacetamide (2.0 ml).

### 2.3. Analysis by LC-APCI-MS

Liquid chromatography-atmospheric-pressure chemical-ionisation mass spectrometry (LC-APCI-MS) analysis was performed using a Lichrosorb RP8 (100  $\times$  3 mm I.D.) column (Chrompack, Millharbour, UK) fitted with a 0.5- $\mu\text{m}$  pre-column filter. The mobile phase was an acetonitrile-water-acetic acid linear gradient: solvent A, 15:85:0.25; solvent B, 85:15:0.25 (v/v). At time 0, 8, 16, 17, 30, 31 min the

percentage solvent B was 4.3, 50, 60, 85, 85, 4.3, respectively.

The mobile phase was delivered at 0.6 ml/min by a Spectra-Physics SP8800-020 tertiary pump (San-Jose, CA, USA). Injections (50  $\mu\text{l}$ ) were made using a Gilson 231XL autosampler (Villiers-le-Bel, France) fitted with a 200  $\mu\text{l}$  Rheodyne loop. A Spectroflow 757 UV detector set at 254 nm (Kratos, Manchester, UK) was connected in series between the HPLC system and the mass spectrometer. The time axis of the UV analog trace was adjusted to allow for the delay between the two detectors in series.

The VG Platform “Classic” benchtop mass spectrometer (Fisons Instruments, Manchester, UK) was operated in the positive-ion atmospheric-pressure chemical-ionisation mode. The instrument was initially tuned on the mobile phase background ions. Tuning was then optimised on a PET cyclic trimer standard (2 mg/ml in acetonitrile) injected directly via a 500  $\mu\text{l}$  Rheodyne loop. Typical tuning parameters were as follows: corona 3.22 kV, high voltage lens 0 kV, extraction 20 V, focus 25 V, source temperature 120°C, APCI probe temperature 600°C, low mass resolution 14.3, high mass resolution 14.9, ion energy 0.9 V, ion energy ramp 0 and multiplier 650. The instrument was calibrated over a mass range 50–1800 using a mixture of polyethylene glycol (PEG) 300, 600, 1000 and 1540, at a scan time of 5 s.

## 3. Results

### 3.1. Optimisation of LC-APCI-MS conditions

Initial calibration and tuning of the VG Platform was carried out at low APCI probe temperatures most suited to the PEG calibrant. At these low temperatures, flow injection of the PET trimer standard produced no significant ions and this prevented optimisation of the instrument. A change of mobile phase to methanol gave a sufficiently strong protonated molecular ion for tuning purposes, as a result of which it was discovered that a probe temperature in the range 500–600°C gave maximum sensitivity. A

temperature at the high end of this range i.e. at 600°C was selected. A return to the original mobile phase (acetonitrile–water–acetic acid) also gave a strong protonated molecular ion at this high probe temperature. The temperature profile for the PET trimer is shown in Fig. 1.

### 3.2. Chromatograms

Figs. 2 and 3 show the UV and total-ion chromatogram (TIC) obtained for a PET extract. The UV trace showed the characteristic profile reported earlier [6,7] for the cyclic trimer followed by decreasing amounts of the tetramer through to the octamer. Comparison of Figs. 2 and 3 show the TIC trace to be considerably inferior to the detection by UV. In contrast, Fig. 4 shows the reconstructed ion chromatograms for the protonated molecular ions of the PET cyclic trimer, tetramer, pentamer, hexamer and heptamer where the oligomers can be clearly observed. It was noted that each cyclic oligomer was preceded by a second, smaller peak giving rise to a second series of oligomers of 44 mass units higher than the first. This series is also shown in Fig. 4. Diode-array analysis showed that all the peaks had a very similar absorption

spectrum indicating a common chromophore (data not shown).

### 3.3. Mass Spectra

Spectra for the PET cyclic trimer through to the heptamer are shown in Fig. 5. Spectra for the corresponding LC peaks for the second oligomer series are shown in Fig. 6. Fig. 5 shows clearly the expected series of cyclic PET oligomers and Fig. 6 shows the homologous series at 44 mass units higher. Ions at  $m/z$  193 and 385 can be seen in many of the spectra and these are attributed to the protonated PET base unit (the  $n = 1$  “monomer”) and dimer, respectively.

## 4. Discussion

### 4.1. PET cyclic oligomer series

As a polyester of terephthalic acid (TPA) and monoethylene glycol (MEG), the main oligomer fraction extracted from food grade PET is expected to be the series  $[TPA]_m[MEG]_n$ . The cyclic oligomers (where  $m = n$ ) predominate [7]. There are two commercially important routes to

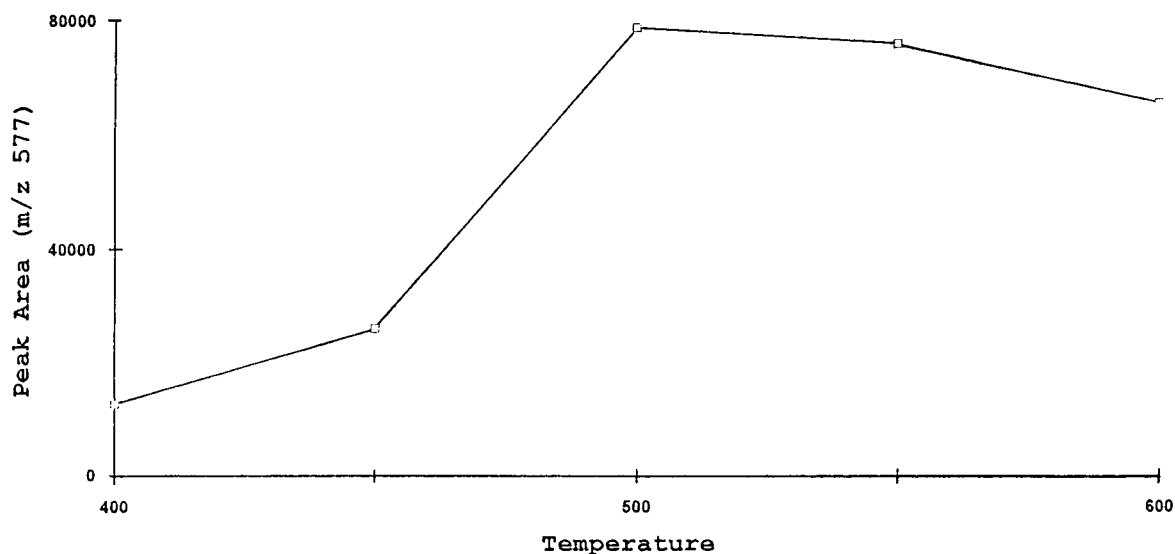


Fig. 1. Effect of APCI probe temperature on ion sensitivity;  $x$ -axis: probe temperature (°C),  $y$ -axis: peak area for  $m/z$  577 for constant mass of PET cyclic trimer flow injected.

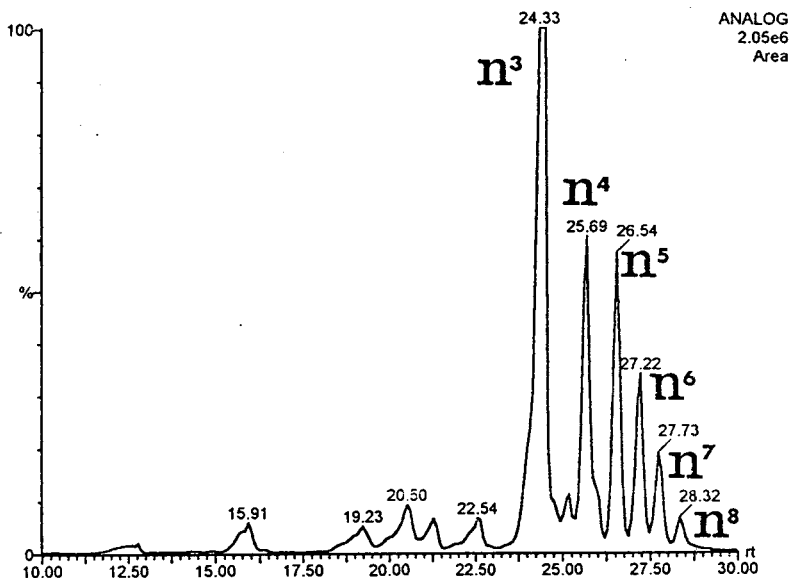


Fig. 2. LC-UV trace for PET extract; x-axis: retention time (min); y-axis; UV response at 254 nm. Peak assignment cyclic PET oligomers:  $n^3$  = trimer,  $n^4$  = tetramer,  $n^5$  = pentamer,  $n^6$  = hexamer,  $n^7$  = heptamer,  $n^8$  = octamer.

PET [1]. One involves the direct esterification of terephthalic acid with ethylene glycol to form a mixture comprising largely of the intermediate monomer bis(2-hydroxyethyl) terephthalate (BHET) and its linear oligomers. The alternative

route starts at dimethyl terephthalate and uses transesterification with MEG to form BHET. Both routes then form PET by prepolymerisation and polycondensation of the BHET reaction mass.

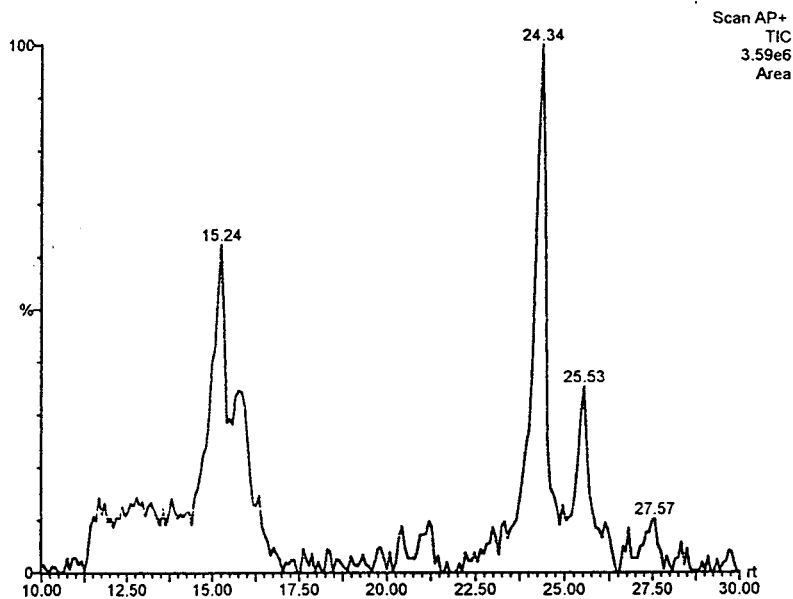


Fig. 3. LC-APCI-MS TIC chromatogram for PET extract; x-axis: retention time (min); y-axis: total ion current (normalised).

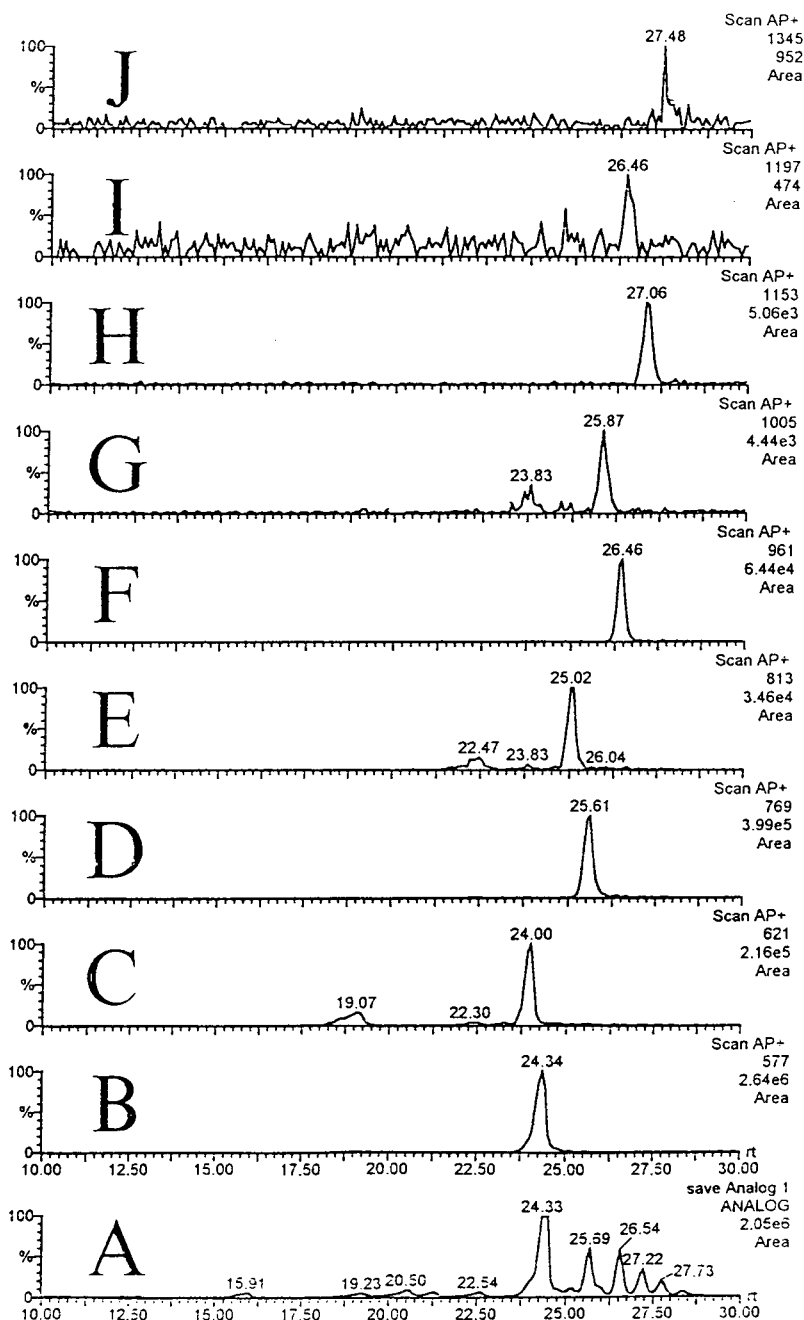


Fig. 4. LC-APCI-MS SIM traces for PET extract; x-axis: retention time (min); y-axis: selected ion intensity (reconstructed and normalised). (A) Analog trace at 254 nm, (B) cyclic trimer at  $m/z$  577, (C) DEG-trimer at 621, (D) tetramer at 769, (E) DEG-tetramer at 813, (F) pentamer at 961, (G) DEG-pentamer at 1005, (H) hexamer at 1153, (I) DEG-hexamer at 1197, (J) heptamer at 1345 (for formula see Table 1).

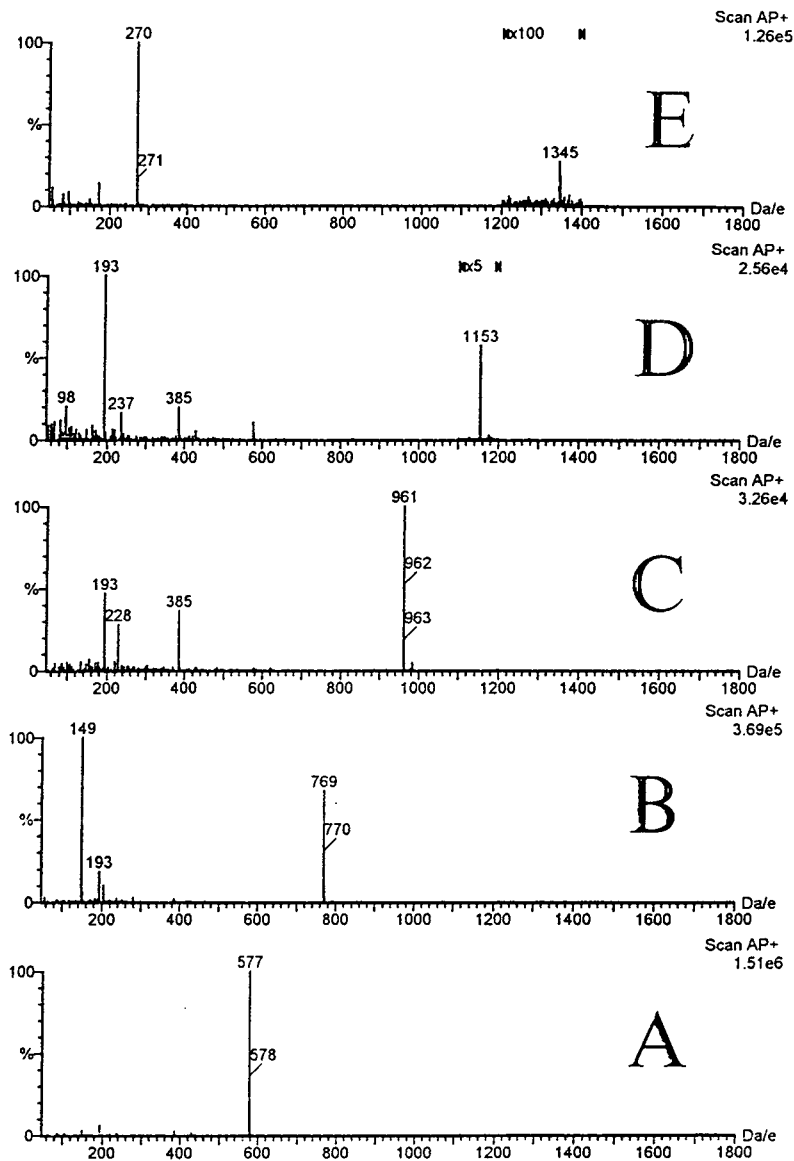


Fig. 5. LC-APCI-MS spectra for cyclic PET oligomers;  $x$ -axis:  $m/z$  ratio;  $y$ -axis: ion intensity (normalised, note that magnification has been used at the top end of the spectra for the weaker, high-molecular-mass, substances). (A) Trimer, (B) tetramer, (C) pentamer, (D) hexamer, (E) heptamer.

In the solid state polycondensation process, PET is heated above its glass transition temperature but below its crystalline melting point, in an inert atmosphere or in vacuo to increase the molecular mass of the polymer [8]. This process does not remove entirely the low-molecular-mass oligomers, however, since the molecular mass

distribution for condensation polymers is characterised by the most probable distribution. The equilibrium distribution is reached by ester interchange reactions which can be quite rapid in the melt, with equilibrium reached within 10 min [9]. Thus, there is always a fraction of low-molecular-mass oligomers present.

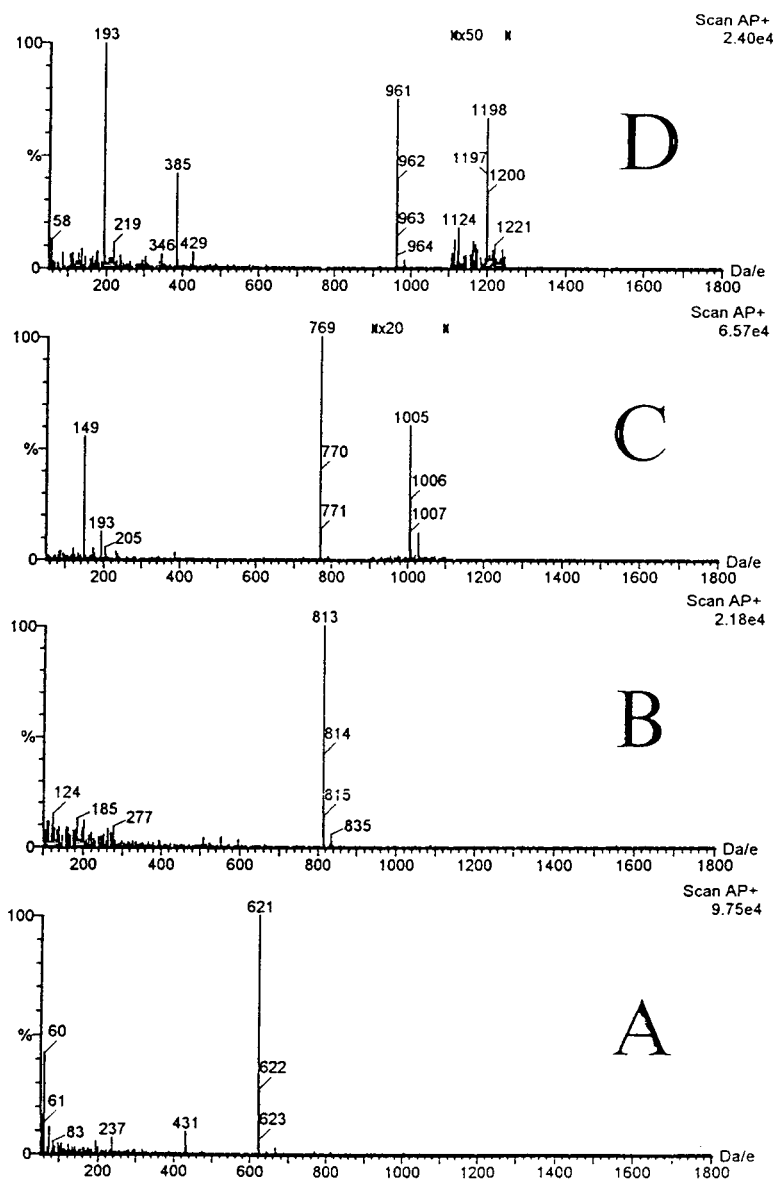


Fig. 6. LC-APCI-MS spectra for cyclic DEG-PET oligomers; x-axis:  $m/z$  ratio; y-axis: ion intensity (normalised, magnification used, see legend Fig. 5). (A) Trimer, (B) tetramer, (C) pentamer, (D) hexamer.

The MS results agree with the expectations above and confirmed that the main extractable fraction from PET comprised the cyclic oligomers. LC-APCI-MS analysis resulted in tentative molecular masses for the peaks present in Fig. 4 and these masses along with the oligomer formulae are given in Table 1. Characteristic

spectra of the cyclic oligomers from the trimer to the heptamer were obtained (Fig. 5).

#### 4.2. Identity of the second oligomer series

A second homologous series of substances 44 mass units higher than each PET oligomer was

Table 1  
PET cyclic oligomer series

Oligomer	Formula (+H <sup>+</sup> )	Protonated molecular mass
<i>PET oligomers</i>		
[TPA] <sub>3</sub> [MEG] <sub>3</sub>	C <sub>30</sub> H <sub>25</sub> O <sub>12</sub>	577.13
[TPA] <sub>4</sub> [MEG] <sub>4</sub>	C <sub>40</sub> H <sub>33</sub> O <sub>16</sub>	769.17
[TPA] <sub>5</sub> [MEG] <sub>5</sub>	C <sub>50</sub> H <sub>41</sub> O <sub>20</sub>	961.21
[TPA] <sub>6</sub> [MEG] <sub>6</sub>	C <sub>60</sub> H <sub>49</sub> O <sub>24</sub>	1153.25
[TPA] <sub>7</sub> [MEG] <sub>7</sub>	C <sub>70</sub> H <sub>57</sub> O <sub>28</sub>	1345.30
<i>Second oligomer series with one DEG in place of MEG</i>		
[TPA] <sub>3</sub> [MEG] <sub>2</sub> [DEG] <sub>1</sub>	C <sub>32</sub> H <sub>29</sub> O <sub>13</sub>	621.12
[TPA] <sub>4</sub> [MEG] <sub>3</sub> [DEG] <sub>1</sub>	C <sub>42</sub> H <sub>37</sub> O <sub>17</sub>	813.23
[TPA] <sub>5</sub> [MEG] <sub>4</sub> [DEG] <sub>1</sub>	C <sub>52</sub> H <sub>45</sub> O <sub>21</sub>	1005.24
[TPA] <sub>6</sub> [MEG] <sub>5</sub> [DEG] <sub>1</sub>	C <sub>62</sub> H <sub>53</sub> O <sub>25</sub>	1197.23

observed eluting prior to each oligomer. It is postulated (Table 1) that these are substances similar to the oligomers but with one MEG unit replaced by a diethylene glycol (DEG) unit. These results confirm those reported in the literature [7,10] where the secondary series of peaks was suspected of being cyclic oligomer ethers. The high temperature and acid conditions of PET polymerisation can cause the formation of traces of diethylene glycol from MEG – a process of etherification with elimination of water from two MEG molecules [8]. As a diol, DEG is capable of participating in the polymerisation process and so is incorporated into oligomer and polymer chains. The formation of DEG is closely controlled since it can have adverse effects on the chemical stability and physical properties of the polymer [8]. A typical DEG content would be quite low at 1–2% by mass of polymer [1] and this is the reason why the second oligomer series (with DEG incorporated) is relatively minor. Statistically, the likelihood of replacing 2 MEG units with DEG is very small and the failure to detect a third oligomer series is not unexpected.

#### 4.3. Advantages of LC-APCI-MS

There are very few published papers dealing with LC-MS analysis of PET oligomers and reaction by-products. Milon [10] extracted the PET film from a microwave susceptor and ana-

lysed the extract by plasmaspray LC-MS in the negative-ion mode using acetonitrile with formic acid as the mobile phase. Milon observed that an unusually high probe tip temperature of 370°C was required and could only confirm the cyclic trimer and tetramer. The tetramer gave a poor peak shape and low ion abundance. There was a severe loss of sensitivity at the lower tip temperature of 290°C and the cyclic tetramer was then not observed. In the TIC mode the LC-MS procedure [10] was at least 10-times less sensitive than LC-UV and this agrees with the findings here.

More recently, Guarini et al. [11] examined depolymerisation reaction mixtures obtained by the glycolysis of PET, again using negative-ion thermospray. With acetonitrile and ammonium acetate as mobile phase, they observed negative-ion mass spectra with ions from both electron attachment and acetate attachment. The sensitivity was not changed on varying the source temperature between 150 and 200°C – although higher temperatures led to reduced sensitivity. The authors reported that the TIC was noisy due to high intensity background ions and sensitivity was poorer than with the UV detector. In the SIM mode, sensitivity was comparable with that of the UV detector. Mass spectra of oligomers larger than the linear TPA<sub>2</sub>MEG<sub>2</sub>DEG<sub>1</sub> were too weak for unambiguous interpretation. Sensitivity was improved by the reaction of terminal hydroxyl groups with perfluoroanhydrides and



oligomers up to the linear tetramer were observed for derivatised samples with good full-scan spectra obtained for 50  $\mu\text{g}$  of glycolysis mixture injected.

In comparison, the work reported here observed cyclic PET oligomers up to the heptamer plus a minor series of related cyclic oligomers. To the authors knowledge, this is the first time that PET oligomers above the cyclic tetramer have been confirmed by positive-ion LC-MS. On the question of sensitivity, the SIM chromatograms and spectra shown in Figs. 4 and 5 correspond to 25  $\mu\text{g}$  (trimer) down to 0.6  $\mu\text{g}$  (heptamer) injected. The advantages of LC-APCI-MS as an MS techniques over thermospray are therefore clearly demonstrated.

## References

- [1] R.E. Richard, W.H. Boon, M.L. Martin-Shultz and E.A. Sisson, in G.D. Andrews and P.M. Subramanian (Editors), *Emerging Technologies in Plastics Recycling*, (ACS Symp. Ser. No. 513), American Chemical Society, Washington, DC, 1992, pp. 196–204.
- [2] L. Castle, *Packaging Tech. Sci.*, 7 (1994) 291.
- [3] L. Castle, A. Mayo, C. Crews and J. Gilbert, *J. Food Protect.*, 52 (1989) 337.
- [4] P.A. Tice, *Food Addit. Contam.*, 5 (1988) 373.
- [5] S. Bajic, D.R. Doerge, S. Lowes and S. Preece, *Am. Lab.*, (1993) 40B.
- [6] T.H. Begley and H.C. Hollifield, *J. Assoc. Off. Anal. Chem.*, 72 (1989) 468.
- [7] W.R. Hudgins, K. Theurer and T. Mariani, *J. Appl. Polym. Sci.: Appl. Polym. Symp.*, 34 (1978) 145.
- [8] K. Ravindranath and R.A. Mashelkar, in A. Whelan and J.L. Craft (Editors), *Developments in Plastics Technology*, Vol. 2, Elsevier Applied Science (Developments Series), London and New York, 1985, pp. 1–42.
- [9] K. Ravindranath and R.A. Mashelkar, *Polym. Eng. Sci.*, 24 (1984) 30.
- [10] H. Milon, *J. Chromatogr.*, 554 (1991) 305.
- [11] A. Guarini, G. Gianfranco and R. Po, *J. Chromatogr.*, 647 (1993) 311.



# Development of an instrumental configuration for pseudo-electrochromatography–electrospray mass spectrometry

Silvio E.G. Dekkers, Ubbo R. Tjaden\*, Jan van der Greef

*Division of Analytical Chemistry, Leiden/Amsterdam Center for Drug Research, Leiden University, P.O. Box 9502, 2300 RA Leiden, Netherlands*

---

## Abstract

The development of an instrumental configuration for the application of the electric field in pseudo-electrochromatography is described. To increase detection sensitivity and selectivity, special attention has been paid to the hyphenation of PEC with electrospray ionization mass spectrometry. Problems encountered in previous instrumental configurations like formation of gas bubbles have been overcome by using liquid junctions to apply the electric field over the column. Some sulfonamides and a nonapeptide have been used as test compounds to compare pseudo-electrochromatography with micro-liquid chromatography. The characteristic features of pseudo-electrochromatography on retention behaviour and separation efficiency are demonstrated.

---

## 1. Introduction

The coupling of separation methods based on electromigration principles, like e.g. capillary zone electrophoresis (CZE) with electrospray ionization mass spectrometry (ESI-MS) is mostly concerned with the transfer of ions in solution to ions in the gas phase [1]. Because of its high efficiency, CZE is favoured for the analysis of complex mixtures. The combination of CZE with ESI-MS increases the selectivity and expands the application range of CZE. The increasing use of CZE–ESI-MS for the analysis of drugs [2], biochemicals [3] and biomacromolecular compounds (peptides, proteins and nucleotides) [4–7] might argue for this powerful combination. However, although the high efficiencies obtained

in CZE result in high mass fluxes, the mass flows are still limited and, therefore, the sample-concentration detection limits are disappointing. This is caused by the small dimensions in CZE in conjunction with the low flow-rate induced by the voltage applied. ESI-MS is characterized as a mass-flow sensitive detection system functioning according to concentration-sensitive principles [8]. Combination of CZE with sample-concentration techniques or enhancement of loadability is necessary for the hyphenation of CZE with mass-spectrometric detection to reach its full potential.

Micro-packed bed liquid chromatography ( $\mu$ LC) can serve as an example of a micro-separation method which has acceptable loadabilities despite its small dimensions when compared with CZE and open-tubular LC. It has been demonstrated that a decrease of column

---

\* Corresponding author.

diameter leads to increased mass sensitivity in sample-limited situations [9]. Although the loadability of  $\mu$ LC is higher when compared with CZE the separation efficiency of  $\mu$ LC expressed as a function of the theoretical plate number is almost two orders of magnitude lower than of CZE. Another limitation with regard to the use of  $\mu$ LC is that in the separation of complex mixtures, gradient elution conditions or the use of ion-pairing or ion-exchanging agents in the mobile phase are often needed to deliver acceptable analysis times and good resolutions. Such conditions are not always compatible with good mass-spectrometric performance. A technique which is a good compromise between the high separation efficiency of CZE and the high loadability of  $\mu$ LC is pseudo-electrochromatography (PEC). The strategy behind the development of PEC in our group was to increase selectivity without impairing possible hyphenation with mass-spectrometric detection techniques as has been demonstrated by Verheij et al. [10] and Hugener et al. [11]. The pressure-assisted variant of electrochromatography, which has been described by Tsuda [12,13], has been developed to suppress bubble formation in electrochromatography (EC) [14–16]. In EC the transport of the mobile phase in packed capillaries is induced by the same principles as known from CZE. An electroosmotic flow is generated by the application of a voltage over the column. Similar to CZE, in EC the possibility of reversal of the voltage polarity is limited by the electroosmotic flow in combination with the electrophoretic behaviour of the compounds of interest. Due to the corresponding reversal of the direction of the electroosmotic flow, electroneutral and positively charged compounds will not migrate in the direction of the column outlet in that case. Although the use of surface-modifying additives in the mobile phase like fluorinated hydrocarbons [17] enables to manipulate the direction of the electroosmotic flow, this leads to a decrease of electrospray ionization efficiency and contamination of the ion source.

However, by superimposing the electroosmotic flow on a pressure-induced hydrodynamic flow, the choice of applied voltage and its polari-

ty is completely free. Moreover, there are no constraints upon the pH used. This approach results in a stable flow that is only limited by the back pressure of the column. This intrinsic packed-bed property does not limit the flow generated by a voltage applied along the column. The voltage applied introduces a plug-like flow profile that is superimposed on the parabolic hydrodynamic flow profile. Through the implementation of a plug flow in a hydrodynamic flow the efficiency can be increased. As a result, a decrease of analysis time while maintaining good separation performance for electroneutral compounds can be obtained.

The aim of this study was the development of a trouble-free instrumental setup enabling to examine PEC and to couple this separation technique to ESI-MS. The described configuration has been used to evaluate the characteristic advantages of PEC in comparison with  $\mu$ LC using sulfonamides and a synthetic peptide as test compounds. Examples are given to demonstrate the potential of PEC in reducing the analysis time, increasing the selectivity and improving the efficiency.

## 2. Experimental

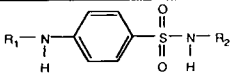
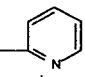
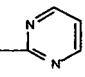
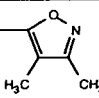
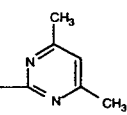
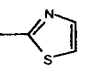
### 2.1. Materials

Analytical grade methanol, acetonitrile, acetic acid (HAc) and a solution of 25% ammonia (Baker, Deventer, Netherlands) were used. Water was purified with a Milli-Q apparatus (Millipore, Bedford, MA, USA). Trifluoroacetic acid (TFA) was purchased from Merck (Darmstadt, Germany). The sulfonamides (Table 1) came from Sigma (St. Louis, MO, USA). The nonapeptide was synthesized at the Biochemical Department of the University Hospital Leiden.

### 2.2. Equipment

In Fig. 1 the instrumental setup used for the PEC–UV and PEC–ESI-MS experiments is outlined. A micro-gradient pump (Brownlee Labs, Santa Clara, CA, USA) operating in the con-

Table 1  
Molecular structures of some sulfonamides

		
	R <sub>1</sub> —	—R <sub>2</sub>
sulfanilamide	H—	—H
sulfadiazine	H—	—CO—CH(CH <sub>3</sub> ) <sub>2</sub>
sulfapyridine	H—	
sulfadiazine	H—	
sulfafurazol	H—	
sulfadimidine	H—	
succinylsulfathiazol	$\begin{matrix} \text{H}_2\text{C}-\text{CO}- \\   \\ \text{H}_2\text{C}-\text{COOH} \end{matrix}$	

stant-pressure mode was used for solvent delivery. The pump was connected to a Valco C14W internal volume (60/150 nl) micro-injector (Valco Instruments, Houston, TX, USA) by a PEEK capillary (400 mm × 308 μm I.D.) to protect the pump for electrical damage. The micro-injector was kept at ground potential to enable safe injections. The column used was a fused-silica capillary of 250 mm × 220 μm I.D., slurry packed with Nucleosil 100-5C8 (Macherey-Nagel, Düren, Germany). At both sides some packing material was removed with a micro-drill and glass-wool plugs were inserted serving as frits.

A 100 mm × 75 μm I.D. × 170 μm O.D. fused-silica capillary was used as transfer line between the injector and the column. The transfer capillary was inserted into the column and gently pressed against the glass-wool plug, thus minimizing extra-column band broadening (see Fig. 1). These connections were placed in high-pressure buffer vials containing platinum electrodes which were connected to a high-voltage power supply (CZE 1000R, Spellman, USA). The detection capillary was installed in the same way. Between the inner column wall and the external wall of the transfer and detection capil-

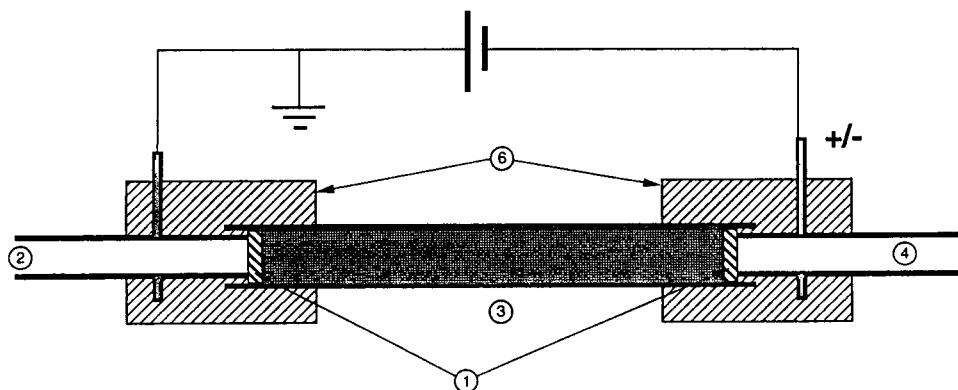


Fig. 1. Schematic diagram of the electrical contact between the power supply and the column with the use of liquid junctions and high-pressure buffer vials. (1) Glass-wool frit, (2) inlet capillary, (3) capillary column, (4) outlet capillary, (6) high-pressure buffer vial.

lary there existed an angular space of 25  $\mu\text{m}$  width in which the buffer penetrates. In this way the electrical contact between the platinum electrodes and the column has been realized.

### 2.3. UV absorbance detection

An LKB 2151 (Bromma, Sweden) variable-wavelength detector set at 254 nm was used to monitor the column effluent. The detector cell was created by burning off the polyimide coating of the fused-silica capillary over a length of 5 mm. The detector cell was placed in a custom-made detector cell housing. The distance from the column end to the detector was 125 mm.

### 2.4. Electrospray mass spectrometric detection

Mass-spectrometric detection was performed using an SSQ 710 single-quadrupole instrument (Finnigan MAT, San José, CA, USA). Scanning was performed in the multiple-ion detection mode. Coupling with PEC was done using the Whitehouse–Fenn-type electrospray interface (Finnigan MAT). The detection capillary was inserted in the stainless-steel electrospray needle. The polyimide coating at the end of the fused-silica capillary was burned off over a length of 10 mm and polished to provide a stable spray. The sheath liquid consisted of a mixture of methanol and 0.5 M acetic acid (95:5, v/v) and provided the electrical contact between the fused-silica capillary and the stainless-steel electrospray needle, which was connected to ground. The sheath liquid was delivered at a flow-rate of 0.75  $\mu\text{l}/\text{min}$  by a syringe pump (Harvard Apparatus, Edinbridge, UK). A nitrogen flow kept at 150°C was used as drying gas.

### 2.5. Packing procedure of the micro-columns

Columns were packed with an air-actuated pump (DSHF-302, Haskel, Burbank, CA, USA). Fused-silica capillary (220  $\mu\text{m}$  I.D.  $\times$  350  $\mu\text{m}$  O.D.) (SGE, Melbourne, Australia) was cut to the desired length. The end of the capillary was inserted into a piece of PEEK tubing (25 mm  $\times$  400  $\mu\text{m}$  I.D.), which was tightened in a

zero dead volume nut. A metal frit was used to prevent the packing material from leaving the column during the packing procedure. The other end of the column was connected to a custom-made slurry reservoir of 1.5 ml that was magnetically stirred. The slurry was prepared by dispersing 40 mg packing material in 5 ml acetonitrile. After the slurry was homogenized in an ultrasonic bath for 5 min, 1.5 ml was transferred into the mixing chamber, after which the column was connected with the outlet pointing upwards. After activating the stirrer the pressure was slowly increased to fill up the column with acetonitrile. After five minutes the column was turned upside down and the pressure was rapidly increased to 600 bar. It took about two minutes to reach the set pressure. Pressure was maintained for one hour, after which it was slowly released, over a period of almost one hour. Before use the columns were flushed with water followed by the buffer solution used in the described experiments.

## 3. Results and discussion

### 3.1. Optimization of the instrumental setup

The first experimental configuration used for the PEC experiments was a modified version of the setup as described by Verheij et al. [10]. The micro-injector and the zero dead nuts were used as electrodes to apply the potential over the column. This did not result in a sufficiently stable system, the major problem being the generation of gasses due to electrolysis at the injector, the zero dead nuts and the metal frits. To circumvent the problems induced by the production of gasses, the electrical field was disconnected from the injector by use of a palladium decoupler while the zero dead nut was made from palladium. The high diffusion coefficient for molecular hydrogen in palladium enables the transport of any produced hydrogen from within the system to the ambient air, as has been successfully applied in CZE by Kok [18,19]. However, in our hands the use of such a decoupler did not lead to a significant improvement with regard to the

elimination of gas bubbles, probably due to the limited hydrogen-capture capacity of the Pd decoupler. For this reason, it was decided to investigate the potential of liquid junctions for the application of the electric field over the column. The open contact between the electrodes and the packing material in the column generates in fact an electrical split, and therefore a loss of analyte may occur. Nevertheless, with the configuration described here, a stable flow without disturbing gas bubbles could be realized.

### 3.2. Coupling to MS

Sulfonamides are ionizable compounds, which offers the possibility to apply a separation technique using the electrophoretic characteristics of these compounds in conjunction with the hydrophobic characteristics of this class of compounds. The analysis of sulfonamides using mass-spectrometric detection has been described by various authors who were using different separation techniques, such as CZE [20], SFC [21] and LC [20,22–24]. Because of their wide-spread use these compounds are often found in food products, like meat, milk and fish. The analysis technique of choice must be able to cope with the different sample matrices and to deal with

the specific impurities. The majority of the papers dealing with the analysis of sulfonamides with LC–MS describes the use of a mobile-phase gradient to obtain acceptable analysis times and resolution [21–24]. The generation of reproducible gradient systems appeared to be problematic in case of miniaturized systems. Therefore, no comparison between PEC and gradient elution in  $\mu$ LC could be made. Besides, from our experience it was known that a mobile-phase gradient influences the electrospray process, and as a consequence the ionization efficiencies are affected. PEC offers the possibility to manipulate the separation process, to improve the selectivity and to speed up the analysis without modifying the composition of the mobile phase. In Fig. 2 it is demonstrated that with PEC it is possible to speed up the analysis without any loss in resolution. Fig. 2a shows a reversed-phase  $\mu$ LC–UV trace of three sulfonamides. Sulfafurazol and sulfadiazamide are retained twice as long as sulfanilamide. The long residence times of sulfafurazol and sulfadiazamide in the column lead to unacceptable band broadening. Manipulation of the voltage in PEC resulted in acceptable analysis times while a good resolution was maintained, as demonstrated in Fig. 2b. An additional but not less important effect of speed-

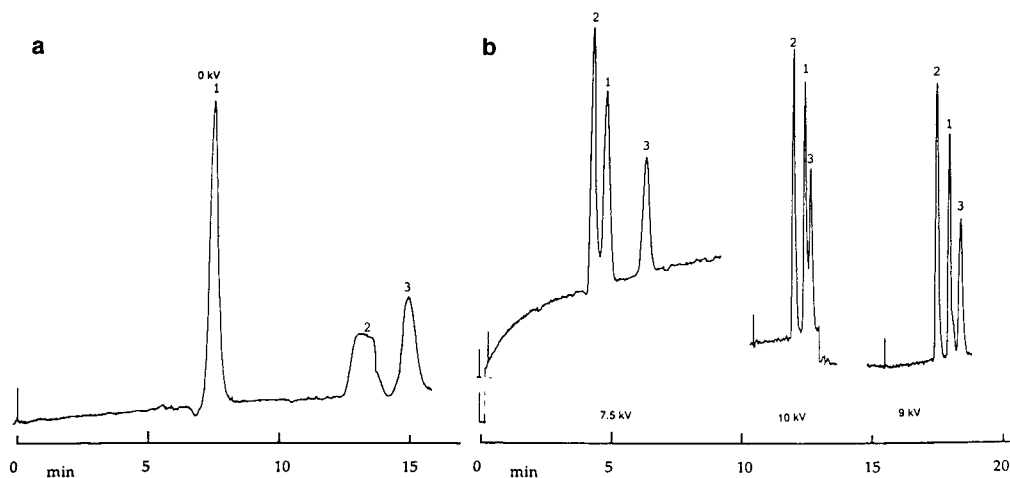


Fig. 2. Chromatograms showing the improvement of peak shapes after applying different voltages in the PEC mode: (a) without and (b) with the application of a voltage. Peaks: 1 = sulfanilamide, 2 = sulfafurazol, 3 = sulfadiazamide. Conditions: mobile phase 4 mM ammonium acetate–methanol pH 5 (60:40, v/v) (adjusted with trifluoroacetic acid), column length 23.5 cm, flow-rate 1  $\mu$ l/min, pressure drop 50 bar, UV-absorbance detection at a wavelength of 254 nm.

ing up the analysis is that the mass flow of the analytes is increased, resulting in lower concentration-detection limits. The different voltages applied over the column were set at their value just prior to injection and switched off when the analysis was done. In this way reproducible runs could be performed. Nevertheless, it has been observed that with longer analysis times some time might be needed before reproducible retention times are obtained. This effect has also been described in the literature [11,25]. Still, PEC appeared to be a good alternative for gradient elution in reducing the analysis times, particularly when mass-spectrometric detection is involved.

In Fig. 3 the coupling of PEC to the mass spectrometer is demonstrated. In the described configuration, there exists a voltage drop over the transfer capillary from the column to the mass spectrometer. This voltage drop is of the same magnitude as that applied over the column and opposite relative to the mass spectrometer. The voltage over the transfer capillary induces a local electroosmotic flow that can be ten times higher than in the packed bed of the column [26]. As a consequence, the mobile phase is more or less dragged out from the packed bed, thus reducing the back pressure of the column. Operating the pump in the constant-flow mode increased the baseline noise under these conditions, for which reason the constant-pressure mode was preferred. As a result the hydrodynamic contribution to the total flow through the column has been increased. The reduction of the analysis time is thus an indirect effect of the voltage applied and is not due to the electrophoresis of the sulfonamides that electromigrate in opposite direction. This electrophoretic behaviour in the detection capillary is not of major concern for the separation process, which can be seen by considering the elution order of the compounds. Although its charge is less positive, the acidic succinylsulfathiazol elutes in front of sulfanilamide and sulfathiazole when the voltage is applied. When the migration order would be determined by the voltage drop existing in the detection capillary, this cannot be the case. This demonstrates that the selectivity in PEC can be

tuned using both the hydrophobic and electrophoretic properties of the compounds to manipulate the separation process.

As mentioned above, not only increased loadability and tunable selectivity belong to the features of PEC, but also the improvement of the separation efficiency [15]. Because an electroosmotic flow is most effectively generated at higher pH values, an alkaline mobile phase is chosen to demonstrate this effect in PEC. Combination of both flow profiles decreases the contribution of convective mixing effects, resulting in less band broadening in comparison with the normal  $\mu$ LC mode. The plate height to velocity curve is shifted to higher velocities and presumably has a larger optimum value [26]. In the example shown in Fig. 4, a nonapeptide with a negative charge of minus three at pH 8 has been used. Because of its high charge the electrophoretic velocity of the nonapeptide almost counterbalances the electroosmotic flow. Therefore, the change in retention is minimal, implying that the increase of the plate number by a factor of two in PEC is mainly caused by the effect of the electroosmotic flow on the flow profile. Unfortunately, a substantial electrical split takes place at the liquid junction on the injection side of the column caused by the high electrophoretic mobility of the nonapeptide. As a consequence, the increase of efficiency as demonstrated in Fig. 4 did not lead to improved detection limits. In a closed separation system without liquid junctions, no electrical split will take place, and the gain in efficiency will also result in an improved concentration sensitivity.

#### 4. Conclusions

PEC appears to be an interesting alternative for isocratic as well as gradient  $\mu$ LC, especially when mass-spectrometric detection is involved. In contrast with LC gradient elution, no compatibility problems with respect to the performance of the electrospray ionization process have been observed. The use of a configuration with liquid junctions in PEC–UV allows to study the net effects of the application of an electric field



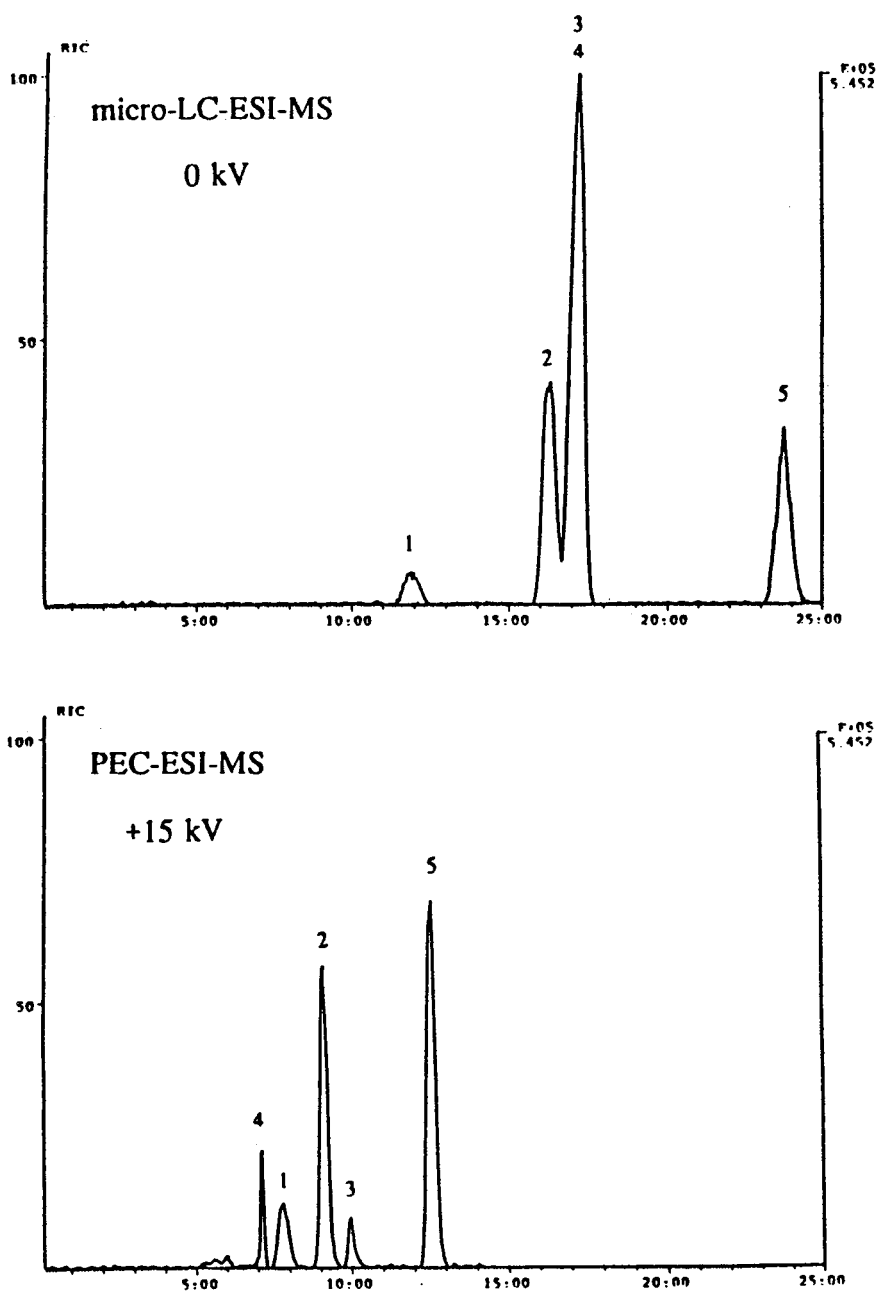


Fig. 3. Comparison of  $\mu$ LC with PEC applying mass spectrometric detection. Conditions: column length 21 cm, all other conditions as described in Fig. 2. Peaks: 1 = sulfanilamide, 2 = sulfathiazol, 3 = sulfapyridine, 4 = succinylsulfathiazol, 5 = sulfadimidine.

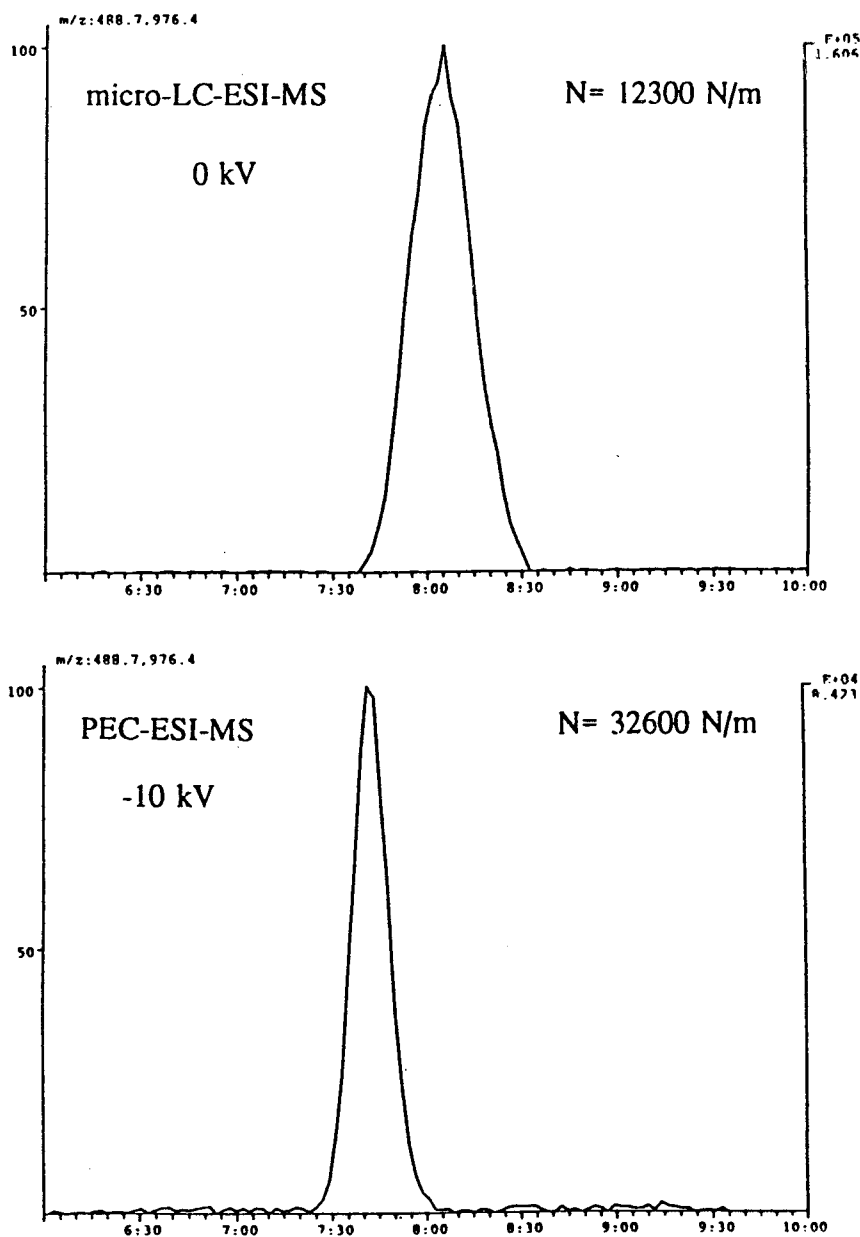


Fig. 4. Effect of the application of a negative voltage of  $-10$  kV over the column in the PEC-ESI-MS mode (lower trace) in comparison with  $\mu$ LC-ESI-MS (upper trace). Conditions: pH 8 (adjusted with ammonium hydroxide), all other conditions as described in Fig. 3.

on the retention behaviour. Our findings indicate that decoupling of the electric circuit used for PEC is not necessary to obtain a stable electro-spray. This offers the possibility to insert the

column outlet directly into the atmospheric-pressure ionization source as described by Hunt et al. [27], thereby minimizing extra-column band broadening introduced by connection devices

and possible electrical split at the liquid junctions. A closed configuration for PEC is currently under investigation.

## References

- [1] P. Kebarle and L. Tang, *Anal. Chem.*, 65 (1993) 972.
- [2] I.M. Johansson, R. Pavelka and J.D. Henion, *J. Chromatogr.*, 559 (1991) 515.
- [3] J.W. Jorgenson and K.D. Lukacs, *Anal. Chem.*, 53 (1981) 1298.
- [4] R.D. Smith, J.A. Olivares, N.T. Nguyen and H.R. Udseth, *Anal. Chem.*, 60 (1988) 436.
- [5] J. Loo, H.R. Udseth and R. Smith, *Anal. Biochem.*, 179 (1989) 404.
- [6] E.D. Lee, W. Murck, J. Henion and T. Covey, *Biomed. Environ. Mass Spectrom.*, 18 (1989) 844.
- [7] L.J. Deterding, C.E. Parker, J.P. Perkins, M.A. Moseley and J.W. Jorgenson, *J. Chromatogr.*, 554 (1991) 329.
- [8] A.P. Bruins, *Mass Spectrom. Rev.*, 10 (1991) 53.
- [9] P. Kucera, *J. Chromatogr.*, 198 (1980) 93.
- [10] E.R. Verheij, U.R. Tjaden, W.M.A. Niessen and J. van der Greef, *J. Chromatogr.*, 554 (1991) 339.
- [11] M. Hugener, A.P. Tinke, W.M.A. Niessen, U.R. Tjaden and J. van der Greef, *J. Chromatogr.*, 647 (1993) 375.
- [12] T. Tsuda, *Anal. Chem.*, 59 (1987) 521.
- [13] T. Tsuda, *Anal. Chem.*, 60 (1988) 1677.
- [14] J.W. Jorgenson and K.D. Lukacs, *J. Chromatogr.*, 218 (1981) 209.
- [15] J.H. Knox and I.H. Grant, *Chromatographia*, 24 (1987) 135.
- [16] S. Otsuka and L. Litowski, *Anal. Biochem.*, 102 (1980) 419.
- [17] A. Emmer, M. Jansson and J. Roeraade, *J. Chromatogr.*, 547 (1991) 554.
- [18] W.Th. Kok, *Anal. Chem.*, 65 (1993) 1853.
- [19] W.Th. Kok, *Anal. Chem.*, 65 (1993) 2497.
- [20] J.R. Perkins, C.E. Parker and K.B. Tomer, *J. Am. Soc. Mass Spectrom.*, 3 (1992) 139.
- [21] J.R. Perkins, D.E. Games, J.R. Startin and J. Gilbert, *J. Chromatogr.*, 540 (1991) 239.
- [22] S. Pleasance, P. Blay, M.A. Quilliam and G. O'Hara, *J. Chromatogr.*, 558 (1991) 155.
- [23] J. Abián, M.I. Churchwell and W.A. Korfmacher, *J. Chromatogr.*, 629 (1993) 267.
- [24] J.D. Henion, B.A. Thomson and D.H. Dawson, *Anal. Chem.*, 54 (1982) 451.
- [25] T. Tsuda, *Anal. Chem.*, 60 (1988) 1677.
- [26] T. Tsuda, K. Nomura and G. Nakagawa, *J. Chromatogr.*, 248 (1982) 241.
- [27] D.F. Hunt, R.A. Henderson, J. Shabonowitz, K. Sakaguchi, H. Michel, N. Seveliz, A.L. Cox, E. Apella and V.H. Engelhard, *Science*, 255 (1992) 1261.



## Performance of an electrospray-interfaced thermospray ion source in hyphenated techniques

R.A.M. van der Hoeven, B.A.P. Buscher, U.R. Tjaden\*, J. van der Greef

*Division of Analytical Chemistry, Leiden/Amsterdam Center for Drug Research, Leiden University, P.O. Box 9502, 2300 RA Leiden, Netherlands*

---

### Abstract

The performance of a custom-made electrospray interface coupled with a thermospray ion source is described, using tetraalkylammonium salts and lysozyme as test compounds. Optimal conditions are created by using a heated sampling capillary, increasing the pumping capacity in the ion source and by changing the shape of the repeller to conical. Under these conditions the performance of the interface, with respect to sensitivity, is comparable with previously described systems using low flow-rates. However, due to the use of a heated sampling capillary flow-rates up to 100  $\mu\text{l}/\text{min}$  can be used. Examples of coupling electrospray with capillary electrophoresis and micro-LC in negative ionization mode are given. As test compounds inositol phosphates and acyl-coenzyme A compounds are used.

---

### 1. Introduction

Since 1984, when electrospray ionization (ESI) in combination with mass spectrometry was first reported by Yamashita and Fenn [1] and Aleksandrov et al. [2] simultaneously, ESI has become a powerful tool in detecting intact multiple protonated molecules up to  $M_r$  60 000 by the use of constant infusion of protein containing solutions. Using low flow-rates makes it interesting to couple ESI with capillary electrophoresis (CE) [3] and micro-LC [4]. The compounds of interest vary from small ionic species, like human growth hormones, to polypeptides and proteins. Interfacing in hyphenated

techniques has resulted in the development of various types of ESI interfaces. The ideal system should cover the sensitivity, efficiency, stability and applicability of all different systems. Unfortunately, such a device does not exist. In the first generation ESI interfaces, like the Whitehouse–Fenn type [5], the flow-rate is limited to a few microlitres per minute with a rapid decrease in signal when increasing the flow-rate. Working in negative ionization mode is difficult, due to corona discharge. The use of chlorinated solvent [6] or oxygen as a bath gas [7] can partly overcome this problem, giving a more stable signal. Working at higher flow-rates, especially using aqueous solvents, limits the use of both microbore and conventional LC coupled with ESI. Part of this problem can be solved by working with a nebulizing gas, forming a so-

---

\* Corresponding author.

called ionspray [8], or when using aqueous solvents to suppress the corona discharge with sulphur hexafluoride [9]. A bad response at higher flow-rates can be attributed to insufficient drying of the formed electrospray, due to the increasing droplet size, as described by Vestal [10]. Actually, there are two ways to solve this problem: (1) increasing the drying capacity by heating the spray with a heated sheath gas [11] and (2) using a heated sampling capillary, as shown by Chowdhury et al. [12]. Nowadays, ESI interfaces are commercially available which more or less overcome the flow-rate problem.

As the ESI source may be a simple metal capillary at elevated voltage relative to a counter electrode, we investigated the possibilities of coupling such a device to a TSP ion source which acts as an intermediate pressure region. A closely related approach was recently described by Jackett and Moini [13], using a flanged ESI adapter mounted to the TSP ion source, in-line with the quadrupole axis.

We describe the use of the original configuration of the TSP ion source, replacing the TSP vaporizer probe by a flanged heated stainless-steel capillary, which fits in the ion source, implying that the heated capillary is mounted at a 90° angle with respect to the quadrupole axis. A low positive or negative voltage at the repeller, depending on the ionization mode, pushes ions into the mass spectrometer. In the configuration tested, the shape of the repeller has been changed to conical, to obtain better sensitivity in the higher mass range. The use of a heated capillary makes it possible to achieve a good performance in positive as well as in negative ionization mode, even at flow-rates of 100  $\mu\text{l}/\text{min}$ . Although this is a simple and inexpensive ESI interface, sensitivities are comparable to other ESI interfaces.

Examples of both high- and low-molecular-mass compounds at high and low flow-rates are shown. The coupling is illustrated with both CE and micro-LC. For this purpose, examples are chosen which include chemically and thermally unstable compounds, such as inositol phosphates in CE-MS mode and some acyl-coenzyme A

compounds using micro-LC, both examples in negative ionization mode.

## 2. Experimental

### 2.1. Interface

All experiments were performed on a Finnigan MAT (San Jose, CA, USA) TSQ-70. The custom-made electrospray interface fits in the thermospray ion source as is shown in Fig. 1.

Depending on the ionization mode, the ESI needle assembly is kept at either  $-3$  or  $+3$  kV towards the heated sampling capillary, which is kept at earth potential. The TSP ion source is also kept at earth potential. The heated capillary consists of a 1/16 in. O.D., 0.5 mm I.D. stainless-steel capillary with a length of 0.09 m, which fits in the ion source by means of a Vespel connector. The sampling capillary together with the heater unit is connected with a nut to a flange and is made as a removable probe. The capillary can be heated up to 300°C. The working temperatures of the heated capillary and the ion source during the experiments were 175 and 150°C, respectively. The best operation was performed by using a conical-shaped repeller and by replacing the original rotary pump (UNO 16, 16 m<sup>3</sup>/h, Balzers, Asslar, Germany) by a pump

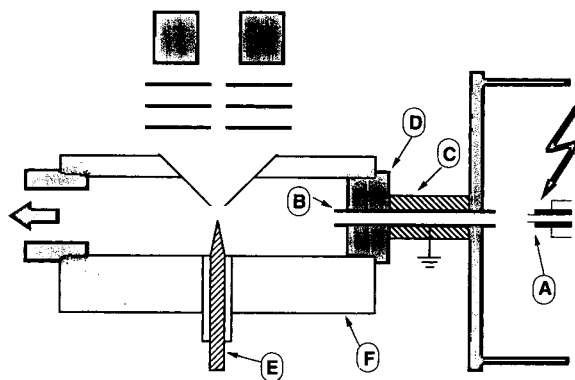


Fig. 1. Schematic diagram of the custom-made electrospray interface: (A) electrospray needle assembly, (B) sampling capillary, (C) heater assembly, (D) vespel connector, (E) conical-shaped repeller, (F) thermospray ion source block.

with higher capacity (E2M28, 28 m<sup>3</sup>/h, Edwards, UK).

## 2.2. Characterization

For the characterization of the custom-made ESI interface in the low mass range a mixture of tetraalkylammonium salts was used, while in the high mass range lysozyme was applied. All chemicals were dissolved in a mixture of methanol and water containing 1% acetic acid (80:20, v/v).

To characterize the use of higher flow-rates, tetraalkylammonium salts were used, with and without the use of nitrogen as a nebulizing gas.

In the constant-infusion mode experiments were performed with a syringe pump (Harvard Apparatus, South Natick, MA, USA). Flow injection experiments (FIA), using tetraoctylammonium bromide (TOA) ( $M_r$  466.4) as test compound, were done at a flow-rate of 1  $\mu$ l/min using a Phoenix 20 CU syringe pump (Carlo Erba, Rodano, Italy) in combination with a Valco CI4W micro-injector with an injection volume of 60 nl (Valco Instruments, Houston, TX, USA). Methanol–water (80:20, v/v) containing 1% acetic acid was used as a liquid sheath flow during all experiments to serve as an electrical contact.

## 2.3. Micro-LC–MS

For the coupling of micro-LC with MS (for the determination of acyl-coenzyme A compounds), a Phoenix 20 CU syringe pump was used to deliver the solvent. A C<sub>8</sub> slurry-packed fused-silica column, 100 mm  $\times$  220  $\mu$ m I.D., was directly connected to a Valco CI4W micro-injector with an injection volume of 60 nl. To eliminate dead volumes, a 170  $\mu$ m O.D., 75  $\mu$ m I.D. fused-silica capillary was inserted in the column towards the glass-wool frit. The 170  $\mu$ m O.D. fused-silica fits in the needle assembly. The mobile phase consisted of a mixture of acetonitrile–0.05 M ammonium/water (10:90, v/v), at a flow-rate of 2  $\mu$ l/min in combination with a sheath flow, delivered by a syringe pump,

of 2  $\mu$ l/min of acetonitrile–0.05 M ammonium acetate/water (90:10, v/v).

## 2.4. CE–MS

For the coupling of CE to MS, the fused-silica capillary, O.D. 170  $\mu$ m, I.D. 100  $\mu$ m and  $l$  = 0.85 m, was inserted into the stainless-steel needle assembly in such a way that the tip of the fused-silica slightly sticks out of the stainless-steel needle. For the best performance the polyimide coating has been removed from the tip of the fused-silica protruding from the needle assembly.

A programmable injector (Prince, Lauerlabs, Emmen, Netherlands) was used to control the injection and the high voltage. The working voltage was –28 kV towards the needle assembly at –3 kV. To eliminate the electroosmotic flow (EOF), the fused-silica was coated with polyacrylamide [10], and also pressure of 10 mbar was applied. As CE buffer a mixture of methanol and ammonium acetate in water (10 mM, pH 5.0) (10:90, v/v) was used. The sheath flow had the same ionic strength and was composed of methanol and ammonium acetate in water (100 mM, pH 5.0) (90:10, v/v) delivered by a syringe pump with a flow-rate of 2  $\mu$ l/min.

## 2.5. Chemicals

Methanol, acetonitrile and acetic acid (Baker, Deventer, Netherlands) were of HPLC grade. Water was purified with a Milli-Q apparatus (Millipore, Bedford, MA, USA). Ammonium acetate was purchased from Merck (Darmstadt, Germany). Tetraalkylammonium (TAA) salts were obtained from Aldrich (Steinheim, Germany). Coenzyme A derivatives and lysozyme came from Sigma (St. Louis, USA) and inositol phosphates from Perstorp (Perstorp, Sweden).

## 3. Results and discussion

The aim of this study was to develop an ESI interface that could compete with commercially available ESI interfaces regarding sensitivity and

costs, and that should cover a wide range of applicable flow-rates. The basis of our design was a thermospray (TSP) ion source. In fact, the original TSP probe has been replaced by a flange with a sampling capillary with 500  $\mu\text{m}$  I.D., separating the ambient-pressure region from the low-pressure region. The ions are extracted out of the ion source at a 90° angle with respect to the quadrupole axis. Changing from TSP to ESI takes less than one hour.

As a starting point an unchanged TSP ion source, in combination with the original 16  $\text{m}^3/\text{h}$  rotary pump, was chosen. Replacement with a rotary pump with higher capacity (28  $\text{m}^3/\text{h}$ ) resulted in an improved performance, which was tested with TAA salts. The increased pumping speed had little influence on the optimum repeller voltage, but ion intensity increased due to reduced ion-source pressure, and consequently resulted in a reduced energy distribution of the expanded ions out of the sampling capillary. The

shape of the repeller did not affect sensitivity for TAA ions. However, in the high mass range using lysozyme as a test compound, far better results could be achieved with a conical-shaped repeller instead of a flat one. A five-fold increase in sensitivity was reached. The conical shape results in a totally different field in the expanded jet, capable of extracting higher-mass molecules more efficiently. In Fig. 2 the mass spectrum of 1 pmol lysozyme consumed, infused at 1  $\mu\text{l}/\text{min}$ , is shown. The molecular mass determined after deconvolution was  $14\,303 \pm 3$ , which is in close agreement with the theoretical value.

The satellite peaks can be identified as phosphate or sulfate clusters, which has been described earlier by Chowdhury et al. [15]. With this setup, the limit of detection for lysozyme could be estimated as 100 fmol consumed. This is in agreement with the sensitivity obtained with the Whitehouse–Fenn interface [5], which has been in use for a few years in our laboratory.

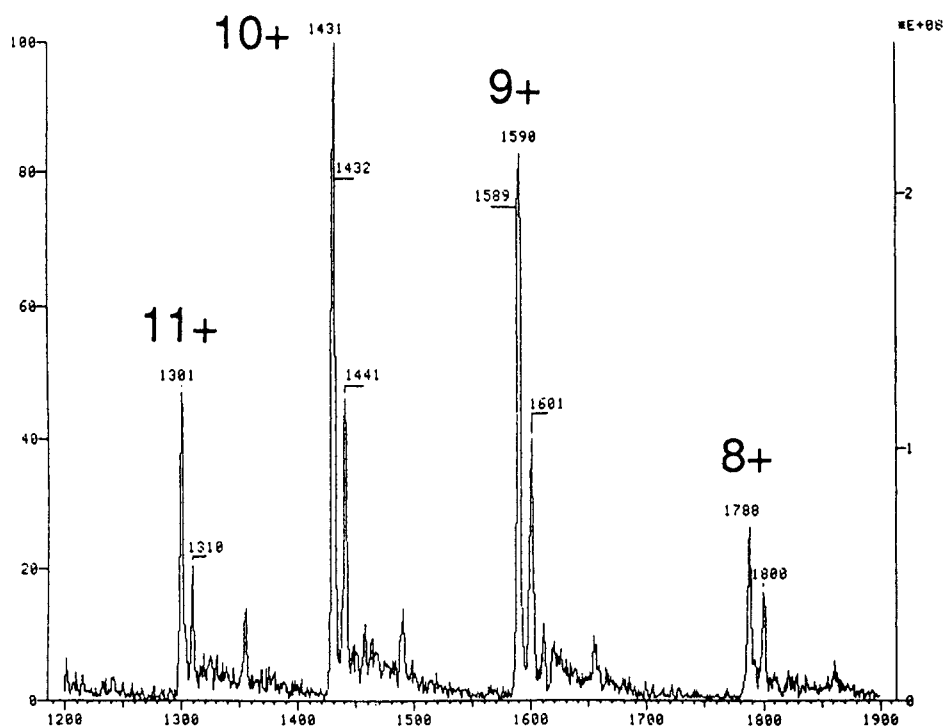


Fig. 2. Electrospray mass spectrum of lysozyme obtained with constant infusion of 1 pmol/ $\mu\text{l}$  in methanol–water (80:20, v/v) +1% acetic acid.



Thermal-induced dissociation of multiply protonated peptides, as shown by Rockwood et al. [16], has not yet been observed. This is probably due to the limited heat capacity of the used sampling capillary. Another way of inducing fragmentation in ESI is known as nozzle-skimmer-induced fragmentation [17]. Using the same ion-source configuration, only in TSP mode, increasing the repeller voltage is used to get structural information. Until now it was not possible to observe the same phenomenon in the ESI mode. This subject is still under investigation at the moment.

At higher flow-rates the cone form at the tip of the needle assembly will be changed drastically, but due to Rayleigh instabilities, small droplets will be formed. Vestal [10] made a prediction of the droplet diameter to be proportional to the  $2/3$  power of the flow-rate, with diameters on the order of 1–2  $\mu\text{m}$  at 1  $\mu\text{l}/\text{min}$  and about 100–200  $\mu\text{m}$  at 1  $\text{ml}/\text{min}$ . The drying capacity of the surrounding air is insufficient for complete dissolution of the bigger droplets, which consequently results in a decrease of the signal. Methods to overcome this problem are mentioned in the literature [11,12].

By means of a heated capillary, the useful flow-rate can already be extended to 100  $\mu\text{l}/\text{min}$ . As a consequence, the signal will be reduced by a factor of four. This was tested with tetraoctylammonium bromide (TOA) as a test compound in constant-infusion mode, as well as in FIA experiments.

Using nitrogen as nebulizing gas, the signal is more stable using flow-rates of 25  $\mu\text{l}/\text{min}$  and higher; also the signal even increases in comparison with no nebulizing gas. With a liquid flow-rate of 25  $\mu\text{l}/\text{min}$ , using nebulizing gas, subsequent injections of 215 fmol TOA, scanning from  $M_r$  100 to 500, gave a standard deviation of 5%, at a signal-to-noise ratio of 10.

### 3.1. Application to micro-LC–MS

Acyl-coenzyme A compounds are highly polar, and chemically and thermally unstable, so soft-ionization techniques are required for identification. Recently, Norwood et al. [18] and

Millington et al. [19] described a method for determination of several acyl-coenzyme A compounds using continuous-flow (CF) fast atom bombardment (FAB)-MS in the positive ionization mode. The mass spectra show, besides the protonated molecule, a lot of fragmentation. The reported detection limits are in the range of 50–100 pmol. We investigated the possibilities of using the described ESI in combination with micro-LC for the determination of some acyl-coenzyme A compounds in negative ionization mode. No attempts have been made to optimize the system with respect to eluent composition for separation and mass spectrometric sensitivity. Acetyl-coenzyme A (A-CoA) and 3-hydroxy-3-methylglutaryl-coenzyme A (MG-CoA) have been used as test compounds. These compounds can only be separated using low percentages of organic solvent, which are in fact less favourable conditions for ESI. Application of a sheath flow with a high percentage of organic solvent enables the detection of A-CoA and MG-CoA at low picomolar levels, as is illustrated in Fig. 3.

Detection is based on deprotonated and doubly deprotonated molecules. Under the above-mentioned conditions, doubly deprotonated molecules are favoured. The optimal repeller voltage is the same for both species. No thermal fragmentation has been observed under these conditions, even not while heating the sampling capillary up to 250°C. MS–MS measurements should be used to obtain structural information.

Optimization of separation and mass spectrometric sensitivity of the acyl-coenzyme compounds is still under investigation, using micro-LC and pseudo-electrochromatography (PEC) [20]. The separation efficiency in micro-LC can be improved by changing the pH in combination with the application of gradient elution, as already described by Norwood et al. [18].

### 3.2. Capillary electrophoresis–mass spectrometry

The described interface allows the combination with extremely low flow-rate separation techniques as is demonstrated in the following example.

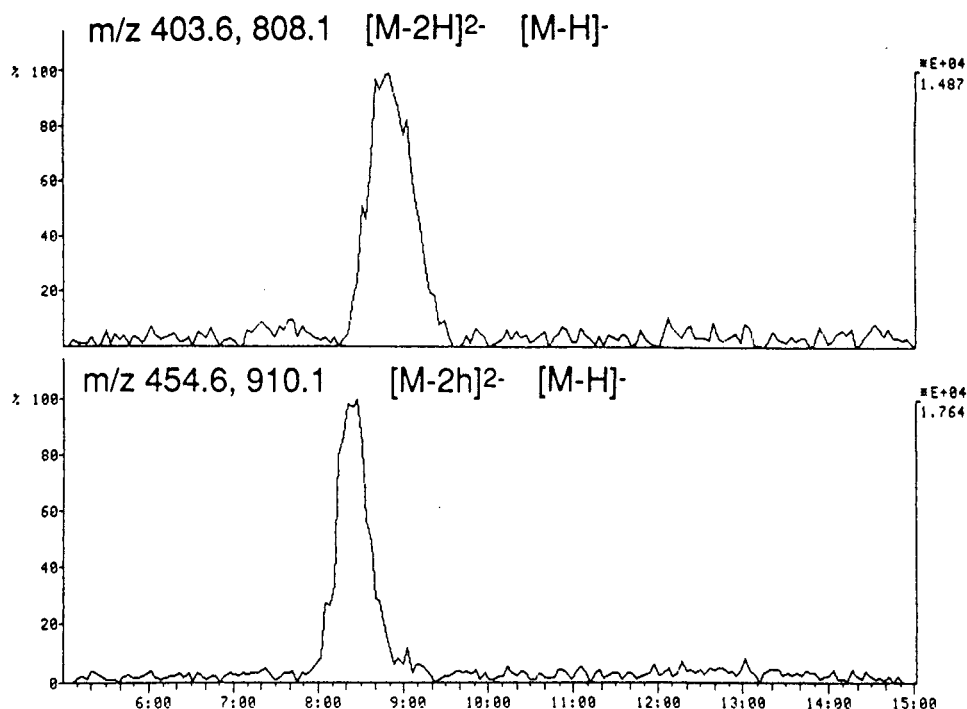


Fig. 3. Micro-LC-MS of 5 pmol injected each of A-CoA and MG-CoA separated on a  $C_8$  slurry-packed column, using acetonitrile–0.05 M ammonium acetate in water (10:90, v/v) as eluent.

Capillary electrophoresis is a suitable technique for the separation of underivatized inositol phosphates at low pH, due to their strong ionic character. Mass spectrometric detection of inositol phosphates is described by Sherman et al. [21] and Walton and Hughes [22], using static FAB-MS, with detection limits in the nanomolar range. It has been demonstrated that mass spectrometry is a reliable and sensitive method of detecting inositol phosphates in the negative ionization mode using capillary electrophoresis [23]. In the configuration with the ESI needle assembly acting as cathode at  $-3$  kV towards the anode at  $-28$  kV, electromigration and the electroosmotic flow (EOF) are in opposite directions. Suppression of the EOF was achieved by coating the fused-silica capillary with polyacrylamide [14].

Preferably, the CE buffer and the sheath liquid should have the same composition. Never-

theless, hardly any signal could be detected in the negative ionization mode using a buffer composition of methanol–ammonium acetate in water (10 mM, pH 5.0) (30:70, v/v). Constant-infusion experiments showed that best sensitivity for inositol phosphates could be obtained with percentages of organic solvents of 80–100%, observing deprotonated molecules. Therefore, it was decided to keep the percentage organic solvent in the CE buffer as low as possible and in the sheath liquid as high as possible, while maintaining the ionic strength the same in both cases. Without any problem concerning stability and sensitivity, buffer compositions as mentioned in this study could be used. In Fig. 4, the electropherogram of a mixture of inositol phosphates is given. In this case 9 pmol of each component is injected. The differences in response factors of the inositol phosphates can be explained by the fact that mass spectrometric

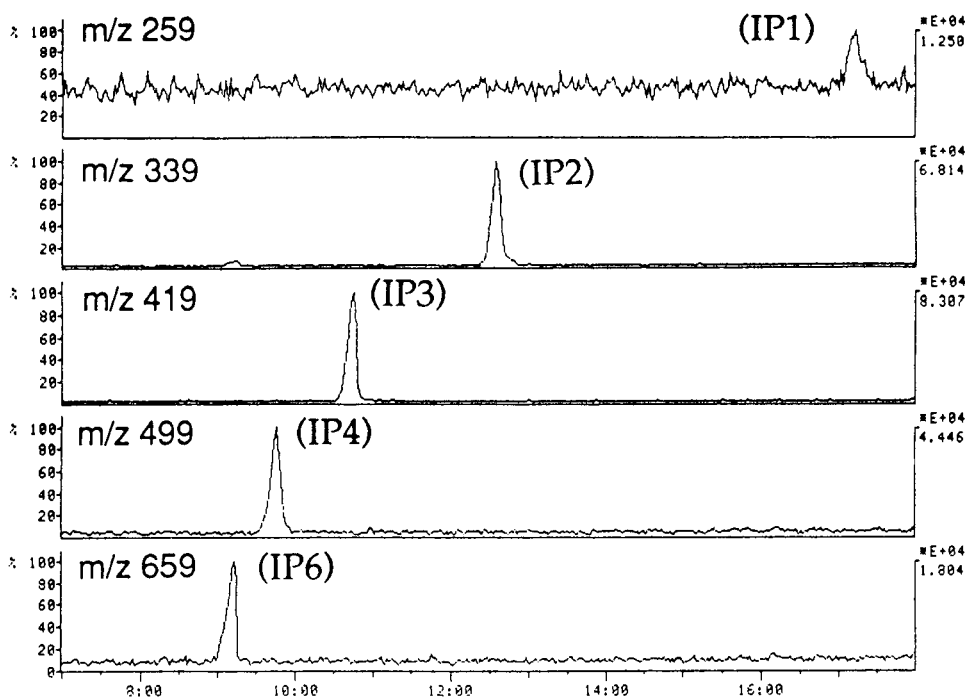


Fig. 4. Electropherogram of a test mixture of inositol phosphates. Amount injected: 9 pmol of each compound.

detection occurred in the MID mode, in which procedure only the singly charged ions were involved.

#### 4. Conclusions

The custom-made electrospray interface in combination with a thermospray ion source offers sensitivities comparable with the Whitehouse–Fenn ESI interface, used in our laboratory, with respect to low flow-rates for low, as well as, high molecular masses. Extraction of ions out of the ion source, by means of a conical-shaped repeller, at a 90° angle with respect to the quadrupole axis, is quite effective. Until now no thermal-induced or repeller-induced fragmentation is observed.

Additionally, flow-rates up to 100  $\mu\text{l}/\text{min}$  can be used without severe loss of signal, due to the heated sampling capillary.

Working in negative ionization mode is not affected by corona discharge. Therefore, the interface is flexible for coupling CE, micro-LC and LC with split. This is illustrated by the coupling of CE–MS for detection of inositol phosphates, obtaining low picomolar detection limits, and micro-LC–MS for determination of intact acyl-coenzyme A compounds.

#### Acknowledgement

The authors wish to thank Hans Robbers of the Department of Fine Mechanics for his skilful help in the development of the interface.

#### References

- [1] M. Yamashita and J.B. Fenn, *J. Phys. Chem.*, 88 (1984) 4451.

- [2] M.L. Aleksandrov, L.N. Gall, V.N. Krasnov, V.I. Nikolaev, V.A. Pavlenko and A. Shkurov, *Dokl. Akad. Nauk SSSR*, 277 (1984) 379.
- [3] R.D. Smith, J.A. Olivares, N.T. Nguyen and H.R. Udseth, *Anal. Chem.*, 60 (1988) 436.
- [4] M.J. Huddleston, R.S. Annan, M.F. Bean and S.A. Carr, *J. Am. Soc. Mass Spectrom.*, 4 (1993) 710.
- [5] C.M. Whitehouse, R.N. Dreyer, M. Yamashita and J.B. Fenn, *Anal. Chem.*, 57 (1985) 675.
- [6] K. Hiraoka and I. Kudaka, *Rapid Commun. Mass Spectrom.*, 6 (1992) 265.
- [7] M. Yamashita and J.B. Fenn, *J. Phys. Chem.*, 88 (1984) 4671.
- [8] A.P. Bruins, T.R. Covey and J.D. Henion, *Anal. Chem.*, 59 (1987) 2642.
- [9] M.G. Ikonomou, A.T. Blades and P. Kebarle, *J. Am. Soc. Mass Spectrom.*, 2 (1991) 497.
- [10] M.L. Vestal, in K.G. Standing and W. Ens (Editors), *Methods and Mechanisms for Producing Ions from Large Molecules*, Plenum Press, New York, 1991, pp. 157–170.
- [11] M.G. Ikonomou and P. Kebarle, *J. Am. Soc. Mass Spectrom.*, 5 (1994) 791.
- [12] S.K. Chowdhury, V. Katta and B.T. Chait, *Rapid Commun. Mass Spectrom.* 4 (1990) 81.
- [13] S. Jackett and M. Moini, *Rev. Sci. Instrum.*, 65 (1994) 591.
- [14] S. Hjerten, *J. Chromatogr.*, 347 (1985) 191.
- [15] S.K. Chowdhury, V. Katta, R.C. Beavis and B.T. Chait, *J. Am. Soc. Mass Spectrom.*, 1 (1990) 382.
- [16] A.L. Rockwood, M. Busman, H.R. Udseth and R.D. Smith, *Rapid Commun. Mass Spectrom.*, 5 (1991) 582.
- [17] Y. Shida, K. O'Hara, L.J. Deterding, C.E. Parker and K.B. Tomer, *The 40th ASMS Conference on Mass Spectrometry and Allied Topics*, Washington, DC, 1992, p. 1351.
- [18] D.L. Norwood, A.B. Christine and D.S. Millington, *J. Chromatogr.*, 527 (1990) 289.
- [19] D.S. Millington, D.L. Norwood and Naoki Kodo, *J. Chromatogr.*, 562 (1991) 47.
- [20] M. Hugener, A.P. Tinke, W.M.A. Niessen, U.R. Tjaden and J. van der Greef, *J. Chromatogr.*, 647 (1993) 375.
- [21] W.R. Sherman, K.E. Ackermann, R.A. Berger, B.G. Gish and M. Zinbo, *Biomed. Environ. Mass Spectrom.*, 13 (1986) 333.
- [22] T.J. Walton and S.Y. Hughes, *Rapid Commun. Mass Spectrom.*, 7 (1993) 555.
- [23] B.A.P. Buscher, R.A.M. van der Hoeven, U.R. Tjaden and J. van der Greef, *J. Chromatogr. A*, 712 (1995) 235.



ELSEVIER

Journal of Chromatography A, 712 (1995) 219–225

JOURNAL OF  
CHROMATOGRAPHY A

# On-line coupling of micellar electrokinetic chromatography to electrospray mass spectrometry

M.H. Lamoree, U.R. Tjaden\*, J. van der Greef

*Division of Analytical Chemistry, Leiden/Amsterdam Center for Drug Research, Leiden University, P.O. Box 9502, 2300 RA Leiden, Netherlands*

## Abstract

The possibility of selectivity enhancement in capillary electrophoresis–mass spectrometry (CE–MS) by hyphenating micellar electrokinetic chromatography (MEKC) and electrospray mass spectrometry (MS) is described for two quaternary ammonium compounds. Direct coupling of MEKC to MS is hazardous because of the contamination of the ion source due to presence of an excess of micelle forming agent in the MEKC buffer. Therefore, a coupled-capillary setup with the possibilities of voltage switching and buffer renewal has been designed. Such a system allows on-line heartcutting of the zones of interest in the MEKC capillary with subsequent transfer via a second capillary to the mass spectrometer.

## 1. Introduction

Since the introduction of micellar electrokinetic chromatography (MEKC) by Terabe et al. [1,2], the scope of capillary electrophoretic separation techniques has broadened significantly. The additional separation mechanism of MEKC, based on the differential partition between the micellar phase and the surrounding aqueous phase, introduces new possibilities concerning the analysis of neutral compounds that cannot be separated by capillary zone electrophoresis (CZE), and concerning the analysis of ionic compounds that prove to be difficult to separate on the basis of their electrophoretic properties only. In the recent past, MEKC has found many applications, ranging from the analysis of ionic and non-ionic compounds in a single run [3], bases, nucleosides and oligonucleotides

[4], peptides [5] and proteins [6] to the determination of drug metabolites in urine [7], hereby demonstrating its value in the field of pharmaceutical and bioanalysis. For an overview of the application of MEKC in pharmaceutical analysis, see Nishi and Terabe [8].

For capillary zone electrophoresis–mass spectrometry (CZE–MS), the choice of buffers to achieve a particular separation is limited to the more volatile ones, such as ammonium acetate and triethylamine. As a consequence of this restriction, selectivity tuning for CZE–MS is not as straightforward as it is for CZE in combination with other detection techniques, where buffer additives mostly do not interfere with detection.

Direct coupling of MEKC to MS with the aim of selectivity enhancement in the separation step is hazardous because of the influence of the micelles in the MEKC buffer on MS performance, resulting in loss of sensitivity and ion

\* Corresponding author.

source contamination [9]. However, the combination of these two techniques is very interesting from the viewpoint of selectivity enhancement for capillary electrophoresis combined with MS for the analysis of compounds difficult to separate with CZE.

In this paper attention is focused on the coupling of MEKC to electrospray MS, with the aim of selectivity enhancement for capillary electrophoretic separation techniques coupled to mass spectrometry. In analogy to the phase system switching approach in liquid chromatography [10], a strategy which enables the separation of the micelles or any other buffer additive from the analytes prior to mass spectrometric detection has been followed. In order to achieve this, a coupled-capillary setup with the possibilities of voltage switching and buffer renewal has been developed, which allows heart-cutting of the zones of interest in the MEKC capillary with subsequent transfer via a second capillary to the MS. The system is described for two model compounds of the quaternary ammonium type that are difficult to separate by CZE, and will be evaluated regarding the use for other separation techniques that are difficult to couple to mass spectrometry.

## 2. Experimental

### 2.1. Experimental setup

A programmable injector for capillary electrophoresis (PrInCE, Lauerlabs, Emmen, Netherlands) was used for pressurized injection and power supply at the inlet of the capillary in which MEKC was performed. The capillary setup consisted of two fused-silica capillaries (SGE, Ringwood, Australia), that were coupled via an open liquid junction. Capillary dimensions were 575 mm  $\times$  75  $\mu$ m I.D. for the first capillary, in which MEKC was carried out, and 325 mm  $\times$  75  $\mu$ m I.D. for the second capillary, where the capillary zone electrophoretic transfer of the analytes to the mass spectrometer was effected. The custom-made liquid junction coupling device was constructed from a 7.5  $\times$  7.5  $\times$  2.5 mm piece

of polyethylene with two perpendicular channels with different diameters drilled in it. The narrow bore channel functioned to keep the capillaries perfectly aligned opposite each other, with an opening between them as small as possible to enable liquid flow from the buffer reservoir. To provide free buffer contact at the junction a wide bore channel perpendicular to the first was drilled.

The junction was placed in a custom-made perspex connection buffer vial, which had a built-in electrode with a connection to an external power supply (Spellman CZE 1000R, Plainview, NY, USA). With an outlet buffer exchange unit (Butler, Lauerlabs, Emmen, Netherlands) the buffer in the connection vial could be changed from MEKC buffer to CZE buffer, depending on the stage of analysis. The experimental setup is schematically represented in Fig. 1.

An SSQ 710 single-quadrupole mass spectrometer (Finnigan MAT, San José, CA, USA) equipped with an electrospray interface (Analytica of Branford, USA) was used in the positive ion mode. For electrical contact at the tip of the electrospray needle a sheath liquid was used, delivered at a flow-rate of 1  $\mu$ l  $\text{min}^{-1}$  by a Model 2400 syringe pump (Harvard Apparatus, Edinbridge, UK). Nitrogen was used as drying gas. The electrospray tip was held at ground potential, while the electrospray counterelectrode was set at  $-4.0$  kV. The analytes were monitored in the multiple ion detection (MID) mode, using 0.2 s per mass.

### 2.2. Micellar electrokinetic chromatography

The buffer used to obtain a micellar electrokinetic separation was a mixture of ammonium acetate buffer (10 mM, pH 4.5) and methanol (3:2, v/v). As the micelle forming agent, sodium dodecylsulphate (SDS) at a concentration of 25 mM was added to the ammonium acetate buffer. For MEKC–UV experiments, a Spectra 100 UV–Vis absorbance detector (Spectra-Physics, Mount View, CA, USA) was used at a wavelength of 210 nm.

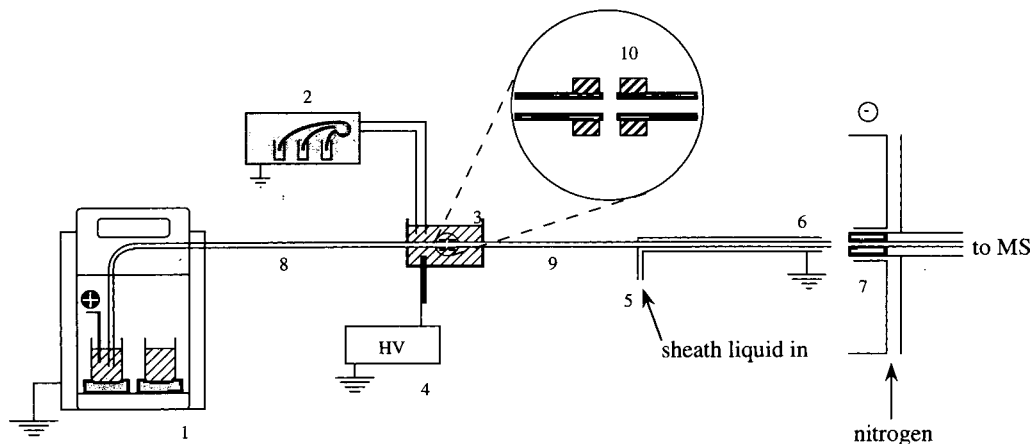


Fig. 1. Schematic representation of the MEKC–MS setup: (1) programmable injector for capillary electrophoresis with internal high-voltage power supply; (2) outlet buffer exchange unit; (3) custom-made perspex connection vial with electrode connection; (4) external high-voltage power supply; (5) inlet for the sheath liquid; (6) grounded electro spray needle; (7) electro spray sampling capillary; (8) MEKC capillary; (9) CZE capillary; (10) capillary coupling device.

### 2.3. Capillary zone electrophoretic transfer of the analytes to the mass spectrometer

Transfer of the analytes via the second capillary to the mass spectrometer was carried out with a solution of ammonium acetate buffer (50 mM, pH 4.5) and methanol (3:2, v/v). The sheath liquid, necessary to maintain electrical contact at the electro spray tip, also consisted of ammonium acetate (100 mM, pH 4.5) and methanol (1:4, v/v).

### 2.4. Chemicals

Mepenzolate and pipenzolate (for chemical structures, see Fig. 2) were obtained from Sigma (St. Louis, MO, USA). SDS was purchased from Serva Feinbiochemica (Heidelberg, Germany),

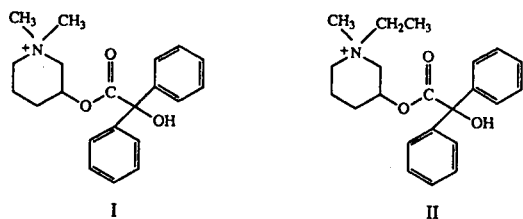


Fig. 2. Chemical structures of the compounds studied. I = mepenzolate,  $M_r = 340.2$ ; II = pipenzolate,  $M_r = 354.2$ .

and ammonium acetate was from Merck (Darmstadt, Germany). Methanol and acetic acid were analytical grade, obtained from Biosolve (Barnveld, Netherlands) and Baker (Deventer, Netherlands), respectively.

In all experiments deionized water was used, obtained with a Milli-Q system (Millipore, Bedford, MA, USA). All samples were dissolved in the MEKC buffer.

## 3. Results and discussion

The direct coupling of MEKC to mass spectrometric detection is hazardous because of the contamination of the ion source due to the presence of an excess of micelle forming agent in the MEKC buffer. In order to overcome the problems associated with introduction of, in this case, SDS into the mass spectrometer, a coupled-capillary setup with the possibilities of voltage switching and buffer renewal has been developed. With this system, a MEKC separation with mass spectrometric detection can be achieved without causing contamination of the ion source, thus ensuring long-term stable operation of the mass spectrometer.

With the coupled-capillary setup described here, MEKC–MS can be divided in three stages.

The first is the actual MEKC separation in the first capillary, followed by a transfer of the zones of interest to the second capillary. Subsequently, the micelles are separated from the analytes by means of CZE.

In Fig. 3, the principle of this approach is represented schematically. Throughout the whole procedure the electrospray tip is held at ground potential and a stable electrospray is established. Before the analysis is started, the first capillary and the connection vial are filled with the MEKC buffer, while the second capillary is filled with the CZE buffer. After pressurized injection of the sample, +15 kV is applied at the inlet of the MEKC capillary, while the connection vial is placed at -10 kV (step I in Fig. 3). The negative voltage applied at the connection vial is necessary to preserve an electroosmotic flow in the second capillary from the electrospray tip towards the connection vial, thus preventing any MEKC buffer constituent from entering the second capillary. At the moment

that the first compound of interest reaches the end of the MEKC capillary, which is depicted in step II, the voltages on the MEKC capillary inlet and the connection vial are switched off. With the outlet buffer exchange unit (see Fig. 1) the connection vial is emptied and the MEKC buffer is replaced by CZE buffer. In this way, a continuous buffer system in the connection vial and the second capillary is established. Ideally, the CZE buffer and the electrospray sheath liquid should be of the same composition in order to obtain optimum electrophoretic performance with regard to plate numbers and resolution, but the relatively high water content in the CZE buffer prohibited the establishment of a stable electrospray for a prolonged period of time. For that reason, a choice was made for a sheath liquid with higher organic modifier content and an ammonium acetate buffer of high concentration to make up for differences in conductivity between the CZE buffer and the sheath liquid. After replacement of the buffer in

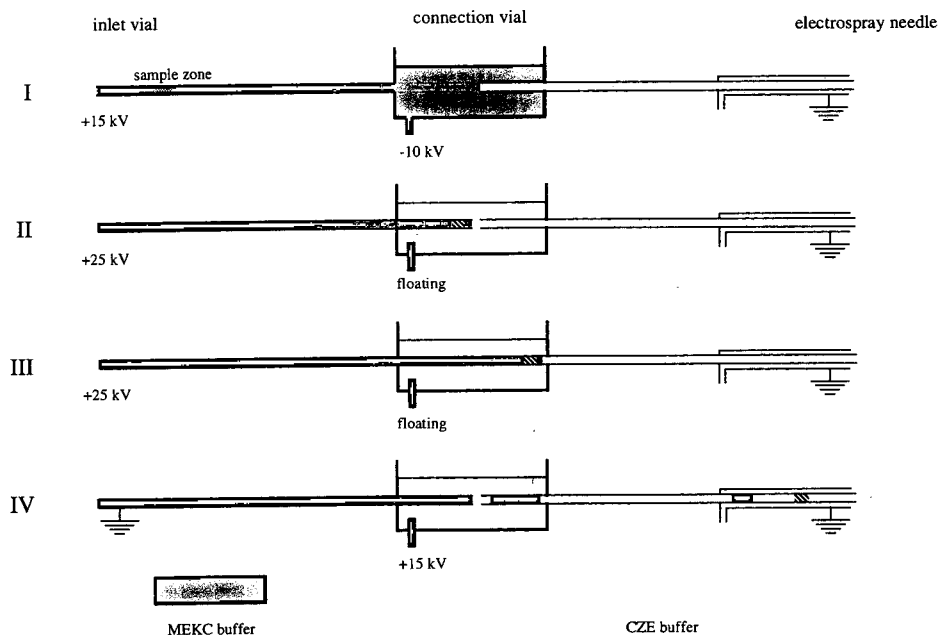


Fig. 3. Schematic representation of the principle of buffer exchange and voltage switching for the coupling of MEKC to MS. For reasons of clarity the capillary coupling device has not been drawn in the picture (see Fig. 1). See text for a detailed explanation of the procedure.



the connection vial, a voltage of +25 kV is applied at the MEKC capillary inlet, while the voltage in the connection vial is not controlled externally. Regarding the passage of the analytes through the liquid junction interface it can be stated that no losses occur. This is based on the effect that the electric field lines are in the direction of the transfer capillary, which has been realized by using the transfer capillary end as the cathodic end. For this reason the center electrode in the connection vial is floating during the passage of analytes through the liquid junction. When the connection vial would not be disconnected physically from the external high-voltage power supply, it would serve as an additional ground, resulting in an electrical split between the connection vial and the second capillary. When the analytes are transferred over the liquid junction into the second capillary, a situation represented in step III in Fig. 3, the voltage at the inlet of the MEKC capillary is switched off. In step IV, a voltage of +15 kV is applied at the connection vial via the external high-voltage power supply, and capillary zone electrophoretic transport of the analytes to the mass spectrometer is effected.

The electrophoretic transfer of the analytes to the mass spectrometer (represented by step IV) can be regarded as conventional CZE of a zone that has been heartcut from the MEKC capillary. The positively charged analytes that have already been separated in the MEKC step migrate further towards the electrospray tip as a result of their own electrophoretic mobility and the electroosmotic flow. The negatively charged SDS micelles have an electrophoretic mobility in the direction of the connection vial, which may be overcome by the larger electroosmotic flow. From our experiments so far it has not become completely clear what happens with the SDS plug, apart from that it does not reach the electrospray tip within reasonable time (<1 h) and does not disturb the electrospray process. We assume that at the boundaries of the heartcut zone in the second capillary the micelles break up due to dilution of the zone in the CZE buffer where no SDS is present. Below the critical micellar concentration of 8 mM (in aqueous

solution) the micelles are disrupted and the SDS exists as free anions in solution.

In the experiments described here, charged analytes have been used to characterize the system, but obviously MEKC is extremely suitable for the separation of neutral compounds that cannot be separated by CZE. In that case, transfer of the analytes to the MS is based solely on electroosmotic flow, ionization for mass spectrometric detection has to take place in the electrospray process.

The choice of the CZE buffer has proven to be of the utmost importance with regard to the maintenance of the electrophoretic peaks in the CZE capillary. The transfer of a zone from the MEKC capillary to the CZE capillary can be considered as the injection of a sample plug containing several types of ions (sodium, dodecylsulphate, ammonium, acetate, the analytes, and their counterions). When the ionic strength of the CZE buffer is chosen too low, severe fronting of the analyte occurs [11] and difficulties may arise for the assignment of electrophoretic peaks. To overcome this problem, the concentration of ammonium acetate in the CZE buffer was taken significantly higher than that in the MEKC buffer.

An important parameter to influence the separation is the use of an organic modifier to control the extent of interaction between the analytes and the micelles. This has been reported extensively in the literature [12–15], and is especially useful in the coupling with electrospray mass spectrometry, because of the greater spray stability when spraying organic solvents such as methanol.

Another aspect that needs attention is the timing of the events. When MEKC is carried out too long, the analytes will migrate into the connection vial and are lost for mass spectrometric detection. However, when the MEKC time is chosen too short, a large plug of MEKC buffer enters the CZE capillary before the compounds of interest are transferred, which might seriously hamper the electrophoretic transport of the analytes, and even result in introduction of SDS into the MS. From this viewpoint it is also clear that only a small separation window from the

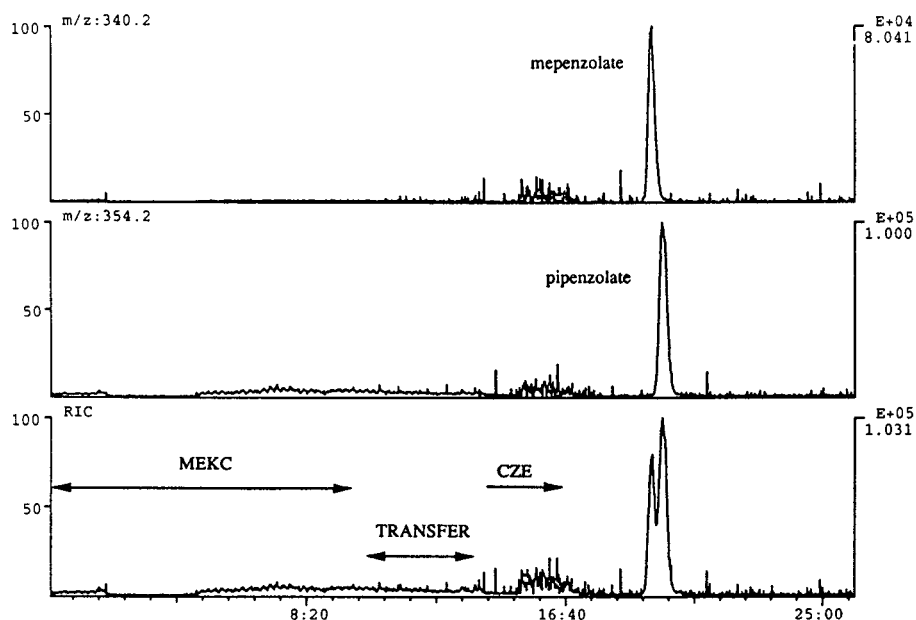


Fig. 4. Mass electropherogram obtained after 9 min MEKC, 3 min transfer and subsequent CZE transport of a mixture of mepenzolate ( $m/z$  340.2) and pipenzolate ( $m/z$  354.2) in a concentration of  $8 \mu\text{g/ml}$  of each compound. The analytes were dissolved in the MEKC buffer, and the volume injected was approximately 25 nl, corresponding to an injected amount of 200 pg.

MEKC capillary can be transferred to the CZE capillary. In practice, this means that only transfer of analytes that are just resolved is feasible.

In Fig. 4 the mass electropherogram is shown that was obtained after 9 min MEKC and 3 min transfer of the zone of interest to the CZE capillary, carried out according to the procedure described above. The injected sample consisted of mepenzolate and pipenzolate in a concentration of  $8 \mu\text{g/ml}$  each, and was prepared in MEKC buffer. The injected volume was approximately 25 nl, corresponding to an injected amount of 200 pg of each compound. The noise at  $t = 16$  min is probably due to sodium that is logically present in the sample plug as a counterion for the dodecylsulphate ions. From the reconstructed ion current it can be seen that the two compounds are not completely resolved. That this is a problem that arises from the procedure of transferring the analytes to the second capillary can be concluded from the electropherogram obtained with MEKC–UV experiments (Fig. 5) for which an identical buffer composition was used. This electropherogram

shows baseline separation of mepenzolate and pipenzolate.

It should be noted that the efficiencies obtained with the coupled-capillary system are

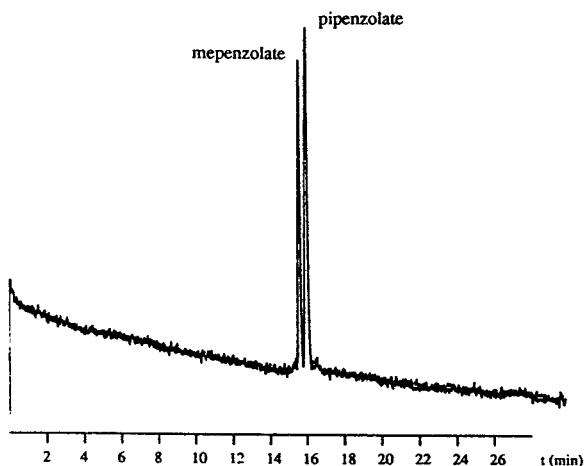


Fig. 5. MEKC–UV electropherogram showing baseline resolution of mepenzolate and pipenzolate. The injected amount was 0.5 ng per compound. Experimental conditions: capillary,  $750 \text{ mm} \times 75 \mu\text{m}$  I.D. fused-silica (600 mm to detector); voltage, +30 kV; UV detection at 210 nm.

lower than those obtained with the single-capillary MEKC–UV setup. One reason is that the applied voltage in the former case was 25 kV, while in the latter setup 30 kV was used. Since the efficiencies are directly proportional to the applied voltage, it may be expected that the resolution will differ. Taking into account the different applied voltages, a loss in efficiency of about 20% should be observed. In fact, the efficiencies differ about 50%. This can be explained by additional band broadening in the coupled-capillary setup caused by the application of the liquid junction, and partly by the diffusion of the zones in the rather long time needed to empty the connection vial from MEKC buffer and refill it with CZE buffer. Optimization of both these aspects is currently under development.

#### 4. Conclusions

The coupled-capillary approach described here enables the micellar electrokinetic separation coupled to mass spectrometric detection of charged analytes that are difficult to separate by capillary zone electrophoresis. During the experiments, no detrimental effects of the presence of SDS on MS performance has been observed, ensuring long-term stable operation conditions. The application of this system to the separation of neutral compounds is currently under investigation.

Analogous to the phase system switching developed in our laboratory [10], the setup used throughout these experiments opens up possibilities for other capillary electrophoretic separation systems which cannot be directly coupled to the mass spectrometer due to the presence of certain buffer additives that are necessary to obtain the required separation. In future research, special attention will be paid to separation systems utilizing chiral separators such as cyclodextrins. Obviously, the coupling of chiral separation systems to mass spectrometry is of

great interest in pharmaceutical analysis, because of the necessity of unequivocal mass determination of analytes paired to the inability of the mass spectrometer of discrimination between two enantiomers which are not electrophoretically resolved.

#### Acknowledgements

We wish to thank Hans Robbers of the Division of Fine Mechanics for the construction of the connection vial and Lauerlabs (Emmen, Netherlands) for the use of the Butler outlet exchange buffer unit.

#### References

- [1] S. Terabe, K. Otsuka, K. Ichikawa, A. Tsuchiya and T. Ando, *Anal. Chem.*, 56 (1984) 111.
- [2] S. Terabe, K. Otsuka and T. Ando, *Anal. Chem.*, 57 (1985) 834.
- [3] R.A. Wallingford and A.G. Ewing, *J. Chromatogr.*, 441 (1988) 299.
- [4] A.S. Cohen, S. Terabe, J.A. Smith and B.L. Karger, *Anal. Chem.*, 59 (1987) 1021.
- [5] J. Liu, K.A. Cobb and M. Novotny, *J. Chromatogr.*, 519 (1990) 189.
- [6] M.A. Strege and A.L. Lagu, *Anal. Biochem.*, 210 (1993) 402.
- [7] M. Tomita, T. Okuyama, S. Sato and H. Ishizu, *J. Chromatogr.*, 621 (1993) 249.
- [8] H. Nishi and S. Terabe, *J. Pharm. Biomed. Anal.*, 11 (1993) 1277.
- [9] J. Varghese and R.B. Cole, *J. Chromatogr. A*, 652 (1993) 369.
- [10] J. van der Greef, W.M.A. Niessen and U.R. Tjaden, *J. Chromatogr.*, 474 (1989) 5.
- [11] F.E.P. Mikkers, F.M. Everaerts and Th.P.E.M. Verheggen, *J. Chromatogr.*, 169 (1979) 1.
- [12] J. Gorse, A.T. Balchunas, D.F. Swaile and M.J. Sepaniak, *J. High Resolut. Chromatogr. Chromatogr. Commun.*, 11 (1988) 554.
- [13] T. Yashima, A. Tsuchiya, O. Morita and S. Terabe, *Anal. Chem.*, 64 (1992) 2981.
- [14] P. Lukkari, H. Vuorela, M.-L. Riekkola, *J. Chromatogr. A*, 655 (1993) 317.
- [15] S. Takeda, S. Wakida, M. Yamane, A. Kawahara and K. Higashi, *Anal. Chem.*, 65 (1993) 2489.





ELSEVIER

Journal of Chromatography A, 712 (1995) 227–234

JOURNAL OF  
CHROMATOGRAPHY A

# Combined liquid–liquid electroextraction–isotachopheresis for loadability enhancement in capillary zone electrophoresis–mass spectrometry

E. van der Vlis, M. Mazereeuw, U.R. Tjaden\*, H. Irth, J. van der Greef

*Division of Analytical Chemistry, Center for Bio-Pharmaceutical Sciences, Leiden/Amsterdam Center for Drug Research, Leiden University, P.O. Box 9502, 2300 RA Leiden, Netherlands*

## Abstract

Combined liquid–liquid electroextraction (EE) and isotachopheresis (ITP) as a fast on-line focusing step in capillary zone electrophoresis (CZE) prior to electrospray mass spectrometric (ESP-MS) detection is described. Very high electric field strengths can be applied owing to the low conductivity of the organic phase, which results in high migration rates. Liquid–liquid electroextraction enables the fast extraction of analyte ions into a small buffer volume, whereas ITP is used to focus the analytes away from the liquid–liquid interface. As a result, ITP starts with a small sample volume containing the extracted ions. After reaching the steady state within several minutes, CZE separation follows. Clenbuterol, salbutamol, terbutaline and fenoterol were used as model compounds. Concentration detection limits of pure solutions down to  $2 \cdot 10^{-9}$  mol/l for clenbuterol, salbutamol and terbutaline, and  $5 \cdot 10^{-9}$  mol/l for fenoterol have been achieved using on-line EE–ITP–CZE–ESP-MS.

## 1. Introduction

The coupling of capillary zone electrophoresis (CZE) to mass spectrometric detection (MS) is advantageous as it combines the high separation power of CZE and the high selectivity of MS detection. However, sample loadability and concentration sensitivity in CZE still limit its use as a separation technique prior to MS detection. Different attempts have been made to enhance sensitivity in CZE by employing sample concentrating techniques prior to the CZE separation, including chromatographic and isotachopheretic preconcentration [1].

Isotachopheresis (ITP) has proven to be a very useful technique for sample enrichment on-

line with CZE [2–11]. As the focusing time in ITP is determined mainly by the concentration of constituents and related to this the electric field strength, the mobility of the analyte and the migration path length, the time needed for the concentration of very large sample volumes is generally longer than 1 h [12,13]. Such long focusing times are undesirable in routine analyses.

Another approach is the use of liquid–liquid extraction as an off-line sample-handling technique prior to CZE [14]. Low detection limits are obtained using chloroform for the extraction of doxorubicin from plasma. A back-extraction to 5 mmol/l phosphoric acid resulted in an extract of low ionic strength compared to the CZE buffer. As a result, analyte stacking during electrokinetic sample injection occurred.

\* Corresponding author.

For several decades it has been known that by using an electric field in liquid–liquid extraction processes on an industrial scale the mass transfer in the extraction of ionic compounds is increased [15–21]. So far, the use of this so-called electroextraction has been limited to bulk processes only. Recently, this principle has been adapted and applied to a miniaturized scale in combination with CZE [22]. The on-line use of combined EE–ITP enabled the fast extraction of charged compounds from large volumes of organic solvents (up to several millilitres) into a 100- $\mu$ m I.D. fused-silica capillary owing to the extremely high local field strength. Automation could easily be accomplished, as the whole procedure was performed in a single capillary.

This paper describes the use of on-line EE–ITP as a novel focusing technique for the improvement of sample concentration detection limits in CZE–MS. Some  $\beta$ -agonists have been used as test compounds. After EE into the terminating buffer of the ITP system only a few minutes are required to reach the steady state.

## 2. Experimental

### 2.1. Chemicals

All chemicals used were of analytical grade. Aqueous solutions were prepared using water purified with a Milli-Q system (Millipore, Bedford, MA, USA). Ethyl acetate (EtOAc), potassium hydroxide, ammonium acetate and acetic acid were obtained from Merck (Darmstadt, Germany), methanol from Biosolve (Barneveld, Netherlands),  $\beta$ -alanine from Aldrich (Steinheim, Germany), crystal violet from Janssen Chimica (Beerse, Belgium), clenbuterol hydrochloride, terbutaline sulphate and fenoterol hydrobromide (Fig. 1) from Sigma (St. Louis, MO, USA). Salbutamol sulphate (Fig. 1) was kindly donated by TNO Institute (Zeist, Netherlands).

The leading buffer and sheath liquid consisted of 50 mmol/l ammonium acetate solution adjusted to pH 5 with 3.3 mol/l acetic acid solution–methanol (20:80, v/v). The terminating

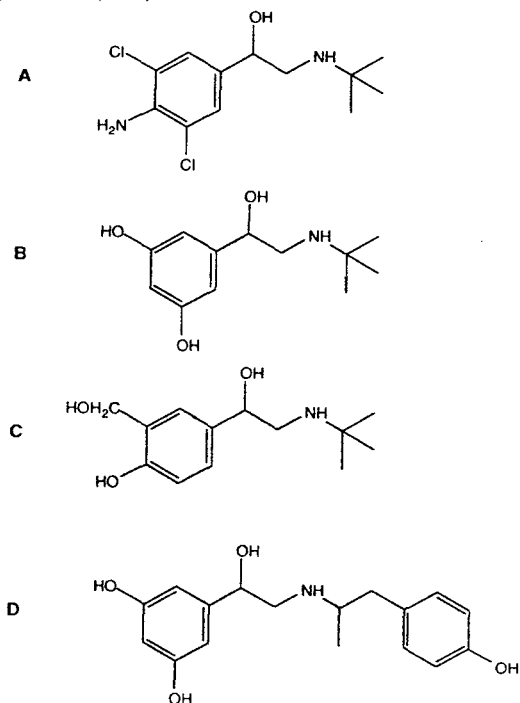


Fig. 1. Chemical structures of clenbuterol,  $M_r$  276.1 (A); terbutaline,  $M_r$  225.1 (B); salbutamol,  $M_r$  239.2 (C); fenoterol,  $M_r$  303.1 (D).

buffer consisted of a 12 mmol/l  $\beta$ -alanine solution adjusted to pH 5 with 3.3 mol/l acetic acid solution–methanol (85:15, v/v). Standard solutions of the  $\beta$ -agonists were made in saturated EtOAc. For this purpose a 10 mmol/l  $\beta$ -alanine solution, adjusted to pH 5 with 3.3 mol/l acetic acid solution, was extracted with EtOAc. Stock solutions of the cationic species were made in water–methanol (50:50, v/v) to a concentration of  $10^{-2}$  mol/l. Methanol was used for further dilution of the stock solutions to a concentration of  $10^{-4}$  mol/l. Finally, saturated EtOAc was used for further dilution of the obtained methanol solutions.

### 2.2. Apparatus

Fig. 2 is a schematic representation of the experimental setup described hereafter. A programmable injection system (Prince, Lauerlabs, Emmen, Netherlands) with the possibility of regulating and fine-tuning both the pressure and

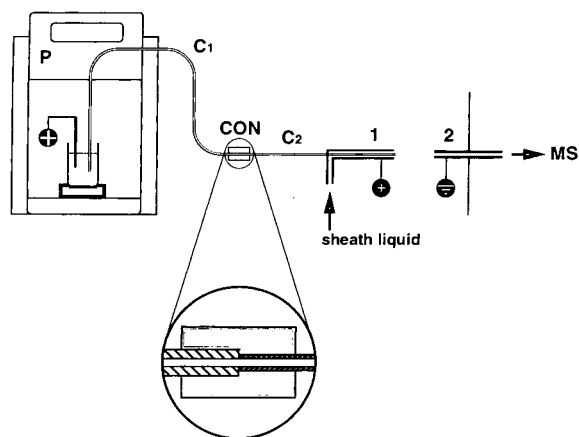


Fig. 2. Schematic representation of the EE-ITP-CZE-MS set-up consisting of a programmable injector (P), a 100- $\mu\text{m}$  I.D., 375- $\mu\text{m}$  O.D. untreated fused-silica capillary (C1) connected to a 100- $\mu\text{m}$  I.D., 170- $\mu\text{m}$  O.D. untreated fused-silica capillary (C2) by means of a laboratory-made transparent polyethylene connector (CON). Capillary C2 is inserted into the stainless-steel needle assembly of the electrospray needle (1) which is positioned opposite to the heated sampling capillary (2).

the voltage. The current was recorded in the low  $\mu\text{A}$ -range. EE-ITP-CZE took place in a 70 cm  $\times$  100  $\mu\text{m}$  I.D. untreated fused-silica capillary (SGE, Ringwood, Vic., Australia) with an O.D. of 375  $\mu\text{m}$ , which was coupled to a 20-cm length of untreated fused-silica capillary (BGB Analytik) with equal I.D., but with an O.D. of 170  $\mu\text{m}$ . The coupling of the two capillaries was achieved using a laboratory-made connector of transparent polyethylene (Fig. 2). The 170- $\mu\text{m}$  O.D. capillary was inserted into the stainless-steel needle assembly of the electrospray needle, after burning off several millimetres of the polyimide-coating of the end of the capillary (Fig. 3).

All experiments were performed on a TSQ-70 triple quadrupole mass spectrometer (Finnigan MAT, San Jose, CA, USA) using a laboratory-made electrospray interface which was positioned in the thermospray ion source. Fig. 3 is a schematic representation of the interface. The electrospray needle was kept at +3 kV, whereas the heated sampling capillary was kept at ground potential. The temperatures of the sampling capillary and of the ion source were 175

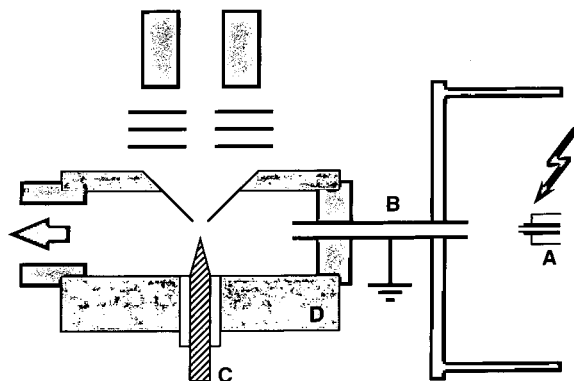


Fig. 3. Schematic representation of the laboratory-made electrospray interface showing the electrospray needle assembly (A), the heated sampling capillary (B), the conical-shaped repeller (C) and the thermospray ion source (D).

and 150°C, respectively. The repeller electrode was set at +30 V. A sheath flow of 1  $\mu\text{l}/\text{min}$ , delivered by a Model 2400 syringe pump (Harvard Apparatus, Edinbridge, UK), was used for optimal electrospray conditions. Protonated analytes were monitored in selected-ion monitoring (SIM) mode, using 0.2 s per mass.

### 2.3. EE-ITP-CZE procedure

Fig. 4 shows the different stages of the procedure, as well as the positioning of the capillary and the electrode. The capillary is conditioned for 10 min daily with water, aqueous potassium hydroxide (0.25 mol/l), water and leading buffer, respectively. Next, the capillary was filled with leading buffer. The 4-ml sample vials were made of glass. Platinum rod electrodes were used for both the anode and the cathode.

#### Step 1

A terminating buffer zone of approximately 15 mm is introduced hydrodynamically at 30 mbar for 18 s at the anodic side of the capillary.

#### Step 2

The capillary inlet is placed in the sample vial containing the EtOAc sample solution (Fig. 4, A1). EE is started by applying a voltage of +10 kV during 1 min (Fig. 4, A2), followed by an additional 9 min at +10 kV in combination with

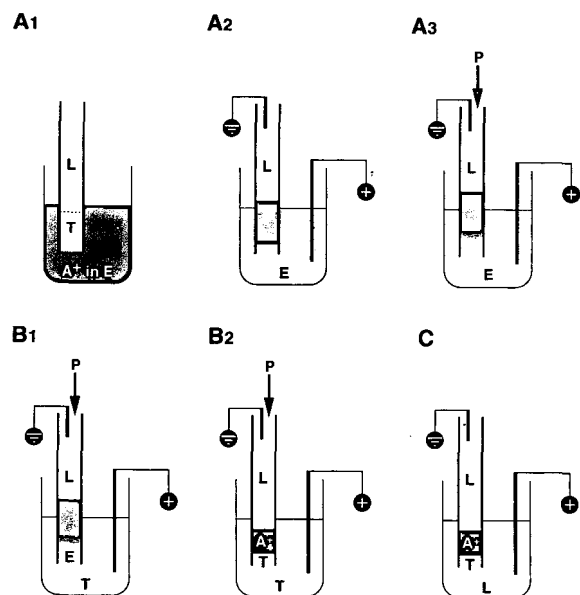


Fig. 4. Step-wise representation of the EE-ITP-CZE procedure. (A1) The capillary, filled with leading buffer (L) and terminating buffer (T), is placed in the ethyl acetate (E) sample solution containing the cationic analyte molecules ( $A^+$ ). (A2) Electroextraction (EE) is performed by applying a voltage. (A3) During EE, using a pressure-induced counterflow (P) in the direction of the arrow, the sample solution is electroextracted. (B1) The analytes are focused by means of pressure-induced counterflow ITP, after the capillary is placed in the terminating buffer vial. (B2) During ITP the remaining EtOAc plug is pushed out of the capillary, while reaching the steady state. (C) The capillary is placed in the leading buffer vial and CZE starts.

an 8-mbar pressure-induced counterflow to avoid entrance of EtOAc into the capillary (Fig. 4, A3). The analyte molecules start to migrate through the interface between the organic phase and the buffer system and continue to migrate through the terminating buffer zone. Simultaneously, the analytes are focused between terminating buffer and leading buffer. Thus, ITP is performed simultaneously and in conjunction with EE.

#### Step 3

Next, the capillary inlet is placed into the terminating buffer vial. By applying a voltage of +15 kV during 1 min using an 8-mbar pressure-induced counterflow, the analytes that are still present in the terminating buffer zone are accel-

erated in the direction of the leading buffer, away from the interface between EtOAc and the buffer system.

#### Step 4

ITP continues at +9 kV during 6 s. A 50-mbar pressure-induced counterflow is used to push the EtOAc plug still present in the capillary towards the capillary outlet (Fig. 4, B1).

#### Step 5

Until the current reaches  $4.0 \mu\text{A}$ , ITP proceeds at +9 kV combined with a 23-mbar pressure-induced counterflow to push out the greater part of the terminating buffer while maintaining a steady state. This step usually takes less than 1 min (Fig. 4, B2).

#### Step 6

CZE is started and performed in leading buffer [23] by applying a voltage of +21 kV (Fig. 4C).

### 3. Results and discussion

#### 3.1. Theoretical aspects of electroextraction-isotachopheresis

The power of EE-ITP is a result of the high local electric field strength in EtOAc. Pure EtOAc hardly conducts electric current. By saturating EtOAc with an aqueous electrolyte solution, the conductivity of the organic phase is slightly increased while the solubility of ionic species improves considerably. This results in a somewhat higher conductivity of the organic phase. Still, the conductivity is about 1000 times lower than that of the terminating buffer of the ITP system [22]. As a consequence of the application of an electric field, transport of charge via the migration of ions originating from the aqueous phase takes place. As the conductivity of EtOAc compared to that of the buffer system is low, the greater part of the applied potential difference exists over the EtOAc zone. This results in a high local electric field strength which is the driving force of migration of ions (Eq. 1),



$$v = \mu \cdot E \quad (1)$$

in which  $v$  is the ion migration rate,  $\mu$  the electrophoretic mobility and  $E$  the electric field strength. As can be calculated [22], the electric field strength in the EtOAc sample can reach 45 kV/cm when applying a voltage of +10 kV over a 90-cm length fused-silica capillary with an I.D. of 100  $\mu\text{m}$ . As the electric field strength is the driving force behind ion migration, the consequence of mass transfer in general is an electric current, usually referred to as driving current. All ionic compounds in an electric field contribute to the total current. Although the driving current during EE–ITP is generally lower than 0.8  $\mu\text{A}$  using a voltage of +10 kV, the extraction rate of the analyte ions from the organic solvent is high owing to the high electric field strength. Even ITP is already in an advanced stage after 10 min of EE with a driving current below 0.8  $\mu\text{A}$ , owing to the short migration path length of 15 mm. As described earlier [22,24], the number of ions  $[N(t)]$  of a single species  $i$  extracted from the organic phase during time  $t$  considering a zero electroosmotic flow and a constant electric field strength is

$$N(t) = S \cdot E_{\text{EtOAc}} \mu_i c_i t \quad (2)$$

where  $c_i$  is the total concentration of ionic species  $i$ ,  $E_{\text{EtOAc}}$  is the constant electric field strength in the EtOAc zone and  $S$  is the area of the liquid–liquid interface, which equals the cross section of the capillary. During EE, the electroosmotic flow is counterbalanced by a pressure-induced counterflow and can thus be neglected. As reported previously [22], in extreme situations the electric field strength in the EtOAc zone at the end of exhaustive EE will be 6% higher than the initial value. This justifies the assumption that the electric field strength is independent of time and can be considered constant.

During EE EtOAc enters the capillary as a result of the induced electroosmotic flow in the capillary. As EtOAc enters the capillary the electric current, and consequently the mass transfer, declines. Thus, a maximum mass transfer is obtained at a maximum driving current.

Hence, a pressure-induced counterflow is applied to counterbalance the electroosmotic flow, hereby preventing the entrance of EtOAc into the capillary. In order to obtain reproducible EE performance, a stable liquid–liquid interface is required [22]. Therefore, EtOAc is allowed to enter the capillary during the first minute of EE. Then, a pressure-induced counterflow is applied to push the liquid–liquid interface back to several millimetres above the tip of the capillary during the remaining 9 min of EE. Initial optimization was carried out using the cationic dye crystal violet, allowing visual monitoring of the whole procedure.

### 3.2. EE–ITP–CZE–MS

Measurement of the protonated  $\beta$ -agonists was performed using a SIM method [23]. Fig. 5 shows mass electropherograms obtained after CZE–MS analysis of a hydrodynamically injected volume of 50 nl of a  $10^{-5}$  mol/l solution of clenbuterol, salbutamol, terbutaline and fenoterol in water. When a voltage of +26 kV was applied at the anodic electrode, an increase in the voltage of the electrospray needle tip from +2.6 kV to +5.1 kV was observed. This phenomenon was reported earlier [25]. The peak height of fenoterol, as can be seen from Fig. 5, is 2–3 times lower than the peak heights of the other  $\beta$ -agonists. This can be explained by the lower proton affinity and related to this a lower ionization efficiency of fenoterol. Coupling of the two fused-silica capillaries by means of a laboratory-made transparent polyethylene connector (Fig. 2) did not influence the separation efficiency significantly. Plate numbers up to 100 000 could be achieved, which is comparable to the separation efficiency reported in a similar setup using a single 100- $\mu\text{m}$  I.D. capillary in combination with the same leading buffer and sheath liquid [23]. This enables the use of capillaries with a thick silica wall at the injector side of the CE system. When applying EE, the use of fused-silica capillaries with thick capillary walls is recommended as electric field strengths of up to 50 kV/cm can be obtained, which may easily lead

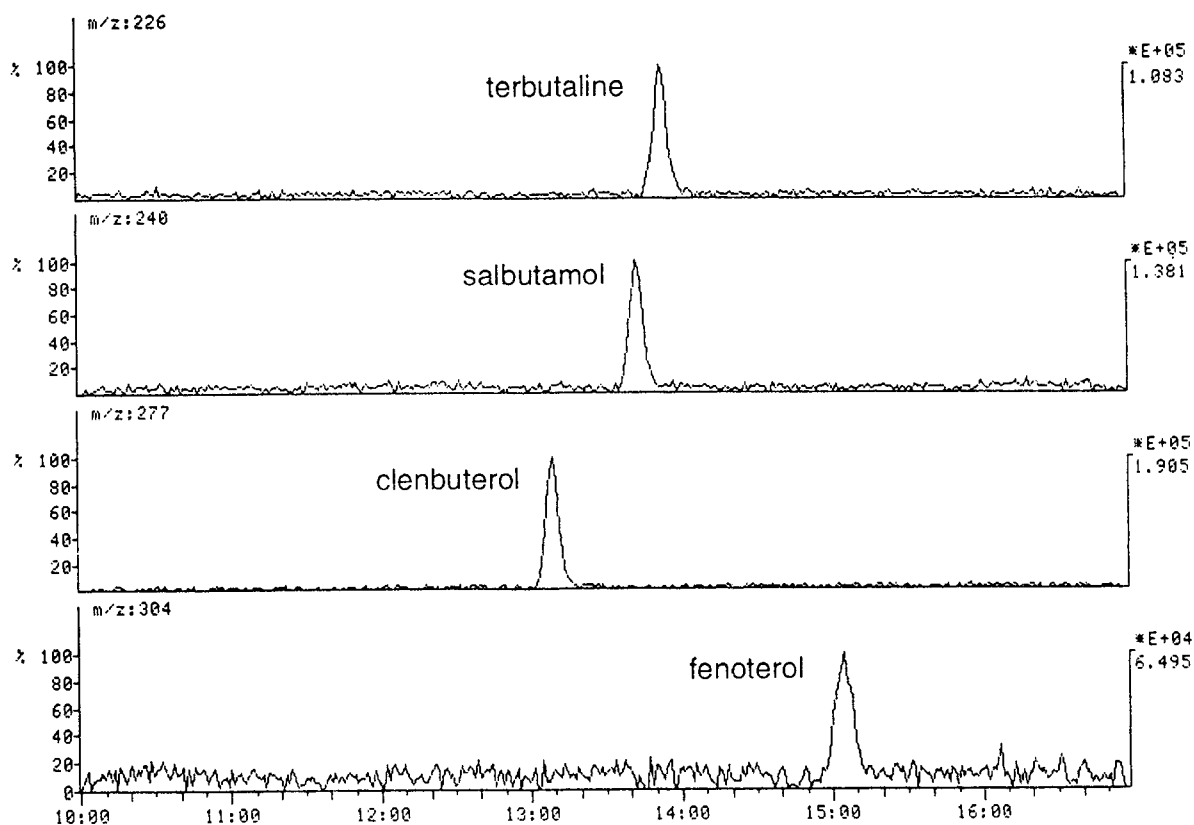


Fig. 5. Mass electropherograms of terbutaline ( $m/z$  226), salbutamol ( $m/z$  240), clenbuterol ( $m/z$  277) and fenoterol ( $m/z$  304) obtained after CZE-MS analysis of 50 nl of a  $10^{-5}$  mol/l  $\beta$ -agonist mixture in water which was injected hydrodynamically.

to electric discharges through the capillary wall and subsequent damage of the capillary.

Fig. 6 shows mass electropherograms obtained after EE-ITP-CZE-MS of 4 ml of a  $5 \cdot 10^{-9}$  mol/l  $\beta$ -agonists mixture in saturated EtOAc sample. Fenoterol has a migration time of 15 min 14 s. The peak at 13 min 11 s at  $m/z$  304 is related to an impurity [23]. This was verified by EE-ITP-CZE-MS-MS of a 4-ml sample of a  $10^{-7}$  mol/l agonist mixture in saturated EtOAc. Clenbuterol, salbutamol and terbutaline are characterized by water loss and subsequent loss of butene, whereas fenoterol is characterized by a fragment at  $m/z$  135. This specific fragment from fenoterol is also obtained after performing collision-induced dissociation in a single quadrupole MS [26,27]. The peak at  $m/z$  304 at 13 min 11 s did not show the specific  $m/z$  135

fragment after collision. MS-MS fragmentation information could still be obtained after EE-ITP-CZE of a 4-ml sample at a concentration of  $10^{-8}$  mol/l of the  $\beta$ -agonists in saturated EtOAc. Concentration detection limits for clenbuterol, salbutamol and terbutaline were  $2 \cdot 10^{-9}$  mol/l, whereas  $5 \cdot 10^{-9}$  mol/l could be obtained for fenoterol. In spite of the low recoveries (4–6%) the use of EE-ITP-CZE-MS (Fig. 6) clearly shows a gain in concentration sensitivity of about 2000 compared to CZE-MS (Fig. 5). From previous reports [22,23] it is demonstrated that the time needed (10 min) for complete EE and subsequent ITP-focusing of a 300- $\mu$ l volume of a saturated EtOAc standard solution equals the time needed to focus an 870-nl aqueous standard solution using ITP-CZE. This clearly demonstrates the high concentrating power of EE.

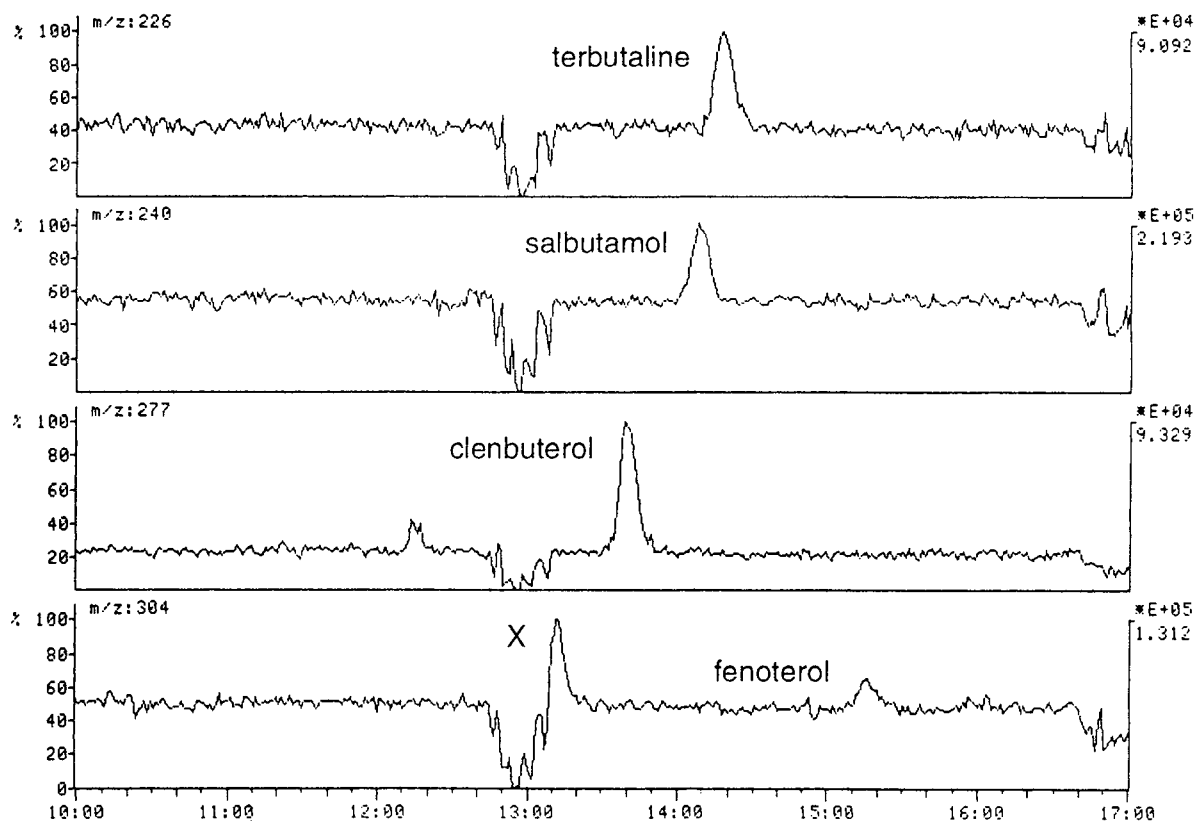


Fig. 6. Mass electropherograms of terbutaline ( $m/z$  226), salbutamol ( $m/z$  240), clenbuterol ( $m/z$  277) and fenoterol ( $m/z$  304) obtained after EE-ITP-CZE-MS analysis of 4 ml of a  $5 \cdot 10^{-9}$  mol/l  $\beta$ -agonist mixture in saturated EtOAc. The peak indicated as "X" is related to an impurity.

Relative standard deviations (R.S.D.s) for EE of a 4-ml sample of a single batch of a  $5 \cdot 10^{-9}$  mol/l mixture of the four  $\beta$ -agonists in saturated EtOAc are less than 12% ( $n = 3$ ). When using sample volumes of more than 1 ml, the diffusion rate of the analyte ions in the EtOAc sample will be the limiting factor for the EE recovery. As EE of ions from the EtOAc sample occurs along the electric field lines, only the sample section between the tip of the capillary and the electrode is extracted. As a result, local exhaustion of only a small part of the total sample volume occurs. Diffusion of ions from the surrounding section into the exhausted section will eventually increase the EE recovery. However, diffusion is a rather slow process. Mixing of a sample of several millilitres during EE might be an option

to increase the EE recovery within an equal period of time.

#### 4. Conclusions

It has been demonstrated that electroextraction in combination with isotachopheresis is a fast technique for sample concentration in capillary electrophoresis-mass spectrometry, with great potential. The high concentrating power of electroextraction enables the extraction of ions into a small volume of terminating buffer prior to ITP. Therefore, only several minutes of ITP is needed to focus the extracted ions between terminating buffer and leading buffer. Application of EE-ITP-CZE prior to MS detection

results in a high concentration sensitivity, as it enables the use of very large sample volumes. Although only standard solutions were used, the results obtained clearly illustrate the concentrating power of EE–ITP. The application of EE–ITP–CZE–MS to the analysis of biological samples is under investigation.

### Acknowledgements

The authors wish to thank the Foundation for Quality Guarantee of the Veal Calf Sector (SKV, Netherlands) for funding, and Mr. R.A.M. van der Hoeven for his skilful help in the mass spectrometric experiments.

### References

- [1] C.A. Monnig and R.T. Kennedy, *Anal. Chem.*, 66 (1994) 280R.
- [2] D.S. Stegehuis, U.R. Tjaden and J. van der Greef, *J. Chromatogr.*, 591 (1992) 341.
- [3] D.S. Stegehuis, H. Irth, U.R. Tjaden and J. van der Greef, *J. Chromatogr.*, 538 (1992) 393.
- [4] N.J. Reinhoud, U.R. Tjaden and J. van der Greef, *J. Chromatogr.*, 641 (1993) 155.
- [5] N.J. Reinhoud, U.R. Tjaden and J. van der Greef, *J. Chromatogr. A*, 653 (1993) 303.
- [6] F. Foret, V. Sustacek and P. Bocek, *J. Microcol. Sep.*, 2 (1990) 229.
- [7] D. Kaniansky and J. Marák, *J. Chromatogr.*, 498 (1990) 191.
- [8] V. Dolnik, K.A. Cobb and M. Novotny, *J. Microcol. Sep.*, 2 (1990) 127.
- [9] D. Kaniansky, J. Marák, V. Madajová and E. Simunicová, *J. Chromatogr.*, 638 (1993) 137.
- [10] F. Foret, E. Szoko and B.L. Karger, *J. Chromatogr.*, 608 (1992) 3.
- [11] P. Jandik and R. Jones, *J. Chromatogr.*, 546 (1991) 431.
- [12] V. Dolnik, M. Deml and P. Bocek, *J. Chromatogr.*, 320 (1985) 89.
- [13] M. Mazereeuw, U.R. Tjaden and J. van der Greef, *J. Chromatogr. A*, 677 (1994) 151.
- [14] N.J. Reinhoud, U.R. Tjaden, H. Irth and J. van der Greef, *J. Chromatogr.*, 574 (1992) 327.
- [15] T.C. Scott, *Sep. Purif. Methods*, 18 (1989) 65.
- [16] P.V.R. Iyer and H. Sawistowski, in G.V. Jeffreys (Editor), *Proc. Int. Solvent Extr. Conf.*, Lyon, 8–14 September, 1974, Society of Chemical Industry, London, Vol. 2, 1974, p. 1029.
- [17] T. Usami, Y. Enokida and A. Suzuki, *J. Nucl. Sci. Technol.*, 30 (1993) 51.
- [18] G. Scibona, P.R. Danesi and C. Fabiani, *Ion Exch. Solvent Extr.*, 8 (1981) 95.
- [19] P.J. Bailes, *Ind. Eng. Chem. Process Des. Dev.*, 20 (1981) 564.
- [20] G. Stewart and J.D. Thornton, *Ind. Chem. Eng. Symp. Ser.*, 26 (1967) 29.
- [21] J.D. Thornton, *Birmingham Univ. Chem. Eng. J.*, (1976) 6.
- [22] E. van der Vlis, M. Mazereeuw, U.R. Tjaden, H. Irth and J. van der Greef, *J. Chromatogr. A*, 687 (1994) 333.
- [23] M.H. Lamoree, N.J. Reinhoud, U.R. Tjaden, W.M.A. Niessen and J. van der Greef, *Biol. Mass Spectrom.*, 23 (1994) 339.
- [24] R.L. Chien and D.S. Burgi, *Anal. Chem.*, 64 (1992) 489A.
- [25] J.R. Perkins and K.B. Tomer, *Anal. Chem.*, 66 (1994) 2835.
- [26] L. Debrauwer and G. Bories, *Rapid Commun. Mass Spectrom.*, 6 (1992) 382.
- [27] L. Debrauwer, G. Delous and G. Bories, *Chromatographia*, 36 (1993) 218.



ELSEVIER

Journal of Chromatography A, 712 (1995) 235–243

JOURNAL OF  
CHROMATOGRAPHY A

# Analysis of inositol phosphates and derivatives using capillary zone electrophoresis–mass spectrometry

B.A.P. Buscher<sup>a</sup>, R.A.M. van der Hoeven<sup>a</sup>, U.R. Tjaden<sup>a,\*</sup>, E. Andersson<sup>b</sup>,  
J. van der Greef<sup>a</sup>

<sup>a</sup>Division of Analytical Chemistry, Leiden/Amsterdam Center for Drug Research, University of Leiden, P.O. Box 9502,  
2300 RA Leiden, Netherlands

<sup>b</sup>Perstorp Regeno, S-284 80 Perstorp, Sweden

## Abstract

Capillary zone electrophoresis (CZE) has been combined with mass spectrometric detection for the separation and determination of inositol phosphates (IPs). Apart from IP1 through IP6 (inositol mono- through hexakisphosphate), an IP3 derivative has been analyzed and identified. The detection limits achieved are in the low micromolar range corresponding to an injected amount of ca. 900 fmol. In addition, an IP3 spiked plasma sample was analyzed after sample pretreatment using ultrafiltration.

## 1. Introduction

Inositol phosphates (IPs) are important compounds in biochemistry (1,4,5-inositol trisphosphate) [1], agriculture (phytic acid) [2] and pharmaceutical science (1,2,6-inositol trisphosphate) [3]. From their chemical structures (Fig. 1A) it can be concluded that IPs are negatively charged and contain neither chromophores nor fluorophores. For many years, separation of IPs has been performed using liquid (ion-pair, ion-exchange) [4] and gas chromatography (after derivatization) [5]. However, capillary zone electrophoresis (CZE) appeared to be more appropriate and faster for the separation of IPs [6,7]. So far, CZE of IPs using indirect UV detection

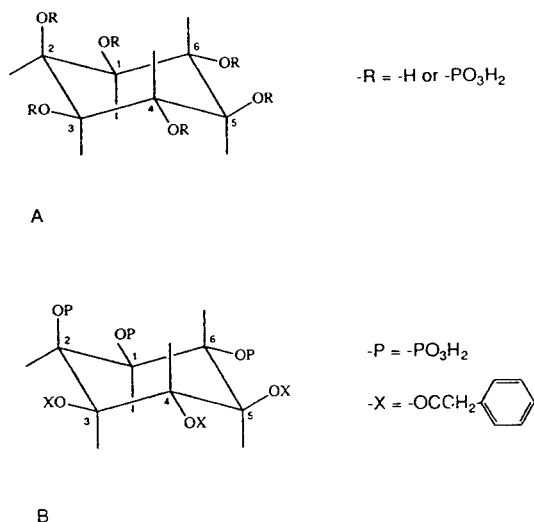


Fig. 1. Chemical structure of inositol phosphates: inositol mono- ( $M_r$  260), bis- ( $M_r$  340), tris- ( $M_r$  420), tetrakis- ( $M_r$  500) and hexakisphosphate ( $M_r$  660) (A) and phenylacetate-IP3 (PIP3) ( $M_r$  774) (B) in the hydrated form.

\* Corresponding author.

has been described. Indirect detection techniques, based on either UV absorbance, fluorescence or amperometric detection, have the disadvantage of increased noise levels and therefore relatively high detection limits. Next to CZE separation of IPs, capillary isotachopheresis (CITP) with conductivity detection has been described [8]. In CITP quantitation of low concentrations is rather limited because zone length instead of peak area or peak height of a compound is related to the amount in the sample volume injected. Sensitive detection of IPs is still problematic. Therefore, alternative detection methods have to be developed for their determination.

Until now, mass spectrometric detection of IPs has been performed using either continuous-flow fast atom bombardment (CF-FAB) or gas chromatography–electron impact ionization mass spectrometry (GC–EI-MS) after per-trimethylsilyl derivatization of the analytes [9]. The detection limits were ca. 10 nmol for 1,4,5-inositol trisphosphate and 1,4-inositol bisphosphate (CF-FAB) and 0.1 pmol for 1-inositol monophosphate (GC–EI-MS).

On-line capillary electrophoresis–mass spectrometry (CE–MS) has been described first in 1987 by Olivares et al. [10]. Since then, quite a number of publications on CE–MS have appeared. Thus far, three types of interfaces have been used for on-line CE–MS, i.e. CF-FAB [11], electrospray [12–16] and ionspray [17]. In addition, CE has been coupled with matrix-assisted laser desorption ionization (MALDI)-MS in the off-line mode [18].

This paper describes the mass spectrometric detection of IPs in the negative ionization mode after CZE separation, without the need of analyte derivatization. The developed method is also applicable for a synthesized IP3 derivative and its impurities with respect to both structure confirmation/elucidation and determination of the synthesis yield. A custom-made electrospray interface was used for the introduction of the column effluent into the mass spectrometer. In order to suppress electroosmotic flow, the capillary wall was coated with polyacrylamide [19].

## 2. Experimental

### 2.1. Chemicals

Acetic acid p.a. and methanol were obtained from J.T. Baker (Deventer, Netherlands). Ammonium acetate p.a. was purchased from Merck (Darmstadt, Germany). All IPs, e.g. inositol monophosphate (2-IP1) as dicyclohexylammonium salt and inositol bis- (1,2-IP2), tris- (1,2,6-IP3), tetrakis- (1,2,5,6-IP4), hexakisphosphate (IP6) and phenylacetate-IP3 (PIP3) (Fig. 1B) as sodium salts, were supplied by Perstorp Pharma (Perstorp, Sweden). For the preparation of the stock solutions of the analytes and buffer solutions, deionized water was used (Milli-Q system, Millipore, Bedford, MA, USA). For the polyacrylamide coating, 3-(trimethoxysilyl)propylmethacrylate, 98% (Janssen, Beerse, Belgium), tetramethylethylenediamine (TEMED) and ammonium persulphate (Bio-Rad, Richmond, CA, USA) and acrylamide (Merck-Schuchardt, Hohenbrunn, Germany) were used.

### 2.2. Procedures

#### Sample pretreatment

An amount of 500  $\mu$ l of blank plasma, spiked to concentrations of either 20 or 200  $\mu$ M IP3 was applied to AMICON sets (Amicon, Danvers, USA), consisting of a donor and acceptor compartment separated by filter with cut-off of  $M_r$  30 000. Ultrafiltration was performed using an ultracentrifuge type JA-20 (Beckman, Fullerton, CA, USA) with fixed angle rotor (34°) at 2000 g for 30 min. The ultrafiltrate was injected into the CZE capillary.

#### Capillary coating

Before the fused-silica capillaries (BGB, Rothenfluh, Switzerland) were coated, they were rinsed for 5 min with 0.1 M sodium hydroxide p.a. (Merck), Milli-Q water and ethanol p.a. (Merck). Subsequently, the polyacrylamide coating procedure according to Hjerten [19] was performed.

### 2.3. Capillary zone electrophoresis

The experiments were performed using a programmable injection system and power supply (Prince, Lauerlabs, Emmen, Netherlands). The electrophoresis buffer was prepared freshly every day and consisted of ammonium acetate (10 mM, pH 5)–methanol (90:10, v/v). The length of the fused-silica capillaries (100  $\mu\text{m}$  I.D. and 170  $\mu\text{m}$  O.D., unless stated otherwise) was 0.85 m. At the capillary inlet, a voltage of  $-28$  kV and in conjunction, a pressure of 10 mbar was applied. Before each run, the capillary was rinsed with electrophoresis buffer for 2 min. Pressurized (200 mbar) sample injection was applied for 0.10 min, corresponding to 250 nl (75  $\mu\text{m}$  I.D.) or 450 nl (100  $\mu\text{m}$  I.D.)

### 2.4. Electrospray mass spectrometry

All experiments were carried out on a triple quadrupole mass spectrometer (Finnigan MAT TSQ-70) equipped with a custom-made electrospray interface that fitted in the thermospray source [20]. Most of the experiments were done in the negative ionization mode: the electrospray (ES) needle was kept at  $-3.5$  kV with respect to the grounded heated sampling capillary. When operated in the positive ion mode, the ES needle was set at  $+3.5$  kV. The sampling capillary and the ion source were kept at 175 respectively 150°C. A slightly negative voltage was applied on the repeller for signal optimization of all ions. After removal of the polyimide layer at the capillary tip, the outlet of the fused-silica capillary was inserted into the stainless-steel needle assembly, slightly ahead of the needle tip. The sheath liquid consisted of ammonium acetate (100 mM, pH 5)–methanol (10:90, v/v) delivered at a flow-rate of 1–2  $\mu\text{l}/\text{min}$  by a Model 2400 syringe pump (Harvard Apparatus, Edinbridge, UK).

### 2.5. Nuclear magnetic resonance

The  $^{31}\text{P}$  NMR spectrum of 2 mg phenylacetate-IP3, dissolved in 0.5 ml  $^2\text{H}_2\text{O}$ ,

was obtained on a Bruker DMX-600 spectrometer (Karlsruhe, Germany).

## 3. Results and discussion

### 3.1. Capillary zone electrophoresis

Depending on the number of phosphate groups, IPs (Fig. 1) have multiple negative charges resulting in high electrophoretic mobilities in the direction of the anode. As the electroosmotic flow (EOF) is in the cathodic direction, net electrophoretic velocities are rather low, implying unacceptably long migration times. Therefore, the EOF must be suppressed using capillaries with either a static or dynamic coating of the wall. In first instance, hydroxypropylmethylcellulose (HPMC), a neutral hydrophilic polymer, was added to the electrophoresis buffer. However, this compound appeared to be incompatible with mass spectrometric detection because of contamination of the ion source. Moreover, the HPMC coating was destroyed when using an organic modifier, e.g. methanol or acetonitrile, as additive in the electrophoresis buffer. The polyacrylamide coating described by Hjerten [19] appeared to be a good alternative. This coating is static, which reduces the risk of ion-source contamination. Furthermore, the coating is compatible with the use of organic modifiers in the electrophoresis buffer and the EOF is substantially reduced. As a consequence of EOF suppression, CZE of IPs has been performed with reversed polarity: the capillary inlet is at  $-28$  kV and the outlet (ES needle) at  $-3.5$  kV.

For the coupling of CZE and MS via an electrospray interface, a buffer must be chosen which is a compromise between aqueous (favourable for CZE of IPs) and non-aqueous (favourable for ES-MS). As CZE buffer, ammonium acetate was chosen, which was appropriate regarding the separation of IPs as well as the required volatility for ES-MS. In order to increase the buffer volatility even more, both methanol and isopropanol were examined as

additives. At comparable modifier content, isopropanol gave longer migration times of the IPs than methanol, caused by its higher viscosity. Therefore, methanol was chosen as modifier.

Resuming, both the not completely suppressed EOF in the cathodic direction (capillary inlet) and the organic modifier as buffer additive lead to an increase of the migration times of the IPs. To compensate for this effect, pressure-assisted CZE can be performed. Compared with conventional CZE, this may lead to decreased efficiencies, caused by the hydrodynamic flow profile. Nevertheless, during all experiments a slight pressure was applied in addition to the high voltage.

### 3.2. Electrospray-mass spectrometry

In order to investigate the electrospray performance and signal intensity as a function of the sheath liquid composition continuous-infusion-ES-MS experiments of PIP3 were carried out in the negative and positive ionization mode. The electrospray technique is most stable at high organic modifier content, whereas the CZE separation of IPs is optimal without any organic modifier in the buffer at all. The highest organic modifier content in the CZE buffer which was still acceptable in terms of migration times and peak shape appeared to be 30% methanol. Therefore, an initial sheath liquid of ammonium acetate (10 mM, pH 5)–methanol (70:30, v/v) was chosen for the continuous infusion of PIP3 in the negative ionization mode. Although the spray performance appeared to be satisfactory, the IP3 derivative could not be detected at all. In the positive ionization mode with the same sheath liquid composition, however, a mass spectrum of PIP3 could be obtained. The spectrum mainly consisted of the  $[M + H]^+$ ,  $[M + NH_4]^+$  and  $[M + Na]^+$  peaks (not shown). In the negative ionization mode, a mass spectrum could not be acquired, unless the sheath liquid contained at least 90% organic modifier. The spectrum principally showed the  $[M - H]^-$  peak of PIP3 and some impurities. Therefore, all experiments have been performed in the negative ionization mode using a sheath liquid consisting

of ammonium acetate (100 mM, pH 5)–methanol (10:90, v/v). In addition to the ES-MS experiments, ES-MS–MS of PIP3 in the negative ionization mode was investigated. The observed loss of 98 u corresponds to the cleavage of one  $H_3PO_4$  from the IP3 derivative.

Besides for PIP3, a mass spectrum for 50  $\mu M$  IP3 has also been obtained in the continuous-infusion mode (Fig. 2). The main peak observed is  $[M - H]^-$  ( $m/z$  419). ES-MS–MS experiments of IP3 gave results comparable to those for PIP3: the loss of 98 u, corresponding with  $H_3PO_4$ . Based on the results obtained during the continuous-infusion experiments the initial conditions in the CZE–ES-MS experiments could be readily chosen.

### 3.3. Capillary zone electrophoresis–electrospray mass spectrometry

When the outlet of the CZE capillary was inserted in the electrospray needle and a high voltage of  $-28$  kV was applied, the voltage on the needle tip increased from  $-3.5$  to ca.  $-4.2$  kV. This phenomenon has also been observed by Perkins and Tomer [21], who explained it as a result of conductivity through the column. This increase of the ES voltage was even more pronounced when samples with high conductivity (e.g. plasma) were analyzed. In that case, a total breakdown of the electrospray was observed which necessitated the use of lower voltages, e.g.  $-20$  kV instead of  $-28$  kV.

Based on the results obtained with the continuous-infusion ES-MS experiments of PIP3 a multiple-ion detection (MID) procedure was designed. CZE–ES-MS of a concentrated (2 mM) and a 1:10 diluted solution of PIP3 was carried out. Fig. 3 shows that in the concentrated sample (Fig. 3A) more impurities than in the 1:10 diluted sample (Fig. 3B) can be detected. The impurity with  $m/z$  575 has come below the limit of detection in Fig. 3B. By injecting the IP3 derivative and impurities at lower concentrations, the peak shape of the analytes was substantially improved (Fig. 3B). Next to the impurities with  $m/z$  809 and 851, a PIP3 adduct has been detected. The ratios of the impurities and



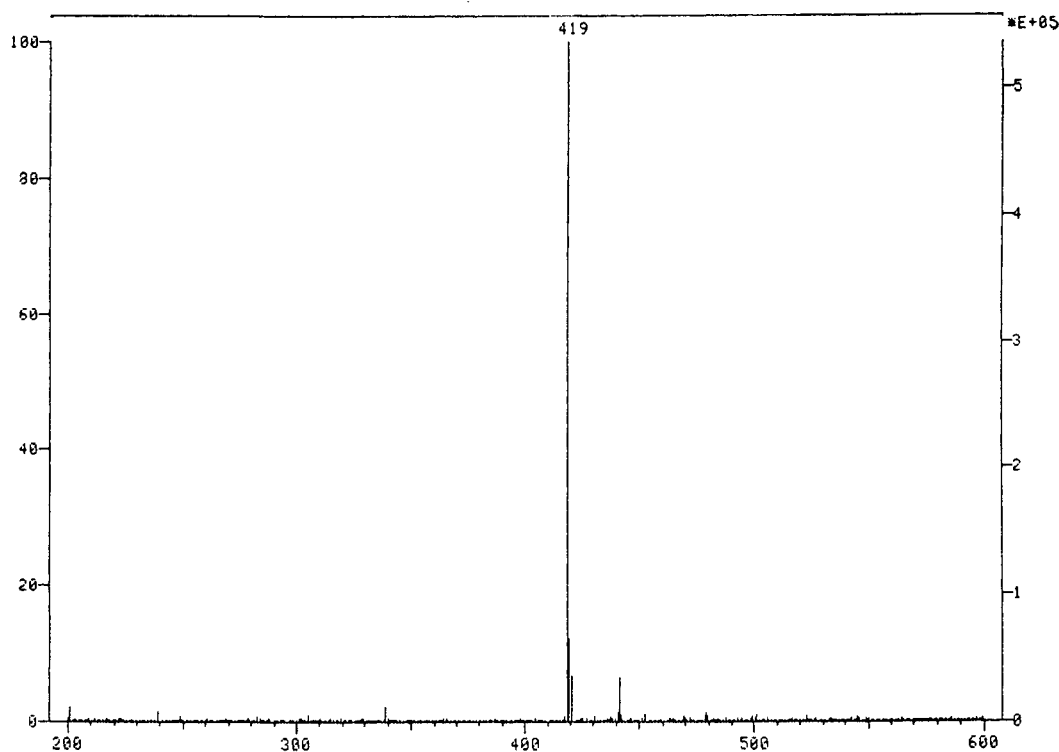


Fig. 2. Electrospray mass spectrum of 1,2,6-inositol trisphosphate in the continuous-infusion mode. Conditions: sheath liquid, ammonium acetate (100 mM, pH 5)–methanol (10:90, v/v), 2  $\mu$ l/min; concentration IP3, 50  $\mu$ M.

PIP3 adduct appear to differ depending on the concentration injected. Probably, the ionization characteristics are dependent on the local conductivities. So far, the masses of the IP3 derivative and the impurities could be determined using CZE–ES–MS. In addition, CZE–ES–MS–MS of PIP3 and some impurities has been performed for further structure elucidation. Fig. 4 shows possible structures for some of the impurities. Structure proposals are based on (i) the mass determination (MS), (ii) the presence of  $H_3PO_4$  in the molecules (MS–MS) and (iii) on the migration times (electrophoretic mobilities) in the mass electropherogram.

For the determination of the synthesis yield, the peak area of PIP3 was compared with the peak areas of the impurities. Using this parameter, the synthesis yield was 74–85%, depending on the injected analyte concentration. One has to realize, however, that the IP3 derivative and the impurities do not have exactly the same

response factors. Unfortunately, these factors cannot be determined as the analytes as such are not available. Nevertheless, assuming equal response factors the purity of PIP3 can be estimated. A complementary technique, NMR, has been performed to confirm the estimated purity. The NMR integrals of the main compound were compared with those of the (P-containing) impurities: the calculated purity was 80%. This is in good agreement with the CZE–MS results, which makes this value quite reliable.

A mixture of IP1, IP2, IP3, IP4 and IP6, all at a concentration of ca. 20  $\mu$ M, was analyzed using CZE–ES–MS. IP5, which is the first degradation product of IP6, was not present in the mixture because, in contrast to the other IPs, IP5 is rather unstable. The result is depicted in Fig. 5. The  $[M - H]^-$  ions of IP1 to IP4 and IP6 have been detected. Most of the peaks are symmetrical. At higher concentrations, however, e.g. 200  $\mu$ M, fronting (IP3–IP6) and tailing (IP1) peaks

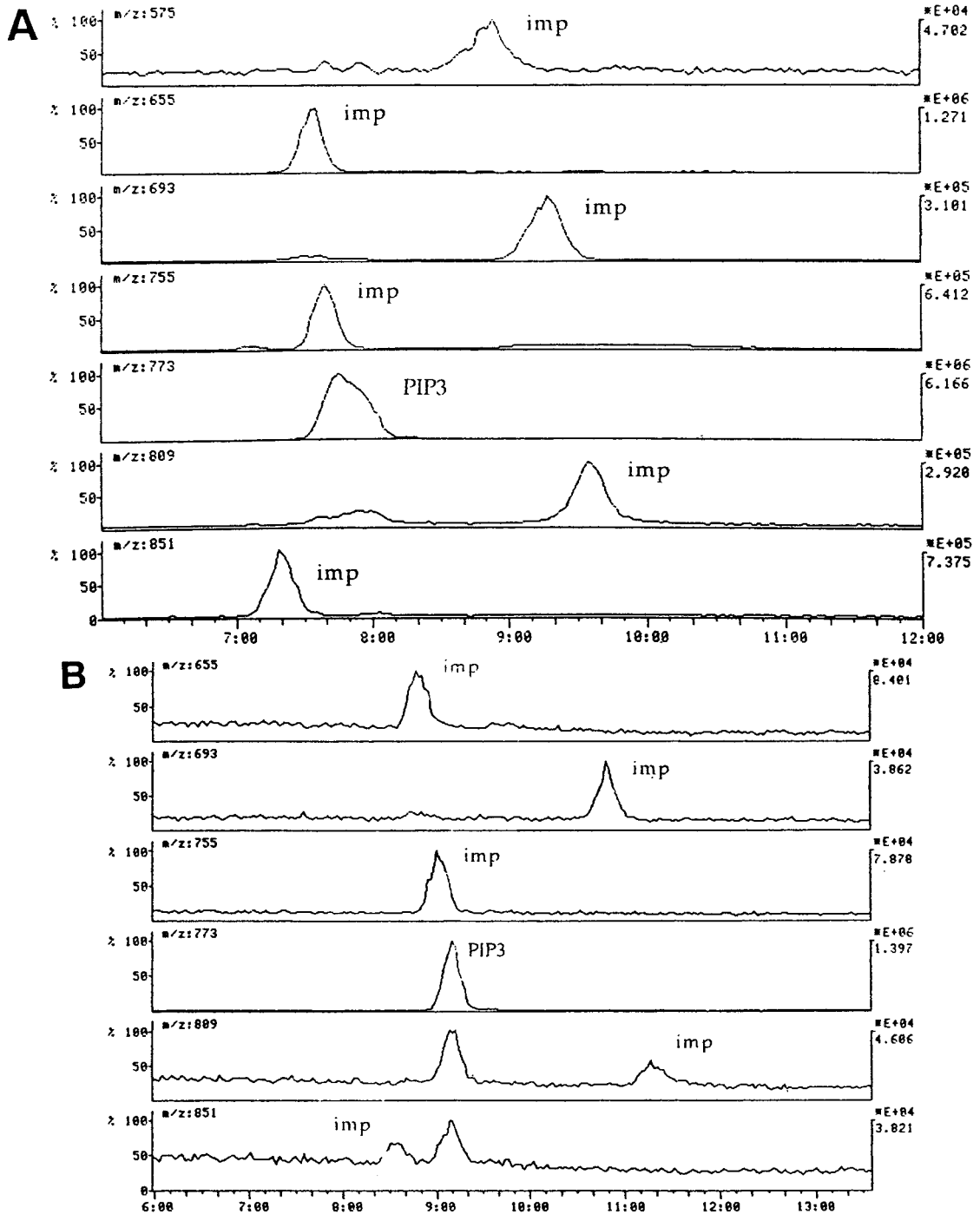


Fig. 3. Mass electropherogram of PIP3 and its impurities. Conditions: polyacrylamide-coated fused-silica capillary, 75 μm I.D., 150 μm O.D.; high-voltage capillary inlet, -28 kV; pressure, 25 mbar; height difference between capillary inlet and ES needle, 5 cm; concentration IP3 derivative, 2 mM (A), respectively 200 μM (B).

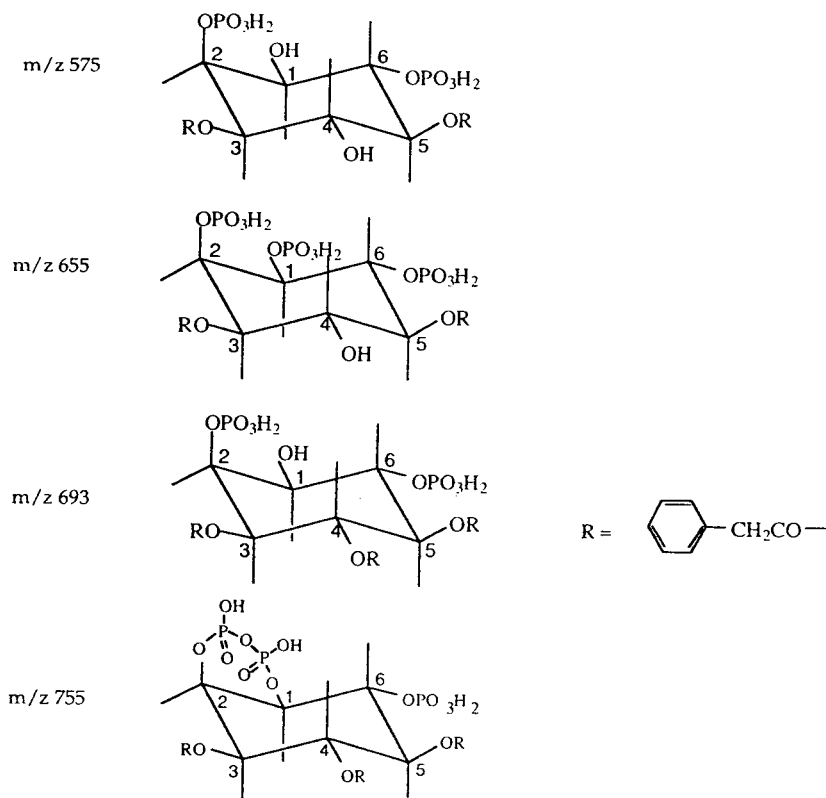


Fig. 4. Structure elucidation of impurities of PIP3.

were more pronounced, which is the result of electromigration dispersion. Only IP2, with an electrophoretic mobility similar to the background electrolyte, had a symmetrical peak shape.

Qualitatively, the developed method appeared to be reproducible: during several days the same mass electropherogram has been obtained. Regarding the quantitative aspects, however, there are some deficiencies. Inter-day reproducibility with respect to the sensitivity is not completely satisfying, which can be overcome by using an internal standard. Furthermore, sensitivity differences between the IPs were observed: at a comparable concentration, the signal-to-noise ratios of the IPs differed substantially, implying different detection limits for the different IPs. Possibly, this is the consequence of working under MID conditions, considering the singly charged ions only. For IP2 and IP3, a con-

centration of  $2 \mu M$  (absolute amount 0.9 pmol) could still be detected, whereas the detection limits for IP1, IP4 and IP6 are between 2 and  $20 \mu M$ .

### 3.4. Bioanalytical aspects

Eventually, IP3 and its derivatives have to be determined in plasma and urine samples, requiring a sensitive determination method. Preliminary results show that the developed method can be used for the analysis of IP3 in plasma. After the plasma sample was spiked with IP3 to a concentration of  $200 \mu M$  and pretreated by ultrafiltration, the ultrafiltrate was injected into the CZE capillary. Although the free fraction of IP3 in plasma is below 10%, a mass electropherogram of the ultrafiltrate could be obtained by using CZE-MS-MS (Fig. 6). A loss of 98 and

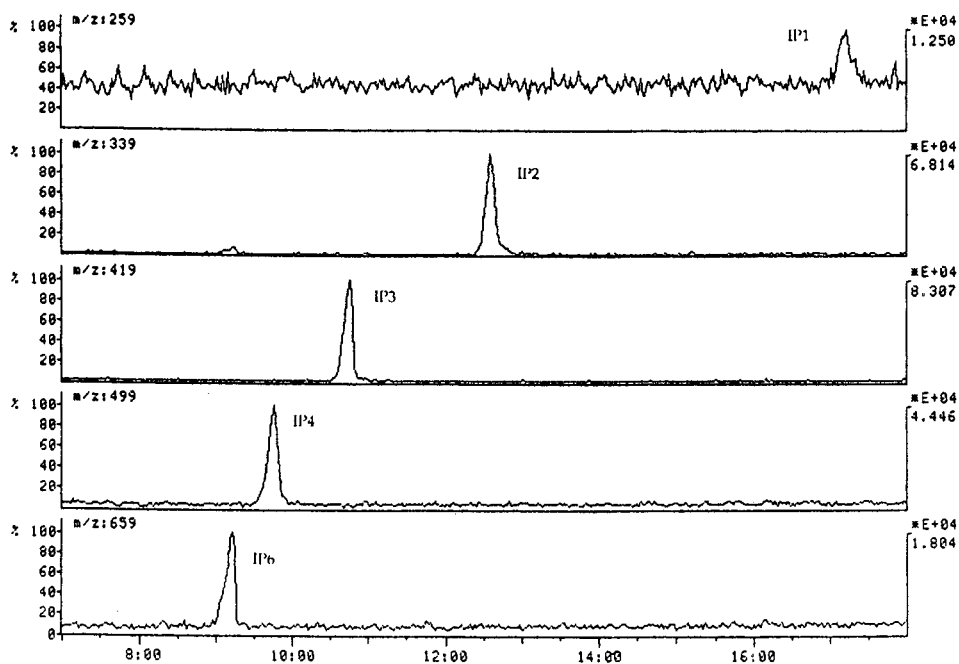


Fig. 5. Mass electropherogram of IP1, IP2, IP3, IP4 and IP6. Conditions: high-voltage capillary inlet,  $-28$  kV; pressure, 10 mbar; concentrations inositol phosphates,  $20 \mu\text{M}$ .

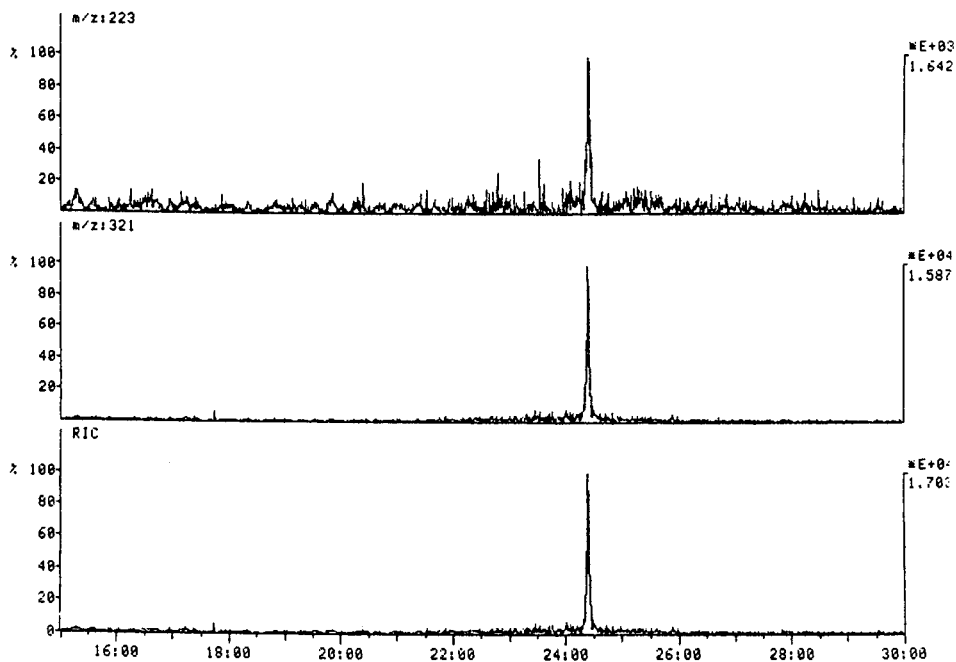


Fig. 6. CZE-ES-MS-MS of IP3 in plasma, pretreated with ultrafiltration. Conditions: high-voltage capillary inlet,  $-20$  kV; pressure, 10 mbar; concentration of IP3 in plasma,  $200 \mu\text{M}$ .

196 u has been observed, which correlates with a subsequent loss of  $H_3PO_4$  (twice).

The developed method can be applied for the determination of IP3 in plasma, but IP3 concentrations in real-life samples will be in the nanomolar range. In order to improve the method for bioanalysis, the protein binding of IP3 must be decreased substantially to increase the recovery of the sample pretreatment. A second approach will be the application of a concentrating technique prior to CZE. For this purpose, isotachopheresis (ITP) can be combined with CZE [13,22–25].

#### 4. Conclusions

The developed method, using CZE–ES-MS (–MS), appears to be applicable for the determination of IPs and analogues without the need of derivatization. The structures of a synthesized IP3 derivative and its impurities have been confirmed and elucidated. The yield of the IP3 synthesis could be well estimated.

Preliminary results show that the determination of IP3 in plasma can be performed after a sample pretreatment consisting of ultrafiltration. For the bioanalysis of real-life samples, however, the sensitivity must be improved. Therefore, future research will be devoted to improvement of the recovery of the sample pretreatment by breaking the plasma protein–analyte bond. Furthermore, on-line concentrating techniques will be considered.

#### References

- [1] M.J. Berridge, *Sci. Am.*, 253 (1985) 124.
- [2] W. Haug and H.-J. Lantsch, *J. Sci. Food Agric.*, 34 (1983) 1423.
- [3] H. Irth, M. Lamoree, G.J. de Jong, U.A.Th. Brinkman, R.W. Frei, R.A. Kornfeldt and L. Persson, *J. Chromatogr.*, 499 (1990) 617.
- [4] J. Meek, *Proc. Natl. Acad. Sci. USA*, 83 (1986) 4162.
- [5] C.W. Ford, *J. Chromatogr.*, 333 (1985) 167.
- [6] A. Henshall, M.P. Harrold and J.M.Y. Tso, *J. Chromatogr.*, 608 (1992) 413.
- [7] B.A.P. Buscher, H. Irth, E. Andersson, U.R. Tjaden and J. van der Greef, *J. Chromatogr. A*, 678 (1994) 145.
- [8] P. Blatny, F. Kvasnicka and E. Kenndler, *J. Chromatogr. A*, 679 (1994) 345.
- [9] W.R. Sherman, K.E. Ackerman, R.A. Berger, B.G. Gish and M. Zinbo, *Biomed. Environ. Mass Spectrom.*, 13 (1986) 333.
- [10] J.A. Olivares, N.T. Nguyen, C.R. Yonker and R.D. Smith, *Anal. Chem.*, 59 (1987) 1232.
- [11] R.D. Minard, D. Chin-Fatt, P. Curry, Jr. and A.G. Ewing, Presented at the 36th ASMS Conference on Mass Spectrometry and Allied Topics, June 5–10, 1988, San Francisco, CA, ASMS, Santa Fe, NM, p. 950.
- [12] W.M.A. Niessen, U.R. Tjaden and J. van der Greef, *J. Chromatogr.*, 636 (1993) 3.
- [13] M.H. Lamoree, N.J. Reinhoud, U.R. Tjaden, W.M.A. Niessen and J. van der Greef, *Biol. Mass Spectrom.*, 23 (1994) 339.
- [14] A.J. Tomlinson, L.M. Benson, J.W. Gorrod and S. Naylor, *J. Chromatogr. B*, 657 (1994) 373.
- [15] W. Weinmann, C. Maier, K. Baumeister, M. Przybylski, C.E. Parker and K.B. Tomer, *J. Chromatogr. A*, 664 (1994) 271.
- [16] K.J. Rosnack, J.G. Stroh, D.H. Singleton, B.C. Guarino and G.C. Andrews, *J. Chromatogr. A*, 675 (1994) 225.
- [17] F.Y.L. Hsieh, J. Cai and J. Henion, *J. Chromatogr. A*, 679 (1994) 206.
- [18] P.A. van Veelen, U.R. Tjaden, J. van der Greef, A. Ingendoh and F. Hillenkamp, *J. Chromatogr.*, 647 (1993) 367.
- [19] S. Hjerten, *J. Chromatogr.*, 347 (1985) 191.
- [20] R.A.M. van der Hoeven, B.A.P. Buscher, U.R. Tjaden and J. van der Greef, *J. Chromatogr.*, 712 (1995) 211.
- [21] J.R. Perkins and K.B. Tomer, *Anal. Chem.*, 66 (1994) 2835.
- [22] D.S. Stegehuis, H. Irth, U.R. Tjaden and J. van der Greef, *J. Chromatogr.*, 538 (1991) 393.
- [23] N.J. Reinhoud, U.R. Tjaden and J. van der Greef, *J. Chromatogr.*, 627 (1993) 263.
- [24] N.J. Reinhoud, U.R. Tjaden and J. van der Greef, *J. Chromatogr. A*, 653 (1993) 303.
- [25] D. Kanianski and J. Marak, *J. Chromatogr.*, 498 (1990) 191.





ELSEVIER

Journal of Chromatography A, 712 (1995) 245–252

---

---

JOURNAL OF  
CHROMATOGRAPHY A

---

---

# Optimization of conditions for the analysis of a peptide mixture and a tryptic digest of cytochrome *c* by capillary electrophoresis–electrospray-ionization mass spectrometry with an improved liquid-sheath probe

J. Fred Banks, Jr.

*Analytica of Branford, Inc., 29 Business Park Drive, Branford, CT 06405, USA*

---

## Abstract

Capillary electrophoresis (CE) has been interfaced with a quadrupole mass spectrometer using electrospray (ES) ionization in order to rapidly analyze a peptide mixture and a tryptic map of cytochrome *c*. A sheath liquid probe has been developed which allows the easy connection of CE with ES and the manipulation of important experimental parameters such as the position of the CE column exit relative to the sheath flow tube exit. In addition, the atmospheric region of the ion source has been modified so that glass windows replace the walls of the chamber, and the electrospray process itself is fully visible during operation. Detection limits for a biologically active peptide, leucine enkephalin, were determined to be 200 fmol in the scan mode of operation and 1.5 fmol in the selected-ion monitoring mode of operation.

---

## 1. Introduction

Electrospray (ES) ionization has become widely used as an interface between liquid chromatography (LC) separation techniques and mass spectrometry (MS) detection. The reasons for this success include the ability of ES ionization sources to both ionize and desolvate from solution the analytes of interest. Frequently, these compounds are polar, fragile, thermally-labile species which are subject to decomposition by conventional ionization methods. The “soft” ionization process of ES allows for the creation of ions and successful transfer from the liquid to the gas phase of important biological species,

such as proteins, which weigh up to several hundred thousand daltons.

Alternatively, the use of ES ionization for mass detection with capillary electrophoresis (CE) has not yet become well-established even though it has been demonstrated on quadrupole [1–7], magnetic sector [8,9], Fourier transform ion cyclotron resonance (FTICR) [10] and time-of-flight (TOF) machines [11]. The primary reason for this is the additional technical challenges associated with CE–ES coupling. First, the outlet of the CE column is fused-silica, a dielectric material which itself cannot be electrically incorporated into the ES-MS system. Electrical connection with the CE column outlet is

mandatory for both the CE and the ES processes. Secondly, the buffers most commonly employed with CE separations are aqueous and high in salt concentrations. Both of these solution characteristics are unsuitable for ES operation.

An initial solution for this dilemma was offered by Smith and co-workers [1–3] with the use of a co-axial sheath flow arrangement which provides for both the electrical connection and the addition of a solution more amenable to ES ionization. Since that time, other techniques have been developed which accomplish these goals as well. These arrangements include: (i) the use of a metal-coated, sharpened CE column outlet [4,12], (ii) the use of a gold wire electrode inserted into the CE column outlet [11], and (iii) a liquid-junction interface [6,13]. The metal-coated CE column tip has the advantage that no sheath flow is needed and thus no sample dilution occurs. It has the disadvantages, however, that ES compatible buffers must be used with the CE separation and that specialized CE columns must be prepared. The use of an inserted gold wire electrode requires neither sheath flow nor a specialized CE column. It does, however, imply the somewhat cumbersome and challenging correct placement of the electrode as well as the use of ES compatible buffers with the CE separation. Finally, the liquid-junction technique uses an additional buffer reservoir to electrically isolate the dielectric CE column outlet and a conductive metal ES needle. This method requires the careful alignment of CE column outlet and ES needle.

Because of the inherent advantages and ease of operation of the sheath flow approach, we have developed a convenient probe based on this concept and used it to demonstrate the separation by CE of biologically active peptides with ES-MS detection using a quadrupole instrument. Most importantly, this probe incorporates a translation device which gives the user the ability to easily adjust the CE column exit relative to the sheath flow tube exit so that this crucial parameter can be easily optimized for maximal performance. In addition, the atmospheric chamber where ES actually occurs has been

modified so that windows are present, and the ES process can be viewed during operation.

## 2. Experimental

### 2.1. CE

The CE instrument used was an ATI (Boston, MA, USA) crystal 300 model with a four-position sampler. The CE column was fabricated from fused-silica, 75  $\mu\text{m}$  I.D.  $\times$  365  $\mu\text{m}$  O.D. from Polymicro Technologies (Phoenix AZ, USA) and was 1 meter in length. A potential of 30 kV was used for all separations except for the tryptic map where 15 kV was used. The sheath flow was delivered with a Harvard Apparatus Model 11 syringe pump (South Natick, MA, USA) and was pure methanol in all cases.

### 2.2. ES

The electrospray ionization source (Fig. 1) was from Analytica (Branford, CT, USA). This system was unaltered from its original form except for the use of a new CE–ES probe. Large windows on three sides of the atmospheric region of the source (P1) allowed for the visualization of the electrospray process itself and greatly aided in the optimization of instrumental conditions necessary to obtain good results. The source was used with the CE column exit at ground potential, the cylinder electrode ( $V_{\text{cyl}}$ ) at  $-2500$  volts (V), the endplate electrode ( $V_{\text{end}}$ ) at  $-3700$  V and the capillary entrance ( $V_{\text{cap}}$ ) at  $-4500$  V. The use of a dielectric capillary having metal coating on both ends to transfer the ions generated from atmosphere into vacuum is important in this case as it allows for the CE column exit to be maintained at ground potential. ES source designs which depend on the application of a positive voltage to the spray needle itself have two disadvantages when CE is used. First, the CE column exit must be floated at the required ES potential (several kV) causing the resulting electric field applied to the CE capillary to be the difference between the applied CE voltage and the ES voltages. Secondly,



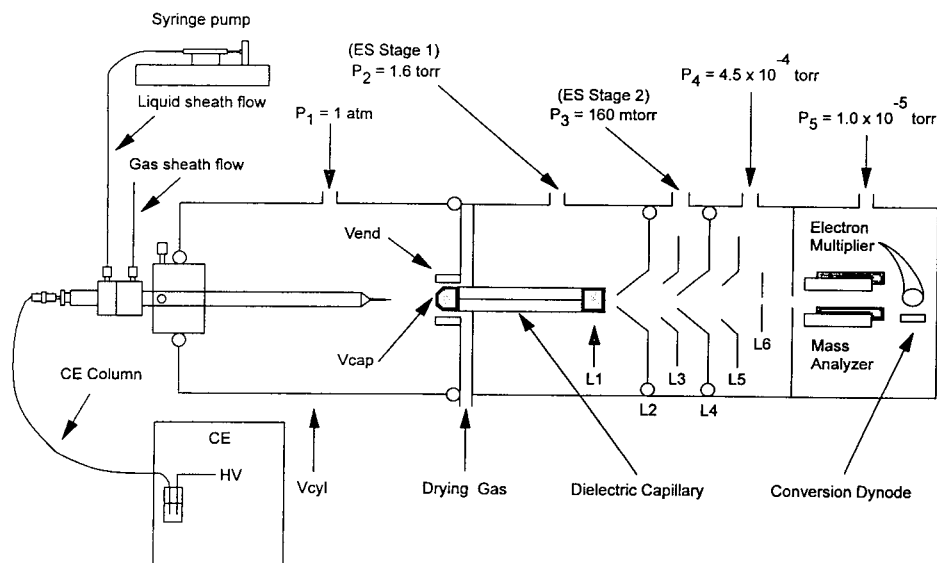


Fig. 1. Schematic of CE-ES-MS system.

if the ES source is operational during the injection phase and subsequent vial movements, the sample loaded on the capillary will have a tendency to migrate back out of the capillary entrance and be diluted in the final run buffer before the voltage can be applied to the run buffer. This phenomena has the potential to greatly reduce sensitivity, make quantitation difficult and degrade the separation quality.

The sheath flow CE probe which was constructed consisted of a 3-layer coaxial arrangement where the CE column exit was the center or first layer. The second layer or sheath liquid flow needle was a piece of stainless-steel tubing, 0.0160 in. I.D.  $\times$  0.0280 in. O.D., and was just large enough to allow passage of the CE fused-silica capillary. The third layer or gas flow needle was another piece of stainless-steel tubing, 0.0325 in. I.D.  $\times$  0.0425 in. O.D. The modest gas flow used (50 ml/min) served only to cool the needle and did not affect the electrospray process itself. This gas flow may find additional use with negative ion ES where a bath gas of SF<sub>6</sub> or O<sub>2</sub> is helpful to suppress the occurrence of a corona discharge in the source. Most importantly, this probe allows for the easy manipulation of the relative distance between the CE column exit

and the sheath flow tube exit through the use of an incorporated translation device which does not apply torsional stress to the CE column during adjustment.

### 2.3. MS

The mass spectrometer used was an HP 5989A MS Engine from Hewlett-Packard (Palo Alto, CA, USA). ES control was accomplished through the use of a digital interface. In the scan mode of operation, the  $m/z$  range was scanned from 100–1000  $m/z$  units at the rate of 1000  $m/z$  per second (s). One sample was collected at each 0.1  $m/z$  point with an integration time of 100  $\mu$ s. In the selected-ion monitoring (SIM) mode of operation, the  $m/z$  value selected was used with a dwell time of 100 ms.

### 2.4. Materials

Buffers were prepared from distilled water obtained from a Barnstead NANOpure II (Boston, MA, USA) system. Acetic acid, ULTREX II Ultrapure Reagent Grade, was purchased from J. T. Baker (Phillipsburg, NJ, USA). Methanol was obtained from Mallinckrodt

(Paris, KY, USA). All solvents were filtered through Nylon 66 membranes from the Anspec (Ann Arbor, MI, USA). Peptide and protein samples were purchased from Sigma (St. Louis, MO, USA) as was trypsin and ammonium carbonate.

## 2.5. Methods

The cytochrome *c* tryptic map was prepared by dissolving 1 mg or 80 nmoles of horse heart cytochrome *c* in 200  $\mu$ l of a 50 mmol solution of ammonium carbonate buffer (pH = 8.1 by ammonium hydroxide addition). Then 2  $\mu$ l of a 1 mg/ml solution of trypsin (in the same buffer as above) was added to the solution. The mixture was incubated for 14 h at 37°C. The reaction was halted by the addition of 1  $\mu$ l of trifluoroacetic acid and the resultant mixture lyophilized and reconstituted in the same volume of water.

## 3. Results and discussion

### 3.1. CE buffer composition

The first experimental variable examined was the effect of CE buffer salt concentration. In all cases, acetic acid was used as a CE buffer due to its volatility. Fig. 2 shows the effect in the MS total ion current (TIC) of a separation of peptides when using 0.010, 0.050 and 0.100 M acetic acid in water as the CE buffer. Here, 500 fmol of each peptide were applied to the CE column while the mass analyzer was scanned from 100–1000 *m/z* units. Several observations on this data are noteworthy. As the concentration of acetic acid was increased, the overall migration times for the peptides increased slightly, due to an associated decrease in the electro-osmotic flow through the column. Also, although the peak widths did not change, the migration times of the analytes were differentially affected by the increasing buffer concentration so that varying

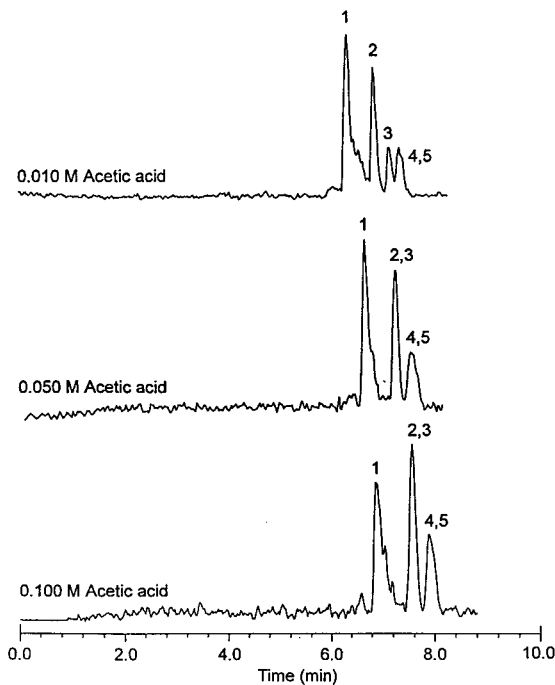


Fig. 2. Effect of acetic acid concentration in the CE buffer on MS TIC from a peptide separation. Peaks: 1 = angiotensin II; 2 = Val-Tyr-Val; 3 = leucine enkephalin; 4 = Gly-Tyr; and 5 = methionine enkephalin.

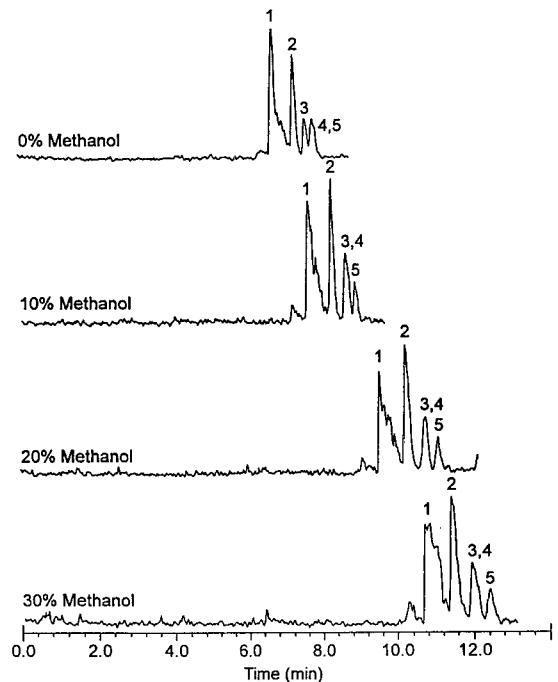


Fig. 3. Effect of methanol content in 0.010 M acetic acid buffer on MS TIC from peptide separation. Peaks as in Fig. 2.

instances of co-migration of peaks occurred. This might be used to an advantage in certain situations, but it was unable to improve the quality of the separation in this case. The results shown here are essentially in agreement with those of Moseley et al. [7] where the use of 0.010 M acetic acid was found to be optimum as well.

Fig. 3 shows the TIC for the separation of the same peptide mixture from above but with varying amounts of methanol in a 0.010 M acetic acid buffer. Again, a number of observations are noteworthy. First, the use of increasing amounts of methanol clearly increased the migration times of the analytes. This is the result of zeta potential alterations and viscosity increase due to the presence of methanol and has been previously demonstrated by others [14]. Also, the peak widths steadily broadened with increasing amounts of methanol. In conclusion, the addition of methanol had only negative effects on the resolution of the peaks or the quality of the separation, thus further supporting the use of a sheath flow probe which does not require the addition of methanol to the CE buffer directly.

### 3.2. Applied pressure

Fig. 4 shows the effect on the TIC of the same peptide mixture when additional pressure was applied on the CE column during the separation. The CE buffer used was 0.010 M acetic acid in water with no methanol. This effect was investigated since the ES has the potential to apply a slight vacuum on the CE column exit resulting in a net forward flow. Also, the CE column inlet must be aligned to be level with the CE column outlet and the ES system to prevent siphoning. This is sometimes difficult, although not in this case, due to the constraints of the CE system and the result may be that the particular CE unit cannot be made level with the ES system. This effect can be duplicated by the application of pressure as is done here. The results show that as the pressure was increased, the migration times of all the species decreased as expected. Also, the resolution and quality of the separation decreased as well. These results are not unexpected since the application of pressure in-

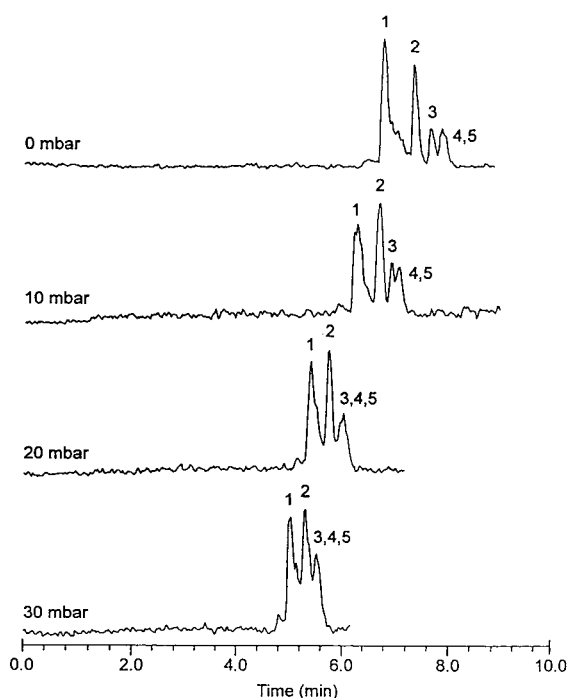


Fig. 4. Effect of applied back pressure on MS TIC from peptide separation. Peaks as in Fig. 2.

duces the LC-type parabolic flow profile that CE normally avoids.

### 3.3. Sheath flow-rate

The sheath flow is expected to dilute the CE sample zone as it passes concentrically around the CE column effluent and mixes with it. This effect was investigated by varying the sheath flow (100% methanol) rate and measuring the signal in the TIC as the leucine enkephalin ion ( $m/z = 556$ ) eluted. This signal was plotted against the sheath flow-rate in Fig. 5 and shows that increasing the sheath flow definitely decreased the ion signal measured. Because only sheath flow-rate values of 2–8  $\mu\text{l}/\text{min}$  could produce a stable electrospray, measured data were limited to this range. Comparing the ion signal at the flow-rate of 2  $\mu\text{l}/\text{min}$  and 8  $\mu\text{l}/\text{min}$  (4  $\mu\text{l}/\text{min}$  being the optimum in terms of ease of use and stability), suggested that the signal loss due to dilution of the sample zone by the sheath flow was just

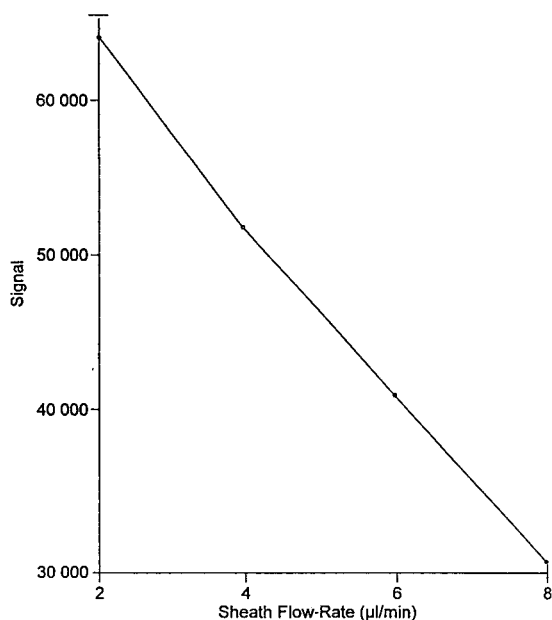


Fig. 5. Effect of sheath flow-rate (100% methanol) on leucine enkephalin ion signal. Peaks as in Fig. 2.

greater than a factor of two over the range studied.

### 3.4. Relative position of CE column exit

The only major physical adjustment which substantially affected performance when using the sheath flow system was the position of the CE column exit relative to the sheath flow exit. The electrospray is in fact defined by the physical dimensions of the sheath layer tube exit (diameter and edge thickness), and the CE column exit must be positioned so as to not interfere with the spray formation process. If the CE column is positioned too far out of the sheath flow tube then a stable spray cannot be maintained. Similarly, if the CE column exit is positioned too far towards the inside of the sheath flow tube, then again a stable spray cannot be maintained and additionally, the CE effluent is diluted greatly in the sheath flow and may even undergo some electrochemical degradation [3]. At this point the ion signal falls to zero. Fig. 6 shows the signal obtained from triplicate applications of leucine enkephalin to the CE column (optimum

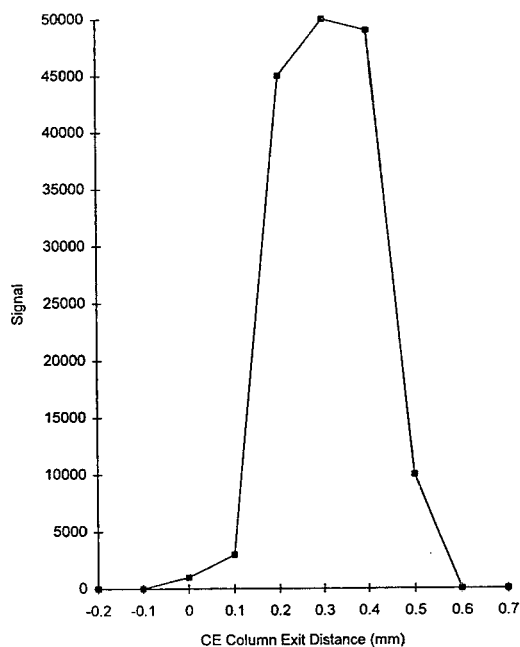


Fig. 6. Effect of distance between CE column and sheath flow tube exits. “+” values indicate that the CE column is protruding beyond the sheath tube and “-” values indicate that the CE column is retracted inside the sheath tube.

buffer conditions used) with varying distances between the CE column exit and the sheath flow tube exit. The best position for the CE column exit was found to be 0.30 mm protruding from the sheath tube. This result is supported by the work of others [3,5,7,9] who have found similar optimal distances ranging from 0.20 mm to 1.0 mm. While the previous investigators have found slight differences in the optimal position, it is important to note that all agree that the determination and maintenance of the correct relative position of the CE column exit is important to achieving satisfactory results.

### 3.5. Sensitivity

In order to determine the sensitivity of this system, leucine enkephalin was applied to the column in varying amounts while the mass spectrometer was operated in both the SIM and scan modes of operation. In the SIM mode (100 µs dwell time), the smallest amount of sample

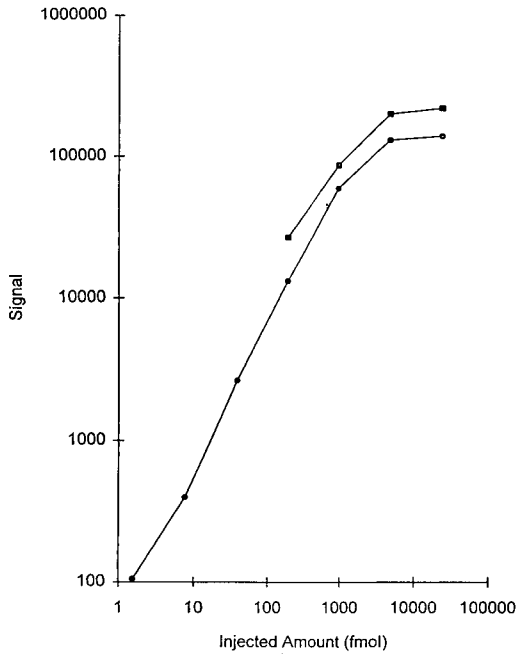


Fig. 7. Ion signal from leucine enkephalin in scan (■) and SIM (●) mode vs. amount injected.

which was detectable above the background noise at  $S/N = 3$  was 1.5 fmol. In the scan mode (100–1000  $m/z$  units at 0.1  $m/z$  intervals) the smallest amount of sample which gave rise to a visible peak in the TIC was 200 fmol. These data are plotted together in Fig. 7. Fig. 8 shows an

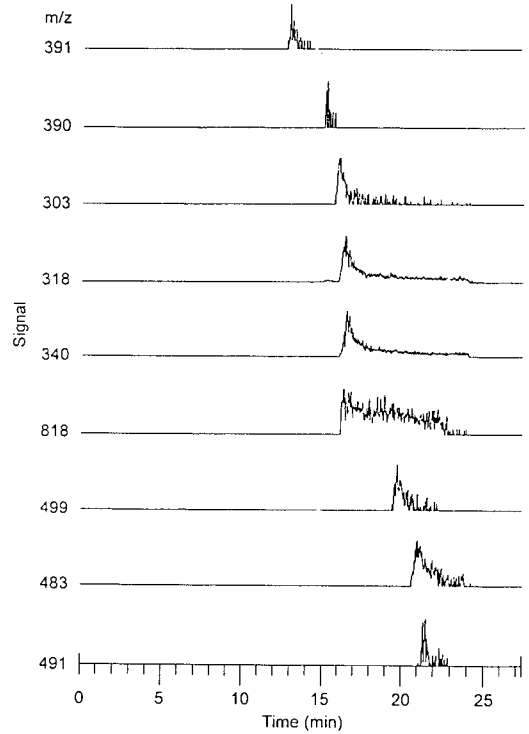


Fig. 9. Reconstructed ion currents from selected  $m/z$  values of a tryptic digest of cytochrome *c* separated by CE.

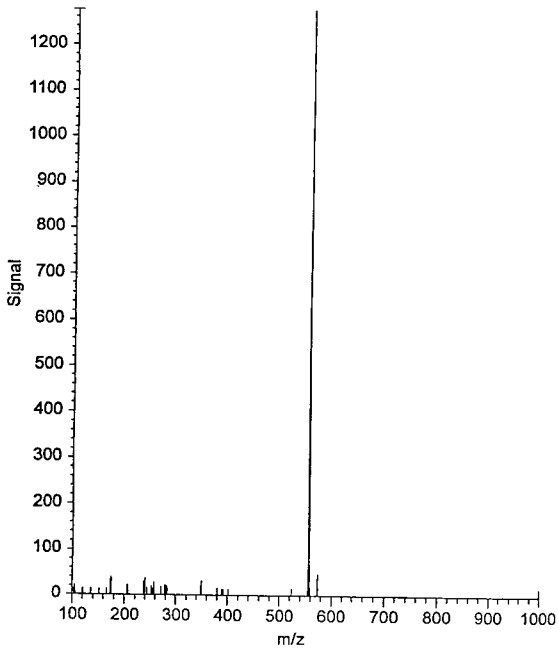


Fig. 8. Average of scans acquired during elution of 200 fmol injection of leucine enkephalin.

Table 1  
Relationship between molecular mass, charge state and observed  $m/z$  peak

Observed $m/z$ peak	Charge state	Molecular mass
391	+2	779
390	+3	1168
303	+2	604
318	+2	634
340	+2	678
818	+2	1635
499	+3	1496
483	+2	964
491	+3	1471

average of scans which were acquired during the elution of the 200 fmol application of leucine enkephalin. The molecular ion at 556  $m/z$  units is clearly visible.

### 3.6. MS analysis of a tryptic map

In order to demonstrate the use of this system with a likely application, cytochrome *c* was digested with trypsin and the resultant products subjected to analysis by CE–ES–MS. This tryptic map is represented in Fig. 9, where the reconstructed ion currents (RIC) from selected  $m/z$  values are shown for the major peptides present in the cytochrome *c* (horse) trypsin digest. All the expected peptide fragments as seen by others [15] were present. The amount of material applied to the CE column was equivalent to 1 pmol of the original protein and the relationship between the observed  $m/z$  peaks and the molecular mass of the fragments is shown in Table 1.

## 4. Conclusions

In these studies, it has been shown that an improved sheath liquid probe can provide for the easy and convenient interfacing of CE with ES–MS. The effects of dilution of the sample zone by the sheath liquid were shown to be minimal over the range studied. Furthermore, the addition of an organic modifier to the CE buffer, which is required with the use of most non-sheath CE–ES–MS probes, has proven to degrade the separation, as has the addition of back pressure on the CE column. This type of pressure can be unintentionally applied if the CE

column entrance is higher than the CE column exit due to instrumental constraints. Using the SIM mode of operation, as little as 1.5 fmol of leucine enkephalin could be detected by CE–ES–MS. Finally, this system was used to detect the peptide fragments from 1 pmol of a tryptic digest of cytochrome *c* when separated by CE.

## References

- [1] J.A. Olivares, N.T. Nguyen, C.R. Yonker and R.D. Smith, *Anal. Chem.*, 59 (1987) 1230.
- [2] J.A. Olivares, N.T. Nguyen, C.R. Yonker and R.D. Smith, *Anal. Chem.*, 60 (1988) 436.
- [3] R.D. Smith, C.J. Barinaga and H.R. Udseth, *Anal. Chem.*, 60 (1988) 1948.
- [4] J.H. Wahl and R.D. Smith, *J. Cap. Elec.*, 1 (1994) 62.
- [5] J.R. Perkins and K. Tomer, *J. Cap. Elec.*, 1 (1994) 231.
- [6] E.D. Lee, W. Muck, J.D. Henion and T.R. Covey, *J. Chromatogr.*, 458 (1988) 313.
- [7] M.A. Moseley, J.W. Jorgenson, J. Shabanowitz, D.F. Hunt and K.B. Tomer, *J. Am. Soc. Mass Spectrom.*, 3 (1992) 289.
- [8] J.R. Perkins and K.B. Tomer, *Anal. Chem.*, 66 (1994) 2835.
- [9] A.J. Tomlinson, L.M. Benson and N. Stephen, *J. Cap. Elec.*, 1 (1994) 127.
- [10] S.A. Hofstadler, J.H. Wahl, R. Bakhtair, G.A. Anderson, J.E. Bruce and R. Smith, *J. Am. Soc. Mass Spectrom.*, 5 (1994) 894.
- [11] L. Fang, R. Zhang, E.R. Williams and R.N. Zare, *Anal. Chem.*, 66 (1994) 3696.
- [12] J.H. Wahl, D.C. Gale and R.D. Smith, *J. Chromatogr. A*, 659 (1994) 217.
- [13] E.D. Lee, W. Muck, T.R. Covey and J.D. Henion, *Anal. Chem.*, 18 (1989) 844.
- [14] S. Fujiwara and S. Honda, *Anal. Chem.*, 59 (1987) 487.
- [15] Y. Takada, K. Nakayama, M. Yoshida and M. Sakairi, *Rapid Commun. Mass Spectrom.*, 8 (1994) 93.



ELSEVIER

Journal of Chromatography A, 712 (1995) 253–268

JOURNAL OF  
CHROMATOGRAPHY A

# Mass spectral analyses of microcystins from toxic cyanobacteria using on-line chromatographic and electrophoretic separations<sup>☆</sup>

K.P. Bateman<sup>a,b</sup>, P. Thibault<sup>b,\*</sup>, D.J. Douglas<sup>b</sup>, R.L. White<sup>a</sup>

<sup>a</sup>Chemistry Department, Dalhousie University, Halifax, NS, B3H 4J3 Canada

<sup>b</sup>Institute for Marine Biosciences, National Research Council of Canada, 1411 Oxford Street, Halifax, NS, B3H 3Z1 Canada

## Abstract

The application of capillary electrophoresis and of reversed-phase liquid chromatography coupled to electrospray mass spectrometry is presented for the analysis of microcystins isolated from toxic strains of *Microcystis aeruginosa*. The separation performance of these two techniques is compared in terms of both sensitivity and of resolution of closely related microcystins. Quantitation of microcystin-LR present at low  $\mu\text{g/ml}$  concentrations in cell extracts is demonstrated using both techniques. A marked advantage of capillary electrophoresis over liquid chromatography was its ability to resolve different desmethyl microcystin-LR analogues. Identification of these positional isomers was facilitated using capillary electrophoresis combined with tandem mass spectrometry (MS–MS). Rationalization of fragment ions observed in MS–MS spectra of microcystins was made possible through comparison with <sup>15</sup>N labelled microcystins obtained from stable isotope feeding experiments. The potential of tandem mass spectrometry in providing selective detection of microcystins in cell extracts, and in structural characterization of novel microcystins, was also investigated.

## 1. Introduction

Microcystins are unusual cyclic peptides produced by toxic strains of the cyanobacteria *Microcystis*, *Anabaena*, *Nostoc*, and *Oscillatoria* [1,2]. These peptides are potent hepatotoxins [3–5] causing substantial disruption of the liver architecture, rearrangement of cellular organelles, and reorganization of microfilaments [6–10]. In contrast to other forms of algal poisoning, this type of intoxication is characterized by the appearance of a dark mottled liver, swollen with blood to twice its normal weight [2]. Acute dosage in mice can lead to rapid death of the

animal between 30 min and 3 h, and the LD<sub>50</sub> in a mouse (intraperitoneal injection) is 40–800  $\mu\text{g/kg}$  [11–14]. More recently, microcystins have been shown to be specific inhibitors of protein phosphatases 1 and 2A [15–17] and to also act as tumor promoters [18,19]. Changes in the balance of the phosphorylation and dephosphorylation reactions of proteins is thought to be a key element in the modifications of the microfilament structures and hepatocyte morphology [4–10]. In view of their toxicity and the world-wide occurrence of toxic cyanobacterial blooms, microcystins thus present a serious global health problem in water supplies, both for livestock and humans [20–22].

The microcystins belong to a family of cyclic heptapeptides with the general structure cyclo-D-

\* Corresponding author.

\* NRCC: 38100.





reduced sample sizes. The present report describes the use of LC and CE combined with electrospray mass spectrometry (ESMS) for the identification and quantitation of microcystins in extracts of different strains of *Microcystis aeruginosa*. Tandem mass spectrometry combined with either LC or CE separations was used to characterize the structures of previously unknown microcystins.

## 2. Experimental

### 2.1. Chemicals

Microcystin-LR was obtained from ICN Biomedicals (Aurora, OH, USA). HPLC-grade acetonitrile and methanol were obtained from Caledon Laboratories (Georgetown, Canada). Distilled and deionized (18 M $\Omega$ ) water (Milli-Q water systems, Millipore, Bedford, MA, USA) was used in the preparation of samples and buffer solutions.

### 2.2. Cell cultures

*Microcystis aeruginosa* strains PCC 7820 (Pasteur Culture Collection, Paris, France) and UTEX LB 2385 (The Culture Collection of Algae, University of Texas at Austin, TX, USA) were grown in BG-11 [43] culture medium under fluorescent illumination (Cool-White) on a 12 h:12 h light:dark cycle at 20°C. Stable isotope feeding experiments used <sup>15</sup>N-labelled NaNO<sub>3</sub> at a concentration of 1 g/l (97.5 at%, MSD isotopes, Montreal, Canada) as a substitute for the unlabelled nitrate in BG-11.

### 2.3. Extraction of microcystins

Cell material was sonicated for 10 min in 25% methanol (0.5 g/50 ml wet weight) and the sonicated slurry was stirred for 20 min to permit optimum extraction. After centrifugation at 3000 g for 10 min the supernatant was collected and the pellet re-extracted. The supernatant was concentrated using a rotary evaporator to approximately 10 ml. The concentrated superna-

tant was applied to a pre-conditioned C<sub>18</sub> Sep-Pak column (Waters, Milford, MA, USA). The cartridge was washed with water (2 × 10 ml) and microcystins were eluted with 100% methanol (2 × 10 ml). The methanol was removed using a Speedvac concentrator, and the residue stored at -10°C until required. Samples were dissolved in 40% aqueous methanol for analysis.

### 2.4. High-performance liquid chromatography with UV detection

All HPLC–UV experiments were performed using a Hewlett-Packard (Palo Alto, CA, USA) HP1090 Series II liquid chromatograph equipped with a ternary DR5 solvent delivery system, an HP1040A diode-array detector, and an HP7994A data system. Microcystins were separated on a 2.1 × 250 mm Vydac 218TP52 column (Vydac Separation group, Hisperia, CA, USA) using a linear gradient elution of 10–60% acetonitrile (0.1% trifluoroacetic acid) in 20 min, followed by a 5 min hold at 60% acetonitrile. The UV absorbance was monitored at both 214 and 238 nm, but full UV spectra were acquired once a chromatographic peak was detected. Sample injection volumes were typically 10  $\mu$ l.

### 2.5. Capillary electrophoresis with UV detection

Analyses of microcystins by CE–UV were achieved using a P/ACE System 2100 (Beckman Instruments, Fullerton, CA, USA). The instrument was equipped with a variable-wavelength UV detector using through-column optics. The system was interfaced directly to an MS-DOS computer (80386 processor) using a Beckman System Gold dedicated software package. Separations were performed using bare fused-silica capillaries (Polymicro Technologies, Phoenix, AZ, USA) previously coated with an aqueous solution of 5% (w/v) hexadimethrine bromide (Polybrene, Aldrich Chemicals, Milwaukee, WI, USA), and 2% (w/v) ethylene glycol (Aldrich). Separations using dynamically coated capillaries were conducted using 50- $\mu$ m I.D. × 107-cm

length (100 cm to detector) columns with 1 M formic acid buffer. The CE–UV analyses were performed using polarity reversal by applying a voltage of –30 kV at the injector end of the capillary.

## 2.6. Mass spectrometry

Mass spectra were obtained using a Perkin–Elmer SCIEX API/III<sup>+</sup> triple quadrupole mass spectrometer (Thornhill, Canada) equipped with a fully articulated, pneumatically assisted nebulization probe and an atmospheric pressure ionization source operated in electrospray (ionspray) mode. LC–ESMS analyses used the same chromatographic system as that described above except that a flow splitter was mounted after the HPLC column, thus allowing a flow-rate of only 15  $\mu\text{l}/\text{min}$  to the mass spectrometer. All CE–ESMS experiments were performed using an ATI Unicam Crystal CE System (Madison, WI, USA). A separate power supply (Glassman EH Series, Glassman, Whitehouse Station, NJ, USA) was used to provide an electrospray voltage of 5 kV. The CE–ESMS interface is based on a coaxial column arrangement [54] which was subsequently modified in our laboratory [51]. A more detailed description of the interface configuration has been presented elsewhere [52].

Mass spectral acquisition was performed using a dwell time of 4 ms per step of 1 dalton in full mass scan mode or 100 ms per channel in selected ion monitoring (SIM) experiments. Product ion spectra obtained from combined CE–MS–MS and LC–MS–MS analyses were obtained using collisional activation with argon target gas in the second (RF-only) quadrupole. Collision energies were typically 50 eV in the laboratory frame of reference, and the collision gas thickness was  $3.5 \cdot 10^{15}$  atoms/cm<sup>2</sup>. Tandem mass spectra were acquired using dwell times of 3 ms per step of 0.2 daltons in full-scan mode or 80 ms per channel in multiple reaction monitoring (MRM) experiments. A MacIntosh Quadra 950 computer was used for instrument control, data acquisition, and data processing.

## 3. Results and discussion

### 3.1. LC–UV and LC–ESMS analyses of cyanobacterial extracts

The LC–UV separation of microcystins extracted from *Microcystis aeruginosa* PCC 7820 is shown in Fig. 2. A non-specific response profile was generated by monitoring UV absorbance at 214 nm (Fig. 2a), whereas more selective detection of potential microcystins was achieved using a wavelength of 238 nm, corresponding to the chromophore of the unconjugated diene of the Adda residue (Fig. 2b). Microcystin-LR is observed in Fig. 2b as an intense peak eluting at 17.4 min, and other potential microcystins were

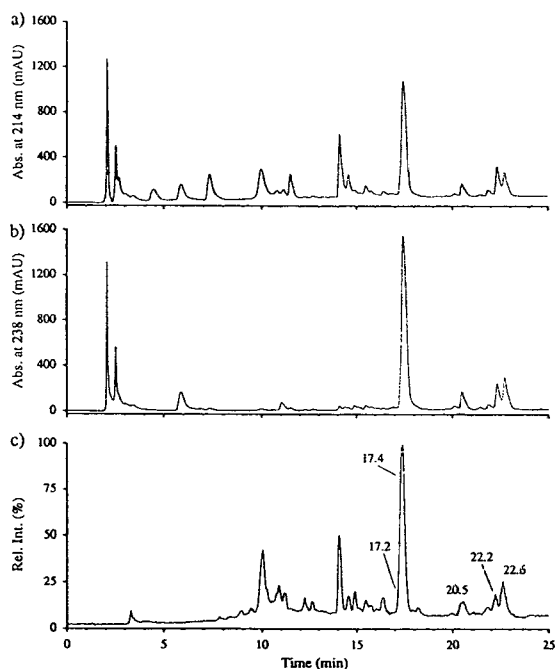


Fig. 2. Analysis of an extract from *M. aeruginosa* PCC 7820 using LC–UV at 214 nm (a), 238 nm (b), and LC–ESMS under full mass scan acquisition ( $m/z$  400–1100) (c). Conditions: injection of 10  $\mu\text{l}$  of a methanolic extract on a Vydac 218TP52 HPLC column, 0.2 ml/min flow-rate, linear gradient of 10–60% aqueous acetonitrile (0.1% trifluoroacetic acid), LC–ESMS conditions used a post-column splitter allowing only 15  $\mu\text{l}/\text{min}$  flow-rate to the mass spectrometer.

observed between 20 and 23 min. However, no structural assignments of these compounds could be made, due to the lack of available standards. In addition to the typical absorption at 238 nm, the UV spectra of several of these suspected microcystins showed characteristic features suggesting the presence of aromatic amino acids. For example, the peak eluting at 22.6 min in Fig. 2b showed a strong absorption band at 280 nm characteristic of a tryptophan residue.

The total ion chromatogram (TIC), obtained by LC–ESMS analysis of the same algal extract, is shown in Fig. 2c. The TIC corresponding to the full mass scan acquisition ( $m/z$  400–1100) gave a profile qualitatively similar to that of the LC–UV at 214 nm (Fig. 2a). Some of the early eluting peaks observed between 3 and 8 min in Fig. 2a, were not detected in the LC–ESMS analysis, and were possibly compounds with molecular masses outside the selected scan range. Examples of extracted mass spectra taken from the LC–ESMS analysis shown in Fig. 2c are presented in Fig. 3. The mass spectrum of microcystin-LR (Fig. 3b) is dominated by ions corresponding to singly and doubly protonated molecules,  $[M + H]^+$  and  $[M + 2H]^{2+}$ , at  $m/z$  996 and 498, respectively.

Tentative structural assignments of other microcystin structures could be deduced from molecular mass measurements taken from the extracted mass spectra. For example, Fig. 3a shows the mass spectrum of a potential microcystin corresponding to a desmethyl analogue of microcystin-LR ( $m/z$  982). This compound eluted at 17.2 min in Fig. 2c, and appeared as a shoulder on the microcystin-LR peak. Three different desmethyl microcystin-LR isomers have been reported in the literature, including desmethyl-Adda-LR [12], dehydroalanine-LR [12,36,47] and D-aspartic acid-LR [36,41,46]. Unfortunately, it was not possible to further determine the identity of this desmethylated analogue, nor was it possible to establish whether the sample contained more than one isomer. The peak detected at 20.5 min (Fig. 3c) showed an intense  $[M + H]^+$  ion at  $m/z$  1003, and was consistent with microcystin-LY [55].

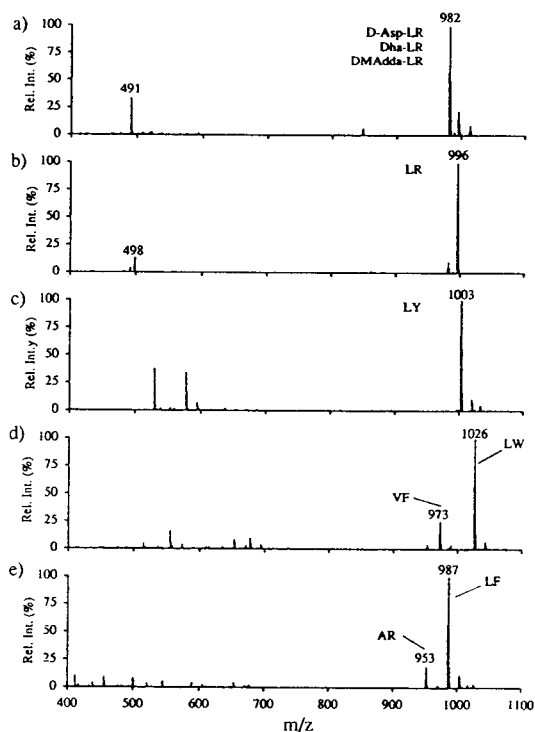


Fig. 3. Extracted mass spectra for peaks eluting at 17.2 (a), 17.4 (b), 20.5 (c), 22.2 (d), and 22.6 min (e) in Fig. 2c.

Two co-eluting microcystins, for which abundant  $[M + H]^+$  ions were observed at  $m/z$  953 and 987 (Fig. 3e), were tentatively assigned as microcystin-AR [12] and microcystin-LF [56], respectively. Finally, the extracted mass spectrum for the peak detected at 22.2 min is presented in Fig. 3d, and shows two  $[M + H]^+$  ions at  $m/z$  973 and 1026. As mentioned above, the UV spectrum for this peak showed a typical absorption band at 280 nm characteristic of a tryptophan residue. The higher molecular mass component at  $m/z$  1026 was tentatively assigned as microcystin-LW. To the best of our knowledge, no report has documented thus far the production of this microcystin from cultures of *M. aeruginosa* or any other toxic cyanobacteria. The molecular mass of the smaller component observed at  $m/z$  973 in Fig. 3d could not be matched with that of any of the known microcystins [21], and further

experiments using tandem mass spectrometry (see following section) were required to provide insights on the structure of this compound.

### 3.2. Tandem mass spectrometric characterization of microcystins

In the absence of suitable standards, information on the retention times, UV absorbances, and molecular masses is not sufficient to confirm the structures of the different microcystins. The application of tandem mass spectrometric techniques to the sequencing of cyclic peptides, such as microcystins, is a well-established analytical technique in many laboratories [57]. Rinehart et al. [21] have developed a protocol using MS and MS–MS for the sequencing and structural assignment of microcystins involving: (1) precise molecular mass measurements using high-resolution FAB/MS; (2) determination of the amino acids present by NMR and gas chromatography–mass spectrometry (GC–MS); (3) linearization of the peptide by treatment with  $O_3$ ,  $NaBH_4$ , and HCl; (4) assignment of the structure of the cyclic and linear peptides using tandem mass spectrometry. They observed fragment ions characteristic of microcystins, which could be used to support structural assignments [12,21].

Alternatively, tandem mass spectra can be obtained for cyanobacterial extracts using combined LC–MS–MS [37]. In the present investigation we have used this approach to confirm the identities of suspected microcystins. In order to assist the assignment of structures of fragment ions observed in the MS–MS spectra of microcystins, the  $m/z$  values were compared with those obtained from MS–MS spectra of  $^{15}N$  labelled analogues isolated after stable-isotope feeding experiments. The MS–MS spectra of selected precursor ions of microcystin-LR and of its  $^{15}N$  analogue, obtained from LC–MS–MS analyses of appropriate extracts of *M. aeruginosa* PCC 7820, are presented in Fig. 4a and b, respectively. Under the present experimental conditions, the formation of intense fragment ions from the singly charged  $[M + H]^+$  precursor ion required collisional activation with argon at collision energies of at least 50 eV. Valuable

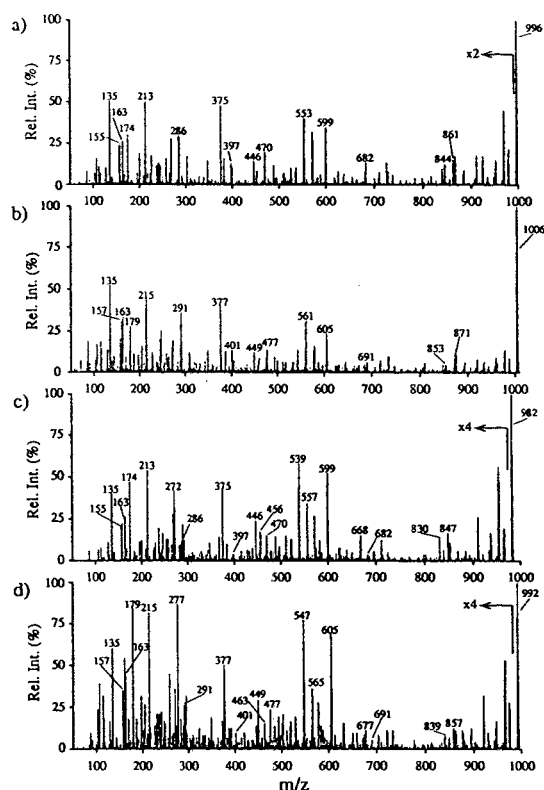


Fig. 4. Extracted product ion spectra from the LC–MS–MS analysis of an extract of *M. aeruginosa* PCC 7820 grown on natural nitrate and culture media fortified with  $^{15}N$ . Product ion of  $m/z$  995.5 from microcystin-LR (a),  $m/z$  1005.5 from  $^{15}N$  microcystin-LR (b),  $m/z$  981.5 from desmethyl microcystin-LR (c), and  $m/z$  991.5 from  $^{15}N$  desmethyl microcystin-LR (d). Conditions: chromatographic conditions as for Fig. 2, collisional activation was achieved using argon target gas at 50 eV collision energy and a collision gas thickness of  $3.5 \cdot 10^{15}$  atoms/cm<sup>2</sup>.

sequence information could also be deduced from the  $[M + 2H]^{2+}$  ion at lower collision energies, although the intensity of this precursor ion was substantially lower than that of the singly protonated molecule.

Fragment ions observed for microcystin-LR arose predominantly from consecutive cleavages of peptide bonds [12,21,57]. Such fragment ions thus provide information concerning different peptide segments of the original molecule, and can be used to verify possible sites of substitution in other microcystins. The sequence information and  $m/z$  values obtained from the MS–MS

spectra of microcystin-LR are conveniently summarized in Table 1. Assignment of the fragment ions and their corresponding structures was further confirmed by the mass shift observed for the  $^{15}\text{N}$  analogue. The  $^{15}\text{N}$  isotopically enriched extract has an  $[\text{M} + \text{H}]^+$  ion at  $m/z$  1005.5 for microcystin-LR, confirming the expected incorporation of ten atoms of  $^{15}\text{N}$ . The number of nitrogen atoms for each fragment ion could be deduced from the difference in  $m/z$  values observed from the two MS–MS spectra.

The MS–MS spectrum of the desmethyl microcystin-LR (Fig. 4c) and that of its  $^{15}\text{N}$  analogue (Fig. 4d) show a similar series of sequence ions, with the exception that the fragment ion at  $m/z$  553 (Fig. 4a) is now shifted to  $m/z$  539, consistent with the proposal that this ion contains one residue lacking a methyl group. Closer examination of Fig. 4c indicated that major fragment ions bearing the Mdha residues at  $m/z$

213 and 375 remained unshifted, indicating that this residue is not the site of desmethylation. However, the fragment ion  $m/z$  286 containing a Masp residue (Fig. 4a) was partly displaced to  $m/z$  272, indicating that in some (not all) of the desmethyl analogues, the Masp residue was replaced by Asp. Interestingly, much less intense fragment ions were also observed at  $m/z$  199, 361, and 286, suggesting that substitution of a methyl group could also take place at the Mdha residue. This proposal was further supported by observations made during CE–ESMS analysis of this extract (see following section).

A characteristic feature of the MS–MS spectra of microcystins is the presence of a set of common fragment ions [15]. As discussed earlier, the variation in the known microcystins is largely due to substitution of two specific amino acids in the cyclic structure (Fig. 1). Fragment ions corresponding to the more conserved por-

Table 1

Assignment of fragment ions observed in product ion spectra of natural and  $^{15}\text{N}$  enriched microcystin-LR and desmethyl microcystin-LR

Fragment ions	Microcystin-LR		Desmethyl microcystin-LR	
	$^{14}\text{N}$	$^{15}\text{N}$	$^{14}\text{N}$	$^{15}\text{N}$
$\text{PhCH}_2\text{CH}(\text{OMe})^+$	135	135	135	135
$[\text{Mdha-Ala} + \text{H}]^+ \text{ }^a$	155	157	155	157
$[\text{C}_{11}\text{H}_{14}\text{O} + \text{H}]^+$	163	163	163	163
$[\text{Arg} + \text{NH}_3 + \text{H}]^+$	174	179	174	179
$[\text{Glu-Mdha} + \text{H}]^+$	213	215	213	215
$[\text{Arg-Masp} + \text{H}]^+ \text{ }^b$	286	291	286	291
$[\text{Arg-Asp} + \text{H}]^+$	–	–	272	277
$[\text{C}_{11}\text{H}_{14}\text{O-Glu-Mdha} + \text{H}]^+$	375	377	375	377
$[\text{Glu-Mdha-Ala-Leu} + \text{H}]^+$	397	401	397	401
$[\text{C}_{11}\text{H}_{14}\text{O-Glu-Mdha-Ala} + \text{H}]^+$	446	449	446	449
$[\text{Arg-Asp-Leu-Ala} + \text{H}]^+$	–	–	456	463
$[\text{Arg-Masp-Leu-Ala} + \text{H}]^+$	470	477	470	477
$[\text{Arg-Asp-Leu-Ala-Mdha} + \text{H}]^+$	–	–	539	547
$[\text{Arg-Masp-Leu-Ala-Mdha} + \text{H}]^+$	553	561	553	561
$[\text{Adda-Arg-Masp} + \text{H}]^+ \text{ }^c$	599	605	599	605
$[\text{Glu-dha-Ala-Leu-Masp-Arg} + \text{H}]^+$	–	–	668	677
$[\text{Glu-Mdha-Ala-Leu-Masp-Arg} + \text{H}]^+$	682	691	682	691
$[\text{C}_{11}\text{H}_{14}\text{O-Glu-Dha-Ala-Leu-Masp-Arg} + \text{H}]^+$	–	–	830	839
$[\text{C}_{11}\text{H}_{14}\text{O-Glu-Mdha-Ala-Leu-Masp-Arg} + \text{H}]^+$	844	853	844	853
Loss of $\text{PhCH} = \text{CH}(\text{OMe})$	861	871	847	857

<sup>a</sup> Mdha = N-methyldehydroalanine.

<sup>b</sup> Masp =  $\beta$ -methylaspartic acid.

<sup>c</sup> Adda = 3-amino-9-methoxy-2,6,8-trimethyl-10-phenyldeca-4,6-dienoic acid.

tion of the molecule can thus be used as possible diagnostic ions for the identification of microcystins. These ions include  $\text{PhCH}_2\text{CH}(\text{OMe})^+$  ( $m/z$  135),  $[\text{Glu-Mdha} + \text{H}]^+$  ( $m/z$  213), and  $[\text{C}_{11}\text{H}_{14}\text{O-Glu-Mdha} + \text{H}]^+$  ( $m/z$  375), see Fig. 4 and Table 1. Suspected microcystins would be expected to give rise to at least one of these ions in the product ion MS–MS spectra of their corresponding  $[\text{M} + \text{H}]^+$  ions. Conversely, it is possible to use one of these three fragment ions in precursor-ion scan mode to identify putative microcystins present in cell extracts. An example of this approach is presented in Fig. 5, obtained by analysis of an extract from *M. aeruginosa* PCC 7820 by direct flow injection. In this case, the third quadrupole Q3 was set to transmit the characteristic microcystin fragment at  $m/z$  135, formed in the RF-only collision cell Q2, while the first quadrupole Q1 was scanned over the range  $m/z$  950–1050. In addition to the expected microcystin-LR at  $m/z$  995.5, other precursor ions of  $m/z$  135 were also observed at  $m/z$  952.5, 972.5, 986.5, 981.5, 1002.5, 1009.5, and 1025.5. Tentative assignments were proposed above for some of these compounds based on data available from both LC–UV and LC–ESMS analyses. The only exceptions to this were the compounds

at  $m/z$  972.5, 1009.5, and 1025.5, which could not be matched with any of the known microcystins. In order to confirm the structure of previously assigned microcystins, and to provide further structural information on other related hepatotoxins, additional experiments using combined LC–MS–MS were undertaken.

Examples of product ion spectra for  $m/z$  987.5, 972.2, 1009.5, and 1025.5, obtained from LC–MS–MS analysis of an extract of *M. aeruginosa* PCC 7820, are presented in Fig. 6. The MS–MS spectrum of the microcystin shown in Fig. 6a was consistent with that of microcystin-LF. The observation of characteristic fragment ions at  $m/z$  135, 213, and 375 supported the proposal that this compound was a microcystin. The presence of a phenylalanine residue at position Z in the microcystin structure (Fig. 1) was substantiated by the observation of intense fragment ions at  $m/z$  544, 673, and 836. The structures and assignment of some of the fragment ions observed for microcystin-LF are presented in Table 2, together with data extracted from MS–MS spectra of other microcystins analyzed in this study.

Information obtained from the MS–MS spectra of microcystin-LR, -LF, and isomers of

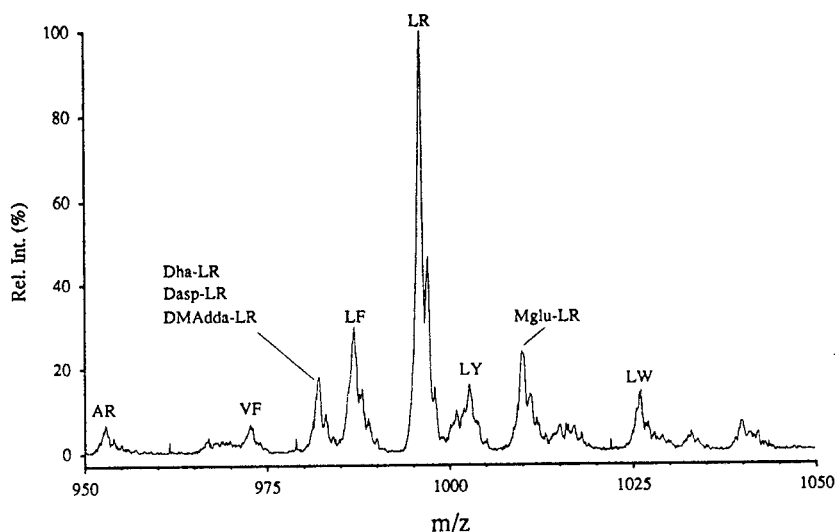


Fig. 5. Precursor ion spectrum of  $m/z$  135 obtained from the direct flow injection of  $2 \mu\text{l}$  of an extract of *M. aeruginosa* PCC 7820. MS–MS conditions as for Fig. 4.

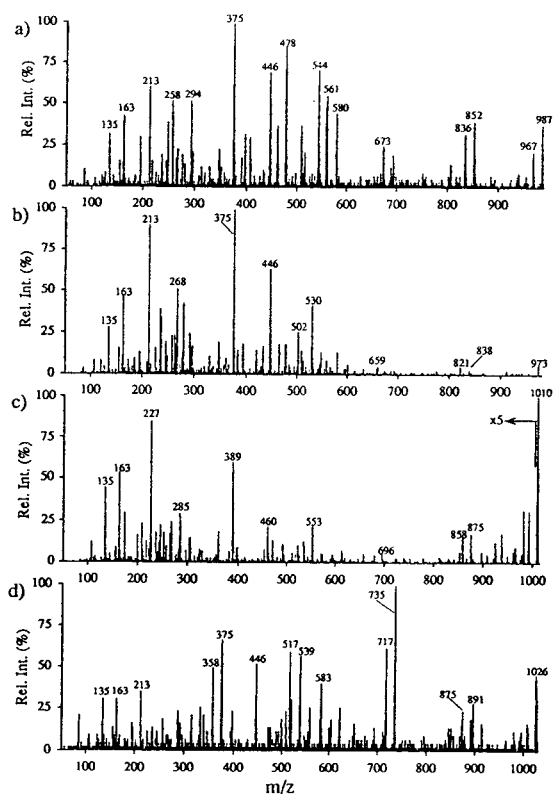


Fig. 6. Extracted MS–MS spectra from the LC–MS–MS analysis of an extract of *M. aeruginosa* PCC 7820. Product ion spectra for  $m/z$  987.5 (a), 972.5 (b), 1009.5 (c), and 1025.5 (d). Conditions as for Fig. 4.

desmethyl-LR was used to suggest possible structures for other suspected microcystins. Of particular interest to the present investigation was the observation of three previously unknown microcystins at  $m/z$  972.5 (Fig. 6b), 1009.5 (Fig. 6c), and 1025.6 (Fig. 6d). As mentioned in the previous section, the last compound was presumed to be microcystin-LW. This proposal was further supported by the observation of fragment ions at  $m/z$  583, 735, and 875 (Table 2, Fig. 6d), which confirmed the presence of a tryptophan residue at position Z in Fig. 1. Peptides containing this amino acid give rise to characteristic immonium and indole ions at  $m/z$  159 and 130, respectively.

The MS–MS spectrum of the compound with  $[M + H]^+$  at  $m/z$  1009.5 (Fig. 6c, Table 2) was consistent with a microcystin-LR containing a

methylated Glu residue (Mglu). The occurrence of a Glu methyl ester of microcystin-LR has been previously reported in species of *Anabaena flos aquae* CYA 83/1 [58], but not from *M. aeruginosa*. Based on this information alone, it is, however, not possible to ascertain whether the incorporation of the extra methyl group takes place on the carboxylic acid or the  $\alpha$ -carbon of Glu or even on the amide nitrogen. Finally, the product ion spectrum of  $m/z$  972.5 is presented in Fig. 6b. Fragment ions observed for this compound suggest that the X and Z position (Fig. 1) are both substituted. The presence of arginine, which is usually characterized by a fragment ion at  $m/z$  174, could not be observed for this microcystin. Comparison of this MS–MS spectrum with that of microcystin-LF (Fig. 6a, Table 2) revealed similar fragment ion patterns displaced by 14 Da. More particularly, fragment ions at  $m/z$  530, 659, and 822 (Table 2, Fig. 6b) suggests that this microcystin could contain valine and phenylalanine at position X and Z, respectively (Fig. 1). Further confirmation of this hypothesis will require more elaborate studies involving preparative HPLC, NMR spectroscopy, and amino acid analyses of purified fractions.

### 3.3. CE–MS and CE–MS–MS analyses of cell extracts

The application of CE–UV to the confirmation of microcystins in fractions collected from preparative HPLC linked with the protein phosphatase assay, was recently demonstrated by Bořand et al. [39]. The concentration detection limit was estimated to be approximately  $3 \mu\text{g/ml}$  (30 nl injection) for microcystin-LR analyzed by CE–UV with detection at 200 nm. Separation of microcystins was performed using a Tris buffer with pH 6. However, when coupled to ESMS this buffer can lead to substantial chemical noise and associated loss in sensitivity. Different electrophoretic conditions were therefore developed for the separation of microcystins by CE–ESMS.

Previous investigations using CE–ESMS with acidic buffers and capillaries coated with cationic polymers such as hexadimethrine bromide, have

Table 2

Characteristic fragment ions observed for different microcystins analyzed by LC–MS–MS

Assignment <sup>a</sup>	m/z values					
	AR	LF	LY	LW	VF	Mglu-LR
[M + H] <sup>+</sup>	953	987	1003	1026	973	1010
Loss of PhCH = CH(OMe)	818	852	868	891	838	875
PhCH <sub>2</sub> CH(OMe) <sup>+</sup>	135	135	135	135	135	135
[C <sub>11</sub> H <sub>14</sub> O + H] <sup>+</sup>	163	163	163	163	163	163
[Glu-Mdha + H] <sup>+</sup>	213	213	213	213	213	227
[C <sub>11</sub> H <sub>14</sub> O-Glu-Mdha + H] <sup>+</sup>	375	375	375	375	375	389
[C <sub>11</sub> H <sub>14</sub> O-Glu-Mdha-Ala + H] <sup>+</sup>	446	446	446	446	446	460
[Arg-Masp-Ala-Ala-Mdha + H] <sup>+</sup>	510	–	–	–	–	–
[Arg-Masp-Ala-Ala-Mdha-Glu + H] <sup>+</sup>	639	–	–	–	–	–
[Arg-Masp-Ala-Ala-Mdha-Glu-C <sub>11</sub> H <sub>14</sub> O + H] <sup>+</sup>	801	–	–	–	–	–
[Phe-Masp-Leu-Ala-Mdha + H] <sup>+</sup>	–	544	–	–	–	–
[Phe-Masp-Leu-Ala-Mdha-Glu + H] <sup>+</sup>	–	673	–	–	–	–
[Phe-Masp-Leu-Ala-Mdha-Glu-C <sub>11</sub> H <sub>14</sub> O + H] <sup>+</sup>	–	836	–	–	–	–
[Tyr-Masp-Leu-Ala-Mdha + H] <sup>+</sup>	–	–	559	–	–	–
[Tyr-Masp-Leu-Ala-Mdha-Glu + H] <sup>+</sup>	–	–	688	–	–	–
[Tyr-Masp-Leu-Ala-Mdha-Glu-C <sub>11</sub> H <sub>14</sub> O + H] <sup>+</sup>	–	–	852	–	–	–
[Trp-Masp-Leu-Ala-Mdha + H] <sup>+</sup>	–	–	–	583	–	–
[CO-Masp-Leu-Ala-Mdha-Glu-C <sub>11</sub> H <sub>14</sub> O + H] <sup>+</sup>	–	–	–	735	–	–
[Trp-Masp-Leu-Ala-Mdha-Glu-C <sub>11</sub> H <sub>14</sub> O + H] <sup>+</sup>	–	–	–	875	–	–
[Phe-Masp-Val-Ala-Mdha + H] <sup>+</sup>	–	–	–	–	530	–
[Phe-Masp-Val-Ala-Mdha-Glu + H] <sup>+</sup>	–	–	–	–	659	–
[Phe-Masp-Val-Ala-Mdha-Glu-C <sub>11</sub> H <sub>14</sub> O + H] <sup>+</sup>	–	–	–	–	822	–

<sup>a</sup> The bold amino acids correspond to positions X and Z in Fig. 1.

enabled identification of a number of peptides, glycopeptides, and proteins in the low femtomole range [53,59]. Such cationic coatings not only reduce the extent of solute–wall interactions but also reverse the direction of the electroosmotic flow (anodal flow), a situation which can magnify the velocity differences amongst those analytes having electrophoretic mobilities in the opposite direction. Furthermore, it is possible to manipulate the electroosmotic flow by varying the acidity of the electrolyte in order to enhance the resolution of analytes having similar electrophoretic mobilities. Preliminary CE–UV experiments, using 50  $\mu\text{m} \times 107$  cm capillaries coated with 5% hexadimethrine bromide and 2% ethylene glycol, indicated that the electroosmotic flow varied from  $6.7 \cdot 10^{-8}$  to  $4.3 \cdot 10^{-8}$   $\text{m}^2 \text{V}^{-1} \text{s}^{-1}$  for concentrations of formic acid ranging from 0.1 to 2.0 M. For the same range of formic acid concentration, the electrophoretic mobility of microcystin-LR was typically  $7.4 \cdot 10^{-9}$   $\text{m}^2 \text{V}^{-1}$

$\text{s}^{-1}$  in the opposite direction. Optimized conditions, in terms of both separation efficiencies and analysis time, were achieved using 1.0 M formic acid, and yielded plate counts in the order of 800 000 for microcystin-LR standards based on measurements of peak width at half height. Such electrophoretic conditions were also found to be compatible with the operation of electro-spray ionization.

The CE–ESMS analysis of a 10  $\mu\text{g}/\text{ml}$  standard of microcystin-LR is shown in Fig. 7. Under the specified conditions, microcystin-LR is observed as a sharp peak migrating at 8.95 min in Fig. 7b. Two peaks corresponding to desmethyl microcystin-LR were also observed, at 8.98 and 9.09 min in the extracted ion chromatogram obtained from the same analysis (Fig. 7a). The fact that this toxin standard contains sizable amounts of the desmethyl analogue probably reflects the difficulty in separating these closely related compounds by chromatographic meth-



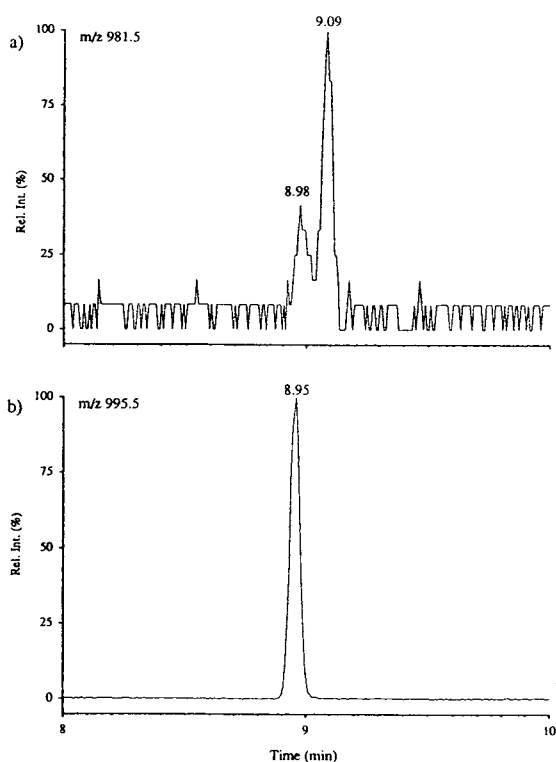


Fig. 7. CE-ESMS analysis of 10  $\mu\text{g/ml}$  microcystin-LR standard using SIM for  $m/z$  981.6 (a) and 995.6 (b). Conditions: fused-silica column 1.0 m  $\times$  50  $\mu\text{m}$  I.D. coated with 5% Polybrene, 2% ethylene glycol, 20 nl injection, 1.0 M formic acid electrolyte, sheath liquid: 25% aqueous methanol (0.2% formic acid) at a flow-rate of 7  $\mu\text{l/min}$ .

ods. Purification of microcystin-LR from cell extracts using reversed-phase HPLC is thus likely to result in a product containing trace amounts of desmethyl microcystin-LR, and qualitative analysis with complementary separation techniques such as CE must be done to evaluate purity of commercially available standards.

CE-ESMS analysis (using selected ion monitoring) of a cyanobacterial extract obtained from *M. aeruginosa* UTEX LB 2385 is shown in Fig. 8. The reconstruction ion electropherogram corresponding to the sum of intensities of  $m/z$  121.1, 135.1, 692.5, 981.5, 995.5, 1007.5, 1027.5, 1041.5, is shown in Fig. 8a. In order to facilitate identification of potential hepatotoxins present in complex extracts, mass spectral ionization conditions were selected to promote the

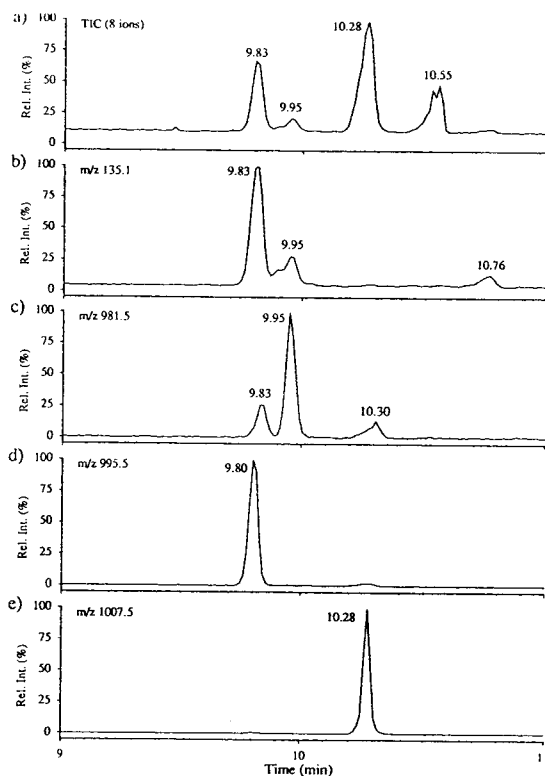


Fig. 8. CE-ESMS analysis of a methanol extract from *M. aeruginosa* UTEX LB 2385 using SIM for the sum of ion current for  $m/z$  121.1, 135.1, 692.5, 981.5, 995.5, 1007.5, 1027.5, 1041.5 (a). Extracted ion chromatograms for 135.1 (b), 981.5 (c), 995.5 (d), 1007.5 (e). Conditions as for Fig. 7, except that a voltage of 100 V was applied at the orifice.

formation of characteristic fragment ions common to most microcystins. Fragmentation reactions leading to a loss of 134, or conversely the formation of  $m/z$  135 from the Adda residue, were found to be a common feature in the mass spectra of the microcystins (Fig. 4). The formation of these fragment ions was promoted by increasing the voltage of the skimmer/orifice lens to 100 V. The extracted ion chromatogram for  $m/z$  135 is shown in Fig. 8b, and reveals the presence of at least four putative microcystins.

The extracted ion electropherograms for  $m/z$  981.5 and 995.5 are shown in Figs. 8c and 8d, respectively. Interestingly, the electropherogram for  $m/z$  981.5 (Fig. 8c) shows three resolved peaks migrating at 9.8, 9.9, and 10.2 min. As will

be discussed later, these peaks were found to be closely related isomers differing only in the position of a methyl group (Fig. 1). Peaks identified in the  $m/z$  135 trace under these conditions matched those of microcystin-LR and its desmethyl analogues. Only the desmethyl microcystin-LR with the lowest abundance does not show a peak in the  $m/z$  135 electropherogram. As will be mentioned later, this compound was found to contain a modified desmethyl Adda residue, and thus could not form the characteristic  $m/z$  135 fragment ion. The small peak observed in the extracted ion chromatogram of  $m/z$  995.5 (Fig. 8d) at 10.3 min is possibly due to a geometrical isomer of microcystin-LR. Previous investigations have shown the presence of a (Z) Adda isomer of microcystin-LR in extracts of *M. viridis* [60]. It is noteworthy that this additional peak was not observed in the LR standard analyzed under the same conditions (Fig. 7b).

In several cases, compounds devoid of the Adda residue did not give rise to a fragment ion at  $m/z$  135. Such discrimination is illustrated in Fig. 8e for an unknown component with  $[M+H]^+$  at  $m/z$  1007.5, present in the *M. aeruginosa* UTEX LB extract, and for which no significant signal was observed in the  $m/z$  135 trace. The formation of a  $m/z$  135 fragment ion can be used as a screening method for monitoring microcystins in cell extracts. However, one must be aware that microcystins present at low concentrations ( $<20$  pg) may not be detected in this way, and although the majority of microcystins produce the  $m/z$  135 ion, this might not be a valid generalization for all related hepatotoxins.

In order to identify individual isomers of desmethyl microcystin-LR, further experiments using CE in combination with tandem mass spectrometry were undertaken. Previous analyses of cyanobacterial extracts have identified three desmethylated microcystins, differing only in the site of demethylation (Fig. 1) [12,36,41,46,47]. Because of sensitivity considerations, CE-MS-MS analyses were achieved using multiple reaction monitoring mode (MRM). As mentioned earlier, microcystins produce characteristic fragment ions which can be used to confirm the amino acid sequence

assignments (Figs. 4 and 6, Tables 1 and 2). Proper selection of reaction channels enabled identification of each desmethyl microcystin-LR isomer identified in Fig. 8c. The observation of fragment ions differing by 14 Da from those of microcystin-LR suggested possible sites of substitution. For example, substitution of the Adda residue by a desmethyl homologue will give rise to a fragment ion at  $m/z$  121 instead of  $m/z$  135. Similarly, substitution on the Masp residue will be indicated by a  $[\text{Arg-Asp} + \text{H}]^+$  fragment ion at  $m/z$  272 instead of  $m/z$  286, whereas a demethylation of the Mdha residue will be reflected by the observation of a fragment ion at  $m/z$  361, corresponding to  $[\text{C}_{11}\text{H}_{14}\text{O-Glu-Dha} + \text{H}]^+$ .

The analysis of the same methanol extract as

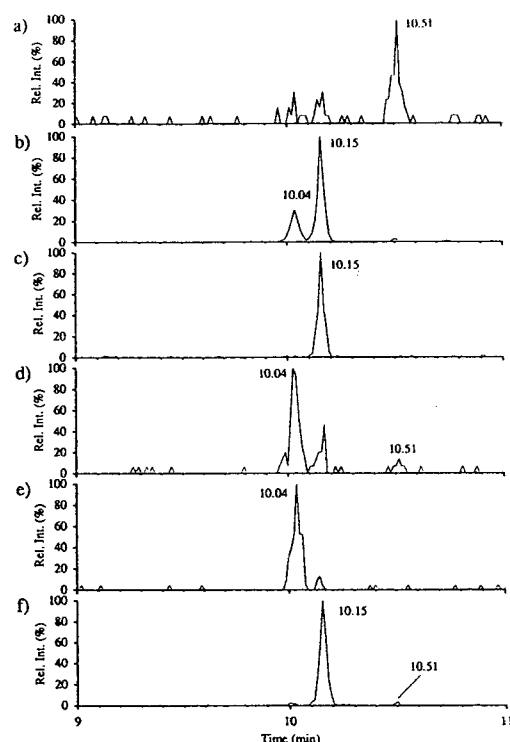


Fig. 9. CE-MS-MS analysis of a methanol extract from *M. aeruginosa* UTEX LB 2385 using multiple reaction monitoring for transitions 981.6  $\rightarrow$  121.1 (a), 981.6  $\rightarrow$  135.1 (b), 981.6  $\rightarrow$  272.3 (c), 981.6  $\rightarrow$  286.3 (d), 981.6  $\rightarrow$  361.3 (e), and 981.6  $\rightarrow$  375.3 (f). Electrophoretic and MS-MS conditions as for Fig. 7 and 4, respectively.

used in Fig. 8 is presented in Fig. 9 for the dissociation of the precursor ion  $m/z$  981.6 using CE–MS–MS in MRM mode. The transitions monitored for the Adda residue (Figs. 9a and 9b) show one peak at 10.5 min for the desmethylated isomer ( $m/z$  121) and two peaks at 10.0 and 10.2 min for the two isomers containing the Adda residue ( $m/z$  135). The second component migrating at 10.2 min was found to contain an Asp residue, based on the ion profile obtained for transitions leading to the formation of  $m/z$  272 (Fig. 9c). The desmethyl microcystins-LR containing a Masp residue were observed at 10.0 and 10.5 min in Fig. 9d. It is noteworthy that because of the high abundance of the second component, the peak observed at 10.2 min in Fig. 9d is probably due to the  $[\text{Glu-Mdha-Ala} + \text{H}]^+$  fragment ion at  $m/z$  285. The final two transitions used in the MRM experiments (Figs. 9e and 9f) enabled identification of Dha-microcystin-LR. The transition  $982 \rightarrow 361$  showed one peak at 10.0 min for the expected  $[\text{C}_{11}\text{H}_{14}\text{O-Glu-dha} + \text{H}]^+$  fragment ion, whereas Fig. 9f shows a prominent signal at 10.2 min accompanied by a weaker peak at 10.5 min for the two remaining microcystins, bearing the Mdha residue.

### 3.4. Quantitation of microcystin-LR by LC–ESMS and CE–ESMS

The amount of microcystin-LR present in extracts of *M. aeruginosa* cells was determined using both LC–ESMS and CE–ESMS operating in SIM mode. The dependence of peak area on sample concentration was examined for a fixed injection volume of microcystin-LR (10  $\mu\text{l}$  for LC and 20 nl for CE). Fig. 10 shows typical calibration curves for these two techniques. In both cases, good linearity with correlation coefficient  $r^2 > 0.9990$  was found over concentrations ranging from two to three orders of magnitude. The insets in Fig. 10 correspond to traces obtained for concentrations approaching the detection limits. The LC–ESMS chromatogram corresponding to the on-column injection of 500 pg (0.05  $\mu\text{g}/\text{ml}$ ) of microcystin-LR, using SIM, for  $m/z$  995.5 gave a signal to noise ( $S/N$ ) ratio of

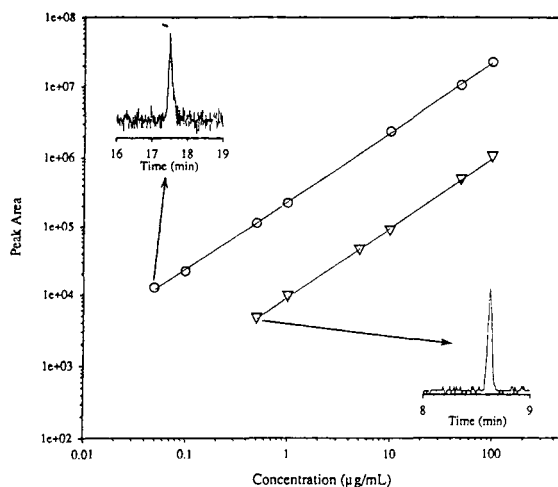


Fig. 10. Calibration plots of concentration versus peak areas for the analysis of microcystin-LR using LC–ESMS (circles),  $r^2 = 0.9992$ , and CE–ESMS (triangles),  $r^2 = 0.9994$ . Insets show the peak profiles at the lowest concentration analyzed by both techniques.

approximately 5:1. In fact, the actual amount of microcystin-LR introduced to the mass spectrometer was approximately 50 pg (50 fmol), taking into account that a post-column split of 1:10 was used.

In comparison, the electropherogram obtained for a 20 nl injection of a 0.5  $\mu\text{g}/\text{ml}$  solution of microcystin-LR gave a  $S/N$  ratio of approximately 10:1. In this case, the detection limit for CE–ESMS was estimated as 0.2  $\mu\text{g}/\text{ml}$  for an actual injection of 4 pg (4 fmol) of microcystin-LR. Despite the lower injection sizes typically used in zone electrophoresis format, the concentration detection limit observed for CE–ESMS was found to be higher than that of LC–ESMS by less than an order of magnitude. On the other hand, the mass detection limit observed for CE–ESMS was found to be higher by at least an order of magnitude compared to that of LC–ESMS. The enhanced signal strength observed here is attributed to the higher separation efficiencies obtainable with CE–ESMS. For typical 20 nl injection (17% of the capillary volume), plate counts obtained for microcystin-LR were approximately 230 000 over the concentration range examined.

Such high separation efficiencies imposed considerable demands on the mass spectrometer for analyses requiring broader acquisition mass ranges. CE–ESMS analysis conducted under full mass scan acquisition ( $m/z$  400–1200) required a concentration of 5  $\mu\text{g}/\text{ml}$  of microcystin-LR in order to obtain a meaningful mass spectrum, whereas similar-quality information could be obtained for solutions ten times less concentrated using LC–ESMS. The relatively high concentration detection limit of CE has been one of the limitations of the present method. However, recent experiments performed in this laboratory using capillary isotachopheresis pre-concentration have shown promising results for enhancing the concentration detection limit of microcystin-LR analyzed subsequently using zone electrophoresis. Results from these studies will be presented separately.

The concentration of microcystin-LR present in the two strains of *M. aeruginosa* investigated was determined using both LC–ESMS and CE–ESMS. For similar weights of biomass extracted, higher concentrations of microcystin-LR were consistently found in extracts of cells from the UTEX LB 2385 strain. Quantitative analyses ( $n = 3$ ) of extracts of this strain, performed using SIM acquisition mode, showed concentrations of microcystin-LR of  $11.8 \pm 0.9 \mu\text{g}/\text{ml}$  (using CE–ESMS), and  $8.0 \pm 0.3 \mu\text{g}/\text{ml}$  (using LC–ESMS). When converted in terms of weight equivalent of cells extracted, these concentrations represent 110–150  $\mu\text{g}$  of microcystin-LR per gram of wet cyanobacterial cells. In contrast, the corresponding amounts of microcystin-LR in extracts of cells from PCC 7820 were  $4.3 \pm 0.5 \mu\text{g}/\text{ml}$  using CE–ESMS and  $2.8 \pm 0.1 \mu\text{g}/\text{ml}$  for LC–ESMS. Such concentrations actually represent 6–10  $\mu\text{g}$  per gram of wet cyanobacterial cells. As observed, concentrations determined using CE–ESMS were consistently 25% higher than those obtained using LC–ESMS. These results were considered to be in acceptable agreement with each other, considering that these analyses were performed on different occasions, one month apart. The higher relative standard deviations observed for concentrations obtained with CE–ESMS were associated with the use of unsealed

vials, thus allowing more extensive evaporation of the sample solvent. Minimization of sample handling errors, evaporation of solvent, and other associated sources of uncertainties, can be minimized using suitable internal standards spiked in the original cell extract.

#### 4. Conclusions

Microcystins present at low  $\mu\text{g}/\text{ml}$  levels in cell extracts of *M. aeruginosa* were analyzed directly by LC–ESMS and CE–ESMS. Analyses performed in selected ion monitoring mode provided detection limits ( $S/N$  3:1) in the order of 50 nM for microcystin-LR using LC–ESMS and 200 nM for analyses conducted with CE–ESMS. Mass spectral detection provided enhanced selectivity compared to UV detection, and meaningful spectra were generally obtained for microcystins present at levels as low as 500 nM in extracts of *M. aeruginosa* cells using LC–ESMS. One distinct advantage of CE–ESMS over LC–ESMS was the possibility of separating isomers differing only in the position of a single methyl group on the microcystin backbone structure. CE–ESMS analyses obtained using capillaries dynamically coated with hexadimethrine bromide and ethylene glycol enabled identification of three desmethyl isomers of microcystin-LR, differing in the Adda, Masp, or Mdha residue. Further characterization of these positional isomers was performed using CE in combination with tandem mass spectrometry.

Selective identification of microcystins present in extracts of toxic cyanobacterial cells was facilitated using a precursor-ion scan of  $m/z$  135, a fragment ion characteristic of the Adda residue. Suspected microcystins were subsequently analyzed using LC–MS–MS to obtain amino acid sequence information, and to identify possible sites of amino acid substitution. Rationalization of fragment ions observed in the MS–MS spectra of microcystins was possible using methanolic extracts of cell cultures of *M. aeruginosa* grown on natural and  $^{15}\text{N}$ -labelled nitrate nutrients. More importantly, the present investigation has emphasized the potential of CE and LC in

combination with tandem mass spectrometry for the identification of known and potentially novel microcystins. In particular, this study has shown evidence for two previously unknown hepatotoxins, microcystin-LW and microcystin-VF, in extracts of *M. aeruginosa* PCC 7820.

### Acknowledgements

The authors would like to thank Dr. Judy Needham for providing methanol extracts of *M. aeruginosa* cells used in the preliminary development stages of this study. The technical assistance of Melanie Hoare in preparing cell cultures is also gratefully acknowledged. K.P.B. would like to acknowledge funding from the Walter C. Summer Fellowship.

### References

- [1] G.A. Codd and G.K. Poon, in L.J. Rogers and J.G. Gallon (Editors), *Biochemistry of the Algae and Cyanobacteria*, Clarendon Press, Oxford, 1988, p. 283.
- [2] W.W. Carmichael, in A.T. Tu (Editor), *Handbook of Natural Toxins*, Marcel Dekker, New York, 1988, p. 121.
- [3] J.A.O. Meriluoto, S.E. Nygård, A.M. Dahlem and J.E. Eriksson, *Toxicon*, 28 (1990) 1439.
- [4] H.W. Siegelman, W.H. Adams, R.D. Stoner and D.N. Slatkin, in E.P. Ragelis (Editor), *Seafood Toxins*, American Chemical Society, Washington, DC, 1984, p. 407.
- [5] M.T.C. Runnegar, R.G. Gerdes and I.R. Falconer, *Toxicon*, 29 (1991) 43.
- [6] W.C. Theiss, W.W. Carmichael, J. Wyman and R. Bruner, *Toxicon*, 26 (1988) 603.
- [7] M.T.C. Runnegar, J. Andrews, R.G. Gerdes and I.R. Falconer, *Toxicon*, 25 (1987) 1235.
- [8] J.E. Eriksson, G.I.L. Paatero, J.A.O. Meriluoto, G.A. Codd, G.E.N. Kass, P. Nicotera and S. Orrenius, *Exp. Cell Res.*, 185 (1989) 86.
- [9] A.S. Dabholkar and W.W. Carmichael, *Toxicon*, 25 (1987) 285.
- [10] M.T.C. Runnegar and I.R. Falconer, *Toxicon*, 24 (1986) 109.
- [11] W.W. Carmichael, J.W. He, Z.R. He and Y.M. Juan, *Toxicon*, 26 (1988) 1213.
- [12] M. Namikoshi, K.L. Rinehart, R. Sakai, R.R. Stotts, A.M. Dahlem, V.R. Beasley, W.W. Carmichael and W.R. Evans, *J. Org. Chem.*, 57 (1992) 866.
- [13] A. Kungsuwan, T. Noguchi, S. Matsunaga, M.F. Watanabe, S. Watabe and K. Hashimoto, *Toxicon*, 26 (1988) 119.
- [14] J.A.O. Meriluoto, A. Sandström, J.E. Eriksson, G. Remaud, A.G. Craig and J. Chattopadhyaya, *Toxicon*, 27 (1989) 1021.
- [15] D.M. Toivola, J.E. Eriksson and D.L. Brautigam, *FEBS Lett.*, 344 (1994) 175.
- [16] R.E. Honkanen, J. Zwiller, R.E. Moore, S. Daily, B.S. Khatra, M. Dukelow and A.L. Boynton, *J. Biol. Chem.*, 265 (1990) 19401.
- [17] C. MacKintosh, K.A. Beattie, S. Klumpp, P. Cohen and G.A. Codd, *FEBS Lett.*, 264 (1990) 187.
- [18] R. Nishiwaki-Matsushima, S. Nishiwaki, T. Ohta, S. Yoshiawa, M. Suganuma, K.-I. Harada, M.F. Watanabe and H. Fujiki, *Jpn. J. Cancer Res.*, 82 (1991) 993.
- [19] R. Nishiwaki-Matsushima, T. Ohta, S. Nishiwaki, M. Suganuma, K. Kohyama, T. Ishikawa, W.W. Carmichael and H. Fujiki, *J. Cancer Res. Clin. Oncol.*, 118 (1992) 420.
- [20] W.W. Carmichael, *Sci. Am.*, January (1994) 78.
- [21] K.L. Rinehart, M. Namikoshi and B.W. Choi, *J. Appl. Phycol.*, 6 (1994) 159.
- [22] W.W. Carmichael, *J. Appl. Bacteriol.*, 72 (1992) 445.
- [23] D.P. Botes, C.C. Viljoen, H. Kruger, P.L. Wessels and D.H. Williams, *S. Afr. J. Sci.*, 78 (1982) 378.
- [24] D.P. Botes, A.A. Tuinman, P.L. Wessels, C.C. Viljoen, H. Kruger, D.H. Williams, S. Santikarn, R.J. Smith and S.J. Hammond, *J. Chem. Soc. Perkin Trans. 1*, (1984) 2311.
- [25] D.P. Botes, C.C. Viljoen, H. Kruger, P.L. Wessels and D.H. Williams, *Toxicon*, 20 (1982) 1037.
- [26] K.L. Rinehart, K.-I. Harada, M. Namikoshi, C. Chen and C.A. Harvis, *J. Am. Chem. Soc.*, 110 (1988) 8557.
- [27] W.W. Carmichael, V. Beasley, D.L. Bunner, J.N. Eloff, I. Falconer, P. Gorham, K.-I. Harada, T. Krishnamurthy, M. Yu, R.E. Moore, K.L. Rinehart, M. Runnegar, O.M. Skulberg and M. Watanabe, *Toxicon*, 26 (1988) 971.
- [28] A.T.R. Sim and L. Mudge, *Toxicon*, 31 (1993) 1179.
- [29] T.W. Lambert, M.P. Boland, C.F.B. Holmes and S.E. Hrudehy, *Environ. Sci. Technol.*, 28 (1994) 753.
- [30] W.W. Carmichael and P.E. Bent, *Appl. Environ. Microbiol.*, 41 (1981) 1383.
- [31] L.A. Lawton, D.L. Campbell, K.A. Beattie and G.A. Codd, *Lett. Appl. Microbiol.*, 11 (1990) 205.
- [32] F.S. Chu, X. Huang and R.D. Wei, *J. Assoc. Off. Anal. Chem.*, 73 (1990) 451.
- [33] P.S. Gathercole and P.G. Thiel, *J. Chromatogr.*, 408 (1987) 435.
- [34] J.A.O. Meriluoto, J.E. Eriksson, K.-I. Harada, A.M. Dahlem, K. Sivonen and W.W. Carmichael, *J. Chromatogr.*, 509 (1990) 390.
- [35] K.-I. Harada, M. Suzuki, A.M. Dahlem, V.R. Beasley, W.W. Carmichael and K.L. Rinehart, *Toxicon*, 26 (1988) 433.
- [36] R. Luukkainen, K. Sivonen, M. Namikoshi, M. Färdig,

- K.L. Rinehart and S.I. Niemela, *Appl. Environ. Microbiol.*, 59 (1993) 2204.
- [37] C. Edwards, L.A. Lawton, K.A. Beattie, G.A. Codd, S. Pleasance and G.J. Dear, *Rapid Commun. Mass Spectrom.*, 7 (1993) 714.
- [38] C.F.B. Holmes, *Toxicon*, 29 (1991) 469.
- [39] M.P. Boland, M.A. Smillie, D.Z.X. Chen and C.F.B. Holmes, *Toxicon*, 31 (1993) 1393.
- [40] D.Z.X. Chen, M.P. Boland, M.A. Smillie, H. Klix, C. Ptak, R.J. Andersen and C.F.B. Holmes, *Toxicon*, 31 (1993) 1407.
- [41] T. Krishnamurthy, L. Szafraniec, D.F. Hunt, J. Shabanowitz, J.R. Yates, C.R. Hauer, W.W. Carmichael, O. Skulberg, G.A. Codd and S. Missler, *Proc. Natl. Acad. Sci. USA*, 86 (1989) 770.
- [42] D.P. Botes, P.L. Wessels, H. Kruger, M.T.C. Runnegar, S. Santikarn, R.J. Smith, J.C.J. Barna and D.H. Williams, *J. Chem. Soc. Perkin Trans. 1*, (1985) 2747.
- [43] I.M. Birk, U. Matern, I. Kaiser, C. Martin and J. Weckesser, *J. Chromatogr.*, 449 (1988) 423.
- [44] I.M. Birk, R. Dierstein, I. Kaiser, U. Matern, W.A. König, R. Krebber and J. Weckesser, *Arch. Microbiol.*, 151 (1989) 411.
- [45] K. Sivonen, W.W. Carmichael, M. Namikoshi, K.L. Rinehart, A.M. Dahlem and S.I. Niemela, *Appl. Environ. Microbiol.*, 56 (1990) 2650.
- [46] K.-I. Harada, K. Matsuura, M. Suzuki, M.F. Watanabe, S. Oishi, A.M. Dahlem, V.R. Beasley and W.W. Carmichael, *Toxicon*, 28 (1990) 55.
- [47] K. Sivonen, M. Namikoshi, W.R. Evans, M. Färdig, W.W. Carmichael and K.L. Rinehart, *Chem. Res. Toxicol.*, 5 (1992) 464.
- [48] F. Kondo, Y. Ikai, H. Oka, N. Ishikawa, M.F. Watanabe, M. Watanabe, K.-I. Harada and M. Suzuki, *Toxicon*, 30 (1992) 227.
- [49] G.K. Poon, L.J. Griggs, C. Edwards, K.A. Beattie and G.A. Codd, *J. Chromatogr.*, 628 (1993) 215.
- [50] M. Namikoshi, K.L. Rinehart, A.M. Dahlem and V.R. Beasley, *Tetrahedron Lett.*, 30 (1989) 4349.
- [51] S. Pleasance, P. Thibault and J. Kelly, *J. Chromatogr.*, 591 (1992) 325.
- [52] S.J. Locke and P. Thibault, *Anal. Chem.*, 66 (1994) 3436.
- [53] S. Pleasance and P. Thibault, in P. Camillieri (Editor), *Capillary Electrophoresis, Theory and Practice*, CRC Press, Boca Raton, FL, 1993, p. 311.
- [54] R.D. Smith, J.A. Olivares, N. Nguyen and H.R. Udseth, *Anal. Chem.*, 60 (1988) 436.
- [55] R.D. Stoner, W.H. Adams, D.N. Slatkin and H.W. Siegelman, *Toxicon*, 27 (1989) 825.
- [56] S.M.F.O. Azevedo, W.R. Evans, W.W. Carmichael and M. Namikoshi, *J. Appl. Phycol.*, 6 (1994) 261.
- [57] K. Eckart, *Mass Spectrom. Rev.*, 13 (1994) 23.
- [58] K. Sivonen, O.M. Skulberg, M. Namikoshi, W.R. Evans, W.W. Carmichael and K.L. Rinehart, *Toxicon*, 30 (1992) 1465.
- [59] J.F. Kelly, S.J. Locke, L. Ramaley and P. Thibault, *J. Chromatogr. A*, in press.
- [60] K.I. Harada, K. Ogawa, K. Matsuura, H. Murata, M. Suzuki, M.F. Watanabe, Y. Itezo and N. Nakayama, *Chem. Res. Toxicol.*, 3 (1990) 473.



ELSEVIER

Journal of Chromatography A, 712 (1995) 269–284

---

---

JOURNAL OF  
CHROMATOGRAPHY A

---

---

# Industrial applications of capillary zone electrophoresis–mass spectrometry

Michel W.F. Nielen

*Akzo Nobel Central Research, Department of Analytical Chemistry and Environmental Analysis, P.O. Box 9300,  
6800 SB Arnhem, Netherlands*

---

## Abstract

Capillary zone electrophoresis was coupled on-line via a tricoaxial sheath flow interface with a benchtop quadrupole mass spectrometer (CZE–MS) equipped with a (pneumatically assisted) electrospray ionization source. Experimental parameters were optimized for operation in the negative-ion scan mode. The system was applied to the fingerprinting of an alkylsulphate detergent, to the identification of an impurity in a chloramine-T disinfectant, to the characterization of a complex polyethoxylated alkylphosphate emulgator, to the analysis of phenoxy acid herbicides and to the impurity profiling of MCP. The optimized system was found to fully maintain the CZE separation performance, showing up to 1 million theoretical plates for the low-molecular-mass analytes studied. The sensitivity in the full-scan mode was typically in the picogram range and sufficient for the separation and identification of minor impurities in these industrial chemicals, down to the 0.1% level. In addition, the feasibility of on-column transient isotachopheresis (ITP–CZE–MS) under high electroosmotic flow conditions has been demonstrated for sample preconcentration and subsequent identification of trace impurities.

---

## 1. Introduction

Initially, capillary zone electrophoresis (CZE) [1] was mainly applied to biochemical analyses, but since 1989 its separation power has been demonstrated in the other fields of chemical analysis as well [2,3]. The ability of CZE to resolve mixtures which are hard to separate by other (chromatographic) methods puts a strong demand on the coupling of CZE with identification methods such as mass spectrometry (MS). As a rule CZE–MS coupling must be performed on-line because of the small elution volumes

(nanolitres) of the zones which migrate through the capillary.

The on-line coupling of CZE with electrospray (ESI)-MS was demonstrated for the first time by Olivares et al. [4], followed by Lee et al. [5] for the coupling with pneumatically-assisted electrospray (ionspray, ISP). The developments in on-line CZE–MS, including the coupling with continuous-flow fast atom bombardment (FAB)-MS, have been described in two recent reviews [6,7]. From our literature survey of on-line CZE–MS, covering 100 publications in the period 1987–1994, we concluded that (a)

(pneumatically-assisted) electrospray and (b) coaxial interface designs are being preferred, (c) about 85% of the CZE–MS work described so far is about positive-ion CZE–MS and, (d) most of the applications are in the biochemistry field; the other applications deal with (a.o.) drugs, metabolites, toxins, dyes and pesticides. Negative-ion electrospray CZE–MS is obviously more demanding, especially when the stability of the ESI is concerned. The onset of corona discharge has been reported to occur at significantly lower field strengths in negative-ion ESI of aqueous solutions versus positive-ion operation because of the fact that electrons can easily emanate from the edges of the stainless-steel electrospray capillary held at high negative potentials [8,9]. Especially in CZE–MS with coaxial sheath flow interfaces, the electrical contact at the CZE capillary outlet with the negative ESI potential might aggravate an unstable situation [9].

Other major concerns in on-line CZE–MS coupling are the maintenance of the separation integrity and the poor (concentration) sensitivity. The former can be realized by proper interface designs and good operating conditions (see below), and the latter covers the most important current research topics in CZE–MS: improvement of the concentration sensitivity via increased sample loadability of the CZE capillary using isotachophoretic principles [10], improvement of the ionization efficiency using sheathless electrospray interfaces and small I.D. (5–10  $\mu\text{m}$ ) capillaries [11,12] and the use of highly sensitive ion-trap mass spectrometers [13].

In this work, a commercial benchtop CZE–MS system was used based on a quadrupole MS equipped with an atmospheric pressure source, pneumatically-assisted electrospray ionization, and a tricoaxial CZE–MS interface. This system was applied to the analysis of a variety of industrial chemicals: the fingerprinting of a sodium alkylsulphate detergent, the analysis of the disinfectant chloramine-T, the characterization of a complex polyethoxylated alkylphosphate emulgator and the analysis of phenoxy acid herbicides and related impurities. In all cases the MS was operated in the negative-ion scan mode.

The results obtained show good separation performance, up to 1 million theoretical plates,

and adequate stability and sensitivity for the identification of impurities (down to the 0.1% level) in these products.

## 2. Experimental

### 2.1. Apparatus

A Lauerlabs (Emmen, Netherlands) Model PRINCE capillary electrophoresis system was used, equipped with an F.u.G. (Rosenheim, Germany) Model HCN 35-35000 power supply, operated in the constant voltage mode. CZE was performed in 80–125 cm  $\times$  50–75  $\mu\text{m}$  I.D., 375  $\mu\text{m}$  O.D. fused-silica capillaries from Polymicro Technologies (Phoenix, AZ, USA), from which the first 30 cm were thermostated in the oven at 30°C. Samples were introduced into the capillary via the controlled pressure system, typically at 40 mbar during 0.1 min, unless stated otherwise. The CZE system was interfaced with a VG-Platform (Fisons Instruments VG–Biotech, Altrincham, UK) mass spectrometer equipped with an API source and a tricoaxial CZE–MS interface with pneumatically-assisted electrospray ionization. The drying and the nebulizing gas were both nitrogen. Depending on the application, the flows of the drying and the nebulizing gas varied between 40 and 150 and 30 and 45 l/h, respectively, the source temperature between 40 and 60°C, the electrospray voltage was –3 to –4 kV, the HV lens –0.2 kV and the cone voltage varied between –15 and –90 V; the multiplier was set at 650 V. The mass spectrometer was calibrated in the positive-ion mode using a mixture of PEG–ammonium adducts.

The make-up liquid, iso-propanol–water (4:1), was provided by an Applied Biosystems (San Jose, CA, USA) Model 140B syringe pump at 5–10  $\mu\text{l}/\text{min}$ . The pump was equipped with a capillary fused-silica restrictor yielding a back-pressure of approx. 80 bar in order to guarantee a stable microflow.

### 2.2. Chemicals

Water was purified in an Alpha-Q (Millipore, Bedford, MA, USA) apparatus. The detergent



Teepol HB7 was obtained from Sigma (St. Louis, MO, USA). Mesityloxyde, chloramine-T, the phenoxy acid herbicides, MCPP and the polyethoxylated alkylphosphate were from laboratory stock. All other chemicals were analytical grade and obtained from J.T. Baker (Deventer, Netherlands).

### 2.3. Methods

The electrophoretic mobilities, the coefficient of electroosmotic flow, and the plate numbers were calculated using the equations in Ref. [14]. New CZE capillaries were flushed with 1 M NaOH, water and finally with the buffer under investigation. In between subsequent analyses the CZE capillary was flushed with buffer only.

## 3. Results and discussion

### 3.1. General considerations

For a successful operation of a CZE–MS system with a tricoaxial interface at least the following critical parameters must be taken into account: (a) the stability of the CZE current via the sheath electrode; (b) the composition and flow-rate of the sheath liquid; (c) the compatibility of the CZE buffer; (d) the relative position of the three capillaries at the probe tip; (e) the flow-rates of the drying and the nebulizing gas; and (f) sample discrimination. The impact of some of these parameters on stability and sensitivity might be rather different from one CZE–MS design to the other and will be discussed here for the particular instrument as described in section 2.

Following the suggestions of Straub and Voyksner [15] we obtained an improved electrospray stability for isopropanol–water versus a methanol sheath flow and a better sensitivity (up to two-fold) at 5  $\mu$ l/min as compared with 10  $\mu$ l/min. From a compatibility point of view, the best CZE buffer would be volatile and contain a significant percentage of organic solvent (ideally the buffer would be the same as the sheath liquid; in particular situations, e.g. in on-line ITP–CZE–MS [10], they even must have the

same composition) in order to assure efficient mixing with the sheath flow at the probe tip, and a low conductivity, the latter providing a more efficient electrospray ionization [16,17] and might be an alternative to the use of very small I.D. (5–10  $\mu$ m) CZE capillaries [11,12]. As in LC–MS, however, such an ideal CZE–MS buffer often differs significantly from the ideal CZE buffer, in practice a good compromise has thus to be found for each application.

In agreement with Varghese and Cole [9] we found protruding capillaries to provide the best sensitivity, but in contrast with their work we obtained adequate stability even with protruding capillaries. Probably a tapered end of the CZE capillary [7] would give better mixing characteristics at the probe tip, but we still did not use that option since the tip would be more fragile.

Many authors [e.g. 13,18] report about the aspirating effect of the coaxial nebulizing gas which might cause the introduction of air during the injection in the CZE system and which introduces a laminar flow inside the CZE capillary during the actual electrophoretic separation. We observed such an aspirating effect at very high nebulizing gas flows (above 50 l/h) only. Actually the reverse situation is true in the design of our API source: a small restriction in the drying gas exhaust tube causes a small overpressure which generates a laminar flow in the direction of the CZE inlet vial and hinders the injection process. In order to study the impact on the CZE performance, the following experiment was carried out. In a first series of experiments the tricoaxial probe was outside the API source while the ESI voltage was off and the nebulizing gas was on. In the second series of experiments the probe was inside the API source with the ESI voltage still off, but with both the drying and the nebulizing gas on. The electroosmotic flows and the plate numbers were determined using a neutral marker, mesityloxyde, which was detected half-way the CZE capillary by UV absorbance. Care was taken to assure that the liquid level in the inlet vial was at the same height as the probe tip in both cases. From the results of the second series of experiments relative to the first series, i.e. relative to the situation outside the API source, it was concluded

that the impact of the pressure-induced flow on the plate number and the electroosmotic flow was significant: with 50  $\mu\text{m}$  and 75  $\mu\text{m}$  I.D. capillaries the electroosmotic flows were reduced to 95 and 85%, respectively, and the plate numbers were reduced to 70% and 5%, respectively. Fortunately, our CZE apparatus is capable of programming either a positive or a negative pressure on the inlet vial during the electrophoretic separation, thus we can compensate for a deviation from atmospheric pressure in the source. Nevertheless 50  $\mu\text{m}$  I.D. (or even smaller I.D.) CZE capillaries are to be preferred, also because of the lower conductivity. The negative impact of the pressure-induced flow on the injection can be simply overcome by switching off the gases during the injection [13]. In addition one should switch off the ESI voltage during pressure injection in order to avoid sample discrimination.

To summarize, for this particular CZE–MS system we recommend the parameters and settings for negative-ion CZE–MS as shown in Table 1. Using these settings it is possible to fully maintain the CZE separation performance, even up to 1 million theoretical plates as shown in the following application.

### 3.2. Fingerprinting of linear alkylsulphates

Linear alkylsulphates are widely used in detergent formulations. Usually they are complex mixtures of components with the anionic group in common but with different lengths of the alkylchain. Fingerprinting of these detergents is necessary in order to assess the particular application area. Liquid chromatography (LC) has

been used for this purpose for many years. Apart from difficulties in obtaining baseline resolution, another problem is the absence of a suitable chromophoric group for UV-absorbance detection.

However, the use of on-line LC–MS with an ion spray interface has shown to be a good alternative for detection problems in this particular field [19,20]. We used the separation power of CZE for the analysis of a commercial detergent, Teepol HB7 [21]. Using a UV-absorbing background electrolyte, we were able to detect the negative peaks as a characteristic fingerprint (actually five fingers indeed) of this detergent featuring baseline resolution, plate numbers of up to 440 000 and an analysis time of 3 min only [21]. The peaks were identified by standard addition and found to represent  $\text{C}_9$ – $\text{C}_{13}$  alkylsulphates. These results were confirmed later by others who also showed the effect of the buffer cation in these separations [22]. It was demonstrated by Smith et al. [23] that sodium dodecylsulphate is very well amenable to CZE–MS. In this work we have studied the use of CZE–MS for the fingerprinting and the identification of the commercial  $\text{C}_9$ – $\text{C}_{13}$  alkylsulphate sample. We used a 50  $\mu\text{m}$  I.D. CZE capillary with a 10 mM ammonium acetate buffer of pH 8.9 and a voltage of 30 kV. The actual voltage difference was 34 kV (400 V/cm) because of the ESI voltage of  $-4$  kV.

A 1:1000 dilution of the detergent with the electrophoresis buffer was made and injected at 40 mbar during 0.1 min, followed by the injection of a similar plug of buffer. Next, the CZE voltage, the ESI voltage and the gases were switched on and the MS started scanning from

Table 1

Guidelines for negative-ion CZE–MS using the system as described in section 2

1. Monitor your CZE current during CZE–MS.
2. Use 50  $\mu\text{m}$  (or smaller) I.D. CZE capillaries.
3. Use a nebulizing gas flow of 30 l/h and a drying gas flow lower than 50 l/h.
4. Avoid a height difference between the liquid level in the CZE inlet vial and the probe tip.
5. Use a stable sheath flow of iso-propanol–water (4:1) at 5  $\mu\text{l}/\text{min}$ .
6. Remove the polyimide outerlayer of the CZE capillary at the probe tip and protrude the CZE capillary 0.2–0.3 mm relative to the sheath flow capillary, and protrude the sheath flow capillary 0.8–1 mm relative to the nebulizing gas capillary.
7. Switch off the drying and the nebulizing gas and the ESI voltage during injection.

100 to 300 amu in 0.5 s. Fig. 1 shows both the total ion current (TIC) and the reconstructed ion electropherograms (RIE) of the  $[M - H]$  ions indicated. The fingerprint can be easily recognized from the TIC, i.e. even without any prior knowledge of the composition. The separation of the individual components is quite satisfactory. The analysis time has almost doubled as compared with our previous work [21] because of the longer CZE capillary and the lower electroosmotic flow in the ammonium acetate buffer versus the sodium veronal buffer. However, the most striking result here is the identification of the  $C_8$  ( $[M - H]$  at  $m/z$  209) and  $C_{14}$  ( $[M - H]$  at  $m/z$  293) homologues in this detergent sample which were not found before. In order to support the identification, the same sample was analyzed under different cone voltage settings thus promoting in-source CID fragmentation patterns. All components showed the  $[HSO_4]^-$  ion ( $m/z$  97) upon in-source CID, in addition to their characteristic  $[M - H]^-$  ions. The overall performance of the CZE-MS system was investigated with the same detergent but at a lower concentration and a smaller injection volume (20 mbar, 0.1 min of a 2000  $\times$  dilution). The MS was scanned over a smaller range at high speed, 215–300 amu in 0.2 s. The total ion current thus obtained (Fig. 2) is really amazing: ultra-high resolution and plate numbers ranging from 700 000 to 1 000 000 (except for  $C_{10}$  alkylsulphate: 330 000). Two additional peaks were observed in between the homologues, which represent, possibly, branched alkylsulphates. When dispersion in CZE is diffusion-limited only, the plate number equation is according to Ref. [1]:  $N = mV/2D$ , in which  $N$  is the plate number,  $m$  the mobility,  $V$  the voltage difference over the capillary and  $D$  the diffusion coefficient. The plate numbers and mobilities obtained here correspond with calculated diffusion coefficients in the order of  $0.8 \cdot 10^{-5}$ – $1.2 \cdot 10^{-5}$   $cm^2 s^{-1}$ , which are very realistic for low-molecular-mass analytes like these. Thus it can be concluded that the theoretically maximum attainable plate number in CZE can be realized in this CZE-MS system provided that the instrument is optimized using the guidelines in Table 1 and overloading

of the CZE capillary is being avoided. This linear alkylsulphate application provides very reproducible results and is currently used as an overall performance standard for negative-ion CZE-MS in our laboratory.

### 3.3. Analysis of chloramine-T

Chloramine-T is widely used as a disinfectant in e.g. the food industry. It can be analyzed by CZE in its anionic form. CZE-MS was carried out using a 75  $\mu m$  I.D. fused-silica capillary and a sheath flow-rate of 10  $\mu l/min$ , i.e. the CZE-MS system was not optimized yet with regard to the guidelines in Table 1. A solution of 0.1 mg/ml chloramine-T in buffer was prepared and injected by a pressure of 40 mbar, 0.1 min, which corresponds to 2 ng. The CZE voltage was switched on and the MS was scanned from 70 to 500 amu in 0.5 s. The total ion current (TIC) and the reconstructed ion electropherogram (RIE) are shown in Fig. 3 (left). Despite the non-optimized conditions, a sharp symmetrical peak, showing 120 000 theoretical plates, could be observed in the TIC and is very obvious from the reconstructed ion electropherogram. The detection limit using the reconstructed ion electropherogram would be 100 pg (scan mode). In an attempt to detect the impurities in chloramine-T, an excess (10 mg/ml) was injected and analyzed by CZE-MS under the same conditions. The total ion current (Fig. 3, right) clearly shows an impurity around 8 min. This result is in good agreement with preliminary CZE-UV studies which also showed one impurity in the electropherogram estimated at the 0.1% level relative to chloramine-T. In the present CZE-MS experiment this corresponds to an injected amount of 200 pg. The impurity was identified using the background subtracted mass spectra shown in Fig. 4. The spectrum of chloramine-T (Fig. 4, lower left) shows the negative ion at  $m/z$  204 and the isotope cluster of one chlorine atom. The impurity (Fig. 4, upper left) has a negative ion at  $m/z$  170 and contains no chlorine at all. The analysis was repeated at an (absolutely) higher cone voltage ( $-60$  vs.  $-16$  V) in order to generate in-source CID fragmentation patterns.

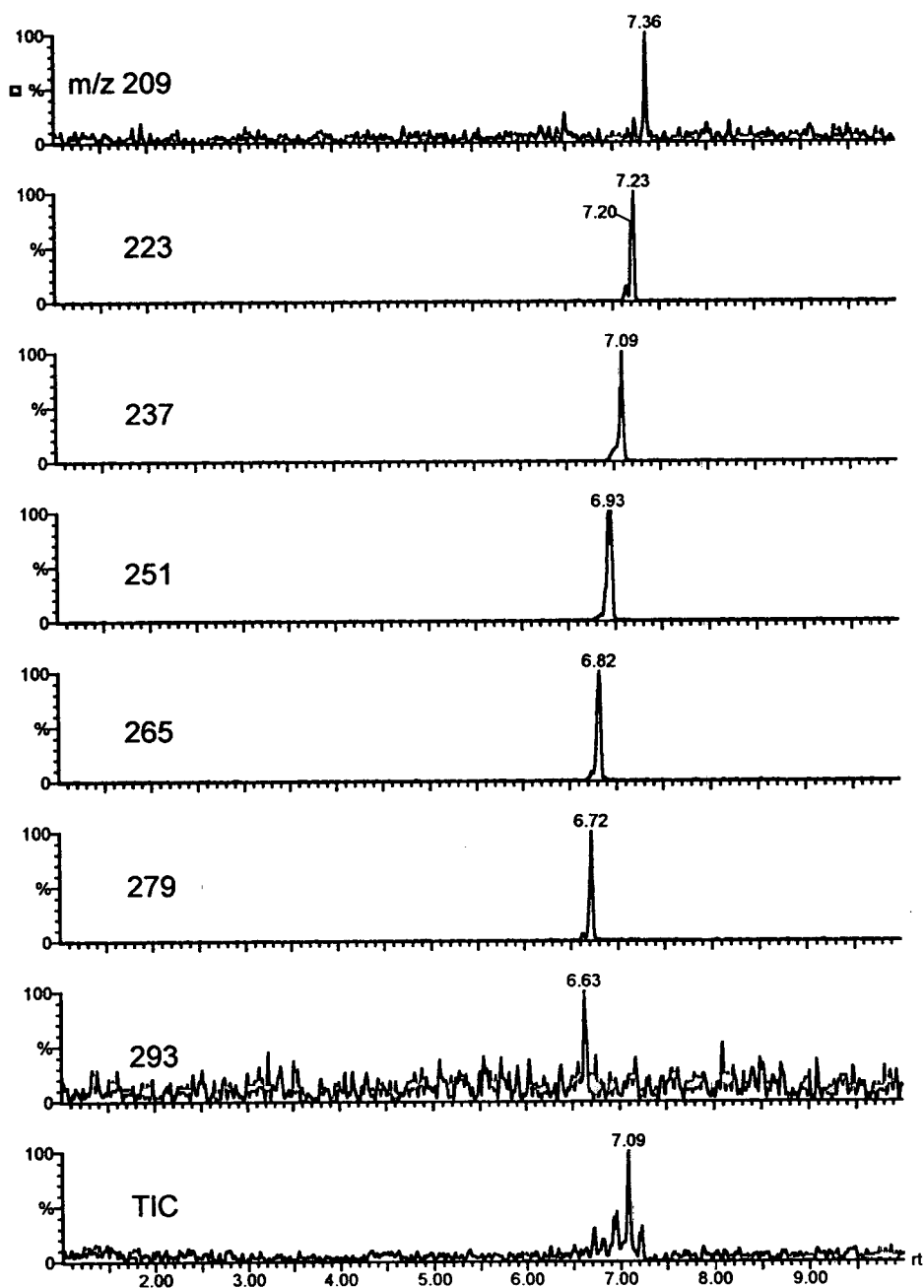


Fig. 1. The analysis of Teepol HB7 by full-scan negative-ion CZE-MS. Total ion current (TIC) and reconstructed ion electropherograms (RIE) of the  $[M - H]^-$  ions indicated. Conditions: injection of a 1:1000 dilution with electrophoresis buffer by pressure (40 mbar, 0.1 min); CZE in a 85 cm  $\times$  50  $\mu$ m I.D. fused-silica capillary using a 10 mM ammonium acetate buffer pH 8.9, constant voltage 30 kV; sheath flow, 5  $\mu$ l/min isopropanol-water (4:1); ESI voltage, -4 kV; cone voltage, -30 V; source, 50°C; drying gas, 50 l/h; nebulizing gas, 30 l/h; scan range, 100–300 amu in 0.5 s. Other conditions, see text.

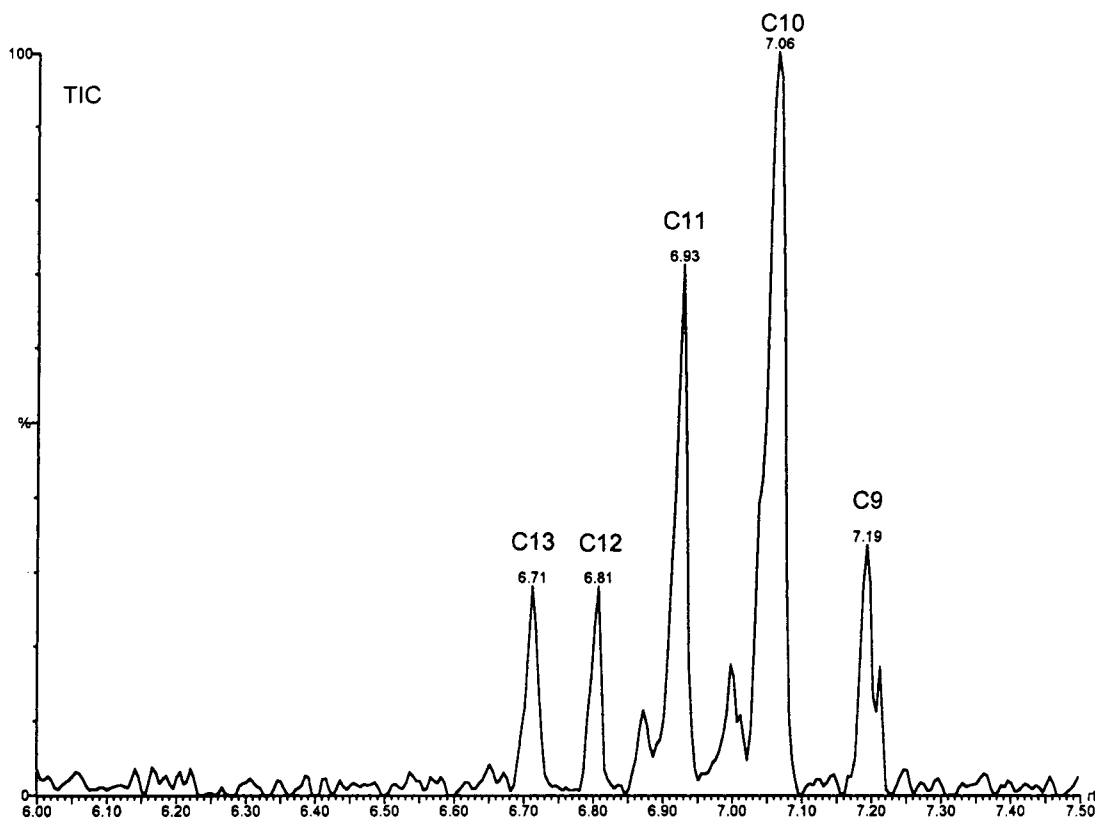


Fig. 2. Total ion current (TIC) showing ultra high-performance CZE-MS of  $C_9$ - $C_{13}$  linear alkylsulphates. Injection of a 1:2000 dilution of Teepol HB7 (20 mbar, 0.1 min). Scan range, 215–300 amu in 0.2 s. Other conditions, see Fig. 1.

The spectra thus obtained (Fig. 4, lower right) indicate that  $m/z$  170 is also a decomposition product in the chloramine-T spectrum. The decomposition pathways are rather different: the chloramine-T spectrum shows a.o. benzene and toluene, while the impurity spectrum (Fig. 4, upper right) shows a.o. the loss of  $SO_2$ . Despite of the dissimilarities in the fragmentation patterns, the most likely identity of the impurity is the decomposition product toluenesulfonamide, formed by the exchange of a chlorine by a hydrogen atom, thus yielding an  $[M - H]^-$  ion at  $m/z$  170 without any chlorine atoms.

#### 3.4. Characterization of a polyethoxylated alkylphosphate

Polyethoxylated alkylphosphates are used as emulgators and exhibit, a.o., antistatic proper-

ties, which are very useful in specific applications. As in the detergent analysis, these products consist of complex mixtures and detailed knowledge of the constituents is required. In the present case, we knew already the presence of phosphor from XRF analysis and the presence of alkyl and ethylene oxide units from NMR analysis. A first attempt with flow injection negative-ion electrospray MS, i.e. without CZE, confirmed the presence of more than 20 components, representing polyethoxylated decyl- and dodecyl-phosphates. Polyethoxylated alkylphosphates cannot be analyzed directly via GC, and LC analysis suffers from detection problems and requires gradient elution. Mono- and dialkylphosphates are weak acids which can be, respectively, double and single negatively charged, depending on the pH of the CZE buffer. We used a 75  $\mu$ m I.D. capillary and a

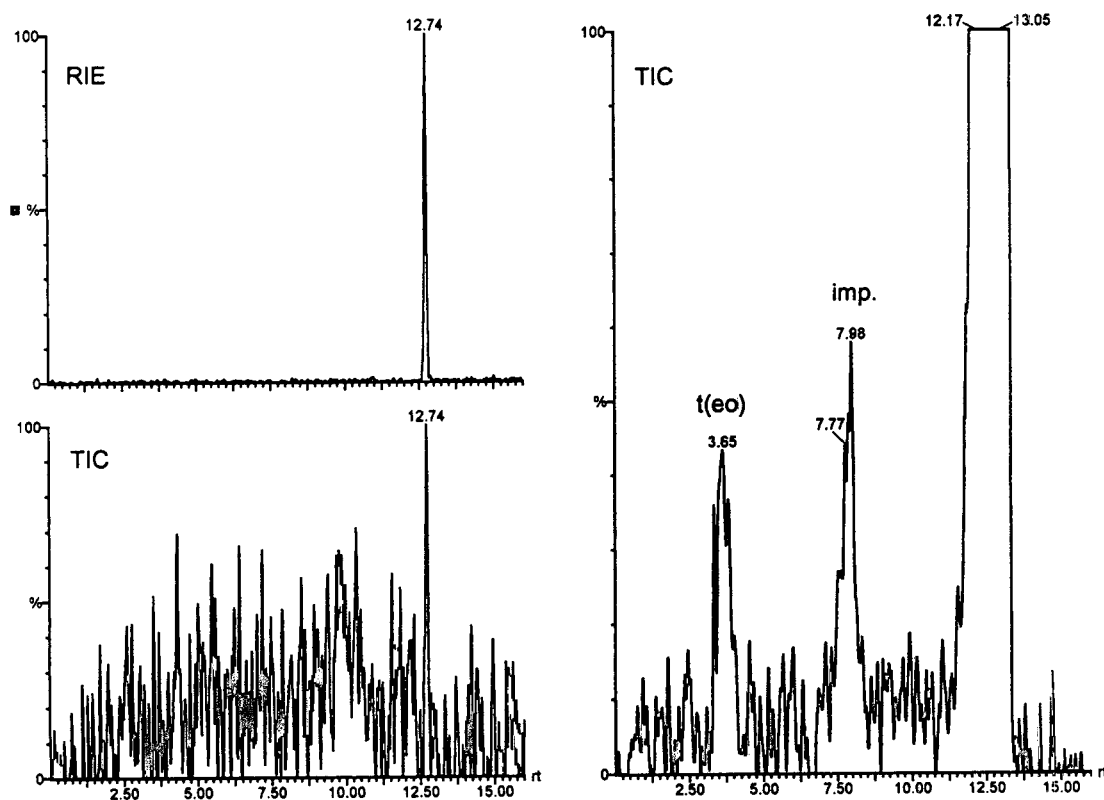


Fig. 3. The analysis of chloramine-T by full-scan negative-ion CZE-MS. Lower left, total ion current (TIC) after injection of a solution of 0.1 mg/ml in buffer (40 mbar, 0.1 min); upper left, reconstructed ion electropherogram (RIE,  $m/z$  204 + 206) of the same analysis. Right, total ion current (TIC) after injection of a 10 mg/ml solution. Conditions: CZE in a 90 cm  $\times$  75  $\mu$ m I.D. fused-silica capillary using a buffer of 10 mM ammonium acetate pH 10; constant voltage, 30 kV; sheath flow, isopropanol-water (4:1) at 10  $\mu$ l/min; ESI voltage, -3.4 kV; cone voltage, -16 V; source, 60°C; drying gas, 150 l/h; nebulizing gas, 45 l/h; scan range, 70–500 amu in 0.5 s. Other conditions, see text.

buffer of 10 mM ammonium acetate (pH 9)-methanol (4:1) in order to obtain sufficient solubility and resolution. The presence of methanol and the relatively high potassium content of the sample decreased the electroosmotic flow as expected, but in conjunction with the overpressure in the ion source (cf. above) rather long analysis times were obtained (> 30 min). Therefore, the pressure-induced laminar flow in the direction of the inlet vial was compensated by programming a pressure of 25 mbar on the inlet vial during the actual CZE separation. Note that the CZE-MS system was not optimized yet with regard to the guidelines in Table 1 and was

scanned from 220 to 1000 amu in 0.5 s. The total ion current thus obtained is shown in Fig. 5 (bottom). About 12 peaks can be easily distinguished, and in between them a few additional minor peaks can be seen. The mass spectra of these peaks showed all  $[M - H]^-$  ions, corresponding with ethoxylated decylphosphates (higher peaks) and ethoxylated dodecylphosphates (smaller peaks). Using the mass spectral data, summed ion electropherograms were reconstructed for both series (Fig. 5, middle and top). The decylphosphates showed 0–15, and the dodecylphosphates 0–12 ethylene oxide units, together 29 components. Looking for even high-

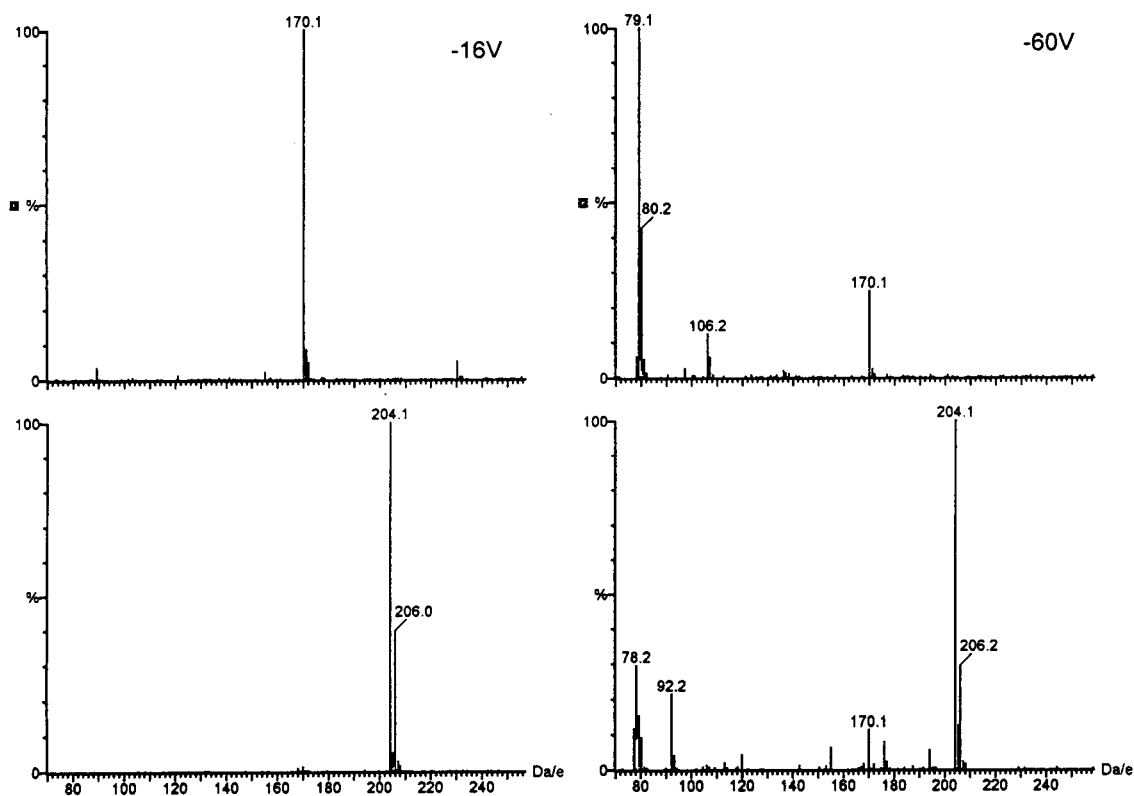


Fig. 4. Background subtracted mass spectra of chloramine-T (lower spectra) and the impurity (upper spectra) using, left, the conditions of Fig. 3 and, right, an (absolutely) higher cone voltage,  $-60$  V vs.  $-16$  V.

er degrees of ethoxylation, the total ion current was further examined at shorter migration times (i.e. at higher apparent mobilities but lower electrophoretic mobilities). Thus all spectra between 8 and 12.5 min were combined and background subtracted, giving the mass spectrum of Fig. 6. Apart from the higher ethoxylated decyl- and dodecylphosphates, a series of didecylphosphates having 0–14 ethylene oxide units showed up in this spectrum. Dialkylphosphates can be single charged only, so it is not surprising that even the lower ethoxylated didecylphosphates appear in the electropherogram before (i.e. at lower electrophoretic mobilities than) the double charged mono-alkylphosphates. To summarize, although a first look at the total ion current showed only about 15 resolved peaks, up to 45

individual components could be identified in this sample using CZE-MS.

### 3.5. Analysis of phenoxy acid herbicides and impurity profiling of MCPP

MCPP, 2-(2-methyl-4-chlorophenoxy)propionic acid, belongs to the group of phenoxy acids, and is widely used in agriculture as a selective herbicide. Formulations of these herbicides can be analyzed by capillary gas chromatography [24] but derivatization of the carboxyl group is required. Liquid chromatography can be applied directly but might not give sufficient resolution for the analysis of related impurities [24]. CZE, on the other hand, shows baseline resolution for the separation of the structurally

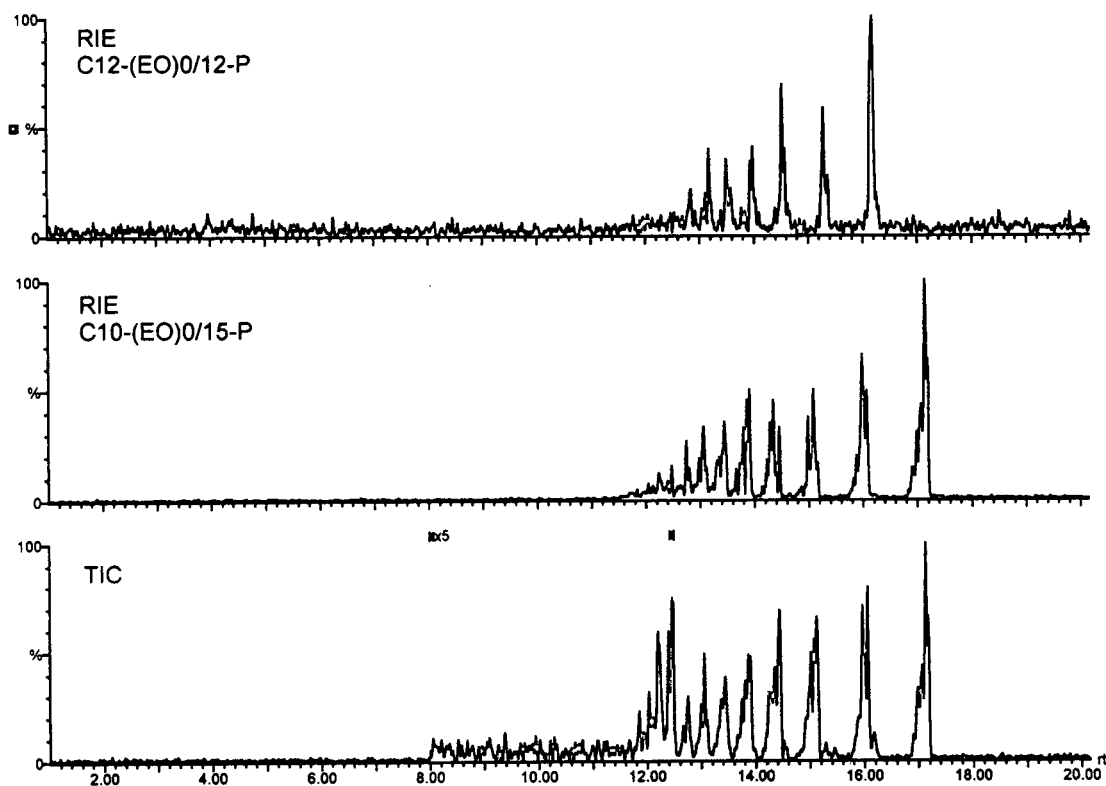


Fig. 5. The characterization of a polyethoxylated alkylphosphate by full-scan negative-ion CZE-MS. Bottom, the total ion current (TIC); middle, the reconstructed ion electropherogram (RIE) of the decyl-polyethoxylated phosphates; and top, the RIE of the dodecyl-polyethoxylated phosphates. Conditions: injection of a 10 mg/ml solution in buffer by a pressure of 40 mbar, 0.1 min; CZE in a 90 cm  $\times$  75  $\mu$ m I.D. fused-silica capillary using a buffer of 10 mM ammonium acetate (pH 9)-methanol (4:1); constant voltage, 30 kV and 25 mbar pressure on the inlet vial during the actual electrophoretic separation; sheath flow, isopropanol-water (4:1) at 5  $\mu$ l/min; ESI voltage, -3 kV; cone voltage, -25 V; source, 60°C; drying gas, 100 l/h; nebulizing gas, 30 l/h; scan range, 220–1000 amu in 0.5 s. Other conditions, see text.

similar phenoxy acid herbicides MCP, 2,4-DP, MCPA and 2,4-D (for structures, see Fig. 7), provided that the pH of the electrophoresis buffer is chosen correctly [25,26]. In our previous work we have studied the separation of phenoxy acid herbicides and analyzed the impurities in MCP using the entire different selectivities as obtained after the addition of different types of cyclodextrines to the CZE buffer [25]. Identification was simply done via standard addition of known impurities to the MCP samples with subsequent analyses using the different CZE buffer systems. The feasibility of CZE coupled with ion spray mass spectrometry for the detection of 2,4-D was demon-

strated by Lee et al. [27], who separated some phenoxy acids (including 2,4-D) using a high acetonitrile content in the buffer, and detected them in the single-ion recording (SIR) mode.

In the present study, a mixture containing 20 ppm (corresponding to 80 pg) of MCP, 2,4-DP, MCPA and 2,4-D was pressure-injected and analyzed using the CZE-MS system in full-scan negative-ion mode, optimized according to the guidelines in Table 1. The reconstructed ion electropherograms are shown in Fig. 8. Baseline separation and high plate numbers were obtained (300 000–500 000 theoretical plates), versus 240 000 plates in the CZE-UV system (cf. Ref. [25]). The higher plate numbers in CZE-



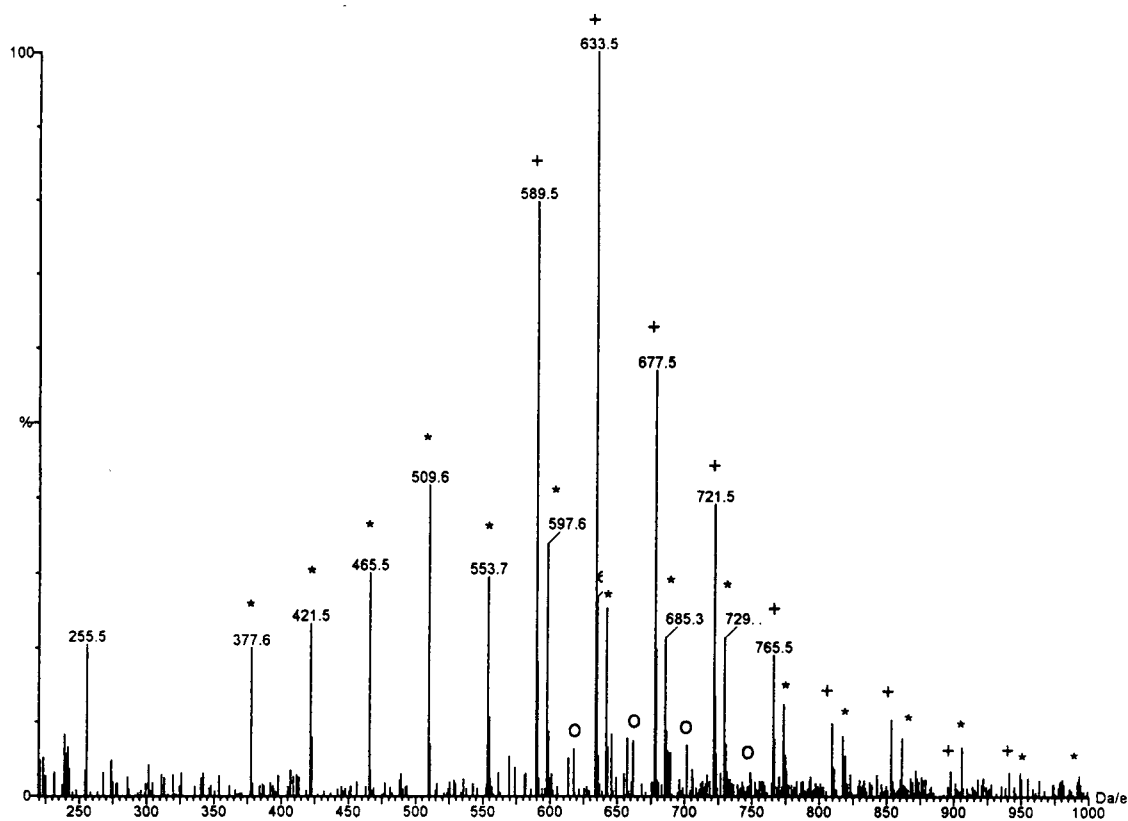


Fig. 6. Background subtracted mass spectrum combined from the data between 8 and 12.5 min in the total ion current of Fig. 5. Symbols: + =  $C_{10}(EO)_{8-16}$  phosphates; O =  $C_{12}(EO)_{8-11}$  phosphates; \* =  $C_{10}/C_{10}(EO)_{0-14}$  phosphates.

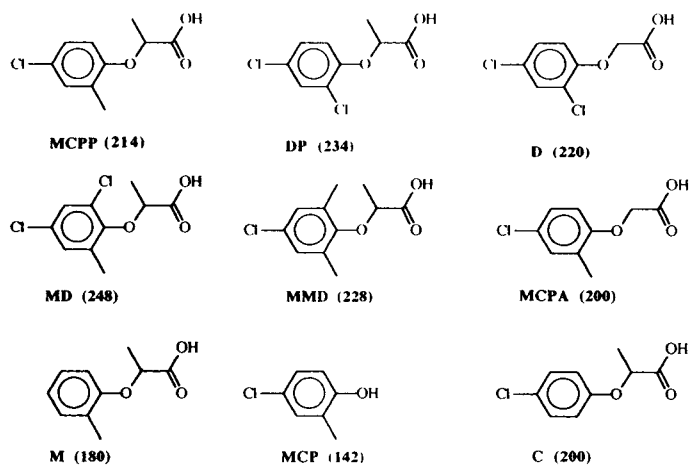


Fig. 7. Structures of MCPP and related compounds (molecular mass in brackets).

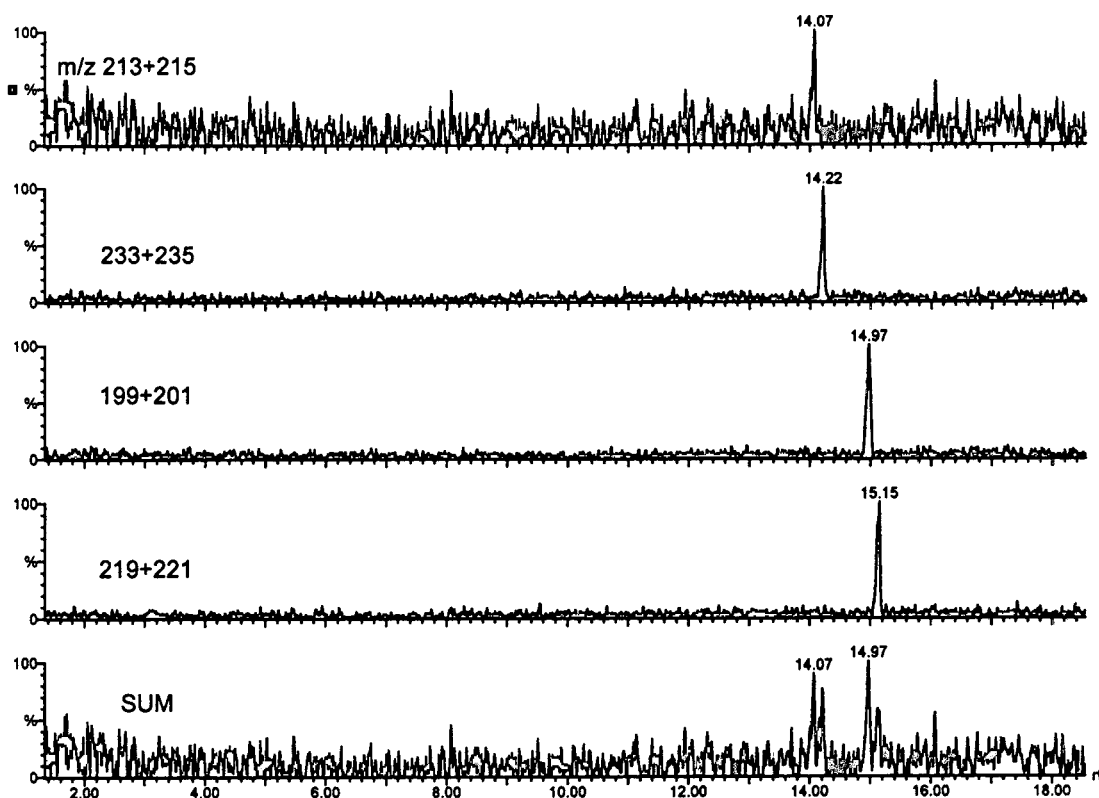


Fig. 8. The analysis of phenoxy acid herbicides by full-scan negative-ion CZE-MS. Reconstructed ion electropherograms (RIE) of the  $[M - H]^-$  ions indicated. Conditions: injection of  $20 \mu\text{g/ml}$  ( $80 \text{ pg}$ ) of each herbicide (in buffer) by pressure of  $40 \text{ mbar}$ ,  $0.1 \text{ min}$ , followed by injection of a similar plug of buffer; CZE in a  $87 \text{ cm} \times 50 \mu\text{m}$  I.D. fused-silica capillary using a buffer of  $10 \text{ mM}$  ammonium acetate pH 4.8; constant voltage,  $30 \text{ kV}$ ; sheath flow, isopropanol-water (4:1) at  $5 \mu\text{l/min}$ ; ESI voltage,  $-4 \text{ kV}$ ; cone voltage,  $-25 \text{ V}$ ; source,  $50^\circ\text{C}$ ; drying gas,  $50 \text{ l/h}$ ; nebulizing gas,  $31 \text{ l/h}$ ; scan range,  $100\text{--}300 \text{ amu}$  in  $0.5 \text{ s}$ . Other conditions, see text.

MS versus CZE-UV might be attributed to the lower buffer concentration (less Joule heating) used in the present work. The detection limits as calculated from the reconstructed ion electropherograms are typically in the order of  $20 \text{ pg}$ , except for MCPP whose  $[M-H]$ -ion, 213, is very close to a persistent background ion at  $m/z$  212. It might be estimated that approximately  $120 \text{ pg}$  of each herbicide will be required in order to distinguish these four peaks in the total ion current (TIC). The background subtracted mass spectra are shown in Fig. 9. The number of chlorine atoms can be readily seen from the isotope distributions around both the  $[M - H]^-$

ions and the main in-source CID decomposition products, the corresponding phenoxy ions.

Next, an excess of an MCPP sample ( $10 \text{ mg/ml}$ ) was injected and analyzed by CZE-MS in order to identify the impurities. In the past, MD, MCPA and M, were found to be present in the range of  $0.1\text{--}1.3\%$  relative to MCPP by CZE-UV [25]. The total ion current and reconstructed ion electropherograms are shown in Fig. 10. A huge peak of MCPP can be seen preceded by a peak at  $7.7 \text{ min}$ , which corresponds to neutral analytes migrating under the influence of the electroosmotic flow only, a peak at  $13.1 \text{ min}$ , and a small peak at  $15.6 \text{ min}$ . The background

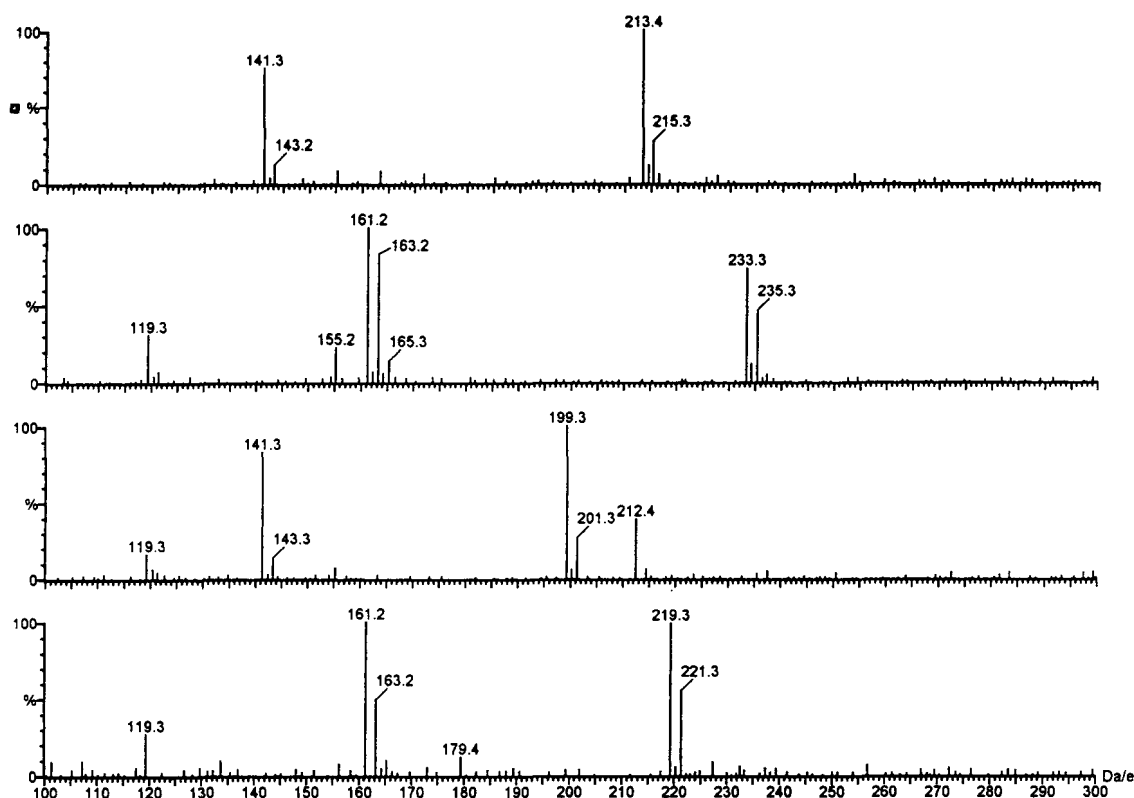


Fig. 9. Background subtracted mass spectra of the four phenoxy acid herbicides in Fig. 8. Top, MCPP; upper middle, DP; lower middle, MCPA; below, D.

subtracted mass spectra of these peaks are shown in Fig. 11. The neutral impurity (Fig. 11, top) shows an  $[M - H]^-$  ion at  $m/z$  141 and one chlorine atom (note that  $m/z$  119 and 212 are background ions). MCP is a good candidate which will behave as a neutral analyte indeed at pH 4.8. The next mass spectrum (Fig. 11, middle) shows at least four compounds which co-migrate at the rear of the MCPP peak and which show extremely narrow peaks (2 s width) in the reconstructed ion electropherograms of Fig. 10. The spectrum contains ions which correspond to a mixture of the MCPA and DP spectra (cf. Fig. 9), extended with  $m/z$  127, 179 and 107. The latter two do not contain any chlorine, making M a good candidate. The ion at 127 does contain one chlorine and must be an acid because of its position in the electropherogram. The impurity

C ( $M_r$  200) will be a good candidate thus providing a nice demonstration of the value of the CID decomposition product at 127, since the parent compound has the same  $[M - H]^-$  ion at  $m/z$  199 and the same chlorine cluster as one of the other impurities, MCPA. The very high plate numbers (2–4 million theoretical plates!) of these compounds are due to a transient isotachophoretic effect [28], as follows. In short, when a sample contains a high concentration of a high mobility co-ion and the CZE buffer ion has a lower mobility than the sample ion, transient isotachopheresis takes place in which the sample co-ion acts as the leading ion and the CZE buffer co-ion as the terminating ion. The sample ion, having a mobility in between, will be focussed in a narrow band as long as the isotachophoretic conditions are maintained. The present situation

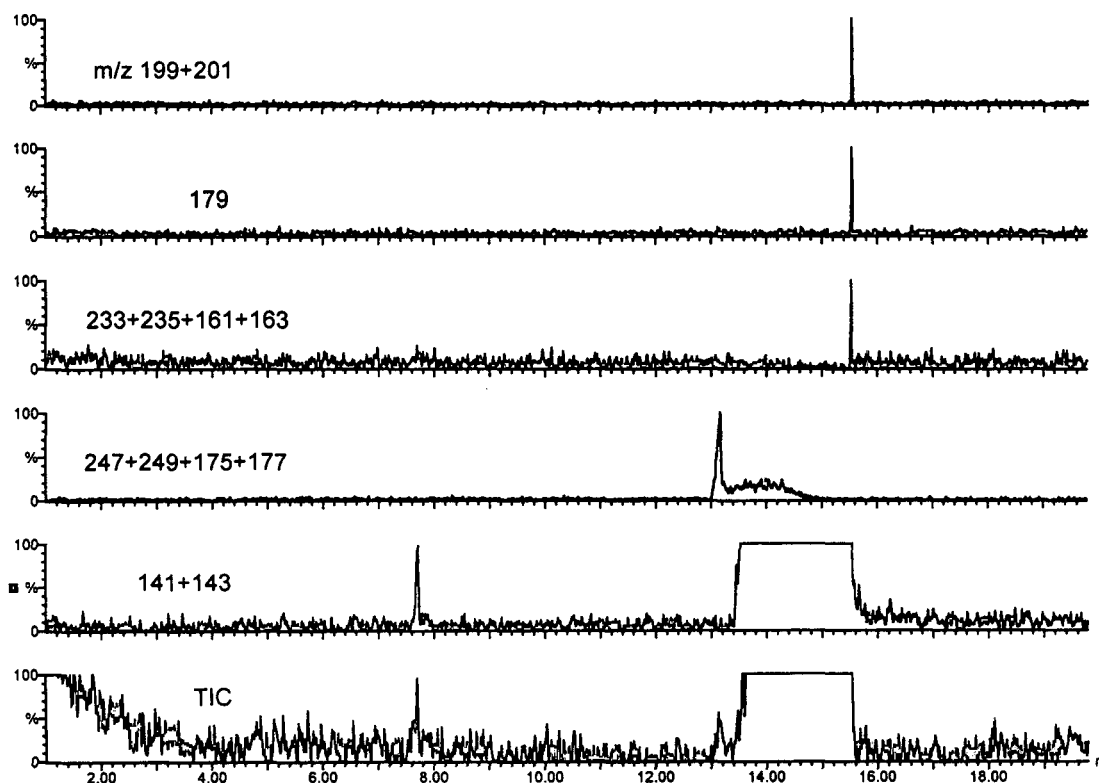


Fig. 10. Impurity profiling of MCPP by full-scan negative-ion CZE-MS. Reconstructed ion electropherograms (RIE) of the  $[M - H]^-$  ions indicated and total ion current (TIC). Injection of 10 mg/ml (in acetonitrile-methanol-CZE buffer, 1:2:2) by pressure of 40 mbar, 0.1 min, followed by injection of a plug of buffer. Other conditions, see Fig. 8 and text.

is different from Ref. [28] because of the presence of a strong electroosmotic flow in a direction opposite to the electrophoretic migration. Nevertheless similar principles apply in such a situation [29], the only difference being that the excess co-ion in the sample should be a low mobility ion and the CZE buffer should contain the high mobility ion. In our case, the excess of MCPP represents the excess (0.05 M) sample co-ion having a low electrophoretic mobility, while the acetate CZE buffer ion (0.01 M) represents the high electrophoretic mobility ion. The impurities M, C, MCPA and DP have electrophoretic mobilities in between MCPP and acetate and will be focussed during the transient isotachophoretic stage. On the other hand, impurities migrating close to the front of MCPP might be broadened, as can be seen in the

reconstructed ion electropherograms of Fig. 10. The spectrum of the broadened peak (Fig. 11, below) shows a mixture of  $[M - H]^-$  ions at  $m/z$  247 and 227, with corresponding fragment ions at  $m/z$  175 and 155, the former having two chlorine and the latter only one chlorine atom. MD and MMD will be good candidates for these impurities. The spectrum of the main component, MCPP, was already shown in Fig. 9. It is interesting to note that apart from the MD, MCPA and M impurities found in the past [25] after spiking of the sample, additional impurities (C, DP, MCP and MMD) were identified now by CZE-MS. In-source CID was essential for their identification and transient isotachophoretic focussing provided the signal-to-noise ratio required for the identification of the trace impurities C and DP, which were not detectable in

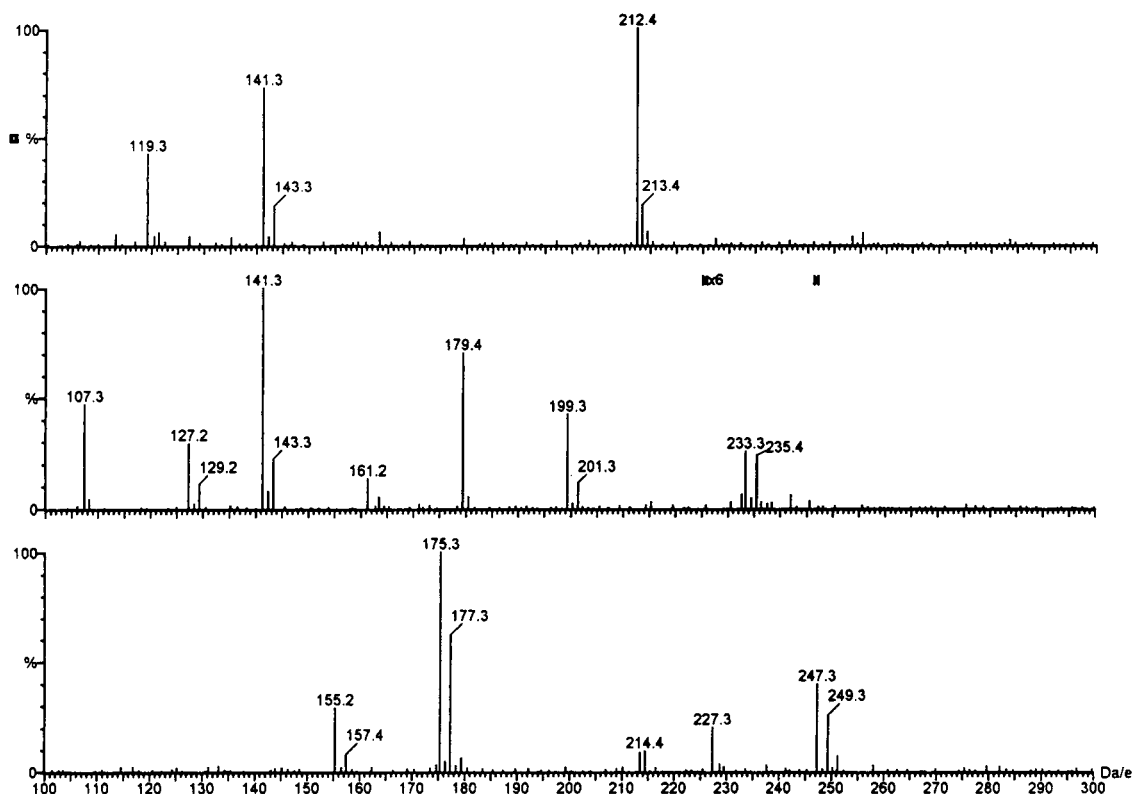


Fig. 11. Background subtracted mass spectra of the impurities in MCPP. Top, spectrum of neutral impurity (MCP) migrating at 7.7 min; middle, spectrum of impurities (MCPA, DP, M, C) migrating at 15.6 min; and bottom, spectrum of impurities (MD, MMD) migrating at 13.1 min in the total ion current (TIC) of Fig. 10.

the CZE–UV approach, i.e. which were present at levels significantly lower than 0.1% relative to MCPP.

#### 4. Conclusions

CZE–MS can be successfully applied to realistic chemical analyses in an industrial research environment. The benchtop system used shows good stability and sensitivity in the negative-ion scan mode, particularly when critical operating parameters are taken into account and optimized. In that case the CZE separation performance is not compromised at all: the reconstructed electropherograms showed plate numbers up to 1 million, even higher than those in comparable CZE–UV studies.

The sensitivity, typically in the picogram range under full-scan conditions, enabled the identification of unknown minor impurities down to the 0.1% level in the examples shown. In addition, transient ITP–CZE–MS under high electroosmotic flow conditions, yielding extremely narrow peaks (up to 4 million theoretical plates), was found to be very useful for on-column preconcentration and subsequent identification of trace impurities ( $\ll 0.1\%$ ).

#### References

- [1] J. Jorgenson and K.D. Lukacs, *Anal. Chem.*, 53 (1981) 1298.
- [2] S.F.Y. Li, *Capillary Electrophoresis, Principles, Practice and Applications*, Elsevier, Amsterdam, 1992.

- [3] C.A. Monnig and R.T. Kennedy, *Anal. Chem.*, 66 (1994) 280R.
- [4] J.A. Olivares, N.T. Nguyen, C.R. Yonker and R.D. Smith, *Anal. Chem.*, 59 (1987) 1232.
- [5] E.D. Lee, W. Muck, J.D. Henion and T.R. Covey, *J. Chromatogr.*, 458 (1988) 313.
- [6] W.M.A. Niessen, U.R. Tjaden and J. van der Greef, *J. Chromatogr.*, 636 (1993) 3.
- [7] R.D. Smith, J.H. Wahl, D.R. Goodlett and S.A. Hofstadler, *Anal. Chem.*, 65 (1993) 574A.
- [8] F.M. Wampler, A.T. Blades and P. Kebarle, *J. Am. Soc. Mass Spectrom.*, 4 (1993) 289.
- [9] J. Varghese and R.B. Cole, *J. Chromatogr.*, 639 (1993) 303.
- [10] M.H. Lamoree, N.J. Reinhoud, U.R. Tjaden, W.M.A. Niessen and J. van der Greef, *Biol. Mass Spectrom.*, 23 (1994) 339.
- [11] J.H. Wahl, D.R. Goodlett, H.R. Udseth and R.D. Smith, *Electrophoresis*, 14 (1993) 448.
- [12] J.H. Wahl, D.C. Gale and R.D. Smith, *J. Chromatogr. A*, 659 (1994) 217.
- [13] J.D. Henion, A.V. Mordehai and J. Cai, *Anal. Chem.*, 66 (1994) 2103.
- [14] M.W.F. Nielen, *J. Chromatogr.*, 542 (1991) 173.
- [15] R.F. Straub and R.D. Voyksner, *J. Am. Soc. Mass Spectrom.*, 4 (1993) 578.
- [16] A.J. Tomlinson, L.M. Benson and S. Naylor, *LC·GC*, 12 (1994) 122.
- [17] A.J. Tomlinson, L.M. Benson and S. Naylor, *J. High Resolut. Chromatogr.*, 17 (1994) 175.
- [18] R. Kostianen, A.P. Bruins and V.M.A. Hakkinen, *J. Chromatogr.*, 634 (1993) 113.
- [19] J.J. Conboy, J.D. Henion, M.W. Martin and J.A. Zweigenbaum, *Anal. Chem.*, 62 (1990) 800.
- [20] D.D. Popenoe, S.J. Morris, P.S. Horn and K.T. Norwood, *Anal. Chem.*, 66 (1994) 1620.
- [21] M.W.F. Nielen, *J. Chromatogr.*, 588 (1991) 321.
- [22] S. Chen and D.J. Pietrzyk, *Anal. Chem.*, 65 (1993) 2770.
- [23] R.D. Smith, C.J. Barinaga and H.R. Udseth, *Anal. Chem.*, 60 (1988) 1948.
- [24] C. Sanchez-Brunete, S. Perez and J.L. Tadeo, *J. Chromatogr.*, 522 (1991) 235.
- [25] M.W.F. Nielen, *J. Chromatogr.*, 637 (1993) 81.
- [26] M.W.F. Nielen, *Trends Anal. Chem.*, 12 (1993) 345.
- [27] E.D. Lee, W. Muck, J.D. Henion and T.R. Covey, *Biomed. Environ. Mass Spectrom.*, 18 (1989) 844.
- [28] T.J. Thompson, F. Foret, P. Vouros and B.L. Karger, *Anal. Chem.*, 65 (1993) 900.
- [29] M.W.F. Nielen, in D. Barcelo (Editor), *Environmental Analysis, Techniques, Applications and Quality Assurance*, Elsevier, Amsterdam, 1993.

**END OF SPECIAL ISSUE**





# Quality Assurance for Environmental Analysis

Method Evaluation within the Measurements and Testing Programme (BCR)

Edited by Ph. Quevauviller, E.A. Maier and B. Griepink

Techniques and Instrumentation in Analytical Chemistry, Volume 17

Quality assurance (QA) for environmental analysis is a growing feature of the nineties as is illustrated by the number of QA guidelines and systems which are being implemented nowadays. This book focuses on the technical aspects of quality assurance. The techniques used in different analytical fields are critically reviewed and existing tools for evaluating their performance are described. Particular reference is made to the activities of the Measurements and Testing Programme (BCR) of the European Commission towards the improvement of quality control of environmental analysis.

**Contents:** 1. Quality assurance for environmental analysis (Ph. Quevauviller *et al.*). 2. Development of ICPMS and ID-ICPMS with the determination of Pb and Hg in environmental matrices as an example (M. Campbell). 3. Detection of sources of error in the determination of Cr in environmental matrices by FAAS and ETAAS (G. Rauret *et al.*). 4. Analysis of environmental and biological samples by atomic spectroscopic methods (M. Hoenig, M.F. Gunn). 5. Validation of neutron activation analysis techniques (K. Heydorn). 6. Flow-through (bio)chemical sensors in environmental analysis (M.D. Luque de Castro, M. Válcárcel). 7. Fiber optical sensors applied to field measurements (C. Cámara *et al.*). 8. Chromium speciation in environmental and biological

samples (K. Vercoetere, R. Cornelis). 9. Determination of aluminium species in natural waters (B. Fairman, A. Sanz-Medel). 10. Selenium speciation analyses in water and sediment matrices (C. Cámara *et al.*). 11. Antimony speciation in water (M.B. de la Calle-Guntiñas *et al.*). 12. Arsenic speciation in environmental matrices (A. Amran *et al.*). 13. Mercury speciation in biological matrices (I. Drabæk, Å Iverfeldt). 14. Speciation analysis of organolead compounds. Status and future prospects (R. Lobinski *et al.*). 15. Speciation analysis of organotin by GC-AAS and GC-AES after extraction and derivatization (W.M.R. Dirx *et al.*). 16. High performance liquid chromatography - isotope dilution - inductively coupled plasma - mass spectrometry for lead and tin speciation in environmental samples (S.J. Hill *et al.*). 17. Speciation of organotin compounds in environmental samples by GC-MS (R. Morabito *et al.*). 18. Development of supercritical fluid extraction procedures for the determination

of organotin compounds in sediment (J.M. Bayona). 19. Hydride generation for speciation analyses using GC/AAS (R. Ritsema *et al.*). 20. Single and sequential extraction schemes for trace metal speciation in soil and sediment (A.M. Ure *et al.*). 21. Methods for the determination of chlorinated biphenyls in air (M. Morosini, K. Balschmitter). 22. Sample handling and determination of carbamate pesticides and their transformation products in various matrices (M. Honing *et al.*). 23. Method development for the determination of polycyclic aromatic hydrocarbons (PAHs) in environmental matrices (J. Jacob). 24. Method validation for the determination of dioxins (T. Rymen). Subject index.

©1995 670 pages Hardbound  
Price: Dfl. 475.00 (US\$279.50)  
ISBN 0-444-89955-3

## ORDER INFORMATION

**ELSEVIER SCIENCE**  
Customer Service Department  
P.O. Box 211  
1000 AE Amsterdam  
The Netherlands  
Fax: +31 (20) 485 3432

For USA and Canada:  
**ELSEVIER SCIENCE**  
Customer Service Department  
P.O. Box 945, New York  
NY 10159-0945  
Fax: +1 (212) 633 3764

US\$ prices are valid only for the USA & Canada and are subject to exchange rate fluctuations; in all other countries the Dutch guilder price (Dfl.) is definitive. Customers in the European Union should add the appropriate VAT rate applicable in their country to the price(s). Books are sent postfree if prepaid.



**ELSEVIER**

An imprint of Elsevier Science

AVAILABLE AT YOUR FINGERTIPS:

NOW AVAILABLE:

# THE ELSEVIER SCIENCE COMPLETE CATALOGUE ON INTERNET

# THE ELSEVIER SCIENCE COMPLETE CATALOGUE 1995 ON CD-ROM

These catalogues feature all journals, books and major reference works from Elsevier Science. Furthermore they allow you to access information about the electronic and CD-ROM products now published by Elsevier Science.

Demonstration examples of some of these products are included.

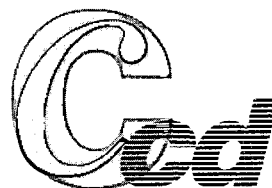
### Features include:

#### ELSEVIER SCIENCE



Catalogue on INTERNET

#### ELSEVIER SCIENCE



Catalogue on CD-ROM

- All the journals, with complete information about journal editors and editorial boards
- Listings of special issues and volumes
- Listings of recently published papers for many journals
- Complete descriptions and contents lists of book titles
- Clippings of independent reviews of published books
- Book series, dictionaries, reference works
- Electronic and CD-ROM products
- Demonstration versions of electronic products
- Free text search facilities
- Ordering facilities
- Print options
- Hypertext features

### Extra features with the Catalogue on Internet

- Alerting facility for new & forthcoming publications
- Updated monthly

**ELSEVIER SCIENCE  
COMPLETE CATALOGUE  
INTERNET: TRY IT TODAY!**

gopher to: gopher.elsevier.nl  
WWW: http://www.elsevier.nl/

**CD-ROM** (published yearly, free of charge)

**Please contact:**

Customer Service Department  
Tel: +31 (20) 485 3757  
Fax: +31 (20) 485 3432  
e-mail: [nlinfo-f@elsevier.nl](mailto:nlinfo-f@elsevier.nl)



ELSEVIER



PERGAMON



NORTH  
HOLLAND



EXCERPTA  
MEDICA

## PUBLICATION SCHEDULE FOR THE 1995 SUBSCRIPTION

*Journal of Chromatography A and Journal of Chromatography B: Biomedical Applications*

MONTH	J–J <sup>a</sup>	A	S	O	N	D
Journal of Chromatography A	689–708/1	708/2 709/1 709/2 710/1	710/2 711/1 711/2	712/1 712/2		
Bibliography Section	713		714/1			714/2
Journal of Chromatography B: Biomedical Applications	663–669	670/1 670/2	671/1 + 2	672/1 672/2	673/1 673/2	674/1 674/2

<sup>a</sup> Vol. 701 (Cumulative Indexes Vols. 652–700) expected in December.

### INFORMATION FOR AUTHORS

(Detailed *Instructions to Authors* were published in *J. Chromatogr. A*, Vol. 657, pp. 463–469. A free reprint can be obtained by application to the publisher, Elsevier Science B.V., P.O. Box 330, 1000 AH Amsterdam, Netherlands.)

**Types of Contributions.** The following types of papers are published: Regular research papers (full-length papers), Review articles, Short Communications and Discussions. Short Communications are usually descriptions of short investigations, or they can report minor technical improvements of previously published procedures; they reflect the same quality of research as full-length papers, but should preferably not exceed five printed pages. Discussions (one or two pages) should explain, amplify, correct or otherwise comment substantively upon an article recently published in the journal. For Review articles, see inside front cover under Submission of Papers.

**Submission.** Every paper must be accompanied by a letter from the senior author, stating that he/she is submitting the paper for publication in the *Journal of Chromatography A* or *B*.

**Manuscripts.** Manuscripts should be typed in **double spacing** on consecutively numbered pages of uniform size. The manuscript should be preceded by a sheet of manuscript paper carrying the title of the paper and the name and full postal address of the person to whom the proofs are to be sent. As a rule, papers should be divided into sections, headed by a caption (e.g., Abstract, Introduction, Experimental, Results, Discussion, etc.). All illustrations, photographs, tables, etc., should be on separate sheets.

**Abstract.** All articles should have an abstract of 50–100 words which clearly and briefly indicates what is new, different and significant. No references should be given.

**Introduction.** Every paper must have a concise introduction mentioning what has been done before on the topic described, and stating clearly what is new in the paper now submitted.

**Experimental conditions** should preferably be given on a *separate* sheet, headed "Conditions". These conditions will, if appropriate, be printed in a block, directly following the heading "Experimental".

**Illustrations.** The figures should be submitted in a form suitable for reproduction, drawn in Indian ink on drawing or tracing paper. Each illustration should have a caption, all the *captions* being typed (with double spacing) together on a *separate sheet*. If structures are given in the text, the original drawings should be provided. Coloured illustrations are reproduced at the author's expense, the cost being determined by the number of pages and by the number of colours needed. The written permission of the author and publisher must be obtained for the use of any figure already published. Its source must be indicated in the legend.

**References.** References should be numbered in the order in which they are cited in the text, and listed in numerical sequence on a separate sheet at the end of the article. Please check a recent issue for the layout of the reference list. Abbreviations for the titles of journals should follow the system used by *Chemical Abstracts*. Articles not yet published should be given as "in press" (journal should be specified), "submitted for publication" (journal should be specified), "in preparation" or "personal communication".

Vols. 1–651 of the *Journal of Chromatography*; *Journal of Chromatography, Biomedical Applications* and *Journal of Chromatography, Symposium Volumes* should be cited as *J. Chromatogr.* From Vol. 652 on, *Journal of Chromatography A* (incl. Symposium Volumes) should be cited as *J. Chromatogr. A* and *Journal of Chromatography B: Biomedical Applications* as *J. Chromatogr. B*.

**Dispatcn.** Before sending the manuscript to the Editor please check that the envelope contains four copies of the paper complete with references, captions and figures. One of the sets of figures must be the originals suitable for direct reproduction. Please also ensure that permission to publish has been obtained from your institute.

**Proofs.** One set of proofs will be sent to the author to be carefully checked for printer's errors. Corrections must be restricted to instances in which the proof is at variance with the manuscript.

**Reprints.** Fifty reprints will be supplied free of charge. Additional reprints can be ordered by the authors. An order form containing price quotations will be sent to the authors together with the proofs of their article.

**Advertisements.** The Editors of the journal accept no responsibility for the contents of the advertisements. Advertisement rates are available on request. Advertising orders and enquiries can be sent to: Elsevier Science, Advertising Department, The Boulevard, Langford Lane, Kidlington, Oxford, OX5 1GB, UK; Tel: (+44) (0) 1865 843565; Fax (+44) (0) 1865 843952. *USA and Canada:* Weston Media Associates, Dan Lipner, P.O. Box 1110, Greens Farms, CT 06436-1110, USA; Tel (203) 261 2500; Fax (203) 261 0101. *Japan:* Elsevier Science Japan, Ms Noriko Kodama, 20-12 Yushima, 3 chome, Bunkyo-Ku, Tokyo 113, Japan; Tel (+81) 3 3836 0810; Fax (+81) 3 3839 4344.

# Flow-Through (Bio)Chemical Sensors

By M. Valcárcel and M.D. Luque de Castro

Techniques and Instrumentation in Analytical Chemistry Volume 16

Flow-through sensors are more suitable than classical probe-type sensors for addressing real (non-academic) problems. The external shape and operation of flow-through (bio)chemical sensors are of great practical significance as they facilitate sample transport and conditioning, as well as calibration and sensor preparation, maintenance and regeneration, all of which result in enhanced analytical features and a wider scope of application. This is a systematic presentation of flow-through chemical and biochemical sensors based on the permanent or transient immobilization of any of the ingredients of a (bio)chemical reaction (i.e. the analyte, reagent, catalyst or product) where detection is integrated with the analytical reaction, a separation process (dialysis, gas diffusion, sorption, etc.) or both.

The book deals critically with most types of flow-through sensors, discussing their possibilities and shortcomings to provide a realistic view of the state-of-the-art in the field. The large numbers of figures, the wealth of literature references and the extensive subject index complement the text.

## Contents: 1. Sensors in Analytical Chemistry.

Analytical chemistry at the turn of the XXI century. Analytical information. What

is a sensor? Sensors and the analytical process. Types of sensors. General features of (bio)chemical sensors. (Bio)chemical sensors and analytical properties. Commercial availability. Trends in sensor development.

## 2. Fundamentals of Continuous-Flow (Bio)Chemical Sensors.

Definition. Classification. The active microzone. Flow-through cells. Continuous configurations. Regeneration modes. Transient signals. Measurement modes. The role of kinetics. Requirements for proper sensor performance.

## 3. Flow-Through Sensors Based on Integrated Reaction and Detection.

Introduction. Flow-through sensors based on an immobilized catalyst. Flow-through immunosensors. Flow-through sensors based on an immobilized reagent. Flow-through sensors based on an *in situ* produced reagent.

## 4. Flow-Through Sensors Based on Integrated Separation and Detection.

Introduction. Integrated gas diffusion and detection. Integrated liquid-liquid separation and detection. Integrated retention and detection. Flow-through sensors for multideterminations based on integrated retention and detection. Ion-selective electrodes (ISEs) and ion-sensitive field-effect transistors (ISFETs).

## 5. Flow-Through Sensors Based on Integrated Reaction, Separation and Detection.

Introduction. Integration of gas-diffusion, reaction and detection. Integration of dialysis, reaction and detection. Integration of sorption, reaction and detection. **Index.**

©1994 332 pages Hardbound  
Price: Dfl. 355.00 (US\$ 208.75)  
ISBN 0-444-89866-2

## ORDER INFORMATION

**ELSEVIER SCIENCE**  
Customer Service Department  
P.O. Box 211  
1000 AE Amsterdam  
The Netherlands  
Fax: +31 (20) 485 3432

For USA and Canada:

**ELSEVIER SCIENCE**  
Customer Service Department  
P.O. Box 945, New York  
NY 10159-0945  
Fax: +1 (212) 633 3764

US\$ prices are valid only for the USA & Canada and are subject to exchange rate fluctuations; in all other countries the Dutch guilder price (Dfl.) is definitive. Customers in the European Union should add the appropriate VAT rate applicable in their country to the price(s). Books are sent postfree if prepaid.



**ELSEVIER**

An imprint of Elsevier Science



0021-9673(19950929)712:1;1-W

- 7 2538